Engineering Design Reliability

HANDBOOK

Copyright 2005 by CRC Press LLC

Engineering Design Reliability

HANDBOOK

Edited by
Efstratios Nikolaidis
Dan M. Ghiocel
Suren Singhal

CRC PRESS

Boca Raton London New York Washington, D.C.

Copyright 2005 by CRC Press LLC

Library of Congress Cataloging-in-Publication Data

Engineering design reliability handbook / edited by Efstratios Nikolaidis, Dan M. Ghiocel, Suren Singhal
p. cm.
Includes bibliographical references and index.
ISBN 0-8493-1180-2 (alk. paper)
1. Engineering design—Handbooks, manuals, etc. 2. Reliability (Engineering)—Handbooks, manuals, etc. I. Nikolaidis, Efstratios. II. Ghiocel, Dan M. III. Singhal, Suren.

TA174.E544 2004
620'.00452—dc22 2004045850

This book contains information obtained from authentic and highly regarded sources. Reprinted material is quoted with permission, and sources are indicated. A wide variety of references are listed. Reasonable efforts have been made to publish reliable data and information, but the author and the publisher cannot assume responsibility for the validity of all materials or for the consequences of their use.

Neither this book nor any part may be reproduced or transmitted in any form or by any means, electronic or mechanical, including photocopying, microfilming, and recording, or by any information storage or retrieval system, without prior permission in writing from the publisher.

All rights reserved. Authorization to photocopy items for internal or personal use, or the personal or internal use of specific clients, may be granted by CRC Press LLC, provided that $1.50 per page photocopied is paid directly to Copyright Clearance Center, 222 Rosewood Drive, Danvers, MA 01923 USA. The fee code for users of the Transactional Reporting Service is ISBN 0-8493-1180-2/05/$0.00+$1.50. The fee is subject to change without notice. For organizations that have been granted a photocopy license by the CCC, a separate system of payment has been arranged.

The consent of CRC Press LLC does not extend to copying for general distribution, for promotion, for creating new works, or for resale. Specific permission must be obtained in writing from CRC Press LLC for such copying.

Direct all inquiries to CRC Press LLC, 2005 N.W. Corporate Blvd., Boca Raton, Florida 33431.

Trademark Notice: Product or corporate names may be trademarks or registered trademarks, and are used only for identification and explanation, without intent to infringe.

Visit the CRC Press Web site at www.crcpress.com

© 2005 by CRC Press LLC

No claim to original U.S. Government works
International Standard Book Number 0-8493-1180-2
Library of Congress Card Number 2004045850
Printed in the United States of America 1 2 3 4 5 6 7 8 9 0
Printed on acid-free paper

Copyright 2005 by CRC Press LLC

Engineering Design Reliability Handbook

Abstract

Probabilistic and other nondeterministic methods for design under uncertainty are becoming increasingly popular in the aerospace, automotive, and the ocean engineering industries because they help them design more competitive products. This handbook is an integrated document explaining the philosophy of nondeterministic methods and demonstrating their benefits on real life problems.

This handbook is for engineers, managers, and consultants in the aerospace, automotive, civil, industrial, nuclear, and ocean engineering industries who are using nondeterministic methods for product design, or want to understand these methods and assess their potential. Graduate students and professors in engineering departments at U.S. and foreign colleges and universities, who work on nondeterministic methods, will find this book useful too.

This handbook consists of three parts. The first part presents an overview of nondeterministic approaches including their potential, and their status in the industry, the government and the academia. Engineers and managers from companies, such as General Motors, General Electric, United Technologies, and Boeing, government agencies, such as NASA centers and Los Alamos and Sandia National Laboratories, and university professors present their perspectives about the status and the future of nondeterministic methods and propose steps for enabling the full potential of these methods.

In the second part, the handbook presents recent advances in nondeterministic methods. First theories of uncertainty are presented. Then computational tools for assessing the uncertainty in the performance and the safety of a system, and for design decision making under uncertainty are presented. This part concludes with a presentation of methods for reliability certification.

The third part demonstrates the use and potential of nondeterministic methods by presenting real life applications in the aerospace, automotive and ocean engineering industries. In this part, engineers from the industry and university professors present their success stories and quantify the benefits of nondeterministic methods for their organizations.

Copyright 2005 by CRC Press LLC

Dedications

To my parents, George Nikolaidis and Theopisti Nikolaidis

Efstratios Nikolaidis

To my father, Professor Dan Ghiocel
President of the Romanian Academy of Technical Sciences
Civil Engineering Division

Dan M. Ghiocel

To my parents, my wife, Adesh, and children Rashi and Sara,
and to all-too-important mentors, colleagues, and friends

Suren Singhal

Copyright 2005 by CRC Press LLC

Preface

If one does not reflect, one thinks oneself master of everything;
but when one does reflect, one realizes that one is a master of nothing.

Voltaire

In today's competitive business environment, decisions about product design involve significant uncertainty. To succeed in this environment, one should replace traditional deterministic approaches for making design decisions with a new risk-based approach that uses rigorous models to quantify uncertainty and assess safety. Probabilistic and other nondeterministic methods for design under uncertainty are becoming increasingly popular in the aerospace, automotive, civil, defense and power industries because they help design safer and cheaper products than traditional deterministic approaches. The term "nondeterministic methods" refers to methods that account explicitly for uncertainties in the operating environment, the material properties and the accuracy of predictive models. The foundation of nondeterministic methods includes theories of probability and statistics, interval arithmetic, fuzzy sets, Dempster-Shafer theory of evidence and Information-Gap theory. Nondeterministic methods have helped companies such as General Electric, United Technologies, General Motors, Ford, DaimlerChrysler, Boeing, Lockheed Martin, and Motorola improve dramatically their competitive positions and save billions of dollars in engineering design and warranty costs. While nondeterministic methods are being implemented in the industry, researchers are making important advances on various fronts including reliability-based design, decision under uncertainty and modeling of uncertainty when data are scarce.

Companies need to educate their designers and managers about the advantages and potential of nondeterministic methods. Professors need to educate their students about nondeterministic methods and increase the awareness of administrators about the importance and potential of these methods. To respond to this need, we put together this handbook, which is an integrated document explaining the philosophy and the implementation of nondeterministic methods and demonstrating quantitatively their benefits.

This handbook is for engineers, technical managers, and consultants in the aerospace, automotive, civil, and ocean engineering industries and in the power industry who want to use, or are already using, nondeterministic methods for product design. Professors and students who work on nondeterministic methods will find this book useful too.

This handbook consists of three parts. The first part presents an overview of nondeterministic approaches including their potential and their status in the industry, academia and national labs. Engineers and managers from companies such as Boeing, United Technologies, General Motors and General Electric, government agencies, such as NASA, Los Alamos and Sandia National Laboratories of the Department of Energy, and university professors present their perspectives about the status and future of nondeterministic methods and propose steps for enabling the full potential of these methods. In the second part, the handbook presents the concepts of nondeterministic methods and recent advances in

Copyright 2005 by CRC Press LLC

the area of nondeterministic methods including theories of uncertainty, computational tools for assessing and validating reliability, and methods for design decision-making under uncertainty. The third part demonstrates the use and potential of nondeterministic methods on applications in the aerospace, automotive, defense and ocean engineering industries. In this part, engineers from the industry and university researchers present success stories and quantify the benefits of nondeterministic methods for their organizations.

A fundamental objective of the book is to provide opinions of experts with different background, experience and personality. Therefore, there are several chapters in the book written by experts from academia, national laboratories or the industry with diverse, and occasionally conflicting, views on some issues. We believe that presenting diverse opinions makes the book content richer and more informative and benefits the reader.

We are grateful to all the authors who contributed to this book. We appreciate the considerable amount of time that the authors invested to prepare their chapters and their willingness to share their ideas with the engineering community. The quality of this book depends greatly on the quality of the contributions of all the authors. We also acknowledge CRC Press for taking the initiative to publish such a needed handbook for our engineering community. In particular, we wish to thank Cindy Carelli, Jay Margolis, Helena Redshaw, and Jessica Vakili for their continuous administrative and editorial support.

Efstratios Nikolaidis
The University of Toledo

Dan M. Ghiocel
Ghiocel Predictive Technologies, Inc.

Suren Singhal
NASA Marshall Space Flight Center

Copyright 2005 by CRC Press LLC

About the Editors

Dr. Efstratios Nikolaidis is a professor of mechanical, industrial, and manufacturing engineering at the University of Toledo, Ohio. His research has focused on reliability-based design optimization of aerospace, automotive, and ocean structures, theories of uncertainty, and structural dynamics. He has published three book chapters, and more than 100 journal and conference papers, mostly on nondeterministic approaches.

Dr. Dan M. Ghiocel is the Chief Engineering Scientist of Ghiocel Predictive Technologies Inc., in Rochester, New York that is a small business specialized in nondeterministic modeling for high-complexity engineering problems. Since 2001, Dr. Ghiocel is also Adjunct Professor at Case Western Reserve University, in Cleveland, Ohio. Dr. Ghiocel has accumulated a large experience in probabilistic approaches for civil nuclear facilities and jet engine systems. He is a member with leading responsibilities in several prestigious technical committees and professional working groups, including AIAA, SAE, and ASCE.

Dr. Suren Singhal is a nationally and internationally recognized leader in the field probabilistic methods and technology. He has initiated new committees, panels, and forums in nondeterministic and probabilistic approaches. He has led development of state-of-the-art probabilistic technology and documents dealing with diverse aspects such as cultural barriers and legal issues.

Copyright 2005 by CRC Press LLC

Contributors

Frank Abdi
Alpha STAR Corp
Long Beach, California, U.S.A.

Joshua Altmann
Vipac Engineers & Scientists Ltd.
Port Melbourne, Australia

Andre T. Beck
Universidade Luterana do Brazil
Canoas, Brazil

Yakov Ben-Haim
Technion-Israel Institute of Technology
Haifa, Israel

Jane M. Booker
Los Alamos National Laboratory
Los Alamos, New Mexico, U.S.A.

Jeffrey M. Brown
U.S. Air Force
AFRL Wright-Patterson Air Force Base, Ohio, U.S.A.

Christian Bucher
Bauhaus-University Weimar
Weimar, Germany

John A. Cafeo
General Motors Corporation
Warren, Michigan, U.S.A.

Brice N. Cassenti
Pratt & Whitney
East Hartford,
Connecticut, U.S.A.

Tina Castillo
Alpha STAR Corporation
Long Beach, California, U.S.A.

Christos C. Chamis
NASA Glenn Research Center
Cleveland, Ohio, U.SA.

Kyung K. Choi
The University of Iowa
Iowa City, lowa, U.S.A.

William (Skip) Connon
U.S. Army Aberdeen Test Center
Aberdeen Proving Ground,
Maryland, U.S.A.

Thomas A. Cruse
Vanderbilt University
Nashville, Tennessee, U.S.A.

Armen Der Kiureghian
University of California
Berkeley, California, U.S.A.

Xuru Ding
General Motors Corporation
Warren, Michigan, U.S.A.

Joseph A. Donndelinger
General Motors Corporation
Warren, Michigan, U.S.A.

Mike P. Enright
Southwest Research Institute
San Antonio, Texas, U.S.A.

Simeon H. K. Fitch
Mustard Seed Software
San Antonio, Texas, U.S.A.

Eric P. Fox
Veros Software
Scottsdale, Arizona, U.S.A.

Dan M. Frangopol
University of Colorado
Boulder, Colorado, U.S.A.

Jeffrey S. Freeman
The University of Tennessee
Knoxville, Tennessee, U.S.A.

Dan M. Ghiocel
Ghiocel Predictive Technologies
Pittsford, New York, U.S.A.

James A. Griffiths
General Electric Company
Evendale, Ohio, U.S.A.

Copyright 2005 by CRC Press LLC

Mircea Grigoriu
Cornell University
Ithaca, New York, U.S.A.

Jon C. Helton
Sandia National Laboratories
Albuquerque, New Mexico, U.S.A.

Luc J. Huyse
Southwest Research Institute
San Antonio, Texas, U.S.A.

Cliff Joslyn
Los Alamos National Laboratory
Los Alamos, New Mexico, U.S.A.

Lambros S. Katafygiotis
Hong Kong University of Science and Technology
Kowloon, Hong Kong

Dimitri B. Kececioglu
The University of Arizona
Tucson, Arizona, U.S.A.

Artemis Kloess
General Motors Corporation
Warren, Michigan, U.S.A.

Robert V. Lust
General Motors Corporation
Warren, Michigan, U.S.A.

Michael Macke
Bauhaus-University Weimar
Weimar, Germany

Sankaran Mahadevan
Vanderbilt University
Nashville, Tennessee, U.S.A.

Kurt Maute
University of Colorado
Boulder, Colorado, U.S.A.

Laura A. McNamara
Los Alamos National Laboratory
Los Alamos, New Mexico, U.S.A.

David Mease
University of Pennsylvania
Philadelphia, Pennsylvania U.S.A.

Robert E. Melchers
The University of Newcastle
Callaghan, Australia

Zissimos P. Mourelatos
Oakland University
Rochester, Michigan, U.S.A.

Rafi L. Muhanna
Georgia Institute of Technology
Savannah, Georgia, U.S.A.

Robert L. Mullen
Case Western Reserve University
Cleveland, Ohio, U.S.A.

Prasanth B. Nair
University of Southampton
Southampton, U.K.

Vijayan N. Nair
University of Michigan
Ann Arbor, Michigan, U.S.A.

Raviraj Nayak
General Motors Corporation
Warren, Michigan, U.S.A.

Daniel P. Nicolella
Southwest Research Institute
San Antonio, Texas, U.S.A.

Efstratios Nikolaidis
The University of Toledo
Toledo, Ohio, U.S.A.

Ahmed K. Noor
Old Dominion University
Hampton, Virginia, U.S.A.

William L. Oberkampf
Sandia National Laboratories
Albuquerque, New Mexico, U.S.A.

Shantaram S. Pai
NASA Glenn Research Center
Cleveland, Ohio, U.S.A.

Jeom K. Paik
Pusan National University
Busan, Republic of Korea

Costas Papadimitriou
University of Thessaly
Volos, Greece

Alan L. Peltz
U.S. Army Materiel Systems Analysis Activity
Aberdeen Proving Ground, Maryland, U.S.A.

Chris L. Pettit
U.S. Naval Academy
Annapolis, Maryland, U.S.A.

Kadambi Rajagopal
The Boeing Company
Canoga Park, California, U.S.A.

Copyright 2005 by CRC Press LLC

David S. Riha
Southwest Research Institute
San Antonio, Texas, U.S.A.

David G. Robinson
Sandia National Laboratories
Albuquerque, Albu Mexico, U.S.A.

Michael J. Scott
University of Illinois at Chicago
Chicago, Illinois, U.S.A.

Youngwon Shin
Applied Research Associates.
Raleigh, North Carolina, U.S.A.

Edward Shroyer
The Boeing Company
Huntington Beach, California, U.S.A.

Thomas J. Stadterman
U.S. Army Materiel Systems Analysis Activity
Aberdeen Proving Ground, Aberdeen, Maryland, U.S.A.

Agus Sudjianto
Ford Motor Company
Dearborn, Michigan, U.S.A.

Robert H. Sues
Applied Research Associates.
Raleigh, North Carolina, U.S.A.

Jun Tang
University of Iowa
Iowa City, Iowa, U.S.A.

Ben H. Thacker
Southwest Research Institute
San Antonio, Texas, U.S.A.

Anil Kumar Thayamballi
Chevron Texaco Shipping Company LLC
San Francisco, California, U.S.A.

Palle Thoft-Christensen
Aalborg University
Aalborg, Denmark

Sviatoslav A. Timashev
Russian Academy of Sciences
Ekaterinburg, Russia

Tony Y. Torng
The Boeing Company
Huntington Beach, California, U.S.A.

Robert Tryon
Vextec Corporation
Brentwood, Tennessee, U.S.A.

Jonathan A. Tschopp
General Electric Company
Evendale, Ohio, U.S.A.

Jian Tu
General Motors Corporation
Warren, Michigan, U.S.A.

Eric J. Tuegel
U.S. Air Force
AFRL Wright-Patterson Air Force Base, Ohio, U.S.A.

Erik Vanmarcke
Princeton University
Princeton, New Jersey, U.S.A.

Chris J. Waldhart
Southwest Research Institute
San Antonio, Texas, U.S.A.

(Justin) Y.-T. Wu
Applied Research Associates.
Raleigh, North Carolina, U.S.A.

Byeng D. Youn
University of Iowa
Iowa City, Iowa, U.S.A.

Copyright 2005 by CRC Press LLC

Contents

Copyright 2005 by CRC Press LLC

Copyright 2005 by CRC Press LLC

Part III: Applications

Copyright 2005 by CRC Press LLC

Copyright 2005 by CRC Press LLC

Disclaimer

The views and opinions expressed in this book are strictly those of the contributors and the editors and they do not necessarily reflect the views of their companies, their organizations, or the government.

Copyright 2005 by CRC Press LLC

I

Status and Future of Nondeterministic Approaches (NDAs)

Copyright 2005 by CRC Press LLC

Copyright 2005 by CRC Press LLC

1

Brief Overview of the Handbook

Efstratios Nikolaidis
The University of Toledo

Dan M. Ghiocel
Ghiocel Predictive Technologies

1.1 Introduction

This handbook provides a comprehensive review of nondeterministic approaches (NDA) in engineering. The review starts by addressing general issues, such as the status and future of NDA in the industry, government, and academia, in Part I. Then the handbook focuses on concepts, methods, and recent advances in NDA, in Part II. Part III demonstrates successful applications of NDA in the industry.

1.1.1 Part I: Status and Future of Nondeterministic Approaches

Uncertainties due to inherent variability, imperfect knowledge, and errors are important in almost every activity. Managers and engineers should appreciate the great importance of employing rational and systematic approaches for managing uncertainty in design. For this purpose, they need to understand the capabilities of NDA and the critical issues about NDA that still need to be addressed. Managers and engineers should also be aware of successful applications of NDA in product design. Researchers in academia, national labs, and research centers should know what areas of future research on NDA are important to the industry.

The first part of the handbook addresses the above issues with an overview of NDA that includes the capabilities of these approaches and the tools available. This part explains what should be done to enable the full potential of NDA and to transition these approaches from research to engineering design. In Part I, technical managers from the government (Chapters 2 and 3), industry (Chapters 4 and 5), and academia and national laboratories (Chapters 6 and 7) present their perspectives on the potential of NDA technology. We believe that the information presented in this part will help the engineering community understand and appreciate the potential and benefits of the application of NDA to engineering design and help technical managers deploy NDA to improve the competitive positions of their organizations.

1.1.2 Part II: Nondeterministic Modeling: Critical Issues and Recent Advances

The second part of the book presents critical issues that are important to the implementation of NDA to real-life engineering problems, and recent advances toward addressing these issues. These issues include:

Copyright 2005 by CRC Press LLC

1. What are the most important sources of uncertainty in engineering design?
2. What are the most suitable theories of uncertainty and mathematical tools for modeling different types of uncertainty?
3. How do we model uncertainty in quantities that vary with time and space, such as the material properties in a three-dimensional structure, or the particle velocity in a turbulent flow-field?
4. What tools are available for uncertainty propagation through a component or a system, and for reliability assessment? What tools are available for estimating the sensitivity of the reliability of a system to uncertainties in the input variables and for identifying the most important variables?
5. How do we make decisions in the presence of different types of uncertainty?
6. How do we validate the reliability of a design efficiently?

Part II consists of a total of 20 chapters. This part is divided into three groups. The first group studies types of uncertainties and theories and tools for modeling uncertainties. The second group presents computational tools for reliability assessment, propagation of uncertainty through a component or system, and decision making under uncertainty. The third group presents methods for reliability validation using tests.

Following is a summary of the chapters in each group.

1.1.2.1 Uncertainty and Theories of Uncertainty

Chapter 8 studies existing taxonomies of uncertainty in a design decision problem. Then it proposes a new taxonomy of uncertainties that are present in the stages of the solution of a design decision problem. This taxonomy is based on the sources of uncertainty. The stages of a decision include framing of the decision, predicting the outcomes and evaluating the worth of the outcomes according to the decision-maker's preferences. The chapter also examines different types of information that can be used to construct models of uncertainty. Chapter 9 presents a general theory of uncertainty-based information. The term "uncertainty-based information" implies that information is considered a reduction of uncertainty. Theories of uncertainty, such as probability, possibility, and Dempster-Shafer evidence theory, are branches of the general theory of uncertainty-based information. The chapter presents measures for characterizing uncertainty and measures of the amount of uncertainty. Chapter 10 presents Dempster-Shafer evidence theory. The authors of this chapter argue that evidence theory can be more suitable than probability theory for modeling epistemic uncertainty. A principal reason is that evidence theory does not require a user to assume information beyond what is available. Evidence theory is demonstrated and contrasted with probability theory on quantifying uncertainty in an algebraic function of input variables when the evidence about the input variables consists of intervals. Chapters 11 and 12 present theories that are suitable for design in the face of uncertainty when there is a severe deficit in the information about uncertainty. Chapter 11 presents information-gap decision theory, which is based on the theory of robust reliability. Another method is to use an interval for each uncertain variable to characterize uncertainty. Chapter 12 presents an efficient method for computing narrow intervals for the response of a component or system when uncertainty is modeled using intervals. In many design problems, information about uncertainty is obtained mainly from experts. Chapter 13 presents a rigorous approach for eliciting, documenting, and analyzing information from experts.

1.1.2.2 Reliability Assessment and Uncertainty Propagation

The second group of chapters presents tools for propagating uncertainty through a component or system (that is, quantifying the uncertainty in the response given a model of the uncertainty in the input variables), and for assessing the reliability of a component or system. The chapters also present methods for the design of components and systems that account directly for reliability. These chapters focus on methods and tools that are based on probability theory and statistics.

First, two numerical approaches for element reliability analysis are examined in which uncertainties are modeled using random vectors. Chapter 15 presents methods for reliability assessment of systems and illustrates these methods with numerous examples involving civil engineering structures.

Copyright 2005 by CRC Press LLC

First- and second-order reliability methods are employed for this purpose. Chapter 16 presents a class of probability density functions that have a fundamental basis in quantum physics. The chapter explains that these probabilistic models have considerable potential for applications to reliability analysis of components and systems. Chapters 14 and 15 are confined to time-invariant problems. Chapters 17 and 18 study time-variant reliability problems in which the excitation on a structure and/or its strength vary with time. Chapter 17 primarily considers structures whose strength is constant. This chapter presents methods for modeling the excitation, finding the statistics of the response, and the failure probability. Chapter 18 provides a thorough review of methods for calculating the reliability of structures whose strength varies with time.

One way to reduce the computational cost associated with reliability assessment is to replace the deterministic model that is used for predicting the response of a system or component with a response surface. Chapter 19 presents different response surface approximation methods. These methods are widely used in the industry and are effective for stochastic problems with a small number of random variables, e.g., less than ten. Chapter 20 presents Monte Carlo simulation methods. These methods are applicable to a broad range of problems, including both time-invariant and time-variant problems. Uncertainties can be modeled using random vectors, stochastic processes, or random fields (random functions of space variables and/or time). This chapter also includes useful discussions on the use of Monte Carlo simulation in conjunction with hierarchical models for stochastic approximation, application of static, sequential and dynamic sampling, and computation of probabilities for high-dimensional problems. Chapter 21 presents stochastic finite element methods. These methods can be used to analyze the uncertainty in a component or system, when the uncertainty in the input is described using random fields. Thus, the methods allow one to accurately model the spatial variation of a random quantity, such as the modulus of elasticity in a structure. These methods convert a boundary value problem with stochastic partial differential equations into a system of algebraic equations with random coefficients. This system of equations can be solved using different numerical techniques including Monte Carlo simulation, or first- and second-order reliability methods, to compute the probability distribution of the performance parameters of a system or component and its reliability. Bayesian methods are useful for updating models of uncertainty, or deterministic models for predicting the performance of a component or system, using sampling information. Chapter 22 is concerned with statistical modeling and updating of structural models as well as their use for predicting their response and estimating their reliability.

1.1.2.3 Engineering Decision under Uncertainty

The results of nondeterministic approaches are useful for making design decisions under uncertainty. Chapters 23 and 24 present tools for decision making. Chapter 23 introduces and illustrates the concepts of utility theory and tools for assessment of the expected utility. These tools can aid decisions in the presence of uncertainty and/or decisions with multiple objectives. Chapter 24 presents methods for reliability-based design optimization. These methods account explicitly for the reliability of a system as opposed to traditional deterministic design, which accounts for uncertainty indirectly using a safety factor and design values of the uncertain variables. The methods and their advantages over deterministic design optimization methods are illustrated with problems involving civil and aerospace engineering systems and microelectromechanical systems (MEMS).

1.1.2.4 Reliability Certification

Validation of the reliability of a design through tests is an important part of design. Chapter 25 presents accelerated life testing methods for reliability validation. Chapter 26 provides a review of tools for constructing and testing models of uncertainty.

Often, we cannot afford to perform a sufficient number of physical tests to validate the reliability of a design. Chapter 27 presents a rigorous method for reducing dramatically the number of the tests required for reliability validation by testing a small set of nominally identical systems selected so as to maximize the confidence in the estimate of the reliability from the test.

Copyright 2005 by CRC Press LLC

1.1.3 Part III: Applications

After providing a general overview of NDA and explaining the concepts and the tools available, the handbook demonstrates how these approaches work on real-life industrial design problems in Part III. This part reports successful applications of NDA in the following companies: Alpha STAR Corporation; Applied Research Associates, Inc.; Boeing; General Electric; General Motors Corporation; Ghiocel Predictive Technologies, Inc.; Mustard Seed Software; Pratt & Whitney; Shevron Shipping Company, LLC; Vipac Engineers & Scientists LTD; and Vextec Corporation. This part consists of 18 chapters. Success stories of reliability analysis and reliability-based optimization are presented and the benefits from the use of NDA are quantified.

Copyright 2005 by CRC Press LLC

2

Perspectives on Nondeterministic Approaches

Ahmed K. Noor
Old Dominion University

2.1 Introduction

Increasingly more complex systems are being built and conceived by high-tech industries. Examples of future complex systems include the biologically inspired aircraft with self-healing wings that flex and react like living organisms, and the integrated human robotic outpost (Figure 2.1). The aircraft is built of multifunctional material with fully integrated sensing and actuation, and unprecedented

Copyright 2005 by CRC Press LLC

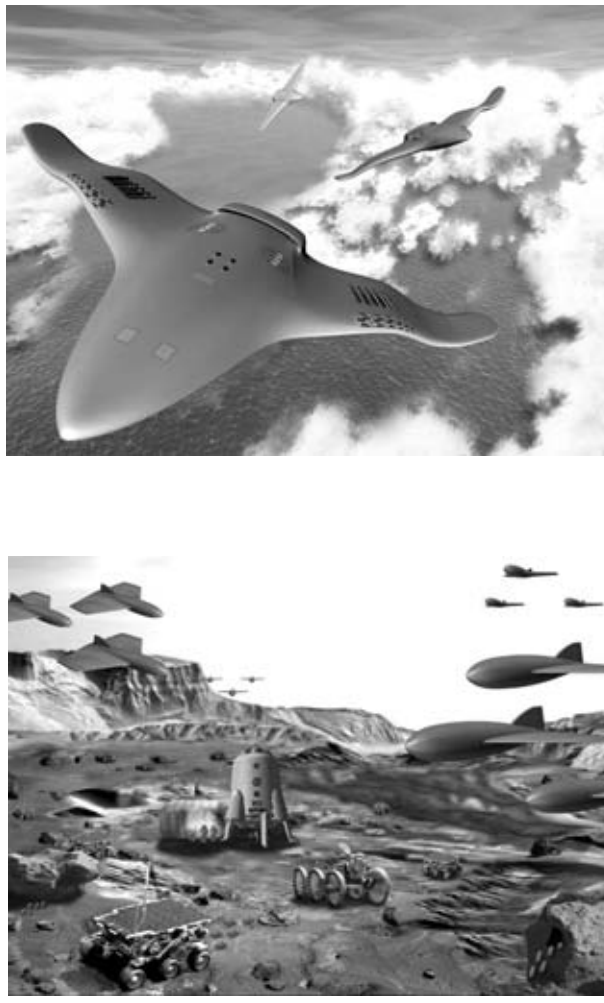

FIGURE 2.1 Examples of future complex systems: (a) biologically inspired aircraft and (b) human-robotic outpost.

levels of aerodynamic efficiencies and aircraft control. The robots in the outpost are used to enhance the astronauts' capabilities to do large-scale mapping, detailed exploration of regions of interest, and automated sampling of rocks and soil. They could enhance the safety of the astronauts by alerting them to mistakes before they are made, and letting them know when they are showing signs of fatigue, even if they are not aware of it.

Engineers are asked to design faster, and to insert new technologies into complex systems. Increasing reliance is being made on modeling, simulation and virtual prototyping to find globally optimal designs that take uncertainties and risk into consideration. Conventional computational and design methods are inadequate to handle these tasks. Therefore, intense effort has been devoted in recent years to nontraditional and nondeterministic methods for solving complex problems with system uncertainties.

Although, the number of applications of nondeterministic approaches in industry continues to increase, there is still some confusion—arising from ill-defined and inconsistent terminology, vague language, and misinterpretation—present in the literature.

An attempt is made in this chapter to give broad definitions to the terms and to set the stage for the succeeding chapters.

Copyright 2005 by CRC Press LLC

2.1.1 Definitions of Uncertainty

Uncertainty is an acknowledged phenomenon in the natural and technological worlds. Engineers are continually faced with uncertainties in their designs. However, there is no unique definition of uncertainty. A useful functional definition of uncertainty is: the information/knowledge gap between what is known and what needs to be known for optimal decisions, with minimal risk [1–3].

2.1.2 Brief Historical Account of Uncertainty Modeling

Prior to the twentieth century, uncertainty and other types of imprecision were considered unscientific, and therefore were not addressed. It was not until the beginning of the twentieth century that statistical mechanics emerged and was accepted as a legitimate area of science. It was taken for granted that uncertainty is adequately captured by probability theory. It took 60 years to recognize that the conceptual uncertainty is too deep to be captured by probability theory alone and to initiate studies of nonprobabilistic manifestations of uncertainty, as well as their applications in engineering and science. In the past two decades, significant advances have been made in uncertainty modeling, the level of sophistication has increased, and a number of software systems have been developed. Among the recent developments are the perception-based information processing and methodology of computing with words (Figure 2.2).

2.1.3 Chapter Outline

The overall objective of this chapter is to give a brief overview of the current status and future directions for research in nondeterministic approaches. The number of publications on nondeterministic approaches has been steadily increasing, and a vast amount of literature currently exists on various aspects and applications of nondeterministic approaches. The cited references are selected for illustrating the ideas presented and are not necessarily the only significant contributions to the subject. The discussion in this chapter is kept on a descriptive level; for details, the reader is referred to the cited literature.

The topics of the succeeding sections include types of uncertainties and uncertainty measures; managing uncertainties; nondeterministic analysis approaches; enhancing the modeling and simulation technologies; verification and validation of numerical simulations; risk management process; key

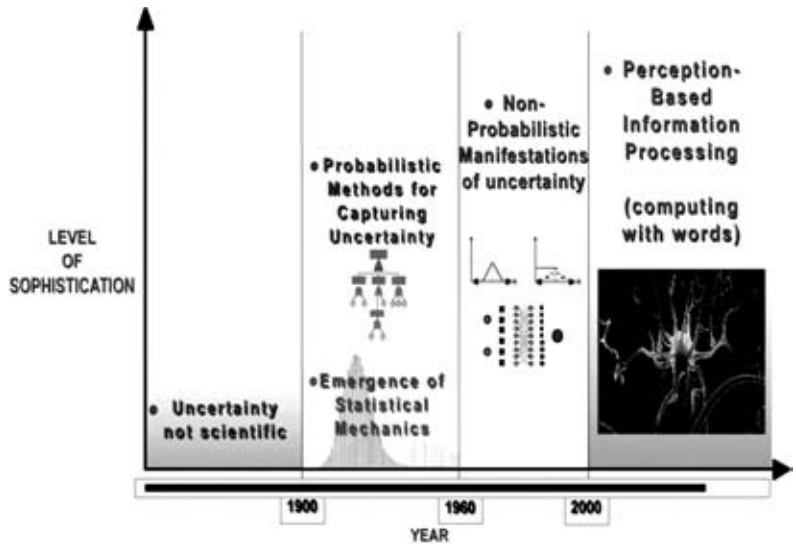

FIGURE 2.2 Evolution of uncertainty modeling.

Copyright 2005 by CRC Press LLC

components of advanced simulation and modeling environments; nondeterministic approaches research and learning networks.

2.2 Types of Uncertainties and Uncertainty Measures

A number of different uncertainty representations and classifications have been proposed. Among these are [1,3–5]:

- The two-type classification — aleatory and epistemic uncertainty in the modeling and simulation process. *Aleatory* uncertainty (originating from the Latin *aleator* or *aleatorius,* meaning dice thrower) is used to describe the inherent spatial and temporal variation associated with the physical system or the environment under consideration as well as the uncertainty associated with the measuring device. Sources of aleatory uncertainty can be represented as randomly distributed quantities. Aleatory uncertainty is also referred to in the literature as variability, irreducible uncertainty, inherent uncertainty, and stochastic uncertainty.

  Epistemic uncertainty (originating from the Greek *episteme*, meaning knowledge) is defined as any lack of knowledge or information in any phase or activity of the modeling process. Examples of sources of epistemic uncertainty are scarcity or unavailability of experimental data for fixed (but unknown) physical parameters, limited understanding of complex physical processes or interactions of processes in the engineering system, and the occurrence of fault sequences or environment conditions not identified for inclusion in the analysis of the system.

  An increase in knowledge or information, and/or improving the quality of the information available can lead to a reduction in the predicted uncertainty of the response of the system. Therefore, epistemic uncertainty is also referred to as reducible uncertainty, subjective uncertainty, and model form uncertainty.
- The two-type classification — uncertainty of information and uncertainty of the reasoning process
- The three-type classification — fundamental (or aleatory), statistical, and model uncertainties. The statistical and model uncertainties can be viewed as special cases of the epistemic uncertainty described previously.
- The three-type classification—variabilities, epistemic uncertainty, and errors.
- The six-type classification with the following six types of uncertainties (Figure 2.3):
  - Probabilistic uncertainty, which arises due to chance or randomness
  - Fuzzy uncertainty due to linguistic imprecision (e.g., set boundaries are not sharply defined)
  - Model uncertainty, which is attributed to a lack of information about the model characteristics
  - Uncertainty due to limited (fragmentary) information available about the system (e.g., in the early stage of the design process)
  - Resolutional uncertainty, which is attributed to limitation of resolution (e.g., sensor resolution)
  - Ambiguity (i.e., one-to-many relations)

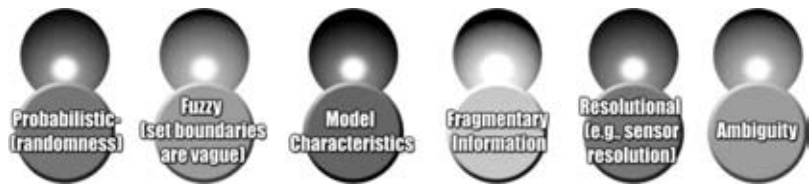

FIGURE 2.3 Six types of uncertainties.

Copyright 2005 by CRC Press LLC

FIGURE 2.4 Disciplines involved in uncertainty management.

In this classification, the probabilistic uncertainty is the same as the aleatory uncertainty of the first classification; and the remaining five types can be viewed as epistemic uncertainties.

2.3 Managing Uncertainties

While completely eliminating uncertainty in engineering design is not possible, reducing and mitigating its effects have been the objectives of the emerging field of uncertainty management. The field draws from several disciplines, including statistics, management science, organization theory, and inferential thinking (Figure 2.4).

In developing strategies for managing uncertainties, the following items must be considered [1]:

- Developing formal, rigorous models of uncertainty
- Understanding how uncertainty propagates through spatial and temporal processing, and decision making
- Communicating uncertainty to different levels of the design and development team in meaningful ways
- Designing techniques to assess and reduce uncertainty to manageable levels for any given application
- Being able to absorb uncertainty and cope with it in practical engineering systems

2.4 Nondeterministic Analysis Approaches: Categories

Depending on the type of uncertainty and the amount of information available about the system characteristics and the operational environments, three categories of nondeterministic approaches can be identified for handling the uncertainties. The three approaches are [6–12] (Figure 2.5) probabilistic analysis, fuzzy-set approach, and set theoretical, convex (or antioptimization) approach. In probabilistic analysis, the system characteristics and the source variables are assumed to be random variables (or functions), and the joint probability density functions of these variables are selected. The main objective of the analysis is the determination of the reliability of the system. (Herein, reliability refers to the successful operation of the system.)

Copyright 2005 by CRC Press LLC

FIGURE 2.5 Three categories of nondeterministic approaches.

If the uncertainty is because of a vaguely defined system and operational characteristics, imprecision of data, and subjectivity of opinion or judgment, fuzzy-set treatment is appropriate. Randomness describes the uncertainty in the occurrence of an event (such as damage or failure).

When the information about the system and operational characteristics is fragmentary (e.g., only a bound on a maximum possible response function is known), then convex modeling is practical. Convex modeling produces the maximum or least favorable response and the minimum or most favorable response of the system under the constraints within the set-theoretic description.

2.4.1 Bounding Uncertainties in Simulation Models

Current synthesis approaches of simulation models involve a sequence of four phases (Figure 2.6):

1. Selection of the models, which includes decisions about modeling approach, level of abstraction, and computational requirements. The complexities arise due to:
   - Multiconstituents, multiscale, and multiphysics material modeling
   - Integration of heterogeneous models

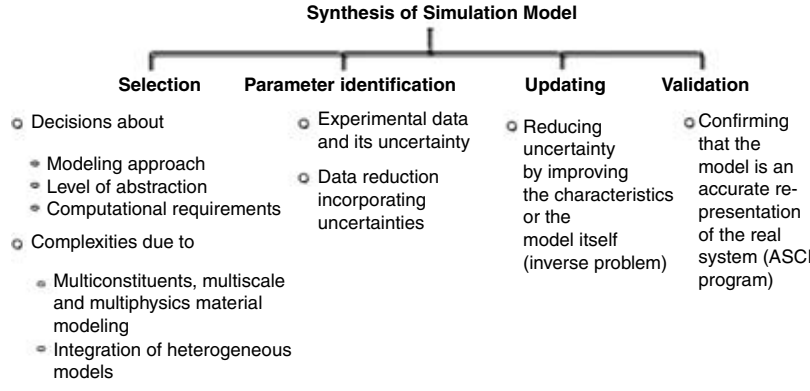

FIGURE 2.6 Four phases involved in the synthesis of simulation models.

Copyright 2005 by CRC Press LLC

2. Parameter identification. Data reduction techniques are used that incorporate uncertainties
3. Model updating, or reducing uncertainty by improving either the model characteristics or the model itself
4. Validation, in the sense of confirming that the model is an accurate representation of the real system

2.4.2 Quality Control and Uncertainty Management in the Modeling and Simulation of Complex Systems

The estimation of total uncertainty in the modeling and simulation of complex systems involves: (1) identification and characterization of the sources of uncertainty, variability, and error; (2) uncertainty propagation and aggregation; and (3) uncertainty quantification. [4,5,13]

Herein, uncertainty is defined as the epistemic uncertainty — a deficiency in any phase of the modeling process due to lack of knowledge (model form or reducible uncertainty), increasing the knowledge base can reduce the uncertainty. The term "variability" is used to describe inherent variation associated with the system or its environment (irreducible or stochastic uncertainty). Variability is quantified by a probability or frequency distribution. An error is defined as a recognizable deficiency that is not due to lack of knowledge. An error can be either acknowledged (e.g., discretization or round-off error) or unacknowledged (e.g., programming error). Uncertainty quantification is discussed in a succeeding subsection.

2.5 Enhancing the Modeling and Simulation Technologies

The synergistic coupling of nondeterministic approaches with a number of key technologies can significantly enhance the modeling and simulation capabilities and meet the needs of future complex systems. The key technologies include virtual product development for simulating the entire life cycle of the engineering system, reliability and risk management, intelligent software agents, knowledge and information, high-performance computing, high-capacity communications, human–computer interfaces, and human performance.

2.5.1 Advanced Virtual Product Development Facilities

Current virtual product development (VPD) systems have embedded simulation capabilities for the entire life cycle of the product. As an example, the top-level system process flow for a space transportation system is shown in Figure 2.7. In each phase, uncertainties are identified and appropriate measures are

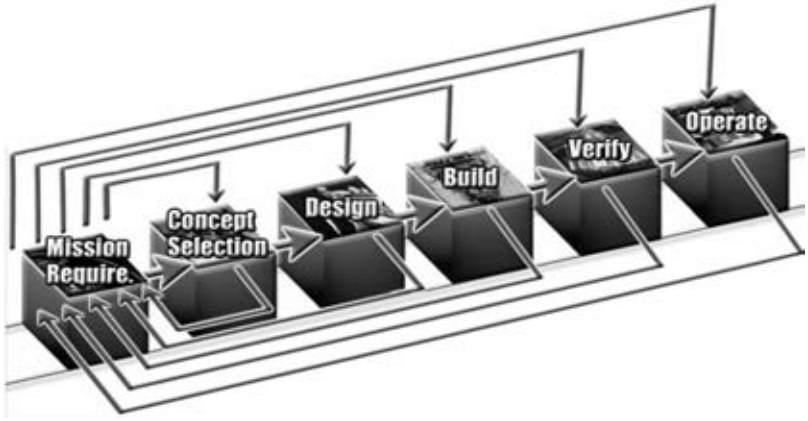

FIGURE 2.7 Top-level system process flow for a space transportation system.

Copyright 2005 by CRC Press LLC

taken to mitigate their effects. Information technology will change the product development from a sequence of distinct phases into a continuous process covering the entire life cycle of the product with full interplay of information from beginning to end and everywhere throughout.

2.5.2 Safety Assessment

Safety assessment encompasses the processes and techniques used to identify risks to engineering systems and missions. The evaluation and identification of risk are based on:

- Probabilistic risk assessment
- Fault tree analysis
- Hazard analysis and failure mode effect analysis coupled with engineering judgment

2.5.3 Uncertainty Quantification

Special facilities are needed for performing uncertainty quantification on large-scale computational models for complex engineering systems. Uncertainty quantification covers three major activities[4,5,13] (Figure 2.8):

1. *Characterization of uncertainty* in system parameters and the external environment. This involves the development of mathematical representations and methods to model the various types of uncertainty. Aleatory uncertainty can generally be represented by a probability or frequency distribution when sufficient information is available to estimate the distribution. Epistemic uncertainty can be represented by Bayesian probability, which takes a subjective view of probability as a measure of belief in a hypothesis. It can also be represented by modern information theories, such as possibility theory, interval analysis, evidence theory (Dempster/Shafer), fuzzy set theory, and imprecise probability theory. These theories are not as well developed as probabilistic inference.
2. *Propagation of uncertainty* through large computational models. The only well-established methodology for uncertainty propagation is based on probability theory and statistics. Use of response surfaces for approximation of the performance of a component or a system can increase the efficiency of this methodology. Nonprobabilistic approaches, which are based on possibility theory,

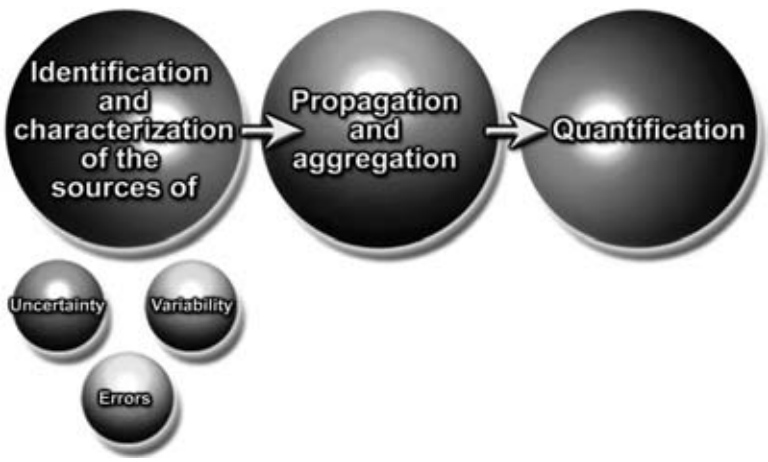

FIGURE 2.8 Major activities involved in uncertainty quantification.

Copyright 2005 by CRC Press LLC

Dempster-Shafer evidence theory, and imprecise probability, are currently investigated. These approaches can be useful when limited data is available about uncertainty.

3. *Verification and validation of the computational models*, and incorporating the uncertainty of the models themselves into the global uncertainty assessment. The verification and validation process is described in the succeeding section.

2.6 Verification and Validation of Numerical Simulations

Quantifying the level of confidence, or reliability and accuracy of numerical simulations has recently received increased levels of attention in research and engineering applications. During the past few years, new technology development concepts and terminology have arisen. Terminology such as virtual prototyping and virtual testing is now being used to describe computer simulation for design, evaluation, and testing of new engineering systems.

The two major phases of modeling and simulation of an engineering system are depicted in Figure 2.9. The first phase involves developing a conceptual and mathematical model of the system. The second phase involves discretization of the mathematical model, computer implementation, numerical solution, and representation or visualization of the solution. In each of these phases there are epistemic uncertainties, variabilities and errors [5,14].

Verification and validation are the primary methods for building and quantifying confidence in numerical simulations. *Verification* is the process of determining that a model implementation, and the solution obtained by this model, represent the conceptual/mathematical model and the solution to the model within specified limits of accuracy. It provides evidence or substantiation that the conceptual model is solved correctly by the discrete mathematics embodied in the computer code. Correct answer is provided by highly accurate solutions. *Validation* is the process of substantiating that a computational model within its domain of applicability possesses a satisfactory range of accuracy in representing the real system, consistent with the intended application of the model. Correct answer is provided by experimental data.

Validation involves computing validation metrics to assess the predictive capability of the computational models, based on distributional predication and available experimental data or other known information.

The development of such metrics is a formidable task, and is the focus of intense efforts at present. Model validation is intimately linked to uncertainty quantification, which provides the machinery to perform the assessment of the validation process.

FIGURE 2.9 Verification and validation of numerical simulations.

Copyright 2005 by CRC Press LLC

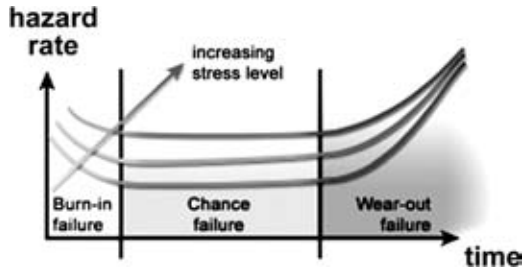

FIGURE 2.10 Failure rate over the lifetime of a component—reliability bathtub curves.

2.7 Availability, Reliability, and Performance

2.7.1 Availability

Availability of a component (or a system) is defined as the probability that the component (or system) will perform its intended functions at a given time, under designated operating conditions, and with a designated support environment. It is an important measure of the component (or system) performance—its ability to quickly become operational following a failure. Mathematically, availability is a measure of the fraction of the total time a component (or a system) is able to perform its intended function.

2.7.2 Reliability

Reliability is defined as the probability that a component (or a system) will perform its intended function without failure for a specified period of time under designated operating conditions. Failure rate or hazard rate is an important function in reliability analysis because it provides a measure of the changes in the probability of failure over the lifetime of a component. In practice, it often exhibits a bathtub shape [15–30] (see Figure 2.10).

Reliability assessment includes selection of a reliability model, analysis of the model, calculation of the reliability performance indices, and evaluation of results, which includes establishment of confidence limits and decision on possible improvements (Figure 2.11).

2.7.3 Performance

Reliability and availability are two of four key performance measures of a component (or a system). The four measures of performance are:

1. Capability: Ability to satisfy functional requirements
2. Efficiency: Ability to effectively and easily realize the objective

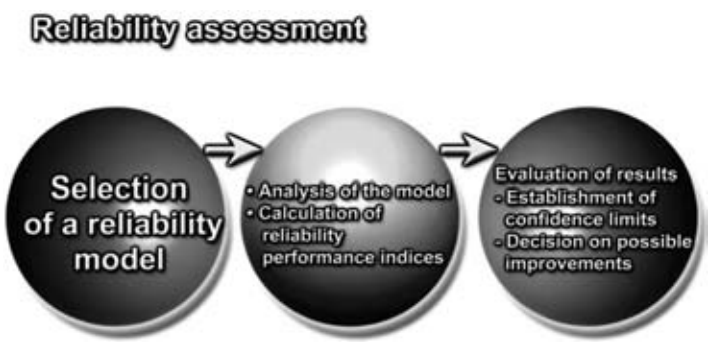

FIGURE 2.11 Reliability assessment.

Copyright 2005 by CRC Press LLC

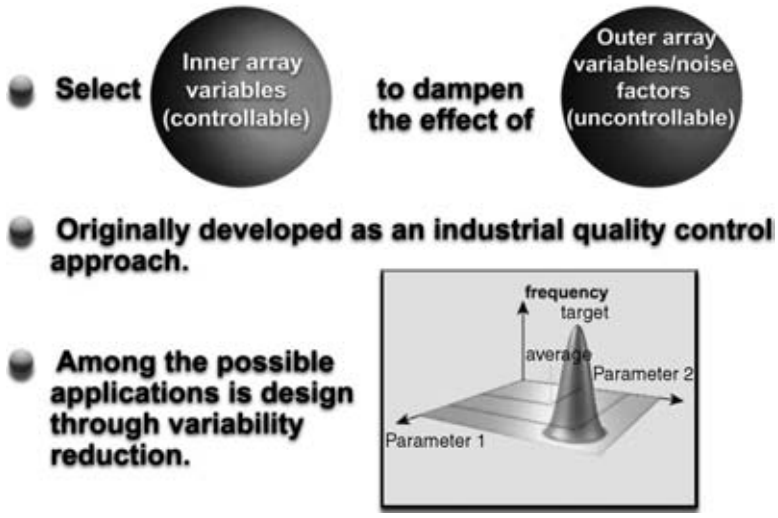

FIGURE 2.12 Taguchi's method.

3. Reliability: Ability to start and continue to operate
4. Availability: Ability to operate satisfactorily when used under specific conditions (in the limit it is the operating time divided by the sum of operating time plus the downtime)

2.7.4 Design of Experiments

These are systematic techniques for investigating (all possible) variations in system performance due to changes in system variables [31].

Two categories of system variables can be identified, namely, (1) inner-array variables, which are controllable; and (2) outer-array variables (also called noise factors), which are functions of environmental conditions and are uncontrollable. Three categories of techniques can be identified: (1) regression analysis, (2) statistical methods, and (3) Taguchi's method [32].

In Taguchi's method, the controllable variables are selected in such a way as to dampen the effect of the noise variables on the system performance. The method was originally developed as an industrial total quality control approach. Subsequently, it has found several other applications, including design optimization through variability reduction (Figure 2.12).

2.8 Response Surface Methodology (RSM)

RSM is a set of mathematical and statistical techniques designed to gain a better understanding of the overall response by designing experiments and subsequent analysis of experimental data. [33] It uses empirical (nonmechanistic) models, in which the response function is replaced by a simple function (often polynomial) that is fitted to data at a set of carefully selected points. RSM is particularly useful for the modeling and analysis of problems in which a response of interest is influenced by several variables and the objective is to optimize the response.

Two types of errors are generated by RSM. The first are random errors or noise, which can be minimized through the use of minimum variance based design. The second is bias or modeling error, which can be minimized using genetic algorithms.

RSM can be employed before, during, or after regression analysis is performed on the data. In the design of experiments it is used before, and in the application of optimization techniques it is used after regression analysis.

Copyright 2005 by CRC Press LLC

FIGURE 2.13 Tasks involved in the risk management process.

2.9 Risk Management Process

Risk is defined as the uncertainty associated with a given design, coupled with its impact on performance, cost, and schedule. Risk management is defined as the systems engineering and program management tools that can provide a means to identify and resolve potential problems [14,18,34,35].

The risk management process includes the following tasks (Figure 2.13):

- Risk planning: development of a strategy for identifying risk drivers
- Risk identification: identifying risk associated with each technical process
- Risk analysis: isolating the cause of each identified risk category and determining the effects

The combination of risk identification and risk analysis is referred to as risk assessment:

- Risk handling: selecting and implementing options to set risk at acceptable levels
- Risk monitoring: systematically tracking and evaluating the performance of risk handling actions

2.10 Robustness

Robustness is defined as the degree of tolerance to variations (in either the components of a system or its environment). A robust ultra-fault-tolerant design of an engineering system is depicted. The performance of the system is relatively insensitive to variations in both the components and the environment. By contrast, a nonrobust design is sensitive to variations in either or both (Figure 2.14).

An example of a robust, ultra-fault-tolerant system is the Teramac computer, which is a one-terahertz, massively parallel experimental computer built at Hewlett-Packard Laboratories to investigate a wide range of computational architectures. It contains 22,000 (3%) hardware defects, any one of which could prove fatal to a more conventional machine. It incorporates a high communication bandwidth that enables it to easily route around defects. It operates 100 times faster than a high-end single processor workstation (for some of its configurations); see Figure 2.15.

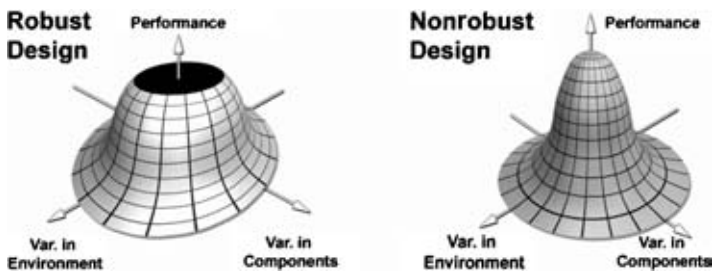

FIGURE 2.14 Robust and nonrobust designs.

Copyright 2005 by CRC Press LLC

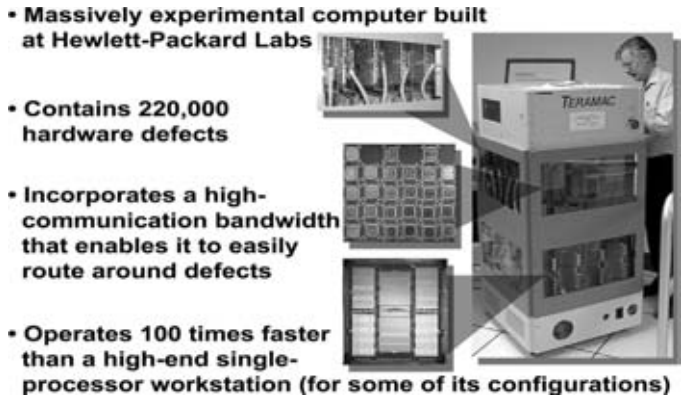

FIGURE 2.15 Teramac configurable custom computer.

2.11 Commercial Software Systems

A number of commercial codes have been developed to enable quantifying the variability and uncertainty in the predictions, as well as performing probabilistic design, reliability assessment, and process optimization. Examples of these codes are NESSUS, DARWIN, ProFES, UINPASS, GENOA, DAKOTA, and structural engineering reliability analysis codes such as CalREL, OpenSees, FERUM, and FSG. Also, some of the deterministic analysis codes, like ANSYS and MSC Nastran, are adding probabilistic tools to enable incorporating uncertainties into the analysis.

NESSUS and DARWIN were developed by Southwest Research Institute. NESSUS (Numerical Evaluation of Stochastic Structures Under Stress) integrates reliability methods with finite element and boundary element methods. It uses random variables to model uncertainties in loads, material properties, and geometries [36,37]. DARWIN (Design Assessment of Reliability With Inspection) predicts the probability of fracture of aircraft turbine rotor disks [38,39]. ProFES (Probabilistic Finite Element System) was developed by Applied Research Associates, Inc [40,41]. It performs probabilistic simulations using internal functions. It can also be used as an add-on to the commercial finite element codes or CAD programs. UNIPASS (Unified Probabilistic Assessment Software System) was developed by Prediction Probe, Inc [42,43]. It can model uncertainties, compute probabilities, and predict the most likely outcomes—analyzing risk, identifying key drivers, and performing sensitivity analysis. GENOA was developed by Alpha Star Corporation [44]. It is an integrated hierarchical software package for computationally simulating the thermal and mechanical responses of high-temperature composite materials and structures. It implements a probabilistic approach in which design criteria and objectives are based on quantified reliability targets that are consistent with the inherently stochastic nature of the material and structural properties.

DAKOTA (Design Analysis Kit for Optimization and Terascale Applications) was developed by Sandia National Labs [45]. It implements uncertainty quantification with sampling, analytic reliability, stochastic finite element methods, and sensitivity analysis with design of experiments and parameter study capabilities.

2.12 Key Components of Advanced Simulation and Modeling Environments

The realization of the full potential of nondeterministic approaches in modeling and simulation requires an environment that links diverse teams of scientists, engineers, and technologists. The essential components of the environment can be grouped into three categories: (1) intelligent tools and facilities, (2) nontraditional methods, and (3) advanced interfaces.

Copyright 2005 by CRC Press LLC

2.12.1 Intelligent Tools and Facilities

These include high fidelity – rapid modeling, life-cycle simulation and visualization tools, synthetic immersive environment; automatic and semiautomatic selection of software and hardware platforms, computer simulation of physical experiments, and remote control of these experiments. The visualization tools should explicitly convey the presence, nature, and degree of uncertainty to the users. A number of methods have been developed for visually mapping data and uncertainty together into holistic views. These include the methods based on using error bars, geometric glyphs, and vector glyphs for denoting the degree of statistical uncertainty. There is a need for creating new visual representations of uncertainty and error to enable a better understanding of simulation and experimental data. In all of the aforementioned tools, extensive use should be made of intelligent software agents and information technology (Figure 2.16).

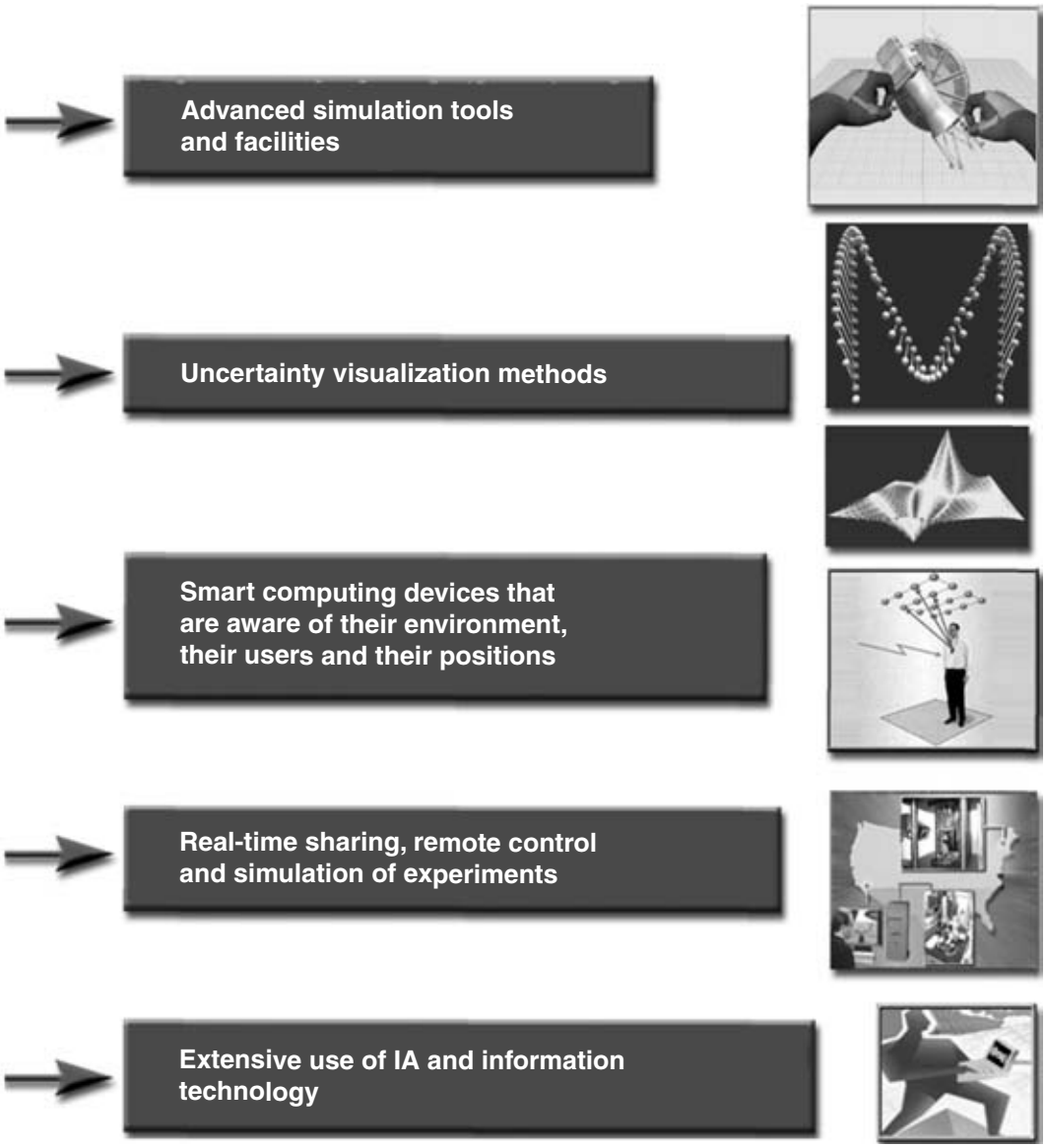

FIGURE 2.16 Intelligent tools and facilities.

Copyright 2005 by CRC Press LLC

2.12.2 Nontraditional Methods

These include multi-scale methods, strategies for highly coupled multi-physical problems, and nondeterministic approaches for handling uncertainty in geometry, material properties, boundary conditions, loading, and operational environments.

2.12.3 Advanced Human–Computer Interfaces

Although the WIMP (windows, icons, menus, pointing devices) paradigm has provided a stable global interface, it will not scale to match the myriad of factors and uses of platforms in the future collaborative distributed environment. Recent work has focused on intelligent multimodal human–computer interfaces, which synthetically combine human senses, enable new sensory-motor control of computer systems, and improve dexterity and naturalness of human–computer interaction [46,47]. An interface is referred to as intelligent if it can:

- Communicate with the user in human language
- Perform intelligent functions
- Adapt to a specific task and user

Intelligent interfaces make the interaction with the computer easier, more intuitive, and more flexible.

Among the interface technologies that have high potential for meeting future needs are perceptual user interfaces (PUIs), and brain–computer (or neural) interfaces (BCIs). PUIs integrate perceptive, multimodal, and multimedia interfaces to bring human capabilities to bear in creating more natural and intuitive interfaces. They enable multiple styles of interactions, such as speech only, speech and gesture, haptic, vision, and synthetic sound, each of which may be appropriate in different applications. These new technologies can enable broad uses of computers as assistants, or agents, that interact in more human-like ways.

A BCI refers to a direct data link between a computer and the human nervous system. It enables biocontrol of the computer—the user can control the activities of the computer directly from nerve or muscle signals. To date, biocontrol systems have utilized two different types of bioelectric signals: (1) electroencephalogram (EEG) and (2) electromyogram (EMG). The EEG measures the brain's electric activity and is composed of four frequency ranges, or states (i.e., alpha, beta, delta, and theta). The EMG is the bioelectric potential associated with muscle movement. BCI technologies can add completely new modes of interaction, which operate in parallel with the conventional modes, thereby increasing the bandwidth of human–computer interactions. They will also allow computers to comprehend and respond to the user's changing emotional states—an important aspect of affective computing, which has received increasing attention in recent years. Among the activities in this area are creating systems that sense human affect signals, recognize patterns of affective expression, and respond in an emotionally aware way to the user; and systems that modify their behavior in response to affective cues. IBM developed some sensors in the mouse that sense physiological attributes (e.g., skin temperature and hand sweatiness), and special software to correlate those factors to previous measurements to gauge the user's emotional state moment to moment as he or she uses the mouse.

Future well-designed multimodal interfaces will integrate complementary input modes to create a synergistic blend, permitting the strengths of each mode to overcome weaknesses in the other modes and to support mutual compensation of recognition errors.

2.13 Nondeterministic Approaches Research and Learning Network

The realization of the full potential of nondeterministic approaches in the design and development of future complex systems requires, among other things, the establishment of research and learning networks. The networks connect diverse, geographically dispersed teams from NASA, other government labs, university consortia, industry, technology providers, and professional societies (Figure 2.17). The

Copyright 2005 by CRC Press LLC

FIGURE 2.17 Nondeterministic approaches research and learning network.

activities of the networks include development of online learning facilities, such as interactive virtual classrooms (Figure 2.18), on nondeterministic approaches.

A European network, SAFERELNET, was established in 2001 to provide safe and cost-efficient solutions for industrial products, systems facilities, and structures across different industrial sectors. The focus of the network is on the use of reliability-based methods for the optimal design of products, production facilities, industrial systems, and structures so as to balance the economic aspects associated with providing preselected safety levels, with the associated costs of maintenance and availability. The approaches used include modeling

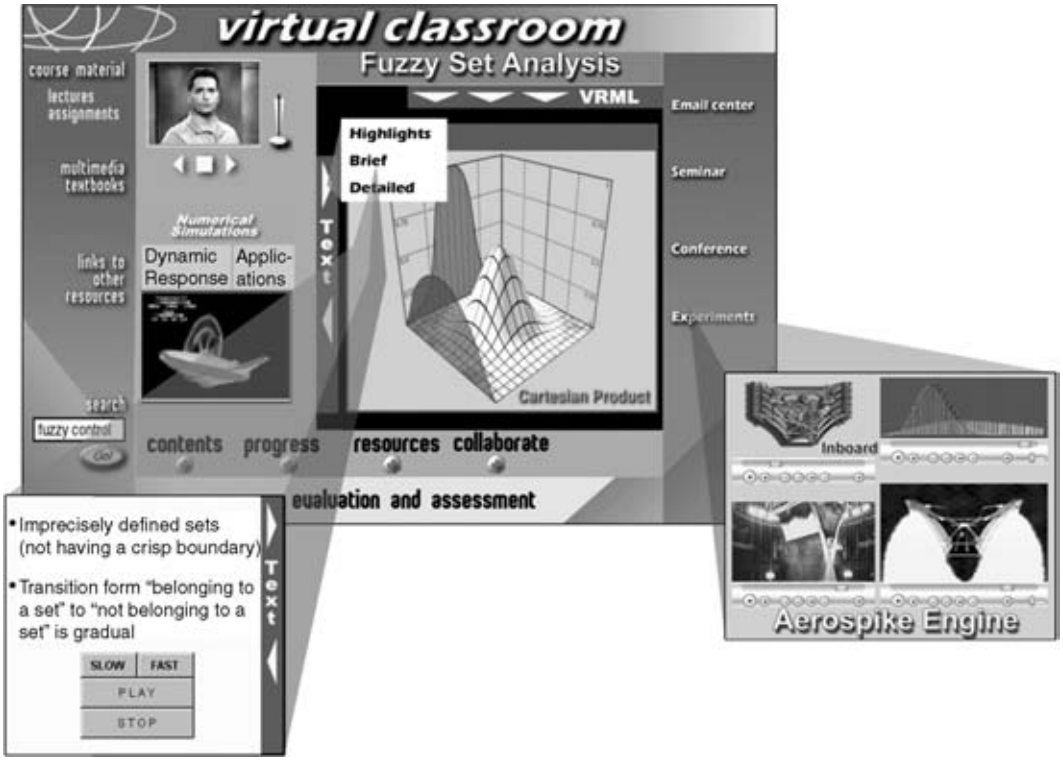

FIGURE 2.18 Interactive virtual classroom.

Copyright 2005 by CRC Press LLC

the reliability of the system throughout its lifetime, and an assessment of the impact of new maintenance and repair schemes on system safety, cycle costs, reliability, serviceability and quality.

2.14 Conclusion

A brief overview is presented of the current status and future directions for research in nondeterministic approaches. Topics covered include definitions of uncertainty, a brief historical account of uncertainty modeling; different representations and classifications of uncertainty; uncertainty management; the three categories of nondeterministic approaches; enhancing the modeling and simulation technologies; verification and validation of numerical simulations; reliability, availability, and performance; response surface methodologies; risk management process; key components of advanced simulation and modeling environments; and nondeterministic approaches research and learning network.

Nondeterministic approaches are currently used as integral tools for reliability, safety, and risk assessments in many industries, including aerospace, nuclear, shipbuilding, and construction.

Future complex engineering systems and information-rich environment will provide a wide range of challenges and new opportunities. The environment will be full of inherent uncertainties, vagueness, noise, as well as conflicts and contradictions. In the next few years, it is expected that the cost effectiveness of nondeterministic approaches tools will be more widely appreciated and, consequently, nondeterministic approaches will become an integral part of engineering analyses and simulations.

References

1. Katzan, H. Jr., *Managing Uncertainty: A Pragmatic Approach*, Van Nostrand Reinhold, New York, 1992.
2. Ben-Haim, Y., *Information-Gap Decision Theory: Decisions Under Severe Uncertainty*, Academic Press, St. Louis, 2001.
3. Natke, H.G. and Ben-Haim, Y., Eds., *Uncertainty: Models and Measures,* John Wiley & Sons, New York, 1998.
4. Oberkampf, W.L., Helton, J.C., and Sentz, K., Mathematical Representation of Uncertainty, presented at Non-Deterministic Approaches Forum, Seattle, WA, April 16–19, 2001, Paper No. 2001-1645, AIAA.
5. Oberkampf, W.L. et al., Error and Uncertainty in Modeling and Simulation, *Reliability Engineering and System Safety*, 75, 333–357, Elsevier Science, New York, 2002.
6. Elishakoff, I. and Tasso, C., Ed., *Whys and Hows in Uncertainty Modeling: Probability, Fuzziness and Anti-optimization,* Springer Verlag, 2000.
7. Soares, C.G., *Probabilistic Methods for Structural Design*, Kluwer Academic Publishers, New York, 1997.
8. Sundararajan, C.R., Ed., *Probabilistic Structural Mechanics Handbook: Theory and Industrial Applications*, Chapman & Hall, New York 1995.
9. Elishakoff, I., *Probabilistic Methods in the Theory of Structures*, John Wiley & Sons, New York, 1999.
10. Elishakoff, I., Possible Limitations of Probabilistic Methods in Engineering, *Applied Mechanics Reviews*, 53, 19–36, 2000.
11. Zadeh, L. and Kacprzyk, J., *Fuzzy Logic for the Management of Uncertainty*, John Wiley & Sons, New York, 1991.
12. Dimitriv, V. and Korotkich, V., Eds., *Fuzzy Logic: A Framework for the New Millennium*, Physica Verlag, New York, 2002.
13. Wojtkiewicz, S.F. et al., Uncertainty Quantification in Large Computational Engineering Models, Paper No. 2001-1455, AIAA.
14. Oberkampf, W.L. and Trucano, T.G., Verification and Validation in Computational Fluid Dynamics, *Progress in Aerospace Sciences*, 38, 209–272, Elsevier Science, New York, 2002.

Copyright 2005 by CRC Press LLC

15. Modarres, M., Kaminskiy, M., and Krivtsov, V., *Reliability Engineering and Risk Analysis: A Practical Guide*, Marcel Dekker, New York, 1999.
16. Ramakumar, R., *Engineering Reliability: Fundamentals and Applications*, Prentice Hall, Englewood Cliffs, NJ, 1993.
17. Knezevic, J., *Reliability, Maintainability and Supportability: A Probabilistic Approach*, McGraw-Hill, New York, 1993.
18. Dhillon, B.S., *Design Reliability: Fundamentals and Applications*, CRC Press, Boca Raton, FL, 1999.
19. Andrews, J.D. and Moss, T.R., *Reliability and Risk Assessment*, ASME Press, New York, 2002.
20. Balakrishnan, N. and Rao, C.R., Eds., *Advances in Reliability, Volume 20*, Elsevier Science and Technology Books, New York, 2001.
21. Birolini, A., *Reliability Engineering: Theory and Practice*, Springer-Verlag Telos, New York, 2001.
22. Blischke, W.R. and Murthy, D.N.P., Eds., *Case Studies in Reliability and Maintenance*, John Wiley & Sons, New York, 2002.
23. Haldar, A. and Mahadevan, S., *Probability, Reliability, and Statistical Methods in Engineering Design*, John Wiley & Sons, New York, 1999.
24. Hoang, P., *Recent Advances in Reliability and Quality Engineering*, World Scientific Publishing, River Edge, 1999.
25. Hobbs, G.K., Ed., *Accelerated Reliability Engineering: Halt and Hass*, John Wiley & Sons, New York, 2000.
26. Kuo, W. et al., *Optimal Reliability Design: Fundamentals and Applications*, Cambridge University Press, New York, 2001.
27. O'Connor, P.D.T., *Practical Reliability Engineering*, Wiley John & Sons, New York, 2002.
28. Wasserman, G.S., *Reliability Verification, Testing, and Analysis in Engineering Design*, Marcel Dekker, New York, 2002.
29. Elsayed, E.A., *Reliability Engineering*, Prentice Hall, Boston, 1996.
30. Hignett, K.C., *Practical Safety and Reliability Assessment*, Routledge, New York, 1996.
31. Coleman, H.W. and Steele, W.G., Jr., *Experimentation and Uncertainty Analysis for Engineers*, John Wiley & Sons, New York, 1999.
32. Roy, R.K., *A Primer on the Taguchi Method,* John Wiley & Sons, New York, 1990.
33. Cornell, J.A., *How to Apply Response Surface Methodology*, ASQ Quality Press, Milwaukee, WI, 1990.
34. Haimes, Y.Y., *Risk Modeling, Assessment, and Management*, John Wiley & Sons, New York, 1998.
35. Bedford, T. and Cooke, R., *Probabilistic Risk Analysis: Foundations and Methods*, Cambridge University Press, Cambridge, MA, 2001.
36. Riha, D.S. et al., Recent Advances of the NESSUS Probabilistic Analysis Software for Engineering Applications, presented at the *Structures, Structural Dynamics and Materials Conference and Exhibit Non-Deterministic Approaches Forum,* Denver, CO, April 22–25, 2002, Paper No. 2002-1268, AIAA.
37. Southwest Research Institute, NESSUS Reference Manual, version 7.5, 2002, (http://www.nessus.swri.org).
38. Wu, Y.T. et al., Probabilistic Methods for Design Assessment of Reliability with Inspection (DARWIN), presented at the *Structures, Structural Dynamics and Materials Conference and Exhibit Non-Deterministic Approaches Forum,* Atlanta, GA, April 3–6, 2000, Paper No. 2000-1510, AIAA.
39. Southwest Research Institute, DARWIN User's Guide, version 3.5, 2002, (http://www.darwin.swri.org).
40. Cesare, M.A. and Sues, R.H., ProFES Probabilistic Finite Element System — Bringing Probabilistic Mechanics to the Desktop, presented at the *Structures, Structural Dynamics and Materials Conference and Exhibit Non-Deterministic Approaches Forum,* St. Louis, MO, April 12–15, 1999, Paper No. 99-1607, AIAA.
41. Aminpour, M.A. et al., A Framework for Reliability-BASED MDO of Aerospace Systems, presented at *Structures, Structural Dynamics and Materials Conference and Exhibit Non-Deterministic Approaches Forum,* Denver, CO, April 22–25, 2002, Paper No. 2002-1476, AIAA.
42. UNIPASS Training Problem Guide, version 4.5, Prediction Probe, Inc., Newport Beach, CA, 2003.

Copyright 2005 by CRC Press LLC

43. UNIPASS Software Specification, version 4.5, Prediction Probe, Inc., Newport Beach, CA, 2003.
44. Abdi, F. and Minnetyan, L., Development of GENOA Progressive Failure Parallel Processing Software Systems, NASA CR No.1999-209404, December 1999.
45. Eldred, M.S. et al., DAKOTA, A Multilevel Parallel Object-Oriented Framework for Design Optimization, Parameter Estimation, Uncertainty Quantification, and Sensitivity Analysis, Version 3.0 Reference Manual, Sandia Technical Report SAND 2001-3515, April 2002.
46. Maybury, M.T. and Wahlster, W., Eds., *Readings in Intelligent User Interfaces*, Morgan Kaufman Publishers, San Francisco, 1998.
47. Carroll, J.M., Ed., Human-Computer Interaction in the New Millennium, ACM Press, New York, 2002.

Copyright 2005 by CRC Press LLC

3

Transitioning NDA from Research to Engineering Design

Thomas A. Cruse
Vanderbilt University

Jeffrey M. Brown
Air Force Research Laboratory, Propulsion Directorate, Components Branch (AFRL/PRTC), Wright-Patterson AFB,

3.1 Introduction

Nondeterministic analysis (NDA) is taken to be the set of technologies that recognize the inherent uncertainties in the model, data, allowables, or any other knowledge that might be applied to predict the reliability of a system or element in the system. Reliability refers to the probability that a design goal can and will be achieved. Given the breadth of NDA, the authors will address a subset of those NDA methods that we deem likely to be most useful in system design.

Within that subset, one can broadly state that there are two classes of NDA methods: (1) those for which a first-order representation (mean and variance) of the uncertain behavior is sufficient and (2) those for which a much higher degree of fidelity is required. The latter are typically needed for the formal processes of certification and apply largely to high-performance systems with human life risk factors that have a high reliability. This review focuses on the latter for their relevance to highly reliable mechanical systems for which accuracy in NDA is needed.

The review begins with a vision for the kind of new design environment in which NDA is central. NDA requires a systems perspective to a much larger degree than do traditional design processes. The new design environment is seen to be more dependent on a comprehensive and consistent

0-8493-1180-X/04/$0.00+$1.50

© 2004 by CRC Press LLC

Copyright 2005 by CRC Press LLC

interaction of data, modeling, updating, and system model validation than past design practices based on margins to assure reliability. The authors see the need for a new, integrating software framework and a variety of new NDA and NDA-supporting tools operating within that framework to support the full transition of NDA to design. A concept for the framework and possible NDA-supporting tools is presented.

NDA has been used in design practice for systems requiring a high degree of reliability, such as disks in turbine engines for commercial engines through statistically-based design limits for certain failure modes. The review includes a historical review of probabilistic method development that clearly indicates the transition from statistical margins to the current, but still limited use of probabilistic finite elements methods for NDA of structural response. The review then summarizes some pertinent literature on various NDA tools that might be used within this design environment.

The use of NDA in design is clearly still in transition. Some tools and strategies have been successfully developed and are being used in structural design today. Other areas of design from thermal response to aerodynamic performance to material behavior are in early stages of transition. The authors identify some issues and challenges that remain as topics to be worked in order to support the complete transition of NDA to design. Items that are briefly discussed include the design environment software framework, developing more generalized yet rational confidence intervals that have meaning in the context of complex system design, the need for systematic error analysis for the various NDA tools, NDA model verification and validation strategies, linkage of NDA with traditional reliability analysis tools, and the still-important issue of the cost of NDA at the systems level.

3.2 The Future Nondeterministic Design Environment

To a great extent, current NDA methods for system design are not based on physics-of-failure modeling at the system level. The real need for advanced design systems is for comprehensive, multi-physics modeling of system behavior. In only this way can the designer truly trade performance, reliability, quality, and cost metrics as functions of all the design variables.[‡]

Multi-physics modeling with fidelity sufficient for NDA is likely to involve the interactions of multiple physics-based computational algorithms. Given the fact that the design variables and the models themselves have uncertainties a NASA-funded study by the first author concluded that a new design environment was needed to support NDA [1]. Such a design environment must provide for generalized data storage, retrieval, and use by the appropriate physical models. The basic elements of the NDA design process are represented in Figure 3.1. The following paragraphs describe some of the proposed tool sets that might be found in a generalized NDA design environment (see Figure 3.2):

- *Information input.* In the past, data for probabilistic modeling was in the form of statistical data represented by analytical or empirical distribution functions and their parameters. For the future, input will include a much broader range of information. Such NDD information that is subjective or "fuzzy" is envisioned as a critical element in NDA. The elicitation of such fuzzy input is a critical element in the process such that expert bias and prior assumptions do not overly influence the representation of the information.
- *Information fusion.* This critical junction is where one must convert disparate forms of information into a common basis for modeling. A critical element in the technology requirements here is the

[‡] Design variables will herein always refer to random variables over which the designer has control. Such random variables may have physical dependencies such as material properties with temperature dependencies. Other variables may have strong statistical dependencies or correlations. The treatment of these conditions is beyond the scope of this chapter but the authors recognize how critical it is that these dependencies be recognized by any NDA methods. In all cases, the analyst is urged to formulate the physics at a primitive enough level to achieve physical and thus statistical independencies of the variables whenever possible.

Copyright 2005 by CRC Press LLC

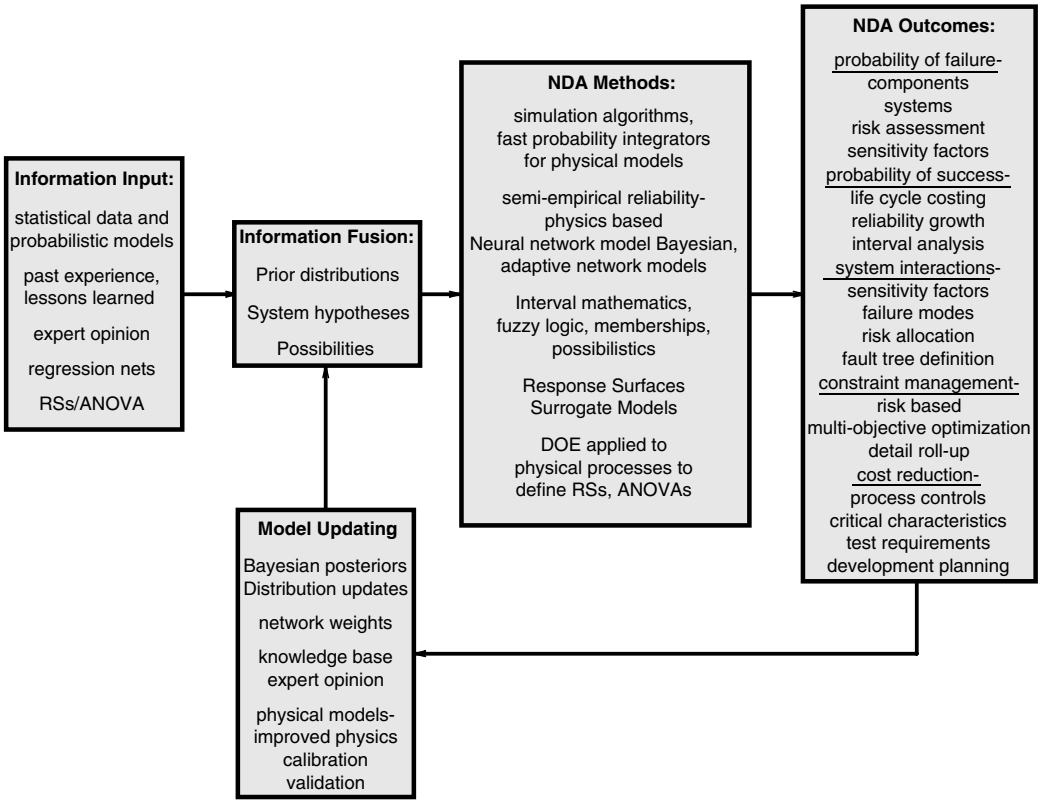

FIGURE 3.1 Elements of the nondeterministic design (NDD) process [1].

translation of properly acquired fuzzy input into sensible probabilistic representations. It is also the place where new information is used to update prior information.

- *NDA methods.* The comments herein address some key current and future NDA elements. Semi-empirical, physics-based modeling of systems using various network algorithms is likely to be important, especially for large systems. Fuzzy logic and its attendant elements of membership functions and possibilistic analysis are not likely to be used for the formal analysis part of the overall design system but are likely to be used for representations of expert-opinion-based input or hyperparametric input models. Response surface (RS) modeling or surrogate (simplified physics) models are likely to be intrinsic to NDD. All probabilistic methods use such models in one way or another. DOE approaches or Taylor series approaches are variations on RS methods. The use of DOE to construct such surfaces from empirical data is seen as an alternative to network models, although the technologies may merge.
- *NDA outcomes.* This is the heart of the design process valuation. A proper NDA design environment in the other entities in this diagram will yield much more useful information for making decisions for design stages from conceptual design to detailed design.
- *Model updating.* A critical element in any design process is updating. Good design operations have evolved means for capturing past experience for new designs. Quantitative risk management programs allow for updating the assumed statistics used in the previous modeling. Bayes' theorem can be used to combine prior distribution models with new data when both the prior model and the new data must be combined. In most data-driven designs, replacing the old dataset with the new one will do the data updating. Model updates will typically also be done by replacement,

Copyright 2005 by CRC Press LLC

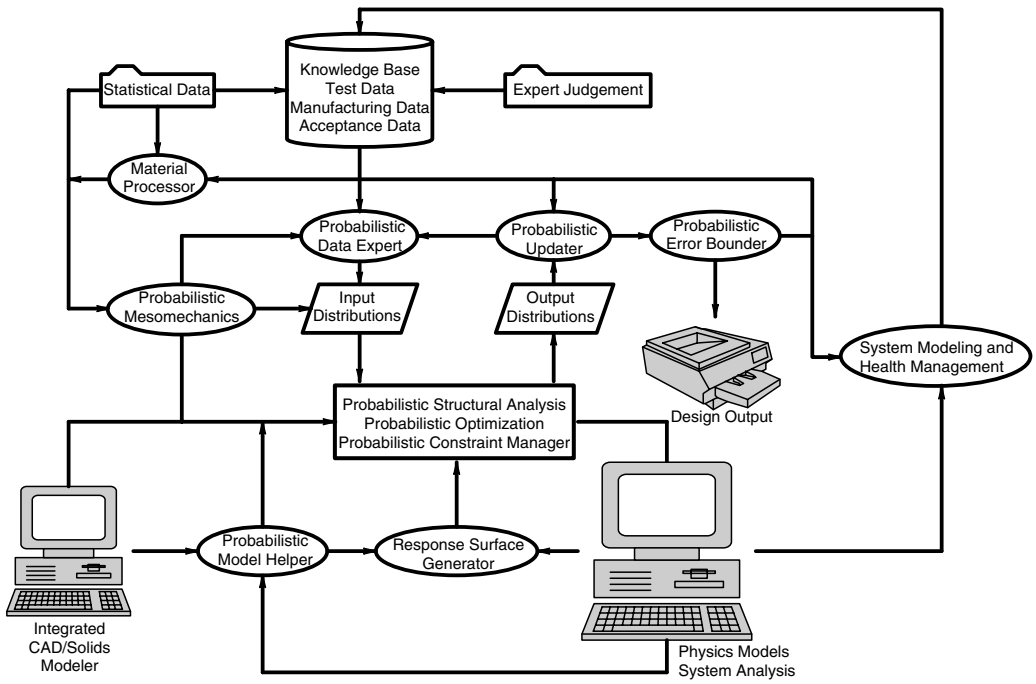

FIGURE 3.2 Integrated nondeterministic design environment.

although there are Bayesian model updating strategies appropriate to certain classes of network models where one cannot validate individual modeling elements. Certainly, the validation process for the physics-based models will lead to model updates. An integrated NDD environment to support these process elements was proposed in [1]. A major challenge in NDA for design is the development of a software framework that supports tool sets with a high degree of interoperability and data transparency for multi-physics modeling of system behavior. The following paragraphs describe some of the proposed toolsets that might be found in a generalized NDA design environment.

- *Probabilistic Data Expert (PDE).* The PDE provides a systematic means for merging disparate forms of "data" into probabilistic design. The data ranges from subjective expert opinions to raw data such as specimen specific fatigue test data. The PDE relies on nontraditional methods for integrating "fuzzy data" based on qualitative information [2]. The major technology needs here are in creating tools for automating the data acquisition and integration processes.
- *Probabilistic Updater (PU).* The NDD process for total life-cycle design from concept to field deployment for complex systems generally involves reliability growth processes of one form or another. Early in the design process, the reliability characteristics of the subsystems are either not known or crudely known. Testing during development should focus on those results that are most effective either in demonstrating greater reliability or increasing the assurance (reducing the uncertainty) in the reliability prediction. One can envision a generalized tool that will provide intelligent ways to update the current reliability and assurance intervals (akin to statistical confidence intervals) taking into account new information and data. These intervals are discussed in Reference 3. Bayesian updating of statistical models can be used for certain automated model updates involving the combination of expertise-driven priors with new data or information. However, other updating strategies are likely needed for large system models where the outcomes are used to assess the quality of the model.

Copyright 2005 by CRC Press LLC

- *Probabilistic Error Bounds (PEB).* Many system design processes have allowed for generalized levels of comfort in product performance— so-called "fuzzy" nondeterministic output. However, both the commercial workplace and the demands of government acquisitions have transformed aerospace vehicle design requirements from nonanalytical reliability bases to specified levels of "demonstrated" reliability that may include both test and analytical bases. A key and, as yet, not addressed and fundamentally critical need is to be able to compute rational reliability error prediction bounds for the various algorithms likely to be used in an advanced aerospace vehicle and propulsion design. Error bounds are needed that span the analysis spectrum from the physics approximations, to the response surface or surrogate models used to represent the physics, to the specific probabilistic algorithms deployed. In fact, it is likely that engineers will need to deploy hybrid combinations of the current probabilistic methods (e.g., RS, fast probability integration (FPI), Monte Carlo (MC) importance sampling) for large system design problems. Error identification, tracking, accountability, and bounds are required for the full process. Such error modeling is seen to be a part of the total model verification and validation process.
- *Response Surface Generator (RSG).* All current probabilistic algorithms for any but the most trivial problems use a "response surface" or surrogate model to describe the component, subsystem, or system-level behavior as a function of the design variables. Thus, it is a surface in the N-dimensional design space of the problem. In fact, it is increasingly likely to be a union of many such hyper-surfaces that can be used for complex system design. An example of a powerful algebraic system for manipulation of RSs that could be easily extended to nondeterministic design is seen at the Rockwell Science Center link: http://www.rsc.rockwell.com/designsheet/.
- Two methods are currently employed to generate RSs; these are the Taylor series method and the design of experiments (DOE) method [4]. The former is more likely to be employed near a critical design point, while the latter is more often used to span a wider range of the design space. Fast probability methods such as the fast probability integrator (FPI) algorithms [5] or importance sampling (a Monte Carlo simulation strategy) are performed using the RS and do not directly use the actual detailed simulation. As such, the RS methods are highly effective over a range of design levels from conceptual to final. A generalized "tool" for effective development and representation of RSs is needed that will interface both to probabilistics and to the closely related field of multidisciplinary optimization (MDO). Further, the *PEB* tool and the *RSG* tool should be able to work together to adaptively build optimal RS strategies that combine computational efficiency with minimizing the probabilistic approximation errors for large system design problems.
- *Probabilistic Model Helper.* A major limitation in the deployment of NDD analysis methods is the current burden that the analyst be a skilled "probabilistic engineer." Such individuals at this time are probably numbered in the low dozens and are scattered between software firms, universities, government labs, and industry. The field is not one that has received much attention in academic curricula, although the topic is now covered in the most recent undergraduate mechanical design texts. Further, the process of preparing and interpreting a probabilistic design problem involves the inclusion and assessment of many more sources of information and decisions regarding the analysis strategy. Nontraditional methods provide a real basis for the development and deployment of intelligent systems to work as probabilistic "robots" or assistants. The approach will likely require significant use of adaptive networks, software robots, genetic algorithms, expert systems, and other nontraditional methods.
- *Probabilistic Mesomechanics.* Significant progress has been achieved since the early attempts at what was called "level 3" probabilistic material modeling as part of the original NASA Probabilistic Structural Analysis Methods (PSAM) contract.[§] Demonstration problems have shown the ability

[§] Dr. Chris Chamis of NASA/GRC was the driving inspiration for this NASA-funded effort led by the Southwest Research Institute in San Antonio, TX, with partners including the Marc Analysis Research Corporation and Rocketdyne Inc.

Copyright 2005 by CRC Press LLC

to link material processing simulation software with micromechanical models of material behavior at the mesoscale (grain size, grain orientation, flow stress, dislocation density) to predict statistical distributions of material fatigue strength [6, 7]. Such probabilistic modeling advances lend real credibility to the notion of engineered materials that goes well beyond the simpler notions associated with composite material systems. Probabilistic mesomechanics tools that can support the PDE tool or feed "data" directly into the material data distributions are required. Automated, intelligent systems are envisioned with the capability to forward model material processing to define scatter in properties as well as sensitivity links to the independent process and material primitive variables. Further, the inverse problem of optimizing the processing and design of the material microstructure provides the ultimate in an "engineered materials" design capability.

- *System Reliability Interface.* The aerospace system design environment of the future requires the ability to interface multiple models of multiple subsystems in an efficient and accurate manner. Each failure mode of the system has its own probabilistic model in terms of a response surface or surrogate model representation of the physical problem together with the associated nondeterministic design variable descriptions. Current system reliability technology focuses on traditional block-diagram forms for representing system reliability. Each block is typically represented by point estimates of reliability that are not linked to the underlying physics or to the distribution and confidence in the underlying variables. Physics based system modeling provides an information-based opportunity for linking the key design parameters and physics-based models together from the sub-system/component level to the full system level. Intelligent systems can be developed for linking the information and propagating it to the various "top-level" events in order to provide a powerful environment for calculating and managing system level reliability.
- *Health Management System.* Health management (HM) is a philosophy that merges component and system level Health Monitoring concepts, consisting of anomaly detection, diagnostic and prognosis technologies, with consideration to the design and maintenance arenas [8]. Traditionally, system health monitoring design has not been an integral aspect of the design process. This may be partly due to the fact a cost/benefit model of a HM system configuration has not yet been fully realized. Without a doubt, HM technology must "buy" its way into an application. Hence, the need exists to extend the utility of traditional system reliability methods to create a virtual environment in that HM architectures and design trade-offs can be evaluated and optimized from a cost/benefit standpoint. This capability should be present both during the design stage and throughout the life of the system. A new HM design strategy should allow inclusion of sensors and diagnostic/prognostic technologies to be generated in order to produce an enhanced realization of component design reliability requirements at a very early stage. Life-cycle costs can be reduced through implementation of health monitoring technologies, optimal maintenance practices, and continuous design improvement. To date, these areas have not been successfully linked with nondeterministic design methods to achieve cost/benefit optimization at the early design stage.

3.3 Probabilistic Methods in Transition for Systems Design

3.3.1 Current Nondeterministic Design Technology

A simplified overview of nondeterministic design (NDD) must address both empirical and predictive reliability methods. NDA is, formally, a member of the latter. However, one cannot ignore the former because NDA relies at some level on empirical modeling for model input or model validation. NDD also includes system safety and reliability analysis tools such as failure modes and effects analysis (FMEA), criticality analysis (CA), and fault tree analysis (FTA) [9]. One of the major future transition elements for NDA is bringing more analysis into the qualitative reliability and risk assessment processes.

Empirical reliability has primarily focused on determining the fitting parameters for two classical statistical models—the exponential and Weibull distributions [10–12]—although the normal and log

Copyright 2005 by CRC Press LLC

normal distributions are also used. The exponential distribution is used to represent the average failure rate for large populations of similar devices or over many hours of operation of a complex system, generally reported as the mean time between failures (MTBF) or the uniform failure rate ($MTBF^{-1}$). This distribution has most often been applied to modeling the reliability of electronic components that have been through a burn-in usage.

The exponential reliability model does not address the physics of failure. For example, an electrical motor design may fail due to armature fatigue, wear, or other mechanical failure mode. Over a long period of time, the occurrences of these failure modes average out to a single MTBF value. Some effort has been made to convert this purely empirical reliability model to one having some physics effects reflected in the MTBF [13].

The Weibull distribution is generally used to represent mechanical failure modes as it combines the features of wear-out failure rates with single-point (brittle) failure modes [14]. All such empirical models rely on sound statistical methods to infer the proper set of parameters for any reliability model that is to be used along with the supporting data [15, 16].

System safety and reliability analysis [9] is widely used and is closely linked to NDD despite its largely qualitative nature. FMEA is a bottoms-up assessment process based on identifying all of the "important" (perhaps as defined in a criticality analysis [CA] process) failure modes for each subsystem or component and estimating the consequences of subsystem or component failure. FMEA is often used to define corrective actions necessary to eliminate or significantly reduce the failure likelihood or consequences (risk). However, a quantitative extension of the standard FMEA would take advantage of the computational reliability predictions coming from NDA used in design. FMEA can provide more insight than NDA into nonquantitative design issues that can affect product reliability.

Fault tree analysis (FTA) [17] is a top-down reliability assessment based on a specified "top" failure event. FTA then seeks to define all of the causes for the top event by breaking down each cause into its causes and so on until the "bottom" of the fault tree is defined. Point probability estimates can be applied to each event in the tree and these are logically combined using "and" and "or" gates to define the probability of the top event. FTA is also qualitative in nature as far as the tree elements and structures are concerned. Experience with product design and product reliability are important in getting useful and comprehensive FEMA and FTA models for systems. Neither FMEA nor FTA is a physics-of-failure based NDD tool.

Probabilistic risk assessment (PRA) [18] is a reliability tool that was largely developed within the nuclear power industry. PRA typically uses Monte Carlo simulation to combine the statistics of the key, physical variables that combine to cause failure. Often, the reliability problem is posed as a basic stress vs. strength problem such as for fatigue and fracture problems [19]. Following the Challenger accident, NASA made a significant commitment to the use of PRA for the high criticality failure modes for the launch system (e.g., [Reference 20]) and the space station. PRA has also been used for various NDD problems in the turbine engine field for many years [21, 22].

3.3.2 Some Transition History

Mechanical system reliability has evolved in multiple paths owing to the unique elements of mechanical system design, at least as one can see them historically. The two paths can be traced in the design of civil structures such as buildings and bridges, and the design of aircraft and propulsion structures. The first category is driven by issues deriving from the high degree of redundancy in most civil structures and by the attendant use of building codes with specified safety factors. The probabilistic elements of civil structure design have come about largely due to two forms of highly stochastic loadings—earthquakes and sea loads (for offshore structures).

Aircraft and propulsion designs have been driven by the specifics of fatigue and fracture mechanics damage processes. While aircraft are subject to stochastic loading conditions, the large loading conditions are better defined than in civil structures, as the designer controls the stall limits of the airfoil and hence the greatest aerodynamic load that can be seen. Stochastic elements of structural reliability problems for

Copyright 2005 by CRC Press LLC

aircraft and propulsion structures are dominated by scatter in the fatigue and crack growth rate characteristics of the materials.

Traditional design for all civil and aerospace structures has been controlled primarily through the use of safety factors or other forms of design margins. Such factors or margins are deterministic in nature but their magnitudes are typically driven by past experience that includes the stated loading or material stochasticity, along with the full range of less important stochastic design variables. There are only two main reasons for changing this, largely successful, design experience. One is economical: design factors and margins are conservative in most cases and the degree of conservancy is not well established. Further, the margins do not reflect the differing degrees of controls on design variations that are a part of the proper design process. All of this costs money and reduces the performance of the system through excess weight or unnecessarily stringent controls.

A key rationale for NDD is its ability to support the design of new systems with new materials or components for that the experience base is lacking, as compared to traditional systems. As material performance is pushed in electronic and mechanical systems, the need for a new design paradigm has become more evident. The past reliance on successful experience and the use of incremental design evolution does not adequately serve the current marketplace. Further, the "customer" in the general sense is no longer willing to pay the price of designs that do not account for intrinsic variability in process or performance.

The following paragraphs seek to provide a limited overview of some of the principal developments that have brought us to the point we are today, where reliability based design is poised to become the new design paradigm for consumer products through advanced aerospace systems.

3.3.2.1 Early Developments

An early interest in the development of reliability was undertaken in the area of machine maintenance. Telephone trunk design problems [23, 24] are cited in a more recent reliability text [25]. Renewal theory was developed as a means of modeling equipment replacement problems by Lotkar [26].

Weibull made a substantial contribution to mechanical system reliability through the development of the extreme value statistic now named after him [27]. His was the first practical tie of the physics of failure to a mathematical model. The model derived from the general extreme value statistical models expounded by Gumbel [28]. The Weibull model contains the concept of brittle failure mechanics that states that any critically sized defect failure causes the entire structure to fail and can be derived as the statistics of failures of the weakest link in a series of links.

3.3.2.2 Use of Weibull Models in Aircraft Engine Field Support

Mechanical failures in gas turbine engine components are driven by specific wear-out modes, including fatigue, creep, crack growth, wear, and interactions of these modes. The components may be bearings, shafts, blades, pressurized cases, or disks. For nearly 30 years, the Weibull reliability model has been successfully used to develop maintenance and field support plans for managing reliability problems defined by field experience. Such methods also have been used successfully in establishing warranty plans for new equipment sales as well as spare parts requirements.

Much of the effectiveness of the developed methods is shrouded in the mist of proprietary data and protectionism. However, it is clear that these specific modes of mechanical system failures are often very well correlated using the Weibull model. The Weibull model has demonstrated the ability to accurately predict subsequent failures from a population based on surprisingly few data points.

The Air Force sponsored some of the more recent work using the Weibull model and the results of the study are in the public domain [14]. This chapter serves as a useful introduction to the use of the Weibull model for various mechanical systems. A more comprehensive examination of the model, along with other models of mechanical reliability is the text by Kapur and Lamberson [10]. There has been considerable growth in the Weibull model applications industry in recent years, as various industries have found ways to use these methods.

Copyright 2005 by CRC Press LLC

A very powerful application of the Weibull method is in probabilistic risk assessment (PRA) for demonstrated mechanical reliability problems [18]. The earliest and probably most extensive use of PRA for large field problems has been in civil transport gas turbine engine field problems [21, 22]. Since about 1978, the Federal Aviation Administration has required the engine manufacturers to use Weibull-based PRA as the basis for setting flight limits on engine components with known field fracture potential. Again, it is the accuracy of the Weibull model to correlate the relevant failure modes on the basis of a few, early failures that allows one to use the model to confidently predict future field failure probabilities. One can then implement the necessary inspection plans that will insure that no actual failures will occur.

Another field application of the Weibull probability model is the prediction of safe operating limits in the field based on successful experimental data. The method is sometimes referred to as a Weibull-Bayesian method. The Weibull-Bayesian method was applied to the problem of safe operating limits for the Space Shuttle auxiliary power unit turbine wheels [29] as part of the return-to-flight studies performed following the Space Shuttle Challenger tragedy.

3.3.2.3 Civil Engineering-Based Reliability Developments

The principal structures that are most closely linked to reliability modeling are those located offshore or in earthquake-prone areas. In both cases, standard design factors do not provide adequate margins nor do they provide sufficient linkage to the actual failure conditions that can occur in specific structural configurations. The notion of a design margin, however, has led to the successful development and use of various probabilistic design methods for these structures.

The stress conditions in complex structures can be computed for various loading conditions, using the extensive computational modeling capabilities that have been available for design modeling since the 1960s. If one can efficiently compute the variability in the stresses due to the stochastic loads, then the design margin between the variable stresses and the variable material strengths can be established. That simple idea underlies much of the developments of reliability design methods for civil structures [30].

The essential feature of these methods is computing the variability of the design response. In simple terms, the variability can be taken to be the statistical "variance" or standard deviation measures. The variance is the second-moment of the statistical distribution of a random variable, while the mean of the distribution is the first moment. The stochastic margin between the stress and the strain was formulated as a reliability index by Cornell [31]. The relation between the reliability index and the safety margin for structural design was then proposed [32].

The original formulation of the reliability index was shown by [33, 34] to give differing reliability indices for the same safety factor, depending only on the algebraic forms of the same relations. The proper reliability index that is invariant to the algebraic form of the safety margin was then given by Hasofer and Lind [35] and by Ang and Cornell [36]. The reliability index for Gaussian functions of stress and strength is directly related to the variance in these two variables, as well as their mean values.

3.3.2.4 Probability Integration Algorithms

Later work in structural reliability has been directed toward computing the reliability index for more complicated structural problems. The failure problem is stated in terms of limit states that separate the safe design from the failed design where the independent variables are the design variables of member size, strength, and loading conditions. The limit states are generally nonlinear functions of the design variables and must be linearized at some design state in order for a reliability index to be computed. The first and enduring algorithm for this problem is that of Rackwitz and Fiessler [37].

One of the major developments in NDA is concerned with the accurate prediction of the reliability of the structural system and not just the variance or reliability index for the design. The earlier NDA design methods are generally referred to as second-moment methods, indicating that the answer is given in terms of the second statistical moment of the problem. To compute an estimated reliability of the performance of the system for low levels of probability, one needs to compute reliability functions for nonGaussian functions. Such computations use approximations that convert the actual probability data for each design variable into "equivalent" Gaussian or normal distributions. The first major improvement

Copyright 2005 by CRC Press LLC

to the Rackwitz-Fiessler algorithm was the three-parameter distribution model introduced by Chen and Lind [38]. Wu [39] contributed a further refinement of this algorithm. Applications of the new reliability algorithms have been extensive in the past several years. New and more accurate algorithms than the original Rackwitz-Fiessler algorithm were developed [40] and applied to complex structural systems [41, 42]. These algorithms are now generally referred to as "fast probability integration (FPI)" algorithms.

3.3.3 Finite Element Based Probabilistic Analysis

The principal, general-purpose NDA tool is based on finite element methods (FEM). Two general approaches have been developed for structural mechanics modeling: stochastic finite element methods and probabilistic finite element methods. The former is a second-moment method in which two coupled systems of matrix equations are created, one giving the response and one giving the variance in the response. Stochastic FEM is not suitable for probability calculations in the same way that second-moment methods are not suitable. The response is not a linear function of the random design variables, the variables are typically not normally distributed, and the probability estimates are not suitable for higher performance design problems.

One of the pioneering probabilistic code developments was work sponsored by the NASA (then) Lewis Research Center under the probabilistic structural analysis methods (PSAM) contract effort [43, 44]. The work was done at Southwest Research Institute (SwRI). A number of early papers were generated that document the probabilistic FEM code referred to as NESSUS (Nonlinear Evaluation of Stochastic Structures under Stress).

The NESSUS probabilistic FEM analysis is based on what is known as the advanced mean value (AMV) and AMV+ algorithms. The starting point for these algorithms is the deterministic FEM analysis done at the mean value design point (all random design conditions are set to their mean values). Each RV (again for now assume independence for convenience of the current discussion) is then perturbed a small amount based on its coefficient of variation (COV) to get a linear response surface. [Note: Quadratic and log-mapped RSs can also be used.] Based on the linear RS and design allowable for the performance function of interest, a limit state is generated from which a first-order reliability calculation can be made, as discussed earlier. Nonnormal RVs are mapped according to the Rosenblatt transformation to equivalent normals, using the Wu-FPI algorithm [5].

The Wu-FPI algorithm provides the design point or most probable point (MPP) in terms of the values for each RV. A new deterministic FEM analysis is done at the MPP. While the response changes from the initially approximated value, the AMV algorithm assumes that the probability associated with the selected limit state does not change in this updating step at the probability level for the original MPP. A spreadsheet example of the AMV algorithm is contained in Reference 45. A number of test problems confirmed the viability of the AMV algorithm as a much more accurate result than the usual first-order reliability results [46, 47].

The AMV+ algorithm is an iterative extension of AMV by reinitiating the RS approximation at the current design point; the updating based on the AMV process is continued until a convergence criterion is met. For a deeper discussion of the AMV+ algorithm, see Reference 48. Numerous applications of the NESSUS software and algorithms have been made including static stress [49], rotor dynamics [50], vibration [51], nonlinear response [52], and optimization [53]. NESSUS also provides a wide variety of probability integration algorithms, system reliability, and user-defined analysis models [54].

Other probabilistic FEM codes have been developed over the same time period. A good approach is to combine probabilistic methods with existing deterministic FEM codes. An excellent example of this is the ProFES product [55, 56]. The ProFES system is a three-dimensional graphical analysis environment that allows the analyst to perform a variety of response surface model developments for standard commercial FEM software systems. ProFES provides a variety of response surface simulations including first- and second-order methods and direct Monte Carlo simulation.

CalREL is another shell-type program with a variety of operating modes [57]. This probabilistic structural analysis code can be run in a stand-alone mode or in conjunction with other deterministic FEM codes. The probability algorithms are similar to those in ProFES and NESSUS in those first- and

Copyright 2005 by CRC Press LLC

second-order reliability computations are facilitated. First-order reliability calculations can be made for series systems while Monte Carlo simulation is available for more general systems problems.

The two major U.S. turbine engine manufacturers have each developed their own probabilistic FEM approaches to NDA for design. The codes are proprietary and not much has been published on them. However, the general approach in each is to use deterministic FEM codes in support of a design of experiments (DOE) approach for defining a response surface (RS) model of the physical variable or limit state of interest. Monte Carlo simulation is then performed on the RS model using the statistical models for each of the design variables.

The RS approaches generally have been developed to avoid the use of fast probability integration (FPI) algorithms, which some view as unreliable and a source of modeling error [60]. Both of these issues are relevant and a challenge to those developing and using FPI algorithms to provide meaningful convergence assurance and error estimation algorithms in support of these clearly faster algorithms.

The RS methods contain their own modeling error issues that have not been addressed in the reported literature. Largely the companies rely on standard RS fitting statistics to assure a "good" fit. However, such fitting is done in a global sense and likely does not apply at the so-called design point where the limiting failure values of the RV are dominant. Thus, further work on error bounding for RS methods is still needed to support NDA transition to design.

3.4 Other NDA Tools: A Transition Assessment

The previous section addressed some NDA methods that are currently being used to support design. A number of potential NDA technologies were reviewed in Reference 1 as possible contributors to the NDD environment. As such, these methods are in earlier stages of transition to design or are still being assessed by various investigators. The following paragraphs summarize those reviews.

3.4.1 Neural Networks [61–66]

Neural nets (NN) have the ability to represent physical responses somewhat like a Response Surface used in design. A NN model training process is used to establish nodal weights and biases. In general, NN weights do not conform to specific physical variables. A NN would be used to model an RS only if one had datasets and not a physical model. However, the statistical method for constructing RSs is more robust as far as sorting out noise from model behavior and for giving statistics that can be used in constructing assurance intervals for error analysis when applying the RS. As pointed out in [61], NNs rapidly lose their attractiveness for large numbers of NN nodes.

Reference 62 summarizes various uses of networks for data mining. Such applications may be valuable when constructing data models for NDD based on extensive test data. An interesting example of the use of NNs to model a combination of experimental data and varying types of modeling results for airfoil design is given in Reference 63. These authors use the NN as an effective way to solve the inverse problem for finding a RS from disparate data sources. The also report that their strategy for training results in nodal weights that can be tied to specific design variables.

A Bayesian network is one in that the nodal weights represent conditional event probabilities, as discussed in Reference 65. Such modeling appears to be useful for large system reliability problems and provides a direct means for simulating the top event and knowing its probabilistic design variable causes. They state that the Bayesian network method is preferable to Monte Carlo for system simulation for the additional information on conditional probabilities that is gained.

The literature suggests that an important NDA role for NNs is to be found in the proposed Model Helper and Data Expert tools. The application of NNs with a strategy to tie the nodal weights to physical variables appears to be an effective data mining strategy to support probabilistic input. Bayesian networks appear to be useful for system reliability modeling. Finally, NNs have a valid and important role in the data gathering and interpretation role in System Health Management. It does not seem likely that standard NNs will be used in the ND design analysis algorithms.

Copyright 2005 by CRC Press LLC

3.4.2 Fuzzy Theory [67–80]

Fuzzy logic is a potential NDA tool. Reference 80 compares probabilistic and fuzzy modeling for reliability. Fuzzy set theory and the closely related field of possibilistics have been touted for NDA. We do not support that position. Fuzzy systems are based on the mathematics of fuzzy set theory. The above references provide an adequate introduction to these fields. Generally speaking, fuzzy systems are used where so-called "crisp" probabilistic models do not exist, such as in linguistic representations. Characteristic mathematical models are assigned to fuzzy functions that are then combined using fuzzy logic. All input variables to the mathematical-physical model are given fuzzy representations and the physical model is written using the "algebra" of "fuzzy logic" to yield "fuzzy output." As in the paper by Rao [81], one finds that fuzzy physics is violated physics. That is, one loses the constraints of the physical model under fuzzy logic formulations. The only advice offered by that author is that one must impose one's physical intuition to properly understand the results. This is not scalable as a problem-solving strategy for large problems.

Reference 71 applies fuzzy logic to classical reliability engineering. The authors contend that this is the right approach to problems where the input is estimated from engineering experience and judgment. They also contend that this is the right way to represent degraded states of operation, given that the word "degraded" is subjective. However, work at the Los Alamos National Lab [2] has shown that one can take fuzzy input such as these authors refer to and convert that input into probabilistic distributions so that one can perform robust probabilistic calculations on these fuzzy-derived distributions.

Bezdek and Pal [69] are quoted as saying that "fuzzy models belong wherever they can provide collateral or competitively better information about a physical process." Bezdek and Pal give an example case wherein two bottles of water are lying in the desert and are found there by a very thirsty wanderer. The first bottle has a membership in the set of potable waters of 0.91 while the other has a probability of being potable that is 0.91. In the first case, the water shares a high degree of characteristics in common with potable water while the second has a 9% chance of being totally nonpotable (poison!). Which do *you* drink?

Fuzzy input is an important capability for NDA-based design. However, mathematically rigorous probabilistic algorithms are required as the processing element for de-fuzzified input data to support complex system designs. Fuzzy logic might be deployed in program management decision and risk prediction tools.

3.4.3 Interval Arithmetic [82–85]

This topic appears to be much more interesting to nondeterministic design. Interval arithmetic operates under some very precise algebraic rules and does not lead to systems that violate physics. In fact, interval arithmetic was developed as a way of representing floating point arithmetic errors. As cited in Reference 82, interval arithmetic is now released as a new variable type in the Sun Microsystems Fortran compiler.

Elishakoff and co-workers have applied interval methods to some structural analysis problems. Reference 86 combines interval analysis with stochastic finite element methods (second-moment method) to structural frames. Elishakoff applied strict interval analysis methods to computing the range of structural natural frequencies in Reference 87.

In a related technology to interval methods, Elishakoff and co-workers have utilized what they refer to as convex modeling [88] to compute one-sided bounds on structural behaviors such as natural frequencies and buckling loads [89]. The method is based on defining bounds on uncertain parameters as convex sets bounded by ellipsoids. For such cases, convex methods can be used to compute a corresponding convex set of results, or upper bounds.

Interval methods provide a formal mathematical treatment for problems where (1) no input information can be defined beyond upper and lower bounds for design variables and where (2) response ranges are desired for preliminary design purposes. Such methods may be worth considering as part of the required error bounds work proposed herein. Interval arithmetic may offer, especially as a data

Copyright 2005 by CRC Press LLC

type, the opportunity to do rapid analysis of the output range for design problems. The major concern with interval methods is that the intervals may be too large to be useful for NDD.

3.4.4 Response Surface Methods

There appears to be some confusion here over terminology as applied to probabilistic design. Probabilistic designers have used Taylor series expansions of the physical response of systems in terms of the design variables to construct locally linear (first-order) and locally quadratic (second-order) polynomial fits to model results. Such representations are updated as the "design point" moves through the design space (so-called advanced mean value [AMV] algorithm). This approach might best be called the local-RS approach.

A second approach, and one currently favored by the major turbine engine companies, derives from classical statistics [90, 91]. These RS methods have been developed as part of experimental statistics wherein the experiment is designed with varying patterns of high-low values for each identified parameter that can be changed. Mathematical methods are then used to define the RS that is most likely that defined by the experiment and the statistics of variance regarding that fit. One also determines the independence or coupling of the variables in the modeled physical response. The use of certain experimental designs leads to first-order surfaces (with interactions) or second- and higher-order surfaces.

While the use of RSs by the turbine engine manufacturers is based on fitting a response surface to deterministic and not to random (i.e., experimental) system responses, the users define their approach as an RS approach consistent with statistical derivations. The reason they use this terminology is that they use a variety of experimental designs (DOE) to select the points in the design space that are used to evaluate the response and from that the first- or second-order surface (with all interaction terms) is fitted. Such an RS method might best be called the DOE-RS method.

The key in all cases is that the RS is a representation of what is probably a model of the physical system. The specific fitting algorithm and probability algorithm define the errors in the nondeterministic results. The two RS approaches have different characteristics in terms of accuracy (local and global) and efficiency.

3.4.5 Nondeterministic Optimization [79, 92–100]

All optimization algorithms can and should be nondeterministically applied. Two design environment references [99, 100] clearly indicate this combination is the future for NDD. Nonprobabilistic elements in optimization can be in the objective function or in the constraints. The issues related to the use of nontraditional optimization strategies (nongradient, for example) such as genetic algorithms and simulated annealing have nothing to do with nondeterministic issues. They have a lot to do with the size, complexity, and the nature of the design environment [96, 97].

3.4.6 Design of Experiments [74, 101]

DOE strategies seek to define an RS by selecting a subset of a full factorial design procedure in order to reduce the experimental cost. The actual patterns are particular to various statisticians and practitioners. The second element is the separation of variables into controlled variables and noise or uncontrolled variables. When trying to target manufacturing processes using Taguchi strategies, one seeks to minimize process variability caused by noise factors. Commercial packages exist that simplify the DOE process (e.g., Reference 102).

3.4.7 Expert Systems

Expert systems are at the heart of an increasing number of applications including the fuzzy logic control systems, as previously discussed. Dedicated expert systems will be important parts of NDA methods deployed to support future design environments and system health monitoring [8, 103].

Copyright 2005 by CRC Press LLC

3.5 Transition Issues and Challenges

3.5.1 Overview

Much of the NDA technology needed to support complex system design for high reliability exists today. Some transition success has been achieved, primarily in areas where reliability is a premium. The following items discussed in this section are not roadblocks to NDA transition but they do represent, at least to these authors, some of the key items that require continuing or new efforts.

The transition issues include the need for a new design environment, verification and validation strategies for NDA models, error estimation models or bounds for NDA methods, linkage of NDA to traditional reliability and safety assessment methods, and the cost of NDA methods for significant (real) design problems. The issue of the design environment was addressed at the outset of this review; essentially, there is a need for a comprehensive information-based operating environment or software framework that supports the comprehensive system design process. Traditional design methods based on margins have worked in the context of individual design environments where design information sharing is very limited. NDA for design is highly dependent on consistent data modeling of common random variables that span the total system problem. The following topics briefly discuss other issues and challenges for NDA transition to design.

3.5.2 Verification and Validation of NDA Methods

Verification and Validation (VV) are critical issues for the modeling and simulation tools used for design—both for deterministic and probabilistic approaches. The Defense Department has published requirements for VV for modeling and simulation [104]. The defined terms for VV are the following.

- *Verification:* the process of determining that a model implementation accurately represents the developer's conceptual description and specifications.
- *Validation:* the process of determining the degree to which a model is an accurate representation of the real world from the perspective of the intended uses of the model.

These are generally accepted definitions within the VV community with variations only in the specific words used [105, 106]. Thus, verification refers to determining if the code does what was intended while validation refers to determining if the code/model represent real physics. Verification is typically done by reference of code output to benchmark solutions with analytical results, while validation is done by reference of code output to experimental results, where the key physics are operative.

We will not address verification issues beyond the need for error estimation requirements for some of the NDA methods. That topic will be addressed in the next subsection. The remainder of this subsection is devoted to the issue of NDA model validation. We propose that NDA model validation will provide a statistical measure of the agreement between the NDA prediction and available test data. We will further suggest that validation for system reliability problems must be inherently modular in nature.

Validation issues for deterministic modeling have been addressed in great detail by the computational mechanics community (e.g., Reference 105) and by the computational fluid mechanics community [107]. The Department of Energy is also active in developing specific modeling strategies to define quantitative measures of model validation [108–110]. This latter set of references demonstrates that validation can result in (1) an efficient use of experimental validation tests and (2) a statistical model for the uncertainty in the deterministic model. The latter can be used as statistical error models in a probabilistic application of the model as alluded to in Reference 3.

To date, no one has defined a comprehensive VV approach to NDA for design. However, we can suggest the elements that need to be included in such an approach. We will not address the issue of validating the deterministic models, *per se*, as we believe such validation needs have been recognized in past design practices.

Copyright 2005 by CRC Press LLC

- *Validate the deterministic models used for nondeterministic system response.*

These models may be based on the full deterministic analysis methods used to support NDA modeling or they may be based on using reduced-order models such as a derived RS [4] or AMV-type of RS [40] that are used as surrogates for the complete computational model. Typically, the issue here that differs significantly from the deterministic models is the need to validate "off-design" or "off-nominal" conditions.

The usual deterministic method validation process involves comparing a deterministic model to experimental results for selected test condition(s). Such testing is most likely to involve design variable conditions quite close to the nominal or expected values of those design variables. The critical reliability condition that drives the design, however, results from off-nominal values of the RVs that dominate the system failure probability.

Thus, a deterministic model may be "validated" at a nominal set of design variables, typically using some calibration factor. In margin-based design practices, it is good practice to assure that the calibration results in a conservative response condition when the reliability issues are considered. Such a calibration approach is unable to determine to what extent the physics of the response are properly modeled for the off-nominal but critical design condition that drives the system reliability.

- *Validate the deterministic model at off-nominal design conditions.*

Ideally, off-nominal validation should be performed at the values of the critical RVs that define the limiting reliability condition for the system design. However, it is likely that such off-nominal testing is impractical. Thus, some compromise must be made and judgment used to extrapolate from the test conditions for the critical RVs to the limiting reliability condition. As discussed in the Confidence Interval subsection, the off-nominal validation process must define the deterministic model errors for both the nominal and off-nominal conditions. The recommended approach is given in the following item.

- *Establish the statistical uncertainties in the deterministic models [110].*

The referenced approach uses probabilistic modeling to propagate uncertainties in the prediction using statistical models for those RVs whose values are not controlled in the testing. The approach also recognizes that the experimental results must themselves have defined uncertainties associated with experimental error. The result is a statistical measure of the probability of having a valid model by a likelihood function comparison of the experimental results with scatter and the NDA model with random factors for the experiment.

Extension of this approach to off-nominal conditions is likely to involve many fewer data points than one might expect for nominal validation testing. This is a practical recognition of the difficulties of performing off-nominal testing. As discussed in a recent Sandia VV report [106], there are practical limits to the cost of VV that dictate sometimes more pragmatic approaches. Nonetheless, it is critical to model the confidence one has in such cost-limited approaches to the experimental validation effort.

Thus, one must define the potential modeling uncertainty using some confidence interval method. That topic is addressed herein in the next subsection. Much further work is required to develop practical deterministic model validation methods that include the off-nominal conditions.

- *Validate the input probabilistic models being used to describe the RVs.*

Typically, such a validation effort will amount to establishing statistical confidence intervals on model parameters. However, it is not yet established how to represent the validation of the probability distribution itself in terms of the probability distributions themselves. Further work is needed on this subject.

- *Validate the total system model.*

The system model validation issue involves two steps. First, one must validate the individual NDA elements based on the individual RVs and statistics used for each. This modular approach would be based on the above validation recommendations. The second element is to perform sufficient system level testing to validate the RV interactions between the system elements. The process must assure that all of the key interaction variables are defined and that valid statistical measures and confidence interval models are represented in the system model. This system-level testing can be done using intermediate system-level testing that addresses blocks of the total system and their interactions.

Copyright 2005 by CRC Press LLC

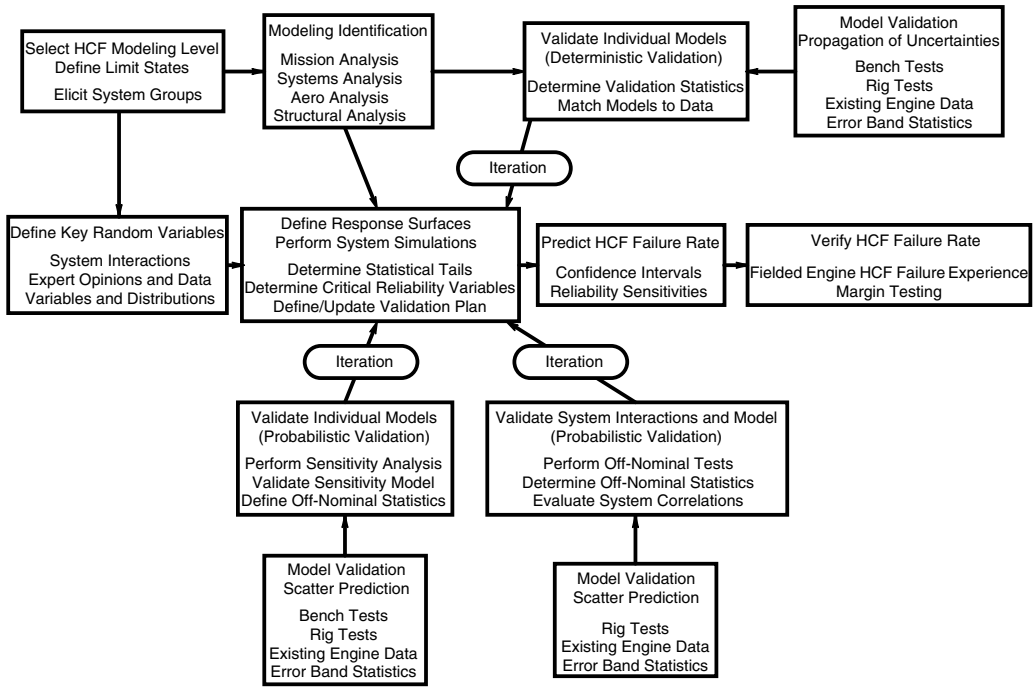

FIGURE 3.3 Notion of probabilistic validation: an HCF design process example.

A suggested logic diagram for validating a probabilistic high cycle fatigue design system is proposed in Figure 3.3. The figure shows the likely iterations that would be needed to update models, especially the error representations. Considerable effort is clearly required to develop a comprehensive validation strategy for each NDA design problem. One can see some of the key elements in the recommended approach used in a recently presented study on probabilistic disk design by Pratt & Whitney [111]. The final validation often must be by reference to a set of actual field reliability data for existing designs.

This approach, used in the reference Pratt & Whitney study combines the modular validation steps for individual NDA elements, with a total system reliability prediction. This is the only practical approach for problems where system level reliability testing is impractical. This is true of most, if not all, real design problems for reliability-critical systems.

3.5.3 NDA Error Estimation

The previous section outlined the VV issues with reference to the usual design analysis tools used in NDA of systems. In addition to these tools, the use of NDA for design must also include statistical measures of algorithm errors in the NDA probabilistic elements. These have been identified in the appropriate sections of this chapter and we will simply summarize them here. In all NDA methods reviewed by these authors, no such error estimations for probabilistic algorithms have been developed. This discussion must be classified as a verification effort where one is comparing actual computational performance of certain NDA elements as compared to benchmark or analytical results.

- *Probability integration algorithms.* The FPI algorithms in existence have varying levels of robustness and accuracy (e.g., References 5, 60). The user must be provided with automated ways of assuring robustness for the particular RV distributions. The final probability of failure result must include a margin for the FPI algorithm error. Monte Carlo simulation errors due to truncation must also be accounted for in RS NDA algorithms.

Copyright 2005 by CRC Press LLC

The use of any FPI algorithm must be supported by established limits on which types of distributions for which the method is robust. Additionally, FPI and MC algorithms must be accompanied by error prediction bounds that can be used in a general approach to confidence interval analysis.

- *RS errors.* The RS approach is suggested in two areas of NDA for design. One is the RS used as a surrogate for the physical or computational model that is too large for application with Monte Carlo methods. As developed by Pratt & Whitney, statistical error measures have been used to validate a RS in a global sense [58] but not at the design point where the probability of failure is being driven.
  The RS method must be implemented in such a way that the error between the surrogate model and the full computational model can be estimated. Often, this amounts to a single deterministic analysis at the most probable point (MPP) at the failure condition. The RS modeling error must be factored into the final reliability prediction in a manner consistent with all modeling errors.
- *Validation errors.* The Sandia National Laboratory validation effort includes statistical measures of the deterministic modeling errors [110]. The Sandia approach includes the important contribution of experimental errors in model validation. More is needed to extend this approach to the off-nominal conditions that are required for probabilistic model validation.
  A statistical model that captures both the experimental and computational modeling error must be defined for each tool and the design regime in which it is being used. This modeling error must be included in the final confidence interval as a statistical distribution.
- *Unknown-unknown errors.* One cannot model what one cannot conceive of as a failure mode for complex systems. The only rational way we can conceive of for reducing the contribution of this type of error is by a full integration of NDA methods that are essentially quantitative with the qualitative methods such as FMEA and FTA [9]. At the same time, it is critical that designers reference comprehensive "lessons learned" data or knowledge bases.
  The nondeterministic design environment must provide for a formal linkage between the FMEA processes and the reliability-based design. Failure modes not considered in the normal NDA design process must all be addressed and resolved. Field failure data records must also be reviewed for any failure modes not considered and such modes resolved for the new design.

3.5.4 Confidence Interval Modeling

The use of NDA for design results in reliability predictions that are the expected value(s) of the system performance. The design data used to generate the expected level of system performance includes probability distributions and their parameters, deterministic models of the physical processes, and system models that tie the variables and the physical process models together. Typically, each of these elements is treated as "truth." Some of the questions one can raise regarding each of these design elements that affect our confidence in the predicted outcome are the following:

- *Incomplete data to fully define the probability distributions being used in the NDA modeling.* Statistically speaking, one can only express the probability of making an error in accepting a certain probability distribution to model individual data sets. The assumption is that the distribution giving the highest statistical evaluation of fitting data is "correct" although any mathematical model is just that—a model. There are many other statistical issues here that go well beyond what can be addressed by this simple discussion.
- *Incomplete data to fully define the parameters used in the probability distributions.* Assuming for now that there are physical grounds for selecting a given distribution, the datasets used to fit the parameters of that distribution are always finite. Our confidence in the values for application of NDA near the center of the distribution is greater than our confidence if the design conditions are near the tails of the data.

Copyright 2005 by CRC Press LLC

NDA for design to a reliability goal typically determines that the limit condition for that reliability condition involves combinations of the RVs such that some of these RVs are in the tails of their distributions. For design problems, there are at least two primary concerns. The design limit condition may be based on applying the probability distribution for that variable beyond the existing data for that variable. Such extrapolations lead to a high risk or low confidence that either the probability distribution or the parameters are accurate at the extrapolated conditions. At this time, there are no formal statistical methods to treat this uncertainty and *ad hoc* methods are needed.

The second problem of incomplete data is the classical statistical problem of empirical or analytical confidence intervals on the distribution given the fitted parameters [112, 113]. Such confidence intervals expand significantly in the tails of the distributions. Strict adherence to these CIs typically imposes significant burdens of the designer to increase the size of the datasets needed to support design for reliability.

The usual basis for NDA for system design is the application of deterministic models of physics but with uncertainty in the modeling parameters, boundary conditions, geometry, etc. This report has identified model verification and validation as required steps in any design problem. The validation process that has been discussed can be used to derive statistical models that link the models to the experimental results recognizing that both have uncertainties associated with them.

Added to the usual validation requirement is the stated requirement that the physical models must be validated in the off-nominal condition, especially weighted toward the conditions that NDA determines control the system reliability. The report also identifies numerical errors in some of the analytical methods that are used to support NDA such as response surface, fast probability integration, and the Monte Carlo simulation algorithms. The uncertainties of each of these must be incorporated in the CI estimation.

The issue of user or operator errors is also a real modeling problem that is linked to confidence in the reliability prediction. We do not address this issue herein beyond indicating the need for the design process to provide quality assurance steps that assure consistency and reliability of the predicted outcomes. Various manufacturers have different approaches to qualifying users of any design tools. These approaches must be expanded to include NDA.

The last area of uncertainty in the NDA prediction of system reliability is the system model itself. This uncertainty is more deterministic in that the system model validation process must be based on sufficient system level testing to assure that the principal RVs and their linkages between the physical modeling modules are correct. We have already cited the Pratt & Whitney probabilistic design system approach to validating the system level model by reference to past performance data [111]. Such system level NDA model validation is the culmination of the validation process for each of the elements in the system model.

Before NDA can fully transition to the design environment for reliability critical applications, the NDA community must address the full set of confidence issues. We strongly believe that the NDA-based design process must be capable of predicting not only the expected system reliability but also the appropriate bounds on the predicted reliability at some confidence level (in the Bayesian sense not the frequentist sense), and the major random variables that govern both. A notional representation of the operation of such an NDA design system with CIs over the design timeframe is shown in Figure 3.4.

The only appropriate formal basis for the definition of CIs for the totality of the defined confidence issues is the Bayesian belief form of confidence [114]. We have developed a generalized application of this general concept in the context of the Markov Chain Monte Carlo algorithm for a representative systems problem [3]. However, work is needed to define rational design approaches to establishing such Bayesian CIs for system problems that combine the uncertainties in distributions, data, models, and the results of validation. Strict statistical approaches simply are not applicable to this critical problem.

3.5.5 Traditional Reliability and Safety Assessment Methods

One of the major opportunities and challenges for NDA in design is achieving a complete closure with standard reliability and safety assessment methods such as FMEA and FTA modeling. The latter already has been addressed in limited ways in various software packages such as NESSUS [54].

Copyright 2005 by CRC Press LLC

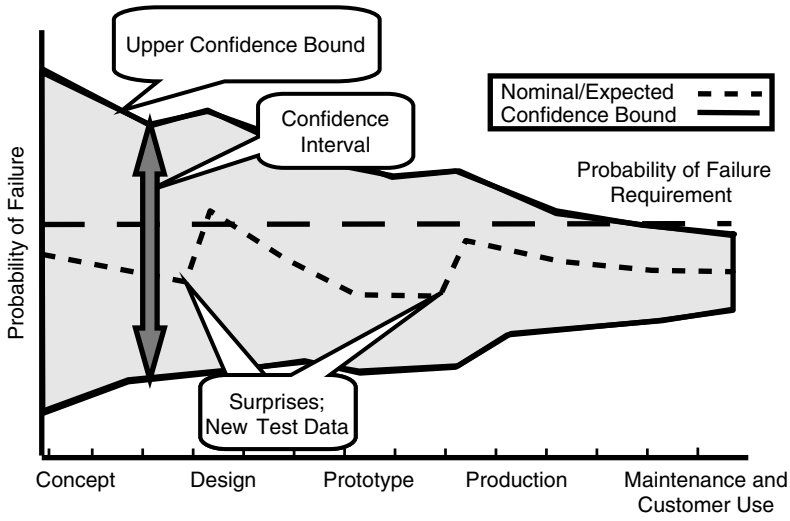

FIGURE 3.4 NDA confidence interval depiction.

A key issue in safety assessment design is the fact that most reliability critical designs begin with a reliability allocation to various subsystems and then to the components themselves. Often, such reliability assessments as are needed to support this kind of top-down reliability allocation approach are based on past hardware data and not on NDA quantitative assessments. Education and communication are required to bring such safety programs into the world of quantitative assessments, with updating methods such as Bayesian methods to achieve consistency between the hardware experience and the quantitative tools coming from NDA technology.

The FMEA process is the most qualitative but provides an important opportunity to address the issues raised by the unknown-unknown reliability problem. That is, the FMEA process, when done properly, has a reasonably high likelihood of identifying a comprehensive set of failure modes—that is its purpose! The FMEA process does not prioritize the failure modes except by reference to operating experience with similar designs. By combining the FMEA and NDA methodologies, one has the ability to be (1) comprehensive in predicting the system reliability, (2) prioritizing by use of the quantitative NDA tools, (3) valid by reference to operating experience, and (4) cost effective by reducing the amount of testing that nonquantitative FMEA results often require.

3.6 Conclusion

The design community is poised on the edge of a major transition from traditional, margin-based design to designs based on NDA. There are many technologies available to support NDA-based design but critical transition issues remain. Some of the transition issues are clearly related to concerns over the cost associated with the need for greater amounts of design data in the appropriate forms for NDA and the greater expense of large NDA models in relation to deterministic design. Nonetheless, there is also a growing understanding that margin-based design is, in many cases, overly conservative such that NDA can result in cost and weight savings in performance critical applications. There is also a growing understanding that NDA methods provide new and critical insights into variable dependencies and interactions that, when properly used, will result in more robust designs.

Acknowledgments

The authors wish to acknowledge the support of the Air Force Research Laboratory, Propulsion Directorate, for the work that underlies this report. The first author also acknowledges the direct support of

Copyright 2005 by CRC Press LLC

Universal Technologies Inc. and Michele Puterbaugh of UTC for her support through the high cycle fatigue program.

References

1. Cruse, T.A., Non-deterministic, Non-traditional Methods (NDNTM), NASA/CR-2001-210976, July 2001.
2. Meyer, M.A. and Booker, J.M., Eliciting and Analyzing Expert Judgment, American Statistical Association and the Society for Industrial and Applied Mathematics, Alexandria, Virginia and Philadelphia, Pennsylvania, 2001.
3. Cruse, T.A. and Brown, J.M., Confidence Intervals for Systems of Random Variables, submitted for publication.
4. Fox, E.P., Issues in Utilizing Response Surface Methodologies for Accurate Probabilistic Design, *Proceedings of the 37th AIAA/ASME/ASCE/AHS/ASC Structures, Structural Dynamics, and Materials Conference,* AIAA-96-1496, April 1996.
5. Wu, Y.-T., Demonstration of a new fast probability integration method for reliability analysis, *J. Engrg. Indus.,* 109, 24–28, 1987.
6. Tryon, R.G., Probabilistic Mesomechanical Fatigue Model, NASA Contractor Report 202342, April 1997.
7. Tryon, R.G. and Cruse, T.A., A Reliability-Based Model to Predict Scatter in Fatigue Crack Nucleation Life, *Fatigue & Fract. Engrg. Matls. & Struct.,* 21, 257–267, 1998.
8. Roemer, M.J. and Kacprzynski, G.J., Advanced Diagnostics and Prognostics for Gas Turbine Engine Risk Assessment ASME/IGTI Turbo-Expo 2000, Munich Germany, 2000-GT-30, May 2000.
9. Lewis, E.E., Introduction to Reliability Engineering, John Wiley & Sons, New York, 1987.
10. Kapur, K.C. and Lamberson, L.R., *Reliability in Engineering Design*, John Wiley & Sons, New York, 1977.
11. Meyer, P.L., *Introductory Probability and Statistical Applications,* Addison-Wesley, Reading, MA, 1970.
12. Cruse, T.A, Ed., *Reliability-Based Mechanical Design,* Marcel Dekker Inc., New York, 1997.
13. Anon., *Handbook of Reliability Prediction Procedures for Mechanical Equipment,* Report Carderock Division NSWC-92/L01, Naval Surface Warfare Center, Bethesda, MD, 1992.
14. Abernethy, R.B., Breneman, J.E., Medlin, C.H., and Reinman, G.L., *Weibull Analysis Handbook,* Air Force Wright Aeronautical Laboratory Report AFWAL-TR-83-2079, 1983.
15. Beck, J.V. and Arnold, K.J., *Parameter Estimation in Engineering and Science,* John Wiley & Sons, New York, 1977.
16. Meeker, W.Q. and Escobar, L.A., *Statistical Methods for Reliability Data,* John Wiley & Sons, Inc., New York, 1998.
17. Kececioglu, D., *Reliability Engineering Handbook,* Vol. 2, Chapter 11: Fault Tree Analysis, Prentice Hall, Englewood Cliffs, NJ, 1991.
18. Kumamoto, H. and Henley, E.J., *Probabilistic Risk Assessment and Management for Engineers and Scientists*, 2nd edition, Chapter 3: Probabilistic Risk Assessment, IEEE Press, 1996.
19. Tryon, R.G., Cruse, T.A., and Mahadevan, S., Development of a reliability-based fatigue life model for gas turbine engine structures, *Engrg. Fract. Mechs.,* 53, 5, pp. 807–828, 1996.
20. Maggio, G. and Fragola, J.R., Combining computational-simulations with probabilistic-risk assessment techniques to analyze launch vehicles, *Proceedings, 1995 Annual R&M Symposium*, pp. 343–348.
21. Cruse, T.A., Engine Components, Practical Applications of Fracture Mechanics, NATA AGARDograph #257, Chapter 2, 1980.
22. Cruse, T.A., Mahadevan, S., and Tryon, R.G., Fatigue Reliability of Gas Turbine Engine Structures, NASA/CR-97-206215.

Copyright 2005 by CRC Press LLC

23. Khintchine, A. Ya., Mathematisches uber die Erwartung von einen offentlicher Schalter, *Matemalliche Sbornik*, 1932.
24. Palm, C., Arbetskraftens Fordelning vid betjaning av automatskiner, *Industritidningen Norden*, 1947.
25. Barlow, R. E. and Proschan, F., *Mathematical Theory of Reliability*, J. Wiley & Sons, New York, p. 1, 1965.
26. Lotka, A.J., A contribution to the theory of self-renewing aggregates with special reference to industrial replacement, *Annual of Mathematical Statistics,* 10, 1–25, 1939.
27. Weibull, W., A statistical theory of the strength of materials, *Proceedings, Royal Swedish Institute of Engineering Research,* 151, Stockholm, Sweden, 1939.
28. Gumbel, E. J., Les valeurs extremes des distributions statistiques, *Annales de l'Institute Henri Poincare,* 4, 2, 1935.
29. Cruse, T. A., McClung, R. C., and Torng, T. Y., NSTS Orbiter Auxiliary Power Unit Turbine Wheel Cracking Risk Assessment, *Journal of Engineering for Gas Turbines and Power,* 114, ASME, pp. 302–308, April 1992.
30. Madsen, H.O., Krenk, S., and Lind, N.C., *Methods of Structural Safety*, Prentice Hall, Englewood Cliffs, NJ, 1986.
31. Cornell, C.A., Bounds on the reliability of structural systems, *J. Structural Division, 93*, American Society of Civil Engineering, pp. 171–200, 1967.
32. Lind, N.C., The design of structural design norms, *J. Structural Mechanics,* 1, 3, pp. 357–370, 1973.
33. Ditlevsen, O., Structural reliability and the invariance problem, Technical Report No. 22, Solid Mechanics Division, University of Waterloo, Ontario, Canada, 1973.
34. Lind, N.C., An invariant second-moment reliability format, Paper No. 113, Solid Mechanics Division, University of Waterloo, Ontario, Canada, 1973.
35. Hasofer, A.M. and Lind, N.C., Exact and invariant second-moment code format, *J. Engineering Mechanics Division,* 100, American Society of Civil Engineers, EM1, pp. 111–121, 1974.
36. Ang, A.H.-S. and Cornell, C.A., Reliability bases of structural safety and design, *J. Structural Division,* 11, American Society of Civil Engineers, pp. 1755–1769, 1974.
37. Rackwitz, R. and Fiessler, B., Structural reliability under combined random load sequences, *J. Engineering Mechanics Division,* 100, American Society of Civil Engineers, pp. 489–494, 1978.
38. Chen, X. and Lind, N.C., Fast probability integration by three-parameter normal tail approximation, *Structural Safety,* 1, pp. 269–276, 1983.
39. Wu, Y.-T., Demonstration of a new, fast probability integration method for reliability analysis, *J. Engineering for Industry,* 109, American Society of Mechanical Engineers, pp. 24–28, 1987.
40. Wu, Y.-T., Millwater, H.R., and Cruse, T.A., Advanced probabilistic structural analysis method for implicit performance functions, *J. of the AIAA,* 28(9), American Institute for Aeronautics and Astronautics, pp. 1663–1669, 1990.
41. Cruse, T.A., Rajagopal, K.R., and Dias, J.B., Probabilistic structural analysis methodology and applications to advanced space propulsion system components, *Computing Systems in Engineering,* 1(2-4), pp. 365–372, 1990.
42. Cruse, T.A., Mahadevan, S., Huang, Q., and Mehta, S., Mechanical system reliability and risk assessment, *AIAA Journal,* 32, 11, pp. 2249–2259, 1994.
43. Cruse, T.A., Burnside, O.H., Wu, Y.–T., Polch, E.Z., and Dias, J.B., Probabilistic structural analysis methods for select space propulsion system structural components (PSAM), *Computers & Structures,* 29, 5, pp. 891–201, 1988.
44. Cruse, T.A., Rajagopal, K.R., and Dias, J.B., Probabilistic structural analysis methodology and applications to advanced space propulsion system components, *Computing Systems in Engineering,* 1,(2–4), pp. 365–372, 1990.
45. Cruse, T.A., Mechanical reliability design variables and models, Chapter 2, in *Reliability-Based Mechanical Design,* T.A. Cruse, Editor, Marcel Dekker, New York, 1997.

Copyright 2005 by CRC Press LLC

46. Wu, Y.–T., Millwater, H.R., and Cruse, T.A., An advanced probabilistic structural analysis method for implicit performance functions, *AIAA Journal,* 28(9), pp. 1663–1669, Sept. 1990.
47. Riha, D.S., Millwater, H.R., and Thacker, B.H., Probabilistic structural analysis using a general purpose finite element program, *Finite Elements in Anal. Des.,* 11, pp. 201–211, 1992.
48. Wu, Y.-T., Computational methods for efficient structural reliability and reliability sensitivity analysis, *AIAA J.,* 32(8), pp. 1717–1723, 1994.
49. Thacker, B.H., Application of advanced probabilistic methods to underground tunnel analysis, *Proceedings of the 10th ASCE Engineering Mechanics Conference,* S. Sture, Editor, Vol. I, pp. 167–170, 1995.
50. Millwater, H.R., Smalley, A.J., Wu, Y.-T., Torng, T.Y., and Evans, B.F., Computational Techniques for Probabilistic Analysis of Turbomachinery, ASME Paper 92-GT-167, June 1992.
51. Cruse, T.A., Unruh, J.F., Wu, Y.-T., and Harren, S.V., Probabilistic structural analysis for advanced space propulsion systems, *J. Eng. Gas Turb. Power,* 112, pp. 251–260, 1990.
52. Millwater, H., Wu, Y., and Fossum, A., Probabilistic Analysis of a Materially Nonlinear Structure, Paper AIAA-90-1099, 31st AIAA/ASME/ASCE/AHS/ASC Structures, Structural Dynamics and Materials Conference, April 1990.
53. Wu, Y.-T. and Wang, W., Efficient probabilistic design by converting reliability constraints to approximately equivalent deterministic constraints, *Trans. Soc. Design Process Sc.,* 2(4), pp. 13–21, 1998.
54. Riha, D.S., Thacker, B.H., Millwater, H.R., and Wu, Y.-T., Probabilistic Engineering Analysis Using the NESSUS Software, Paper AIAA 2000-1512, *Proceedings of the 41st AIAA/ASME/ASCE/ASC Structures, Structural Dynamics, and Materials Conference and Exhibit, AIAA Non-Deterministic Approaches Forum,* Atlanta, Georgia, 3–6 April 2000.
55. Cesare, M.A. and Sues, R.H., ProFES probabilistic finite element system—Bringing probabilistic mechanics to the desktop, *Proceedings of the 40th AIAA/ASME/ASCE/ASC Structures, Structural Dynamics, and Materials Conference and Exhibit, AIAA Non-Deterministic Approaches Forum,* April 1999.
56. Sues, R.H. and Cesare, M., An innovative framework for reliability-based MDO, *Proceedings of the 41st AIAA/ASME/ASCE/ASC Structures, Structural Dynamics, and Materials Conference and Exhibit, AIAA Non-Deterministic Approaches Forum,* Atlanta, Georgia, 3–6 April 2000.
57. Liu, P.-L., Lin, H.-Z., and Der Kiureghian, A., CALREL User Manual, Report No. UCB/SEMM-89/18, Structural Engineering, Mechanics and Materials, Department of Civil Engineering, University of California, Berkeley, CA, 1989.
58. Fox, E.P., The Pratt & Whitney Probabilistic Design System, Paper AIAA-94-1442, *Proceedings of the 35th AIAA/ASME/ASCE/AHS/ASC Structures, Structural Dynamics, and Materials Conference,* 1994.
59. Roth, P.G., Probabilistic Rotor Design System (PRDS), AFRL Contract F33615-90-C-2070 Final Report, General Electric Aircraft Engines, June 1999.
60. Fox, E.P. and Reh, S., On the Accuracy of Various Probabilistic Methods, Paper AIAA-2000-1631, 2000.
61. Wacholder, E., Elias, E., and Merlis, Y., Artificial networks optimization method for radioactive source localization, *Nuclear Technology,* 110, pp. 228–237, May 1995.
62. Harmon, L. and Schlosser, S., CPI plants go data mining, *Chemical Engineering*, pp. 96–103, May 1999.
63. Rai, M.R. and Madavan, N.K., Aerodynamic design using neural networks, *AIAA Journal,* 38(1), January 2000, pp. 173–182.
64. Steppe, J.M. and Bauer, K.W., Jr., Feature saliency measures, *Computers Math. Applic.,* 33(8), pp. 109–126, 1997.
65. Yu, D.C., Nguyen, T.C., and Haddaway, P., Bayesian network model for reliability assessment of power systems, *IEEE Transactions on Power Systems,* 14(2), pp. 426–432, May 1999.
66. Xia, Y. and Wang, J., A general methodology for designing globally convergent optimization neural networks, *IEEE Transactions on Neural Networks,* 9(6), pp. 1331–1343, January-February, 1999.
67. Mendel, J.M., Fuzzy logic systems for engineering: a tutorial, *Proceedings of the IEEE*, Vol. 83, No. 3, 345–377, March 1995.

Copyright 2005 by CRC Press LLC

68. Zadeh, L.A., Outline of a new approach to the analysis of complex systems and decision processes, *IEEE Transactions on Man and Cybernetics*, Vol. SMC-3, No. 1, 28–44, 1973.
69. Bezdek, J. and Pal, S.K., *Fuzzy Models for Pattern Recognition*, IEEE Press, New York, 1992.
70. Jang, J.-S. Roger and Sun, C.-T., Neuro-fuzzy modeling and control, *Proceedings of the IEEE*, 83(3), 378–405, March 1995.
71. Bowles, J.B. and Peláez, C.E., Application of fuzzy logic to reliability engineering, *Proceedings of the IEEE*, 83(3), 435–449, March 1995.
72. Misra, K. B. and Onisawa, T., Use of fuzzy sets theory part II: applications, in *New Trends in System Reliability Evaluation,* Elsevier, Amsterdam, 551–587, 1993.
73. Roy, R., A primer on the Taguchi method, Van Nostrand Reinhold, New York, 1990.
74. Bonissone, P.P., Badami, V., Chiang, K.H., Khedkar, P.S., Marcelle, K.W., and Schutten, M.J., Industrial applications of fuzzy logic at General Electric, *Proceedings of the IEEE*, 83(3), 450–464, March 1995.
75. Procyk, T. and Mamdani, E., A linguistic self-organizing process controller, *Automatica*, 15(1), 15–30, 1979.
76. Zadeh, Lotfi A., Soft Computing and Fuzzy Logic, *IEEE Software*, pp. 48–58, November 1994.
77. Kosko, B., *Neural Networks and Fuzzy Systems: A Dynamical Systems Approach to Machine Language*, Prentice Hall, Englewood Cliffs, NJ, 1991.
78. Karr, C., Genetic algorithms for fuzzy controllers, *AI Expert*, pp. 26–33, Nov. 1991.
79. Mulkay, E.L. and Rao, S.S., Fuzzy heuristics for sequential linear programming, *J. Mechanical Design*, 120, pp. 17–23, March 1998.
80. Chen, S., Nikolaidis, E., and Cudney, H.H., Comparison of probabilistic and fuzzy set methods for designing under uncertainty, Paper AIAA-99-1579, pp. 2660–2674, 1999.
81. Rao, S.S. and Weintraub, P.N., Modeling and analysis of fuzzy systems using the finite element method, Paper AIAA-2000-1633.
82. Walster, G. William, Introduction to interval arithmetic, unpublished note supporting Sun Microsystems compilers for interval programs, May 19, 1997.
83. Alefield, G. and Claudio, D., The basic properties of interval arithmetic, its software realizations and some applications, *Computers and Structures,* 67, pp. 3–8, 1998.
84. Walster, G. William, Interval arithmetic: the new floating-point arithmetic paradigm, unpublished notes from the Fortran Compiler Technology group at Sun Microsystems.
85. Hansen, E.R., *Global Optimization Using Interval Analysis*, Marcel Dekker, Inc., New York, 1992.
86. Köylüoglu, H. Ugur and Elishakoff, I., A comparison of stochastic and interval finite elements applied to shear frames with uncertain stiffness properties, *Computers & Structures,* 67, 91–98, 1998.
87. Qiu, Z.P., Chen, S.H., and Elishakoff, I., Natural frequencies of structures with uncertain but nonrandom parameters, *J. Optimization Theory Appl.,* 86(3), 669–683, 1995.
88. Ben-Haim, Y. and Elishakoff, I., *Convex Models of Uncertainty in Applied Mechanics,* Elsevier Science Publishers, Amsterdam, 1990.
89. Li, Y.W., Elishakoff, I., Starnes, J.H., Jr., and Shinozuka, M., Prediction of natural frequency and buckling load variability due to uncertainty in material properties by convex modeling, *Fields Institute Communications,* 9, 139–154, 1996.
90. Khuri, A. I. and Cornell, J. A., *Response Surfaces,* Marcel Dekker Inc., New York, 1987.
91. Box, G.P. and Draper, N.R., *Empirical Model-Building and Response Surfaces,* J. Wiley & Sons, New York, 1987.
92. Toh, A.T.C., Genetic algorithm search for critical slip surface in multiple-wedge stability analysis, *Can. Geotech. J., 36*, pp. 382–391, 1999.
93. Xia, Y. and Wang, J., A general methodology for designing globally convergent optimization neural networks, *IEEE Transactions on Neural Networks,* 9(6), pp. 1331–1343, January–February, 1999.
94. Mosher, T., Conceptual spacecraft design using a genetic algorithm trade selection process, *J. of Aircraft,* 36(1), pp. 200–208, January–February, 1999.

Copyright 2005 by CRC Press LLC

95. Alberti, N. and Perrone, G., Multipass machining optimization by using fuzzy possibilistic programming and genetic algorithms, *Proc. Inst. Mech. Engrs.,* 213, Part B, pp. 261–273, 1999.
96. Hajela, P., Nongradient methods in multidisciplinary design optimization—status and potential, *J. Aircraft,* 36(1), pp. 255–265, January 1999.
97. Josephson, J.R., Chandrasekaran, B., Carroll, M., Iyer, N., Wasacz, B., Rizzoni, G., Li, Q., and Erb, D.A., An architecture for exploring large design spaces, *Proceedings of the 1998 AAAI,* http://www.aaai.org/.
98. Fogel, D. B., Fukuda, T., and Guan, L., Scanning the Issue/Technology—special issue on computational intelligence, *Proc. IEEE,* 87(9), pp. 1415–1421, September 1999.
99. Bailey, M.W., Irani, R.K., Finnigan, P.M., Röhl, P.J., and Badhrinath, K., Integrated multidisciplinary design, manuscript submitted to AIAA, 2000.
100. Röhl, P.J., Kolonay, R., Irani, M., Sobolewski, R.K., Kao, M., and Bailey, M.W., A federated intelligent product environment, *AIAA-2000-4902*, 2000.
101. Lochner, R.H. and Matar, J.E., *Design for Quality,* Quality Resources, A Division of The Kraus Organization Ltd., White Plains, NY, 1990.
102. Anon., Design-Expert Software Version 6 User's Guide, Stat-Ease, Inc., Minneapolis, MN, 55413-9827.
103. DePold, H.R. and Gass, F.D., The application of expert systems and neural networks to gas turbine prognostics and diagnostics, *J. Engrg. Gas Turbines Power,* 121, pp. 607–612, October 1999.
104. Anon., DoD Modeling and Simulation (M&S) Verification, Validation, and Accreditation (VV&A), Department of Defense Instruction No. 5000.61, April 29, 1996.
105. Roache, P.J., *Verification and Validation in Computational Science and Engineering,* Hermosa Publishing, Albuquerque, NM, 1998.
106. Oberkampf, W.L., Trucano, T.G., and Hirsch, C., Verification, Validation, and Predictive Capability in Computational Engineering and Physics, Sandia National Laboratory Report SAND2003-3769, February 2003.
107. Anon., Guide for the Verification and Validation of Computational Fluid Dynamics Simulations, AIAA Guide G-077-1998.
108. Pilch, M., Trucano, T., Moya, J., Froehlich, G., Hodges, A., and Peercy, D., Guidelines for Sandia ASCI Verification and Validation Plans—Content and Format: Version 2.0, Sandia Report SAND2000-3101, January 2001.
109. Trucano, T.G., Easterling, R.G., Dowding, K.J., Paez, T.L., Urbina, A., Romero, V.J., Rutherford, B.M., and Hills, R.G., Description of the Sandia Validation Metrics Project, Sandia Report SAND2001-1339, July 2001.
110. Hills, R.G. and Trucano, T.G., Statistical Validation of Engineering and Scientific Models: A Maximum Likelihood Based Metric, Sandia Report SAND2001-1783, January 2002.
111. Adamson, J., Validating the Pratt & Whitney Probabilistic Design System, *Proceedings of the 6th Annual/FAA/AF/NASA/Navy Workshop on the Application of Probabilistic Methods to Gas Turbine Engines,* Solomons Island, MD, March 19, 2003.
112. Mann, N.R., Schafer, R.E., and Singpurwalla, N.D., *Methods for Statistical Analysis of Reliability and Life Data,* John Wiley & Sons, New York, 1974.
113. Meeker, W.Q. and Escobar, L.A., *Statistical Methods for Reliability Data,* John Wiley & Sons, New York, 1998.
114. Martz, H.F. and Waller, R.A., Bayesian Reliability Analysis, Reprint Edition, Krieger Publishing Company, Malabar, FL, 1991.

Copyright 2005 by CRC Press LLC

4

An Industry Perspective on the Role of Nondeterministic Technologies in Mechanical Design

Kadambi Rajagopal
Rocketdyne Propulsion and Power, The Boeing Company

4.1 Introduction

Affordable and reliable access to space is a fundamental and necessary requirement to achieve the loftier goals of expanding space exploration. It also plays an important role in achieving the near-term benefits of space-based technologies for mankind. The development, performance, and reliability of liquid rocket propulsion systems have played and will continue to play a critical role in this mission. However, the cost of development of a typical propulsion system in the past was on the order of a few billion dollars. The design approaches using nondeterministic technologies as well as deterministic design space exploration approaches show promise in significantly reducing the development costs and improving the robustness and reliability of newly developed propulsion systems.

Copyright 2005 by CRC Press LLC

4.2 The Business Case

Traditional ideas of application of structural reliability concepts use the probabilistic information of stress and strength (supply and demand) to compute the probability of failure. The probabilistic approach when applied to all facets of structural analysis (not just random vibration) will be a significant change from past practices. In the conventional factor of safety approach to structural design, the probability of failure is neither explicitly calculated nor stated as a design requirement. However, the potential for reducing the development costs of liquid rocket propulsion systems through the use and application of nondeterministic analysis approaches is of great interest in the liquid rocket propulsion industry.

This is illustrated in Figure 4.1 where the high reliability of liquid rocket engines is achieved by extensive testing of the hardware to flush out all the failure modes. This development cycle is typically referred to as "Test-Fail-Fix" cycle. Similar experiences can be found in jet engine as well as in automobile product development. While this approach has proven itself very successful, the new realities of limited budgets have made such an approach not always practical. Further, in addition to cost, the schedule pressures can preclude extensive testing as an avenue for successful product development. It also must be mentioned that in many space use scenarios, it is impossible to duplicate the space environment on ground. The challenge is then to develop product development approaches to achieve the development cost and schedule profile goals shown in Figure 4.1.

A study of the developmental failures in the liquid rocket engine indicates that the failures can be categorized due to three main causes, which are approximately equal in percentage. They are (1) a lack of knowledge of the loading environment, (2) the absence or lack of accuracy in the physics-based models to explain complex phenomena (e.g., combustion-induced high frequency vibration), and (3) lack of understanding of hardware characteristics as manufactured (e.g., unintended defects). (Figure 4.2). Successful robust and reliable product development under the cost and schedule constraints mentioned above requires a new design approach that puts less emphasis on testing. It is in this role that the nondeterministic approaches that explicitly consider *total uncertainty* can play a

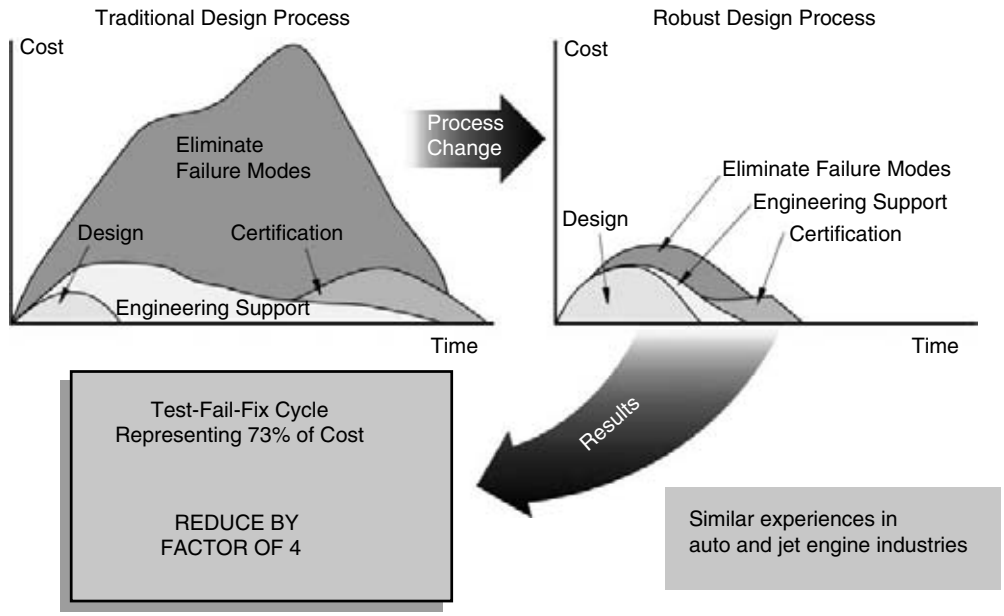

FIGURE 4.1 Historical development cost profile for liquid rocket engine development.

Copyright 2005 by CRC Press LLC

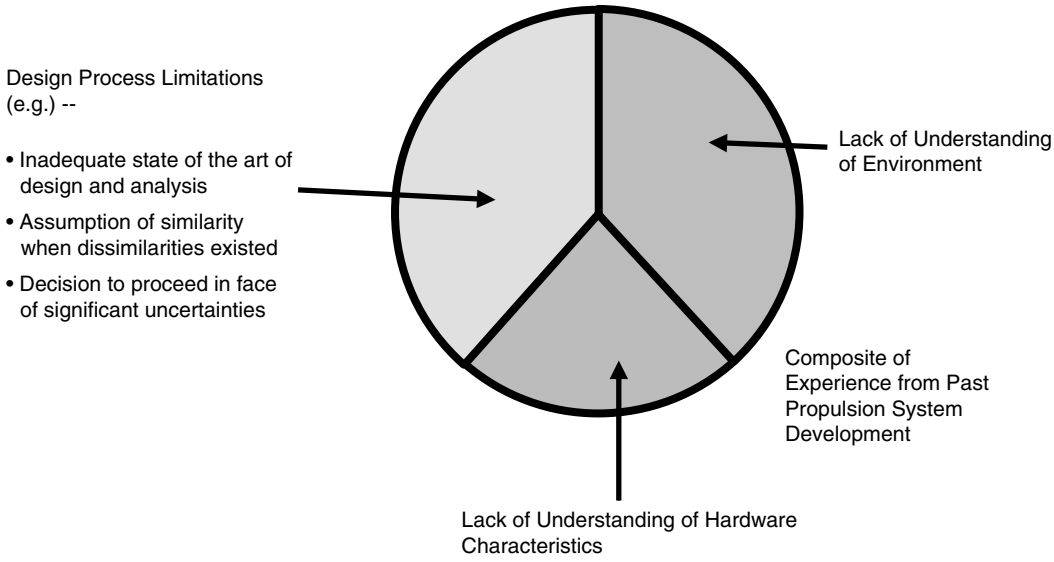

FIGURE 4.2 Categorization of causes of development failures based on historical data.

significant role. The role of epistemic uncertainty (lack of knowledge) resulting in consequences that drive up development cost is significant and comparable to aleatory (system variability) uncertainty based root causes.

Historically, in a typical new engine design, the development testing process works through approximately 25 to 150 failure modes. Most of them are minor but some require major redesign of specific components. The number of failures depends on the technology stretch of the new engine (from past experience), both from engine cycle as well as production process points of view. Considering that the typical engine contains thousands of parts, the majority of the components are designed correctly from the beginning and they perform flawlessly. But the expense of testing is so high, due to cost of fuel, facilities, and expensive hardware, that even this small amount of failures has very high cost consequences. In the population of these failure modes, some of them could be anticipated and prevented by the improved current state-of-the-art analysis technology (e.g., finite element methods, computational fluid dynamics, etc.) leveraging the quantum improvements in the computational speed. Some of the failure modes are the result of complex system interactions, such as fluid structure coupling, high-frequency excitation due to internal turbulent flow, and nozzle side loads generated due to overexpanded nozzle ratios (the nozzle exit pressure is less than the ambient pressure) during ground testing. The current state-of-the-art model based analysis methodology has not advanced enough to predict reliably the loads induced by these phenomena.

It is necessary to make a clear distinction between activities related to automation in design (computer aided design, CAD) that result in significant cost savings and the technologies that reduce the developmental risk because of their ability to operate in the uncertainty space. A successful practical approach to design should leverage advances in both the technologies, as shown in Figure 4.3. The chart should be read by starting at the right quadrant, going up to estimate the number of anticipated failures based on risk anchored by historical records, and moving to the left quadrant to estimate the number of failures and associated development costs. The risk factor as portrayed in Figure 4.3 could be a measure of design risk using rankings on a scale of 0 to 1.0. It could be calculated either by a subjective approach using a scoring method by a panel of experts with experience in very detailed engine categories or using a quantitative approach.

Copyright 2005 by CRC Press LLC

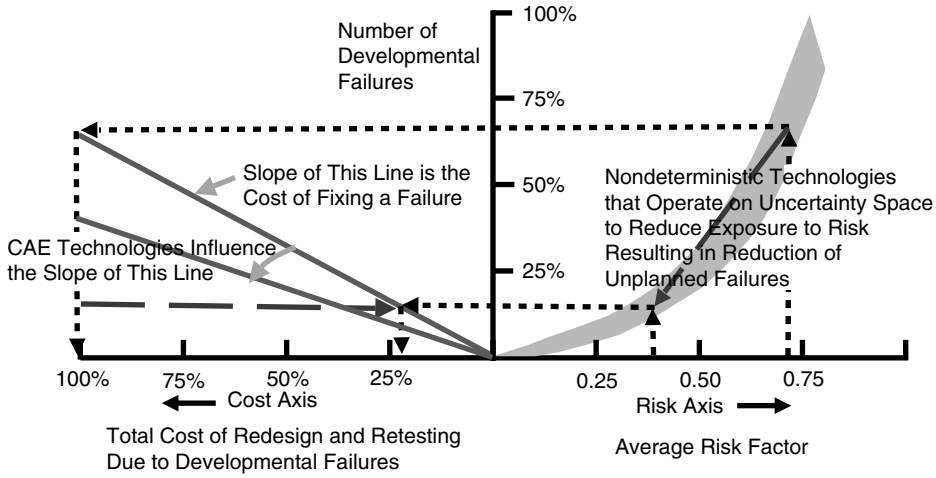

FIGURE 4.3 A scenario that leverages advances in computer aided design and the use of nondeterministic technologies to reduce development risk.

4.3 Strategies for Design Approach for Low-Cost Development

It is clear from the discussion in the previous section that the transient reliability of liquid rocket engines during the development phase has been historically low due to the number of developmental failures. However, it must be emphasized that by the time an engine reaches the certification stage, most of the design errors have been fixed using extensive testing, of course, with the corresponding cost consequence. During the service life, historically the reliability of man rated booster liquid rocket engines has been high enough that there have been no engine-related failures in the manned U.S. Space Program. It is a common occurrence (due to harsh and complex environments) that some of the parts do not meet the life requirements after they have entered into service, thus resulting in expensive inspection and maintenance costs.

So the new tools and approaches on the use of nondeterministic technologies must be tailored to their use in two design phases. During the development stage, the technologies used should provide an approach to reduce the failures using both analysis and testing. They should provide a rigorous quantitative approach for the initial design stages, in which there are significant epistemic and aleatory uncertainties, making the design insensitive, to the extent possible, to these uncertainties. This is referred to as Robust Design. Testing plays an important role during development by contributing to the reduction of epistemic uncertainty. One of the most important challenges that needs to be addressed is in designing a focused test program that maximizes information return with minimal testing. The challenge is a demanding one because the economics of putting a payload in space requires high thrust-to-weight ratios for the engines. This translates into small margins but yet safe operation, and losing an engine even during the development program is not a planned option (e.g., testing until failure occurs).

Once the lack of knowledge has been significantly reduced and the variabilities present in the system due to manufacturing capabilities are estimated and quantified using historical data, the challenge shifts to using a design/analysis approach that further improves the reliability of the engine to very high levels dictated by customer and contractual requirements. This might require redesign of some percentage of parts to meet the high reliability goal. Typically, the very high computed reliability values, as a minimum, will allow for comparative evaluation of competing designs to choose a better design, based on reliability constraints. The goal in this phase is to dramatically reduce service failures.

Copyright 2005 by CRC Press LLC

4.4 Role of Design Space Exploration Approaches (Deterministic and Nondeterministic) in the Product Development Phase

One of the fundamental design approaches to avoiding development failures could be to adopt the philosophy of "anticipate-prevent." This means that engineers must perform numerous "what-if" scenarios to meet the new design philosophy as opposed to "Test-Fail-Fix." The engineers' understanding of the performance of the engine and its components under nominal and off-nominal conditions must be complete. When deterministic technologies are applied to the various "what-if" scenarios, the consequences can be evaluated. Using a nondeterministic approach, for example probability or other uncertainty theories (e.g., Dempster-Shafer theory of evidence), the likelihood of their occurrence can be quantified. In some instances, the uncertainty in the probability statements themselves could be quantified using confidence metrics. The important point is that the effective use of deterministic and nondeterministic technologies can help meet the goals of successful design by understanding the design sensitivities —the word "sensitivity" being used in the most general sense.

The design philosophy is best explained using Figure 4.4 and Figure 4.5. Figure 4.4 describes the design approach in general, and Figure 4.5 goes into the details of the design approach. The design approach does not force the use of all design processes to analyze and design every component. It is common practice that only a subset of available design approaches is used for a large set of components, which inherently have large margins or are not safety critical. However, for safety-critical components with severe failure consequences, the use of all design views to design a robust product is encouraged. This approach has not become universal practice in the industry to the extent one would hope, but the trend in using the design approach has been very encouraging with many instances of success.

The example used in Figure 4.5 is a hypothetical one involving two design variables (X1 and X2) and one response variable. The contours of the response variable are plotted, but in general are not known *a priori*. Each square in the chart represents a particular "view" of the design space using either deterministic or nondeterministic design approaches. It is arranged such that one can proceed from a well-established and widely understood design approach to more recent nondeterministic and robust design approaches. Each circle represents the engineer's knowledge of the behavior of the system under each

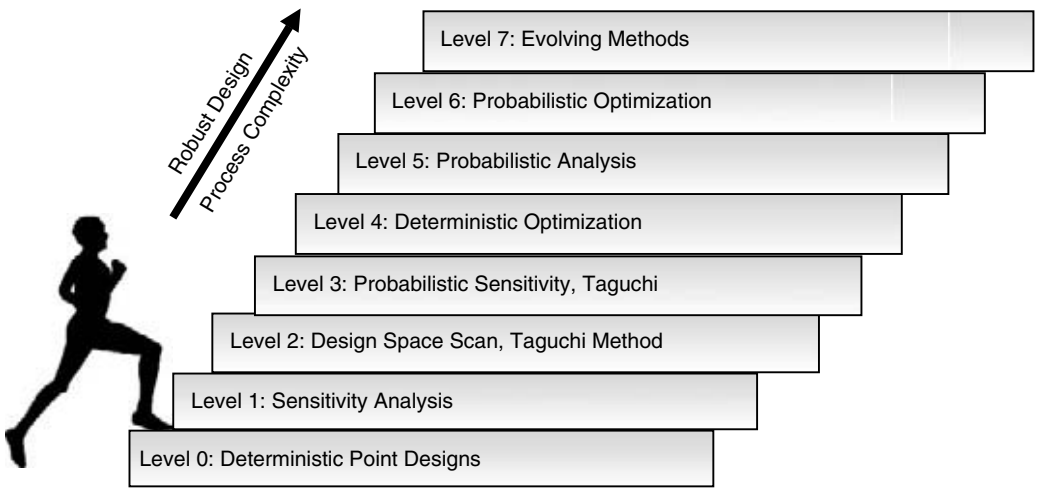

FIGURE 4.4 A design approach use ladder that can systematically improve the understanding of component behavior over the entire design space.

Copyright 2005 by CRC Press LLC

Copyright 2005 by CRC Press LLC

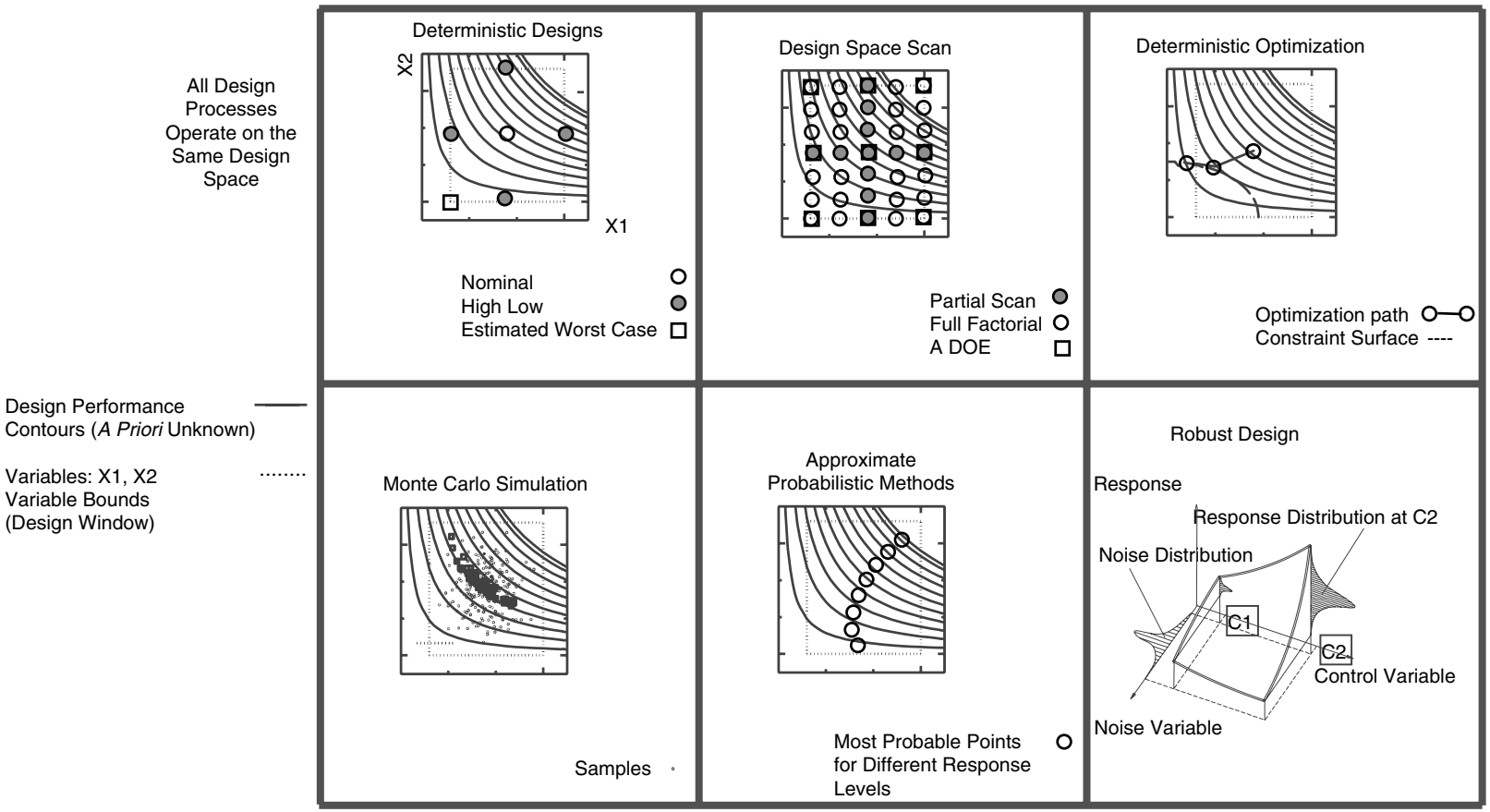

FIGURE 4.5. Multiple views of design space where sampling is performed on the same design space to meet a given "view" objective.

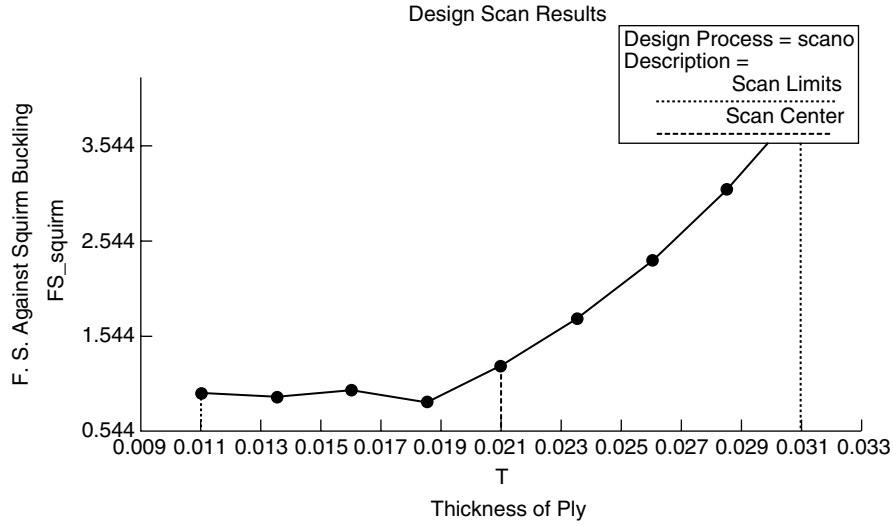

FIGURE 4.6 An example of partial design scan results identifying the nonlinearity in system response.

specific "view." For example, designing a component with conventional, but often heuristically determined worst-case scenario can provide a safe design but it sheds little information on the behavior of the system in nominal or at other "corner" conditions.

The deterministic design space scan is one of the most useful tools in understanding the design space and the potential nonlinearity present in the system. Understanding the extent of the nonlinearity present in the system is very important and in many cases can point to the cause of hardware failures. One can also readily identify nonrobust operating points of the design space from the scan. Frequently, many algorithms in the deterministic optimization or probabilistic analysis fail when significant nonlinearity is present. Even more troubling could be that the algorithms may provide inaccurate answers in the presence of significant nonlinearity and the errors may go unnoticed due to lack of rigorous error bounds with the methods. An example of such a behavior is seen in scan results on metal bellows analysis used in ducting of rocket engines. Figure 4.6 shows the Squirm buckling safety factor as a function of the thickness of each ply for a specific bellow design. Widespread use of such systematic analysis has only been recently made possible due to advances in automation.

While with partial scans one cannot study the interaction effects, one can still obtain valuable information regarding system "sensitivities" and nonlinearity under the umbrella of "Main Effects." When a deterministic scan is performed on noise variables, the results contain the information of tolerance effects or noise effects on performance in the deterministic sense. It is just that a probability measure has not been calculated, which could be done as a second step if sufficient information is available.

Other fractional or full factorial designs can be employed to study the interaction effects, which can be significant. When the dimensionality of the system becomes large, it becomes essential to use more efficient and practical approaches wherein the computational burden can be minimized. The Design of Experiments concept originally developed for physical experiments has been successfully applied to numerical experiments with modifications. The modifications pertain to elimination of the replication present in the original designs, which in the case of numerical experiments adds no new information. The deterministic optimization is widely performed as part of the engineering design process. As practiced by the engineering community, the deterministic optimization process (maximizing performance) does not directly address the question of Robustness (which is the domain of probabilistic optimization), which is defined as performance insensitivity under uncontrollable variations (noise). It has been observed that, in the current economic environment, the customer requirements emphasize equally, if not more, the reliability and robustness over performance.

Copyright 2005 by CRC Press LLC

When low-order statistical moments of responses need to be estimated, Monte Carlo solutions have been used most successfully. The Monte Carlo or other simulation-based methods (such as Latin Hyper Cube) have performed well over a wide class of problems. From several points of view, such as robustness of the algorithm, generality, and simplicity, Monte Carlo simulation is the preferred choice in the industry (including cases that require high reliability numbers) when computational burden is not an issue. When computational expense is prohibitive, approximate probabilistic methods generally referred to as First-Order Reliability Methods (FORMs) have been successfully applied. The word "approximate" is probably controversial as Monte Carlo simulation methods are also approximate. A by-product of FORMs, the most probable point information has the potential for playing an even more important role in defining a focused test matrix, to verify the design. For example, in a focused test scenario, the most probable point information could be used to design tests that can validate the extent of physics model accuracy in the regions of extreme event occurrence by seeding, for example, defects for the purposes of testing.

The Taguchi Analysis-based robust design concepts have been successfully applied in experimentally based design approaches. The use of these concepts in numerical model-based design approaches has been limited. However, the idea of using mathematical optimization techniques to achieve robustness has gained significant attention. Industry and government are making significant research investments in the area of mathematical probabilistic optimization-based technologies and they are discussed later.

4.5 Sensitivity Analysis

The design sensitivity factors have been used extensively to rank the input variables by their importance to performance variables. These factors are finding their way into formal design review meetings. This certainly gives the approving authorities an appreciation of the sensitivity of performance variables to input assumptions and the variable ranking in terms of their importance to satisfying the end requirement. In this context, the sensitivity factors derived from deterministic as well as nondeterministic approaches have been extremely valuable (Figure 4.7). One form of sensitivity factor ranking is based on measuring changes in performance to small perturbations in variables, which is purely deterministic. Because the design space is typically comprised of both input and response variables that span a multidisciplinary domain with a mixture of units, a pure gradient quantity is not of much practical value. Many normalization schemes have been proposed and used but they all have some shortcomings.

Typically, the results are portrayed as a pie or a bar chart with sorted sensitivity factors for each response variable. When this exercise is performed in a multidisciplinary space, they provide sensitivity values across discipline boundaries (e.g., thermal and structures) that have been invaluable. In general, the computed sensitivity factors are a function of the expansion point, which can be varied over the design window to obtain a more realistic assessment of the sensitivity factors over the entire design space. The probabilistic sensitivity factors are measures of the effect of input scatter to output scatter. The measures that have been used are computed such that the probabilistic information is integrated with deterministic sensitivity values (the exact algorithmic detail is a function of definition of the sensitivity measure). Because of the variety of definitions, the sensitivity measures have only been used in a qualitative way to rank the variables. An example of the sensitivity measure obtained for a mildly nonlinear problem with approximately similar coefficients of variation among input design variables is shown in Figure 4.7. When the degree of scatter among the input design variables is markedly different, the differences between deterministic and probabilistic sensitivity measures can be expected to be very high. The use of sensitivity measures in design is a success story as it was used to control variations during an engine development program.

In summary, in the initial stages of design, deterministic as well probabilistic methods that emphasize low-order statistics to screen different concepts are widely used. One practice is to establish safety margins

Copyright 2005 by CRC Press LLC

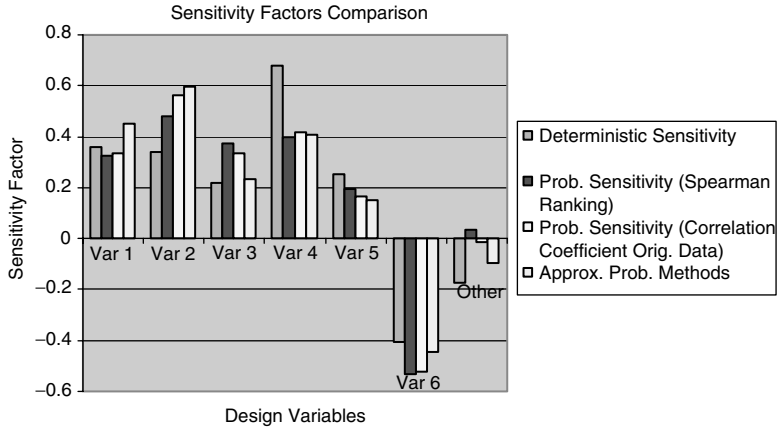

FIGURE 4.7 Comparison of different sensitivity measures for a mildly nonlinear problem with same order of coefficients of variation among input variables.

based on computed standard deviation, with less emphasis on the exact value of the reliability, which is usually designed in to be very high. The computed reliability of the product using probabilistic methods is recomputed, refined, and updated once more reliable data from actual tests is obtained.

4.6 Probabilistic Analysis Approaches

In practice, the use of probabilistic analysis approaches can be categorized based on their use emphasis, either for computing low-order statistics or for computing very high-order reliability quantities. The low-order statistical quantities of choice in the industry are the mean and the standard deviation for the random quantities. This is so because there is a long tradition of defining extreme quantities of design variables as a function of multiples of standard deviation among structural engineers, dynamic loads specialists, material scientists, and thermal analysts.

For the low-order statistics computation, the linear function approximation methods to propagate the "errors" and compute the standard deviation of response quantities have been very successful. However, the industry practice and preference has drifted toward Monte Carlo simulation based approaches to compute the low-order statistics. This is because of the ready availability or ease of writing of Monte Carlo simulation software and the widespread availability of cluster computing. The generality and stability of Monte Carlo simulation methods, the ability to increase the sample size to meet a given error bound, and the availability of high-end cluster computing to obtain quick turnaround are all reasons for its preferred use. It is common practice to perform Monte Carlo simulation on the order of 100 to 5000 sample values (depending on the computational burden in the function evaluation) using the best available knowledge of the input distribution. As an example, this approach has been so successful that detailed uncertainty analysis at the very early stages of engine design are routinely conducted to estimate the uncertainty in engine performance parameters such as thrust, engine mixture ratio, and specific impulse, a measure of engine efficiency (Figure 4.8). When needed for screening purposes, approximate reliability numbers are also computed, either by directly using the simulation results (when enough samples have been run for the required reliability estimate) or by using the computed mean and standard deviation values using the normality assumption for responses.

When more detailed reliability calculations are needed, approximate probabilistic analysis methods have been used. These include the Mean Value First Order (MVFO) method, the First-Order Reliability Method (FORM), the Fast Probability Integration (FPI) method, and many others such as SORM (Second-Order Reliability Method). In the above-mentioned technologies, a form of response function approximation at the region of interest (based on the probability of event occurrence) is fundamental to the algorithmic

Copyright 2005 by CRC Press LLC

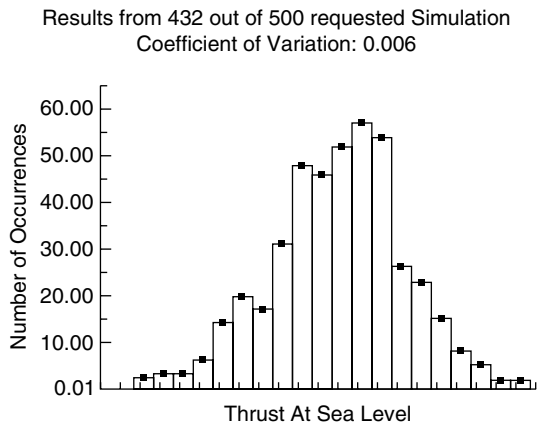

FIGURE 4.8 Example Monte Carlo simulation results from an engine performance model during the conceptual design phase.

approach. On the other hand, explicit computation of a response surface using fractional factorial designs commonly known as Design of Experiments (DOE) has also been widely used. Once the explicit functional form of the approximate response surface is available, it is used in deterministic and probabilistic optimization approaches as well in basic probabilistic analysis using Monte Carlo simulation.

In practice, there are numerous applications in industry where the degree of nonlinearity of the function behavior is moderate. In such cases, the performance of FPI and explicit response surface based applications has been good. An example of the results of probabilistic stress analysis of a turbine blade is shown in Figure 4.9. These methods have been used with success in evaluating the failure risk of products in service with defects or to evaluate the added risk under newly discovered or revised loads after the design is complete.

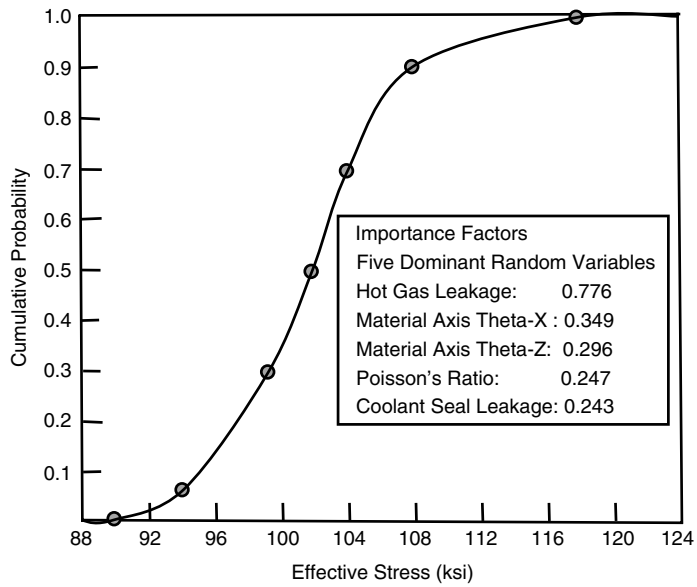

FIGURE 4.9 Example probabilistic stress analysis for a turbo-pump turbine blade using the First-Order Reliability Method.

Copyright 2005 by CRC Press LLC

The use of the above approximate methods for new designs is done on a case-by-case basis where there is prior customer concurrence of the methodology and the input assumptions that will be used in the analysis. The use of the above approximate methods in new designs will become even more widespread if there is a well-established and computationally tractable approach to include the epistemic uncertainty and provide confidence statements or error bounds on the computed reliability values.

4.7 The Need and Role of Multidisciplinary Analysis in Deterministic and Nondeterministic Analysis

All design activities in an industrial setting are multidisciplinary. Traditionally, the design for performance under the purview of each discipline is performed within each discipline, with information and data sharing among disciplines performed manually or in patches of automation. It is increasingly recognized that such an approach results in nonoptimal designs from a systems point of view. Thus, the industry involved in mechanical design in recent years has invested heavily in developing tools, generally component specific, for an effective multidisciplinary analysis. This has cost, schedule, and performance impacts in developing a product in a very positive way.

In the current context, a multidisciplinary analysis is defined as a process wherein consistent data/information is shared across all disciplines for a given realization. That is, as part of the process, a design point set is defined and collected as a specific realization of input design variables and corresponding output response variables spanning multiple disciplines. An example of such an application is illustrated in Figure 4.10, wherein consistent geometry, thermal, structural, and material property data is available for each realization, orchestrated by any design process (see Figure 4.5). The linked sets of models form the basis for deterministic as well as nondeterministic multidisciplinary analysis and optimization. The role of response surface methodology has been effective in system level optimization. In this approach, the response surface models are used in the linked set of models in lieu of computationally intensive models (e.g., computational fluid dynamics) for system optimization.

It is important to recognize the significance of a multidisciplinary linked set of models/codes to an accurate probabilistic analysis. There are uncertainties at all stages of manufacturing and use conditions, as illustrated in Figure 4.11. For an accurate reliability computation, in addition to accounting for those uncertainties, they should be introduced as appropriate numerical models linked to form a multidisciplinary model. This will capture accurately the correlation information through dependency relationships

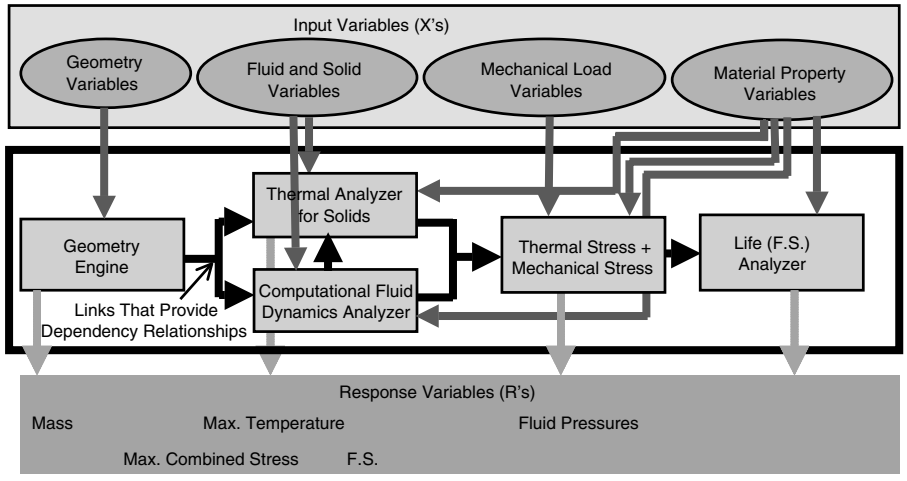

FIGURE 4.10 Example multidisciplinary network of physics-based models connected to form a multidisciplinary design space of input and response variables.

Copyright 2005 by CRC Press LLC

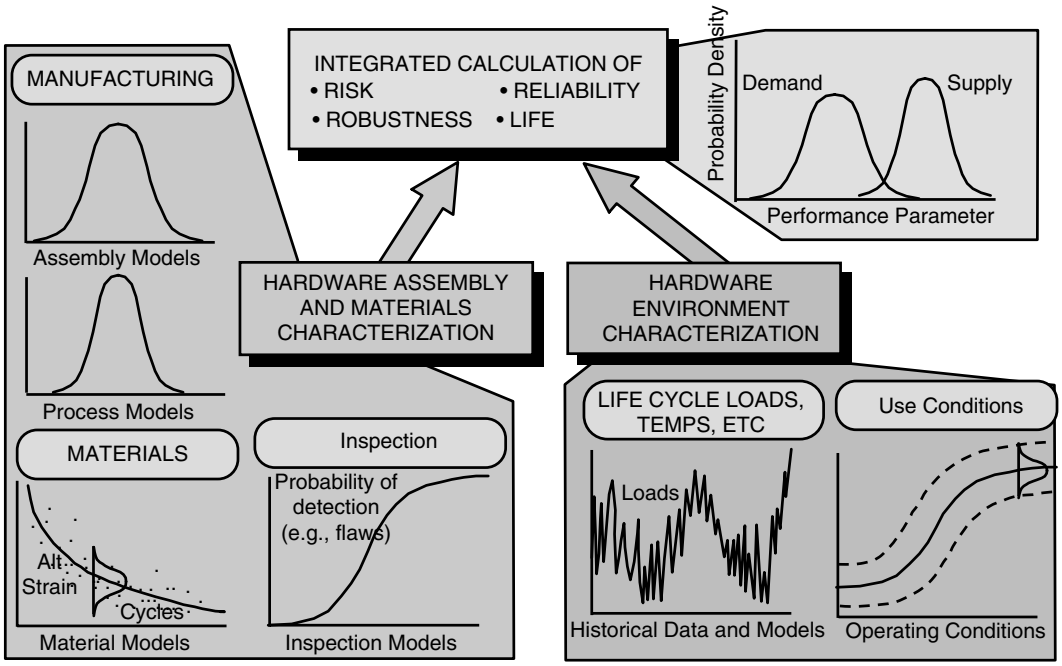

FIGURE 4.11 End structural reliability is affected by uncertainties introduced at all levels of manufacturing and use conditions.

as defined by the multidisciplinary model. The issue of the assumption of independence of random variables in a typical probabilistic analysis is important. Many of the probabilistic tools and codes that are readily available to the industry do not provide effective approaches for treatment of correlated input variables in a probabilistic analysis. In limited instances, tools provide approaches to probabilistic analysis under normality and linear correlation model assumptions. Hence, in the current state of the art, an accurate probabilistic analysis is performed starting with modeling the physical process from a stage that can justify the assumption of using independent input variables. The strategy is then to rely on linked models spanning multiple disciplines to automatically provide the correlation information. When used with Monte Carlo simulation techniques, the use of multidisciplinary models provides the probabilistic information (e.g., variance) for design performance measures across all disciplines for the same computational effort. Further, the approach provides an opportunity to capture accurately the variance information as well as the correlation between intermediate variables.

4.8 Technology Transition and Software Implementation

To use the methodologies described above in an industrial setting, it is essential that commercial-grade software with the current technologies implemented be readily available. Some of the key requirements for efficient software include availability of user-friendly graphic user interfaces for pre- and post-processing of the problem, amenable for nonexpert use, a framework for efficiently linking multidisciplinary models, efficient computational strategies for fast turn around time, implementation of stable algorithms, and a software implementation that allows the user to progress easily from simple to more complex design processes without having to repose the same problem. Satisfying the above requirements is the key to a successful technology transition strategy. A few commercial software programs that satisfy some of these requirements have emerged and others will continue to emerge.

The availability of an integration framework for linking multidisciplinary models has become a reality. Commercial as well as proprietary software programs are now available that can perform over a network

Copyright 2005 by CRC Press LLC

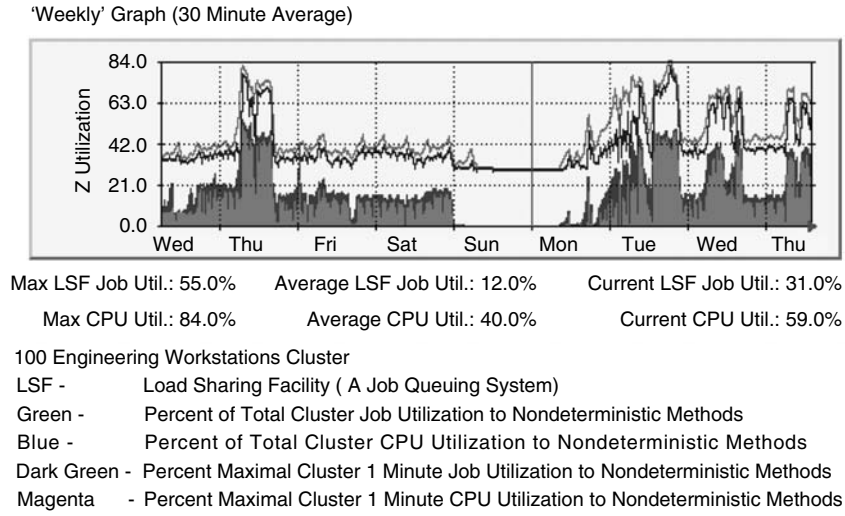

FIGURE 4.12 Typical workload of engineering cluster workstations dominated by analysis performed in support of nondeterministic and deterministic design exploration methods.

of heterogeneous computers with different operating systems, chip architectures, and manufacturers. Systematic use of the design processes mentioned above (such as sensitivity analysis, design scans using factorial designs, Response Surface Methodology, Monte Carlo simulation and its variants, and deterministic and probabilistic optimization) all require an order of magnitude more function evaluations than conventional worst-case analysis based design approaches. Hence, for practical use of the above technologies in industry under ubiquitous schedule constraints, leveraging of the information technology revolution in software and hardware is essential. Many of the algorithms implementing the above design processes can effectively perform parallel computations to reduce the wall clock turnaround time of computer runs. It is not uncommon to utilize hundreds of engineering computer workstations to achieve the required computational speed to solve a design problem. An example of such a use scenario is shown in Figure 4.12. In Figure 4.12, software usage for nondeterministic analysis consumed a significant amount of the available CPU cycles. In general, the use of these newer analysis technologies does not cause any additional cost consequence, as they tend to use otherwise idle machine capacity. Without considering analysis jobs supporting newer approaches to design, in large corporations, the CPU average usage of engineering workstations at user desktops is in single-digit percentage points. The network and software reliability are high enough that in a typical year, hundreds of thousands of analyses can be performed in support of deterministic and nondeterministic analysis approaches.

4.9 Needed Technology Advances

The transition of the powerful array of technology and tools described above to a majority of practicing design engineers in a design shop is a challenging one. It is important to recognize that to have a pervasive impact on the design practice, it is necessary to put the above tools in the hands of integrated product design team engineers who perform most of the product design. It is emphasized that this is the group that must be targeted for technology transition and not the advanced engineering groups comprised of specialists. It is granted that a systematic application of the technologies described above will inevitably result in more reliable and robust products. If successful, it will be a quantum improvement over the current practice. However, there are a number of challenges that still need to be adequately addressed and this section attempts to enumerate them.

Copyright 2005 by CRC Press LLC

At first, a far greater recognition among structural reliability researchers of the role epistemic uncertainty is needed. The structural reliability research should make technology advances that treat both the epistemic and aleatory uncertainty together in the reliability assessment process. The theoretical basis for the developed methodology should provide practicing engineers with a tool that is capable of a more rigorous treatment of lack of knowledge, ignorance, in addition to the treatment of variability.

1. Significant new research in developing new design approaches that optimize/effectively combine analysis model results with focused testing is needed. Frequently, current approaches to testing are reactionary to an observed failure mode. In some instances, the testing is considered an independent verification of design. The suggested new approaches should consider both analysis and testing as part of a unified holistic approach to improve confidence in product performance, which either model or testing alone could not provide.
2. Many sub-elements of the broad research topic described above include a strategy for model calibration across scales (e.g., size effect), design of a test matrix that maximizes information return leveraging or giving adequate credit to analysis model results where appropriate, new forms of confidence measures for combined analysis, and focused test data.
3. Advances in stochastic optimization that will allow engineers to solve optimization problems such as "minimize testing subject to target confidence" or "least uncertainty subject to cost constraint on testing."
4. In addition to the fundamental challenge of understanding the "operational definition" for these methods, all the above will present computational challenges and numerical and "software implementation" issues.

Acknowledgments

Many of the ideas and concepts discussed in this chapter evolved over a period of 20 years while performing technology development research and application efforts. The extensive contributions of my colleagues — Drs. Amitabha DebChaudhury, George Orient, and Glenn Havskjold (in the Structures Technology group at Rocketdyne Division of The Boeing Company) — in developing the methodologies and necessary software is gratefully acknowledged.

Copyright 2005 by CRC Press LLC

5

The Need for Nondeterministic Approaches in Automotive Design: A Business Perspective

John A. Cafeo
General Motors Research and Development Center

Joseph A. Donndelinger
General Motors Research and Development Center

Robert V. Lust
General Motors Research and Development Center

Zissimos P. Mourelatos
Oakland University

5.1 Introduction

This chapter presents the importance of uncertainty characterization and propagation in the execution of the vehicle development process (VDP). While the VDP may be viewed from many perspectives, we consider it to be a series of decisions. In the absence of uncertainty, this series of decisions can, in principle, be posed as a very complex multidimensional optimization problem. Decisions, however, are actions taken in the present to achieve an outcome in the future. Because it is impossible to predict the outcomes of these decisions with certainty, the characterization and management of uncertainty in engineering design are essential to the decision making that is the core activity of the vehicle development process.

Uncertainties are present throughout the vehicle development process—from the specification of requirements in preliminary design to build variation in manufacturing. Vehicle program managers are continually challenged with the task of integrating uncertain information across a large number of functional areas, assessing program risk relative to business goals, and then making program-level decisions. Engineers struggle to develop design alternatives in this uncertain environment and to provide the program managers with credible, timely, and robust estimates of a multitude of design related vehicle performance attributes. Marketplace pressures to continuously shorten the vehicle development process drive the increasing use of mathematical models (as opposed to physical

Copyright 2005 by CRC Press LLC

prototypes) for providing estimates of vehicle performance to support decision-making under uncertainty. For the calculations from the mathematical models to be useful, the decision makers must have confidence in the results. This confidence is formally developed through the model validation process.

In the following sections, we discuss these issues in some depth and illustrate them through a heuristic example. They conclude with a summary and a number of important challenges for embedding nondeterministic approaches in automotive design.

5.2 The Vehicle Development Process

The vehicle development process is the series of actions and choices required to bring a vehicle to market. For domestic (U.S.) vehicle manufacturers, the VDP is structured around a traditional systems engineering approach to product development. The initial phase of the VDP focuses on identifying customer requirements and then translating them into lower-level requirements for various functional activities, including product planning, marketing, styling, manufacturing, finance, and a broad array of engineering disciplines. Work within this phase of the VDP then proceeds in a highly parallel fashion. Engineers design subsystems to satisfy the lower-level requirements; then the subsystems are integrated to analyze the vehicle's conformance to customer requirements and to assess the compatibility of the subsystems. Meanwhile, other functional staffs work to satisfy their own requirements: product planning monitors the progress of the VDP to ensure that the program is proceeding on time and within its budget, marketing ensures that the vehicle design is appropriate to support sales and pricing goals, finance evaluates the vehicle design to ensure that it is consistent with the vehicle's established cost structure, manufacturing assesses the vehicle design to ensure that it is possible to build within the target assembly plant, etc. This is typically the most complex and the most iterative phase of the VDP, as literally thousands of choices and trade-offs are made. Finally, the product development team converges on a compatible set of requirements and a corresponding vehicle design. Engineers then release their parts for production and the vehicle proceeds through a series of preproduction build phases, culminating in the start of production.

Naturally, the VDP is scaled according to vehicle program scope; it is significantly more complex and longer in duration for the design of an all-new family of vehicles than it is for a vehicle freshening with relatively minor changes to feature content and styling cues. At any scale, however, there is an appreciable level of uncertainty at the beginning of the VDP. By the end of the VDP, this level of uncertainty is much lower, and the vehicle is being produced in a manufacturing plant with knowable build variation.

We distinguish between variation and uncertainty as follows. *Variation* is an inherent state of nature. The resulting uncertainty may not be controlled or reduced. Conceptually, variation is easy to incorporate in mathematical models using Monte Carlo simulation. For any number of random variables, the input distributions are sampled and used in the model to calculate an output. The aggregate of the outputs is used to form a statistical description. However, there are challenges in implementation. Monte Carlo simulation requires many evaluations of the mathematical model. If the mathematical models are very complex (e.g., finite element models with hundreds of thousands of elements used for analyzing vehicle structures), it is often prohibitively expensive or impossible to perform a Monte Carlo simulation within the time allotted for the analysis within the VDP.

In contrast to variation, *uncertainty* is a potential deficiency due to a lack of knowledge. In general, this is very difficult to handle. Acquiring and processing additional knowledge, perhaps by conducting experiments or by eliciting information from experts, may reduce uncertainty. The most difficult challenge is that you may not be aware that you do not know some critical piece of information. Thus it is necessary to undertake an iterative process of discovery to reduce uncertainty. It may also be necessary to allocate resources (e.g., people, time, money) to reduce uncertainty, and these allocation decisions are often very difficult given limited resources.

Copyright 2005 by CRC Press LLC

5.3 Vehicle Development Process: A Decision-Analytic View

Uncertainty, then, is our focal point. It is an inherent part of the VDP and we include it here in our decision-analytic view of vehicle development. We begin by discussing the work of Clark and Fujimoto [1] who, alternatively, view the product development process from an information-processing perspective. From this perspective, they identify three key themes:

1. The product development process is a simulation of future production and consumption.
2. Consistency in the details of product development is important.
3. Product integrity is a source of competitive advantage.

"The information-processing perspective focuses on how information is created, communicated, and used and thus highlights critical information linkages within the organization and between the organization and the market [1]."

"Critical information linkages" implies that information must be transferred from people who have it to the decision makers who need it to support critical decisions. Previous studies by Eppinger [2] and Cividanes [3] have focused on information flow within our VDP. Here, we extend this focus beyond the structure of information flow to include the presentation of structured design alternatives to vehicle program decision-makers. That is, rather than focusing on the information linkages, we will focus on the reason for the linkages: making decisions.

At this point it is prudent to discuss the definition of a decision. Although there has been a considerable amount of research into decision-making in engineering design, there is not yet a consensus within the engineering design community as to the definition of a decision. Conceptually, Herrmann and Schmidt [4] view decisions as value-added operations performed on information flowing through a product development team. In contrast, Carey et al. [5] view decisions as strategic considerations that should be addressed by specific functional activities at specific points in the product development process to maximize the market success of the product being developed. While we monitor this work with genuine interest, we subscribe to the explicit and succinct definition from Matheson and Howard [6]:

> "A decision is an irrevocable allocation of resources, in the sense that it would take additional resources, perhaps prohibitive in amount, to change the allocation."

Commonly, we understand that a decision is a selection of one from among a set of alternatives after some consideration. This is illustrated well by Hazelrigg [7] in his discussion of the dialogue between Alice and the Cheshire cat in *Alice in Wonderland*. He notes that in every decision, there are alternatives. Corresponding to these alternatives are possible outcomes. The decision maker weighs the possible outcomes and selects the alternative with the outcomes that he or she most prefers. Although apparently simple, this discussion contains several subtle but powerful distinctions. One of these is that the decision is made according to the preferences of the decision maker—not those of the decision maker's stakeholders, or customers, or team members, or for that matter anyone's preferences but the decision maker's. Another is that the decision maker's preferences are applied not to the alternatives, but to the outcomes.

It is clear that decisions are actions taken in the present to achieve a desired outcome in the future. However, the future state cannot be known or predicted with absolute certainty. This is the reason that incorporating nondeterministic methods into decision-making processes (in our case, into decision making in our VDP) is crucial. Because we cannot know future outcomes with certainty, the outcomes resulting from selection of our alternatives must be expressed in terms of possible future states with some corresponding statement of the likelihood of occurrence. This, then, is the core activity of engineers in our VDP. Design engineers formulate sets of subsystem design alternatives. Development engineers assess the performance of these design alternatives in vehicles, considering uncertainty due to manufacturing build variation, mathematical model fidelity, and variations in customer usage.

Copyright 2005 by CRC Press LLC

5.4 The Decision Analysis Cycle

Decision makers are, by definition, people who have the authority to allocate an organization's resources. In a vehicle development program, these people are typically executives or senior managers. They make decisions (knowingly or not) using the Decision Analysis Cycle (Figure 5.1) described briefly below, and described completely in [6].

The discussion of the phases in the Decision Analysis Cycle contains several precisely defined terms from the language of formal decision analysis [6]. The term "value" is used to describe a measure of the desirability of each outcome. For a business, the value is typically expressed in terms of profit. The term "preferences" refers to the decision-maker's attitude toward postponement or uncertainty in the outcomes of his decision. The three phases of the Decision Analysis Cycle that precede the decision are:

1. *Deterministic Phase.* The variables affecting the decision are defined and related, values are assigned, and the importance of the variables is measured without consideration of uncertainty.
2. *Probabilistic Phase.* Probabilities are assigned for the important variables. Associated probabilities are derived for the values. This phase also introduces the assignment of risk preference, which provides the solution in the face of uncertainty.
3. *Informational Phase.* The results of the previous two phases are reviewed to determine the economic value of eliminating uncertainty in each of the important variables of the problem. A comparison of the value of information with its cost determines whether additional information should be collected.

Decisions are made throughout the VDP using the Decision Analysis Cycle. At the outset of the VDP, the decision makers' prior information consists of all their knowledge and experience. This prior information is then supplemented by the information collected and the outcomes of decisions made throughout the course of the VDP. In the Deterministic Phase, engineers provide decision makers with design alternatives and corresponding performance assessments. Other functional staffs, such as finance, marketing, and manufacturing, also provide their assessments of outcomes corresponding to the engineers' design alternatives, such as potential changes in cost and revenue and required changes to manufacturing facilities. In the Probabilistic Phase, the engineers as well as the other functional staffs augment their assessments to comprehend uncertainties; the application of nondeterministic methods is absolutely essential in this phase.

The Informational and Decision Phases are the domain of the decision makers—the senior managers and executives. These decision makers determine whether to gather additional information or to act based on the value of the information and their risk tolerance. If there are profitable further sources of information, then the decision should be made to gather the information rather than to take action. This

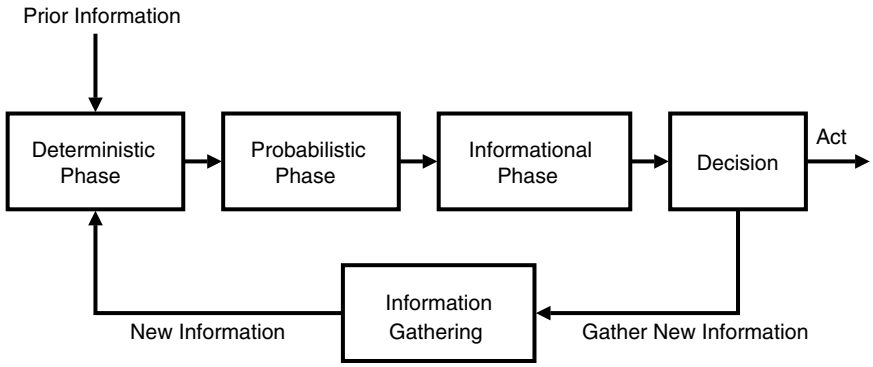

FIGURE 5.1 The Decision Analysis Cycle [6].

Copyright 2005 by CRC Press LLC

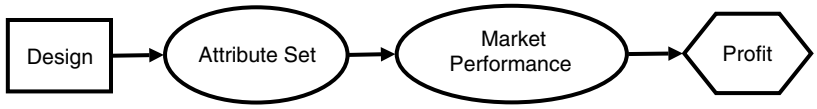

FIGURE 5.2 Abbreviated decision diagram for a design alternative.

cycle can be executed until the value of new analyses and information is less than its cost; then the decision to act will be made.

Another issue that is relevant to incorporating nondeterministic methods into the vehicle development process is the distinction between a good decision and a good outcome.

> "A good decision is based on the information, values and preferences of a decision-maker. A good outcome is one that is favorably regarded by a decision-maker. It is possible to have good decisions produce either good or bad outcomes. Most persons follow logical decision procedures because they believe that these procedures, speaking loosely, produce the best chance of obtaining good outcomes [6]."

This is critical to the idea of a true learning organization. Recriminations because something did not work become pointless. The questions that should be asked include "Was all of the available information used?" or "Was our logic faulty in the decision(s) that we made?" or "Were the preferences of the decision maker properly taken into account in our process?"

We now present a more specific view of decision making in the VDP (Figure 5.2). The rectangular block in this diagram represents the decisions to be made. In the VDP, these are the design alternatives for both the vehicle and its manufacturing system. The ovals in this diagram represent uncertain quantities. In the VDP, we represent the vehicle's Attribute Set and its Market Performance as uncertainties. Finally, the hexagon in this diagram represents the decision maker's value. As would generally be true in business, the value in the VDP is a measure of profit. The arrows in the diagram represent our beliefs about the relationships between our decisions, the relevant uncertainties, and our value. Thus, the interpretation of this diagram is that Profit depends on the vehicle's market performance, which depends on its Attribute Set, which in turn depends on the selection of design alternatives.

The decision diagram shown in Figure 5.2 is applied to the Decision Analysis Cycle shown in Figure 5.1. In the Deterministic Phase, we identify the specific set of design alternatives to be considered and the corresponding set of analytical and experimental methods and tools we will use to relate the design alternatives to their effects on the vehicle's attributes, the vehicle's market performance, and ultimately to the profit generated by selling the vehicle. In the Probabilistic Phase, we characterize the uncertainties in our estimates of the vehicle's attributes and its market performance and use them to examine their effects on profit. In the Information Phase, we examine whether or not it is prudent to allocate additional resources to gather more information (usually through further studies with our analytical tools) to increase our likelihood of realizing greater profit. Finally, in the Decision Phase, the decision maker commits to a course of action developed using the Decision Analysis Cycle.

5.4.1 Illustration: Door Seal Selection

Now let us now begin to illustrate the role of nondeterministic methods in decision making during the vehicle development process. While there are many different types of decisions made during a vehicle development program, here we will begin to discuss decision making in the context of a single vehicle subsystem: a door sealing system. In the following, we introduce the problem. We then continue to discuss this example as we proceed through this chapter.

Copyright 2005 by CRC Press LLC

5.4.1.1 The Door Sealing System

The door seal is typically an elastomer ring that fills the space between the door and the vehicle body. Figure 5.3 illustrates a typical door body and seal cross-section within a cavity. The function of the door seal is to prevent the flow of air, water, and environmental debris into the interior of the vehicle. The door seal is usually larger than the space it must seal. The seal compresses as the door is closed, filling the space and providing some restoring force in the seal to accommodate fluctuations in the size of the door-to-body structure gap due to motion of the door relative to the body. This motion can occur as the result of road loads applied or transmitted to the body and door structures.

Functionally, the door seal must satisfy several customer needs. The first and most obvious is that customers expect the passenger compartment to be sealed against water leaks. Second, customers are annoyed by air leaks and their accompanying wind noise, especially at highway speeds. And third, air leaks can carry dust into the vehicle, causing problems for people with allergies. If this were our only concern, we could fill the space with a very large seal. However, there is a competing objective. The larger the seal, the more force it takes to compress it. We also know that customers like to be able to close the doors with minimum effort. So from this standpoint, we would like the seal to have very little compression when the door is being shut. Thus, the door seal designer must strike a delicate balance when designing the seal and its resultant compression force. If the force is too low, the vehicle will be viewed as poorly designed because of the resulting air and water leaks; if it is too high, the vehicle will be viewed as poorly designed because of the high door-closing effort.

In luxury cars, it is typical to have a door seal system that contains three seals. The primary seal is a continuous bulbous seal, located deep within the door-to-body gap, which completely surrounds the door opening. It can be mounted on either the body or door side of the cavity. The other two seals are usually combined and are located across the top of the door and down the windshield pillar. The upper part of this combined seal is a barrier across the gap between the door and the body while the lower part fills the gap directly below. This provides three barriers to isolate the interior from the exterior environment. In economy cars, it is typical to just use a primary seal which provides one barrier.

The seal cross-section shape and size are dependent on the specific door and body geometry in the cavity when the door is closed. This cross-section is designed to deflect and compress during the door-closing event to seal the cavity while maintaining a good door-closing effort. The material for the seal is

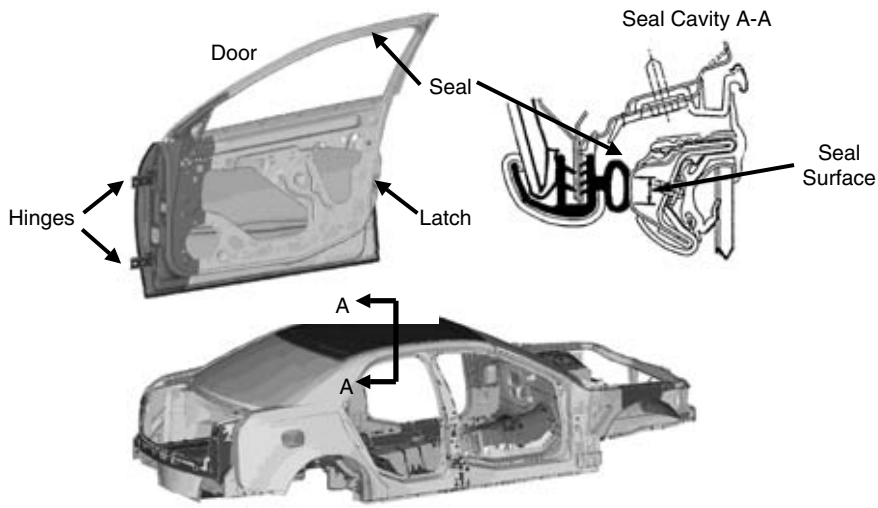

FIGURE 5.3 Finite element representation of a typical door, body, and cavity cross-section showing sealing system.

Copyright 2005 by CRC Press LLC

chosen for both its mechanical and durability properties. Other important design parameters are the location of the hinges and the latching mechanism.

5.4.2 Deterministic Phase

The Deterministic Phase mainly focuses on quantifying the complex relationship between our design decisions (engineering design variables) and our value (profit). We previously presented a simplified view of this relationship in Figure 5.2. However, in reality, it is much more complex. Figure 5.4 provides an expanded and more complete view of decision making in the VDP.

Fundamentally, there are two approaches to managing the complexity of product development decision making. One approach is to decompose the product development system into smaller units; perhaps using product design parameters, product architecture, organizational structure, or tasks in the product development process (as discussed by Browning [8]) as the basis for the decomposition. The enterprise *value* is then decomposed into a set of specific objectives for each of the units so that they can work in parallel to achieve a common enterprise-level goal. This decomposition simplifies decision making in some respects; however, it often leads to sub-optimal results for the enterprise due to insufficient coordination of actions between the units. There is no guarantee that the objectives given to each unit will lead to the greatest benefit for the enterprise. Therefore, if the product development system is to be decomposed, mechanisms must be put in place for rebalancing the objectives allocated to each of the units. Kim et al. [9] have made progress toward developing these rebalancing methods, but this remains a very challenging problem.

The alternative approach is to retain the interconnectivity within the product development system with a fully integrated cross-functional design environment. The benefit of this approach is that decisions are consistently made in the best interest of the enterprise. Its drawback is that it requires a set of engineering design tools that are compatible with one another both in terms of their level of detail and their flow of information. While it can be challenging to conduct these analyses even by assembling a

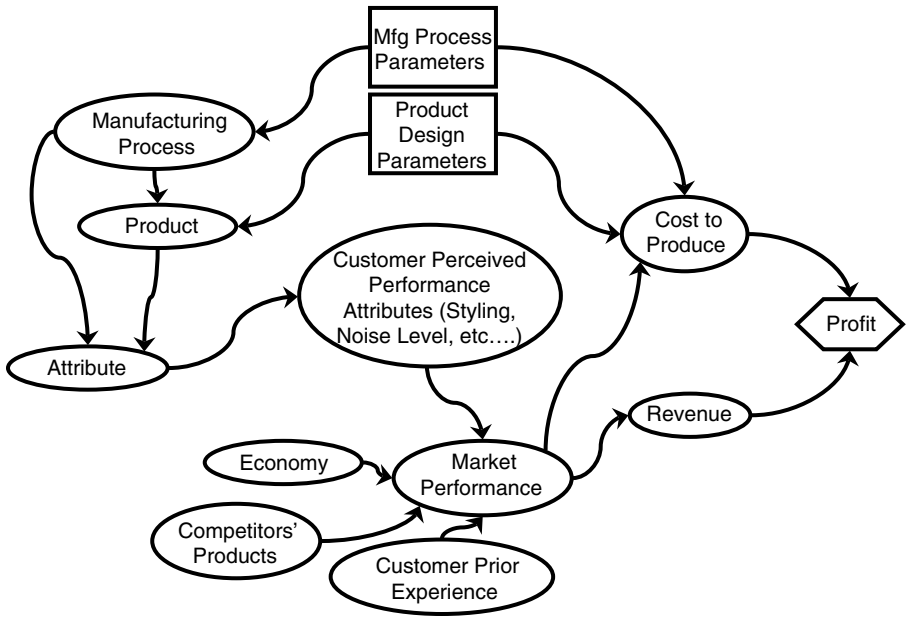

FIGURE 5.4 Detailed decision diagram for a design alternative.

Copyright 2005 by CRC Press LLC

team of cross-functional experts to provide their judgments, recent research suggests that it is now possible to conduct these analyses in a model-based environment using a combination of well-established and emerging technologies.

A number of commercial tools are available for representing the product and the manufacturing process. Mature tools are also available for correlating engineering evaluations of vehicle attributes to customer perceptions, for modeling the effects of the economic climate and of customers' prior experiences on purchase behavior. These tools are usually developed internally by the vehicle manufacturers and are considered proprietary.

More recently, a number of methods have been developed for linking the engineering and business domains by estimating the impacts of engineering designs on cost and revenue. The procedures published by Dello Russo et al. [10] are broadly applicable for cost estimating of new designs and the Technical Cost Modeling process developed by Kirchain [11] is particularly well suited to assessing the cost impacts of implementing new materials and manufacturing processes. Market demand can be estimated using either Discrete Choice Analysis, as discussed by Wassenaar et al. [12] or the S-Model, as demonstrated by Donndelinger and Cook [13]. Competitors' reactions to marketplace changes can, in principle, be simulated using game theoretic methods such as those implemented by Michalek et al. [14] Once market demand and cost are known, revenue and profit can be estimated using conventional financial practices.

Multidisciplinary design frameworks such as those developed by Wassenaar and Chen [15] and Fenyes et al. [16] can be applied to conduct a series of mathematical analyses relating engineering designs to enterprise values with a compatible level of details and information flow. These frameworks are therefore suitable for analysis of design alternatives in the Deterministic Phase of decision making. This type of analysis is necessary but definitely not sufficient for design decision making; the Probabilistic and Information phases of the Decision Analysis Cycle must also be completed before the committed decision maker can reach a decision. We continue with a discussion of the work in subsequent phases of the Decision Analysis Cycle in the next section. But first, let us return to the door seal selection example.

5.4.2.1 Door Seal Selection Continued: Deterministic Phase

In the Deterministic Phase of the Decision Analysis Cycle, we identify the decisions to be made, the value we seek to achieve, and the intermediate quantities that relate our decisions to our value. The decisions that we will study are "Which sealing system and its associated parameters should we choose for a particular new vehicle that we are developing?" and "Are any modifications to our manufacturing facilities required to improve our door attachment process capability?" To begin framing these decisions, we will stipulate that the business plan for the vehicle program has been approved, meaning among other things that the vehicle's architecture and body style have already been chosen and that an assembly plant has already been allocated for production of the vehicle. The strategic decisions under consideration for the door seal at this stage relate to the conceptual design of the door seal system and include the number of seals, the seal's cross-sectional shape, and its material properties. The decisions related to improvement of the door attachment process (hinges and latching system) are also strategic decisions at this stage and will be considered concurrently with the conceptual design of the door seal. The decisions related to detail design of the door seal system are tactical decisions at this stage; however, we may need to consider some of the seal size parameters to be tentative decisions if they are relevant to the selection of the door seal design concept.

The Decision Analysis Cycle begins with the generation of a set of design alternatives to present to the decision maker. There are many methods and theories about the best ways to create sets of alternatives; however, we do not discuss them here. For this discussion, suffice it to say that the set of alternatives will be created by considering a number of door seal designs carried over from similar vehicles and perhaps some innovative new sealing technologies developed by our suppliers or through our internal research and development activities. Then, a manageable list of specific design alternatives can be engineered and analyzed (a coupled and iterative process).

Copyright 2005 by CRC Press LLC

The analyses conducted to relate the design alternatives to their corresponding values follow the VDP decision diagram in Figure 5.4. Decisions about the door seal design concept and the door attachment process capability influence our value of profit through effects on both cost and revenue. The effect on cost can be determined "simply" by conducting a cost estimate. The effect on revenue, however, requires a much more intricate series of analyses.

The first of these analyses covers the synthesis of the vehicle design concept. These analyses are inherently complex because every design engineer on the program is conducting them in parallel. Thus, while one design engineer is developing alternative door seal concepts, another is developing alternative concepts for the inner and outer door panels, and yet another is developing alternative concepts for the door ring on the outside of the body structure. Vehicle concept engineers are faced with the challenging job of integrating each engineer's design alternatives into vehicle-level representations that can then be used to analyze the performance of the various subsystem design concepts at the vehicle level.

Once the vehicle-level design representations are created, all of the relevant vehicle performance attributes can be assessed for each of the design alternatives. For the door seals, these would include assessments of wind noise, water penetration, pollen count, and door-closing effort. Engineers are faced with difficult choices over the construction and use of mathematical models while performing these assessments. In this example, finite element analysis techniques could be applied to model the air and water penetration using seal pressure as a surrogate for air and water leakage. Meanwhile, an energy analysis could be performed to model the door-closing effort. We could construct a variety of models at various levels of complexity, allocating a little or a lot of time and engineering resources in the process. The prudent choice is to construct the model that provides the appropriate level of information and accuracy to the decision maker to support the decision. It may be fruitful to err on the side of simplicity and let the decision maker inform and guide improvement to our modeling in the Information Phase of the Decision Analysis Cycle.

The engineering assessments of the vehicle attributes must be translated into customer terms before they can be used to estimate the market demand for the vehicle. From a technical perspective, the most interesting translation in this example would be for wind noise. The results of the engineering analyses for wind noise are sound pressure levels. These results would then be translated into terms more meaningful to a customer, such as into an Articulation Index (as discussed in Reference [17]) or some company-proprietary metric to reflect the perceived quietness of the vehicle's interior. Most of the results in this example, however, would be mapped into vehicle-level quality measures. Water leaks, high door-closing efforts, and any misalignment of the door relative to the rest of the vehicle will all lead to some warranty claims and will also negatively affect the customer's overall perception of the vehicle's quality. These measures of customer-perceived quality can then be used as inputs to a market demand model that can be used to explore the marketability of each of the design alternatives in terms of changes in the vehicle's market share and in customers' willingness to pay for the vehicles.

At this point, only a few more steps remain. The effects of the economic climate and of customers' prior experiences on the market demand for the vehicle must be considered; however, most decision makers would not consider these to be conditioned upon the performance of the door seal. The discussion of competitive action is more interesting: the changes in the vehicle's market share and in customers' willingness to pay for the vehicle based on the performance of the door seal could be influenced by competitors' actions. If our competitors make significant improvements to the interior quietness or the door-closing efforts in their vehicles, it will likely shift the customers' level of expected performance, meaning that the competitive advantage we would realize by improving our vehicle's interior quietness or door-closing efforts would be decreased. Once these assessments are made, the resulting effects on the vehicle's revenue can be computed. Our value of profit can then be determined as a function of revenue and cost.

Copyright 2005 by CRC Press LLC

5.4.3 Probabilistic Phase

In the Probabilistic Phase, we estimate, encode, and propagate the uncertainties that have been identified as relevant to the design alternative decisions [6]. In the formal decision process discussed in [6], all the uncertainties that have been identified are characterized by the decision maker's subjective probability estimates. This Bayesian approach is consistent with the main objective of the probabilistic phase: to incorporate the element of risk preference into the values corresponding to the design alternatives. Risk is inherent in the decision-making process because of uncertainty, especially the epistemic uncertainty associated with the outcome of future events.

A growing body of formal methodologies is available to aid the decision makers in identifying key uncertainties and in mitigating the risks associated with them. The Design-for-Six-Sigma (DFSS) methodology [18] is frequently applied to this end. DFSS can be applied to identify, prioritize, and monitor both the product attributes critical to satisfying the customers' expectations as well as the uncertainties that pose the greatest challenges in consistently delivering them. Robust Design [19] principles can then be applied to develop subsystem and component designs that are less sensitive to these uncertainties, thereby increasing the likelihood that the designs will satisfy customers' expectations.

The results generated using these methodologies (or, for that matter, the results generated using any mathematical model, whether deterministic or nondeterministic) can be used to augment the decision maker's state of information. However, they are not a direct substitute for the belief-based probability assessments that must be used as the basis for the decision. A decision maker's beliefs about these uncertainties are ultimately based on his general state of information. The extent to which the results of an analytical model are substitutable for a decision maker's beliefs is determined through a process of model validation that is discussed in the next section.

5.4.3.1 Uncertainty Characterization Methods

The previous paragraphs discussed the importance of characterizing and quantifying the uncertainties associated with vehicle attributes. Although probability theory is perhaps the first method that comes to mind when formally characterizing uncertainties, other theories have been proposed and are used in various disciplines. We will overview these here and discuss their relationships. At this point, however, it is still unclear precisely how they fit into the decision analysis framework that we have been discussing. We will discuss this briefly at the end of this section.

Generally, uncertainties can be classified into two general types: (1) aleatory (stochastic or random) and (2) epistemic (subjective) [20–24]. *Aleatory uncertainty* is related to inherent variability. It is irreducible because collecting more information or data cannot decrease it. *Epistemic uncertainty* describes subjectivity, ignorance or lack of information in any phase of the modeling process. It is reducible because it can be decreased with an increased state of knowledge or the collection of more data.

Formal theories for handling uncertainty include evidence theory (or Dempster–Shafer theory) [20,21], possibility theory [25], and probability theory [26]. Evidence theory bounds the true probability of failure with belief and plausibility measures. These measures are mutually dual in the sense that one of them can be uniquely determined from the other. When the plausibility and belief measures are equal, the general evidence theory reduces to the classical probability theory.

Classical probability theory models aleatory uncertainty very efficiently and it is extensively used in engineering when sufficient data is available to construct probability distributions. However, when data is scarce or there is a lack of information, probability theory is not as useful because the needed probability distributions cannot be accurately constructed. For example, during the early stages of product development, the probabilistic quantification of the product's reliability or compliance to performance targets is very difficult due to insufficient statistical data for modeling the uncertainties.

When there is no conflicting evidence or information, we obtain a special subclass of dual plausibility and belief measures called possibility and necessity measures, respectively. As a subclass of the general theory of evidence, the possibility theory can be used to characterize epistemic uncertainty when incomplete data is available. The true probability can be bounded using the possibility theory, based on the

Copyright 2005 by CRC Press LLC

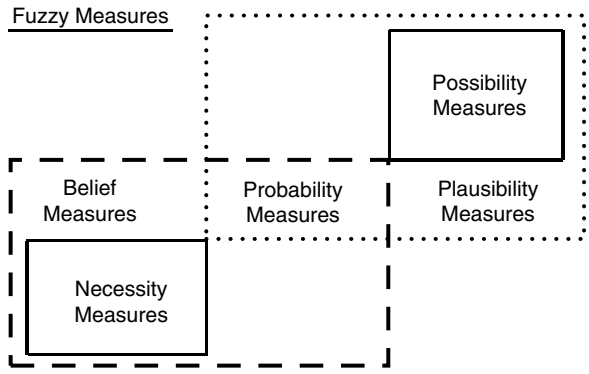

FIGURE 5.5 Fuzzy measures to characterize uncertainty.

fuzzy set approach at various confidence intervals (a-cuts). The advantage of this is that as the design progresses and the confidence level on the input parameter bounds increases, the design need not be reevaluated to obtain the new bounds of the response.

A fuzzy set is an imprecisely defined set that does not have a crisp boundary. It provides, instead, a gradual transition from "belonging" to "not belonging" to the set. The process of quantifying a fuzzy variable is known as *fuzzification*. If any of the input variables is imprecise, it is considered fuzzy and must therefore be fuzzified in order for the uncertainty to be propagated using fuzzy calculus. Fuzzification is done by constructing a possibility distribution, or membership function, for each imprecise (fuzzy) variable. Details can be found in References [27] and [28]. After the fuzzification of the imprecise input variables, the epistemic uncertainty must be propagated through the transfer function in order to calculate the fuzzy response. For that, explicit and implicit formulations are available in the literature [29,31].

In summary, the classical probability theory is a subset of the possibility theory, which in turn is a subset of the evidence theory (Figure 5.5). There is no overlap between the probability and possibility measures, although both are special classes of the plausibility measures. Probability theory is an ideal tool for formalizing uncertainty when sufficient information is available; or equivalently, evidence is based on a sufficiently large body of independent random experiments. When there is insufficient information, possibility theory can be used if there is no conflicting evidence. If there is conflicting evidence, then evidence theory should be used instead. It should be noted that, in practice, it is very common to have conflicting evidence even among "experts." Finally, when evidence theory is used, the belief and plausibility measures can be interpreted as lower and upper probability estimates, respectively.

Now let us return to the issue raised previously. How do these methodologies fit into the formal decision analytic view of vehicle development? Perhaps the most straightforward way is that they can be applied to the models we use within the general guiding framework of the Design-for-Six-Sigma methodology. The results—whether an interval estimate, a probability distribution, or a belief value—are used to inform the decision maker's general state of information. Then, as before, the decision maker assigns subjective probability estimates to the uncertainties and proceeds as outlined in Reference [6].

Alternatively, it might be possible to use the most relevant theory (evidence, possibility, probability) independently for each uncertainty and then combine them in a way where probability is not the overarching framework. We have not explored this in detail and put it forward as a research opportunity.

5.4.3.2 Door Seal Selection Continued: Probabilistic Phase

We stress the importance of the Probabilistic Phase because it extends beyond the identification of a deterministic optimum. We believe that the commonly faced problem of decision makers hesitating to accept the conclusions of deterministic optimization studies is because these studies disregard the uncertainty that is inherent and fundamental to the decision-making process. Robust engineering is gaining

Copyright 2005 by CRC Press LLC

popularity because it offers the promise of mitigating risk through management of uncertainty. The decision analytic approach provides further benefits: it includes provisions for the decision maker's estimates of uncertainty based on his general state of information (vs. the estimates generated by models that are limited by the scope of the models and the assumptions made in constructing them) and it incorporates the decision maker's attitude toward risk. We believe that implementing the decision-analytic approach is a means of bridging this gap between presenting the conclusions of engineering analyses to decision makers and enabling them to commit to a course of action and then to execute it.

The decision maker will consider all the uncertainties shown in Figure 5.4. One key consideration in "product uncertainties" is the probabilities assigned to the selection of the various design alternatives of the chosen interfacing systems. For example, the window opening subsystem can have an effect on both the door's stiffness and its mass, which will in turn affect the door-closing effort and the wind noise. However, the product design parameters still need to be chosen to create various alternatives. In this example, the design parameters are the seal material, thickness, and cross-section geometry. These parameters affect the engineering performance attributes of seal deflection and restoring force for a given load. Other design parameters include the geometry of the cavity between the door and body as well as the type and location of both the upper and lower hinges and the latch mechanism location.

Next, we consider "manufacturing uncertainty." For this example, there are two types of hinges available; one is a bolt-on system and one is a weld-on system. The weld-on system requires less labor in the manufacturing process but can lead to a higher variation in door location. This not only affects the size of the interior cavity between the door and the body (and hence closing efforts and wind noise), but also makes visible the gap that can be viewed between the door and the body from the exterior of the vehicle. The visual consistency, size, and flushness of this gap are known to be very important to the customers' perception of vehicle quality. The manufacturing facility and its processes are thus dependent on the various design alternatives. This description shows the close linkages illustrated in Figure 5.4 between the Manufacturing System, the Product, and the Attribute uncertainties.

During engineering design, the wind noise and door-closing attributes are calculated for the various alternatives. Typically, manufacturing variations are considered in these models. They produce a range or distribution for the wind noise and the door-closing efforts. A further consideration is the math model itself. Any model is an approximation to reality and, as such, there is some uncertainty in the actual number calculated. Therefore, an estimate of the model uncertainty must be included as part of the results. This helps the decision maker understand how well the results can be trusted, which in turn has a critical effect on the subjective probabilities that will be assigned to each alternative. Because this is a critical issue, we discuss it in more detail under the name of model validation in Section 5.4.4.

Each of the other uncertainties detailed in Figure 5.4 is important, deserving a lengthy discussion that we will not include here. Some of the key issues are:

- *Translation uncertainties:* noise in the statistical models used to translate attributes from engineering terms to customer terms; also epistemic uncertainty due to imperfect knowledge of how customers perceive vehicles.
- *Economic uncertainties:* those most relevant to the auto industry include unemployment levels to the extent that they drive the total industry volume, interest rates because they affect affordability through financing and availability of capital for R&D, exchange rates because they affect the relative price position of foreign and domestic vehicles, and oil prices because they can affect customers' choices of vehicle types.
- *Competitive uncertainties:* risks due to the unknown extent to which our competitors will improve their products through performance enhancements, attractive new styling, and addition of new technology and feature content.
- *Cost uncertainties:* changes to the purchase price of parts due to design changes over the product's life cycle, amounts of supplier givebacks due to productivity improvements, fluctuations in raw material prices and exchange rates, and the emergence or decline of suppliers.

Copyright 2005 by CRC Press LLC

5.4.4 Information Phase

In the Information Phase, we use the results of the previous two phases to determine the economic value of eliminating uncertainty in each of the important variables of the problem. A comparison of the value of information with its cost determines whether additional information should be collected. If the decision maker is not satisfied with the general state of information, then he will use the diagram shown in Figure 5.4 (and its subsequent analysis) to determine which uncertainty he needs to reduce. Once the dominant uncertainty is determined, it will be clear what needs to be done to improve the information state. If, for example (referring to Figure 5.4), the "Customer Perceived Performance" attribute is the dominant uncertainty, then a marketing research study of potential customers will be conducted.

Often, a major uncertainty is the estimation of the vehicle attributes corresponding to a specific set of design parameters. These attributes are usually calculated using some mathematical model. This model can take many different forms: a statistical (empirical) model based on measured attributes of previous vehicles, a crude physics- (or first principles-) based model of the attribute, or a detailed physics model. Regardless of the exact type of model, the way to reduce uncertainty is to gain more confidence in the results. This is the issue addressed by the model validation process.

5.4.4.1 Validation of Mathematical Models to Inform the Decision Maker

The purpose of the model validation process is to establish confidence that the mathematical model can predict the reality of interest (the attribute). This helps the builders of the models during the model development phase. It enables them to change parameters or modify assumptions to improve the model's predictive power. It also informs the person using the results from the model and helps them estimate their subjective uncertainty during the decision-making process. Because engineering models that calculate the performance attributes of the vehicle are fundamental to the vehicle design process, we will focus on them and on the attribute uncertainty illustrated in Figure 5.4.

During the product development process, the person responsible for a decision will ask and answer the following two basic questions when presented with model results: (1) "Can I trust this result?" and (2) "Even if I can trust it, is it useful (i.e., does it help me make my decision)?" Most times, there is no formal objective measure of trust. Instead, the trust in the model results is equivalent to trust in the modeler, a subjective measure based on previous experiences. The chief engineer will ask the modeler to assess and report his confidence in the results. But this is difficult without a formal model validation process. What the engineer really needs is an objective measure of confidence to present to the decision maker. This can only be obtained as the product of the model validation process.

Previously we described and advocated a formal decision-making process based on the subjective probabilities of the decision maker. Here we advocate the use of a formal model validation process as a logical, complementary, and necessary way to determine the confidence we have in our models. This inherently statistical process determines the degree to which a model is an accurate representation of the real world from the perspective of the intended uses of the model. It is statistical because this (statistics) is the science developed to deal with the idea of uncertainties.

In practice, the processes of mathematical model development and validation most often occur in concert; aspects of validation interact with and feed back to the model development process (e.g., a shortcoming in the model uncovered during the validation process may require change in the mathematical implementation). It is instructive, therefore, to look at some of the current practices to begin to understand the role that nondeterministic analysis should play in this process. We do this now.

5.4.4.2 Model Validation: Current Practice

Model validation often takes the form of what is commonly called a model correlation exercise. This deterministic process involves testing a piece of hardware that is being modeled and running the model at the nominal test conditions. Typically, only a single set of computational results and one set of test measurements are generated. These results (test and computational) are then compared. Often, the results are overlaid in some way (e.g., graphed together in a two-dimensional plot) and an experienced engineer

Copyright 2005 by CRC Press LLC

decides whether or not they are "close enough" to declare that the model is correlated (this measure of correlation is often referred to as the "viewgraph norm"). On initial comparison, the degree of correlation may be judged to be insufficient. Then the engineer will adjust some of the model parameters in an attempt to make the model results match the test results more closely. If and when sufficient agreement is obtained, the model is accepted as a useful surrogate for further hardware tests.

During this process, several important issues must be considered; these include:

1. This process, as described, implicitly assumes that the test result is the "correct answer" (i.e., a very accurate estimate of reality). In many cases, this may be a good assumption but experience has shown that testing can be prone to error. Consequently, the test used should have a quantified repeatability. Also, every effort must be made to ensure that the test results are free from systematic error. The use of independent test procedures can help here. For example, the dynamic strain results from a strain gage time history can be used to confirm the results from an accelerometer. If the accuracy of the test results cannot be quantified and assured through procedural controls, then replicated experiments should be run to estimate test uncertainty.
2. Changing model parameters to obtain "better" agreement between test and analysis results (calibration) can lead to the false conclusion that the modified model is better than its original version. Often, many model parameters can be chosen that will allow the same level of agreement to be forced. This nonuniqueness means that the engineer must be very disciplined when choosing the calibration parameters. They should only be chosen when there are significant reasons to believe that they are in error and therefore "need" to be calibrated.
3. Experimental data that has been used to adjust the model should not be the sole source of data for establishing the claim that the model is validated. Additional data for model validation should be obtained from further experiments. Ideally, these experiments should be carefully and specifically planned for model validation and represent the design domain over which the model will be used. However, with great care, data from hardware development and prototype tests can sometimes be used as a surrogate for (or an augmentation to) further validation testing.

These issues make it difficult for the engineer to calculate objective confidence bounds for the results of a mathematical model. To do this, a formal model validation process is necessary. Such a process is discussed next.

5.4.4.3 Model Validation: A Formal Process

A validated model has the following characteristics: (1) an estimate of the attribute (the output of the model), (2) an estimate of the bias (or difference between the computer experiments and the field "measured" experiments), (3) a measure of the confidence (tolerance) in the estimate of the bias, and finally (4) full documentation of the model parameters along with the validation process and the data used in the process. The bias and its tolerance measure results from three causes:

1. The approximation assumptions made during the development of the mathematical model
2. The uncertainty in the model parameters, boundary, and initial conditions used when running the computer model
3. The systematic errors present in the measurement and processing of field data

Figure 5.6 shows a process that is capable of producing a validated model having the characteristics described above. This figure is an adaptation of a similar figure given in Reference [32]. Specific modeling and simulation activities are shown with solid lines; while assessment activities are shown with dashed lines. The reality of interest is the particular performance attribute we are calculating (e.g., stress field or modes of vibration). The mathematical model is the result of the conceptual modeling activity.

The computer program is the realization of the mathematical model for implementing the calculations. It takes inputs, boundary conditions, initial conditions, and parameters (both physical and numerical) and produces simulation outcomes. The associated assessment activities are code and

Copyright 2005 by CRC Press LLC

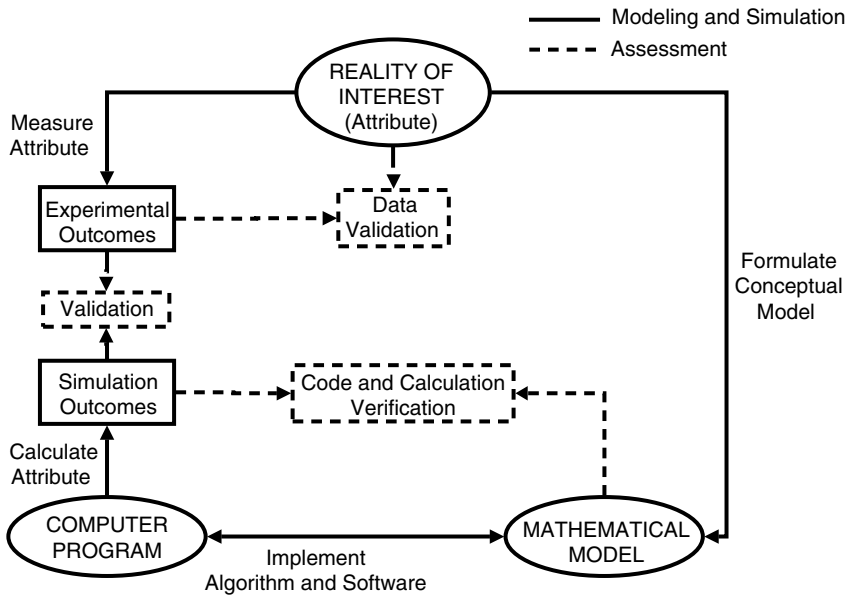

FIGURE 5.6 Block diagram of mathematical model validation and verification outside of the model development context.

calculation verification. Code verification is the process that determines that the computer code is an accurate representation of the discrete mathematical model. Calculation verification is the process that determines the numerical accuracy of code calculations (e.g., numerical error estimation). The main idea here is to make sure that the computer model accurately represents the conceptual mathematical model. A complicating factor from an industrial standpoint is that most models are constructed and exercised with commercial modeling and analysis software packages that are outside the direct control of the engineer.

Finally, the results from carefully designed physical experiments, as well as corresponding computer runs, are gathered and compared. This comparison generates an objective measure of agreement, the bias, and its tolerance bounds. The measure of agreement is what the engineer presents to the decision maker when asked about the validity of the results (see Bayarri et al. [33] for an example).

The decision maker, who has a particular risk tolerance, then decides whether the results are useful for making the decision. This is a critical step. A useful model is one with predictive power that is sufficient for making decisions with respect to the decision maker's risk tolerance. This can only be assessed within the overarching framework of decision making under uncertainty.

Once again, let us return to the door seal selection example.

5.4.4.4 Door Seal Selection Continued: Information Phase

In the Information Phase, the decision maker must decide either to continue collecting information or to commit to a course of action. In this example, the decision would be either to conduct additional analyses and/or experiments in order to better understand the performance and cost of the various door seal design alternatives, or to select a door seal design and authorize any necessary changes to the manufacturing system. "Selection," in the context of this design decision, means that the decision maker irrevocably allocates resources as the result of his or her actions. Thus, the selection of a door seal system would occur in a binding fashion by signing a letter of intent or a contract with a supplier. Likewise "authorization" of changes to the manufacturing system would include signing documents authorizing

Copyright 2005 by CRC Press LLC

the exchange of funds from the vehicle program's budget to the manufacturing facility. Until these actions have occurred, no decisions have been made.

In this illustration, we know that the rubber model we use has some high uncertainty associated with it. Two issues that could cause this high uncertainty are the material properties and the nonlinear model used to analyze the potentially complex cross-section seal deflection characteristics. In this case, the decision maker may find the tolerance bounds on the attribute calculations too wide for the risk tolerance he has. He may ask the engineer to estimate the resource requirements to improve the model to a certain tolerance level. The value of information is the cost of conducting additional analyses relative to the changes we will see in the values of the alternatives as a result of conducting the analyses. A question that can be answered from analyzing the decision diagram shown in Figure 5.4 is: "Would a change in the information cause the decision maker to select a different design alternative?" A change in information that does not change the preference order of the design alternatives (i.e., order in terms of our value from highest to lowest; we prefer more profit to less) is not worth conducting.

It is important to note that the need to improve a predictive model should be driven by the decision it supports, *not* by the engineer who is constructing it. For example, if the dominant uncertainty influencing this decision is the customer perception of wind noise for this vehicle, then the decision maker will allocate his resources to reduce that uncertainty, not to improve the door seal model.

5.5 Concluding Comments and Challenges

In this chapter we have discussed why the use of nondeterministic methods is critical from a business perspective. The VDP can be viewed as a series of decisions that are made by humans in an uncertain and creative environment. Our methods for design need to acknowledge and embrace this reality. We advocate a nondeterministic world view in a predominantly deterministically minded world. However, thinking in terms of a number of possible outcomes with varying probabilities of achieving those outcomes is a skill that very few people have developed. The fact that casinos and lotteries are thriving businesses is a powerful testament to this. Getting entire organizations to the point that they have healthy attitudes about decision making under uncertainty is a major challenge. This includes two key elements. First, they must accurately identify possible future states and encode the uncertainties about their potential occurrences, such that they migrate from "gambling" or overly risk-averse behavior to carefully calculated strategies with favorable reward-to-risk ratios. Second, they must accept the aleatory uncertainties that they cannot control and must migrate from the attitude that "they should have known" to "they could not have known with certainty and they made the best decision that they could at the time." These are cultural changes that cannot be made quickly—but unless they are made, a decision-analytic design framework such as the one we have described cannot flourish.

We have discussed the notion of using subjective probability as the overarching framework for decision analysis. We believe that other uncertainty methods fit within this framework. However, turning this notion around to where another uncertainty methodology is used as the overarching framework should be explored and researched.

While we know that the use of validation metrics is essential to help inform the decision maker, the technology for computing metrics like tolerance bounds for calculated attributes is still an area of research. The main challenge lies in the cost and complexity of the data and calculations that need to be assembled to estimate the tolerance bounds.

Uncertainty in calculating performance is intertwined with uncertainty in setting targets. The use of probability-based specifications in a flow-down and roll-up balancing process requires further research.

Finally, in a large enterprise, it is critical to evenly develop analytical capability across all of the product development disciplines. It would be difficult to operate a decision-making framework with varying levels of underlying mathematical modeling across disciplines. Engineers, for example, might think that marketing has sketchy data, has not really done any detailed analysis, and is just guessing. Marketing,

Copyright 2005 by CRC Press LLC

meanwhile, might think that engineers are overanalyzing some mathematical minutia and are missing some important elements of the big picture. The challenge is to make both sides recognize that they are both partly right and can learn some valuable lessons from each other.

References

1. Clark, K.B. and Fujimoto, T., Product Development Performance—Strategy, Organization, and Management in the World Auto Industry, Harvard Business School, Boston, MA, 1991.
2. Eppinger, S., Innovation at the speed of information, *Harvard Business Review*, 79 (1), 149, 2001.
3. Cividanes, A., Case Study: A Phase-Gate Product Development Process at General Motors, S.M. thesis, Massachusetts Institute of Technology, 2002.
4. Herrmann, J. and Schmidt, L., Viewing product development as a decision production system, in *Proc. ASME Design Eng. Tech. Conf.*, Montreal, Canada, 2002.
5. Carey, H. et al., Corporate decision-making and part differentiation: a model of customer-driven strategic planning, *Proc. ASME Design Eng. Tech. Conf.*, Montreal, Canada, 2002.
6. Matheson, J.E. and Howard, R.A., An Introduction to Decision Analysis (1968), from Readings on The Principles and Applications of Decision Analysis, Strategic Decisions Group, 1989.
7. Hazelrigg, G.A., The cheshire cat on engineering design, submitted to *ASME Journal of Mech. Design*.
8. Browning, T., Applying the design structure matrix to system decomposition and integration problems: a review and new directions, *IEEE Trans. on Eng. Management*, 48 (3), 292, 2001.
9. Kim, H. et al., Target cascading in optimal system design, *Journal of Mechanical Design*, 125(3), 474–480, 2003.
10. Dello Russo, F., Garvey, P., and Hulkower, N., Cost Analysis, Technical Paper No. MP 98B0000081, MITRE Corporation, Bedford, MA, 1998.
11. Kirchain, R., Cost modeling of materials and manufacturing processes, *Encyclopedia of Materials: Science and Technology*, Elsevier, 2001.
12. Wassenaar, H., Chen, W., Cheng J., and Sudjianto, A., Enhancing Discrete Choice Demand Modeling for Decision-Based Design, *Proc. ASME Design Eng. Tech. Conf.*, Chicago, IL, 2003.
13. Donndelinger, J. and Cook, H., Methods for analyzing the value of automobiles, *Proc. SAE Int. Congress and Exposition*, Detroit, MI, 1997.
14. Michalek, J., Papalambros, P., and Skerlos, S., A study of emission policy effects on optimal vehicle design decisions, *Proc. ASME Design Eng. Tech. Conf.*, Chicago, IL, 2003.
15. Wassenaar, H. and Chen, W., An approach to decision-based design with discrete choice analysis for demand modeling, *Journal of Mechanical Design*, 125 (3), 490–497, 2003.
16. Fenyes, P., Donndelinger, J., and Bourassa, J.-F., A new system for multidisciplinary analysis and optimization of vehicle architectures, *Proc. 9th AIAA/ISSMO Symposium on Multidisciplinary Analysis and Optimization*, Atlanta, GA, 2002.
17. Beranak, L.L. and Vér, I.L., *Noise and Vibration Control Engineering—Principles and Applications,* John Wiley & Sons, New York, 1992.
18. Chowdhury, S., *Design for Six Sigma: The Revolutionary Process for Achieving Extraordinary Profits*, Dearborn Trade, 2002.
19. Phadke, M.S., *Quality Engineering Using Robust Design*, Pearson Education, 1995.
20. Oberkampf, W., Helton, J., and Sentz, K., Mathematical representations of uncertainty, *Proc. AIAA/ASME/ASCE/AHS/ASC Structures, Structural Dynamics and Materials Conf.,* Seattle, WA, 2001.
21. Sentz, K. and Ferson, S., Combination of Evidence in Dempster–Shafer Theory, Sandia National Laboratories Report SAND2002-0835, 2002.
22. Klir, G.J. and Yuan, B., *Fuzzy Sets and Fuzzy Logic: Theory and Applications*, Prentice Hall, New York, 1995.
23. Klir, G.J. and Filger, T.A., *Fuzzy Sets, Uncertainty, and Information*, Prentice Hall, New York, 1988.

Copyright 2005 by CRC Press LLC

24. Yager, R.R., Fedrizzi, M., and Kacprzyk, J., Eds., *Advances in the Dempster–Shafer Theory of Evidence*, John Wiley & Sons, New York, 1994.
25. Dubois, D. and Prade, H., *Possibility Theory*, Plenum Press, New York, 1988.
26. Haldar, A. and Mahadevan, S., *Probability, Reliability and Statistical Methods in Engineering Design*, John Wiley & Sons, New York, 2000.
27. Zadeh, L.A., Fuzzy sets as a basis for a theory of possibility, *Fuzzy Sets and Systems*, 1, 3, 1978.
28. Ross, T.J., *Fuzzy Logic with Eng. Applications*, McGraw-Hill, New York, 1995.
29. Chen, L. and Rao, S.S., Fuzzy finite element approach for the vibration analysis of imprecisely defined systems, *Finite Elements in Analysis and Design*, 27, 69, 1997.
30. Mullen, R.L. and Muhanna, R.L., Bounds of structural response for all possible loading combinations, *ASCE Journal of Structural Eng.*, 125(1), 98–106, 1999.
31. Akpan, U.O., Rushton, P.A., and Koko, T.S., Fuzzy probabilistic assessment of the impact of corrosion on fatigue of aircraft structures, Paper AIAA-2002-1640, 2002.
32. Oberkampf, W.L., Sindir, M., and Conlisk, A.T., Guide for the verification and validation of computational fluid dynamics simulations, AIAA G-077-1998, 1998.
33. Bayarri, M.J., Berger, J.O., Higdon, D., Kennedy M.C., Kottas A., Paulo, R., Sacks, J., Cafeo, J.A., Cavendish, J., Lin, C.H., and Tu, J., A framework for validation of computer models, *Proc. of Foundations 2002—A Workshop on Model and Simulation Verification and Validation for the 21st Century*, Johns Hopkins University Applied Physics Lab, Laurel, MD, 2002.

Copyright 2005 by CRC Press LLC

6

Research Perspective in Stochastic Mechanics

Mircea Grigoriu
Cornell University

6.1 Introduction

The response and evolution of mechanical, biological, and other systems subjected to some input can be characterized by equations of the form

$$\mathcal{D}[\mathcal{X}(x,t)] = \mathcal{Y}(x,t), \quad t \geq 0, \quad x \in D \subset \mathcal{R}^d, \tag{6.1}$$

where $\mathcal{D}$ can be an algebraic, integral, or differential operator with random or deterministic coefficients characterizing the properties of the system under consideration, $\mathcal{Y}(x,t)$ denotes an $\mathbb{R}^{d'}$-valued random or deterministic function, and $d, d' \geq 1$ are integers. The output $\mathcal{X}$ depends on the properties of $\mathcal{D}$ and $\mathcal{Y}$ and the initial/boundary conditions, which can be deterministic or random.

Four classes of problems, referred to as stochastic problems, can be distinguished, depending on the systems and input properties: (1) deterministic systems and input, (2) deterministic systems and stochastic input, (3) stochastic systems and deterministic input, and (4) stochastic systems and input. The solution of the problems in these classes requires specialized methods that may involve elementary probabilistic considerations or advanced concepts on stochastic processes.

It has been common to develop methods for solving stochastic problems relevant to a field of applications without much regard to similar developments in related fields. For example, reliability indices developed for structural systems began to be used only recently in geotechnical and aerospace engineering because they were perceived as applicable only to buildings, bridges, and other structural systems [1]. Methods for characterizing the output of mechanical, structural, electrical, and other systems subjected to time-dependent uncertain input have been developed independently although the defining equations for the output of these systems coincide [2, 3].

It is anticipated that the emphasis of future research on stochastic problems will be on the development of methods for solving various classes of problems irrespective of the field of applications. This trend is

Copyright 2005 by CRC Press LLC

a direct consequence of the interdisciplinary nature of current research. A broad range of stochastic problems relevant to different fields can be described by the same equations. For example, the solution of the random eigenvalue problem can be used to find directions of crack initiation in materials with random properties, characterize the frequency of vibration for uncertain dynamic systems, and develop stability criteria for systems with random properties.

This chapter (1) briefly reviews current methods for solving stochastic problems and (2) explores likely future research trends in stochastic mechanics and related fields. The chapter is organized according to the type of Equation 6.1 rather than the field of application in agreement with the anticipated research trends. It includes four sections corresponding to the type of the operator $\mathcal{D}$ and the input $\mathcal{Y}$ in Equation 6.1.

6.2 Deterministic Systems and Input

Initial and boundary value deterministic problems have been studied extensively in engineering, science, and applied mathematics. Engineers and scientists have focused on numerical results, for example, the calculation of stresses and strains in elastic bodies, flows in hydraulic networks, temperatures in material subjected to heat flux, waves in elastic media, and other topics [4, 5]. Applied mathematicians have focused on conditions for the existence and uniqueness of a broad class of partial differential equations [6]. The difference of objectives has resulted in a limited interaction between mathematicians and engineers/scientists. Also, the engineers and scientists have emphasized numerical solutions for Equation 6.1 because applications usually involve complex equations, which rarely admit analytical solutions.

6.2.1 Current Methods

Numerical solutions to problems in science and engineering are commonplace in today's industry, research laboratories, and academia. Together with analytical and experimental methods, numerical simulations are accepted as an invaluable tool for the understanding of natural phenomena and the design of new materials systems, processes, and products.

The *finite element method* reigns supreme as the method of choice in computational solid mechanics, with the boundary element and finite difference methods running substantially far behind. While these methods are extremely powerful and versatile, they are not optimal for all applications. For example, some of the drawbacks of the finite element method are that it always provides a global solution, needs domain discretization, and involves solution of large linear algebraic systems [7].

Global methods providing values of the stress, displacement, and other response functions at all or a finite number of points of the domain of definition of these functions are generally used to solve mechanics, elasticity, physics, and other engineering problems. These methods can be based on analytical or numerical algorithms. The analytical methods have limited value because few practical problems admit closed form solutions and these solutions may consist of slowly convergent infinite series [5]. The finite element, boundary element, finite difference, and other numerical methods are generally applied to solve practical problems. Some of the possible limitations of these numerical methods include: (1) the computer codes used for solution are relatively complex and can involve extensive preprocessing to formulate a particular problem in the required format, (2) the numerical algorithms may become unstable in some cases, (3) the order of the errors caused by the discretization of the continuum and the numerical integration methods used in analysis cannot always be bounded, and (4) the field solution must be calculated even if the solution is needed at a single point, for example, stress concentration, deformations at particular points, and other problems.

6.2.2 Research Needs and Trends

The analysis of complex multidisciplinary applications requires realistic representations for the operator $\mathcal{D}$ and the input $\mathcal{Y}$ in Equation 6.1, as well as efficient and accurate numerical algorithms for solving this equation. Also, methods for estimating or bounding errors related to numerical calculations and

Copyright 2005 by CRC Press LLC

discretization need to be developed and implemented in future algorithms. For example, useful results for the growth of microcracks in aluminum and other materials are possible if the analysis is based on (1) detailed representations of the material microstructure at the grain level and (2) powerful and accurate numerical algorithms for solving discrete versions of Equation 6.1 obtained by finite element or other methods.

Close interaction between engineers, scientists, and applied mathematicians is deemed essential for developing efficient and accurate numerical algorithms for the solution of Equation 6.1 This interaction is expected to deliver numerical algorithms needed to solve complex multidisciplinary applications considered currently in science and engineering.

There are some notable developments in this direction. For example, recent work in applied mathematics is directed toward the estimation of errors generated by various numerical solutions of Equation 6.1. Some of these studies use probabilistic concepts for error quantification [8]. Also, alternative techniques to the traditional numerical methods, referred to as local methods, are currently explored for solving locally some types of partial differential equations. The methods delivers the solution of these partial differential equations at an arbitrary point directly, rather than extracting the response value at this point from the field solution, and are based on probabilistic concepts. The theoretical considerations supporting these solutions are relatively complex. They are based on properties of diffusion processes, Itô's formula for continuous semimartingales, and Monte Carlo simulations [9–12]. However, the resulting numerical algorithms for solution have attractive features. These algorithms are (1) simple to program, (2) always stable, (3) accurate, (4) local, and (5) ideal for parallel computation ([13], Chapter 6).

Consider for illustration the Laplace equation

$$\Delta u(x) = 0, \quad x \in D, \quad u(x) = \xi_r(x), \quad x \in \partial D_r, r = 1, \ldots, m \tag{6.2}$$

where D is an open bounded subset in $\mathbb{R}^d$ with boundaries ∂D_r, $r = 1, \ldots, m$, and ξ_r denote functions defined on these boundaries. If $m = 1$, then D is a simply connected subset of $\mathbb{R}^d$. Otherwise, D is multiply connected.

Denote by B an $\mathbb{R}^d$-valued Brownian motion starting at $x \in D$. The samples of B will exit D through one of the boundaries ∂D_r of D. Figure 6.1 shows three samples of a Brownian motion B in $\mathbb{R}^2$ and their exit points from a multiply connected set D. Let $T = \inf\{t > 0 : B(t) \notin D\}$ denote the first time B starting at $B(0) = x \in D$ exits D. Then, the local solution of this equation is ([13], Section 6.2.1.3)

$$u(x) = \sum_{r=1}^{m} E^x[\xi_r(B(T)) \mid B(T) \in \partial D_r] p_r(x) \tag{6.3}$$

where E^x is the expectation operator corresponding to $B(0) = x$ and $p_r(x)$ denotes the probability that B starting at x exits D through ∂D_r.

For example, let $u(x)$ be the steady-state temperature at an arbitrary point $x = (x_1, x_2)$ of an eccentric annulus

$$D = \left\{(x_1, x_2) : x_1^2 + x_2^2 - 1 < 0, (x_1 - 1/4)^2 + x_2^2 - (1/4)^2 > 0\right\}$$

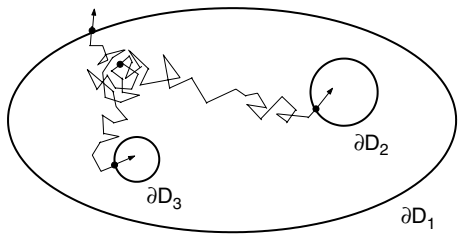

FIGURE 6.1 Local solution of the Laplace equation for a multiply connected domain D in $\mathbb{R}^2$.

Copyright 2005 by CRC Press LLC

in $\mathbb{R}^2$ with boundaries $\partial D_1 = \{(x_1, x_2) : x_1^2 + x_2^2 - 1 = 0\}$ and $\partial D_2 = \{(x_1, x_2) : (x_1 - 1/4)^2 + x_2^2 - (1/4)^2 = 0\}$ kept at the constant temperatures 50 and 0, respectively. The local solution in Equation 6.3 is $u(x) = 50\, p_1(x)$ for any point $x \in D$. Because $p_1(x)$ cannot be found analytically, it has been calculated from samples of B starting at x. The largest error recorded at $x = (0.7,0)$, $(0.9,0)$, $(0,0.25)$, $(0,0.5)$, and $(0,0.75)$ was found to be 2.79% for $n_s = 1{,}000$ independent samples of B with time steps $mit\, \Delta t = 0.001$ or 0.0001. Smaller time steps were used at points x close to the boundary of D. The error can be reduced by decreasing the time step or increasing the sample size. The exact solution can be found in [5] (Example 16.3, p. 296).

6.3 Deterministic Systems and Stochastic Input

Generally, the input to biological, electrical, mechanical, and physical systems is uncertain and can be modeled by stochastic processes. The output of these systems is given by the solution of Equation 6.1 with $\mathcal{D}$ deterministic and $\mathcal{Y}$ random.

Records and physical considerations are used to estimate — at least partially — the probability law of these processes. For example, the symmetry of the seismic ground acceleration process about zero indicates that this process must have mean 0 and that its marginal density must be an even function. It is common to assume that the ground acceleration process is Gaussian although statistics of seismic ground acceleration records do not support this assumption ([14], Section 2.1.4). On the other hand, pressure coefficients recorded in wind tunnels at the eaves of some building models exhibit notable skewness, as demonstrated in Figure 6.2.

The broad range of probability laws of the input processes in these examples show that general Gaussian and nonGaussian models are needed to describe inputs encountered in applications.

6.3.1 Current Methods

Most available methods for finding properties of the output $\mathcal{X}$ of Equation 6.1 have been developed in the framework of random vibration [3, 15]. The methods depend on the system type, which defines the functional form of the operator $\mathcal{D}$ in Equation 6.1, input properties, and required output statistics. For example, the determination of the second-moment output properties for linear systems subjected to white noise involves elementary calculations, and can be based on a heuristic second-moment definition of the driving noise. If the noise is assumed to be Gaussian, then the output $\mathcal{Y}$ is Gaussian so that the probability law of $\mathcal{Y}$ is completely defined by its second-moment properties. On the other hand, there are no general methods for finding the probability law of the output of a linear system subjected to an arbitrary nonGaussian input. Similarly, the probability law of $\mathcal{Y}$ for nonlinear systems can be found only for some special input processes. For example, it can be shown that the marginal distribution of the output of these systems subjected to Gaussian white noise satisfies a partial differential equation, referred to as the Fokker-Planck equation, provided that the white noise input is interpreted as the formal derivative of the Brownian motion or Wiener process ([13], Section 7.3.1.3). Unfortunately, analytical solutions of the Fokker-Planck equation are available only for elementary systems and numerical solutions of this equation are possible

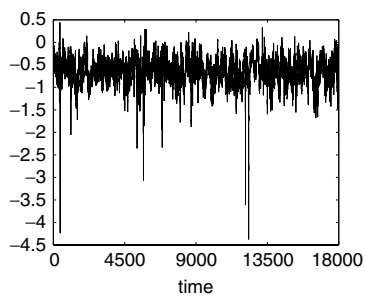

FIGURE 6.2 A record of pressure coefficients.

Copyright 2005 by CRC Press LLC

only for small dimension output processes ([13], Sections 7.3.1.3 and 7.3.1.4). This limitation is the main reason for the development of a variety of heuristic methods for solution; for example, equivalent linearization, moment closure, and other techniques ([13], Sections 7.3.1.1 and 7.3.1.5).

The above exact and approximate methods have been used to model climatic changes, describe the evolution atomic lattice orientation in metals, and perform reliability studies in earthquake engineering and other fields ([13], Sections 7.4.1.1, 7.4.2, 7.4.3, and 7.4.4). Early applications encountered difficulties related to the interpretation of the white noise input as a stationary process with finite variance and correlation time approaching zero. These difficulties have been gradually overcome as differences between physical white noise and mathematical white noise and between the Itô and Stratonovich integrals were understood ([16], Section 5.4.2). A significant contribution to the clarification on these issues has been the available mathematical literature on stochastic differential equations [17].

6.3.2 Research Needs and Trends

There are no general methods for finding the probability law of the output of linear systems subjected to arbitrary nonGaussian input processes and nonlinear systems with Gaussian and nonGaussian input. An additional difficulty relates to the limited number of simple models available for representing non-Gaussian input processes, for example, the process in Figure 6.2. A close interaction between engineers, scientists, and mathematicians is needed to overcome some of these difficulties.

Recent research addresses some of these needs. For example, efficient simple methods have been developed for calculating moments of any order for the state of linear systems driven by a class of non-Gaussian processes defined as polynomials of Gaussian diffusion processes. The analysis is based on properties of diffusion processes and Itô's calculus ([13], Section 7.2.2.3). For example, consider the linear system

$$\ddot{X}(t)+2\zeta\nu\dot{X}(t)+\nu^2 X(t)=\sum_{l=0}^{n} a_l(t)S(t)^l \tag{6.4}$$

where $dS(t)=-\alpha S(t)\,dt+\sigma\sqrt{2\alpha}\,dB(t)$, $\alpha>0$, σ, $\zeta>0$, and $\nu>0$ are some constants, B denotes a Brownian motion, $n\geq 1$ is an integer, and a_l are continuous functions. The process X represents the displacement of a linear oscillator with natural frequency ν and damping ratio ζ driven by a polynomial of the Ornstein-Uhlenbeck process S.

The moments $\mu(p,q,r;t)=E[X(t)^p\,\dot{X}(t)^q\,S(t)^r]$ of order $s=p+q+r$ of $Z=(X,\dot{X},S)$ satisfy the ordinary differential equation

$$\begin{aligned}\dot{\mu}(p,q,r;t)&=p\,\mu(p-1,q+1,r;t)-q\nu^2\mu(p+1,q-1,r;t)\\&\quad-(q\beta+r\alpha)\mu(p,q,r;t)+q\sum_{l=0}^{n}a_l(t)\mu(p,q-1,r+l;t)\\&\quad+r(r-1)\alpha\sigma^2\mu(p,q,r-2;t)\end{aligned} \tag{6.5}$$

at each time t, where $\beta=2\zeta\nu$ and $\mu(p,q,r;t)=0$ if at least one of the arguments p, q, or r of $\mu(p,q,r;t)$ is strictly negative. The above equation results by taking the expectation of the Itô formula applied to the function $X(t)^p\,\dot{X}(t)^q\,S(t)^r$ ([13], Section 4.6).

If $(X,\dot{X},S)$ becomes stationary as $t\to\infty$, the stationary moments of this vector process can be obtained from a system of algebraic equations derived from the above moment equation by setting $\dot{\mu}(p,q,r;t)=0$.

Table 6.1 shows the dependence on damping $\beta=2\zeta\nu$ of the coefficients of skewness and kurtosis of the stationary process X for $\nu^2=1.6$, $\nu^2=9.0$, and the input $\Sigma_{l=0}^{n}a_l(t)S(t)^l$ with $n=2$, $a_0(t)=a_1(t)=0$, $a_2(t)=1$, $\alpha=0.12$, and $\sigma=1$. The skewness and the kurtosis coefficients are increasing functions of β. If the linear system has no damping $(\beta=0)$, these coefficients are 0 and 3, respectively, so that they match the values for Gaussian variables. This result is consistent with a theorem stating roughly that the output

Copyright 2005 by CRC Press LLC

TABLE 6.1 Coefficients of Skewness and Kurtosis of the Stationary Displacement X of a Simple Linear Oscillator Driven by the Square of an Ornstein-Uhlenbeck Process

	Skewness		Kurtosis	
β	$\nu^2 = 1.6$	$\nu^2 = 9.0$	$\nu^2 = 1.6$	$\nu^2 = 9.0$
0	0	0	3	3
0.25	1.87	1.79	9.12	8.45
0.5	2.48	2.34	11.98	11.24
1	2.84	2.72	13.99	13.32
1.5	2.85	2.77	14.51	13.95

of a linear filter with infinite memory to a random input becomes Gaussian as time increases indefinitely ([14], Section 5.2). The linear filter in this example has infinite memory for $\beta = 0$. Similar results are available for linear systems driven by Poisson white noise interpreted as the formal derivative of the compound Poisson process ([13], Section 7.2.2.3). There are some limited research results on the output of nonlinear systems to Gaussian and nonGaussian input. For example, simple tail approximations have been recently found for the output of simple nonlinear systems with additive Lévy noise, interpreted as the formal derivative of α-stable processes [18]. Also, partial differential equations have been developed for the characteristic function of the output of some linear and nonlinear systems subjected to Gaussian white noise ([13], Section 7.3.1.2). These preliminary results need to be extended significantly to be useful in applications.

The Monte Carlo method is general in the sense that it can be used to estimate the probability law of the output for arbitrary systems and input processes. However, its use is limited because the computation time needed to calculate the system output to an input sample is usually excessive in applications. Hence, only a few output samples can be obtained within a typical computation budget so that output properties cannot be estimated accurately. Several methods are currently under investigation for improving the efficiency of current Monte Carlo simulation algorithms. Some of these methods constitute an extension of the classical importance sampling technique for estimating expectations of functions of random variables to the case of stochastic processes, and are based on Girsanov's theorem ([19]). Additional developments are needed to extend the use of these methods from elementary examples to realistic applications. The essentials of the importance sampling method can be illustrated by the following example.

Let $P_s = P(X \in D)$ and $P_f = P(X \in D^c)$ denote the reliability and probability of failure, where $D \subset \mathbb{R}^d$ is a safe set. The probability of failure is

$$P_f = \int_{\mathbb{R}^d} 1_{D^c}(x) f(x)\, dx = E_P[1_{D^c}(X)] \quad \text{or} \quad P_f = \int_{\mathbb{R}^d} \left[1_{D^c}(x)\frac{f(x)}{q(x)}\right] q(x)\, dx = E_Q\left[1_{D^c}(X)\frac{f(X)}{q(X)}\right]$$

where f and q are the densities of X under the probability measures P and Q, respectively. The measure P defines the original reliability problem. The measure Q is selected to recast the original reliability problem in a convenient way. The estimates of P_f by the above two formulas, referred to as direct Monte Carlo and importance sampling, are denoted by $\hat{p}_{f,MC}$ and $\hat{p}_{f,IS}$, respectively.

Let X have independent $N(0, 1)$ coordinates and D be a sphere of radius $r > 0$ centered at the origin of $\mathbb{R}^d$, that is, $D = \{x \in \mathbb{R}^d : \| x \| \le r\}$, for $d = 0$. The density q corresponds to an $\mathbb{R}^d$-valued Gaussian variable with mean $(r, 0, \ldots, 0)$ and covariance matrix $\sigma^2 i$, where $\sigma > 0$ is a constant and i denotes the identity matrix. The probability of failure P_f can be calculated exactly and is 0.053, 0.8414×10^{-4}, and 0.4073×10^{-6} for r = 5, 6, and 7, respectively. Estimates of P_f by direct Monte Carlo simulation based on 10,000 independent samples of X are $\hat{p}_{f,MC}$ = 0.0053, 0.0, and 0.0 for r = 5, 6, and 7, respectively. On the other hand, importance sampling estimates of P_f based on 10,000 independent samples of X are $\hat{p}_{f,IS}$ = 0.0; 0.0009; 0.0053; 0.0050; 0.0050, $\hat{p}_{f,IS} = 0.0001 \times 10^{-4}$; 0.1028×10^{-4}; 0.5697×10^{-4}; 1.1580×10^{-4}; 1.1350×10^{-4}, and $\hat{p}_{f,IS}$ = 0.0; 0.0016×10^{-6}; 0.1223×10^{-6}; 0.6035×10^{-6}; 0.4042×10^{-6} for r = 5, 6, and 7, respectively. The values of $\hat{p}_{f,IS}$ for each value of r correspond to σ = 0.5; 1; 2; 3; 4,

Copyright 2005 by CRC Press LLC

respectively. The direct Monte Carlo method is inaccurate for relatively large values of r, that is, small probabilities of failure. The success of the importance sampling method depends on the density q. For example, $\hat{p}_{f,IS}$ is in error for $d = 10$ and $\sigma = 0.5$ but becomes accurate if σ is increased to 3 or 4. Details on these calculations can be found in ([13] Section 5.4.2.1).

6.4 Stochastic Systems and Deterministic Input

The solution of Equation 6.1 with stochastic operator $\mathcal{D}$ and deterministic input $\mathcal{Y}$ is relevant for many problems in science and engineering. For example, this solution can be used to calculate effective properties for random heterogeneous materials; develop criteria for the stochastic stability of mechanical, biological, and other systems; and examine localization phenomena in nearly periodic systems ([13], Section 8.1).

6.4.1 Current Methods

There is no general methodology for the solution of Equation 6.1 with stochastic operator $\mathcal{D}$ and deterministic input $\mathcal{Y}$. The available methods for solution can be divided in several classes, depending on the form of Equation 6.1, the level of uncertainty in $\mathcal{D}$, and the objective of the analysis. If the uncertainty in $\mathcal{D}$ is small, moments and other properties of the solution $\mathcal{X}$ can be obtained approximately by Taylor series, perturbation, Neumann series, and other methods. These methods are based on relatively simple probabilistic concepts, and can also be used to characterize partially the eigenvalues and eigenfunction of the homogeneous version of Equation 6.1 and calculate approximately effective properties for random heterogeneous materials ([13], Sections 8.3.2, 8.4.2, and 8.5.2.4). On the other hand, methods for evaluating the stability of the stationary solution for a class of equations of the type in Equation 6.1 and assessing the occurrence of localization phenomena are based on properties of diffusion processes and Itô calculus ([13], Sections 8.7 and 8.8).

The Monte Carlo simulation method can be used to estimate the probability law of the solution of the version of Equation 6.1 considered here. The method is general but can be impractical in some applications because of excessive computation time. Also, the use of this method requires one to specify completely the probability law of all random parameters in Equation 6.1 even if only a partial characterization of the output is needed. This requirement may have practical implications because the available information is rarely sufficient to specify the probability law of the uncertain parameters uniquely.

6.4.2 Research Needs and Trends

At least two research areas have to be emphasized in future studies: (1) the development of more powerful probabilistic models for the representation of the uncertain coefficients in Equation 6.1 and (2) the development of general and efficient methods for solving this equation. Research in these areas is essential for the formulation and solution of stochastic problems of the type considered in this section, and requires a close collaboration between engineers, scientists, and applied mathematicians.

Recent work seems to address some of these research needs. For example, new probabilistic models are currently being developed for random heterogeneous materials [20]. Generally, these models are calibrated to the available information consisting of estimates of the first two moments of some material properties, so that there exists a collection of random fields consistent with this information. The selection of an optimal model from this collection has not yet been addressed systematically in a general context. Model selection is a relevant research topic because the properties of the output corresponding to models of $\mathcal{D}$ that are consistent with the available information can differ significantly. For example, suppose that Equation 6.1 has the elementary form

$$Y = \frac{1}{X}, \quad X > 0 \text{ a.s.} \tag{6.6}$$

Copyright 2005 by CRC Press LLC

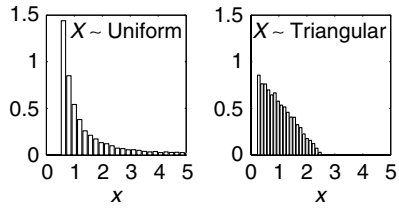

FIGURE 6.3 Histograms of Y for two models of X with the same mean $\mu = 1$, variance $\sigma^2 = a^2/3$, and $a = 0.95$.

where Y can be interpreted as the tip deflection of a cantilever with stiffness X. Suppose that the available information on the uncertain parameter X in $\mathcal{D}$ is limited to the first two moments of X and the requirement that $X > 0$ with probability 1. Let $\mu = E[X]$ and $\sigma^2 = E[(X-\mu)^2]$ denote the mean and variance of X. Hence, any random variable with range in $(0, \infty)$ and first two moments (μ, σ^2) is a valid model for the beam stiffness. Figure 6.3 shows histograms of Y for two models of X with mean $\mu = 1$, variance $\sigma^2 = a^2/3$, and $a = 0.95$. The left plot is for X uniformly distributed in the interval $(1-a, 1+a)$, and the right plot is for X assumed to follow a triangular density in the range $(1-h\sqrt{3}, 1+2h\sqrt{3})$ with the nonzero value at the left end of this interval and $h = a\sqrt{6}$. The histograms of the output Y differ significantly although correspond to models of X that are consistent with the available information.

Similar results can be found in [21], where several random fields are used to represent a two-phase microstructure. The second-moment properties of these fields and the target microstructure nearly coincide. However, other microstructure properties predicted by these fields differ significantly, for example, the density of the diameter of the phases generated by these fields. This lack of uniqueness can have notable practical implications.

There is limited work on the selection of the optimal model from a collection of probabilistic models for $\mathcal{D}$ consistent with the available information.

Also, new methods for finding effective properties of a class of multiphase microstructures described by versions of Equation 6.1 are under development. These methods are based on multiscale analysis, are developed in the context of material science, and involve engineers, scientists, and applied mathematicians [22].

6.5 Stochastic Systems and Input

In most applications, both the operator $\mathcal{D}$ and the input $\mathcal{Y}$ in Equation 6.1 are uncertain. The forms of this equation considered in the previous two sections are relevant for applications characterized by a dominant uncertainty in input or operator. If the uncertainty in both the input and the output is weak, Equation 6.1 can be viewed as deterministic.

6.5.1 Current Methods

Monte Carlo simulation is the only general method for solving Equation 6.1. The difficulties involving the use of this method relate, as stated previously, to the computation time, which may be excessive, and the need for specifying completely the probability law of all random parameters in $\mathcal{D}$ and $\mathcal{Y}$.

Some of the methods frequently applied to find properties of $\mathcal{Y}$ in Equation 6.1 constitute direct extensions of the techniques outlined in the previous two sections. For example, conditional analysis is an attractive alternative when $\mathcal{D}$ depends on a small number of random parameters so that for fixed values of these parameters the methods applied to solve Equation 6.1 with deterministic operator and stochastic input apply. Methods based on Taylor, perturbation, and Neumann series can also be used for finding properties of $\mathcal{X}$ approximately. Other approximate methods for solving Equation 6.1 can be found in ([13] Section 9.2).

Copyright 2005 by CRC Press LLC

Over the past 15 years there have been many studies attempting to extend the finite element and other classical numerical solutions used to solve the deterministic version of Equation 6.1 to the case in which both the operator and the input of this equation are uncertain. Unfortunately, these extensions, referred to as stochastic finite element, finite difference, and boundary element, fell short of expectations. The solutions of Equation 6.1 by these methods are based on (1) approximations of the solution by Taylor, perturbation, or Neumann series for cases in which the uncertainty in $\mathcal{D}$ is small (13], Section 9.2.6); (2) approximations of the solution by polynomial chaos, that is, sums of Hermite polynomials in Gaussian variables [23]; and (3) formulation of the solution as a reliability problem so that FORM/SORM and other approximate methods for reliability analysis can be used for solution [1].

The Monte Carlo simulation method and many of the above approximate methods have been applied to solve a variety of problems from mechanics, physics, environment, seismology, ecology, and other fields. In addition to these methods, alternative solutions have been used to solve particular applications. For example, properties of diffusion processes and the Itô calculus have been used to characterize noise induced transitions in a randomized version of the Verhulst model for the growth of a biological population ([13], Section 9.4.3) and find properties of the subsurface flow and transport in random heterogeneous soil deposits ([13], Section 9.5.3).

6.5.2 Research Needs and Trends

Methods are needed for solving efficiently and accurately Equation 6.1 for a broad range of stochastic operators $\mathcal{D}$ and input processes $\mathcal{Y}$. It may not be possible to develop a single method for solving an arbitrary form of Equation 6.1. The contribution of applied mathematicians to the development of solutions for Equation 6.1 may be essential for advances in this challenging area.

There are some limited developments that provide approximate solutions to Equation 6.1. For example, equations can be developed for the gradients of the solution $\mathcal{X}$ with respect to the uncertain parameters in $\mathcal{D}$. These gradients, referred to as sensitivity factors, and the uncertainty in the random parameters in $\mathcal{D}$ can be used to identify the most relevant sources of uncertainty and calculate approximately properties of the output $\mathcal{X}$. For example, let $X(t; R)$ be the solution of the differential equation

$$dX(t; R) = -R\,X(t; R) + \sigma\,dB(t), \quad t \geq 0, \tag{6.7}$$

where the random variable R with mean μ_r and variance σ_r^2 is strictly positive, σ is a constant, and B denotes a Brownian motion. Consider the first order approximation

$$X(t; R) \approx X(t; \mu_r) + Y(t; \mu_r)(R - \mu_r), \tag{6.8}$$

of the solution of the above equation, where the sensitivity factor $Y(t; \mu_r)$ is the partial derivative $\partial X(t; R)/\partial R$ evaluated at $R = \mu_r$. The sensitivity factor $Y(t; \mu_r)$ is the solution of the differential equation

$$dY(t; \mu_r) = -\mu_r\,Y(t; \mu_r)\,dt - X(t; \mu_r)\,dt \tag{6.9}$$

derived from Equation 6.7 by differentiation with respect to R and setting $R = \mu_r$. The defining equations for $X(t; \mu_r)$ and $Y(t; \mu_r)$ can be considered simultaneously and solved by classical methods of linear random vibration. Figure 6.4 shows the evolution in time of the exact and the approximate variance functions of $X(t; \mu_r)$ and $X(t; R)$, respectively, for $X(0) = 0$, $\sigma = \sqrt{2}$, $\mu_r = 1$, and $\sigma_r = 1.4/\sqrt{12}$. The plots show that the uncertainty in R increases notably the variance of the process X. The use of sensitivity analysis replaces the solution of a differential equation with random coefficients and input with the solution of two differential equations with deterministic coefficients and stochastic input.

Copyright 2005 by CRC Press LLC

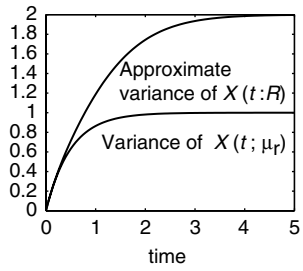

FIGURE 6.4 Exact and approximate variance functions of $X(t; \mu_r)$ and $X(t; R)$.

6.6 Comments

The formulation and solution of the future problems encountered in science and engineering require (1) extensive interaction between experts from different disciplines and (2) methods for solving stochastic problems that focus on the functional form of the defining equations rather than the particular field of application. The contribution of applied mathematicians is considered to be essential for these developments.

Two research directions have been identified as critical. The first relates to the development of probabilistic models capable of representing a broad range of input processes and characteristics of uncertain systems. Moreover, practical methods are needed to select optimal models from a collection of random variables, stochastic processes, and random fields whose members are consistent with the available information. Some useful results have already been obtained in this area.

The second direction relates to the development of efficient and accurate numerical algorithms for solving complex algebraic, differential, and integral equations with random coefficients and input. Significant work is needed in this area.

References

1. Madsen, H.O., Krenk, S., and Lind, N.C., *Methods of Structural Safety,* Prentice Hall, Englewood Cliffs, NJ, 1986.
2. Papoulis, A., *Probability, Random Variables, and Stochastic Processes,* McGraw-Hill, New York, 1965.
3. Soong, T.T. and Grigoriu, M., *Random Vibration of Mechanical and Structural Systems,* Prentice Hall, Englewood Cliffs, NJ, 1993.
4. Crandall, S.H., *Engineering Analysis. A Survey of Numerical Procedures,* McGraw-Hill, New York, 1956.
5. Greenberg, M.D., *Foundations of Applied Mathematics,* Prentice Hall, Englewood Cliffs, NJ, 1978.
6. John, F., *Partial Differential Equations, 4th edition,* Springdf-Verlag, New York, 1982.
7. Brebbia, C.A. and Connor, J.J., *Fundamentals of Finite Element Techniques,* Butterworth, London, 1973.
8. Glimm, J., Uncertainty Quantification for Numerical Simulations, presented at the *SIAM Conference on Computational Science and Engineering,* February 10–13, 2003, San Diego, CA.
9. Chung, K.L. and Williams, R.J., *Introduction to Stochastic Integration,* Birkhäuser, Boston, 1990.
10. Courant, R. and Hilbert, D., *Methods of Mathematical Physics,* Vol. 2, Interscience, New York, 1953.
11. Durrett, R., *Stochastic Calculus. A Practical Introduction,* CRC Press, Boca Raton, FL, 1996.
12. Øksendal, B., *Stochastic Differential Equations,* Springer-Verlag, New York, 1992.
13. Grigoriu, M., *Stochastic Calculus. Applications in Science and Engineering,* Birkhäuser, Boston, 2002.
14. Grigoriu, M., *Applied Non-Gaussian Processes: Examples, Theory, Simulation, Linear Random Vibration, and MATLAB Solutions,* Prentice Hall, Englewood Cliffs, NJ, 1995.

Copyright 2005 by CRC Press LLC

15. Crandall, S.H. and Mark, W.D., *Random Vibration in Mechanical Systems,* Academic Press, New York, 1963.
16. Horsthemke, W. and Lefever, R., Phase transitions induced by external noise, *Physics Letters,* 64A(1), 19–21, 1977.
17. Protteer, P., *Stochastic Integration and Differential Equations,* Springer-Verlag, New York, 1990.
18. Samorodnitsky, G. and Grigoriu, M., Tails of solutions of certain nonlinear stochastic differential equations driven by heavy tailed Lévy motions, *Stochastic Processes and Their Applications,* submitted 2002.
19. Naess, A. and Krenk, S., Eds., *Advances in Nonlinear Stochastic Mechanics,* Kluwer Academic, Boston, 1996.
20. Torquato, S., Thermal conductivity of disordered heterogeneous media form the microstructure, *Reviews in Chemical Engineering,* 4(3 and 4), 151–204, 1987.
21. Roberts, A.P., Statistical reconstruction of three-dimensional porous media from two-dimensional images, *Physical Review E,* 56(3), 3203–3212, 1997.
22. Hornung, U., *Homogenization and Porous Media,* Springer-Verlag, New York, 1997.
23. Ghanem, R.G. and Spanos, P.D., *Stochastic Finite Elements: A Spectral Approach,* Springer-Verlag, New York, 1991.

Copyright 2005 by CRC Press LLC

7

A Research Perspective

David G. Robinson
Sandia National Laboratories

7.1 Background

As with all probability-related methods, nondeterministic analysis (NDA) methods have gone through numerous cycles of interest to management and as topics of investigation by a wide spectrum of engineering disciplines. In concert with these cycles has been the support for research in NDA methods. As always, research funding is ultimately driven by the perceived benefit that decision makers from management and engineering feel is to be gained by the time and money needed to support the inclusion of nondeterministic methods in their project.

The focus of this chapter is a suggested research direction or focus that I believe will result in nondeterministic methods having more value to the broad spectrum of customers and will, as a result, become more tightly woven in the overall systems design and analysis process.

From a broad perspective, future research in the NDA area needs to begin to focus on being applicable across the entire systems design process, through all phases of initial design conception and across the entire system life cycle. Historically, the NDA field has tackled important pieces of the process and a number of very elegant mathematical techniques have been developed. However, there are areas where there remains much to be done. Inherent with these areas is the critical need for direct or indirect customers to see the value added via the application of NDA methods: How are NDA methods going to permit better system level decisions? Will these methods shorten my time to market? How are NDA methods going to provide information regarding trade-off during design?

By its nature the system engineering process is adrift in a sea of information and data: field data on similar components, handbook data on material properties, laboratory test results, engineering experience, etc. A complete "information science" has grown around the collection, storage, manipulation, and retrieval of information. Perversely, as expansive as this information space appears, the information is incomplete. A critical goal of nondeterministic methods is to characterize or quantify this lack of information.

Copyright 2005 by CRC Press LLC

Historically, research into nondeterministic methods has focused on point estimates and amalgamation of those estimates into a point estimate at the system level. To demonstrate the value of NDA methods, researchers must move outside the "point estimate" box. From a broad perspective, challenges facing researchers in the NDA field include:

- Relating lower-level analyses to system level performance through a more objective integration of information and by identifying those aspects of the system where generation of additional information (e.g., focused testing or simulation) will reduce the uncertainty in system performance. The majority of the discussion in this chapter focuses on this particular challenge.
- Characterization of the uncertainty associated with degradation in system performance throughout the life cycle of the system. The integration of temporal system characteristics and spatial properties result in an extremely complicated analysis problem. Yet with the aging civil infrastructure and the increased dependence by military organizations on long-term storage of complex electronics and materials, characterization of time-dependent system behavior is becoming a critically important part of the decision-making process. However, as Niels Bohr noted, prediction is extremely difficult — especially about the future.
- The logical next step is the combination of the first two challenges: development of techniques to combine information from accelerated laboratory tests, results from periodic testing of system articles, and output from computer simulation models to anticipate failure and better plan maintenance support will be a particularly challenging task.

Information comes at a price — nondeterministic methods can be a powerful tool for placing value on this information. Beyond the above challenges, new directions for research in NDA methods are likely to be in support of information science and, in turn, the systems engineering process. The value of all information lies in the ability to reduce the uncertainty associated with the consequences of the solution chosen. Nondeterministic methods provide the potential for answering many questions, including: *What is the likelihood that the system will perform as needed now and in the future, and where should the limited resources be allocated: in materials testing, complex computer modeling, component testing or system testing to be as confident as possible in how the system will perform?*

7.1.1 Critical Element of the Design Process

Systems engineering is a multidisciplinary approach to problem solution that ensures that system requirements are satisfied throughout the entire system life cycle. This approach has gained popularity because of its proven track record in increasing the probability of system success and reducing costs through the entire life of the system.

Figure 7.1 depicts the systems engineering process used by Lockheed-Martin [1]. This is a common approach: "pushing" information down based on top-level requirements while simultaneously "pulling" information up from lower-level analyses. Figure 7.2 is a similar depiction focusing on the application of nondeterministic methods. Top-level requirements drive subsystem requirements, component requirements, etc. Application of nondeterministic methods are often applied to either amalgamate failure modes or integrated with simulation models (e.g., finite element model, electrical circuit simulation). In either case, these models are often supported in turn by complex materials aging models.

Regardless of the particular perspective on system engineering, the critical point is the recognition that resources expended on each subsequent level of indenture are driven by the impact that analysis at the lower level will have on the characterization of the top-level system. The overriding goal is to assess the impact of various uncertainties associated with internal and external variables on the uncertainty in system performance: an estimate in the probability that the system will perform, in conjunction with the confidence that we have in that estimate.

Clearly, a balance must be obtained between the information gained from testing and modeling at various levels of system indenture, the resources required to perform testing and develop models, and the uncertainties associated with predicting system performance. The ability to logically combine information

Copyright 2005 by CRC Press LLC

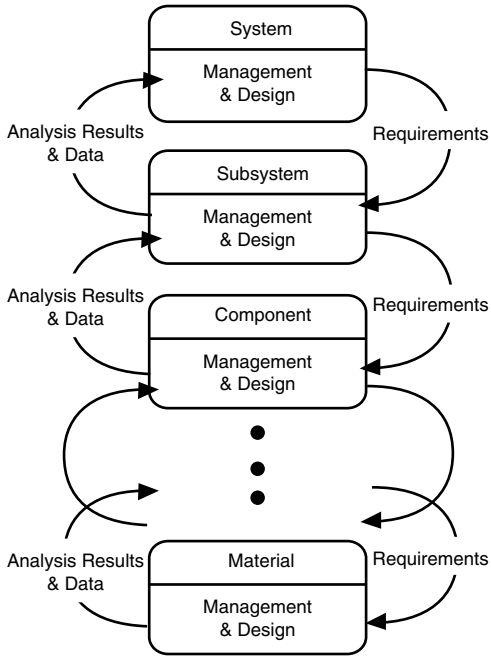

FIGURE 7.1 Systems engineering process.

from these various areas — as well as the organization, characterization, and quantification of this myriad of uncertainties — are critical elements of the system design and analysis processes. Importantly, although the ultimate objective is to obtain accurate predictions, it must be recognized that real merit also exists for simply obtaining more robust solutions than are presently possible (i.e., simply improving the confidence in the estimates of useful life).

7.1.2 The Need for a New Approach

As noted by the Greek philosopher Herodotus in roughly 500 B.C., "A decision was wise, even though it led to disastrous consequences, if the evidence at hand indicated it was the best one to make; and a decision was foolish, even though it led to the happiest possible consequences, if it was unreasonable to expect those consequences." Fundamental to implementing a systems approach will be the need to consider all the evidence at hand through the use of nondeterministic methods, in particular through a Bayesian approach. Classical statistical methods, those based on a frequency approach, permit the combination of point estimates but stumble when confidence in system-level performance must be characterized. In addition, classical Bayesian methods permit the logical combination of test data but do not fully incorporate all available information. Specifically, *classical* Bayesian methods assume that the articles under test are not related in any manner although the articles may be identical. Alternatively, *hierarchical* Bayesian methods permit the relationship between test articles to be explicitly included in the analysis.

In particular, the use of this more modern methodology provides a formal process for synthesizing and "learning" from the data that is in agreement with current information sciences. It permits relevant expert opinion, materials aging, sparse field data, and laboratory failure information to be codified and merged.

In addition to providing an objective means of combining information, Bayesian methods provide a structured tool for robust model development. For example, if laboratory experiments and detailed mathematical simulations are too expensive, empirical models based on data from field measurements and component/subsystem testing can drive model refinement. In addition, this methodology has the potential to address both failures due to aging effects and random failures due to unaccounted-for latent defects.

Copyright 2005 by CRC Press LLC

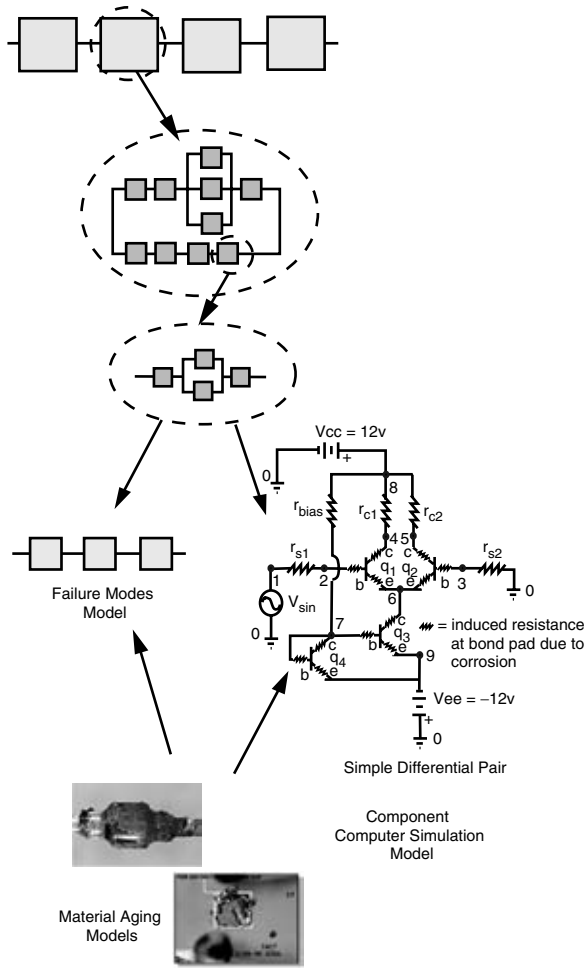

FIGURE 7.2 Systems engineering approach to reliability design.

The foundation for what is referred to today as Bayesian analysis was first formalized by Presbyterian minister Thomas Bayes of Tunbridge Wells, Kent. His article entitled "Essay towards Solving a Problem in the Doctrine of Chances" was published posthumously in 1763 in the *Philosophical Transactions of the Royal Society of London.* However, the work was rediscovered in 1774 by Pierre Laplace and it is his (i.e., Laplace's) formulation that is commonly referred to today as Bayes theorem.

In the early twentieth century, mathematicians became uncomfortable with the concept of only using available information to characterize uncertainty. The concept of long-run relative frequency of an event based on an infinite number of trials became popularized by researchers such as Kolomogorov, Fischer, and Neyman, among others. Practitioners of this latter mathematical philosophy are commonly referred to as Frequentists. However, because it was actually impossible to observe an infinite number of trials, various data transformations (i.e., statistics) were developed. The result has been an array of different statistics for different applications, leading to the cookbook type of statistics commonly practiced today.

At about this same time, Jefferys [2] published one of the first modern books on Bayes theory, uncovering the work by Laplace many years earlier. Unfortunately, the work appeared at the same time that maximum likelihood estimation was being popularized in the literature and much of the potential impact was not realized.

Copyright 2005 by CRC Press LLC

In recent years, the work of Bayes, Laplace, and Jefferys has received increasing attention for a wide variety of related reasons. Information sciences and the rise of decision theory as an aid to management are the most recent additions to the list. For engineers, the high cost of testing has led to a push to investigate some alternative means to extort as much information as possible from existing data.

To appreciate why alternative methods of processing information are important, consider the problem of a bag containing five red balls and seven green balls [3]. On a particular draw we choose a ball, with probability 5/12 and 7/12 of picking a red or a green ball, respectively. If, after the initial selection, the ball is not returned to the bag, then the chance of picking either a green or red ball on the next selection depends on the prior selection. On the other hand, if no information regarding the result of the first selection is available and a green ball is chosen on the second draw, what can be said about the probability of choosing a red or green ball on the first pick? Intuition suggests that the results of the second selection should not influence the probability of choosing a red or green ball on the first draw. However, before answering this, consider the situation where there is only one red ball and one green ball in the bag. Clearly, the information available as a result of the second draw influences the guess as to the first selection. It is this use of information in a *conditional* manner that provides additional insight into problems not otherwise possible and is the key to a Bayesian approach to test plan design and data analysis.

Beyond costly system-level testing, possible information sources include materials testing, subsystem laboratory testing as well as data from similar systems, and finally computer simulations. From the perspective of increasing confidence in the final decision (within budget constraints), it is of immense importance to efficiently use information from all available sources. For example, information from analysis or testing at the subsystem level is commonly used to make system-level assessments because laboratory testing is generally much less expensive than full system testing in an operational environment.

This approach has been particularly appealing for those situations where extensive system testing is impractical for a variety of reasons (e.g., cost of prototype development) or even impossible due to international treaties (e.g., nuclear weapons). While there is no substitute for full-scale testing in a realistic operational environment, it is always difficult to justify not considering data from all relevant sources.

The use of condition-based logic — given this information, then I expect these results — contrasts greatly with the more popular approach — this exact situation has happened many times, so I expect it will happen again — or equivalently — this has never happened before so it will never happen in the future. The application of Bayesian methods, and inductive reasoning in general, permits the analyst to provide answers to a variety of questions with increased confidence. For engineers, Bayesian methods provide a logical, structured approach to assess the likelihood of new events that are outside the current reality and cannot be directly measured.

7.2 An Inductive Approach

From basic probability theory the conditional distribution of variable **Y** given variable **X** is defined as:

$$f(y \mid x) = \frac{f(y, x)}{f_x(x)}$$

where $f(y, x)$ is the joint density function of (**Y**, **X**) and $f_x(x)$ is the marginal density function for random variable **X**. Because we know that: $f(y, x) = f(y)f(x \mid y)$, it follows that:

$$f(y \mid x) = \frac{f(y, x)}{f_x(x)} = \frac{f(y)f(x \mid y)}{f_x(x)} = \frac{f(y)f(x \mid y)}{\int_x f(y, x)dy} = \frac{f(y)f(x \mid y)}{\int_x f(y)f(x \mid y)dy} \tag{7.1}$$

summarizing the foundation of Bayes theorem. The distribution $f(y)$ characterizes random variable **Y** before information about **X** becomes available and is referred to as the *prior* distribution function.

Copyright 2005 by CRC Press LLC

Similarly, the distribution $f(y|x)$ is referred to as the *posterior* distribution. Note also that because $\int_x f(y)f(x|y)dy$ depends only on the **X** and not on **Y**, the integration is simply a normalization constant and therefore:

$$f(y|x) \propto f(y)f(x|y)$$

The distribution $f(x|y) \equiv l(y|x)$ and is referred to as the likelihood function, incorporating information available about **X** into the characterization of **Y**.

In our context, to contrast Bayes theorem with the traditional Frequentist approach, let us characterize a random variable **Y**, probability density function $f(y)$, with for example a parameter vector $\boldsymbol{\theta} = \{\alpha, \beta\}$. From a Frequentist perspective, the parameters α and β are fixed quantities that can be discovered through repeated observation. However, from a Bayesian point of view, parameter $\boldsymbol{\theta}$ is unknown and *unobservable*. Further, the probability that a sequence of values is observed for **Y** is explicitly conditioned on the value that this parameter assumes that:

$$f(y_1, y_2, \ldots, y_n|\boldsymbol{\theta})$$

7.2.1 Family of Bayesian Methods

As previously alluded to, within the family of Bayesian analysis techniques there are two broad frameworks: (1) empirical Bayes and (2) hierarchical Bayes. The classifications "empirical" and "hierarchical" are unfortunately all too common in the literature; all Bayesian methods are empirical in nature and all can be described as being hierarchical in the fashion in which data is accumulated.

Hierarchical Bayes is the more recent addition to the family, is considerably more efficient than the empirical Bayesian approach, and is suggested as the general direction for future research. The hierarchical Bayes approach is also less sensitive to the choice of the prior distribution parameters, typically the focus of a great deal of emotional discussion.

7.2.1.1 Empirical Bayes

The foundation for empirical Bayes — or more specifically, parametric empirical Bayes — has been in place since von Mises in the 1940s, but really came into prominence in the 1970s with the series of papers by Efron and Morris, (see, e.g., [4]). There have been a number of excellent publications in which the authors have made the effort to explain the theory and logic behind empirical Bayes and its relationship to other statistical techniques [5, 6].

Again, consider the random variable **Y**, probability density function $f(y)$, with for example a parameter vector $\boldsymbol{\theta} = \{\alpha, \beta\}$. From an empirical Bayes perspective, **Y** is explicitly conditioned on the value that this parameter assumes that $f(y_1, y_2, \ldots, y_n|\boldsymbol{\theta})$, where $\boldsymbol{\theta} = \{\alpha, \beta\}$ is unknown, unobservable, and the prior beliefs about $\boldsymbol{\theta}$ are estimated from data collected during analysis.

However, some subtle problems exist with the empirical Bayesian approach. First, point estimates for the prior parameters lack consideration for modeling uncertainty. Second, in general, any available data would have to be used once to form a prior and then again as part of the posterior; that is, data would be used twice and result in an overly conservative estimate of the elements of $\boldsymbol{\theta}$.

In general then, empirical Bayesian methods represent only an approximation to a full Bayesian analysis. They do not represent a true Bayesian analysis of the data because a traditional statistical approach is used to estimate the parameters of the prior distribution. Alternatively, in a hierarchical Bayesian approach, data analysis, and all prior and posterior distribution characteristics are estimated in an integrated fashion.

7.2.1.2 Hierarchical Bayes

The distinguishing feature of this Bayesian technique is the hierarchical nature in which information is accumulated. Using the example from the previous section, it is now assumed that the parameter

Copyright 2005 by CRC Press LLC

$\boldsymbol{\theta} = \{\alpha, \beta\}$ is an *unknown* hyperparameter vector described via a prior distribution $f(\boldsymbol{\theta})$. Now it is assumed that $\boldsymbol{\theta}$ is also a random variable and the uncertainty in the hyperparameters is addressed explicitly. For example, the complete Bayesian analysis for characterizing the density function $f(\alpha \mid \mathbf{y})$ requires a description of the vector of random variables $\boldsymbol{\theta} = \{\alpha, \beta\}$ with joint prior distribution:

$$f(\alpha, \beta) = f(\alpha \mid \beta) f(\beta)$$

and joint posterior distribution:

$$\begin{aligned} f(\boldsymbol{\theta} \mid \mathbf{y}) &\propto f(\alpha, \beta) l(\alpha, \beta \mid \mathbf{y}) \\ &= f(\alpha, \beta) f(\mathbf{y} \mid \alpha, \beta) \end{aligned} \tag{7.2}$$

Note that the joint posterior density function $f(\alpha, \beta \mid \mathbf{y})$ can be written as a product of the hyperprior $f(\boldsymbol{\theta})$, the population distribution $f(\alpha \mid \beta)$, and the likelihood function $l(\boldsymbol{\theta} \mid \mathbf{y})$. Under the assumption of an independent and identically distributed set of samples, $\mathbf{y} = \{y_1, \ldots, y_N\}$, an analytical expression for the conditional posterior density of $f(\alpha \mid \beta, \mathbf{y})$, can be easily constructed as the product of the density functions $f(y_i)$.

In the case of conjugate density functions, a solution is available directly. Once an expression for the joint posterior function is found, the marginal posterior distribution can be found through direct evaluation or via integration:

$$f(\alpha \mid \mathbf{y}) = \frac{f(\boldsymbol{\theta} \mid \mathbf{y})}{f(\beta \mid \alpha, \mathbf{y})} = \int f(\alpha, \beta \mid \mathbf{y}) d\beta. \tag{7.3}$$

Because it is rare that either direct evaluation or integration is possible, an alternative is the use of simulation to construct the various conditional density functions:

- Generate a sample of the hyperparameter vector β from the marginal distribution function, $f(\beta \mid \mathbf{y})$.
- Given β, generate a sample parameter vector α from $f(\alpha \mid \beta, \mathbf{y})$.
- A population sample can be then be generated using the likelihood function $l(\mathbf{y} \mid \alpha, \beta)$.

(For a more detailed discussion see the summary by Robinson [7].) Generally, these steps will be difficult to accomplish due to the problems associated with generating samples from complex conditional distributions. A simulation technique particularly suited for this task, Markov Chain Monte Carlo simulation, is introduced in the following section. Two recent applications of hierarchical Bayesian methods in the structural reliability area that utilize this approach are Wilson and Taylor [8] and Celeux et al. [9]. Because of the truly objective fashion with which data is integrated together, further efforts in the hierarchical Bayesian area hold the most promise for further research. A key piece of technology that makes the use of hierarchical Bayesian methods possible is Markov Chain Monte Carlo simulation [10].

7.3 Information Aggregation

Before addressing the challenge of aggregating data from various sources and levels of analysis, it is important to understand a key difference (and benefit) between Frequentist and Bayesian analysis techniques: the interpretation of confidence statements. It is the unique nature with which confidence intervals are interpreted in Bayesian methods that suggests their use in a systems engineering framework by permitting the aggregation of information.

Copyright 2005 by CRC Press LLC

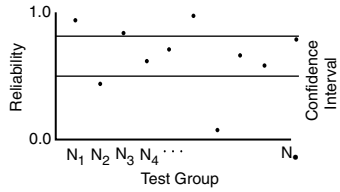

FIGURE 7.3 Confidence intervals: Frequentist.

7.3.1 Confidence Intervals

A Frequentist does not view the system parameters as random variables but rather as *constants* that are unknown. As such, it is not possible to make statements regarding the *probability* that the parameters lie within a particular interval. To characterize confidence intervals from a Frequentist perspective, it is necessary to imagine a very large (potentially infinite) ensemble of tests. All parameters in each group of tests are assumed to be held fixed, with the exception of the parameter of interest (e.g., system reliability). Therefore, the reliability of each group will be different and can be calculated. After an extremely large number of groups are tested and the reliability calculations collected, a fraction of reliability values would fall within a band of reliabilities. This "band" is referred to as a confidence interval for the reliability (see Figure 7.3).

Note that a large number of groups of tests are not actually conducted but are only imagined. It also bears repeating that, because system reliability is not a random variable, it cannot be stated that there is a probability that the true reliability falls within these confidence intervals.

The Bayesian interpretation of confidence intervals is slightly less abstract. Under a Bayesian approach, the reliability of the system is a random variable with density function $f(p)$. The parameters of the density function can be estimated from existing data, as in the case of empirical Bayesian methods, or can also be random variables with associated probability density functions (e.g., hierarchical Bayes).

In any case, because the reliability is a random variable, it is possible to make probability statements regarding the likelihood of the true reliability being in a particular interval as depicted in Figure 7.4. And because the reliability of each subsystem is a random variable, it will be seen that the aggregation of information from various sources and levels of analysis is therefore straightforward.

7.3.2 Data Congeries

A number of authors have suggested methods for combining subsystem and system data into congeries under a Bayesian framework (see, e.g., [11–13]). In general, these papers, along with a number of others, support analysis approaches that permit the collection of test data from a number of levels of system indenture, into an overall estimate of the system reliability. The methods all depend on a combination of analytical techniques for combining test information and inherently depend on assumptions regarding the underlying distribution function.

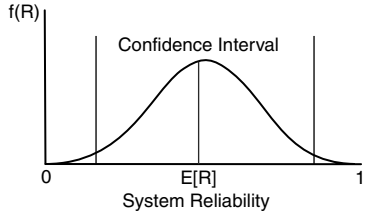

FIGURE 7.4 Confidence intervals: Bayesian.

Copyright 2005 by CRC Press LLC

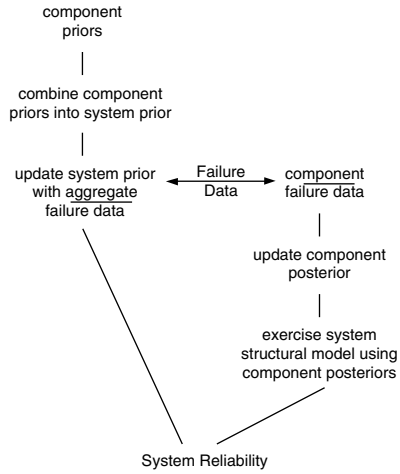

FIGURE 7.5 Data aggregation options.

As noted in the papers above, the aggregation of system and component level data can become involved. In general, the system-level reliability distribution derived from component data is used as a prior for the reliability distribution based on system level data (Figure 7.5). However, when component- and system-level failure and performance information is collected at the same time, aggregation of component data into a system-level analysis may not result in the same reliability prediction as obtained from the system data alone (see, e.g., Azaiez and Bier [14]).

Preliminary efforts in this area are discussed in [7], but considerable work remains. In particular, aggregation issues must be strongly considered as new analysis methods are developed to support time-dependent analysis of material aging and degradation processes.

7.4 Time Dependent Processes

Consideration of potential nondeterministic characteristics of time-dependent processes in concert with a total systems approach is one of the more challenging aspects of future NDA research. There are two critical aspects: (1) the estimation of the current state of the system in the presence of past degradation and, (2) the prediction of future system performance with the expectation of continued aging. The overall goal is to use NDA techniques to improve the ability to *anticipate* the occurrence of a failure, something not possible with deterministic methods (Figure 7.6).

However, before delving into possible research directions, it is important to appreciate the distinction between the failure rate of the underlying time-to-failure distribution and the process failure rate. It is important for the engineer interested in characterizing time-dependent processes (specifically degradation) to understand how each concept applies to the particular problem at hand.

7.4.1 Distribution or Process Model?

An often-confusing aspect of aging/degradation analysis is the distinction between hazard function for the distribution and the failure rate for the underlying degradation process.

Let $N(t)$ denote the number of cumulative failures that occur in the interval (0, t]. The set of points on the timeline associated with occurrence of failures form what is referred to as a *point process.* The expected number of failures in the interval (0, t] is defined as $E[N(t)]$. When addressing the situation

Copyright 2005 by CRC Press LLC

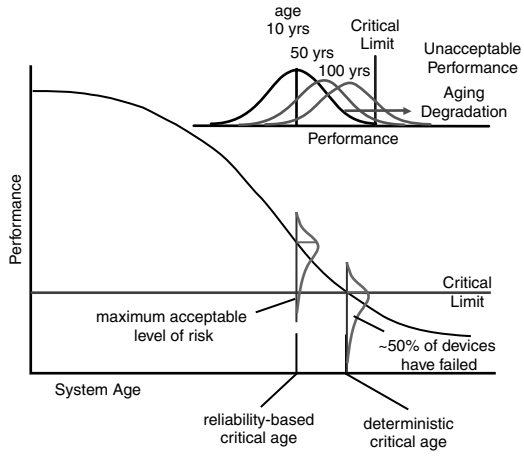

FIGURE 7.6 Anticipation of failure.

that might exist during design, $E[N(t)]$ will be assumed to be a continuous, nondecreasing function and, then, assuming its derivative exists, let

$$\lambda(t) = \frac{dE[N(t)]}{dt}.$$

Therefore, $\lambda(t)$ represents the instantaneous change in the number of failures per unit time; that is, the rate at which failures occur and $\lambda(t)$ is referred to as the *failure rate of the process*. Assuming that simultaneous failures do not occur:

$$\lambda(t) = \lim_{\Delta t \to 0} \frac{P[N(t, t+\Delta t) \geq 1]}{\Delta t} \tag{7.4}$$

For small Δt, $\lambda(t)\Delta t$ is approximately the probability of a failure occurring in the interval $(t, t+\Delta t]$.

Now consider the hazard function: the probability of a failure per unit time occurring in the interval, given that a failure has not already occurred prior to time t. Let the density and distribution functions of the system lifetime **T** be $f(T)$ and $F(T)$, respectively. Define $1-F(T) = \overline{F}(T)$. Then:

$$h(t) = \frac{P[t \leq T \leq t+\Delta t \mid t \leq T]}{\Delta t}. \tag{7.5}$$

Substituting the appropriate expressions and taking the limit yields:

$$h(t) = \lim_{\Delta t \to 0} \frac{\overline{F}(t) - \overline{F}(t+\Delta t)}{\Delta t \overline{F}(t)} = \frac{f(t)}{1-F(t)} \tag{7.6}$$

Thus, we have the instantaneous *failure rate of the distribution* of the system lifetimes.

To compare process and distribution failure rates, suppose for example that we have n units with identical hazard rate characteristics as discussed above. Let $N(t)$ represent the number of units that have failed by time t. Thus, $\{N(t)\}$ represents the point process discussed previously.

Copyright 2005 by CRC Press LLC

The random variable $N(t)$ is then binomially distributed:

$$P[N(t)=k]=\binom{n}{k}F^k(t)[1-F(t)]^{n-k} \qquad k=0,1,\ldots,n \tag{7.7}$$

The expected value of $N(t)$ is given by $nF(t)$, and the rate at which failures occur is:

$$\frac{dE[N(t)]}{dt}=nf(t)$$

the failure rate of the process. However, the failure rate of the distribution is given by $h(t)$.

Care must be taken to ensure which changing failure rate is of interest because the difference between a changing failure rate for the process will be significantly different from the failure rate for the density function. The above discussion focused on continuous parameter systems. Similar results hold for discrete parameter systems.

Significant progress has been made in understanding and characterizing those situations where, in the presence of either growth or degradation, the uncertainties in system parameters and system age are separable. In particular, characterization of the improvement in the probability of system performance as the design process progresses is referred to as reliability growth and has received a great deal of attention in the past few decades. The appreciation that reliability is changing during the course of design has led to a significant decrease in the development time of complex systems and has resulted in greatly improved reliability of deployed systems. Unfortunately, until rather recently, little attention has been paid to the "other end" of the system life cycle — the degradation of system performance.

A large number of publications have dealt with time-dependent system performance for those situations where the uncertainties in physical characteristics are separable from the temporal characteristics. This emphasis has resulted from a number of factors, the foremost being (1) a significant number of real problems fall into this category and (2) the mathematics are within reach of most engineers. The benefit of these applications is clear in many areas (the area of fatigue life, for example); however, a number of substantial gaps remain.

A common theme of previous discussion in this chapter has been the need to incorporate historical data to improve the confidence in the analyses. This need is even more critical when dealing with time-dependent processes; the projection of system performance 10, 30, or even 100 years into the future requires substantial confidence in the ability to characterize *current* system performance. One direction of potentially fruitful research lies in the areas of longitudinal and nonlinear Bayesian analysis. Longitudinal analysis involves repeated measurements on a collection of individuals taken over a period of time. A substantial body of work exists in the area of pharmacokinetics and trajectory analyses of disease incidence and mortality [15, 16].

Another area that holds promise for making significant inroads into this problem is with the continued research into those situations where time is inseparable from the uncertainties. The area of stochastic differential equations holds promise for providing insight into the additional complexities that present themselves in these unique problems. Discussion of this area is left for more qualified hands in other chapters.

7.5 Value of Information

Previous discussion focused on tackling problems from a systems perspective and highlighted the need to develop new methods for bringing data together efficiently from possibly disparate sources. On the other side of the discussion is the decision as to where to focus resources to collection information as efficiently as possible. However, there is no such thing as a free lunch; each laboratory experiment, each flight test brings a new piece of the puzzle — but at a price. Even computer simulations are no longer "free" in the usual sense; some simulations can take on the order of days, making the additional

Copyright 2005 by CRC Press LLC

effort of considering uncertainty costly from a variety of perspectives, including the time to complete a full analysis.

So how does a decision maker decide where to spend his or her resources: additional computer model fidelity or additional computer simulations? On which variables should the experimental tests be focused, and will specific test equipment have to be developed? Clearly, as depicted in Figure 7.7, the value of new information decreases as the uncertainties decrease, and the focus needs to be on where in the process is the most cost-effective way to reduce this uncertainty.

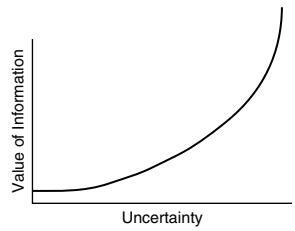

FIGURE 7.7 Value of information.

The expected value of information will be defined as the difference between the benefit or value $u(x, \boldsymbol{\theta})$ of an optimal decision after the data x is available and the value of an optimal decision if the data had not been collected $u(\boldsymbol{\theta})$:

$$EVI = \int_x \left[\int_{\boldsymbol{\upsilon}} u(x, \boldsymbol{\theta}) f(\boldsymbol{\theta} \mid x) d\boldsymbol{\theta} \right] f_x(x) dx - \int_{\boldsymbol{\theta}} u(\boldsymbol{\theta}) f(\boldsymbol{\theta}) d\boldsymbol{\theta} \tag{7.8}$$

The value of information about a parameter $\boldsymbol{\theta}$ depends on the prior distribution characterizing the current information $f(\boldsymbol{\theta})$. The impact of a data x from an experiment on the parameter $\boldsymbol{\theta}$ is found through application of Bayes theorem:

$$f(\boldsymbol{\theta} \mid x) = \frac{f(\boldsymbol{\theta}, x)}{f_x(x)} = \frac{f(\boldsymbol{\theta}) f(x \mid \boldsymbol{\theta})}{\int_{\boldsymbol{\theta}} f(\boldsymbol{\theta}) f(x \mid \boldsymbol{\theta}) d\boldsymbol{\theta}} \tag{7.9}$$

After data is collected (e.g., computer simulation or laboratory experiment), the expected posterior distribution $f(\boldsymbol{\theta} \mid x)$:

$$\begin{aligned} E[f(\boldsymbol{\theta} \mid x)] &= \int_x f(x) f(\boldsymbol{\theta} \mid x) dx \\ &= \int_x f_x(x) \left[\frac{f(\boldsymbol{\theta}) f(x \mid \boldsymbol{\theta})}{f_x(x)} \right] dx \\ &= f(\boldsymbol{\theta}) \end{aligned} \tag{7.10}$$

which indicates that the *expected* uncertainty (as characterized by the posterior) after the data has been collected is fully characterized by the prior distribution. Clearly, information will be gained by the additional data, but the content of that information cannot be anticipated from the information currently available. So what can be discerned about the value of additional information? Consider the well-known situation where $f(\boldsymbol{\theta})$ is Gaussian and the likelihood function $l(\boldsymbol{\theta} \mid x) \equiv f(x \mid \boldsymbol{\theta})$ is also Gaussian. In this case, any additional data cannot increase uncertainty (i.e., increase posterior variance) and, in general, the expected variance of the posterior distribution cannot exceed the prior variance because:

$$V[f(\boldsymbol{\theta})] = E[V[f(\boldsymbol{\theta} \mid x)]] + V[E[f(\boldsymbol{\theta} \mid x)]] \tag{7.11}$$

Copyright 2005 by CRC Press LLC

Unfortunately, this well-known relationship is true only in expectation and can be misleading when it is used to assess the value of specific information. In particular, it can be disconcerting for those who depend on this as an argument to justify additional data that, in general, *additional data does not guarantee a decrease in uncertainty* [17]. For example, a larger posterior variance results in the situation where both prior and likelihood functions are *t*-distributions. Situations can be constructed where the resulting posterior is actually bi-modal, further complicating the characterization of information value.

Clearly, research into how the value of information is measured is necessary. Some efforts have been made in utilizing information theory (e.g., entropy) as a basis for measuring value of additional data. For example, Shannon's measure of entropy can be used to measure the difference between the prior and posterior distributions (defined over common support $\boldsymbol{\Omega}$):

$$V = \int_{\Omega} f(\boldsymbol{\theta} \mid x) \ln\left(\frac{f(\boldsymbol{\theta} \mid x)}{f(\boldsymbol{\theta})} \right) dx \tag{7.12}$$

When discussion turns to the value of information, it is generally assumed that the topic is related to experiments of a physical nature. However, as noted above, there is increased reliance on computer simulation to support characterization of uncertainty. A critical area for research is the identification of efficient computer simulations; what are the minimum scenarios that need to be explored to characterize uncertainty to the required degree of confidence? The need is even greater and the research gap even wider when time dependency is required in the analysis. Some significant inroads have been made, for example, in the area of importance sampling; however, much important research remains.

A great deal of research must be successfully accomplished before a useful tool is available to assist decision makers in assessing the value of information, be it from computer simulations or from laboratory experiments. With the increasing scarcity and escalating cost of information, research in this area will become critical and has the potential to position nondeterministic methods as one of the significant design and analysis tools during the life of a system.

7.6 Sensitivity Analysis

An area closely related to value of information is *sensitivity analysis.* There is a vast quantity of literature related to sensitivity analysis typically based on some form of variance decomposition. Because this is a topic discussed in other chapters, the discussion herein is very limited. It is noted however that a drawback of current sensitivity analysis methods is the limited consideration for *global* sensitivity. The strength of the variance decomposition methods common in the literature lies in the assumption that the uncertainty in the response of a system can be characterized through an at least approximate linear transformation of internal and external uncertainties. Unfortunately, the applicability of such linear relationships is becoming increasingly rare as systems being analyzed and associated models have become increasingly complex (and nonlinear) except under very localized conditions within the problem.

7.7 Summary

The previous discussion focused on those areas of research that I believe must be tackled before nondeterministic methods can enter mainstream use for engineering design and analysis. The emphasis has been on specific topics with a central theme: to have a long-term impact, research in nondeterministic methods must support a systems approach to design and analysis. Clearly, a discussion suggesting that particular areas of research deserve particular attention will be biased toward the perceptions and experience of the

Copyright 2005 by CRC Press LLC

author. In defense of the above discussion, it should be noted that successful progress in any of the areas would have immediate value.

There have been a couple of notable omissions. In particular, an important area not discussed where increased attention would be of immediate value relates to *verification and validation.* This topic is also left in more knowledgeable hands for discussion in another chapter.

Another area that has received a great deal of recent focus in the literature relates to the classification of uncertainty into different categories: that is, probabilistic, possibilistic, epistemic, aleatory, etc. One important objective of these efforts is to provide engineers and decision makers with insight into the role that each of these variables plays in the analysis, with a goal of trying to better model and control these uncertainties. Clearly, the subject of this chapter has been constrained to probabilistic-type random variables but there is considerable promise in investigating possibilistic or fuzzy types of nondeterministic analysis. One benefit of the fuzzy approach is that the methods are relatively immune to the complexity of the system under scrutiny and, as such, hold promise for having a long-term impact. Unfortunately, they remain viewed by some as "fringe" technologies, much as probabilistic-based methods were a few decades ago.

Classification of probabilistic variables into epistemic and aleatory has also received a great deal of attention from the research community. However, similar to classifying variables as "strength" and "stress" variables, there does not seem to be much to be gained in return for the investment because the classification is somewhat arbitrary and can possibly change during the course of a single analysis iteration.

Finally, the growing volume of literature in the nondeterministic methods area guarantees that a contribution in any one of the research topics might have been overlooked and therefore my apologies in advance for my ignorance; the omission of a particular topic is certainly not intended to diminish any research currently in progress.

References

1. Lockheed Missiles and Space Company, Inc., SSD Systems Engineering Manual, Code 66, Sunnyvale, CA, 1994.
2. Jeffreys, H., *Theory of Probability,* 3rd ed., Oxford University Press, 1939.
3. Jaynes, E.T., Clearing up mysteries—the original goal, in *Maximum Entropy and Bayesian Methods in Applied Statistics,* J.H. Justice, Ed., Cambridge University Press, Cambridge, 1989.
4. Efron, B. and Morris, C., Limiting the risk of Bayes and empirical Bayes estimators. Part II: The empirical Bayes case, *J. Am. Stat. Assoc.,* 67, 130, 1972.
5. Deely, J.J. and Lindley, D.V., Bayes empirical Bayes, *J. Am. Stat. Assoc.,* 76, 833, 1981.
6. Casella, G., An introduction to empirical Bayes data analysis, *Am. Stat.*, 39, 753, 1985.
7. Robinson, D., A Hierarchical Bayes Approach to Systems Reliability Analysis, SAND 2001-3513, Sandia National Laboratories, Albuquerque, NM, 2001.
8. Wilson, S. and Taylor, D., Reliability assessment from fatigue micro-crack data, *IEEE Trans. Rel.*, 46, 165, 1997.
9. Celeux, G., Persoz, M., Wandji, J., and Perrot, F., Using Markov chain Monte Carlo methods to solve full Bayesian modeling of PWR vessel flaw distributions, *Rel. Eng. Sys. Safety,* 66, 43, 1999.
10. Gilks, W.R., Richardson, S., and Spiegelhalter, D.J., Eds., *Markov Chain Monte Carlo in Practice,* Chapman & Hall, New York, 1996.
11. Mastran, D., Incorporating component and system test data into the same assessment: A Bayesian approach, *Oper. Res.,* 24, 491, 1976.
12. Mastran, D.V. and Singpurwalla, N.D., A Bayesian estimation of the reliability of coherent structures, *Oper. Res.*, 26, 663, 1978.
13. Martz, H.F. and Waller, R.A., *Bayesian Reliability Analysis*, John Wiley & Sons, New York, 1982, Chap. 11.

Copyright 2005 by CRC Press LLC

14. Azaiez, M. and Bier, V., Perfect aggregation for a class of general reliability models with Bayesian updating, *Appl. Mathematics and Computation,* 73, 281, 1995.
15. Steimer, J.L., Mallet, A., Golmard, J., and Boisieux, J., Alternative approaches to estimation of population pharmacokinetic parameters: comparison with the nonlinear effect model, *Drug Metab. Rev.,* 15, 265, 1985.
17. Carlin, B., Hierarchical longitundal modeling, in *Markov Chain Monte Carlo in Practice,* Gilks, W.R., Richardson, S., and Spiegelhalter, D.J., Eds., Chapman & Hall, New York, 1996, chap. 17.
18. Hammit, J.K., Can more information increase uncertainty?, *Chance,* 8, 15, 1991.

Copyright 2005 by CRC Press LLC

II

Nondeterministic Modeling: Critical Issues and Recent Advances

Copyright 2005 by CRC Press LLC

Copyright 2005 by CRC Press LLC

Copyright 2005 by CRC Press LLC

8

Types of Uncertainty in Design Decision Making

Efstratios Nikolaidis
The University of Toledo

8.1 Introduction

Uncertainty and types of uncertainty are studied in the context of decision making in this chapter. Concepts from decision theory are used to define a measure of information and the notion of uncertainty. The chapter "The Need for Nondeterministic Approaches in Automotive Design: A Business Perspective," in this book, presents a similar approach to study uncertainty in automotive design.

8.1.1 The Role of Uncertainty in Design Decision Making

Decision is an irrevocable allocation of resources to achieve a desired outcome. Three elements of a decision are alternative courses of action (or choices), outcomes of the actions, and payoffs (Figure 8.1). First, the decision maker defines the decision problem; he or she defines the objectives, the criteria, and the alternative actions. The decision maker tries to predict the outcome of an action using a model of reality. Each outcome is characterized by its attributes. The payoff of an outcome to the decision maker depends on these attributes and the decision maker's preferences. The decision maker wants to select the action with the most desirable outcome.

Decisions involve uncertainty. When framing a decision (defining the context of the decision), the decision maker may not know if the frame captures the decision situation at hand. Also, the decision maker may not know all possible courses of action. Often, a decision maker is uncertain about the

Copyright 2005 by CRC Press LLC

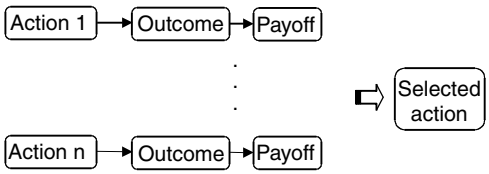

FIGURE 8.1 Decision: Selecting among alternative actions the one with the highest payoff.

outcome of an action, because of a lack of knowledge or inherent randomness. Thus, to the best of the decision maker's knowledge, an action could result in a single outcome, a discrete set of different outcomes, or a continuous range of outcomes (Figure 8.2). Even more challenging are decisions for which the decision maker does not know all possible outcomes of an action. Finally, the decision maker faces uncertainty in assessing the value of the outcomes in a way that is consistent with his or her preferences.

Design of a system or a component, such as a car, is a decision because it involves selection of a design configuration, which is an allocation of resources [1]. The designer is to select the design configuration that will result in the most desirable outcome (e.g., maximize the profit for his or her company).

Example 1: Uncertainty in Design Decisions in Automotive Engineering

The design of an automotive component involves decisions under uncertainty. Figure 8.3a shows two decisions in the design of an automotive component (Figure 8.3b). The objectives of a designer are to (1) find a design with good performance, and (2) minimize the time it takes to find this design. First, a designer determines alternative designs. For simplicity, Figure 8.3a shows only two designs. The designer uses computer-aided engineering (CAE) analysis to predict the performance attributes of these designs (e.g., the stresses or vibration amplitudes at critical locations). The designer must decide whether to select one design or reject both if they fail to meet some minimum acceptable performance targets. In the latter case, he or she must find a new design. In this decision, the designer does not know the true values of the performance attributes of the designs because of:

1. Product-to-product variability
2. Modeling uncertainty and numerical errors in CAE analysis
3. Inability to predict the real-life operating conditions

Because of these uncertainties, the designer builds and tests a prototype and uses the results to decide whether to sign off the design for production or reject it. The test eliminates modeling uncertainty and numerical errors but it introduces measurement errors. Therefore, even after the designer obtains the results of tests, he or she remains uncertain about the true value of the attributes of the design when it will be massively produced. Moreover, when the designer tries to decide whether to sign off or reject the design, he or she is uncertain about the cost and time it will take to find a better, acceptable design.

Decision makers use models of real systems to predict the outcomes of actions. A model is a mathematical expression, $\hat{\mathbf{Y}}(\mathbf{X})$, relating one or more quantities of interest, $\mathbf{Y}$ (e.g., the stiffness of a structure) to a set of measurable variables, $\mathbf{X}$. We use a model to predict the outcome of a design decision

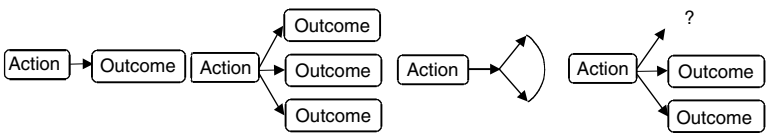

FIGURE 8.2 Decision under certainty (a) and decision under uncertainty (b-d).

Copyright 2005 by CRC Press LLC

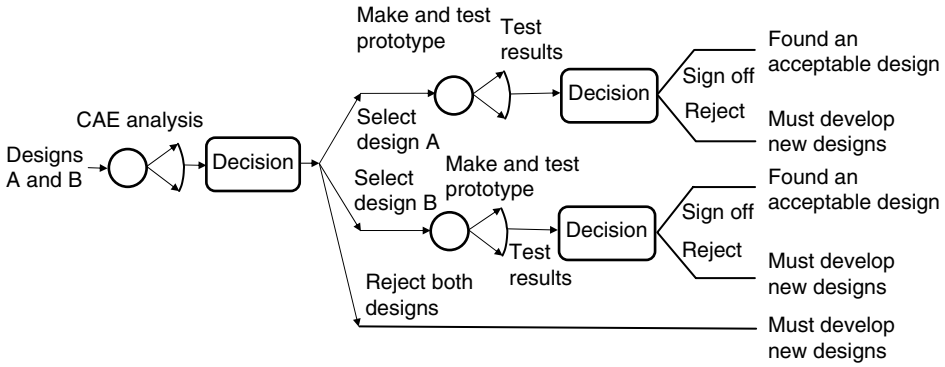

(a)

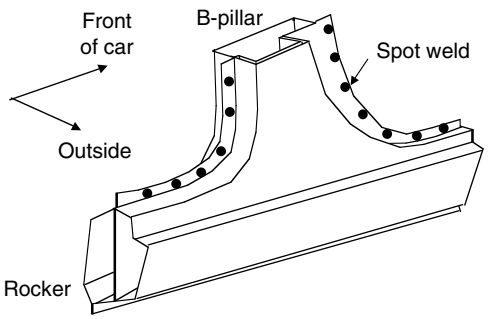

(b)

FIGURE 8.3 Uncertainty in design of an automotive component. (a) Two decisions in design of an automotive component. (b) Automotive component in example 1. *Note*: The decision maker is uncertain of the outcome of the test of the prototype (the measured values of the attributes) before the test. The test can produce a continuous range of values of the attributes.

by predicting the attributes of a selected design (e.g., the stiffness). Figure 8.4 shows the procedure for developing an analytical tool for predicting the outcome of an action. First, a conceptual model of a process or a system is built. This is an abstraction of the system. Then a mathematical model, which is a symbolic model consisting of equations, is constructed based on the analytical model. The equations are solved using a numerical technique to estimate the performance. The figure shows various errors in the analytical prediction of the attributes. These are described in Section 8.2.1.

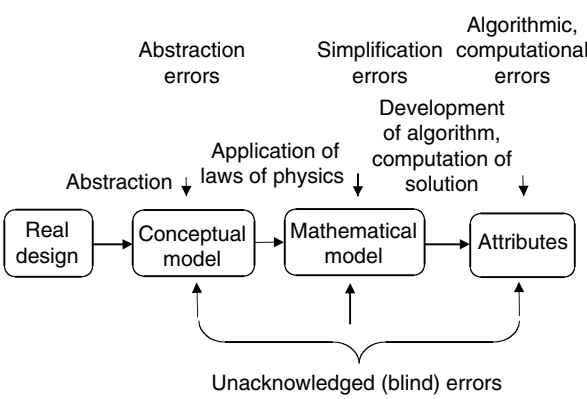

FIGURE 8.4 Analysis of a design to predict its performance.

Copyright 2005 by CRC Press LLC

There is always error in the predictions of analytical tools. Errors result from:

- Use of imperfect model forms (e.g., a linear expression is used, whereas the actual relation between the quantity we want to predict and the variables is nonlinear)
- Variables that affect the outcome of an action but are omitted in the model

The above deficiencies in building models can be due to a poor understanding of the physics of a problem or to intentional simplifications.

The set of variables that affect the outcome of an action can be divided into two subsets: those that are included in a model, $\mathbf{X}$, and those that are missing, $\mathbf{X}'$. Let $\mathbf{Y}(\mathbf{X}, \mathbf{X}')$ be the true relation between the attributes describing the outcome and the uncertain variables. This relation is rarely known; instead, an approximate relation $\hat{\mathbf{Y}}(\mathbf{X})$ is available from an analytical solution and is used as a surrogate of $\mathbf{Y}(\mathbf{X}, \mathbf{X}')$ for making decisions.

Example 2: Developing a Model for Predicting the Response of an Automotive Component

In Example 1, the conceptual model for predicting the performance of a design includes a geometric model, such as a CAD model. The mathematical model is a set of partial differential equations solved by finite element analysis.

Many automotive components consist of thin metal shells fastened by spot welds (Figure 8.3b). An approximate model of a component may replace spot welds with a rigid continuous connection of the flanges of the shells. Then, vector $\mathbf{X}'$ in the previous paragraph includes variables such as the spot weld pitch and diameter, which are missing from the model. Model approximations induce errors, $\varepsilon = \hat{\mathbf{Y}}(\mathbf{X}) - \mathbf{Y}(\mathbf{X}, \mathbf{X}')$, in the response of the component to given loads.

A designer makes decisions when developing a predictive model and solving the model to predict the outcome of an action. The designer has to choose those characteristics of the system or process that should be included in the model, and also choose how to model these characteristics so as to construct a model that is both accurate and affordable. The designer must also choose a numerical algorithm and the parameters of the algorithm (e.g., the step size) so as to compute accurately the attributes of a design at a reasonable cost. Decisions are also involved in solving the model using a numerical algorithm. The payoff of these decisions is a function of (1) the cost of developing and using a predictive model and the solution algorithm, and (2) the information from solving the model to predict the performance. The information could be measured in a simplified manner by the error of the model. A more sophisticated measure of the information a model provides can be the probability that the designer will obtain the most desirable achievable outcome using the model predictions to determine the preferred design [1, p. 341].

8.1.2 Why It Is Important to Study Theories of Uncertainty and Types of Uncertainty

When facing uncertainty, the decision maker cannot select the action that guarantees the most desirable outcome but he or she can select the action with maximum probability to achieve this outcome. To be successful, a decision maker should manage uncertainty effectively, which requires tools to quantify uncertainty. Theories of uncertainty — including probability theory, evidence theory, and generalized information theory — are available for quantifying uncertainty, but there is no consensus as to which theory is suitable in different situations. An important objective of this book is to help readers understand uncertainty and its causes, and the tools that are available for managing uncertainty.

It is important for making good decisions to know all important types of uncertainty and understand their characteristics to construct good models of uncertainty. Decision makers face different types of uncertainty, including uncertainty due to inherent randomness, lack of knowledge, and human intervention. We will see in this chapter that different types of information (e.g., numerical, interval valued or linguistic) are suitable for different types of uncertainty. Understanding different types of uncertainties

Copyright 2005 by CRC Press LLC

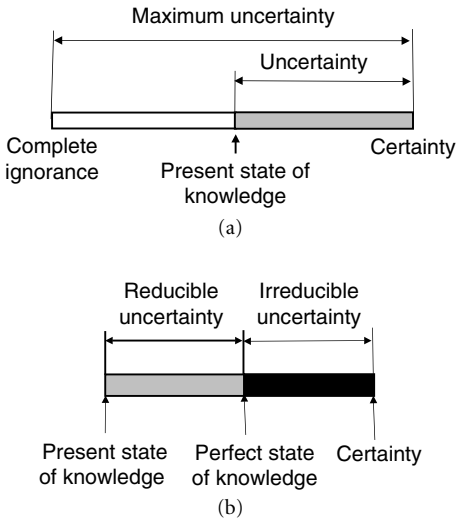

FIGURE 8.5 Illustration of the definition of uncertainty. (a) Uncertainty is the gap between certainty and the present state of knowledge. Information reduces uncertainty. (b) Reducible and irreducible uncertainty.

helps designers allocate resources effectively to collect the most suitable type of information, select the most suitable tools to model uncertainty, and interpret correctly the results of their calculations.

8.1.3 Definition of Uncertainty

We can define uncertainty indirectly based on the definition of certainty. Certainty, in the context of decision theory, is the condition in which a decision maker knows everything needed in order to select the action with the most desirable outcome. This means that, under certainty, the decision maker knows every available action possible and the resulting outcome. Uncertainty is the gap of what the decision maker presently knows and certainty (Figure 8.5a).

When there is complete ignorance, uncertainty is maximum. In this state, the decision maker does not know anything about the likelihood of the outcomes of the alternative actions. Information reduces uncertainty. It helps the decision maker select an action so as to increase the chance of getting the most desirable outcome. When information becomes available to the decision-maker (e.g., sampling information from which the decision maker can estimate the probabilities of alternative actions), uncertainty is reduced. The new state is marked "present state of knowledge" in Figure 8.5a.

Example 3: Uncertainty in Design of the Automotive Component in Example 1

An inexperienced designer knows nothing about the two designs in Figure 8.3. The designer wants to select the best design that meets the targets. But he or she cannot do so because he or she does not know the attributes of the designs. When information from CAE analysis becomes available, some uncertainty is eliminated, which increases the probability that the designer will select the action that will yield the most preferred outcome.

Hazelrigg [1, pp. 340 to 344] defined measures of information and uncertainty by using concepts of decision theory. The amount of information and uncertainty depends on the decision at hand. A measure of the amount of information is the probability that a decision maker's preferred action will lead to the most desired achievable outcome. The preferred action is the one with maximum expected utility, where the utility is determined using the presently known probabilities of the outcomes of the alternative actions. Then Hazelrigg defined the following measure of uncertainty: informational entropy of the decision is the negative natural logarithm of the probability that the preferred choice will *not* result in the most

Copyright 2005 by CRC Press LLC

Hazelrigg's two measures require that the decision maker know all the possible outcomes of each action and can estimate their probabilities.

8.1.4 Objectives and Outline

The objectives of this chapter are to help the reader understand the concept of uncertainty and its significance in decision making, present different categorizations of uncertainty and the types of information for each type of uncertainty. This helps the reader understand which theories of uncertainty and tools for quantifying uncertainty have been designed for each type of uncertainty. These theories and tools are presented in chapters 9 to 12.

This chapter focuses on uncertainties that a designer faces. These uncertainties include uncertainties in simulation to predict the attributes of designs, including their reliability. We appreciated the importance of uncertainties involved in business decisions, such as uncertainties in predicting the demand for a product and the effect of price and marketing on demand. However, these uncertainties are beyond the scope of this chapter.

The chapter starts with a review of various taxonomies of uncertainty. It illustrates these taxonomies on the example of the design of the automotive component in Example 1. The relation between various taxonomies is studied. Then guidelines for what type of information is suitable for each type of uncertainty are presented.

8.2 Taxonomies of Uncertainty and the Relation between These Taxonomies

Uncertainty can be categorized either based on its causes or its nature. There are two main ways for constructing taxonomies of uncertainty. The first primarily considers three sources of uncertainty: inherent randomness, lack of knowledge, and human error. The second way considers the nature of uncertainty.

8.2.1 Taxonomies According to Causes of Uncertainty

Uncertainty is often categorized into aleatory (random) and epistemic. Aleatory uncertainty is due to variability, which is an intrinsic property of natural phenomena or processes. We cannot reduce variability unless we change the phenomenon or the process itself. For example, there is variability in the thicknesses of metal plates produced in an automotive supplier's factory. We cannot reduce variability by collecting data on plate thicknesses. We can only reduce variability by changing the manufacturing process, for example by using better equipment or more skillful operators.

Epistemic uncertainty is a potential deficiency in selecting the best action in a decision (the action with the highest probability of resulting in the most desirable outcome) due to lack of knowledge. Epistemic uncertainty may or may not result in a deficiency; hence the qualifier "potential" is used in the definition. Epistemic uncertainty is reducible; we can reduce it by collecting data or acquiring knowledge. For example, we have reducible uncertainty in predicting the stress in a structure due to deficiencies in the predictive models. Improving our predictive models can reduce this uncertainty. Reducible uncertainty has a bias component. For example, crude finite element models of a structure tend to underestimate deflections and strains.

Example 4: Aleatory and Epistemic Uncertainty in the Design of an Automotive Component

Suppose that the designer of the automotive component in Examples 1 through 3 does not know the probability distribution of the thicknesses of the plates from the supplier's factory. In this example, assume that the only uncertainty is in the thicknesses of the plates. The designer faces both reducible uncertainty

Copyright 2005 by CRC Press LLC

(e.g., does not know the probability distribution of the thickness) and irreducible uncertainty (e.g., even if the designer knew the probability distribution of the thickness, the designer could not know the thickness of a particular plate from the factory). This state is marked as "present state of knowledge" in Figure 8.5b.

The designer starts measuring the thicknesses of plates and estimates the probability distribution of the thickness. As the designer collects more data, the estimated probability distribution of the thickness approaches the true one and the epistemic uncertainty decreases. Eventually, the designer determines the true probability distribution. In this state, which is marked "perfect state of knowledge" in Figure 8.5b, there is no reducible uncertainty because the designer knows all that could be known. However, there is still irreducible (aleatory) uncertainty because the designer cannot know the thickness of a new plate from the factory. The designer can only know that the new plate comes from a known probability distribution.

The best that a decision maker can do in a decision involving only aleatory uncertainty is to determine the true probabilities of the outcomes of the actions. But consider a decision in which there is only epistemic uncertainty. If the decision maker eliminates epistemic uncertainty by collecting information that allows him or her to understand the physics of the problem and construct accurate predictive models, then the decision maker will know the outcomes of the actions.

Several researchers have refined the above taxonomy of uncertainty into aleatory and epistemic types by considering different species within each type and considering other types of uncertainty. Der Kiuregian [2] considered the following four causes of uncertainty in structural analysis and design: (1) inherent variability, (2) estimation error, (3) model imperfection, and (4) human error, as shown in Figure 8.6a. Estimation error is due to incompleteness of sampling information and our inability to estimate accurately the parameters of probabilistic models that describe inherent variability. Model imperfection is due to lack of understanding of physical phenomena (ignorance) and the use of simplified structural models and probabilistic models (errors of simplification). Imperfections in probabilistic models mean errors in the choice of a parameterized probability distribution. Human errors occur in the process of designing, modeling, constructing and operating a system. We can reduce human error by collecting additional data or information, better modeling and estimation, and improved inspection. Cause (1) is irreducible, whereas causes (2) and (3) are reducible. Human error is also reducible. However, human errors tend to occur randomly.

Gardoni et al. [3] developed a methodology for constructing probabilistic models of the capacity of structures, which accounts for both variability and reducible uncertainty. These models consist of three terms: (1) a deterministic model for predicting the capacity of a structure, (2) a correction term for the bias inherent in the model, which is a function of a set of unknown parameters, and (3) a random variable for the scatter in the model. The user of Gardoni's model has to estimate the parameters of the term for the bias and the standard deviation of the term for the scatter using Bayesian methods and using experimental measurements.

Haukass [4] considered inherent variability and measurement error as two components of aleatory uncertainty (Figure 8.6b). He described two types of epistemic uncertainty: modeling and statistical uncertainty. Modeling uncertainty is due to imperfect idealized representations of reality. In Haukass' study, "statistical uncertainty" refers to the uncertainty caused by the inability to predict the parameters of a probability distribution from a sample (for example, to predict the mean value and the standard deviation of the thickness of plates from the factory from a sample of plates). Note that the term "statistical uncertainty" has been also used for aleatory uncertainty by some researchers. Another type of uncertainty is human error.

Haukaas said that the division of aleatory and epistemic uncertainty is not disjunctive; one component of modeling uncertainty is due to missing some random variables in a model and this component is also aleatory uncertainty (Figure 8.6b). Suppose that in the analysis of the automotive component, the designer neglects the spot welds by assuming that the flanges of the shells are rigidly connected. Then the model that he or she uses neglects the variability in the spot weld pitch and diameter as well as the variability due to failed spot welds.

Copyright 2005 by CRC Press LLC

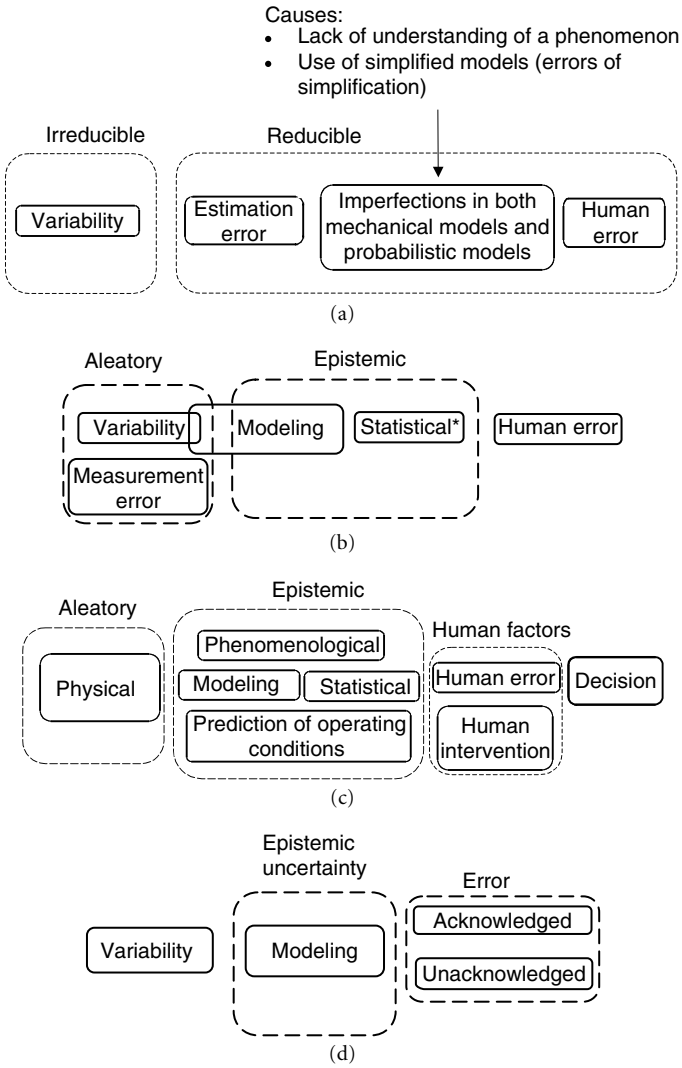

FIGURE 8.6 Taxonomies of uncertainty. (a) Taxonomy of uncertainty by Der Kiureghian [2]. Boxes marked by dashed lines indicate broad categories of uncertainty; solid lines indicate special types within the broad categories. (b) Taxonomy of uncertainty by Haukaas [4]. Modeling uncertainty and variability overlap because modeling uncertainty due to missing random variables in a deterministic model causes variability. *Note*: The term "statistical uncertainty" refers to the uncertainty caused by the inability to predict the parameters of a probability distribution from a sample — it does not refer to variability. (c) Taxonomy of uncertainty by Melchers [5]. (d) Taxonomy by Oberkampf et al. [6]. *Note*: Modeling uncertainty is caused by Vagueness, Nonspecificity and Conflict in the available information.

Melchers [5] considered physical uncertainty as a component of aleatory uncertainty (Figure 8.6c). In addition to physical uncertainty, he described six types of uncertainty:

1. Phenomenological uncertainty (caused by difficulties in understanding and modeling the physics of a novel system)
2. Modeling uncertainty
3. Uncertainty in prediction of the operating conditions, loads, and deterioration of a system during its life
4. Statistical uncertainty

Copyright 2005 by CRC Press LLC

5. Uncertainty due to human factors
6. Decision uncertainty

Melchers divided causes of human error into natural variation in task performance and gross errors. Gross errors occur in tasks within accepted procedures or they are the direct result of ignorance or oversight of the fundamental behavior of systems.

Decision uncertainty is uncertainty in deciding the state of a system, (e.g., deciding if a design whose maximum deflection is given is acceptable).

Oberkampf et al. [6, 7] focused on causes of uncertainty in simulation of physical and chemical processes. He considered (1) variability, (2) epistemic uncertainty, and (3) error (Figure 8.6d). Oberkampf et al. defined epistemic uncertainty as a potential deficiency in any phase of modeling that is due to lack of knowledge. Epistemic uncertainty is caused by incomplete information, which is due to Vagueness, Nonspecificity, and Dissonance (Conflict).These terms will be defined in Section 8.2.2. Epistemic uncertainty was divided into parametric (the analyst does not know the values of the parameters of a system), modeling, and scenario abstraction.

According to Oberkampf et al., error is a recognizable deficiency in modeling that is not due to lack of knowledge. If error is pointed out, it can be corrected or allowed to remain. Error was divided into acknowledged (intentional) and unacknowledged. Discretization errors or round-off errors are examples of acknowledged (intentional) errors. Programming errors, blunders, and mistakes are examples of unacknowledged error.

Oberkampf's definition of error is broader than the definition of human error in other studies presented here. Error includes simplifications of mathematical models and approximations in numerical algorithms. Oberkampf et al. stated that error is not uncertainty because it is not due to lack of knowledge.

Both variability and error cause uncertainty in predicting the outcomes of actions. For example, a designer may be unable to predict if a particular car from an assembly line meets crash requirements because of human errors in the assembly and variability in material properties. The distinction of error and of the effect of epistemic uncertainty is blurred. According to Oberkampf et al., error is a departure from the correct or acceptable modeling procedure. But in many cases there is no consensus of what is an acceptable or correct modeling procedure.

Nowak and Collins [8, pp. 289 to 313] divided causes of uncertainty in building structures into natural and human. Human causes can arise from within the building process and from outside. Examples of the first are errors in calculating loads and load effects and errors in construction, while examples of the second are fires and collisions. Human causes of uncertainty from within the building process occur if one deviates from the acceptable practice, or even if one follows the acceptable practice.

Human errors are defined as deviations from acceptable practice. They can be divided into three types:

1. Conceptual errors, which are departures from the acceptable practice due to lack of knowledge of a particular professional
2. Errors of execution, which are due to carelessness, fatigue, or lack of motivation
3. Errors of intention, (e.g., simplifications in numerical algorithms to reduce computational cost)

Example 5: Different Types of Uncertainty in Automotive Component Design

The following list provides examples illustrating the types of uncertainty presented above.

- *Aleatory uncertainty:* variability in the thicknesses of plates, material properties, spot weld pitch, and diameters of spot welds.
- *Epistemic uncertainty:* uncertainty due to deficiencies in the analytical and mathematical model of a structural component caused by lack of knowledge. Neglecting nonlinearities is an example of a cause of such deficiencies.
- *Blind error:* errors in typing the input data file for finite element analysis, errors in reading stresses and deflections from the output file.
- *Acknowledged error:* a designer assumes that the probability density function of the thickness of a plate is normal without evidence supporting this assumption. The reason is that the designer is under pressure to produce results quickly.

Copyright 2005 by CRC Press LLC

- *Statistical uncertainty:* uncertainty in the mean value and standard deviation of a plate thickness caused by estimating these statistics from a finite sample of measurements. Neglecting the spatial variation in the thickness of a plate is another example of a cause of statistical uncertainty.
- *Measurement error:* errors in measuring the dimensions of plates or spot weld diameters. Errors in measuring the response of a prototype structure to loads.
- *Uncertainty in predicting operating conditions:* uncertainty in predicting the loads on a component during its life.
- *Phenomenological uncertainty:* uncertainty due to the inability to model a new design of the thin wall structure in Figure 8.3b, in which plates are joined by adhesives instead of spot welds.
- *Decision uncertainty:* the component in Examples 1 through 4 was tested under a repeated cyclic loading and a spot weld failed. The designer is uncertain if he or she should consider that the component failed.

8.2.1.1 Importance of Uncertainty Due to Human Errors

Results of surveys show that human error is responsible for the majority of catastrophic failures ([8], p. 292). For example, according to the above reference, 70% of accidents in aviation have been attributed to crew error, and similar results are thought to apply to other industries. Incidents such as Three Mile Island and Chernobyl indicate the importance of human error in the safety of nuclear plants. One cannot obtain an estimate of the failure probability of a system that is indicative of the true failure probability of this system unless one considers uncertainty due to human error. Moreover, if one neglects uncertainty due to human error, one cannot even obtain an estimate of the probability of failure that can be used to compare the safety of designs with different construction types.

8.2.2 Taxonomies According to the Nature of Uncertainty

Studies presented in this subsection consider uncertainty as knowledge deficiency caused by incompleteness in the acquired knowledge. They classify uncertainty according to its cause and the available information.

Zimmermann [9] considered the following causes of uncertainty: lack of information, complexity (which forces one to simplify models of reality), conflicting evidence, ambiguity, measurement error, and subjectivity in forming beliefs. According to Zimmermann, the available information can be numerical, interval-based, linguistic, and symbolic. Numerical information can be nominal (defines objects), ordinal (defines order of objects), and cardinal (in addition to order, it defines differences between ordered objects). An example of nominal numerical information is the plate number of a car, which only defines the particular car. Ordinal information is the ranking of the students in a class based on their performance. This information defines the order of the students in terms of how well they did in the class but does not indicate differences in their performance. Cardinal information is the overall percentage grades of the students in the class — it defines the difference in the performance of the students in addition to their order.

Ayyub [10] presented a comprehensive study of ignorance (lack of knowledge). He divided ignorance into conscious (one is aware of his or her ignorance) and blind ignorance (one does not know that he or she do not know). He considered uncertainty (knowledge incompleteness due deficiencies in acquired knowledge) as a special case of conscious ignorance. He classified uncertainty based on its sources into ambiguity, approximations, and likelihood. Ayyub did not consider conflict as a component of uncertainty. He also explained which theory can handle each type of ignorance.

Klir and Yuan [11] and Klir and Weirman [12] categorized uncertainty on the basis of the type of deficiency in the available information, into vagueness (fuzziness), and ambiguity (Figure 8.7). Ambiguity is a one-to-many relationship. Klir further divided Ambiguity into Conflict and Nonspecificity. We can have Conflict because the same action results in different outcomes (repeated tosses of a die result in different numbers from one to six) or because there is conflicting evidence (three experts provide different estimates of the error in the estimate of the stress in a structure). Nonspecificity occurs when multiple

Copyright 2005 by CRC Press LLC

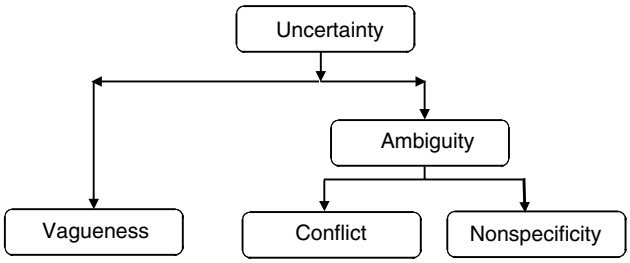

FIGURE 8.7 Taxonomy of uncertainty by Klir and Yuan [11].

outcomes of an action are left unspecified. Fuzziness is the inability to define the boundaries of sets of objects sharing a common property.

Measurements from observations of repeated experiments are often precise but are in conflict. Subjective information from experts is often nonspecific. For example, suppose that we ask an expert for a subjective estimate of the difference between the true value of the stress in a structural component and the predicted value of the stress from a finite element model. It is more likely for the expert to estimate a range for the difference rather than a precise value. The less confident the expert feels about the estimate of the difference, the broader is expected to be the range he or she will provide.

Klir and Weirman have proposed axioms that measures of Conflict and Nonspecificity should satisfy. They also proposed measures for these types as well as a measure of the total uncertainty. These include equations for computing these measures. This is an important contribution because if one disputes the validity of Klir's definitions and measures, then one has to explain which axiom is wrong.

Example 6: Nonspecificity and Vagueness in Error in the Estimate of the Stress in an Automotive Component

The designer estimated the stress in the automotive component described in Examples 1 through 5 using finite element analysis, but does not know the error in the estimate (e.g., the difference between the true value and the estimate of the stress). Figure 8.8a shows a condition called maximum uncertainty, in which the designer does not know anything about the error. The designer asks an expert for an estimate of the error. Often, an expert provides an interval containing the error (Figure 8.8b). This is nonspecific evidence because the exact value of the error is not specified. However, there is no conflict. Finally, the designer conducts an experiment in which he or she measures the stress accurately and determines the exact value of the error for this single experimental validation. Now there is no uncertainty.

Often, an expert will specify the error in the stress in plain English. For example he or she could say that "the error is small." To explain what "small error" means, the expert might specify a few values of the error and the degree to which he considers them small, or construct a plot showing the degree of which the error is small as a function of the value of the error (Figure 8.8c). This is an example of vague or fuzzy evidence. Contrast this case with the case of crisp evidence (the expert provides a sharp boundary between small and not small errors). This latter case is rare because it is difficult to explain why an error of 9.99% is small while and error of 10.01% is not small. Fuzziness in the boundaries of a set is one of the causes of decision uncertainty (see classification by Melchers).

Example 7: Nonspecificity and Conflict in the Thickness of a Plate Selected Randomly from a Batch

A batch of plates is received from the supplier factory. Suppose the designer only knows the range of the thickness based on the factory specifications. Then he or she faces both Nonspecificity and Conflict (Figure 8.9a). There is Nonspecificity because the evidence consists of a range — not a specific value. There is also Conflict because thickness varies from plate to plate in the batch. The designer measures the thicknesses of all the plates in the batch. Now Nonspecificity has been eliminated but Conflict remains for the population that was inspected (Figure 8.9b)

Copyright 2005 by CRC Press LLC

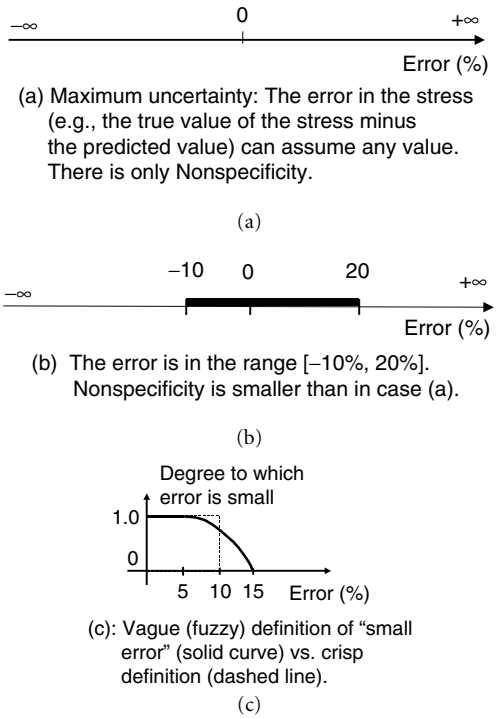

FIGURE 8.8 Illustration of Nonspecificity (a, b), and Vagueness (c).

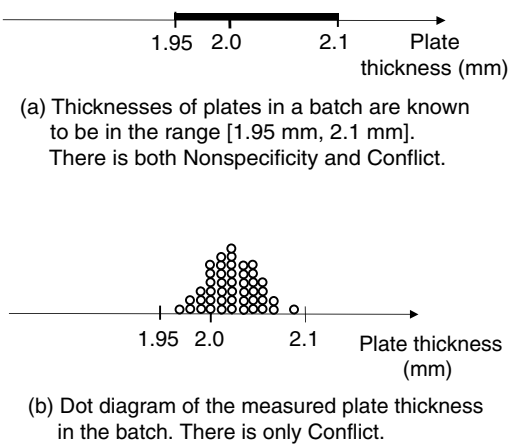

FIGURE 8.9 Nonspecificity and Conflict in the thickness of a plate. Initially there is both Nonspecificity and Conflict (a). After measuring all plate thicknesses there is only Conflict (b).

8.3 Proposed Taxonomy

8.3.1 Types of Uncertainty

Uncertainty in three stages of a decision — namely, framing a decision, predicting the outcomes of actions, and evaluating the payoff of outcomes — will be classified according to its causes. For each type of uncertainty, certain types of information are typically available. These are presented in Section 8.3.2.

Copyright 2005 by CRC Press LLC

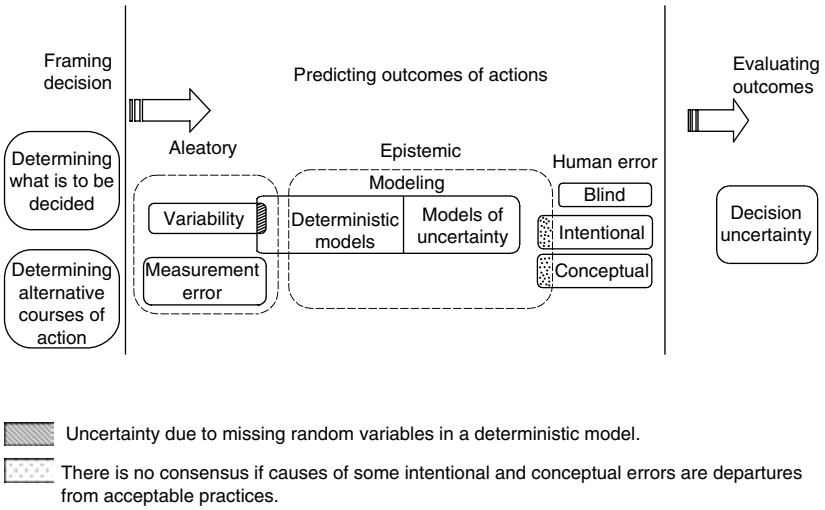

FIGURE 8.10 Proposed taxonomy of uncertainty based on its causes.

8.3.1.1 Framing a Decision

When framing a decision, the decision maker is uncertain if he or she has correctly determined what is to be decided and if all relevant features of the problem are known. For example, although the performance of the automotive component in Figure 8.3b depends on the design of the adjacent beams, a designer neglects this dependence and designs the automotive component in isolation. Moreover, the decision maker is uncertain if he or she has determined all alternative courses of action available. For example the designer of the automotive component may not know all alternative design configurations, which may result in missing the optimum action (the action with highest probability of resulting in the most desirable outcome). This uncertainty is epistemic and is due to lack of creativity and knowledge.

8.3.1.2 Predicting the Outcome of an Action

Here we have the three basic types of uncertainty presented in Section 8.2.1: aleatory, epistemic, and uncertainty due to human error (Figure 8.10). Aleatory uncertainty is caused by variability and measurement error.

We adopt Oberkampf's [6, 7] definition of epistemic uncertainty; epistemic uncertainty is a potential deficiency in any phase of the modeling process that is due to lack of knowledge. There is epistemic uncertainty in both deterministic models for predicting the attributes of a design and in models of uncertainty. As mentioned in the introduction, uncertainty in deterministic models is due to use of incorrect model forms and missing variables. If a probabilistic model of uncertainty is used, uncertainty in models of uncertainty is caused by selecting the wrong type of probability distribution for a random variable or vector and the inability to estimate accurately the parameters of the distribution from a finite sample (Figure 8.10).

The boxes representing variability and epistemic uncertainty in deterministic models partially overlap, indicating that the division of aleatory and epistemic uncertainty is not disjunctive. Specifically, one component of modeling uncertainty is due to missing some random variables in a model and this component is also aleatory uncertainty [4].

Example 8: Uncertainty in Models of Uncertainty in the Design of an Automotive Component

A designer tries to model the probability distribution of the number of defective welds in a component from the numbers of defective welds in a sample of nominally identical components. The designer faces statistical uncertainty. But the sample could be small or nonexistent so that a designer would rely on

Copyright 2005 by CRC Press LLC

first principles-based models, such as a model of the spot welding process, to derive a probability distribution of the number of defective welds in a component. In this case, the designer also faces modeling uncertainty because he or she uses a physics-based model of the spot welding process, which always involves simplifications.

Human error is a departure from accepted procedures. According to Nowak and Collins [8], human error can be divided into execution, intentional, and conceptual errors. The boundary between intentional and conceptual errors and epistemic uncertainty is fuzzy, as mentioned earlier. Sometimes, there is no consensus or dominant view of what acceptable practice is. What one professional considers departure from acceptable practice another professional considers acceptable. For example, many proponents of probability theory consider the use of nonprobabilistic models of uncertainty (e.g., possibility theory or evidence theory) as departure from acceptable practice of modeling uncertainty. Moreover, the definition of acceptable practices changes with time.

8.3.1.3 Evaluating the Payoff of the Outcomes of Actions

Decision makers face uncertainty in assessing the payoffs of outcomes of actions in a way that they are consistent with their preferences. One of the reasons is that decision makers often miss important criteria for determining the payoff of outcomes. Melchers [5] classified this uncertainty as decision uncertainty.

8.3.2 Types of Information

Following are types of information available for quantifying uncertainty:

- *Experimental observations.* These are observed values of the uncertain variables. If the sample size is sufficiently large,[1] then we can construct a reasonable probability distribution using the sample. However, if the sample is small, one must use additional information, such as expert opinion, to model uncertainty.

  When it is impractical to collect data, we could use surrogate data on uncertainties that are similar to the uncertainties we want to model. For example, the probability distribution of the thicknesses of plates from a particular factory can be estimated from measurements on plates from another factory.

  It is impractical to obtain observations for extremely rare or one-time events, such as a catastrophic nuclear accident or a nuclear war. The likelihood of such events can be estimated on the basis of judgment. An alternative approach is to identify all possible failure scenarios that can result in the rare catastrophic event and to estimate the probabilities of these scenarios.

  Observations are not obtainable for future events. Suppose that we want to predict the price of gas in 2020. We cannot rely only on prices from the past to model prices in the future. The reason is that the price of gas as a function of time is a nonstationary, random process.[2] Therefore, in addition to data from the past, we should consider subjective information to construct models of the uncertainty in these events.
- *Intervals.* This information is usually obtained from experts. An expert could provide one interval believed to contain the true value of an uncertain variable or nested confidence intervals containing the true value with certain probabilities. Figure 8.8.b shows an interval that contains the true value of the error in the stress computed from an analytical model.
- *Linguistic information.* This information is obtained from experts. For example, an expert could quantify the error in the stress by saying that "the error is small" (Figure 8.8c).

[1] The required size of a sample depends on the problem. Usually, we can estimate the main body of a probability distribution using 30 experimental observations; but if we want to estimate probabilities of rare events, then we need more experimental observations.

[2] The statistical properties of a nonstationary random process change with shifts in the time origin.

Copyright 2005 by CRC Press LLC

- *First principles-based models of uncertainty.* The type of the probability distribution function of a variable can often be derived from first principles of mechanics or chemistry, and probability. Following are examples of standard probability distributions that were derived from first principles:
  - The Weibull distribution. This distribution models the minimum value of a sample of values drawn from a probability distribution bounded from below. The Weibull distribution is often used for the strength of structures or materials. If the load capacity of a system is the minimum of the capacities of the components and the capacities are statistically independent, then the probability distribution of the load capacity of the system converges to the Weibull distribution as the number of components tends to infinity.
  - An extreme value distribution. There are three distributions, called Type I, Type II, and Type III extreme value distributions. These are used to model the maximum and minimum values of a sample from a population. Type I and Type II extreme value distributions are suitable for modeling loads caused by extreme environmental events, such as storms and earthquakes.
  - The Raleigh distribution. The peaks of a narrowband[3] random process, such the elevation of ocean waves, follow the Raleigh distribution, assuming that the peaks are statistically independent. Thus, a designer may be able to determine the type of the probability distribution governing an uncertain variable without collecting data.
- *Models based on principles of uncertainty.* When little information is available, one can select a model of uncertainty based on principles of uncertainty. These include the principles of maximum uncertainty, minimum uncertainty and uncertainty invariance ([11], pp. 269 to 277).

  The maximum uncertainty principle states that a decision maker should use all the information available but not unwittingly add additional information. Therefore, one should select the model with maximum uncertainty consistent with the available evidence.

Example 9: Modeling Uncertainty in the Stress in a Component When We Only Know the Stress Range

A designer knows that the stress in a particular component, resulting from a given load, is between 10 MPa and 50 MPa. He or she should select the model with maximum uncertainty whose support is the above stress range. In probability theory, uncertainty is measured using Shannon's entropy. According to the maximum uncertainty principle, the designer should use the uniform probability distribution for the stress because this distribution has the largest entropy among all distributions supported by the interval [10 MPa, 50 MPa].

This example is only intended to illustrate the maximum entropy principle. One can question the use of a uniform distribution in this example because there is Nonspecificity type of uncertainty in the stress and because probability cannot account for Nonspecificity [11, p. 259]. When the designer uses a uniform probability distribution, he or she assumes that all values of the stress in the specified range are equally likely. But the evidence does not support this assumption — it only indicates that the stress is in the range [10 MPa, 50 MPa].

- *Tools from numerical analysis for numerical error.* Numerical analysis includes methods to quantify errors in numerical algorithms for solving models. These methods determine the effect of the algorithm parameters (e.g., step size, or the size of a panel) on the error in the solution. Convergence studies also show the effect of the finite element mesh size, or the step size on the solution of a mathematical model.
- *Tools from sampling theory.* Sampling theory [13] provides equations for estimating the probability distributions of the statistics of a sample, such as the sample mean, standard deviation and higher moments of samples drawn from a population.

[3]The energy of a narrowband process is confined in a narrow frequency range.

Copyright 2005 by CRC Press LLC

TABLE 8.1 Types of Information for Types of Uncertainty

Type of Information Type of Uncertainty or Source	Experimental Observations	Interval and Linguistic	Type of Probability Distribution from First Principles	Type of Probability Distribution from Principles of Uncertainty	Numerical Analysis Tools and Results of Convergence Studies	Samplig Theory
Aleatory	X	X	X	X		
Epistemic (predictive deterministic models, models of uncertainty)	X*	X				
Epistemic (parameters of a probabilistic model)	X	X				X
Execution error	X	X				
Error in numerical algorithms		X			X	

**Note*: One should be cautious using experimental observations to update predictive models that are used for a broad range of applications because it is often impractical to obtain a sample that is representative of the population.

8.3.3 Type of Information for Various Types of Uncertainty

Here we explain which types of the information reviewed in the previous subsection should be used for various types of uncertainty. Table 8.1 summarizes the recommendations in this subsection.

8.3.3.1 Information for Aleatory Uncertainty

One should seek experimental observations to model aleatory uncertainty. If there is insufficient data to construct a probability distribution, then a first principles-based model for the type of the probability distribution could be chosen. Then the parameters of the distribution could be estimated using the experimental data. The chapter entitled "The Role of Statistical Testing in NDA" in this book presents methods to construct models of aleatory uncertainty.

In some cases, very limited numerical data or no data is available for aleatory uncertainty. Then information from experts, such as intervals or linguistic information, together with principles of uncertainty (e.g., the maximum entropy principle) can be used for modeling uncertainty. A standard probability distribution can also be used. Subjective probabilistic models can be updated using Bayes' rule when additional information becomes available later. In these cases, aleatory and epistemic uncertainties in probabilistic models coexist.

In some problems, such as gambling problems, one can divide the space of all possible events into elementary events. Moreover, in these problems, there is no reason to assume that the events have different probabilities. For example, there is no reason to assume that the six faces of a die have different probabilities to appear in a roll. According to the principle of insufficient reason, these events should be assumed equiprobable. Then one could estimate the probability of an event based on the number of favorable elementary events normalized by the total number of possible elementary events.

Traditionally, the effect of aleatory uncertainty on the performance of a system was quantified with a probability distribution. For example, the Weibull probability distribution was typically used for the strength or fatigue life. In a modern, bottom-up approach, designers quantify aleatory uncertainty by developing probabilistic models of the input variables or drivers, **X**. Then they calculate the probability distributions in the output variables, **Y**, (e.g., the attributes of a product or the response of a system) using probability calculus together with a model relating the output to the input variables. Chapters 14 to 22 present methods that can be used for this purpose for both static and time-invariant problems.

Copyright 2005 by CRC Press LLC

Table 8.1 summarizes the above recommendations for aleatory uncertainty. Experimental information, interval or linguistic information from experts can be used for aleatory uncertainty. We can determine the type of the probability distribution of a variable from principles of uncertainty or we can use a standard probability distribution.

8.3.3.2 Information for Epistemic Uncertainty

One typically relies on expert opinion for epistemic uncertainty in a predictive model. Experts provide nonspecific information (e.g., intervals instead of exact values) or linguistic information about the variables that describe model uncertainty. For example, it is wiser for an expert to say that the error in the stress in a component is between 0 and 20% rather than to pinpoint the exact value of the error.

Often, we represent the modeling uncertainty of a predictive model with random parameters. For example, we can represent modeling uncertainty in a simplistic way as a random correction coefficient with which we multiply the output of a model to estimate the response of a system. Prior probability distributions of the random parameters are estimated on the basis of judgment and later updated using experimental data and using Bayes rule (see, for example, Cardoni et al. [3] and Chapter 22 "Bayesian Modeling and Updating" in this book). We can use a similar approach to represent modeling uncertainty in a probabilistic model of uncertainty — we can consider the distribution parameters random (e.g., the mean value and the standard deviation), estimate their prior probability distributions, and update these distributions using sampling information.

The above approach can develop reasonable probabilistic models for the epistemic uncertainty in a model for a particular application; for example the prediction of the compressive collapse load of a family of plates with similar geometry and materials. Often, we want to quantify modeling uncertainty in a generic model or modeling practice that is used for a broad range of applications. For example, we want to quantify the modeling uncertainty in loads or load effects for design codes for buildings, bridges or offshore platforms. There are concerns about constructing probabilistic models of uncertainty using experimental data and Bayesian updating for these applications because it is often impractical to obtain a sample of experimental measurements that is representative of the population.

One should primarily rely on expert judgment to model modeling uncertainty in this case, in addition to experimental measurements.

Example 10: Experimental Data on Modeling Error in the Activity Coefficient of a Chemical Solvent

Figure 8.11 shows the errors in the predictions of the activity coefficient of ten chemical solvents. The predictive model was originally developed for 2-propanol but it was used for the ten solvents, which are similar to 2-propanol. This figure was created using data reported by Kubic [14].The vertical axis is the subjective degree to which each solvent is similar to 2-propanol. The horizontal axis is the error in the model

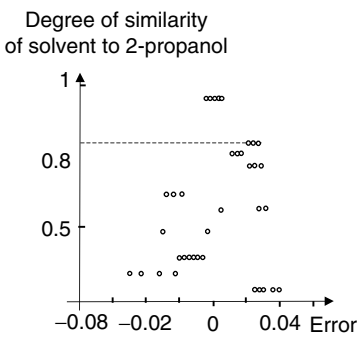

FIGURE 8.11 Errors (discrepancy between predicted and measured values) in activity coefficients for solvents.

Copyright 2005 by CRC Press LLC

predictions. For each solvent, predictions were obtained at different temperatures and the errors are shown as small circles in the figure. The errors for each solvent are on the same horizontal line. It is observed that the errors are different for each solvent and they also vary in a different way as a function of the temperature.

Because the error is not random, one cannot obtain a representative sample of the population of the errors for the ten solvents from the results for a subset of solvents. For example, the errors for the solvent with degree of similarity around 0.8 are clustered around 0.03. None of the results for the errors for the other solvents exhibits similar behavior as the errors in the above solvent. If a designer built a probability distribution of the error using the results in Figure 8.11, then it would be very unlikely that the errors in the predictions for another solvent would fit to the probability distribution. Therefore, the probability distribution for the error developed using the numerical data in the figure would not be useful for constructing a model of the error.

There is epistemic uncertainty in models of uncertainty. We may not know the type of probability distribution of a variable and we may be unable to estimate accurately the parameters of the distribution from a finite sample. One can use expert opinion for the uncertainty in the type of the probability distribution (Table 8.1, third row). Results from theory of sampling [13] are available for modeling the uncertainty in the values of the parameters of a distribution. An alternative approach, which can be used if few experimental measurements are available (e.g., less than 30), is to start with a prior probability distribution of a distribution parameter and update it using experimental measurements and Bayes' rule.

In conclusion, intervals or linguistic information from experts can be used for characterizing epistemic uncertainty (Table 8.1). We can also characterize epistemic uncertainty in predictive models by combining subjective information and experimental measurements for a model that is used for a particular range of applications. Results of theory of sampling are available for modeling uncertainty in the estimates of the parameters of a probabilistic model from a finite sample.

8.3.3.3 Information for Human Errors

We can estimate the frequency of occurrence of execution errors from sampling data. For example, investigations have shown that typical (micro) tasks used in detail structural design have produced an estimate of 0.02 errors per mathematical step on a desktop calculator ([5], p. 40). Sampling data were also used for constructing a histogram of the bending moment capacities of a portal frame computed by different designers.

8.3.3.4 Information for Error in Numerical Solution of Predictive Models

Error in numerical algorithms is easier to quantify than the effect of epistemic uncertainty. Results from numerical analysis and convergence studies help quantify errors due to numerical approximations.

8.4 Chapters in This Book on Methods for Collecting Information and for Constructing Models of Uncertainty

Methods for collecting information, constructing, and testing probabilistic models of uncertainty are presented in Chapter 26 by Fox. Booker's and McNamara's Chapter 13 focuses on elicitation of expert knowledge for quantifying reliability. Theories of uncertainty are presented in Chapter 9 by Joslyn and Booker. Oberkampf and Helton focus on evidence theory in Chapter 10. Two chapters deal with theories and methods for modeling uncertainty when there is a severe information deficit: Ben Haim presents Information Gap theory in Chapter 11, and Muhanna and Mullen present a method using interval arithmetic in Chapter 12. Chapter 22, by Papadimitriou and Katafygiotis, presents Bayesian methods for modeling uncertainty. These methods allow a designer to fuse expert knowledge and experimental data and they are suitable for problems in which limited data is available.

Copyright 2005 by CRC Press LLC

8.5 Conclusion

Uncertainty is important in making design decisions. Because of uncertainty, a decision maker's preferred choice is not guaranteed to result in the most desirable outcome. The best the decision maker can do is to determine the choice that maximizes the odds of getting the most desirable outcome.

To manage uncertainty effectively, a designer should understand all important types of uncertainty. This will enable him or her to allocate resources effectively, to collect the most suitable type of information for each type of uncertainty, and to use the proper theory to quantify each type of uncertainty.

There are three basic types of uncertainty in predicting the outcomes of a decision: aleatory, epistemic, and uncertainty due to human error. The source of aleatory uncertainty is inherent randomness, while the source of epistemic uncertainty is lack of knowledge. There is epistemic uncertainty in deterministic models for predicting the outcome of an action and in models of uncertainty. The latter uncertainty can be in the type of the probability distribution of a random variable and in the parameters of the distribution. Human errors are not due to lack of knowledge and can be corrected if pointed out. Epistemic uncertainty and human error can be reduced by collecting information or by inspection, respectively, whereas aleatory uncertainty cannot be reduced by collecting information.

Aleatory uncertainty is modeled using probability distributions of the driver variables or the response variables of a system.

Sampling data from observations and evidence from experts is usually available for aleatory uncertainty. For epistemic uncertainty, information from experts is suitable. This information is often nonspecific (e.g., consists of intervals or sets of possible outcomes). Sampling information can also be used for epistemic uncertainty in a predictive model for a specific application. Numerical data about the frequency of the effect of gross human errors can be used to construct models of these effects. Errors in numerical solutions of mathematical models can be quantified using tools from numerical analysis and convergence studies.

Acknowledgments

The author wishes to thank Dr. W. Oberkampf and Prof. Z. Mourelatos for reviewing this chapter. The author acknowledges the help of Prof. A. Der Kiureghian in finding publications on types of uncertainty and modeling of epistemic uncertainty using Bayesian updating. The author also wishes to thank Prof. T. Haukass for proving information about human error.

References

1. Hazelrigg, G.A., *Systems Engineering: An Approach to Information-Based Design,* Prentice Hall, Englewood Cliffs, NJ, 1996.
2. Der Kiureghian, A., Measures of Structural Safety under Imperfect States of Knowledge, *J. Structural Eng.,* ASCE, 115(5), 1119–1139, May 1989.
3. Gardoni, P., Der Kiureghian, A., and Mosalam, K.M., Probabilistic Capacity Models and Fragility Estimates for Reinforced Concrete Columns Based on Experimental Observations, *J. Eng. Mechanics,* ASCE, 128(10), 1024–1038, October 2002.
4. Haukass, T., Types of Uncertainties, Elementary Data Analysis, Set Theory, *Reliability and Structural Safety: Lecture Notes,* University of British Columbia, 2003.
5. Melchers, R.E., *Structural Reliability, Analysis and Prediction,* John Wiley & Sons, New York, 1999.
6. Oberkampf, W.L., DeLand, S.M., Rutherford, B.M., Diegert, K.V., and Alvin, K.F., A New Methodology for the Estimation of Total Uncertainty in Computational Simulation, *AIAA Paper No. 99-1612,* 1999.
7. Oberkampf, W.L., DeLand, S.M., Rutherford, B.M., Diegert, K.V., and Alvin, K.F., Error and Uncertainty in Modeling and Simulation, *Reliability Engineering and System Safety,* 75, 333–357, 2002.
8. Nowak, A.S. and Collins, K.R., Uncertainties in the Building Process, in *Reliability of Structures,* McGraw-Hill, New York, 2000.

Copyright 2005 by CRC Press LLC

9. Zimmermann, H.-J., Uncertainty Modelling and Fuzzy Sets, *Uncertainty: Models and Measures,* Proceedings of the International Workshop, Lambrecht, Germany, Akademie Verlag, 1996, 84–100.
10. Ayyub, B., From Dissecting Ignorance to Solving Algebraic Problems, Epistemic Uncertainty Workshop, Sandia National Laboratories, Albuquerque, NM, 2002.
11. Klir, G.J. and Yuan, B., *Fuzzy Sets and Fuzzy Logic*, Prentice Hall, Upper Saddle River, NJ, 1995.
12. Klir, J.G. and Wierman, M.J., *Uncertainty-Based Information*, Physica-Verlag, 1998.
13. Deming, W.E., *Some Theory of Sampling,* Dover, New York, 1966.
14. Kubic, W.,L., "The Effect of Uncertainties in Physical Properties on Chemical Process Design," Ph.D. dissertation, Chemical Engineering Department, Lehigh University, 1987.

Copyright 2005 by CRC Press LLC

9

Generalized Information Theory for Engineering Modeling and Simulation

Cliff Joslyn
Los Alamos National Laboratory

Jane M. Booker
Los Alamos National Laboratory

9.1 Introduction: Uncertainty-Based Information Theory in Modeling and Simulation

Concepts of information have become increasingly important in all branches of science, and especially in modeling and simulation. In the limit, we can view all of science as a kind of modeling. While models can be physical or scale models, more typically we are referring to mathematical or linguistic models, such as $F = ma$, where we measure quantities for mass m and acceleration a, and try to predict another measured quantity force F. More cogently to the readers of this volume, computer simulation models manifest such mathematical formalisms to produce numerical predictions of some technical systems.

A number of points stand out about all models. To quote George Box, "All models are wrong; some models are useful." More particularly:

- All models are necessarily incomplete, in that there are certain aspects of the world which are represented, and others which are not.
- All models are necessarily somewhat in error, in that there will always be some kind of gap between their numerical output and the measured quantities.
- The system being modeled may have inherent variability or un-measurability in its behavior.

Copyright 2005 by CRC Press LLC

In each case, we wish to be able to measure or quantify these properties, that is, the fidelity and accuracy of our models. We therefore care about the concept of "uncertainty" and all its related concepts: How certain can I be: that I am capturing the properties I'm trying to? that I'm making accurate predictions? that the quantities can be confidently accepted?

We refer to **Uncertainty Quantification** (UQ) as this general task of representing amounts, degrees, and kinds of uncertainty in formal systems. In this context, the concept of uncertainty stands in a dual relation to that of "information." Classically, we understand that when I receive some information, then some question has been answered, and so some uncertainty has been reduced. Thus, this concept of information is that it is a reduction in uncertainty, and we call this **uncertainty-based information**.

Through the 20th century, uncertainty modeling has been dominated by the mathematics of probability, and since Shannon and Weaver [1], information has been defined as a statistical measure of a probability distribution. But also starting in the 1960s, alternative formalisms have arisen. Some of these were intended to stand in contrast to probability theory; others are deeply linked to probability theory but depart from or elaborate on it in various ways. In the intervening time, there has been a proliferation of methodologies, along with concomitant movements to synthesize and generalize them. Together, following Klir [2], we call these **Generalized Information Theory** (GIT).

This chapter surveys some of the most prominent GIT mathematical formalisms in the context of the classical approaches, including probability theory itself. Our emphasis will be primarily on introducing the formal specifications of a range of theories, although we will also take some time to discuss semantics, applications, and implementations.

We begin with the classical approaches, which we can describe as the kinds of mathematics that might be encountered in a typical graduate engineering program. **Logical and set-theoretical** approaches are simply the application of these basic formal descriptions. While we would not normally think of these as a kind of UQ, we will see that in doing so, we gain a great deal of clarity about the other methods to be discussed. We then introduce **interval analysis** and the familiar **probability theory** and related methods.

Following the development of these classical approaches, we move on to consider the GIT proper approaches to UQ. What characterizes a GIT approach is some kind of generalization of or abstraction from a classical approach [3]. **Fuzzy systems theory** was the first and most significant such departure, in which Zadeh generalized the classical, Boolean notions of both set inclusion and truth valuation to representations which are a matter of degree.

A fuzzy set can also be seen as a generalization of a probability distribution or an interval. Similarly, a **monotone** or **fuzzy measure** can be seen as a generalization of a probability measure. A **random set** is a bit different; rather than a generalization, it is an extension of a probability measure to set-valued, rather than point-valued, atomic events. Mathematically, random sets are isomorphic to **Dempster-Shafer bodies of evidence**. Finally, we consider **possibility theory**, which arises as a general alternative to classical information theory based on probability. Possibility measures arise as a different special case of fuzzy measures from probability measures, and are generated in extreme kinds of random sets; similarly, possibility distributions arise as a different special case of fuzzy sets, and generalize classical intervals.

The relations among all the various approaches discussed in this chapter is shown in Figure 9.18. This diagram is somewhat daunting, and so we deliberately show it toward the end of the chapter, after the various subrelations among these components have been explicated. Nonetheless, the intrepid reader might wish to consult this as a reference as the chapter develops.

We also note that our list is not inclusive. Indeed, the field is a dynamic and growing area, with many researchers inventing novel formalisms. Rather, we are trying to capture here the primary classes of GIT theories, albeit necessarily from our perspective. Furthermore, there are a number of significant theoretical components that we will mention in Section 9.4 only in passing, which include:

- **Rough sets** as representations of multi-resolutional structures, and are equivalent to classes of possibility distributions

Copyright 2005 by CRC Press LLC

- Higher-order hybrid structures such as **type II** and **level-II** fuzzy sets and **fuzzified Dempster-Shafer theory**; and finally
- **Choquet capacities** and **imprecise probabilities**, which provide further generalizations of monotone measures.

9.2 Classical Approaches to Information Theory

Throughout this chapter we will assume that we are representing uncertainty claims about some system in the world through reference to a universe of discourse denoted $\Omega = \{\omega\}$. At times we can specify that Ω is finite, countable, or uncountable, depending on the context.

9.2.1 Logical and Set Theoretical Approaches

As mentioned above, some of the most classical mathematical representations can be cast as representations of uncertainty in systems, albeit in a somewhat trivial way. But by beginning this way, we can provide a consistent development of future discussions.

We can begin with a simple proposition A, which may or may not be true of any particular element $\omega \in \Omega$. So if A is true of ω, we can say that the truth value of A for ω is 1: $T_A(\omega) = 1$; and if it is false, that $T_A(\omega) = 0$. Because there are two logical possibilities, 0 and 1, the expression $T_A(\omega)$ expresses the uncertainty, that it might be $T_A(\omega) = 0$, or it might be that $T_A(\omega) = 1$.

Surely the same can be said to be true for any function on Ω. But in this context, it is significant to note the following. First, we *can*, in fact, characterize Boolean logic in this way, characterizing a predicate A as a function $T_A : \Omega \mapsto \{0, 1\}$. The properties of this value set $\{0, 1\}$ will be crucial below, and will be elaborated on in many of the theories to be introduced.

Second, we can gather together all the $\omega \in \Omega$ for which T_A is true, as distinguished from all those $\omega \in \Omega$ for which T_A is false, and call this the subset $A \subseteq \Omega$, where $A := \{\omega \in \Omega : T_A(\omega) = 1\}$. It is standard to represent the set A in terms of its characteristic function $\chi_A : \Omega \mapsto \{0, 1\}$, where

$$\chi_A(\omega \in \Omega) = \begin{cases} 1, & \omega \in A \\ 0, & \omega \notin A \end{cases}$$

It is not insignificant that, in fact, $\chi_A \equiv T_A$: the truth value function of the predicate A is equivalent to the characteristic function of the set A. Indeed, there is a mathematical isomorphism between the properties of Boolean logic and those of set theory. For example, the truth table for the logical disjunction ("or") of the two predicates A and B, and the "set disjunction" (union operation) of the two subsets A and B, is shown in Table 9.1. Table 9.2 shows the isomorphic relations among all the primary operations. Graphical representations will be useful below. Letting $\Omega = \{x, y, z, w\}$, Figure 9.1 shows the characteristic function of the subset $A = \{x, z\}$.

TABLE 9.1 Truth Table for Logical Disjunction and Set Disjunction $\cup$

$T_A(\omega)$	$T_B(\omega)$	$T_{A \text{ or } B}(\omega)$	$\chi_A(\omega)$	$\chi_B(\omega)$	$\chi_{A \cup B}(\omega)$
0	0	0	0	0	0
0	1	1	0	1	1
1	0	1	1	0	1
1	1	1	1	1	1

TABLE 9.2 Isomorphisms between Logical and Set Theoretical Operations

Logic		Set Theory	
Negation	$\neg A$	Complement	A^c
Disjunction	A or B	Union	$A \cup B$
Conjunction	A and B	Intersection	$A \cap B$
Implication	$A \rightarrow B$	Subset	$A \subseteq B$

Copyright 2005 by CRC Press LLC

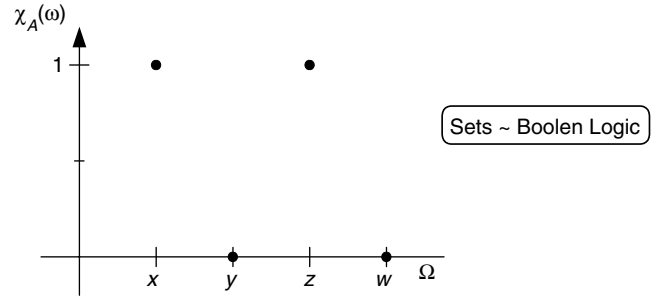

FIGURE 9.1 The crisp set $A = \{x, z\} \subseteq \Omega$.

So far this is quite straightforward, but in so doing we are able to point out the general elements of an uncertainty theory, in particular we can identify:

- The primary objects, in this case sets or propositions, A
- Compound objects as collections of these objects on which the uncertainty can be valued, in this case the power set 2^{Ω}, that is, the set of all subsets of Ω, so that $2^{\Omega} = \{A : A \subseteq \Omega\}$
- A range of possible uncertainty quantities for each element $\omega \in \Omega$ with respect to the object $A \in 2^{\Omega}$, in this case the two binary choices 0 and 1
- Standard operations to combine different objects A and B

The other necessary element is a measure of the total uncertainty or information content $U(A)$ of a particular set or proposition A. For set theory and logic, as well as all the subsequent theories to be presented, such measures are available. Because this is not the primary subject of this chapter, we refer the interested reader elsewhere [4]; nonetheless, for each of the structures we present, we will attempt to identify the community's current best definition for U for that theory. In this case, it is the Hartley measure of information, which is quite simply

$$U_{\text{logic}}(A) = \log_2(|A|), \tag{9.1}$$

where $|\cdot|$ indicates the cardinality of the set. For this and all other uncertainty-based information measures, logarithmic scales are used for their ability to handle addition of two distinct quantities of information, and they are valued in units of bits.

Finally, in each of the cases below, we will identify and observe an **extension principle**, which effectively means that when we generalize from one uncertainty theory to another, then, first, the results from the first must be expressible in terms of special cases of the second, and furthermore the particular properties of the first are recovered exactly for those special cases. However, it is a corollary that in the more general theory, there is typically more than one way to express the concepts that had been previously unequivocal in the more specific theory. This is stated abstractly here, but we will observe a number of particular cases below.

9.2.2 Interval Analysis

As noted, as we move from theory to theory, it may be useful for us to change the properties of the universe of discourse Ω. In particular, in real applications it is common to work with real-valued quantities. Indeed, for many working scientists and engineers, it is always presumed that $\Omega = \mathbb{R}$. The analytical properties of $\mathbb{R}$ are such that further restrictions can be useful. In particular, rather than working with arbitrary subsets of $\mathbb{R}$, it is customary to restrict ourselves to relatively closed sets, specifically closed intervals $I = [I_l, I_u] \subseteq \mathbb{R}$ or half-open intervals $I = [I_l, I_u) \subseteq \mathbb{R}$. Along these lines, it can be valuable to identify

$$\mathcal{D} := \{[a, b) \subseteq \mathcal{R} : a, b \in \mathcal{R}, a \leq b\} \tag{9.2}$$

as the **Borel field** of half-open intervals.

Copyright 2005 by CRC Press LLC

In general, interval-valued quantities represent uncertainty in terms of the upper and lower bounds I_l and I_u. That is, a quantity $x \in \mathbb{R}$ is known to be bounded in this way, such that $x \in [I_l, I_u]$, or $I_l \le x \le I_u$. Because I is a subset of $\mathbb{R}$, it has a characteristic function $\chi_I : \mathbb{R} \mapsto \{0, 1\}$, where

$$\chi_I(x) = \begin{cases} 1, & I_l \le x \le I_u \\ 0, & \text{otherwise} \end{cases}$$

The use of intervals generally is well-known in many aspects of computer modeling and simulation [5].[1] We can also observe the components of interval analysis necessary to identify it as an uncertainty theory, in particular:

- The basic objects are the numbers $x \in \mathbb{R}$.
- The compound objects are the intervals $I \subseteq \mathbb{R}$.
- Note that while the universe of discourse has changed from the general set Ω with all its subsets to $\mathbb{R}$ with its intervals, the valuation set has remained $\{0, 1\}$.
- The operations are arithmetic manipulations, of the form $I * J$ for two intervals I and J, where $* \in \{+, -, \times, \div, \min, \max\}$, etc. In general, we have

$$I * J := \{x * y : x \in I, y \in J\}. \tag{9.3}$$

  For example, we have

$$I + J = [I_l, I_u] + [J_l, J_u] = \{x + y : x \in I, y \in J\} = [I_l + I_u, J_l + J_u].$$

  Note, however, that in general for an operator $*$ we usually have

$$I * J \neq [I_l * I_u, J_l * J_u].$$

- Finally, for uncertainty we can simply use the width of the interval $U_{\text{int}}(I) := |I| = |I_u - I_l|$, or its logarithm

$$U_{\text{int}}(I) := \log_2(|I|). \tag{9.4}$$

The interval operation [1, 2] + [1.5, 3] = [2.5, 5] is shown in Figure 9.2. Note that

$$U([2.5,\ 5]) = \log_2(2.5) = 1.32 > U([1,\ 2]) + U([1.5,\ 3]) = \log_2(1) + \log_2(1.5) = .58.$$

Also note that interval analysis as such is a kind of set theory: each interval $I \subseteq \mathbb{R}$ is simply a special kind of subset of the special universe of discourse $\mathbb{R}$. Thus we can see in Figure 9.2 that intervals have effectively the same form as the subsets $A \subseteq \Omega$ discussed immediately above in Section 9.2.1, in that they are shown as characteristic functions valued on {0, 1} only.

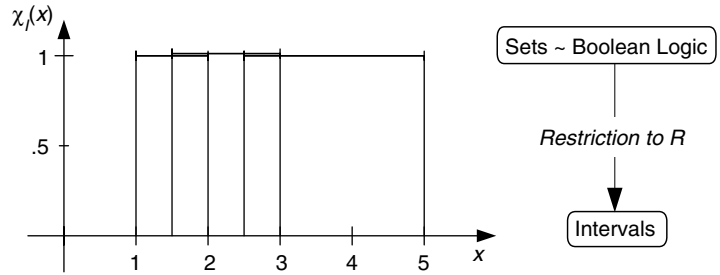

FIGURE 9.2 Interval arithmetic: $[1,2] + [1.5,3] = [2.5,5] \subseteq \mathbb{R}$.

[1]For example, see the journal *Reliable Computing*.

Copyright 2005 by CRC Press LLC

Finally, we can observe the extension principle, in that a number $x \in \mathbb{R}$ can be represented as the degenerate interval $[x, x]$. Then, indeed, we do have that $x * y = [x, x] * [y, y]$.

9.2.3 Probabilistic Representations

By far, the largest and most successful uncertainty theory is probability theory. It has a vast and crucial literature base, and forms the primary point of departure for GIT methods.

Probability concepts date back to the 1500s, to the time of Cardano when gamblers recognized that there were rules of probability in games of chance and, more importantly, that avoiding these rules resulted in a sure loss (i.e., the classic coin toss example of "heads you lose, tails I win," referred to as the "Dutch book"). The concepts were still very much in the limelight in 1685, when the Bishop of Wells wrote a paper that discussed a problem in determining the truth of statements made by two witnesses who were both known to be unreliable to the extent that they only tell the truth with probabilities p_1 and p_2, respectively. The Bishop's answer to this was based on his assumption that the two witnesses were independent sources of information [6].

Mathematical probability theory was initially developed in the 18th century in such landmark treatises as Jacob Bernoulli's *Ars Conjectandi* (1713) and Abraham DeMoiver's *Doctrine of Chances* (1718, 2nd edition 1738). Later in that century, articles would appear that provided the foundations of modern interpretations of probability: Thomas Bayes' "An Essay Towards Solving a Problem in the Doctrine of Chances," published in 1763 [7], and Pierre Simon Laplace's formulation of the axioms relating to games of chance, "Memoire sur la Probabilite des Causes par les Evenemens," published in 1774. In 1772, the youthful Laplace began his work in mathematical statistics and provided the roots for modern decision theory.

By the time of Newton, physicists and mathematicians were formulating different theories of probability. The most popular ones remaining today are the relative frequency theory and the subjectivist or personalistic theory. The latter development was initiated by Thomas Bayes [7], who articulated his very powerful theorem, paving the way for the assessment of subjective probabilities. The theorem gave birth to a subjective interpretation of probability theory, through which a human's degree of belief could be subjected to a coherent and measurable mathematical framework within the subjective probability theory.

9.2.3.1 Probability Theory as a Kind of GIT

The mathematical basis of probability theory is well known. Its basics were well established by the early 20th century, when Rescher developed a formal framework for a conditional probability theory and Jan Lukasiewicz developed a multivalued, discrete logic circa 1930. But it took Kolmogorov in the 1950s to provide a truly sound mathematical basis in terms of measure theory [8].

Here we focus only on the basics, with special attention given to casting probability theory in the context of our general development of GIT.

In our discussions on logic and set theory, we relied on a general universe of discourse Ω and all its subsets $A \in 2^{\Omega}$, and in interval analysis we used $\mathbb{R}$ and the set of all intervals $I \in \mathcal{D}$. In probability theory, we return to a general universe of discourse Ω, but then define a **Boolean field** $\mathcal{E} \subseteq 2^{\Omega}$ on Ω as a collection of subsets closed under union and intersection:

$$\forall A_1, A_2 \in \mathcal{E}, \quad A_1 \cup A_2 \in \mathcal{E}, \quad A_1 \cap A_2 \in \mathcal{E}.$$

Note that while 2^{Ω} is a field, there are fields which are not 2^{Ω}.

We then define a probability measure Pr on $\mathcal{E}$ as a set function $\Pr : \mathcal{E} \mapsto [0, 1]$ where $\Pr(\Omega) = 1$ as a **normalization** condition, and if $A_1, A_2, \ldots$ is a countably infinite sequence of mutually disjoint sets in $\mathcal{E}$ whose union is in $\mathcal{E}$, then

$$\Pr\left(\bigcup_{i=1}^{\infty} A_i\right) = \sum_{i=1}^{\infty} \Pr(A_i).$$

Copyright 2005 by CRC Press LLC

When all of these components are in place, we call the collection $\langle \Omega, \mathcal{E}, \Pr \rangle$ a **probability space**, where we use $\langle \cdot \rangle$ to indicate a general n-tuple, in this case an ordered triple.

We interpret the probability of an event $A \in \mathcal{E}$ as the uncertainty associated with the outcome of A considered as an event. Implicit in this definition are two additional concepts, time, t, and "history" or background information, H, available for contemplating the uncertain events, at t and H. Thus we can also use the revised notation $\Pr(A; H, t)$. Below, we will freely use either notation, depending on the context.

The calculus of probability consists of certain rules (or axioms) denoted by a number determined by $\Pr(A; H, t)$, in which the probability of an event, A, is related to H at time t. When the event A pertains to the ability to perform a certain function (e.g., survive a specified mission time), then $\Pr(A; H, t)$ is known as the product's reliability. This is a traditional definition of reliability, although we must note that treatments outside of the context of probability theory, indeed, outside of the context of any uncertainty-based information theory, are also possible [9].

The quantity $\Pr(A_1 \mid A_2; H, t)$ is known as the conditional probability of A_1, given A_2. Note that conditional probabilities are in the subjunctive. In other words, the disposition of A_2 at time t, were it to be known, would become a part of the history H at time t. The vertical line between A_1 and A_2 represents a supposition or assumption about the occurrence of A_2.

We can also define a function called a **probability distribution** or **density**, depending on the context, as the probability measure at a particular point $\omega \in \Omega$. Specifically, we have $p: \Omega \mapsto [0, 1]$ where $\forall \omega \in \Omega$, $p(\omega) := \Pr(\{\omega\})$. When Ω is finite, then we tend to call p a discrete distribution, and we have

$$\forall A \subseteq \Omega, \quad \Pr(A) = \sum_{\omega \in A} p(\omega),$$

and as the normalization property we have $\sum_{\omega \in \Omega} p(\omega) = 1$.

When $\Omega = \mathbb{R}$, then we tend to use f, and call it a **probability density function** (pdf). We then have

$$\forall A \subseteq \mathbb{R}, \quad \Pr(A) = \int_A f(x)dx,$$

and for normalization $\int_{-\infty}^{\infty} f(x)dx = 1$. In this case, we can also define the **cumulative distribution** as

$$\forall x \in \mathbb{R}, \quad F(x) := \Pr((-\infty, x]) = \int_{-\infty}^{x} f(x)dx,$$

and for normalization $\lim_{x \to \infty} F(x) = 1$.

To make the terminological problems worse, it is common to refer to the cumulative distribution as simply the "distribution function." These terms, especially "distribution," appear frequently below in different contexts, and we will try to use them clearly.

We have now introduced the basic components of probability theory as a GIT:

- The objects are the points $\omega \in \Omega$.
- The compound objects are the sets in the field $A \in \mathcal{E}$.
- The valuation set has become the unit interval $[0, 1]$.

We are now prepared to introduce the operations on these objects, similar to logic and intervals above. First we exploit the isomorphism between sets and logic by introducing the formulation

$$\Pr(A \text{ or } B; H, t) := \Pr(A \cup B; H, t), \quad \Pr(A \text{ and } B; H, t) := \Pr(A \cap B; H, t).$$

Copyright 2005 by CRC Press LLC

The calculus of probability consists of the following three primary rules:

1. **Convexity:** For any event $A \in \mathcal{E}$, we have $0 \le \Pr(A; H, t) \le 1$. Note that this is effectively a restatement of the definition, since $\Pr: 2^{\Omega} \mapsto [0, 1]$.
2. **Addition:** Assume two events A_1 and A_2 that are mutually exclusive; that is, they cannot simultaneously take place, so that $A_1 \cap A_2 = \varnothing$. Then we have

$$\Pr(A_1 \text{ or } A_2; H, t) = \Pr(A_1; H, t) + \Pr(A_2; H, t).$$

   In general, for any two sets $A, B \in \mathcal{E}$, we have

$$\Pr(A_1 \text{ or } A_2; H, t) = \Pr(A_1; H, t) + \Pr(A_2; H, t) - \Pr(A_1 \cap A_2; H, t). \tag{9.5}$$

3. **Multiplication:** Interpreting $\Pr(A_1 \mid A_2; H, t)$ as a quantification of the uncertainty about an event A_1 supposing that event A_2 has taken place, then we have

$$\Pr(A_1 \text{ and } A_2; H, t) = \Pr(A_1 \mid A_2; H, t) \Pr(A_2; H, t).$$

Finally, $\Pr(A_1 \text{ and } A_2; H, t)$ also can be written as $\Pr(A_2 \mid A_1; H, t) \Pr(A_1; H, t)$ because at time t both A_1 and A_2 are uncertain events and one can contemplate the uncertainty about A_1 supposing that A_2 were to be true or vice versa.

To complete the characterization of probability theory as a GIT, we can define the total uncertainty for a discrete as its statistical entropy:

$$U_{\text{prob}}(p) = -\sum_{\omega \in \Omega} p(\omega) \log_2(p(\omega)). \tag{9.6}$$

It is not so straightforward for a continuous pdf, but these concepts are related to variance and other measures of the "spread" or "width" of the density.

9.2.3.2 Interpretations of Probability

The calculus of probability does not tell us how to interpret probability, nor does the theory define what probability means. The theory and calculus simply provide a set of rules by which the uncertainties about two or more events combine or "cohere." Any set of rules for combining uncertainties that are in violation of the rules given above are said to be "incoherent" or inconsistent with respect to the calculus of probability. But it is crucial to note that it is exactly these "inconsistencies" that have spurred much of the work in generalizing the structures reported herein.

Historically speaking, there have been at least 11 different significant interpretations of probability; the most common today are relative frequency theory and personalistic or subjective theory.

Relative frequency theory has its origins dating back to Aristotle, Venn, von Mises, and Reichenbach. In this interpretation, probability is a measure of an empirical, objective, and physical fact of the world, independent of human knowledge, models, and simulations. Von Mises believed probability to be a part of a descriptive model, whereas Reichenbach viewed it as part of the theoretical structure of physics. Because probability is based only on observations, it can be known only *a posteriori* (literally, after observation). The core of this interpretation is in the concept of a random collective, as in the probability of finding an ace in a deck of cards (the collective). In relative frequency theory, $\Pr(A; H, t) = \Pr(A)$; there is no H or t.

Personalistic or subjective interpretation of probability has its origins attributed to Borel, Ramsey, de Finetti, and Savage. According to this interpretation, there is no such thing as a correct probability, an unknown probability, or an objective probability. Probability is defined as a degree of belief, or a willingness to bet: the probability of an event is the amount (say p) the individual is willing to bet, on a two-sided bet, in exchange for \$1, should the event take place. By a two-sided bet is meant staking

Copyright 2005 by CRC Press LLC

$(1-p)$ in exchange for \$1, should the event not take place. Probabilities of one-of-a-kind or rare events, such as the probability of intelligent life on other planets, are easily handled with this interpretation.

The personalistic or subjective probability permits the use of all forms of data, knowledge, and information. Therefore, its usefulness in applications where the required relative frequency data are absent or sparse becomes clear. This view of probability also includes Bayes theorem and comes the closest of all the views of probability to the interpretation traditionally used in fuzzy logic. Therefore, this interpretation of probability can be the most appropriate for addressing the uncertainties in complex decisions surrounding modern reliability problems.

9.2.3.3 Bayes Theorem and Likelihood Approaches for Probability

In 1763, the Reverend Thomas Bayes of England made a momentous contribution to probability, describing a relationship among probabilities of events (A_1 and A_2) in terms of conditional probability:

$$\Pr(A_1 \mid A_2;\ H) = \frac{\Pr(A_2 \mid A_1;\ H)\Pr(A_1;\ H)}{\Pr(A_2;\ H)}.$$

Its development stems from the third "multiplication" axiom of probability defining conditional probability. Bayes theorem expresses the probability that event A_1 occurs if we have observed A_2 in terms of the probability of A_2 given that A_1 occurred.

Historical investigation reveals that Laplace may have independently established another form of Bayes Theorem by considering A_1 as a comprised of k sub-events, $A_{11}, A_{12}, \ldots, A_{1k}$. Then the probability of $A_2, \Pr(A_2;\ H)$ can be rewritten as

$$\Pr(A_2 \mid A_{11};\ H)\Pr(A_{11};\ H) + \Pr(A_2 \mid A_{12};\ H)\Pr(A_{12};\ H) + \cdots + \Pr(A_2 \mid A_{1k};\ H)\Pr(A_{1k};\ H).$$

This relationship is known as the **Law of Total Probability** for two events, A_1 and A_2, and can be rewritten as:

$$\Pr(A_2 = a_2;\ H) = \sum_j \Pr(A_2 = a_2 \mid A_1 = a_{1j};\ H)\Pr(A_1 = a_{1j};\ H),$$

where lower case a values are particular values or realizations of the two events.

The implications of Bayes theorem are considerable in its use, flexibility, and interpretation in that [10]:

- It demonstrates the proportional relationship between the conditional probability $\Pr(A_1 \mid A_2;\ H)$ and the product of probabilities $\Pr(A_1;\ H)$ and $\Pr(A_2 \mid A_1;\ H)$.
- It prescribes how to relate the two uncertainties about A_1: one prior to knowing A_2, the other posterior to knowing A_2.
- It specifies how to change the opinion about A_1 were A_2 to be known; this is also called "the mathematics of changing your mind".
- It provides a mathematical way to incorporate additional information.
- It defines a procedure for the assessor, i.e., how to bet on A_1 should A_2 be observed or known. That is, it prescribes the assessor's behavior before actually observing A_2.

Because of these implications, the use of Bayesian methods, from the application of this powerful theorem, have become widespread as an information combination scheme and as an updating tool, combining or updating the prior information with the existing information about events. These methods also provide a mechanism for handling different kinds of uncertainties within a complex problem by linking subjective-based probability theory and fuzzy logic.

The prior about A_1 refers to the knowledge that exists prior to acquisition of information about event A_1. The fundamental Bayesian philosophy is that prior information is valuable, should be used, and can

Copyright 2005 by CRC Press LLC

be mathematically combined with new or updating information. With this combination, uncertainties can be reduced.

Bernoulli appears to be the first to prescribe uncertainty about A_1 if one were to observe A_2 (but assuming $A_2 = a_2$ has not yet occurred). By dropping the denominator and noting the proportionality of the remaining terms on the right-hand side, Bayes rule becomes:

$$\Pr(A_1 \mid A_2; H) \propto \Pr(A_2 \mid A_1; H) \Pr(A_1; H).$$

However, $A_2 = a_2$ is actually observed, making the left-hand side written as $\Pr(A_1; a_2, H)$. Therefore,

$$\Pr(A_1;\ a_2,\ H) \propto \Pr(A_2 = a_2 \mid A_1 = a_1;\ H) \Pr(A_1 = a_1;\ H).$$

However, there is a problem because $\Pr(A_2 = a_2 \mid A_1 = a_1; H)$ is no longer interpreted as a probability. Instead, this term is called the **likelihood** that $A_1 = a_1$ in light of H and the fact that $A_2 = a_2$. This is denoted $L(A_1 = a_1; a_2, H)$. This likelihood is a function of a_1 for a fixed value of a_2. For example, the likelihood of a test resulting in a particular failure rate would be expressed in terms of $L(A_1 = a_1; a_2, H)$.

The concept of a likelihood gives rise to another formulation of Bayes theorem:

$$\Pr\ (A_1; a_2, H) \propto L(A_1 = a_1; a_2, H) \Pr(A_1 = a_1; H).$$

Here, $\Pr(A_1 = a_1; H)$ is again the *prior probability* of A_1 (i.e., the source for information that exists "prior" to test data (a_2) in the form of expert judgment and other historical information). By definition, the prior represents the possible values and associated probabilities for the quantity of interest, A_1. For example, one decision is to represent the average failure rate of a particular manufactured item. The likelihood $L(A_1 = a_1; a_2, H)$ is formed from data in testing a specified number of items. Test data from a previously made item similar in design forms the prior. $\Pr(A_1; a_2, H)$ is the posterior distribution in the light of a_2 (the data) and H, produced from the prior information and the data.

The likelihood is an intriguing concept but it is not a probability, and therefore does not obey the axioms or calculus of probability. In Bayes theorem, the likelihood is a connecting mechanism between the two probabilities: the prior probability, $\Pr(A_1; H)$, and the posterior probability, $\Pr(A_1; a_2, H)$. The likelihood is a subjective construct that enables the assignment of relative weights to different values of $A_1 = a_1$.

9.2.3.4 Distribution Function Formulation of Bayes Theorem

Bayes theorem has been provided for the discrete form for two random variables representing the uncertain outcomes of two events, A_1 and A_2. For continuous variables X and Y, the probability statements are replaced by pdfs, and the likelihood is replaced by a likelihood function. If Y is a continuous random variable whose probability density function depends on the variable X, then the conditional pdf of Y given X is $f(y \mid x)$. If the prior pdf of X is $g(x)$, then for every y such that $f(y) > 0$ exists, the posterior pdf of X, given $Y = y$ is

$$g(x \mid y; H) = \frac{f(y \mid x;\ H) g(x;\ H)}{\int f(y \mid x;\ H) g(x;\ H) dx},$$

where the denominator integral is a normalizing factor so that $g(x \mid y; H)$, the posterior distribution, integrates to 1 (as a proper pdf).

Alternatively, utilizing the likelihood notation, we have

$$g(x \mid y; H) \propto L(x \mid y; H) g(x; H),$$

so that the posterior is proportional to the likelihood function times the prior distribution.

Copyright 2005 by CRC Press LLC

In this form, Bayes theorem can be interpreted as a weighting mechanism. The theorem mathematically weights the likelihood function and prior distribution, combining them to form the posterior. If these two distributions overlap to a large extent, this mathematical combination produces a desirable result: the uncertainty (specifically, the variance) of the posterior distribution is smaller than that produced by a simple weighted combination, $w_1 g_{\text{prior}} + w_2 L_{\text{likelihood}}$, for example. The reduction in the uncertainty results from the added information of combining two distributions that contain similar information (overlap).

Contrarily, if the prior and likelihood are widely separated, then the posterior will fall in the gap between the two functions. This is an undesirable outcome because the resulting combination falls in a region unsupported by either the prior or the likelihood. In this situation, one would want to reconsider using Bayesian combination and either seek to resolve the differences between the prior and likelihood or use some other combination method such as a simple weighting scheme; for example, consider $w_1 g_{\text{prior}} + w_2 L_{\text{likelihood}}$.

As noted above, a major advantage of using Bayes theorem to combine distribution functions of different information sources is that the spread (uncertainty) in the posterior distribution is reduced when the information in the prior and likelihood distributions are consistent with each other. That is, the combined information from the prior distribution and the data has less uncertainty because the prior distribution and data are two different information sources that support each other.

Before the days of modern computers and software, calculating Bayes theorem was computationally cumbersome. For those times, it was fortunate that certain choices of pdfs for the prior and likelihood produced easily obtained posterior distributions. For example, a beta prior with a binomial likelihood produces a beta posterior whose parameters are simple functions of the prior beta and binomial parameters, as the following example illustrates. With modern computational methods, these analytical shortcuts, called conjugate priors, are not necessary; however, computation still has its difficulties in how to formulate, sample from, and parameterize the various functions in the theorem. Simulation algorithms such as Metropolis-Hastings and Gibbs sampling provide the how-to, but numerical instabilities and convergence problems can occur with their use. A popular simulation technique for simulation and sampling is Markov Chain Monte Carlo (MCMC). A flexible software package for implementation written in Java is YADAS[2] [11].

9.2.3.5 Binomial/Beta Reliability Example

Suppose we prototype a system, building 20 units, and subject these to a stress test. All 20 units pass the test [10]. The estimate of success/failure rates from test data alone is $n_1 = 20$ tests with $x_1 = 20$ successes.

Using just this information, the success rate is 20/20 = 1, and the failure rate is 0/20 = 0. This fundamental reliability (frequentist interpretation of probability) estimate, based on only 20 units, does not reflect the uncertainty in the reliability for the system and does not account for any previously existing information about the units before the test.

A Bayesian approach can take advantage of prior information and provide an uncertainty estimate on the probability of a success, p. Prior knowledge could exist in many forms: expertise of the designers, relevant data from similar systems or components, design specifications, historical experience with similar designs, etc. that can be used to formulate the prior distribution for p, $g(p)$. The beta distribution is often chosen as a prior for a probability because it ranges from 0 to 1 and can take on many shapes (uniform, "J" shape, "U" shape and Gaussian-like) by adjusting its two parameters, n_0 and x_0. That beta prior is denoted as beta(x_0, n_0), and its pdf is:

$$g(p) = \frac{\Gamma(n_0)}{\Gamma(x_0)\Gamma(n_0 - x_0)} x^{x_0 - 1}(1-x)^{n_0 - x_0 - 1}.$$

[2]Yet Another Data Analysis System.

Copyright 2005 by CRC Press LLC

For this example, assume the prior information is in the form of an estimate of the failure rate from the test data done on a similar system that is considered relevant for this new system with $n_0 = 48$ tests on a similar system with $x_0 = 47$ successes.

The new prototype test data forms the likelihood, $L(p; x)$. Because this data represents the number of successes, x_1, in n_1 trials it conforms to the binomial distribution with the parameter of interest for success, p. The beta distribution, $g(p)$, is a conjugate prior when combined with the binomial likelihood, $L(p; x)$, using Bayes theorem. Thus, the resulting, posterior distribution, $g(p \mid x)$ is also a beta distribution with parameters $(x_0 + x_1, n_0 + n_1)$:

$$g(p \mid x) = \frac{\Gamma(n_0 + n_1)}{\Gamma(x_0 + x_1)\Gamma(n_0 + n_1 - x_0 - x_1)} p^{x_0 + x_1 - 1}(1-p)^{n_0 + n_1 - x_0 - x_1 - 1},$$

or

$$g(p \mid x) = \frac{\Gamma(68)}{\Gamma(67)\Gamma(1)} p^{66}(1-p)^{0}.$$

The mean success rate of the beta posterior is

$$\frac{x_0 + x_1}{n_0 + n_1} = \frac{67}{68} = 0.985,$$

or, in terms of a mean failure rate for the beta posterior, approximately $1 - 0.985 = 0.015$ failure rate. The variance of the beta posterior distribution is:

$$\frac{(x_0 + x_1)[(n_0 + n_1) - (x_0 + x_1)]}{(n_0 + n_1)^2 (n_0 + n_1 + 1)} = 0.00021.$$

The engineering reliability community gravitates to the binomial/beta conjugate prior because many of the failures are binomial in nature and the parameters of the prior and posterior can have a reliability-based interpretation: n_0 = number of tests and x_0 = number of successes for the prior parameter interpretation. Similarly, $n_0 + n_1$ = number of pseudo tests and $x_0 + x_1$ = number of pseudo successes for the posterior parameter interpretation, provided these values are greater than 1.

9.3 Generalized Information Theory

We now turn our attention to the sub-fields of GIT proper. Most of these formalisms were developed in the context of probability theory, and are departures, in the sense of generalization from or elaborations, of it. However, many of them are also intricately interlinked with logic, set theory, interval analysis, combinations of these, combinations with probability theory, and combinations with each other. We emphasize again that there is a vast literature on these subjects in general, and different researchers have different views on which theories are the most significant, and how they are related. Our task here is to represent the primary GIT fields and their relations in the context of probability theory and reliability analysis. For more background, see work elsewhere [12–15].

9.3.1 Historical Development of GIT

As mentioned in the introduction, we will describe the GIT sub-fields of fuzzy systems, monotone or fuzzy measures, random sets, and possibility theory. While these GIT sub-fields developed historically in the context of probability theory, each also has progenitors in other parts of mathematics.

Copyright 2005 by CRC Press LLC

In 1965, Lotfi Zadeh introduced his seminal idea in a continuous-valued logic called fuzzy set theory [16, 17]. In doing so, he was recapitulating some earlier ideas in multi-valued logics [13].

Also in the 1960s, Arthur Dempster developed a statistical theory of evidence based on probability distributions propagated through multi-valued maps [18]. In so doing, he introduced mathematical structures that had been identified by Choquet some years earlier, and described as general "capacities." These Choquet capacities [19, 20] are generalizations of probability measures, as we shall describe below. In the 1970s, Glenn Shafer extended Dempster's work to produce a complete theory of evidence dealing with information from more than one source [21]. Since then, the combined sub-field has come to be known as "Dempster-Shafer Evidence Theory" (DS Theory). Meanwhile, the stochastic geometry community was exploring the properties of random variables valued not in $\mathbb{R}$, but in closed, bounded subsets of $\mathbb{R}^n$. The random sets they described [22, 23] turned out to be mathematically isomorphic to DS structures, although again, with somewhat different semantics. This hybrid sub-field involving Dempster's and Shafer's theories and random sets all exist in the context of infinite-order Choquet capacities.

While random sets are defined in general on $\mathbb{R}^n$, for practical purposes, as we have seen, it can be useful to restrict ourselves to closed or half-open intervals of $\mathbb{R}$ and similar structures for $\mathbb{R}^n$. Such structures provide DS correlates to structures familiar to us from probability theory as it is used, for example pdfs and cumulative distributions. It should be noted that Dempster had previously introduced such "random intervals" [24].

In 1972, Sugeno introduced the idea of a "fuzzy measure" [25], which was intended as a direct generalization of probability measures to relax the additivity requirement of additive Equation 9.5. Various classes of fuzzy measures were identified, many of the most useful of which were already available within DS theory. In 1978, Zadeh introduced the special class of fuzzy measures called "possibility measures," and furthermore suggested a close connection to fuzzy sets [26]. It should be noted that there are other interpretations of this relation, and to some extent it is a bit of a terminological oddity that the term "fuzzy" is used in two such contexts [27]. For this reason, researchers are coming to identify fuzzy measures instead as "monotone measures."

The 1980s and 1990s were marked by a period of synthesis and consolidation, as researchers completed some open questions and continued both to explore novel formalisms, but more importantly the relations among these various formalisms. For example, investigators showed a strong relationship between evidence theory, probability theory, and possibility theory with fuzzy measures [28].

One of the most significant developments during this period was the introduction by Walley of an even broader mathematical theory of "imprecise probabilities," which further generalizes fuzzy measures [29].

9.3.2 GIT Operators

The departure of the GIT method from probability theory is most obviously significant in its use of a broader class of mathematical operators. In particular, probability theory operates through the familiar algebraic operators addition + and multiplication ×, as manifested in standard linear algebra. GIT recognizes + as an example of a generalized disjunction, the "or"-type operator, and × as an example of a generalized conjunction, the "and"-type operator, but uses other such operators as well.

In particular, we can define the following operations:

Complement: Let c: $[0, 1] \mapsto [0, 1]$ be a **complement** function when

$$c(0) = 1, \quad c(1) = 0, \quad x \leq y \mapsto c(x) \geq c(y).$$

Norms and Conorms: Assume associative, commutative functions $\sqcap: [0,1]^2 \mapsto [0,1]$ and $\sqcup: [0,1]^2 \mapsto [0,1]$. Because of associativity, we can use the operator notation $x \sqcap y := \sqcap(x, y)$, $x \sqcup y := \sqcup(x, y)$. Further assume that $\sqcup$ and $\sqcap$ are monotonic, in that

$$\forall x \leq y, z \leq w, \quad x \sqcap z \leq y \sqcap w, \quad x \sqcup z \leq y \sqcap w.$$

Copyright 2005 by CRC Press LLC

Then $\sqcap$ is a **triangular norm** if it has identity 1, with $1 \sqcap x = x \sqcap 1 = x$; and $\sqcup$ is a **triangular conorm** if it has identity 0, with $0 \sqcup x = x \sqcup 0 = x$.

While there are others, the prototypical complement function, and by far the most commonly used, is $c(x) = 1 - x$. Semantically, complement functions are used for logical negation and set complementation.

In general, there are many continuously parameterized classes of norms and conorms [13]. However, we can identify some typical norms and conorms that may be familiar to us from other contexts. Below, use $\wedge, \vee$ for the maximum and minimum operators, let $x, y \in [0, 1]$, and let $\lfloor x \rfloor$ be the greatest integer below $x \in \mathbb{R}$, and similarly $\lceil x \rceil$ the least integer above x. Then we have:

Norms:

- **–Min:** $x \wedge y$
- **–Times:** $x \times y$
- **–Bounded Difference:** $x -_b y := (x + y - 1) \vee 0$
- **–Extreme Norm:** $\lfloor x \rfloor \times \lfloor y \rfloor$

Conorms:

- **–Max:** $x \vee y$
- **–Probabilistic Sum:** $x +_p y := x + y - xy$
- **–Bounded Sum:** $x +_b y := (x + y) \wedge 1$
- **–Extreme Conorm:** $\lfloor x \rfloor \times \lfloor y \rfloor$

In general, $\wedge$ is the greatest and $\lfloor x \rfloor \times \lfloor y \rfloor$ the least norm, and $\vee$ is the least and $\lceil x \rceil \times \lceil y \rceil$ the greatest conorm. The relations are summarized in Table 9.3.

9.3.3 Fuzzy Systems

In 1965, Zadeh published a new set theory that addressed the kind of vague uncertainty that can be associated with classifying an event into a set [16, 17]. The idea suggested that *set membership* is the key to decision making when faced with linguistic and nonrandom uncertainty. Unlike probability theory, based upon crisp sets, which demands that any outcome of an event or experiment belongs to a set A or to its complement, A^c, and not both, fuzzy set theory permits such a joint membership. The degree of membership that an item belongs to any set is specified using a construct of fuzzy set theory, a membership function.

Just as we have seen that classical (crisp) sets are isomorphic to classical (crisp) logic, so there is a fuzzy logic that is isomorphic to fuzzy sets. Together, we can thus describe **fuzzy systems** as systems whose operations and logic are governed by these principles. Indeed, it can be more accurate to think of a *process* of "fuzzification," in which a formalism that has crisp, binary, or Boolean choices are relaxed to admit degrees of gradation. In this way, we can conceive of such ideas as fuzzified arithmetic, fuzzified calculus, etc.

9.3.3.1 Fuzzy Sets

Zadeh's fundamental insight was to relax the definition of set membership. Where crisp sets contain objects that satisfy precise properties of membership, fuzzy sets contain objects that satisfy imprecise properties of membership; that is, membership of an object in a fuzzy set can be approximate or partial.

We now introduce the basic formalism of fuzzy sets. First, we work with a general universe of discourse Ω. We then define a **membership function** very simply as any function μ: $\Omega \mapsto [0, 1]$. Note, in particular, that the characteristic function χ_A of a subset $A \subseteq \Omega$ is a membership function, simply because $\{0, 1\} \subseteq [0, 1]$.

TABLE 9.3 Prototypical Norms and Conorms

Triangular Norm	$x \sqcap y$:	$x \wedge y$	$\geq$	$x \times y$	$\geq$	$0 \vee (x + y - 1)$	$\geq$	$\lfloor x \rfloor \times \lfloor y \rfloor$
Triangular Conorm	$x \sqcup y$:	$x \vee y$	$\leq$	$x + y - xy$	$\leq$	$1 \wedge (x + y)$	$\leq$	$\lceil x \rceil \times \lceil y \rceil$

Copyright 2005 by CRC Press LLC

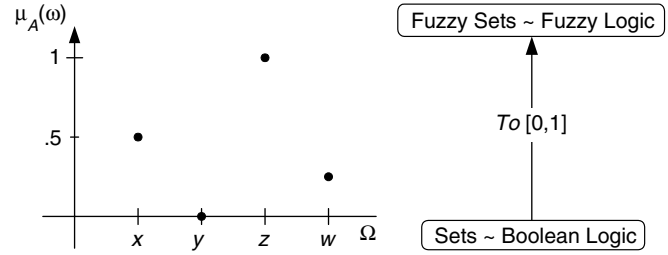

FIGURE 9.3 The fuzzy set $\tilde{A} = \{\langle x, .5\rangle, \langle y, 0\rangle, \langle z, 1\rangle, \langle w, .25\rangle\} \tilde{\subseteq} \Omega$.

Thus, membership functions generalize characteristic functions, and in this way, we can conceive of a **fuzzy subset** of Ω, denoted $\tilde{A} \tilde{\subseteq} \Omega$, as being defined by some particular membership function $\mu_{\tilde{A}}$. For a characteristic function χ_A of a subset A, we interpret $\chi_A(\omega)$ as being 1 if $\omega \in A$, and 0 if $\omega \notin A$. For a membership function $\mu_{\tilde{A}}$ of a fuzzy subset $\tilde{A}$, it is thereby natural to interpret $\mu_{\tilde{A}}(\omega)$ as the *degree* or *extent to which* $\omega \in \tilde{A}$.

Then note especially how the extension principle holds. In particular, consider $\omega_1, \omega_2 \in \Omega$ such that $\mu_{\tilde{A}}(\omega_1) = 0$ and $\mu_{\tilde{A}}(\omega_2) = 1$. In these cases, we can still consider that $\omega_1 \in \tilde{A}$ and $\omega_2 \notin \tilde{A}$ unequivocally.

Below, it will frequently be convenient to denote $\tilde{A}(\omega)$ for $\mu_{\tilde{A}}(\omega)$. Moreover, when $\Omega = \{\omega_1, \omega_2, \ldots, \omega_n\}$ is finite, we can denote a fuzzy subset as a set of ordered pairs:

$$\tilde{A} = \{\langle \omega_1, \tilde{A}(\omega_1)\rangle, \langle \omega_2, \tilde{A}(\omega_2)\rangle, \ldots, \langle \omega_n, \tilde{A}(\omega_n)\rangle\}.$$

Consider the simple example shown in Figure 9.3. For $\Omega = \{x, y, z, w\}$, we might have

$$\tilde{A} = \{\langle x, .5\rangle, \langle y, 0\rangle, \langle z, 1\rangle, \langle w, .25\rangle\},$$

so that z is completely in $\tilde{A}$, y is completely not in $\tilde{A}$, and x and w are in $\tilde{A}$ to the intermediate extents .5 and .25, respectively.

When a membership function actually reaches the line $\mu = 1$, so that $\exists \omega \in \Omega, \tilde{A}(\omega) = 1$, then we call $\tilde{A}$ **normal**. This usage is a bit unfortunate because it may indicate probabilistic additive normalization, so we will try to distinguish this as fuzzy normalization. Fuzzy normalization is also the criterion for $\tilde{A}$ to be a possibility distribution, which we will discuss below in Section 9.3.6.

To continue our characterization of fuzzy sets as a GIT, we need to define the correlates to the basic set operations. Not surprisingly, we will do this through the generalized operators introduced in Section 9.3.2. Below, presume two fuzzy sets $\tilde{A}, \tilde{B} \tilde{\subset} \Omega$. Then we have:

Fuzzy Complement: $\mu_{\tilde{A}^c}(\omega) = c(\tilde{A}(\omega))$
Fuzzy Union: $\mu_{\tilde{A} \cup \tilde{B}}(\omega) = \tilde{A}(\omega) \sqcup \tilde{B}(\omega)$
Fuzzy Intersection: $\mu_{\tilde{A} \cap \tilde{B}}(\omega) = \tilde{A}(\omega) \sqcap \tilde{B}(\omega)$
Fuzzy Set Equivalence: $\tilde{A} = \tilde{B} := \forall \omega \in \Omega, \tilde{A}(\omega) = \tilde{B}(\omega)$
Fuzzy Subsethood: $\tilde{A} \tilde{\subseteq} \tilde{B} := \forall \omega \in \Omega, \tilde{A}(\omega) \leq \tilde{B}(\omega)$

Typically, we use $\sqcup = \vee, \sqcap = \wedge$, and $c(\mu) = 1 - \mu$, although it must always be kept in mind that there are many other possibilities. The extension principle can be observed again, in that for crisp sets, the classical set operations are recovered.

Proposition 7: Consider two crisp subsets $A, B \subseteq \Omega$, and let $\mu_{\tilde{C}} = \chi_A \sqcup \chi_B$, and $\mu_{\tilde{D}} = \chi_A \sqcap \chi_B$ for some general norm $\sqcap$ and conorm $\sqcup$. Then $\mu_{\tilde{C}} = \chi_{A \cup B}$ and $\mu_{\tilde{D}} = \chi_{A \cap B}$.

So again, we have the ideas necessary to cast fuzzy systems as a kind of GIT. As with classical sets, the basic objects are the points $\omega \in \Omega$, but now the compound objects are all the fuzzy subsets $\tilde{A} \tilde{\subseteq} \Omega$, and the valuation is into [0, 1] instead of {0, 1}. The operations on fuzzy sets are defined above.

Copyright 2005 by CRC Press LLC

So now we can introduce the measure of the information content of a fuzzy set. There are at least two important concepts here. First, we can consider the "size" of a fuzzy set much like that of a crisp set, in terms of its cardinality. In the fuzzy set case, this is simply

$$|\tilde{A}| := \sum_{\omega \in \Omega} \tilde{A}(\omega),$$

noting that in accordance with the extension principle, this fuzzy cardinality of a crisp set is thereby simply its cardinality.

We can also discuss the "fuzziness" of a fuzzy set, intuitively as how much a fuzzy set departs from being a crisp set, or in other words, some sense of "distance" between the fuzzy set and its complement [13]. The larger the distance, the "crisper" the fuzzy set. Using Z to denote this quantity, and recalling our fuzzy complement operator above, we have:

$$Z(\tilde{A}) := \sum_{\omega \in \Omega} |\, \tilde{A}(\omega) - c(\tilde{A}(\omega)) \,|,$$

which, when $1-\cdot$ is used for c, becomes:

$$Z(\tilde{A}) = \sum_{\omega \in \Omega} (1 - |\, 2\tilde{A}(\omega) - 1 \,|).$$

Finally, we note the presence of the extension principle everywhere. In particular, all of the classical set operations are recovered in the case of crisp sets, that is, where $\forall \omega \in \Omega, \tilde{A}(\omega) \in \{0, 1\}$.

9.3.3.2 Fuzzy Logic

We saw in Section 9.2.1 that we can interpret the value of a characteristic function of a subset χ_A as the truth value of a proposition T_A, and in this way set theoretical operations are closely coupled to logical operations, to the extent of isomorphism. In classical predicate logic, a proposition A is a linguistic, or declarative, statement contained within the universe of discourse Ω, which can be identified as being a collection of elements in Ω which are strictly true or strictly false.

Thus, it is reasonable to take our concept of a fuzzy set's membership function $\mu_{\tilde{A}}$ and derive an isomorphic fuzzy logic, and indeed, this is what is available. In contrast to the classical case, a fuzzy logic proposition is a statement involving some concept without clearly defined boundaries. Linguistic statements that tend to express subjective ideas and that can be interpreted slightly differently by various individuals typically involve fuzzy propositions. Most natural language is fuzzy, in that it involves vague and imprecise terms. Assessments of people's preferences about colors, menus, or sizes, or expert opinions about the reliability of components, can be used as examples of fuzzy propositions.

So mathematically, we can regard a fuzzy subset $\tilde{A}$ as a fuzzy proposition, and denote $T_{\tilde{A}}(\omega) := \tilde{A}(\omega) \in [0, 1]$ as the extent to which the statement "ω is $\tilde{A}$" is true. In turn, we can invoke the GIT operators analogously to fuzzy set theory to provide our fuzzy logic operators. In particular, for two fuzzy propositions $\tilde{A}$ and $\tilde{B}$ we have:

Negation: $T_{\neg \tilde{A}}(\omega) = c\big(\tilde{A}(\omega)\big)$
Disjunction: $T_{\tilde{A} \text{ or } \tilde{B}}(\omega) = \tilde{A}(\omega) \sqcup \tilde{B}(\omega)$
Conjunction: $T_{\tilde{A} \text{ and } \tilde{B}}(\omega) = \tilde{A}(\omega) \sqcap \tilde{B}(\omega)$
Implication: There are actually a number of expressions for fuzzy implication available, but the "standard" one one might expect is valid: $T_{\tilde{A} \to \tilde{B}}(\omega) = T_{\neg \tilde{A} \text{ or } \tilde{B}}(\omega) = c\big(\tilde{A}(\omega)\big) \vee \tilde{B}(\omega)$

Table 9.4 shows the isomorphic relations among all the primary fuzzy operations. Again, the extension principle holds everywhere for crisp logic. Note, however, that, in keeping with the multi-valued nature of mathematical ideas in the more general theory, the implication operation is only roughly equivalent to the subset relation, and that there are other possibilities. Figure 9.3 shows our simple example again, along with the illustration of the generalization of classical sets and logic provided by fuzzy sets and logic.

Copyright 2005 by CRC Press LLC

TABLE 9.4 Isomorphisms between Fuzzy Logical and Fuzzy Set Theoretical Operations

Fuzzy Logic		Fuzzy Set Theory		GIT Operation
Negation	$\neg\tilde{A}$	Complement	$\tilde{A}^c$	$c(\mu_{\tilde{A}})$
Disjunction	$\tilde{A}$ or $\tilde{B}$	Union	$\tilde{A} \cup \tilde{B}$	$\mu_{\tilde{A}} \sqcup \mu_{\tilde{B}}$
Conjunction	$\tilde{A}$ and $\tilde{B}$	Intersection	$\tilde{A} \cap \tilde{B}$	$\mu_{\tilde{A}} \sqcap \mu_{\tilde{B}}$
Implication	$\tilde{A} \rightarrow \tilde{B}$	Subset	$\tilde{A} \subseteq \tilde{B}$	$c(\mu_{\tilde{A}}) \sqcup \mu_{\tilde{B}}$

9.3.3.3 Comparing Fuzzy Systems and Probability

The membership function $\tilde{A}(\omega)$ reflects an assessor's view of the extent to which $\omega \in \tilde{A}$, an epistemic uncertainty stemming from the lack of knowledge about how to classify ω. The subjective or personalistic interpretation of probability, $\Pr(A)$, can be interpreted as a two-sided bet, dealing with the uncertainty associated with the outcome of the experiment. While this type of uncertainty is usually labeled as random or aleatory, there is no restriction on applying subjective probability to characterize lack of knowledge or epistemic uncertainty. A common example would be eliciting probability estimates from experts for one-of-a kind or never observed events.

However, just because probabilities and fuzzy quantities can represent epistemic uncertainties does not guarantee interchangeability or even a connection between the two theories. As noted above, their axioms are quite different in how to combine uncertainties represented within each theory. Therefore, the linkage between the two theories is not possible by modifying one set of axioms to match the other. Other fundamental properties also differ. It is not a requirement that the sum over ω of all $\tilde{A}(\omega)$ equals one, as is required for summing over all probabilities. This precludes $\tilde{A}(\omega)$ from being interpreted as a probability in general. Similarly, pdfs are required to sum or integrate to one, but membership functions are not. Therefore, membership functions cannot be equated with pdfs either.

At least one similarity of probability and membership functions is evident. Just as probability theory does not tell how to specify $\Pr(A)$, fuzzy set theory does not tell how to specify $\tilde{A}(\omega)$. In addition, specifying membership is a subjective process. Therefore, subjective interpretation is an important common link to both theories.

Noting that $\tilde{A}(\omega)$, as a function of ω, reflects the extent to which $\omega \in \tilde{A}$, it is an indicator of *how likely* it is that $\omega \in \tilde{A}$. One interpretation of $\tilde{A}(\omega)$ is as the likelihood of ω for a fixed (specified) $\tilde{A}$. A likelihood function is not a pdf. In statistical inference, it is the relative degree of support that an observation provides to several hypotheses. Specifying the likelihood is also a subjective process, consistent with membership function definition and the subjective interpretation of probability.

As noted above, likelihoods are mostly commonly found in Bayes theorem. So, Bayes theorem links subjective probability with subjective likelihood. If membership functions can be interpreted as likelihoods, then Bayes theorem provides a valuable link from fuzzy sets back into probability theory. A case is made for this argument [30], providing an important mathematical linkage between probability and fuzzy theories. With two theories linked, it is possible to analyze two different kinds of uncertainties present in the same complex problem. An example application in the use of expert knowledge illustrates how these two theories can work in concert as envisioned by Zadeh [17] can be found in [31]. Additional research is needed to link other GITs so that different kinds of uncertainties can be accommodated within the same problem.

9.3.3.4 Fuzzy Arithmetic

Above we considered the restriction of sets from a general universe Ω to the line $\mathbb{R}$. Doing the same for fuzzy sets recovers some of the most important classes of structures.

In particular, we can define a **fuzzy quantity** as a fuzzy subset $\tilde{I} \tilde{\subseteq} \mathbb{R}$, such that $\mu_{\tilde{I}} : \mathbb{R} \mapsto [0,1]$. Note that a fuzzy quantity is any arbitrary fuzzy subset of $\mathbb{R}$, and as such may not have any particular useful

Copyright 2005 by CRC Press LLC

properties. Also note that every pdf is a special kind of fuzzy quantity. In particular, if $\int_{\mathbb{R}} \mu_{\tilde{I}}(x)dx = 1$, then $\mu_{\tilde{I}}$ is a pdf.

We can discuss another special kind of fuzzy quantity, namely a **possibilistic density** or **distribution function** (again, depending on context), which we will abbreviate as π-df, pronounced "pie-dee-eff." In contrast with a pdf, if $\tilde{I}$ is fuzzy normal, so that $\sup_{x\in\mathbb{R}} \tilde{I}(x) = 1$, then $\tilde{I}$ is a π-df. We note here in passing that where a pdf is a special kind of probability distribution on $\mathbb{R}$, so a π-df is a special kind of possibility distribution on $\mathbb{R}$. This will be discussed in more detail below in Section 9.3.6.

We can also discuss special kinds of π-dfs. When a π-df is convex, so that

$$\forall_{x,y\in\mathbb{R}} \forall_{z\in[x,y]} \tilde{I}(z) \geq \tilde{I}(x) \wedge \tilde{I}(y), \tag{9.8}$$

then $\tilde{I}$ is a **fuzzy interval**. We can also define the **support** of a fuzzy interval as $\mathrm{U}(\tilde{I}) := \{x : \tilde{I}(x) > 0\}$, and note that $\mathbf{U}(\tilde{I})$ is itself a (possibly open) interval. When a fuzzy interval $\tilde{I}$ is unimodal, so that $\exists! x \in \mathbb{R}, \tilde{I}(x) = 1$, then $\tilde{I}$ is a **fuzzy number**, where $\exists!$ means "exists uniquely."

These classes of fuzzy quantities are illustrated in Figure 9.4. Note in particular that the fuzzy quantity and π-df illustrations are cartoons: in general, these need not be continuous, connected, or unimodal. Some of the cases shown here will be discussed further in Section 9.3.6.4.

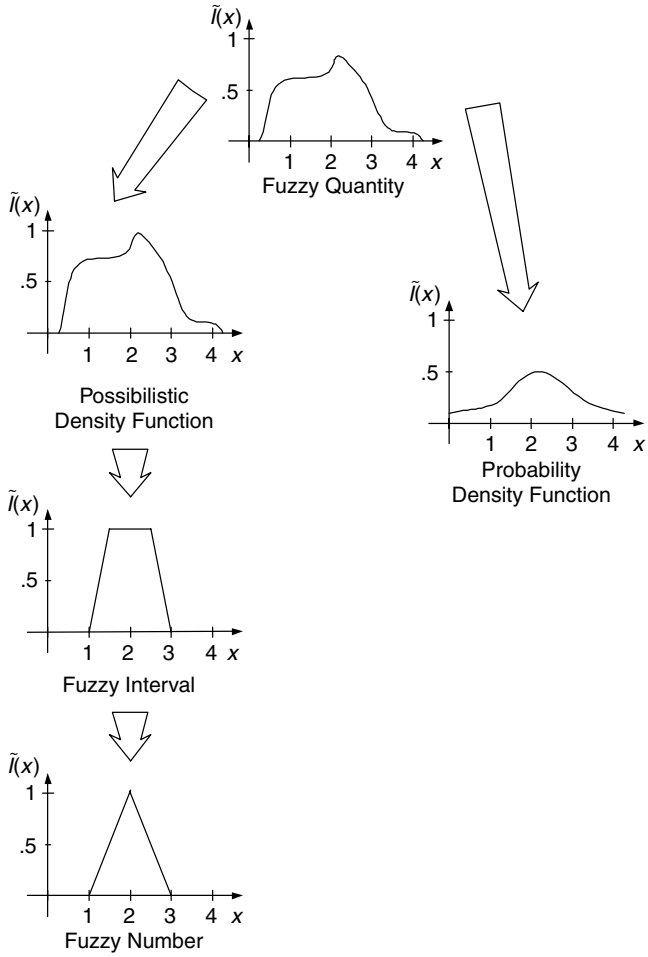

FIGURE 9.4 Kinds of fuzzy quantities.

Copyright 2005 by CRC Press LLC

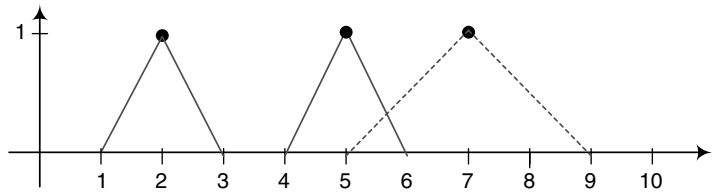

FIGURE 9.5 The fuzzy arithmetic operation [1, 2, 3] + [4, 5, 6] = [5, 7, 9].

Fuzzy intervals and numbers are named deliberately to invoke their extension from intervals and numbers. In particular, if a fuzzy interval $\tilde{I}$ is crisp, so that $\mu_{\tilde{I}}\mathbb{R} \mapsto \{0,1\}$, then $\tilde{I}$ is a crisp interval I with characteristic function $\chi_I = \mu_{\tilde{I}}$. Similarly, if a fuzzy number $\tilde{I}$ is crisp with mode x_0, so that $\tilde{I}(x_0) = 1$ and $\forall x \neq x_0, \tilde{I}(x) = 0$, then $\tilde{I}$ is just the number x_0, also characterized as the crisp interval $[x_0, x_0]$.

So this clears the way for us to define operations on fuzzy intervals, necessary to include it as a branch of GIT. As with crisp intervals, we are concerned with two fuzzy intervals $\tilde{I}, \tilde{J}$, and operations $* \in \{+, -, \times, \div\}$, etc. Then we have $\forall x \in \mathbb{R}$,

$$\mu_{\tilde{I} * \tilde{J}}(x) := \bigsqcup_{x = y * z} \left[\tilde{I}(y) \sqcap \tilde{J}(z) \right], \tag{9.9}$$

for some conorm $\sqcup$ and norm $\sqcap$. Again, the extension principle is adhered to, in that when $\tilde{I}$ and $\tilde{J}$ is crisp, Equation 9.3 is recovered from Equation 9.9.

An example of a fuzzy arithmetic operation is shown in Figure 9.5. We have two fuzzy numbers, each indicated by the triangles on the left. The leftmost, $\tilde{I}$, is unimodal around 2, and the rightmost, $\tilde{J}$, is unimodal around 6. Each is convex and normal, dropping to the x-axis as shown. Thus, $\tilde{I}$ expresses "about 2," and $\tilde{J}$ "about 5," and because they can be characterized by the three quantities of the mode and the x-intercepts, we denote them as

$$\tilde{I} = [1, 2, 3], \quad \tilde{J} = [4, 5, 6].$$

Applying Equation 9.9 for $* = +$ reveals $\tilde{I} + \tilde{J} = [5, 7, 9]$, which is "about 7."

Note how the extension principle is observed for fuzzy arithmetic as a generalization of interval arithmetic, in particular, we have

$$\mathbf{U}(\tilde{I} + \tilde{J}) = [5, 9] = [1, 3] + [4, 6] = \mathbf{U}(\tilde{I}) + \mathbf{U}(\tilde{J}),$$

where the final operation indicates interval arithmetic as in Equation 9.3.

The relations among these classes of fuzzy quantities, along with representative examples of each, is shown in Figure 9.6

9.3.3.5 Interpretations and Applications

Some simple examples can illustrate the uncertainty concept and construction of a fuzzy set, and the corresponding membership function.

First, let Ω be the set of integers between zero and ten, inclusive: $\Omega = \{0, 1, 2, \ldots, 10\}$. Suppose we are interested in a subset of Ω, $\tilde{A}$, where $\tilde{A}$ contains all the *medium* integers of Ω: $\tilde{A} = \{\omega : \omega \in \Omega$ and ω is medium$\}$. To specify $\tilde{A}$, the term "medium integer" must be defined. Most would consider 5 as medium, but what about 7? The uncertainty (or vagueness) about what constitutes a medium integer is what makes $\tilde{A}$ a fuzzy set, and such sets occur in our everyday use (or natural language). The uncertainty of

Copyright 2005 by CRC Press LLC

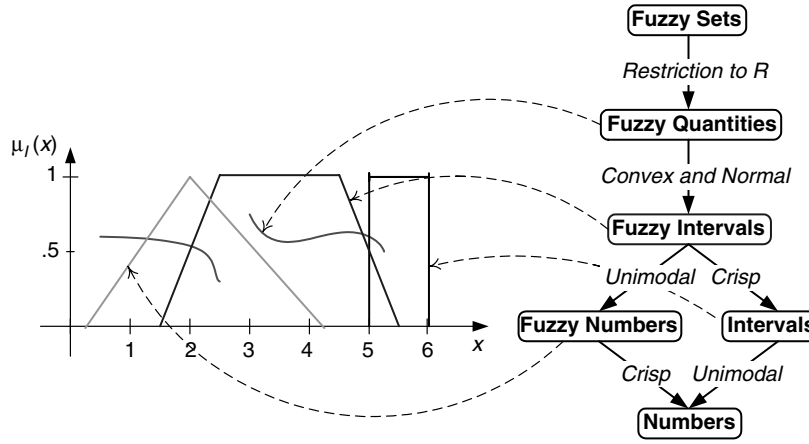

FIGURE 9.6 Fuzzy quantities.

classification arises because the boundaries of $\tilde{A}$ are not crisp. The integer 7 might have some membership (belonging) in $\tilde{A}$ and yet also have some degree of membership in $\tilde{A}^c$. Said another way, the integer 7 might have some membership in $\tilde{A}$ and yet also have some membership in another fuzzy set, $\tilde{B}$, where $\tilde{B}$ is the fuzzy set of large integers in Ω.

For a more meaningful example, assume we have a concept design for a new automotive system, like a fuel injector. Many of its components are also new designs, but may be similar to ones used in the past, implying that partial knowledge exists that is relevant to the new parts, but also implying large uncertainties exist about the performance of these parts and the system. The designer of this system wants to assess its performance based upon whatever information is currently available before building prototypes or implementing expensive test programs. The designer also wants to be assured that the performance is "excellent" with a high confidence. This desire defines a reliability **linguistic variable**. While reliability is traditionally defined as the probability that a system performs its functions for a given period of time and for given specifications, the knowledge about performance (especially new concepts) may only be in the form of linguistic and fuzzy terms.

For example, a component designer may only have access to the information that "if the temperature is too hot, this component won't work very well." The conditions (e.g., "too hot") can be characterized by a fuzzy set, and the performance (e.g., "won't work very well") can also be represented by a fuzzy set. Chapter 11 of Ross, Booker, and Parkinson [15] illustrates how fuzzy sets can be used for linguistic information and then combined with test data, whose uncertainty is probabilistic, to form a traditionally defined reliability.

Combining the probabilistic uncertainty of outcomes of tests and uncertainties of fuzzy classification from linguistic knowledge about performance requires a theoretical development for linking the two theories. Linkage between the probability and fuzzy set theories can be accomplished through the use of Bayes theorem, whose two ingredients are a prior probability distribution function and a likelihood function. As discussed in Section 9.3.3.3, Singpurwalla and Booker [30] relax the convention that the maximum value of $\tilde{A}(\omega)$ is set to 1.0, because that better conforms to the definition of a likelihood. Their theoretical development demonstrates the equivalency of likelihood and membership.

In the example above, if test data exists on a component similar to a new concept design component then probability theory could be used to capture the uncertainties associated with that data set, forming the prior distribution in Bayes theorem. Expert knowledge about the new design in the form of linguistic information about performance could be quantified using fuzzy membership functions, forming the likelihood. The combination of these two through Bayes theorem produces a posterior distribution, providing a probability based interpretation of reliability for the component. See [15] for more details on this kind of approach.

Copyright 2005 by CRC Press LLC

9.3.4 Monotone and Fuzzy Measures

In discussing probability theory in Section 9.2.3, we distinguished the probability measure Pr valued on sets $A \subseteq \Omega$ from the probability distribution p valued on points $\omega \in \Omega$. Then in Section 9.3.3 we characterized the membership functions of fuzzy sets $\tilde{A}$ also as being valued on points $\omega \in \Omega$, and, indeed, that probability distributions and pdfs are, in fact, kinds of fuzzy sets. It is natural to consider classes of measures other than Pr which are also valued on subsets $A \subseteq \Omega$, and perhaps related to other kinds of fuzzy sets.

This is the spirit that inspired Sugeno to define classes of functions he called **fuzzy measures** [25, 32]. Since then, terminological clarity has led us to call these **monotone measures** [33].

Assume for the moment a finite universe of discourse Ω, and then define a monotone measure as a function $\nu : 2^{\Omega} \mapsto [0,1]$, where $\nu(\varnothing) = 0, \nu(\Omega) = 1$, and

$$A \subseteq B \rightarrow \nu(A) \leq \nu(B). \tag{9.10}$$

When Ω is uncountably infinite, continuity requirements on ν come into play, but this will suffice for us for now.

We can also define the **trace** of a monotone measure as the generalization of the concept of a density or distribution. For any monotone measure ν, define its trace as a function $\rho_{\nu} : \Omega \mapsto [0,1]$, where $\rho_{\nu}(\omega) := \nu(\{\omega\})$.

In general, measures are much "larger" than traces, in that they are valued on the space of subsets $A \subseteq \Omega$, rather than the space of the points of $\omega \in \Omega$. So, for finite Ω with $n = |\Omega|$, a trace needs to be valued n times, one for each point $\omega \in \Omega$, while a measure needs to be valued 2^n times, one for each subset $A \subseteq \Omega$. Therefore, it is very valuable to know if, for a particular measure, it might be possible not to know all 2^n values of the measure independently, but rather to be able to calculate some of these based on knowledge of the others; in other words, to be able to break the measure into a small number of pieces and then put those pieces back together again. This greatly simplifies calculations, visualization, and elicitation.

When this is the case, we call such a monotone measure **distributional** or **decomposable**. Mathematically, this is the case when there exists a conorm $\sqcup$ such that

$$\forall A, B \subseteq \Omega, \quad \nu(A \cup B) + \nu(A \cap B) = \nu(A) \sqcup \nu(B). \tag{9.11}$$

It follows that

$$\nu(A \cup B) = \nu(A) \sqcup \nu(B) - \nu(A \cap B).$$

It also follows that when $A \cap B = \varnothing$, then $\nu(A \cup B) = \nu(A) \sqcup \nu(B)$.

Decomposability expresses the idea that the measure can be broken into pieces. The smallest such pieces are just the values of the trace, and thus decomposability is also called "distributionality," and can be expressed as

$$\nu(A) = \bigsqcup_{\omega \in A} \rho_{\nu}(\omega).$$

Finally, we call a monotone measure **normal** when $\nu(\Omega) = 1$. When ν is both normal and decomposable, it follows that

$$\bigsqcup_{\omega \in \Omega} \rho_{\mathbf{v}}(\omega) = 1.$$

So it is clear that every probability measure Pr is a monotone measure, but not vice versa, and the distribution p of a finite probability measure and the pdf f of a probability measure on $\mathbb{R}$ are both traces

Copyright 2005 by CRC Press LLC

of the corresponding measure Pr. Indeed, all of these concepts are familiar to us from probability theory, and are, in fact, direct generalizations of it.

In particular, a probability measure Pr is a normal, monotone measure that is decomposable for the bounded sum conorm $+_b$ (see Section 9.3.2), and whose trace is just the density. Note, however, that because we presume that a probability measure Pr is always normalized, when operating on probability values, the bounded sum conorm $+_b$ becomes equivalent to addition +. For example, when $\sum_{\omega\in\Omega} p(\omega) = 1$, then $\forall \omega_1, \omega_2 \in \Omega, p(\omega_1) +_b p(\omega_2) = p(\omega_1) + p(\omega_2)$. In this way we recover the familiar results for probability theory:

$$\begin{aligned} \Pr(A \cup B) &= \Pr(A) + \Pr(B) - \Pr(A \cap B) \\ A \cap B = \varnothing \ &\rightarrow \Pr(A \cup B) = \Pr(A) + \Pr(B) \\ \Pr(A) + \Pr(A^c) &= 1 \\ \Pr(A) &= \sum_{\omega \in A} p(\omega). \end{aligned} \tag{9.12}$$

Note that a trace $\rho_v : \Omega \mapsto [0,1]$ is a function to the unit interval, and is thus a fuzzy set. This will be important below, as in many instances it is desirable to interpret the traces of fuzzy measures such as probability or possibility distributions as special kinds of fuzzy sets.

A measure of information content in the context of general fuzzy or monotone measures is an area of active research, and beyond the scope of this chapter (see elsewhere for details [33]). Below we consider some particular cases in the context of random sets and possibility theory.

9.3.5 Random Sets and Dempster-Shafer Evidence Theory

In our historical discussion in Section 9.3.1, we noted that one of the strongest threads in GIT dates back to Dempster's work in probability measures propagated through multi-valued maps, and the subsequent connection to Shafer's theory of evidence and random sets. We detail this in this section, building on the ideas of monotone measures.

9.3.5.1 Dempster-Shafer Evidence Theory

In particular, we can identify **belief** Bel and **plausibility** Pl as dual fuzzy measures with the properties of super- and sub-additivity, respectively:

$$\begin{aligned} \mathrm{Bel}(A \cup B) &\geq \mathrm{Bel}(A) + \mathrm{Bel}(B) - \mathrm{Bel}(A \cap B) \\ \mathrm{Pl}(A \cap B) &\leq \mathrm{Pl}(A) + \mathrm{Pl}(B) - \mathrm{Pl}(A \cup B). \end{aligned}$$

Note the contrast with the additivity of a probability measure shown in Equation 9.12. In particular, it follows that each probability measure Pr is both a belief and a plausibility measure simultaneously. Also, while Pr is always decomposable in $+_b$, Bel and Pl are only decomposable under some special circumstances.

Again, in contrast with probability, we have the following sub- and super-additive properties for Bel and Pl:

$$\mathrm{Bel}(A) + \mathrm{Bel}(A^c) \leq 1, \qquad \mathrm{Pl}(A) + \mathrm{Pl}(A^c) \geq 1$$

Also, Bel and Pl are dually related, with:

$$\mathrm{Bel}(A) \leq \mathrm{Pl}(A), \tag{9.13}$$

$$\mathrm{Bel}(A) = 1 - \mathrm{Pl}(A^c), \quad \mathrm{Pl}(A) = 1 - \mathrm{Bel}(A^c). \tag{9.14}$$

Copyright 2005 by CRC Press LLC

So, not only are Bel and Pl co-determining, but each also determines and is determined by another function called a **basic probability assignment** $m : 2^{\Omega} \mapsto [0, 1]$ where $m(\emptyset) = 0$, and

$$\sum_{A \subseteq \Omega} m(A) = 1. \tag{9.15}$$

$m(A)$ is also sometimes called the "mass" of A.

$$\text{Bel}(A) = \sum_{B \subseteq A} m(B), \qquad \text{Pl}(A) = \sum_{B \cap A \neq \emptyset} m(B)$$

We then have the following relations:

$$m(A) = \sum_{B \subseteq A} (-1)^{|A-B|} \text{Bel}(B) = \sum_{B \subseteq A} (-1)^{|A-B|} (1 - \text{Pl}(B^c)), \tag{9.16}$$

where Equation 9.16 expresses what is called a **Möbius inversion**. Thus, given any one of m, Bel, or Pl, the other two are determined accordingly.

Some other important concepts are:

- A **focal element** is a subset $A \subseteq \Omega$ such that $m(A) > 0$. In this chapter, we always presume that there are only a finite number N of such focal elements, and so we use the notation $A_j, 1 \leq j \leq N$ for all such focal elements.
- The **focal set** $\mathcal{F}$ is the collection of all focal elements:

$$\mathcal{F} = \{A_j \subseteq \Omega : m(A_j) > 0\}.$$

- The **support** of the focal set is the global union:

$$\mathbf{U} = \bigcup_{A_j \in \mathcal{F}} A_j.$$

- The **core** of the focal set is the global intersection:

$$\mathbf{C} = \bigcap_{A_j \in \mathcal{F}} A_j.$$

- A **body of evidence** is the combination of the focal set with their masses:

$$\mathcal{S} = \langle \mathcal{F}, m \rangle = \langle \{A_j\}, \{m(A_j)\} \rangle, \qquad 1 \leq j \leq N\,.$$

- Given two independent bodies of evidence $\mathcal{S}_1 = \langle \mathcal{F}_1, m_1 \rangle, \mathcal{S}_2 = \langle \mathcal{F}_2, m_2 \rangle$, then we can use **Dempster combination** to produce a combined body of evidence $\mathcal{S} = \mathcal{S}_1 \oplus \mathcal{S}_2 = \langle \mathcal{F}, m \rangle$, where $\forall A \subseteq \Omega$,

$$m(A) = \frac{\sum_{A_1 \cap A_2 = A} m_1(A_1) m_2(A_2)}{\sum_{A_1 \cap A_2 \neq \emptyset} m_1(A_1) m_2(A_2)}.$$

While Dempster's rule is the most prominent combination rule, there are a number of others available [34].

Copyright 2005 by CRC Press LLC

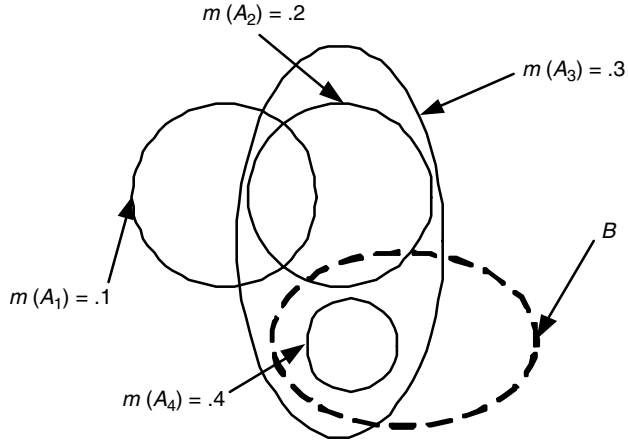

FIGURE 9.7 A Dempster-Shafer body of evidence.

- Assume a body of evidence $\mathcal{S}$ drawn from a finite universe of discourse with $\Omega = \{\omega_i\}$ with $1 \leq i \leq n$. Then if $N = n$, so that the number of focal elements is equal to the number of elements of the universe of discourse, then we call $\mathcal{S}$ **complete** [35].

An example is shown in Figure 9.7. We have:

$$\mathcal{F} = \{A_1, A_2, A_3, A_4\}$$

$$m(A_1) = .1, \quad m(A_2) = .2, \quad m(A_3) = .3, \quad m(A_4) = .4$$

$$\text{Bel}(B) = \sum_{A_j \subseteq B} m(A_j) = m(A_4) = .4$$

$$\text{Pl}(B) = \sum_{A_j \cap B \neq \varnothing} m(A_j) = m(A_2) + m(A_3) + m(A_4) = .2 + .3 + .4 = .9.$$

9.3.5.2 Random Sets

Above we identified the structure $\mathcal{S} = \langle \mathcal{F}, m \rangle = \langle \{A_j\}, \{m(A_j)\} \rangle$ as a body of evidence. When Ω is finite, we can express this body of evidence in an alternative form: instead of a pair of sets ($\mathcal{F}$ and m), now we have a set of pairs, in particular, pairings of focal elements $A_j \in \mathcal{F}$ with their basic probability value $m(A_j)$:

$$\langle \{A_j\}, \{m(A_j)\} \rangle \mapsto \{\langle A_j, m(A_j) \rangle\}.$$

We call this form the **random set** representation of the DS body of evidence.

This alternative formulation is triggered by recalling that $\sum_{A_j \in \mathcal{F}} m(A_j) = 1$, so that m can be taken as a discrete probability distribution or density on the various sets A_j. In other words, we can interpret $m(A_j)$ as the probability that A_j occurs compared to all the other $A \subseteq \Omega$.

Note that despite a superficial similarity, there is a profound difference between a probability measure $\Pr(A)$ and a basic probability assignment $m(A)$. Where it must *always* be the case that for two sets $A, B \subseteq \Omega$, Equation 9.12 must hold, in general there need be *no* relation between $m(A)$ and $m(B)$, other than Equation 9.15, that $\sum_{A \subseteq \Omega} m(A) = 1$.

To explicate this difference, we recall the definition of a **random variable**. Given a probability space $\langle \Omega, \mathcal{E}, \Pr \rangle$, then a function $S: X \mapsto \Omega$ is a random variable if S is "Pr-measurable," so that $\forall \omega \in \Omega$,

Copyright 2005 by CRC Press LLC

$S^{-1}(\omega) \in \mathcal{E}$. S then assigns probabilities to the items $\omega \in \Omega$. Similarly, we can think of a random set simply as a random variable that takes values on *collections* or *sets* of items, rather than points.

General Random Set: $\mathcal{S}: X \mapsto 2^{\Omega} - \{\emptyset\}$ is a random subset of Ω if $\mathcal{S}$ is Pr-measurable: $\forall \emptyset \neq A \subseteq \Omega$ $\mathcal{S}^{-1}(A) \in \Sigma$. m acts as a density of $\mathcal{S}$.

Given this, we can then interpret the DS measures in a very natural way in terms of a random set $\mathcal{S}$:

$$m(A) = \Pr(\mathcal{S} = A),$$

$$\text{Bel}(A) = \Pr(\mathcal{S} \subseteq A),$$

$$\text{Pl}(A) = \Pr(\mathcal{S} \cap A \neq \emptyset).$$

In the remainder of the chapter we will generally refer to random sets, by which we will mean finite random sets, which are isomorphic to finite DS bodies of evidence. Also, for technical reasons (some noted below in Section 9.3.6.2), there is a tendency to work only with the plausibility measure Pl, and to recover the belief Bel simply by the duality relation (Equation 9.14). In particular, for a general random set, we will generally consider its trace specifically as the plausibilistic trace ρ_{Pl}, and thereby have

$$\rho_{\text{Pl}}(\omega_i) = \text{Pl}(\{\omega_i\}) = \sum_{A_j \ni \omega_i} m_j.$$

The components of random sets as a GIT are now apparent. The basic components now are not points $\omega \in \Omega$, but rather subsets $A \subseteq \Omega$, and the compound objects are the random sets $\mathcal{S}$. The valuation set is again [0, 1], and the valuation is in terms of the evidence function m. Finally, operations are in terms of the kinds of combination rules discussed above [34], and operations defined elsewhere, such as inclusion of random sets [36].

9.3.5.3 The Information Content of a Random Set

The final component of random sets as a GIT, namely the measure of the information content of a random set, has been the subject of considerable research. Development of such a measure is complicated by the fact that random sets by their nature incorporate two distinct kinds of uncertainty. First, because they are random variables, they have a probabilistic component best measured by entropies, as in Equation 9.6. But, unlike pure random variables, their fundamental "atomic units" of variation are the focal elements A_j, which differ from each other in size $|A_j|$ and structure, in that some of them might overlap with each other to one extent or another. These aspects are more related to simple sets or intervals, and thus are best measured by measures of "nonspecificity" such as the Hartley measure of Equations 9.1 and 9.4.

Space precludes a discussion of the details of developing information measure for random sets (see [33]). The mathematical development has been long and difficult, but we can describe some of the highlights here.

The first good candidate for a measure of uncertainty in random sets is given by generalizing the nonspecificity of Equations 9.1 and 9.4 to be:

$$U_{\text{N}}(\mathcal{S}) := -\sum_{A_j \in \mathcal{F}} m_j \log_2(|A_j|). \tag{9.17}$$

This has a number of interpretations, the simplest being the expectation of the size of a focal element. Thus, both components of uncertainty are captured: the randomness of the probabilistic variable coupled to the variable size of the focal element.

Copyright 2005 by CRC Press LLC

While this nonspecificity measure U_N captures many aspects of uncertainty in random sets, it does not as well capture all the attributes related to conflicting information in the probabilistic component m, which is reflected in probability theory by the entropy of Equation 9.6. A number of measures have been suggested, including **conflict** as the entropy of the singletons:

$$U_S(\mathcal{S}) := -\sum_{\omega_i \in \Omega} m(\{\omega_i\}) \log_2(m(\{\omega_i\})),$$

and **strife** as a measure of entropy focused on individual focal elements:

$$U_S(\mathcal{S}) := -\sum_{A_j \in \mathcal{F}} m_j \log_2 \left[\sum_{k=1}^{N} m_k \frac{|A_j \cap A_k|}{|A_j|} \right].$$

While each of these measures can have significant utility in their own right, and arise as components of a more detailed mathematical theory, in the end, none of the them alone proved completely successful in the context of a rigorous mathematical development. Instead, attention has turned to single measures that attempt to directly integrate both nonspecificity and conflict information. These measures are not characterized by closed algebraic forms, but rather as optimization problems over sets of probability distributions. The simplest expression of these is given as an **aggregate uncertainty**:

$$U_{AU}(\mathcal{S}) := \max_{p: \forall A \subseteq \Omega, \Pr(A) \leq \mathrm{Pl}(A)} U_{\mathrm{prob}}(p), \tag{9.18}$$

recalling that $\Pr(A) = \sum_{\omega_i \in A} p(\omega_i)$ and $U_{\mathrm{prob}}(p)$ is the statistical entropy (Equation 9.6). In English, U_{AU} is the largest entropy of all probability distributions consistent with the random set $\mathcal{S}$.

9.3.5.4 Specific Random Sets and the Extension Principle

The extension principle also holds for random sets, recovering ordinary random variables in a special case. So, given that random sets are set-valued random variables, then we can consider the special case where each focal element is not, in fact, a set at all, but really just a point, in particular a singleton set. We call such a focal set **specific**:

$$\forall A_j \in \mathcal{F}, \quad |A_j| = 1, \quad \exists! \omega_i \in \Omega, A_j = \{\omega_i\}.$$

When a specific random set is also complete, then conversely we have that $\forall \omega_i \in \Omega, \exists! A_j \in \mathcal{F}, A_j = \{\omega_i\}$.

Under these conditions, the gap between $\mathrm{Pl}(A)$ and $\mathrm{Bel}(A)$ noted in Equation 9.13 closes, and this common DS measure is just a probability measure again:

$$\forall A \subseteq \Omega, \quad \mathrm{Pl}(A) = \mathrm{Bel}(A) = \Pr(A). \tag{9.19}$$

And when $\mathcal{S}$ is complete, the plausibilistic trace reverts to a probability distribution, with $p(\omega_i) = m_j$ for that A_j which equals $\{\omega_i\}$.

As an example, consider Figure 9.8, where $\Omega = \{x, y, z, w\}$, and $\mathcal{F} = \{\{x\}, \{y\}, \{z\}, \{w\}\}$ with m as shown. Then, for $B = \{z, w\}, C = \{y, w\}$, we have

$$\mathrm{Bel}(B) = \mathrm{Pl}(B) = \Pr(B) = .3 + .4 = .7, \quad \Pr(B \cup C) = \Pr(B) + \Pr(C) - \Pr(B \cap C) = .9,$$

and, using vector notation, the probability distribution is $p = \langle .1, .2, .3, .4 \rangle$.

Copyright 2005 by CRC Press LLC

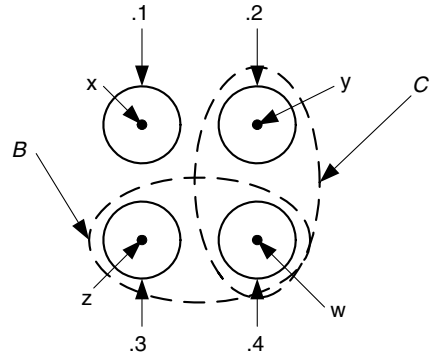

FIGURE 9.8 A specific random set, which induces a probability distribution.

9.3.5.5 Random Intervals and P-Boxes

Above we moved from sets to intervals, and then fuzzy sets to fuzzy intervals. Now we want to similarly move from random sets to **random intervals**, or DS structures on the Borel field $\mathcal{D}$ defined in Equation 9.2. Define a random interval $\mathcal{A}$ as a random set on $\Omega = \mathbb{R}$ for which $\mathcal{F}(\mathcal{A}) \subseteq \mathcal{D}$. Thus, a random interval is a random left-closed interval subset of $\mathbb{R}$. For a random interval, we denote the focal elements as intervals $I_j, 1 \le j \le N$, so that $\mathcal{F}(\mathcal{A}) = \{I_j\}$.

An example is shown in Figure 9.9, with $N = 4$,

$$\mathcal{F} = \{[2.5, 4), [1, 2), [3, 4), [2, 3.5)\},$$

support $\mathbf{U}(\mathcal{F}(\mathcal{A})) = [1, 4)$, and m is as shown.

Random interval approaches are an emerging technology for engineering reliability analysis [37–41]. Their great advantage is their ability to represent not only randomness via probability theory, but also imprecision and nonspecificity via intervals, in an overall mathematical structure that is close to optimally simple. As such, they are superb ways for engineering modelers to approach the world of GIT.

So, random intervals are examples of DS structures restricted to intervals. This restriction is very important because it cuts down substantially on both the quantity of information and computational and human complexity necessary to use such structures for modeling. Even so, they remain relatively complex structures, and can present challenges to modelers and investigators in their elicitation and interpretation. In particular, interpreting the fundamental structures such as possibly overlapping focal elements and basic probability weights can be a daunting task for the content expert, and it can be desirable to interact with investigators over more familiar mathematical objects. For these reasons, we commonly introduce simpler mathematical structures that approximate the complete random interval by representing a portion of their information. We introduce these now.

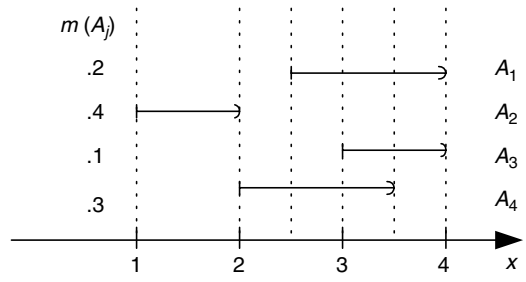

FIGURE 9.9 A random interval.

Copyright 2005 by CRC Press LLC

A probability box, or just a **p-box** [42], is a structure $\mathcal{B} := \langle \underline{B}, \overline{B} \rangle$, where $\underline{B}, \overline{B} : \mathbb{R} \mapsto [0,1]$,

$$\lim_{x \mapsto -\infty} B(x) \to 0, \quad \lim_{x \mapsto \infty} B(x) \to 1, \quad B \in \mathcal{B},$$

and $\underline{B}, \overline{B}$ are monotonic with $\underline{B} \leq \overline{B}$. $\underline{B}$ and $\overline{B}$ are interpreted as bounds on cumulative distribution functions (CDFs). In other words, given $\mathcal{B} = \langle \underline{B}, \overline{B} \rangle$, we can identify the set of all functions $\{F : \underline{B} \leq F \leq \overline{B}\}$ such that F is the CDF of some probability measures Pr on $\mathbb{R}$. Thus each p-box defines such a class of probability measures.

Given a random interval $\mathcal{A}$, then

$$\mathcal{B}(\mathcal{A}) := \langle \text{BEL}, \text{PL} \rangle \tag{9.20}$$

is a p-box, where BEL and PL are the "cumulative belief and plausibility distributions" $\text{PL}, \text{BEL} : \mathbb{R} \mapsto [0, 1]$ originally defined by Yager [43]

$$\text{BEL}(x) := \text{Bel}((-\infty, x)), \quad \text{PL}(x) := \text{Pl}((-\infty, x)).$$

Given a random interval $\mathcal{A}$, then it is also valuable to work with its plausibilistic trace (usually just identified as its trace), where $r_{\mathcal{A}}(x) := \text{Pl}(\{x\})$. Given a random interval $\mathcal{A}$, then we also have that $r_{\mathcal{A}} = \text{PL} - \text{BEL}$, so that for a p-box derived from Equation 9.20, we have

$$r_{\text{A}} = \overline{B} - \underline{B}. \tag{9.21}$$

See details elsewhere [44, 45].

The p-box generated from the example random interval is shown in the top of Figure 9.10. Because $\overline{B}$ and $\underline{B}$ partially overlap, the diagram is somewhat ambiguous on its far left and right portions, but note that

$$\overline{B}((-\infty, 1)) = 0, \quad \underline{B}((-\infty, 2,)) = 0,$$
$$\overline{B}([3, \infty)) = 1, \quad \underline{B}([3.5, \infty)) = 1.$$

The trace $r_{\mathcal{A}} = \overline{B} - \underline{B}$ is also shown.

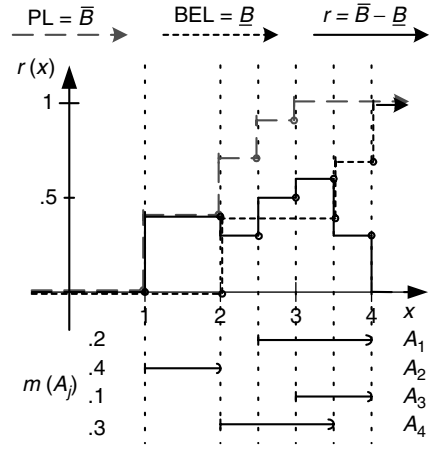

FIGURE 9.10 The probability box derived from a random interval.

Copyright 2005 by CRC Press LLC

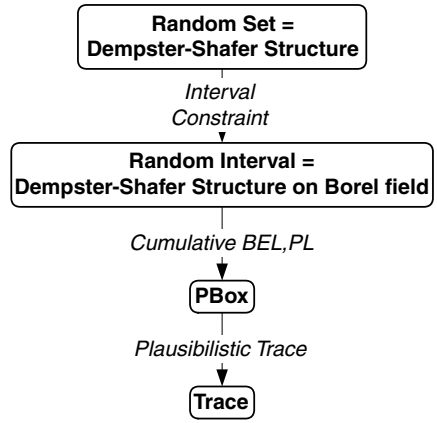

FIGURE 9.11 Relations among random sets, random intervals, p-boxes, and their traces.

So each random interval determines a p-box by Equation 9.20, which in turn determines a trace by Equation 9.21. But conversely, each trace determines an equivalence class of p-boxes, and each p-box an equivalence class of random intervals. In turn, each such equivalence class has a canonical member constructed by a standard mechanism. These relations are diagrammed in Figure 9.11, and see details elsewhere [45].

9.3.6 Possibility Theory

So far, we have discussed classical uncertainty theories in the form of intervals and probability distributions; their generalization to fuzzy sets and intervals; and the corresponding generalization to random sets and intervals. In this section we introduce **possibility theory** as a form of information theory, which in many ways exists as an alternative to and in parallel with probability theory, and which arises in the context of both fuzzy systems and DS theory.

9.3.6.1 Possibility Measures and Distributions

In Section 9.3.4 we identified a probability measure Pr as a normal monotone measure that is decomposable for the bounded sum conorm $+_b$. Similarly, a **possibility measure** Π is a normal, monotone measure that is decomposable for the *maximum* conorm $\vee$. In this way, the familiar results for probability theory shown in Equation 9.12 are replaced by their maximal counterparts for possibility theory. In particular, Equation 9.11 yields

$$\forall A, B \subseteq \Omega, \quad \Pi(A \cup B) \vee \Pi(A \cap B) = \Pi(A) \vee \Pi(B), \tag{9.22}$$

so that from Equation 9.10 it follows that

$$\Pi(A \cup B) = \Pi(A) \vee \Pi(B), \tag{9.23}$$

whether A and B are disjoint or not.

The trace of a possibility measure is called a **possibility distribution** $\pi : \Omega \mapsto [0,1], \pi(\omega) = \Pi(\{\omega\})$. Continuing our development, we have the parallel results from probability theory:

$$\Pi(A) = \bigvee_{\omega \in A} \pi(\omega), \quad \Pi(\Omega) = \bigvee_{\omega \in \Omega} \pi(\omega) = 1.$$

Copyright 2005 by CRC Press LLC

In Section 9.3.5.4 and Figure 9.8 we discussed how the extension principle recovers a "regular" probability measure from a random set when the focal elements are specific, so that the duality of belief and plausibility collapses and we have that $\text{Bel} = \text{Pl} = \text{Pr}$. In a sense, possibility theory represents the opposite extreme case. In a specific random set, all the focal elements are singletons, and are thus maximally small and disjoint from each other. Possibility theory arises in the alternate case, when the focal elements are maximally large and intersecting.

In particular, we call a focal set **consonant** when $\mathcal{F}$ is a nested class, so that $\forall A_1, A_2 \in \mathcal{F}$, either $A_1 \subseteq A_2$ or $A_2 \subseteq A_1$. We can then arbitrarily order the A_j so that $A_i \subseteq A_{i+1}$, and we assign $A_0 := \varnothing$. If a consonant random set is also complete, then we can use the notation

$$\forall 1 \le i \le n, \quad A_i = \{\omega_1, \omega_2, \ldots, \omega_i\} \tag{9.24}$$

and we have that $A_i - A_{i-1} = \{\omega_i\}$.

Whenever a random set is consonant, then the plausibility measure Pl becomes a measure Π. But unlike in a specific random set, where the belief and plausibility become maximally close, in a consonant random set the belief and plausibility become maximally separated, to the point that we call the dual belief measure Bel a **necessity measure**:

$$\eta(A) = 1 - \Pi(A^c).$$

Where a possibility measure Π is characterized by the maximum property by Equation 9.23, a necessity measure η is characterized by

$$\eta(A \cap B) = \eta(A) \wedge \eta(B) \tag{9.25}$$

For the possibility distribution, when $\mathcal{S}$ is complete, and using the notation from Equation 9.24, we have:

$$\pi(\omega_i) = \sum_{j=i}^{n} m_j, \quad m(A_i) = \pi(\omega_i) - \pi(\omega_{i+1}),$$

where $\pi_{n+1} := 0$ by convention.

An example of a consonant random set is shown in Figure 9.12, where again $\Omega = \{x, y, z, w\}$, but now

$$\mathcal{F} = \{\{x\}, \{x, y\}, \{x, y, z\}, \{x, y, z, w\}\}$$

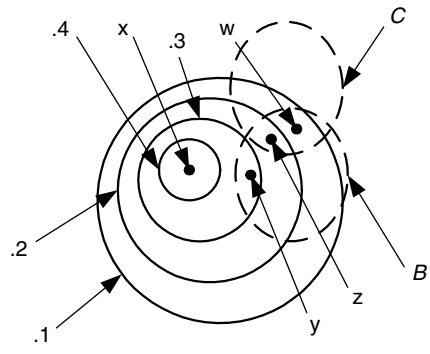

FIGURE 9.12 A consonant, possibilistic random set.

Copyright 2005 by CRC Press LLC

with m as shown. Then, for $B = \{y, z, w\}, C = \{z, w\}$, we have

$$\text{Pl}(B) = .1 + .2 + .3 = .6, \quad \text{Pl}(C) = .1 + .2 = .3,$$
$$\text{Pl}(B \cup C) = .1 + .2 + .3 = .6 = \text{Pl}(B) \vee \text{Pl}(C),$$

thus characterizing Pl as, in fact, a possibility measure Π. We also have, using vector notation, $\pi = \langle 1, .6, .3, .1 \rangle$.

In considering the information content of a possibility measure, our intuition tells us that it would best be thought of as a kind of nonspecificity such as in Equation 9.17. However, while the nonspecificity of a specific random set vanishes, the strife or conflict of a consonant random set does not. Indeed, it was exactly this observation that drove much of the mathematical development in this area, and thus, technically, the information content of a possibility measure is best captured by an aggregate uncertainty such as Equation 9.18.

However, for our purposes, it is useful to consider Equation 9.17 applied to consonant random sets. Under these conditions, we can express Equation 9.17 in terms of the possibility distribution as:

$$U_{\text{N}}(\pi) := \sum_{i=2}^{n} \pi_i \log_2\left(\frac{i}{i-1}\right) = \sum_{i=1}^{n} (\pi_i - \pi_{i+1}) \log_2(i).$$

9.3.6.2 Crispness, Consistency, and Possibilistic Histograms

In the case of the specific random set discussed in Section 9.3.5.4, not only do the belief measure Bel and plausibility measure Pl collapse together to the decomposable probability measure Pr, but also their traces ρ_{Bel} and ρ_{Pl} collapse to the trace of the probability measure ρ_{Pr}, which is just the probability density p.

But the possibilistic case, which is apparently so parallel, also has some definite differences. First, as we saw, the belief and plausibility measures are distinct as possibility Π and necessity η. Moreover, the necessity measure η is not decomposable, and indeed, the minimum operator $\wedge$ from Equation 9.25 is not a conorm. But moreover, the relation between the measure Pl and its trace ρ_{Pl} is also not so simple.

First consider the relation between intervals and fuzzy intervals discussed in Section 9.3.3.4. In particular, regular (crisp) intervals arise through the extension principle when the characteristic function takes values only in $\{0, 1\}$. Similarly, for general possibility distributions, it might be the case that $\pi(\omega_i) \in \{0, 1\}$. In this case, we call π a **crisp possibility distribution**, and otherwise identify a noncrisp possibility distribution as a **proper possibility distribution**. Thus, each fuzzy interval is a general (that is, potentially proper) possibility distribution, while each crisp interval is correspondingly a crisp possibility distribution.

Note that crispness can arise in probability theory only in a degenerate case, because if $\exists \omega_i, p(\omega_i) = 1$, then for all other values, we would have $p(\omega_i) = 0$. We call this case a **certain distribution**, which are the only cases that are both probability and possibility distributions simultaneously.

Now consider random sets where the core is non-empty, which we call **consistent**:

$$\mathbf{C} = \bigcap_{A_j \in \mathcal{F}} A_j \neq \varnothing.$$

Note that all consistent random sets are consonant, but not *vice versa*. But in these cases, the trace ρ_{Pl} is a maximal possibility distribution satisfying

$$\bigvee_{\omega \in \Omega} \rho_{\text{Pl}}(\omega) = 1,$$

Copyright 2005 by CRC Press LLC

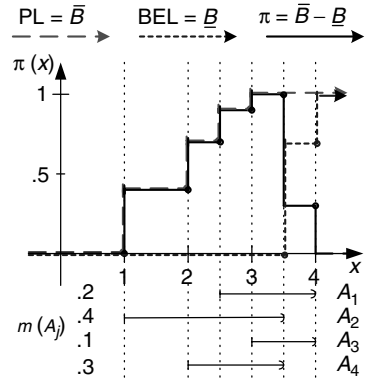

FIGURE 9.13 A consistent random interval with its possibilistic histogram π.

but Pl is not a possibility measure (that is, Equation 9.22 is *not* satisfied). However, it can be shown that for each consistent random set $\mathcal{S}$, there is a unique, well-justified consonant approximation $\mathcal{S}^*$ whose plausibilistic trace is equal to that of $\mathcal{S}$ [44].

When a consistent random interval is shown as a p-box, it also follows that the trace $\bar{B} - \underline{B} = \pi$ is this same possibility distribution. We have shown [44] that under these conditions, not only is $r = \pi$ a possibility distribution, but moreover is a fuzzy interval as discussed in Section 9.3.3.4. We then call π a **possibilistic histogram**.

An example is shown in Figure 9.13, with m as shown. Note in this case the positive core

$$\mathrm{C} = \bigcap_{A_j \in \mathcal{F}} A_j = [3, 3.5),$$

and that over this region, we have $\bar{B} = 1, \underline{B} = 0, r = 1$.

Returning to the domain of general, finite random sets, the relations among these classes is shown in Figure 9.14. Here we use the term "vacuous" to refer to a random set with a single focal element:

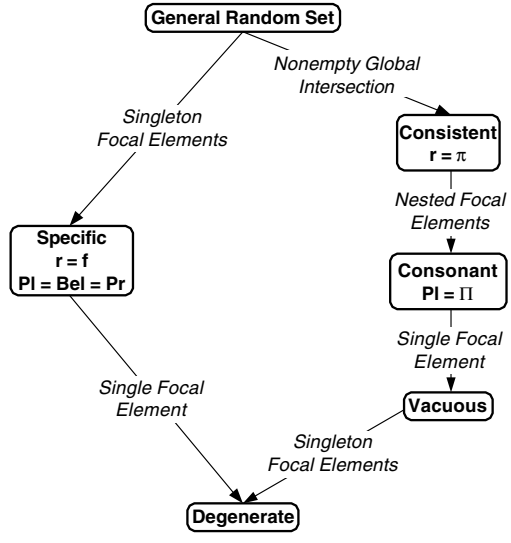

FIGURE 9.14 Relations among classes of random sets.

Copyright 2005 by CRC Press LLC

$\exists A \subseteq \Omega,\ \mathcal{F} = \{A\}$; and "degenerate" to refer to the further case where that single focal element has only one element: $\exists \omega \in \Omega,\ \mathcal{F} = \{\{\omega\}\}$.

9.3.6.3 Interpretations and Applications

Although max-preserving measures have their origins in earlier work, in the context of GIT possibility theory was originally introduced by Zadeh [26] as a kind of information theory strictly related to fuzzy sets. As such, possibility distributions were intended to be measured as and interpreted as linguistic variables.

And, as we have seen, in the context of real-valued fuzzy quantities, it is possible to interpret fuzzy intervals and numbers as possibility distributions. Thus we would hope to use possibility theory as a basis for representing fuzzy arithmetic operations as in Equation 9.8. However, just as there is not a strict symmetry between probabilistic and possibilistic concepts, so there is not a clean generalization here either. In particular, we have shown [45] that the possibilistic properties of fuzzy quantities are not preserved by fuzzy arithmetic convolution operations such as Equation 9.8 outside of their cores and supported.

One of the primary methods for the determination of possibilistic quantities is to take information from a probability distribution and convert it into a possibility distribution. For example, given a discrete probability distribution as a vector $p = \langle p_1, p_2, \ldots, p_n \rangle$, then we can create a possibility distribution $\pi = \langle \pi_1, \pi_2, \ldots, \pi_n \rangle$, where

$$\pi_i = \frac{p_i}{\max p_i}.$$

There are other conversion methods, and an extensive literature, including how the information measure is preserved or not under various transformations [46, 47]. However, one could argue that all such methods are inappropriate: when information is provided in such a way as to be appropriate for a probabilistic approach, then that approach should be used, and *vice versa* [27]. For the purposes of engineering reliability analysis, our belief is that a strong basis for possibilistic interpretations is provided by their grounding in random sets, random intervals, and p-boxes. As we have discussed, this provides a mathematically sound approach for the measurement and interpretation of statistical collections of intervals, which always yield p-boxes, and may or may not yield possibilistic special cases, depending on the circumstances. When they do not, if a possibilistic treatment is still desired, then various normalization procedures are available [48, 49] to transform an inconsistent random set or interval into a consistent or consonant one.

9.3.6.4 Relations between Probabilistic and Possibilistic Concepts

We are now at a point where we can summarize the relations existing between probabilistic and possibilistic concepts in the context of random set theory. To a certain extent, these are complementary, and to another distinct.

Table 9.5 summarizes the relations for general, finite random sets and the special cases of probability and possibility. Columns are shown for the case of general finite random sets, and then the two prominent probabilistic and possibilistic special cases. Note that these describe complete random sets, so that $n = N$ and the indices i on ω_i and j on A_j can be used interchangeably.

In Section 9.3.4 we noted that, formally, all traces of monotone measures are fuzzy sets. Thus, in particular, each probability and possibility distribution is a kind of fuzzy set. In Section 9.3.3.4, we similarly discussed relations among classes of fuzzy quantities, which are fuzzy sets defined on the continuous $\mathbb{R}$. The relations among classes of fuzzy sets defined on a finite space Ω are shown in Figure 9.15, together with examples of each for $\Omega = \{a, b, c, d, e\}$.

Figure 9.16 shows the relations between these distributions or traces as fuzzy sets (quantities defined on the points $\omega \in \Omega$) and the corresponding monotone measures (quantities defined on the subsets $A \subseteq \Omega$). Note that there is not a precise symmetry between probability and possibility. In particular, where probability distributions are symmetric to possibility distributions, probability measures collapse the duality of belief and plausibility, which is exacerbated for possibility.

Copyright 2005 by CRC Press LLC

TABLE 9.5 Summary of Probability and Possibility in the Context of Random Sets

	Random Set	Special Cases: Complete Random Sets, $N=n, i \leftrightarrow j$	
		Probability	Possibility
Focal Sets	Any $A_j \subseteq \Omega$	Singletons: $A_i = \{\omega_i\}$ $\{\omega_i\} = A_i$	Nest: $A_i = \{\omega_1, \ldots, \omega_i\}$ $\{\omega_i\} = A_i - A_{i-1}, A_0 := \varnothing$
Structure	Arbitrary	Finest Partition	Total order
Belief	$\mathrm{Bel}(A) = \sum_{A_j \subseteq A} m_j$	$\Pr(A) := \mathrm{Bel}(A)$	$\eta(A) := \mathrm{Bel}(A)$
Plausibility	$\mathrm{Pl}(A) = \sum_{A_j \cap A \neq \varnothing} m_j$	$\Pr(A) := \mathrm{Pl}(A)$	$\Pi(A) := \mathrm{Pl}(A)$
Relation	$\mathrm{Bel}(A) = 1 - \mathrm{Pl}(A^c)$	$\mathrm{Bel}(A) = \mathrm{Pl}(A) = \Pr(A)$	$\eta(A) = 1 - \Pi(A^c)$
Trace	$\rho_{\mathrm{Pl}}(\omega_i) = \sum_{A_j \ni \omega_i} m_j$	$p(\omega_i) := m(A_j), A_j = \{\omega_i\}$	$\pi(\omega_i) = \sum_{j=i}^{n} m_j$
		$m_i = p_i$	$m_i = \pi_i - \pi_{i+1}$
Measure		$\Pr(A \cup B) = \Pr(A) + \Pr(B) - \Pr(A \cap B)$	$\Pi(A \cup B) = \Pi(A) \vee \Pi(B)$
Normalization		$\sum_i p_i = 1$	$\bigvee_i \pi_i = 1$
Operator		$\Pr(A) = \sum_{\omega_i \in A} p_i$	$\Pi(A) = \bigvee_{\omega_i \in A} \pi_i$
Nonspecificity	$U_{\mathrm{N}}(\mathcal{S}) = \sum_{j=1}^{N} m_j \log_2 \lvert A_j \rvert$		$U_{\mathrm{N}}(\pi) = \sum_{i=2}^{n} \pi_i \log_2 \left[\frac{i}{i-1}\right] = \sum_{i=1}^{n} (\pi_i - \pi_{i+1}) \log_2(i)$
Conflict	$U_{\mathrm{S}}(\mathcal{S}) = -\sum_{i=1}^{n} m(\{\omega_i\}) \log_2(m(\{\omega_i\}))$	$U_{\mathrm{prob}}(p) = -\sum_i p_i \log_2(p_i)$	
Strife	$U_{\mathrm{S}}(\mathcal{S}) = -\sum_{j=1}^{N} m_j \log_2 \left[\sum_{k=1}^{N} m_k \frac{\lvert A_j \cap A_k \rvert}{\lvert A_j \rvert}\right]$	$U_{\mathrm{prob}}(p) = -\sum_i p_i \log_2(p_i)$	
Aggregate Uncertainty	$U_{AU}(\mathcal{S}) = \max_{p: \forall A \subseteq \Omega, \Pr(A) \leq \mathrm{Pl}(A)} U_{\mathrm{prob}}(p)$		

9.4 Conclusion and Summary

This chapter described the basic mathematics of the most common and prominent branches of both classical and generalized information theory. In doing so, we have emphasized primarily a perspective drawing from applications primarily in engineering modeling. These principles have use in many other fields, for example data fusion, image processing, and artificial intelligence.

It must be emphasized that there are many different mathematical approaches to GIT. The specific course of development espoused here, and the relations among the components described, is just one among many. There is a very large literature here that the diligent student or researcher can access.

Moreover, there are a number of mathematical components that properly belong to GIT but space precludes a development of here. In particular, research is ongoing concerning a number of additional mathematical subjects, many of which provide even further generalizations of the already generalized

Copyright 2005 by CRC Press LLC

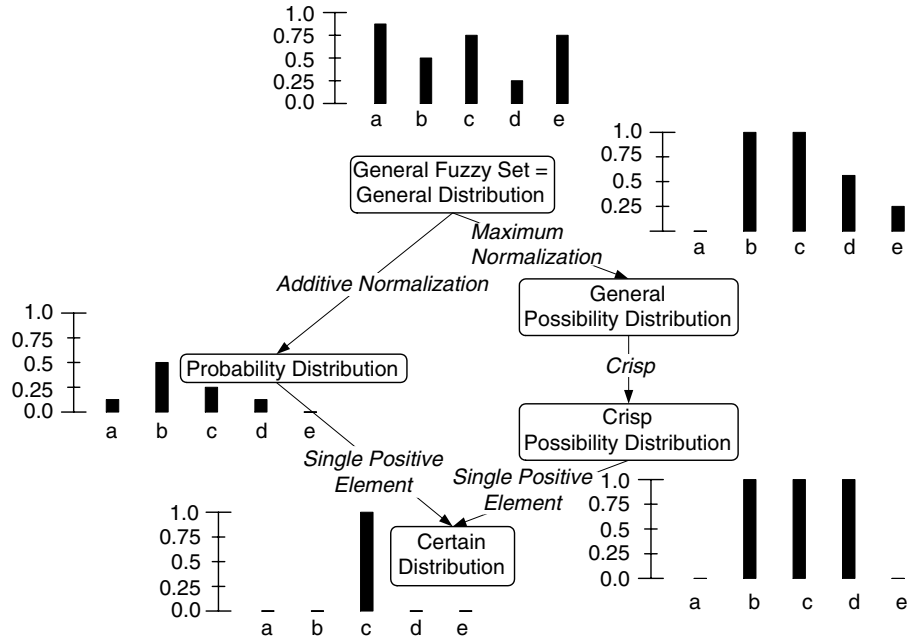

FIGURE 9.15 Relations among classes of general distributions as fuzzy sets.

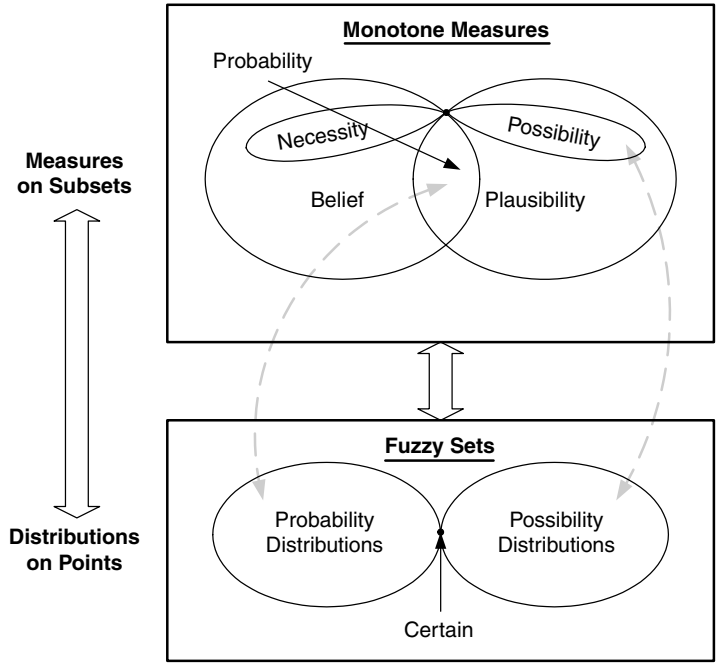

FIGURE 9.16 Relations between distributions on points and measures on subsets.

Copyright 2005 by CRC Press LLC

topics introduced here. These include at least the following:

Rough Sets: Pawlak [50] introduced the structure of a "rough" set, which is yet another way of capturing the uncertainty present in a mathematical system. Let $\mathcal{C} = \{A\} \subseteq 2^{\Omega}$ be a partition of Ω, and assume a special subset $A_0 \subseteq \Omega$ (not necessarily a member of the partition). Then $\mathbf{R}(A_0) := \{\underline{A}_0, \overline{A}_0\}$ is a **rough set** on Ω, where

$$\underline{A}_0 := \{A \in \mathcal{C} : A \subseteq A_0\}, \quad \overline{A}_0 := \{A \in \mathcal{C} : A \cap A_0 \neq \varnothing\}.$$

Rough sets have been closely related to the GIT literature [51], and are useful in a number of applications [52]. For our purposes, it is sufficient to note that $\overline{A}_0$ effectively specifies the support **U**, and $\underline{A}_0$ the nonempty core **C**, of a number of DS structures, and thus an equivalence class of possibility distributions on Ω [53].

Higher-Order Structures: In Section 9.3.3, we described how Zadeh's original move of generalizing from $\{0,1\}$-valued characteristic functions to $[0,1]$-valued membership functions can be thought of as a *process* of "fuzzification." Indeed, this lesson has been taken to heart by the community, and a wide variety of fuzzified structures have been introduced. For example, Type II and Level II fuzzy sets arise when fuzzy weights themselves are given weights, or whole fuzzy sets themselves. Or, fuzzified DS theory arises when focal elements *Aj* are generalized to fuzzy subsets $\tilde{A}_j \tilde{\subseteq} \Omega$. There is a fuzzified linear algebra; a fuzzified calculus, etc. It is possible to rationalize these generalizations into systems for generating mathematical structures [54], and approach the whole subject from a higher level of mathematical sophistication, for example by using category theory.

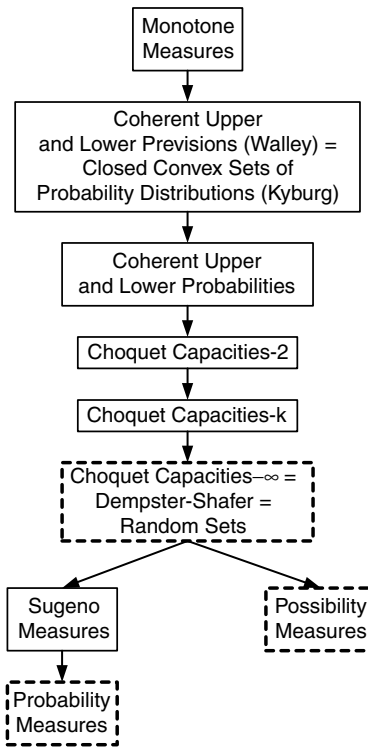

FIGURE 9.17 Relations among classes of monotone measures, imprecise probabilities, and related structures, adapted from [33].

Copyright 2005 by CRC Press LLC

Copyright 2005 by CRC Press LLC

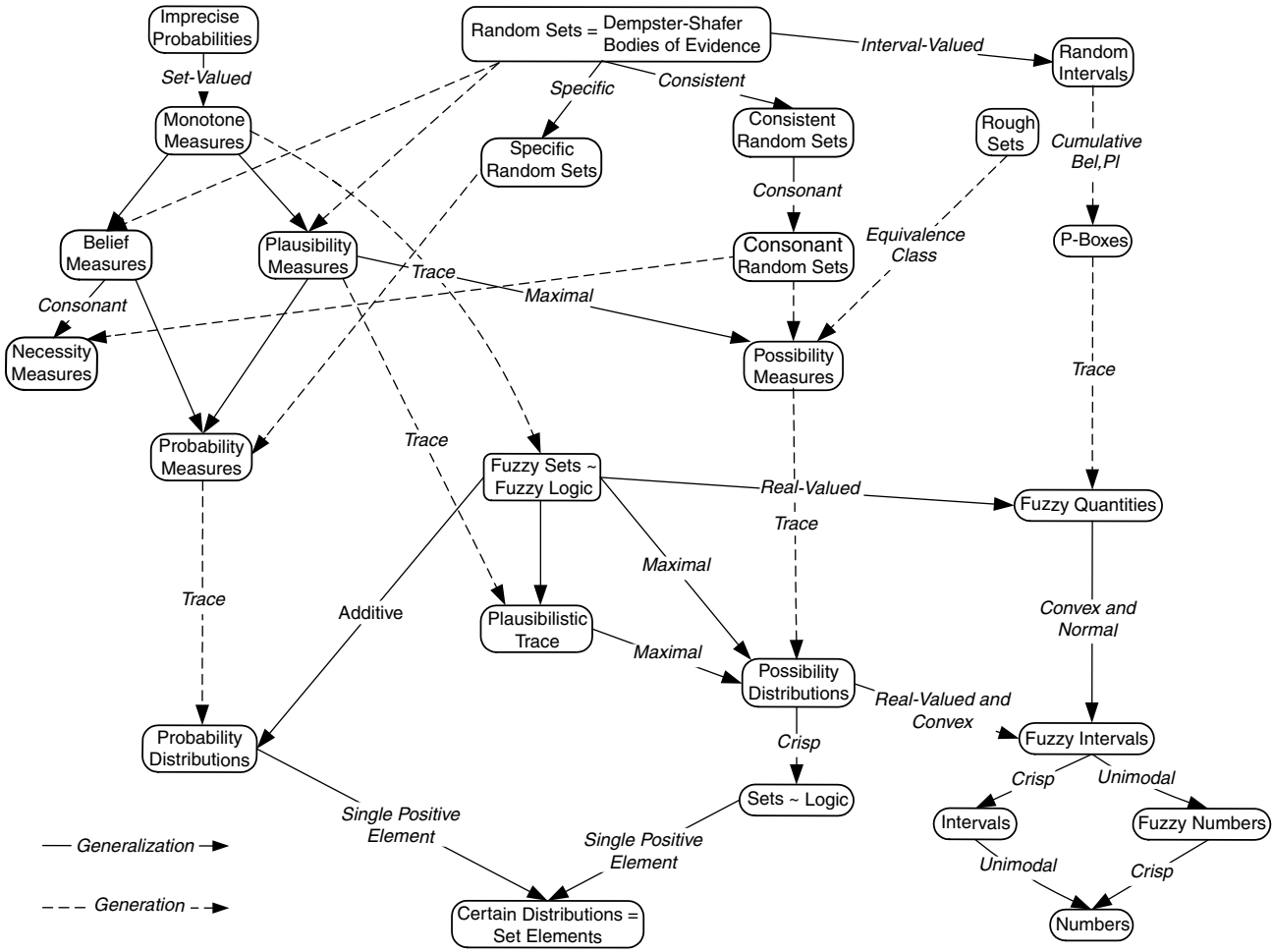

FIGURE 9.18 Map of the various sub-fields of GIT.

Other Monotone Measures, Choquet Capacities, and Imprecise Probabilities: We have focused exclusively on belief and plausibility measures, and their special cases of probability, possibility, and necessity measures. However, there are broad classes of fuzzy or monotone measures outside of these, with various properties worthy of consideration [32]. And while DS theory and random set theory arose in the 1960s and 1970s, their work was presaged by prior work by Choquet in the 1950s that identified many of these classes. Within that context, we have noted above in Section 9.3.1 that belief and plausibility measures stand out as special cases of **infinite order Choquet capacities** [19, 20].

Then, just as monotone measures generalize probability measures by relaxing the additivity property of Equation 9.5, it is also possible to consider relaxing the additivity property of random sets in Equation 9.15, or their range to the unit interval (that is, to consider possibly negative m values), and finally generalizing away from measures on subsets $A \subseteq \Omega$ altogther. Most of the most compelling research ongoing today in the mathematical foundations of GIT concerns these areas, and is described in various ways as **imprecise probabilities** [29] or **convex combinations of probability measures** [33, 55]. Of course, these various generalizations satisfy the extension principle, and thus provide, for example, an alternative basis for the more traditional sub-fields of GIT such as probability theory [56].

Research among all of these more sophisticated classes of generalized measures, and their connections, is active and ongoing. Figure 9.17, adapted from [33], summarizes the current best thought about these relations. Note the appearance in this diagram of certain concepts not explicated here, including previsions, Choquet capacities of finite order, and a class of monotone measures called "Sugeno" measures proper.

We close this chapter with our "grand view" of the relations among most of the structures and classes discussed in Figure 9.18. This diagram is intended to incorporate all of the particular diagrams included earlier in this chapter. Specifically, a solid arrow indicates a mathematical generalization of one theory by another, and thus an instance of where the extension principle should hold. These are labeled with the process by which this specification occurs. A dashed arrow indicates where one kind of structure is generated by another; for example, the trace of a possibility measure yields a possibility distribution.

Acknowledgments

The authors wish to thank the Los Alamos Nuclear Weapons Program for its continued support, especially the Engineering Sciences and Applications Division. This work has also been supported by a research grant from Sandia National Laboratories as part of the Department of Energy Accelerated Strategic Computing Initiative (ASCI).

References

1. Shannon, CE and Weaver, W: (1964) *Mathematical Theory of Communication*, University of Illinois Press, Urbana.
2. Klir, George: (1991) "Generalized Information Theory", *Fuzzy Sets and Systems*, v. **40**, pp. 127–142.
3. Bement, T; Booker, JM; McNulty, S; and N. Singpurwalla: (2003) "Testing the Untestable: Reliaiblity in the 21st Century", *IEEE Transactions in Reliability*, v. **57**, pp. 114–128.
4. Klir, George and Wierman, Mark J: (1997) *Uncertainty-Based Information Elements of Generalized Information Theory,* in: *Lecture Notes in Computer Science*, Creighton University, Omaha.
5. Moore, RM: (1979) *Methods and Applications of Interval Analysis*, in: *SIAM Studies in Applied Mathematics*, SIAM, Philadelphia.
6. Lindley, D: (1987) "Comment: A Tale of Two Wells", *Statistical Science*, v. **2**:1, pp. 38–40.
7. Bayes, T: (1763) "An Essay Towards Solving a Problem in the Doctrine of Chances", *Philosophical Trans. of the Royal Society*, v. **53**, pp. 370–418.

Copyright 2005 by CRC Press LLC

8. Kolmogorov, AN: (1956) *Foundations of the Theory of Probability*, Chelsea, New York.
9. Ben-Haim, Yakov: (2001) *Information-Gap Decision Theory*, Academic Press, London.
10. Sellers, K and Booker, J: (2002) "Bayesian Methods", in: *Fuzzy Logic and Probability Applications: Bridging the*, ed. Ross, Booker, and Parksinson, SIAM, Philadelphia.
11. Graves, T: (2001) "YADAS: An Object-Oriented Framework for Data Analysis Using Markov Chain Monte Carlo", *LANL Technical Report LA-UR-01-4804*.
12. Dubois, Didier and Prade, Henri: (1993) "Fuzzy sets and Probability: Misunderstandings, Bridges and Gaps", in: *Proc. FUZZ-IEEE '93*.
13. Klir, George and Yuan, Bo: (1995) *Fuzzy Sets and Fuzzy Logic*, Prentice-Hall, New York.
14. Klir, George J: (1997) "Uncertainty Theories, Measures, and Principles: An Overview of Personal Views and Contributions", in: *Uncertainty: Models and Measures*, ed. HG Natke and Y Ben-Haim, pp. 27–43, Akademie Verlag, Berlin.
15. Ross, Timothy and Parkinson, J: (2002) "Fuzzy Set Theory, Fuzzy Logic and, Fuzzy Systems", in: *Fuzzy Logic and Probability Applications: Bridging the Gap*, ed. Ross, Booker, and Parksinson, SIAM, Philadelphia.
16. Zadeh, Lotfi A: (1965) "Fuzzy Sets and Systems", in: *Systems Theory*, ed. J. Fox, pp. 29–37, Polytechnic Press, Brooklyn NY.
17. Zadeh, Lotfi A: (1965) "Fuzzy Sets", *Information and Control*, v. **8**, pp. 338–353.
18. Dempster, AP: (1967) "Upper and Lower Probabilities Induced by a Multivalued Mapping", *Annals of Mathematical Statistics*, v. **38**, pp. 325–339.
19. Lamata, MT and Moral, S: (1989) "Classification of Fuzzy Measures", *Fuzzy Sets and Systems*, v. **33**, pp. 243–153.
20. Sims, John R and Wang, Zhenyuan: (1990) "Fuzzy Measures and Fuzzy Integrals: An Overview", *Int. J. of General Systems*, v. **17**:2–3, pp. 157–189.
21. Shafer, Glen: (1976) *Mathematical Theory of Evidence*, Princeton University Press, Princeton, NJ.
22. Kendall, DG: (1974) "Foundations of a Theory of Random Sets", in: *Stochastic Geometry*, ed. EF Harding and DG Kendall, pp. 322–376, Wiley, New York.
23. Matheron, G: (1975) *Random Sets and Integral Geometry*, Wiley, New York.
24. Dempster, AP: (1968) "Upper and Lower Probabilities Generated by a Random Interval", *Annals of Mathematical Statistics*, v. **39**:3, pp. 957–966.
25. Sugeno, Michio: (1972) "Fuzzy Measures and Fuzzy Integrals", *Trans. SICE*, v. **8**:2.
26. Zadeh, Lotfi A: (1978) "Fuzzy Sets as the Basis for a Theory of Possibility", *Fuzzy Sets and Systems*, v. **1**, pp. 3–28.
27. Joslyn, Cliff: (1995) "In Support of an Independent Possibility Theory", in: *Foundations and Applications of Possibility Theory*, ed. G de Cooman et al., pp. 152–164, World Scientific, Singapore.
28. Klir, George and Folger, Tina: (1987) *Fuzzy Sets, Uncertainty, and Information*, Prentice Hall.
29. Walley, P: (1990) *Statistical Reasoning with Imprecise Probabilities*, Chapman & Hall, New York.
30. Singpurwalla, N and Booker, J: (2002) "Membership Functions and Probability Measures of Fuzzy Sets", *Los Alamos Technical Report LAUR 02-0032.*, LANL.
31. Booker, JM and Singpurwalla, N: (2003) "Using Probability and Fuzzy Set Theory for Reliability Assessment", in: *Proc. 21st Int. Modal Analysis Conference (IMAC-XXI)*, pp. 259, Kissimmee FL.
32. Wang, Zhenyuan and Klir, George J: (1992) *Fuzzy Measure Theory*, Plenum Press, New York.
33. Klir, George and Smith, Richard M: (2000) "On Measuring Uncertainty and Uncertainty-Based Information: Recent Developments", *Annals of Mathematics and Artificial Intelligence*, v. **32**:1-4, pp. 5–33.
34. Sentz, Kari and Ferson, Scott: (2002) "Combination Rules in Dempster-Shafer Theory", in: *6th World Multi-Conference on Systemic, Cybernetics, and Informatics.*
35. Joslyn, Cliff: (1996) "Aggregation and Completion of Random Sets with Distributional Fuzzy Measures", *Int. J. of Uncertainty, Fuzziness, and Knowledge-Based Systems*, v. **4**:4, pp. 307–329.
36. Dubois, Didier and Prade, Henri: (1990) "Consonant Approximations of Belief Functions", *Int. J. Approximate Reasoning*, v. **4**, pp. 419–449.

Copyright 2005 by CRC Press LLC

37. Helton, JC and Oberkampf, WL, eds.: (2004) "Special Issue: Alternative Representations of Epistemic Uncertainty", *Reliability Engineering and Systems Safety*, 95:1-3.
38. Joslyn, Cliff and Helton, Jon C: (2002) "Bounds on Plausibility and Belief of Functionally Propagated Random Sets", in: *Proc. Conf. North American Fuzzy Information Processing Society (NAFIPS 2002)*, pp. 412–417.
39. Joslyn, Cliff and Kreinovich, Vladik: (2002) "Convergence Properties of an Interval Probabilistic Approach to System Reliability Estimation", *Int. J. General Systems,* in press.
40. Oberkampf, WL; Helton, JC; Wojtkiewicz, SF, Cliff Joslyn, and Scott Ferson: (2004) "Uncertainty in System Response Given Uncertain Parameters", *Reliability Reliability Engineering and System Safety*, 95:1-3, pp. 11–20.
41. Tonon, Fulvio and Bernardini, Alberto: (1998) "A Random Set Approach to the Optimization of Uncertain Structures", *Computers and Structures*, v. **68**, pp. 583–600.
42. Ferson, Scott; Kreinovich, V; and Ginzburg, L et al.: (2002) "Constructing Probability Boxes and Dempster-Shafer Structures", *SAND Report 2002-4015*, Sandia National Lab, Albuquerque NM, http://www.sandia.gov/epistemic/Reports/SAND2002-4015. pdf.
43. Yager, Ronald R: (1986) "Arithmetic and Other Operations on Dempster-Shafer Structures", *Int. J. Man-Machine Studies*, v. **25**, pp. 357–366.
44. Joslyn, Cliff: (1997) "Measurement of Possibilistic Histograms from Interval Data", *Int. J. General Systems*, v. **26**:1-2, pp. 9–33.
45. Joslyn, Cliff and Ferson, Scott: (2003) "Convolutions of Representations of Random Intervals", in preparation.
46. Joslyn, Cliff: (1997) "Distributional Representations of Random Interval Measurements", in: *Uncertainty Analysis in Engineering and the Sciences*, ed. Bilal Ayyub and Madan Gupta, pp. 37–52, Kluwer.
47. Sudkamp, Thomas: (1992) "On Probability-Possibility Transformations", *Fuzzy Sets and Systems*, v. **51**, pp. 73–81.
48. Joslyn, Cliff: (1997) "Possibilistic Normalization of Inconsistent Random Intervals", *Advances in Systems Science and Applications*, special issue, ed. Wansheng Tang, pp. 44–51, San Marcos, TX, ftp://wwwc3.lanl.gov/pub/users/joslyn/iigss97.pdf.
49. Oussalah, Mourad: (2002) "On the Normalization of Subnormal Possibility Distributions: New Investigations", *Int. J. General Systems*, v. **31**:3, pp. 227–301.
50. Pawlak, Zdzislaw: (1991) *Rough Sets: Theoretical Aspects of Reasoning about Data*, Kluwer, Boston.
51. Dubois, Didier and Prade, Henri: (1990) "Rough Fuzzy Sets and Fuzzy Rough Sets", *Int. J. General Systems*, v. **17**, pp. 191–209.
52. Lin, TY and Cercone, N, eds.: (1997) *Rough Sets and Data Mining: Analysis of Imprecise Data*, Kluwer, Boston.
53. Joslyn, Cliff: (2003) "Multi-Interval Elicitation of Random Intervals for Engineering Reliability Analysis", *Proc. 2003 Int. Symp. on Uncertainty Modeling and Analysis (ISUMA 03)*.
54. Joslyn, Cliff and Rocha, Luis: (1998) "Towards a Formal Taxonomy of Hybrid Uncertainty Representations", *Information Sciences*, v. **110**:3-4, pp. 255–277.
55. Kyburg, HE (1987): "Bayesian and Non-Bayesian Evidential Updating", *Artificial Intelligence*, v. **31**, pp. 271–293.
56. de Cooman, Gert and Aeyels, Dirk: (2000) "A Random Set Description of a Possibility Measure and Its Natural Extension", *IEEE Trans. on Systems, Man and Cybernetics A*, v. **30**:2, pp. 124–130.

Copyright 2005 by CRC Press LLC

10

Evidence Theory for Engineering Applications

William L. Oberkampf
Sandia National Laboratories

Jon C. Helton
Sandia National Laboratories

10.1 Introduction

10.1.1 Background

Computational analysis of the performance, reliability, and safety of engineered systems is spreading rapidly in industry and government. To many managers, decision makers, and politicians not trained in computational simulation, computer simulations can appear most convincing. Terminology such as "virtual prototyping," "virtual testing," "full physics simulation," and "modeling and simulation-based acquisition" are extremely appealing when budgets are highly constrained; competitors are taking market share; or when political constraints do not allow testing of certain systems. To assess the accuracy and usefulness of computational simulations, three key aspects are needed in the analysis and experimental process: computer code and solution verification; experimental validation of most, if not all, of the mathematical models of the engineered system being simulated; and estimation of the uncertainty associated with analysis inputs, physics models, possible scenarios experienced by the system, and the outputs of interest in the simulation. The topics of verification and validation are not addressed here, but these are covered at length in the literature (see, for example, [1–6]). A number of fields have contributed to the development of uncertainty estimation techniques and procedures, such as nuclear reactor safety, underground storage of radioactive and toxic wastes, and structural dynamics (see, for example, [7–18]).

Copyright 2005 by CRC Press LLC

Uncertainty estimation for engineered systems is sometimes referred to as the simulation of nondeterministic systems. The mathematical model of the system, which includes the influence of the environment on the system, is considered nondeterministic in the sense that: (i) the model can produce nonunique system responses because of the existence of uncertainty in the input data for the model, or (ii) there are multiple alternative mathematical models for the system. The mathematical models, however, are assumed to be deterministic in the sense that when all necessary input data for a designated model is specified, the model produces only one value for every output quantity. To predict the nondeterministic response of the system, it is necessary to evaluate the mathematical model, or alternative mathematical models, of the system multiple times using different input data. This presentation does not consider chaotic systems or systems with hysteresis, that is, mathematical models that map a unique input state to multiple output states.

Many investigators in the risk assessment community segregate uncertainty into *aleatory* uncertainty and *epistemic* uncertainty. Aleatory uncertainty is also referred to as variability, irreducible uncertainty, inherent uncertainty, stochastic uncertainty, and uncertainty due to chance. Epistemic uncertainty is also referred to as reducible uncertainty, subjective uncertainty, and uncertainty due to lack of knowledge. Some of the investigators who have argued for the importance of distinguishing between aleatory uncertainty and epistemic uncertainty are noted in [19–32]. We believe the benefits of distinguishing between aleatory and epistemic uncertainty include improved interpretation of simulation results by decision makers and improved ability to allocate resources to decrease system response uncertainty or risk. Note that in the present work we use the term "risk" to mean a measure of the likelihood and severity of an adverse event occurring [13, 33].

Sources of aleatory uncertainty can commonly be singled out from other contributors to uncertainty by their representation as randomly distributed quantities that take values in an established or known range, but for which the exact value will vary by chance from unit to unit or from time to time. The mathematical representation most commonly used for aleatory uncertainty is a probability distribution. When substantial experimental data is available for estimating a distribution, there is no debate that the correct mathematical model for aleatory uncertainty is a probability distribution. Propagation of these distributions through a modeling and simulation process is well developed and is described in many texts (see, for example, [31, 34–38]).

Epistemic uncertainty derives from some level of ignorance about the system or the environment. For this presentation, *epistemic uncertainty* is defined as any lack of knowledge or information in any phase or activity of the modeling process [39]. The key feature stressed in this definition is that the fundamental source of epistemic uncertainty is incomplete information or incomplete knowledge of some characteristic of the system or the environment. As a result, an increase in knowledge or information can lead to a reduction in the predicted uncertainty of the response of the system, all things being equal. Examples of sources of epistemic uncertainty are: little or no experimental data for a fixed (but unknown) physical parameter, a range of possible values of a physical quantity provided by expert opinion, limited understanding of complex physical processes, and the existence of fault sequences or environmental conditions not identified for inclusion in the analysis of a system. For further discussion of the sources of epistemic uncertainty in engineering systems see, for example, [40, 41].

Epistemic uncertainty has traditionally been represented with a random variable using subjective probability distributions. However, a major concern is that when there is little or no closely related experimental data, a common practice is to simply pick some familiar probability distribution and its associated parameters to represent one's belief in the likelihood of possible values that could occur. Two important weaknesses with this common approach are of critical interest when the assessment of epistemic uncertainty is the focus. First, even small epistemic uncertainty in parameters for continuous probability distributions, such as a normal or Weibull, can cause very large changes in the tails of the distributions. For example, there can be orders-of-magnitude change in the likelihood of rare events when certain distribution parameters are changed by small amounts. Second, when epistemic uncertainty is represented as a probability distribution and when there are multiple parameters treated in this fashion, one can obtain misleading results. For example, suppose there are ten parameters in an analysis that are

Copyright 2005 by CRC Press LLC

only *thought* to be within specified intervals; for example, the parameters are estimated from expert opinion, not measurements. Assume each of these parameters is treated as a random variable and assigned the least informative distribution (i.e., a uniform distribution). If extreme system responses correspond to extreme values of these parameters (i.e., values near the ends of the uniform distribution), then their probabilistic combination could predict a very low probability for such extreme system responses. Given that the parameters are only known to occur within intervals, however, this conclusion is grossly inappropriate.

10.1.2 Improved Models for Epistemic Uncertainty

During the past two decades, the information theory and expert systems communities have made significant progress in developing a number of new theories that can be pursued for modeling epistemic uncertainty. Examples of the newer theories include fuzzy set theory [17, 42–46], interval analysis [47, 48], evidence (Dempster-Shafer) theory [49–55], possibility theory [56, 57], and theory of upper and lower previsions [58]. Some of these theories only deal with epistemic uncertainty; most deal with both epistemic and aleatory uncertainty; and some deal with other varieties of uncertainty (e.g., nonclassical logics appropriate for artificial intelligence and data fusion systems [59]).

A recent article summarizes how these theories of uncertainty are related to one another from a hierarchical viewpoint [60]. The article shows that evidence theory is a generalization of classical probability theory. From the perspective of bodies of evidence and their measures, evidence theory can also be considered a generalization of possibility theory. However, in evidence theory and in possibility theory, the mechanics of operations applied to bodies of evidence are completely different [54, 57]. The mathematical foundations of evidence theory are well established and explained in several texts and key journal articles [49–55, 61–64]. However, essentially all of the published applications of the theory are for simple model problems—not actual engineering problems [41, 65–74]. Note that in some of the literature, evidence theory is referred to as the theory of random sets.

In evidence theory there are two complementary measures of uncertainty: belief and plausibility. Together, belief and plausibility can be thought of as defining lower and upper limits of probabilities, respectively, or interval-valued probabilities. That is, given the information or evidence available, a precise (i.e., single) probability distribution cannot be specified. Rather, a range of possible probabilities exists, all of which are consistent with the evidence. Belief and plausibility measures can be based on many types of information or evidence (e.g., experimental data for long-run frequencies of occurrence, scarce experimental data, theoretical evidence, or individual expert opinion or consensus among experts concerning the range of possible values of a parameter or possibility of the occurrence of an event). We believe that evidence theory could be an effective path forward in engineering applications because it can deal with both thoroughly characterized situations (e.g., precisely known probability distributions) and situations of near-total ignorance (e.g., only an interval containing the true value is known).

There are two fundamental differences between the approach of evidence theory and the traditional application of probability theory. First, evidence theory uses two measures—belief and plausibility—to characterize uncertainty; in contrast, probability theory uses only one measure—the probability of an event or value. Belief and plausibility measures are statements about the likelihood related to sets of possible values. There is no need to distribute the evidence to individual values in the set. For example, evidence from experimental data or from expert opinion can be given for a parameter value to be within an interval. Such evidence makes no claim concerning any specific value within the interval or the likelihood of any one value compared with any other value in the interval. In other words, less information can be specified than the least information that is typically specified in applications of probability theory (e.g., the uniform likelihood of all values in the interval).

The second fundamental difference between evidence theory and the traditional application of probability theory is that in evidence theory, the evidential measure for an event and the evidential measure for the negation of an event do not have to sum to unity (i.e., certainty). In probability theory, the measure for an event plus the measure against an event (i.e., its negation) must be unity. This sum to

Copyright 2005 by CRC Press LLC

unity implies that the absence in the evidence for an event must be equivalent to the evidence for the negation of the event. In evidence theory, this equivalence is rejected as excessively restrictive; that is, a weak statement of evidence can result in support for an event, but the evidence makes no inference for the support of the negation of the event.

As a final background comment concerning historical perspective of evidence theory, the theory is philosophically related to the approach of Bayesian estimation. Indeed, many of the originators of evidence theory viewed it as an offshoot of Bayesian estimation for the purpose of more properly dealing with subjective probabilities. There are, however, two key differences. First, evidence theory does not assign any prior distributions to a given state of knowledge (i.e., body of evidence) if none are given. The requirement for such a prior distribution is obviated because all possible probability distributions are allowed to describe the body of evidence. Second, evidence theory does not embody the theme of updating probabilities as new evidence becomes available. In Bayesian estimation, a dominant theme is toward continually improving statistical inference as new evidence becomes available; whereas in evidence theory, the emphasis is on precisely stating the present state of knowledge—not updating the statistical evidence.

10.1.3 Chapter Outline

In the following section (Section 10.2), the mathematical framework of evidence theory is explained and contrasted to the traditional application of probability theory. The definitions of belief and plausibility are given, along with the relationships between them. Also discussed is an important quantity called the basic probability assignment (BPA). A few simple examples are given illustrating the interpretation of the belief and plausibility functions and the BPA. Section 10.3 discusses the application of evidence theory to a simple example problem. The simple system is given by an algebraic equation with two uncertain input parameters and one system response variable. The example is analyzed using the traditional application of probability theory and evidence theory. The discussion of each solution approach stresses the mathematical and procedural steps needed to compute uncertainty bounds in the system response, as well as the similarities and differences between each approach. The analyses using traditional probabilistic and evidence theory approaches are compared with regard to their assessment for the system yielding an unsafe response. The presentation concludes in Section 10.4 with a brief discussion of important research and practical issues hindering the widespread application of evidence theory to large-scale engineering systems. For example, the critical issue of propagating BPAs through a "black box" computer code using input/output sampling techniques is discussed.

10.2 Fundamentals of Evidence Theory

10.2.1 Belief, Plausibility, and BPA Functions

Evidence theory provides an alternative to the traditional manner in which probability theory is used to represent uncertainty by allowing less restrictive statements about "likelihood" than is the case with a full probabilistic specification of uncertainty. Evidence theory can be viewed as a generalization of the traditional application of probability theory. By "generalization" we mean that when probability distributions are specified, evidence theory yields the same measures of likelihood as the traditional application of probability theory. Evidence theory involves two specifications of likelihood—a belief and a plausibility—for each subset of the universal set under consideration. Formally, an application of evidence theory involves the specification of a triple $(\mathcal{S}, \mathbb{S}, m)$, where (i) $\mathcal{S}$ is a set that contains everything that could occur in the particular universe under consideration, typically referred to as the sample space or universal set; (ii) $\mathbb{S}$ is a countable collection of subsets of $\mathcal{S}$, typically referred to as the set of focal elements of $\mathcal{S}$; and (iii) m is a function defined on subsets of $\mathcal{S}$ such that

$$m(\mathcal{E}) > 0 \quad \text{if} \quad \mathcal{E} \in \mathbb{S}, m(\mathcal{E}) = 0 \quad \text{if} \quad \mathcal{E} \subset \mathcal{S} \text{ and } \mathcal{E} \notin \mathbb{S}, \tag{10.1}$$

Copyright 2005 by CRC Press LLC

and

$$\sum_{\mathcal{E}\in\mathbb{S}} m(\mathcal{E}) = 1. \tag{10.2}$$

The quantity $m(\mathcal{E})$ is referred to as the basic probability assignment (BPA), or the mass function, associated with the subset $\mathcal{E}$ of $\mathcal{S}$.

The sets $\mathcal{S}$ and $\mathbb{S}$ are similar to probability theory where one has the specification of a triple ($\mathcal{S}$, $\mathbb{S}$, p) called a probability space, where (i) $\mathcal{S}$ is a set that contains everything that could occur in the particular universe under consideration, (ii) $\mathbb{S}$ is a suitably restricted set of subsets of $\mathcal{S}$, and (iii) p is the function that defines probability for elements of $\mathbb{S}$ (see [75], Section IV.4). In probability theory, the set $\mathbb{S}$ is required to have the properties that (i) if $\mathcal{E}\in\mathbb{S}$, then $\mathcal{E}^C\in\mathbb{S}$, where $\mathcal{E}^C$ is the complement of $\mathcal{E}$, and (ii) if $\mathcal{E}_1, \mathcal{E}_2, \ldots$ is a sequence of elements of $\mathbb{S}$, then $\cup_i\mathcal{E}_i\in\mathbb{S}$ and $\cap_i\mathcal{E}_i\in\mathbb{S}$. Further, p is required to have the properties that (i) if $\mathcal{E}\in\mathbb{S}$, then $0\le p(\mathcal{E})\le 1$, (ii) $p(\mathcal{S}) = 1$, and (iii) if $\mathcal{E}_1, \mathcal{E}_2, \ldots$ is a sequence of disjoint sets from $\mathbb{S}$, then $p(\cup_i\mathcal{E}_i) = \sum_i p(\mathcal{E}_i)$ (see [75], Section IV.3). In the terminology of probability theory, $\mathcal{S}$ is called the sample space or universal set; elements of $\mathcal{S}$ are called elementary events; subsets of $\mathcal{S}$ contained in $\mathbb{S}$ are called events; the set $\mathbb{S}$ itself has the properties of what is called a σ-algebra (see [75], Section IV.3); and p is called a probability measure.

The sample space $\mathcal{S}$ plays the same role in both probability theory and evidence theory. However, the $\mathbb{S}$ set has a different character in the two theories. In probability theory, $\mathbb{S}$ has special algebraic properties fundamental to the development of probability and contains all subsets of $\mathcal{S}$ for which probability is defined (see [75], Section IV.3). In evidence theory, $\mathbb{S}$ has no special algebraic properties (i.e., $\mathbb{S}$ is not required to be a σ-algebra, as is the case in probability theory) and contains the subsets of $\mathcal{S}$ with nonzero BPAs. In probability theory, the function p actually defines the probabilities for elements of $\mathbb{S}$, with these probabilities being the fundamental measure of likelihood. In evidence theory, the function m is *not* the fundamental measure of likelihood. Rather, there are two measures of likelihood, called belief and plausibility, that are obtained from m as described in the next paragraph. The designation BPA for $m(\mathcal{E})$ is almost universally used, but, unfortunately, m does not define probabilities except under very special circumstances. Given the requirement in Equation 10.2, the set $\mathbb{S}$ of focal elements associated with an evidence space ($\mathcal{S}$, $\mathbb{S}$, m) can contain at most a countable number of elements; in contrast, the set $\mathbb{S}$ of events associated with a probability space ($\mathcal{S}$, $\mathbb{S}$, p) can, and essentially always does, contain an uncountable number of elements.

The belief, $Bel(\mathcal{E})$, and plausibility, $Pl(\mathcal{E})$, for a subset $\mathcal{E}$ of $\mathcal{S}$ are defined by

$$Bel(\mathcal{E}) = \sum_{\mathcal{U}\subset\mathcal{E}} m(\mathcal{U}) \tag{10.3}$$

and

$$Pl(\mathcal{E}) = \sum_{\mathcal{U}\cap\mathcal{E}\neq\emptyset} m(\mathcal{U}). \tag{10.4}$$

Conceptually, $m(\mathcal{U})$ is the amount of likelihood that is associated with a set $\mathcal{U}$ that cannot be further assigned to specific subsets of $\mathcal{U}$. Specifically, no specification is implied concerning how this likelihood is apportioned over $\mathcal{U}$. Given the preceding conceptualization of $m(\mathcal{U})$, the belief $Bel(\mathcal{E})$ can be viewed as the minimum amount of likelihood that *must* be associated with $\mathcal{E}$. Stated differently, $Bel(\mathcal{E})$ is the amount of likelihood that must be associated with $\mathcal{E}$ because the summation in Equation 10.3 involves all $\mathcal{U}$ that satisfy $\mathcal{U}\subset\mathcal{E}$. Similarly, the plausibility $Pl(\mathcal{E})$ can be viewed as the maximum amount of likelihood that *could* be associated with $\mathcal{E}$. Stated differently, $Pl(\mathcal{E})$ is the maximum amount of likelihood that could possibly be associated with $\mathcal{E}$ because the summation in Equation 10.4 involves all $\mathcal{U}$ that

Copyright 2005 by CRC Press LLC

intersect $\mathcal{E}$. From the perspective of making informed decisions, the information provided by beliefs and plausibilities is more useful than the information provided by BPAs. This statement is made because a BPA only provides likelihood information that can be attributed to a set, but to none of its subsets. In contrast, a belief provides likelihood information about a set and all its subsets, and a plausibility provides likelihood information about a set and all sets that intersect it.

Belief and plausibility satisfy the equality

$$Bel(\mathcal{E}) + Pl(\mathcal{E}^c) = 1 \tag{10.5a}$$

for every subset $\mathcal{E}$ of $\mathcal{S}$. In words, the belief in the occurrence of an event (i.e., $Bel(\mathcal{E})$) and the plausibility of the nonoccurrence of an event (i.e., $Pl(\mathcal{E}^c)$) must sum to one. In contrast, probability theory relies on the analogous equation

$$p(\mathcal{E}) + p(\mathcal{E}^c) = 1. \tag{10.5b}$$

As is well known, Equation 10.5b states that the likelihood in the occurrence of an event and the likelihood of the nonoccurrence of an event must sum to one. Stated differently, in probability theory, the likelihood for an event is the complement of the likelihood against an event, whereas in evidence theory, there is no such assumption of symmetry.

In evidence theory, it can be shown that

$$Bel(\mathcal{E}) + Bel(\mathcal{E}^c) \leq 1. \tag{10.6}$$

The specification of belief is capable of incorporating a lack of assurance that is manifested in the sum of the beliefs in the occurrence (i.e., $Bel(\mathcal{E})$) and nonoccurrence (i.e., $Bel(\mathcal{E}^c)$) of an event $\mathcal{E}$ being less than one. Stated differently, the belief function is a likelihood measure that allows evidence for and against an event to be inconclusive. For the plausibility function, it can be shown that

$$Pl(\mathcal{E}) + Pl(\mathcal{E}^c) \geq 1. \tag{10.7}$$

The specification of plausibility is capable of incorporating a recognition of alternatives that is manifested in the sum of the plausibilities in the occurrence (i.e., $Pl(\mathcal{E})$) and nonoccurrence (i.e., $Pl(\mathcal{E}^c)$) of an event $\mathcal{E}$ being greater than one. Stated differently, the plausibility function is a likelihood measure that allows evidence for and against an event to be redundant.

10.2.2 Cumulative and Complementary Cumulative Functions

In probability theory, the cumulative distribution function (CDF) and the complementary cumulative distribution function (CCDF) are commonly used to provide summaries of the information contained in a probability space $(\mathcal{S}, \mathbb{S}, p)$. The CCDF is also referred to as the *exceedance risk* curve in risk assessment analyses. Similarly in evidence theory, cumulative belief functions (CBFs), complementary cumulative belief functions (CCBFs), cumulative plausibility functions (CPFs), and complementary cumulative plausibility functions (CCPFs) can be used to summarize beliefs and plausibilities. Specifically, CBFs, CCBFs, CPFs, and CCPFs are defined by the sets of points

$$\mathcal{CBF} = \left\{\left[v, Bel\left(\mathcal{S}_v^c\right)\right], v \in \mathcal{S}\right\} \tag{10.8}$$

$$\mathcal{CCBF} = \left\{[v, Bel(\mathcal{S}_v)], v \in \mathcal{S}\right\} \tag{10.9}$$

$$\mathcal{CPF} = \left\{\left[v, Pl\left(\mathcal{S}_v^c\right)\right], v \in \mathcal{S}\right\} \tag{10.10}$$

$$\mathcal{CCPF} = \left\{[v, Pl(\mathcal{S}_v)], v \in \mathcal{S}\right\}, \tag{10.11}$$

Copyright 2005 by CRC Press LLC

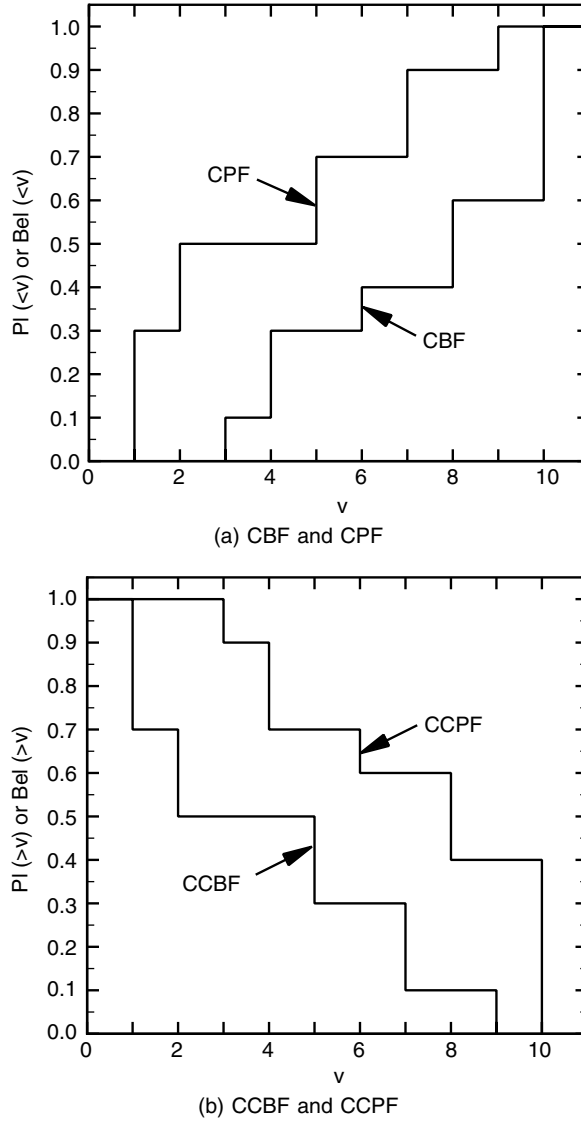

FIGURE 10.1 Example of (a) cumulative belief and plausibility functions and (b) complementary cumulative belief and plausibility functions.

where $\mathcal{S}_v$ is defined as

$$\mathcal{S}_v = \{x : x \in \mathcal{S} \text{ and } x > v\}. \tag{10.12}$$

Plots of the points in the preceding sets produce CBFs, CCBFs, CPFs, and CCPFs (Figure 10.1).

As grouped in Figure 10.1, a CBF and the corresponding CPF occur together naturally as a pair because, for a given value v on the abscissa, (i) the value of the CBF (i.e., $Bel(\mathcal{S}_v^c)$) is the smallest probability for $\mathcal{S}_v^c$ that is consistent with the information characterized by $(\mathcal{S}, \mathbb{S}, m)$ and (ii) the value of the CPF (i.e., $Pl(\mathcal{S}_v^c)$) is the largest probability for $\mathcal{S}_v^c$ that is consistent with the information characterized by $(\mathcal{S}, \mathbb{S}, m)$. A similar interpretation holds for the CCBF and CCPF. Indeed, this bounding relationship occurs for any subset $\mathcal{E}$ of $\mathcal{S}$, and thus $Pl(\mathcal{E})$ and $Bel(\mathcal{E})$ can be thought of as defining upper and lower probabilities for $\mathcal{E}$ [61].

Copyright 2005 by CRC Press LLC

10.2.3 Input/Output Uncertainty Mapping

The primary focus in many, if not most, engineering problems involving uncertainty estimation is on functions

$$y = f(\boldsymbol{x}), \tag{10.13}$$

where

$$\boldsymbol{x} = [x_1, x_2, \ldots, x_n]$$

and the uncertainty in each x_i is characterized by a probability space $(\mathcal{X}_i, \mathbb{X}_i, p_i)$ or an evidence space $(\mathcal{X}_i, \mathbb{X}_i, m_i)$. The elements x_i of $\boldsymbol{x}$ are used to construct the input sample space

$$\mathcal{X} = \{x : x = [x_1, x_2, \ldots, x_n] \in \mathcal{X}_1 \times \mathcal{X}_2 \times \ldots \times \mathcal{X}_n\}. \tag{10.14}$$

When the uncertainty in each x_i is characterized by a probability space $(\mathcal{X}_i, \mathbb{X}_i, p_i)$, this leads to a probability space $(\mathcal{X}, \mathbb{X}, p_X)$ that characterizes the uncertainty in $\boldsymbol{x}$, where $\mathbb{X}$ is developed from the sets contained in

$$\mathbb{C} = \{\mathcal{E} : \mathcal{E} = \mathcal{E}_1 \times \mathcal{E}_2 \times \ldots \times \mathcal{E}_n \in \mathbb{X}_1 \times \mathbb{X}_2 \times \ldots \times \mathbb{X}_n\} \tag{10.15}$$

(see [75], Section IV.6, and [76], Section 2.6) and p_X is developed from the probability functions (i.e., measures) p_i. Specifically, if the x_i are independent and d_i is the density function associated with p_i, then

$$p_X(\mathcal{E}) = \int_{\mathcal{E}} d(\boldsymbol{x})\, dV \tag{10.16}$$

for $\mathcal{E} \in \mathbb{X}$ and

$$d(\boldsymbol{x}) = \prod_{i=1}^{n} d_i(x_i) \tag{10.17}$$

for $\boldsymbol{x} = [x_1, x_2, \ldots, x_n] \in \mathcal{X}$.

In engineering practice, f is often a set of nonlinear partial differential equations that are numerically solved on a computer. The dimensionality of the vector $\boldsymbol{x}$ of inputs can be high in practical problems (e.g., on the order of 50). The analysis outcome y is also often a vector of high dimensionality, but is indicated in Equation 10.13 as being a single system response for notational convenience.

The sample space $\mathcal{X}$ constitutes the domain for the function f in Equation 10.13. In turn, the range of f is given by the set

$$\mathcal{Y} = \{y : y = f(\boldsymbol{x}), \boldsymbol{x} \in \mathcal{X}\}. \tag{10.18}$$

The uncertainty in the values of y contained in $\mathcal{Y}$ derives from the probability space $(\mathcal{X}, \mathbb{X}, p_X)$ that characterizes the uncertainty in $\boldsymbol{x}$ and from the properties of the function f. In concept, $(\mathcal{X}, \mathbb{X}, p_X)$ and f induce a probability space $(\mathcal{Y}, \mathbb{Y}, p_Y)$. The probability p_Y is defined for a subset $\mathcal{E}$ of $\mathcal{Y}$ by

$$p_Y(\mathcal{E}) = p_X(f^{-1}(\mathcal{E})), \tag{10.19}$$

where

$$f^{-1}(\mathcal{E}) = \{x : x \in \mathcal{X} \text{ and } y = f(x) \in \mathcal{E}\}. \tag{10.20}$$

Copyright 2005 by CRC Press LLC

The uncertainty in y characterized by the probability space $(\mathcal{Y}, \mathbb{Y}, p_Y)$ is typically presented as a CDF or CCDF.

Equation 10.19 describes the mapping of probabilities from the input space to probabilities in the space of the system outcome y when the uncertainty associated with the domain of the function is characterized by a probability space $(\mathcal{X}, \mathbb{X}, p_X)$. When the uncertainty in each x_i is characterized by an evidence space $(\mathcal{X}_i, \mathbb{X}_i, m_i)$, the uncertainty in $\boldsymbol{x}$ is characterized by an evidence space $(\mathcal{X}, \mathbb{X}, m_X)$, where (i) $\mathcal{X}$ is defined by Equation 10.14, (ii) $\mathbb{X}$ is the same as the set $\mathbb{C}$ defined in Equation 10.15, and (iii) under the assumption that the x_i are independent, m_X is defined by

$$m_X(\mathcal{E}) = \begin{cases} \prod_{i=1}^{n} m_i(\mathcal{E}_i) & \text{if } \mathcal{E} = \mathcal{E}_1 \times \mathcal{E}_2 \times \ldots \times \mathcal{E}_n \in \mathbb{X} \\ 0 & \text{otherwise} \end{cases} \tag{10.21}$$

for subsets $\mathcal{E}$ of $\mathcal{X}$.

The development is more complex when the x_i are not independent. For a vector $\boldsymbol{x}$ of the form defined in conjunction with Equation 10.13, the structure of $\mathbb{X}$ for the evidence space $(\mathcal{X}, \mathbb{X}, m_X)$ is much simpler than the structure of $\mathbb{X}$ for an analogous probability space $(\mathcal{X}, \mathbb{X}, p_X)$. In particular, the set $\mathbb{X}$ for the evidence space $(\mathcal{X}, \mathbb{X}, m_X)$ is the same as the set $\mathbb{C}$ in Equation 10.15. In contrast, the set $\mathbb{X}$ for an analogous probability space $(\mathcal{X}, \mathbb{X}, p_X)$ is constructed from $\mathbb{C}$ and in general contains an uncountable number of elements rather than the finite number of elements usually contained in $\mathbb{C}$.

For evidence theory, relations analogous to Equation 10.19 define belief and plausibility for system outcomes when the uncertainty associated with the domain of the function is characterized by an evidence space $(\mathcal{X}, \mathbb{X}, m_X)$. In concept, $(\mathcal{X}, \mathbb{X}, m_X)$ and f induce an evidence space $(\mathcal{Y}, \mathbb{Y}, m_Y)$. In practice, m_Y is not determined. Rather, the belief $Bel_Y(\mathcal{E})$ and plausibility $Pl_Y(\mathcal{E})$ for a subset $\mathcal{E}$ of $\mathcal{Y}$ are determined from the BPA m_X associated with $(\mathcal{X}, \mathbb{X}, m_X)$. In particular,

$$Bel_Y(\mathcal{E}) = Bel_X[f^{-1}(\mathcal{E})] = \sum_{\mathcal{U} \subset f^{-1}(\mathcal{E})} m_X(\mathcal{U}) \tag{10.22}$$

and

$$Pl_Y(\mathcal{E}) = Pl_X[f^{-1}(\mathcal{E})] = \sum_{\mathcal{U} \cap f^{-1}(\mathcal{E}) \neq \varnothing} m_X(\mathcal{U}), \tag{10.23}$$

where Bel_X and Pl_X represent belief and plausibility defined for the evidence space $(\mathcal{X}, \mathbb{X}, m_X)$.

Similarly to the use of CDFs and CCDFs in probability theory, the uncertainty in y characterized by the evidence space $(\mathcal{Y}, \mathbb{Y}, m_Y)$ can be summarized with CBFs, CCBFs, CPFs, and CCPFs. In particular, the CBF, CCBF, CPF, and CCPF for y are defined by the sets of points

$$\mathcal{CBF} = \left\{\left[v, Bel_Y\left(\mathcal{Y}_v^c\right)\right], v \in \mathcal{Y}\right\} = \left\{\left[v, Bel_X\left(f^{-1}\left(\mathcal{Y}_v^c\right)\right)\right], v \in \mathcal{Y}\right\} \tag{10.24}$$

$$\mathcal{CCBF} = \{[v, Bel_Y(\mathcal{Y}_v^c)], v \in \mathcal{Y}\} = \{[v, Bel_X(f^{-1}(\mathcal{Y}_v^c))], v \in \mathcal{Y}\} \tag{10.25}$$

$$\mathcal{CPF} = \left\{\left[v, Pl_Y\left(\mathcal{Y}_v^c\right)\right], v \in \mathcal{Y}\right\} = \left\{\left[v, Pl_X\left(f^{-1}\left(\mathcal{Y}_v^c\right)\right)\right], v \in \mathcal{Y}\right\} \tag{10.26}$$

$$\mathcal{CCPF} = \{[v, Pl_Y(\mathcal{Y}_v^c)], v \in \mathcal{Y}\} = \{[v, Pl_X(f^{-1}(\mathcal{Y}_v^c))], v \in \mathcal{Y}\}, \tag{10.27}$$

where

$$\mathcal{Y}_v = \{y : y \in \mathcal{Y} \text{ and } y > v\} \tag{10.28}$$

$$\mathcal{Y}_v^c = \{y : y \in \mathcal{Y} \text{ and } y \leq v\}. \tag{10.29}$$

Copyright 2005 by CRC Press LLC

Plots of the points contained in $\mathcal{CBF}$, $\mathcal{CCBF}$, $\mathcal{CPF}$, and $\mathcal{CCPF}$ produce a figure similar to Figure 10.1 and provide a visual representation of the uncertainty in y in terms of belief and plausibility.

The beliefs and plausibilities appearing in Equation 10.24 through Equation 10.27 are defined by sums of BPAs for elements of $\mathbb{X}$. For notational convenience, let $\mathcal{E}_j$ denote the jth element of $\mathbb{X}$ for the evidence space $(\mathcal{X}, \mathbb{X}, m_X)$. Such a numbering is possible because $\mathbb{X}$ is countable due to the constraint imposed by Equation 10.2. For $v \in \mathcal{Y}$, let

$$\mathcal{ICBF}_v = \left\{ j : \mathcal{E}_j \subset f^{-1}\left(\mathcal{Y}_v^c\right) \right\} \tag{10.30}$$

$$\mathcal{ICCBF}_v = \{ j : \mathcal{E}_j \subset f^{-1}(\mathcal{Y}_v) \} \tag{10.31}$$

$$\mathcal{ICPF}_v = \left\{ j : \mathcal{E}_j \cap f^{-1}\left(\mathcal{Y}_v^c\right) \neq \varnothing \right\} \tag{10.32}$$

$$\mathcal{ICCPF}_v = \{ j : \mathcal{E}_j \cap f^{-1}(\mathcal{Y}_v) \neq \varnothing \}. \tag{10.33}$$

In turn, the beliefs and plausibilities in Equation 10.24 through Equation 10.27 are defined by

$$Bel_Y\left(\mathcal{Y}_v^c\right) = Bel_X\left(f^{-1}\left(\mathcal{Y}_v^c\right)\right) = \sum_{j \in \mathcal{ICBF}_v} m_X(\mathcal{E}_j) \tag{10.34}$$

$$Bel_Y(\mathcal{Y}_v) = Bel_X(f^{-1}(\mathcal{Y}_v)) = \sum_{j \in \mathcal{ICCBF}_v} m_X(\mathcal{E}_j) \tag{10.35}$$

$$Pl_Y\left(\mathcal{Y}_v^c\right) = Pl_X\left(f^{-1}\left(\mathcal{Y}_v^c\right)\right) = \sum_{j \in \mathcal{ICPF}_v} m_X(\mathcal{E}_j) \tag{10.36}$$

$$Pl_Y(\mathcal{Y}_v) = Pl_X(f^{-1}(\mathcal{Y}_v)) = \sum_{j \in \mathcal{ICCPF}_v} m_X(\mathcal{E}_j). \tag{10.37}$$

The summations in Equation 10.34 through Equation 10.37 provide formulas by which the CBF, CCBF, CPF, and CCPF defined in Equation 10.24 through Equation 10.27 can be calculated. In practice, determination of the sets in Equation 10.24 through Equation 10.27 can be computationally demanding due to the computational complexity of determining f^{-1}. For example, if f corresponds to the numerical solution of a system of nonlinear PDEs, there will be no closed form representation for f^{-1} and the computation of approximate representations for f^{-1} will require many computationally demanding evaluations of f. Section 10.3.3.4 gives a detailed example of how Equation 10.24 through Equation 10.27 are calculated in a simple example. The issue of convergence of sampling was recently addressed in [77], where it was established that, as the number of samples increases, even with minimal assumptions concerning the nature of f, convergence to the correct belief and plausibility of the system response is ensured.

10.2.4 Simple Conceptual Examples

The theoretical fundamentals given above can be rather impenetrable, even to those well grounded in the theoretical aspects of probability theory. We believe two of the reasons evidence theory is difficult to grasp are the following. First, evidence theory has *three* likelihood measures — belief, plausibility, and BPA functions — any one of which can determine the other two. In probability theory there is only one, the probability measure p. Second, the conversion of data or information into a BPA in evidence theory seems rather nebulous and confusing compared to the construction of probability measures in probability theory. In practice, this conversion and its representation in probability theory is simplified by using probability density functions (PDFs) as surrogates for the corresponding probability measures. For example, in probability theory if one assumes a "noninformative prior" then a uniform PDF is chosen. Or, if one has a histogram of experimental data, it is rather straightforward to construct a PDF. To aid in understanding evidence theory and how it compares with probability theory, the following two simple conceptual examples (similar to those given in [53], p. 75–76) are given.

Copyright 2005 by CRC Press LLC

Example 1

Children are playing with black and white hollow plastic Easter eggs. The children place a chocolate candy in each black Easter egg and put nothing into each white Easter egg. A parent appears and says, "I will secretly put one or more of your various Easter eggs in a paper bag. Tell me what is the probability (these are very precocious children) of you drawing out a black Easter egg from the paper bag (which you cannot see into)?"

The universal set X contains the two possible outcomes: $\{B, W\}$, where B indicates a black egg with chocolate, and W indicates a white egg without chocolate.

A probabilistic solution would traditionally assume that, according to the Principle of Insufficient Reason, there is an equal likelihood of drawing out a black egg and a white egg. Therefore, the answer to the question would be: "There is a 0.5 probability of getting a black egg."

An evidence theory solution would assign the BPA of the universal set a value of 1, which can be written as $m(X) = 1$. Because nothing is known about what this parent might do concerning putting white vs. black eggs in the bag, a BPA of zero is assigned to each possible event: $m(B) = 0$ and $m(W) = 0$. Using Equations 10.3 and 10.4, one computes that $Bel(B) = 0$ and $Pl(B) = 1$ for drawing out a black egg. Therefore, an evidence theory approach would answer the question: "The probability is between 0 and 1 for getting a black egg."

Example 2

The same children are playing with plastic Easter eggs and the same parent shows up. However, this time, the parent paints some of the plastic Easter eggs gray and places chocolates into some of the gray eggs, out of sight of the children. The parent now says, "I have put ten Easter eggs into a paper bag, which you cannot see into. In the bag there are two black eggs (with chocolates), three white eggs (without chocolates), and five gray eggs that may or may not contain a chocolate. Tell me what is the probability of drawing out an egg with a chocolate?"

The universal set X can be written as $\{B, W, G\}$; B and W are as before, and G is a gray egg which may or may not have a chocolate. A probabilistic solution could be based on the probabilities

$$p(B) = 0.2,\ p(W) = 0.3,\ p(G) = 0.5\,.$$

In addition, according to the Principle of Insufficient Reason, each gray egg containing a chocolate, G_w, has a probability of 0.5, and each gray egg without a chocolate, G_{wo}, has a probability of 0.5. Therefore, they would assign a probability of 0.25 to the likelihood that a gray egg with chocolate would be drawn. The probabilistic answer to the question would then be: "The probability of getting a chocolate from the bag is $p(\mathrm{B}) + 0.25 = 0.45$."

The evidence theory solution would assign the following BPAs

$$m(B) = 0.2,\ m(W) = 0.3,\ m(G_w, G_{wo}) = 0.5\,.$$

With the use of Equations 10.3 and 10.4, the belief for getting a chocolate, *Bel(C)*, and plausibility for getting a chocolate, *Pl(C)*, can be computed:

$$Bel(C) = Bel(B, G_w) = 0.2,\ Pl(C) = Pl(B, G_w) = 0.2 + 0.5 = 0.7.$$

Therefore, an evidence theory answer to the question would be: "There is a probability between 0.2 and 0.7 of getting a chocolate from the bag."

Copyright 2005 by CRC Press LLC

10.2.4.1 Observations

First, on these simple examples, it can be seen, hopefully, that evidence theory accurately represents the range in probabilities that are consistent with the given data; no additional assumptions concerning the given data are imposed. Stated differently, traditional application of probability theory leads one to assign probabilities to all events of the universal set, thereby forcing one to make assumptions that are not supported by the evidence. Evidence theory allows one to assign basic probabilities to *sets* of elements in the universal set, thus avoiding unjustified assumptions. Concern might be expressed that the range of probabilities with evidence theory is so large that little useful information is gained with the approach to aid in the decision-making process. The response to this is that when large epistemic uncertainty is present, the decision maker should be clearly aware of the range of probabilities, rather than having assumptions buried in the analysis disguise the probabilities. If high-consequence decisions are involved instead of chocolates, it is imperative that the decision maker understand the probabilities and resulting risks. If the highest possible risks are unacceptable to the decision maker, then resources must be made available to reduce the epistemic uncertainty.

Second, in these examples the inappropriate use of the Principle of Insufficient Reason, particularly in Example 1, is obvious. However, the assumption, without justification, of a uniform PDF in engineering analyses is very common. Sometimes the assumption is made with the caveat that, "For the first pass through the analysis, a uniform PDF is assumed." If the decision maker acts on the "first pass analysis" and a refined analysis is never conducted, inappropriate risks could be the result. Or, the more common situation might occur: "The risks appear acceptable based on the first pass analysis, and if the funds and schedule permit, we will conduct a more refined analysis in the future." Commonly, the funds and schedule are consumed with "more pressing issues."

10.3 Example Problem

The topics covered in this section are the following. First, an algebraic equation will be given (Section 10.3.1), which is a model for describing the response of a simple nondeterministic system. The nondeterministic character of the system is due to uncertainty in the parameters embodied in the algebraic model of the system. Second, the uncertainty of the response of the system will be estimated using the traditional application of probability theory (Section 10.3.2) and evidence theory (Section 10.3.3). Comparisons will be made (Section 10.3.4) concerning the representation of uncertainty using each approach. Third, in the solution procedure using evidence theory, the steps are described for converting the information concerning the uncertain parameters into input structures usable by evidence theory. A detailed discussion will be given for propagating input uncertainties represented by BPAs through the system response function and computing belief and plausibility measures in the output space.

10.3.1 Problem Description

The following equation is a simple special case of the input/output mapping indicated in Equation 10.13:

$$y = f(a,b) = (a+b)^a. \tag{10.38}$$

The parameters a and b are the analysis inputs and are the only uncertain quantities affecting the system response. Parameters a and b are independent; that is, knowledge about the value of one parameter implies nothing about the value of the other. Multiple expert sources provide information concerning a and b, but the precision of the information is relatively poor. Stated differently, there is scarce and conflicting information concerning a and b, resulting in large epistemic uncertainty. All of the sources for a and b are considered equally credible.

Copyright 2005 by CRC Press LLC

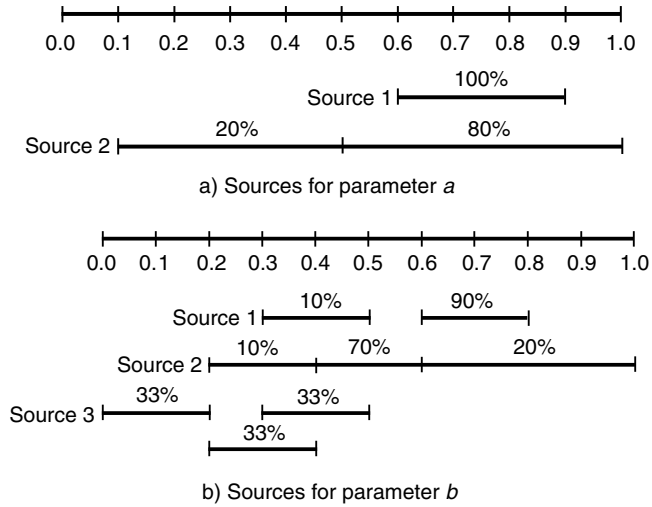

FIGURE 10.2 Information from each source for parameters *a* (upper) and *b* (lower). (Originially published in *Investigation of Evidence Theory for Engineering Applications,* Oberkampf, W.L. and Helton, J.C., 4th Nondeterministic Approaches Forum, Denver, AIAA-2002-1569. Copyright © 2002 by the American Institute of Aeronautics and Astronautics, Inc. Reprinted with permission.)

For parameter *a*, two sources provide information. Source 1 states that he believes that the actual, or true, value lies in the interval [0.6, 0.9]. Source 2 states that, in her opinion, the actual value is in one of two contiguous intervals: in the interval [0.1, 0.5] with a 20% level of subjective belief, or in the interval [0.5, 1.0] with a 80% level of subjective belief. (Note: For clarity, an adjective such as "subjective" or "graded" with the term "belief" is used to designate the common language meaning for "belief." When "belief" is used without such adjectives, reference is being made to the belief function in evidence theory.)

For parameter *b*, three sources provide information. Source 1 states that the actual value could lie in one of two disjoint intervals: in the interval [0.3, 0.5] with a 10% level of subjective belief, or in the interval [0.6, 0.8] with a 90% level of subjective belief. Source 2 states that the actual value could be in one of three contiguous intervals: [0.2, 0.4] with a 10% level of subjective belief, [0.4, 0.6] with a 70% level of subjective belief, and [0.6, 1.0] with a 20% level of subjective belief. Source 3 states that he believes that three experimental measurements he is familiar with should characterize the actual value of *b*. The three experimental realizations yielded: 0.1 ± 0.1, 0.3 ± 0.1, and 0.4 ± 0.1. He chooses to characterize these measurements, that is, his input to the uncertainty analysis, as three intervals: [0.0, 0.2], [0.2, 0.4] and [0.3, 0.5], all with equal levels of subjective belief. (See [74] for a description of more complex subjective belief statements.)

The input data for *a* and *b* for each source are shown graphically in Figure 10.2a and b, respectively.

To complete the statement of the mathematical model of the system, the system response *y* is considered to be unsafe for values of *y* larger than 1.7. It is desired that both the traditional and evidence theory approaches be used to assess what can be said about the occurrence of $y > 1.7$. Although the example problem may appear quite simple to some, the solution is not simple, or even unique, because of the poor information given for the parameters. It will be seen that both methods require additional assumptions to estimate the occurrence of $y > 1.7$. Some of these assumptions will be shown to dominate the estimated safety of the system.

Figure 10.3 presents a three-dimensional representation of $y = f(a, b)$ over the range of possible values of *a* and *b*. Several level curves, or response contours, of *y* are shown (i.e., loci of [*a*, *b*] values that produce equal *y* values). The rectangle defined by $0.1 \le a \le 1$ and $0 \le b \le 1$ is referred to as the input product space.

Copyright 2005 by CRC Press LLC

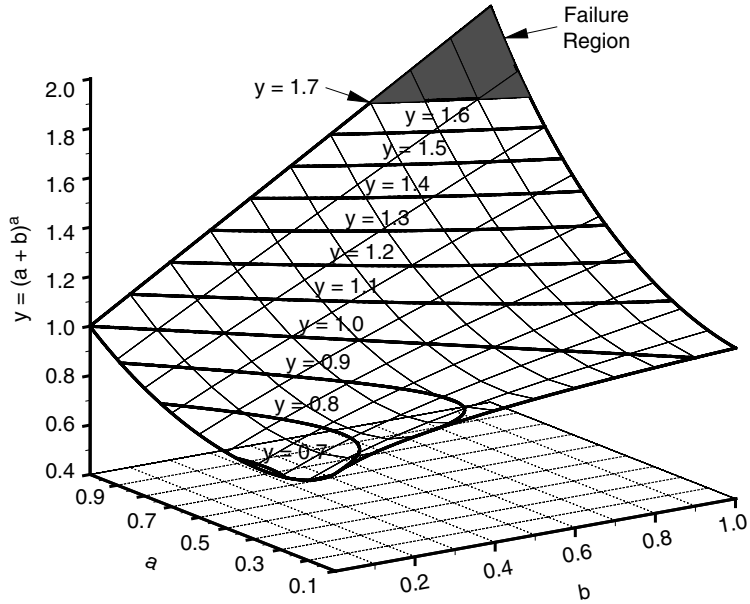

FIGURE 10.3 Three-dimensional representation of $y = (a + b)^a$ on the rectangle defined by $0.1 \le a \le 1$ and $0 \le b \le 1$. (Originially published in *Investigation of evidence theory for engineering applications,* Oberkampf, W.L. and Helton, J.C., 4th Non-Deterministic Approaches Forum, Denver, AIAA-2002-1569. Copyright © 2002 by the American Institute of Aeronautics and Astronautics, Inc. Reprinted with permission.)

10.3.2 Traditional Analysis Using Probability Theory

10.3.2.1 Combination of Evidence

The information concerning a from the two sources is written as

$$\mathcal{A}_1 = \{a : 0.6 \le a \le 0.9\} \tag{10.39}$$

$$\mathcal{A}_2 = \begin{Bmatrix} a : 0.1 \le a \le 0.5 \text{ with } 20\% \text{ belief} \\ a : 0.5 \le a \le 1.0 \text{ with } 80\% \text{ belief} \end{Bmatrix}. \tag{10.40}$$

Thus, the set

$$\mathcal{A} = \mathcal{A}_1 \cup \mathcal{A}_2 = \{a : 0.1 \le a \le 1\} \tag{10.41}$$

contains all specified values for a.

Similarly, the information for b from the three sources is written as

$$\mathcal{B}_1 = \begin{Bmatrix} b : 0.3 \le b \le 0.5 \text{ with } 10\% \text{ belief} \\ b : 0.6 \le b \le 0.8 \text{ with } 90\% \text{ belief} \end{Bmatrix} \tag{10.42}$$

$$\mathcal{B}_2 = \begin{Bmatrix} b : 0.2 \le b \le 0.4 \text{ with } 10\% \text{ belief} \\ b : 0.4 \le b \le 0.6 \text{ with } 70\% \text{ belief} \\ b : 0.6 \le b \le 1.0 \text{ with } 20\% \text{ belief} \end{Bmatrix} \tag{10.43}$$

$$\mathcal{B}_2 = \begin{Bmatrix} b : 0.0 \le b \le 0.2 \text{ with } 33\% \text{ belief} \\ b : 0.2 \le b \le 0.4 \text{ with } 33\% \text{ belief} \\ b : 0.3 \le b \le 0.5 \text{ with } 33\% \text{ belief} \end{Bmatrix}. \tag{10.44}$$

Copyright 2005 by CRC Press LLC

Thus, the set

$$\mathcal{B} = \mathcal{B}_1 \cup \mathcal{B}_2 \cup \mathcal{B}_3 = \{b : 0 \le b \le 1\} \tag{10.45}$$

contains all specified values for b.

Given that each of the sources of information specifies only intervals of values, the traditional probabilistic analysis is implemented by assuming that a and b are uniformly distributed over each of their specified intervals. This is a significant assumption beyond what was given for the state of knowledge concerning a and b. The only claim from the expert sources is that the actual value is contained in specified intervals, *not* that all values over each of the intervals are equally likely. Other specifications of probability are possible, e.g., the intervals specified by each source could be divided into a finite number of subintervals, and probability density distributions (PDFs) could be defined for each of the subintervals. However, this is essentially never done. The specification of uniform distributions over each interval is the most common technique used to convert intervals of possible values to PDFs.

Let $[r_i, s_i]$, $i = 1, 2, \ldots n$, denote the specified intervals for a parameter from a given source. Let g_i be the graded level of belief associated with the interval $[r_i, s_i]$, expressed as a decimal. Then the resultant density function d is given by

$$d(v) = \sum_{i=1}^{n} \delta_i(v) g_i / (s_i - r_i), \tag{10.46}$$

where

$$\delta_i(v) = \begin{cases} 1 & \text{for } v \in [r_i, s_i] \\ 0 & \text{otherwise.} \end{cases} \tag{10.47}$$

For parameter a, n has values of 1 and 2 for sources 1 and 2, respectively. For parameter b, n has values of 2, 3, and 3 for sources 1, 2, and 3, respectively.

Because it is given that each source of information is equally credible, the resultant density functions for each source are simply averaged. Thus, if $d_{A1}(a)$ and $d_{A2}(a)$ denote the density functions for sources 1 and 2 for variable a, the resultant combined density function is

$$d_A(a) = \sum_{i=1}^{2} d_{Ai}(a)/2. \tag{10.48}$$

Similarly, the resultant combined density function for b is

$$d_B(b) = \sum_{i=1}^{3} d_{Bi}(b)/3, \tag{10.49}$$

where $d_{B1}(b)$, $d_{B2}(b)$, and $d_{B3}(b)$ denote the density functions from sources 1, 2, and 3, respectively. The density functions $d_A(a)$ and $d_B(b)$ in Equation 10.48 and Equation 10.49 effectively define the probability space used to characterize the uncertainty in a and b, respectively.

10.3.2.2 Construction of Probabilistic Response

Each possible value for y in Equation 10.38 derives from multiple vectors $\mathbf{c} = [a, b]$ of possible values for a and b. For example, each contour line in Figure 10.3 derives from multiple values of $\mathbf{c}$ that produce the same value of y. The set

$$\mathcal{C} = \mathcal{A} \times \mathcal{B} = \{\mathbf{c} = [a, b] : a \in \mathcal{A}, b \in \mathcal{B}\} \tag{10.50}$$

Copyright 2005 by CRC Press LLC

contains all possible values for **c**. Because it is given that a and b are independent, the PDF for $\mathcal{C}$ is given by

$$d_C(\mathbf{c}) = d_A(a)d_B(b) \tag{10.51}$$

for $\mathbf{c} = [a, b] \in \mathcal{C}$. For notational convenience, the probability space used to characterize the uncertainty in $\mathbf{c} = [a, b]$ will be represented by $(\mathcal{C}, \mathbb{C}, p_C)$.

Possible values for a and b give rise to possible values for y through the relationship in Equation 10.38. In particular, the set $\mathcal{Y}$ of all possible values for y is given by

$$\mathcal{Y} = \{y : y = f(a, b) = (a + b)^a, [a, b] \in \mathcal{C}\}. \tag{10.52}$$

With a probability-based approach, the uncertainty in y is represented by defining a probability distribution over $\mathcal{Y}$. Ultimately, the probability distribution associated with $\mathcal{Y}$ derives from the nature of the mapping $y = f(a, b)$ and the probability distributions over $\mathcal{A}$ and $\mathcal{B}$.

The probability $p_Y(\mathcal{E})$ of a subset $\mathcal{E}$ of $\mathcal{Y}$ can be formally represented by

$$p_Y(\mathcal{E}) = \int_{\mathcal{E}} d_Y(y)dy = p_C(f^{-1}(\mathcal{E})), \tag{10.53}$$

where d_Y denotes the density function associated with the distribution of y, $p_C(f^{-1}(\mathcal{E}))$ denotes the probability of the set $f^{-1}(\mathcal{E})$ in $\mathcal{C} = \mathcal{A} \times \mathcal{B}$, and

$$f^{-1}(\mathcal{E}) = \{\mathbf{c} : \mathbf{c} = [a, b] \in \mathcal{C} = \mathcal{A} \times \mathcal{B} \text{ and } y = f(a, b) \in \mathcal{E}\}. \tag{10.54}$$

A closed-form representation for the density function d_Y can be derived from f, d_A and d_B. However, in real analysis problems, this is rarely done due to the complexity of the function and distributions involved. The relations in Equation 10.53 are presented to emphasize that probabilities for subsets of $\mathcal{Y}$ result from probabilities for subsets of $\mathcal{C}$.

An alternative representation for $p_Y(\mathcal{E})$ is given by

$$\begin{aligned} p_Y(\mathcal{E}) &= \int_{\mathcal{Y}} \delta_E(y) d_Y(y) dy \\ &= \int_{\mathcal{C}} \delta_E[f(a, b)] d_A(a) d_B(b) da\, db, \end{aligned} \tag{10.55}$$

where

$$\delta_E(y) = \begin{cases} 1 & \text{if } y \in \mathcal{E} \\ 0 & \text{otherwise.} \end{cases} \tag{10.56}$$

The preceding representation underlies the calculations carried out when a Monte Carlo or Latin Hypercube sampling procedure is used to estimate $p_Y(\mathcal{E})$ [78–80].

As indicated in Section 10.2.2, CCDFs provide a standard way to summarize probability distributions and provide an answer to the following commonly asked question: "How likely is y to be this large or larger?" The defining equation for a CCDF is analogous to Equation 10.25 and Equation 10.27 for CCBFs and CCPFs, respectively, in evidence theory. Specifically, the CCDF for y is defined by the set of points

$$\mathcal{CCDF} = \{[v, p_Y(\mathcal{Y}_v)], v \in \mathcal{Y}\} = \{[v, p_C(f^{-1}(\mathcal{Y}_v))], v \in \mathcal{Y}\} \tag{10.57}$$

for $\mathcal{Y}_v$ defined in Equation 10.28. The CCDF for the function $y = f(a, b)$ defined in Equation 10.38 and the probability space $(\mathcal{C}, \mathbb{C}, p_C)$ introduced in this section is presented in Section 10.3.4.

Copyright 2005 by CRC Press LLC

10.3.3 Analysis Using Evidence Theory

10.3.3.1 Construction of Basic Probability Assignments for Individual Inputs

The BPAs for $\mathcal{A}$ and $\mathcal{B}$ are obtained by first defining BPAs for $\mathcal{A}_1$ and $\mathcal{A}_2$, and $\mathcal{B}_1$, $\mathcal{B}_2$, and $\mathcal{B}_3$. This is done using the information for a and b from each source (see Equation 10.39, 10.40 and Equation 10.42 through Equation 10.44). A convenient representational device for BPAs associated with interval data can be obtained with the use of lower triangular matrices. This representation, an extension of that used in [81], is constructed as follows. For each uncertain parameter, an interval is identified that contains the range of the parameter when all of the sources of information for that parameter are combined. The range of each parameter is divided into as many contiguous subintervals as needed to describe the interval value information from each of the sources; that is, any specified interval of values for the parameter is equal to the union of a subset of these contiguous intervals. The columns of the lower triangular matrix are indexed by taking the lower value of each subinterval, and the rows are indexed by taking the upper value of each subinterval.

To represent this lower triangular matrix of potential nonzero BPAs, let $l_1, l_2, \ldots l_n$ be the lower values for the n subintervals, where $l_1 \le l_2 \ldots \le l_n$. Let $u_1, u_2, \ldots u_n$ be the upper values of the subintervals, where $u_1 \le u_2 \ldots \le u_n$. Consistent with the contiguous assumption, the intervals can be expressed as $[l_1, l_2]$ $[l_2, l_3], \ldots [l_n, u_n]$ with $l_n \le u_n$, or equivalently as $[l_1, u_1], [u_1, u_2], \ldots [u_{n-1}, u_n]$ with $l_1 \le u_1$. Let $m([l_i, u_j])$ be the BPA for the subinterval $[l_i, u_j]$. The $n \times n$ lower triangular matrix can then be written as

$$\begin{array}{cccccc} & l_1 & l_2 & l_3 & \cdots & l_n \\ u_1 & m([l_1,u_1]) & & & & \\ u_2 & m([l_1,u_2]) & m([l_2,u_2]) & & & \\ u_3 & m([l_1,u_3]) & m([l_2,u_3]) & m([l_3,u_3]) & & \\ \vdots & \vdots & \vdots & \vdots & \ddots & \\ u_n & m([l_1,u_n]) & m([l_2,u_n]) & m([l_3,u_n]) & \cdots & m([l_n,u_n]). \end{array} \tag{10.58}$$

Specifically, m in the preceding matrix defines a BPA for $\mathcal{S} = \{x : l_1 \le x \le u_n\}$ provided (i) the values for m in the matrix are nonnegative and sum to 1, and (ii) $m(\mathcal{E}) = 0$ if $\mathcal{E} \subset \mathcal{S}$ and $\mathcal{E}$ does not correspond to one of the intervals with a BPA in the matrix. In essence, this representation provides a way to define a BPA over an interval when all noncontiguous subintervals are given a BPA of zero. When only the diagonal elements of the matrix are nonzero, the resultant BPA assignment is equivalent to the specification of a discrete probability space. For this space, the set $\mathbb{S}$ contains the null set and all sets that can be generated by forming unions of the intervals $[l_1, l_2), [l_2, l_3), \ldots [l_n, u_n]$. Note that half-open intervals are assumed so that the intersection of any two intervals will be the null set. Conversely, from the structure of the matrix it can be seen that the precision of the information decreases as the distance from the diagonal increases. For example, the least precise statement of information appears in the lower-left element of the matrix with the definition of the BPA $m[l_1, u_n]$.

In the present example, the sets $\mathcal{A}$ and $\mathcal{B}$ correspond to the intervals [0.1, 1] and [0, 1], respectively. The corresponding matrices for $\mathcal{A}$ and $\mathcal{B}$ are

$$\begin{array}{cccccc} & 0.1 & 0.5 & 0.6 & 0.9 & \\ 0.5 & m_A([0.1,0.5]) & & & & \\ 0.6 & m_A([0.1,0.6]) & m_A([0.5,0.6]) & & & \\ 0.9 & m_A([0.1,0.9]) & m_A([0.5,0.9]) & m_A([0.6,0.9]) & & \\ 1.0 & m_A([0.1,1.0]) & m_A([0.5,1.0]) & m_A([0.6,1.0]) & m_A([0.9,1.0]) & \end{array} \tag{10.59}$$

Copyright 2005 by CRC Press LLC

and

$$
\begin{array}{cccccccc}
 & 0.0 & 0.2 & 0.3 & 0.4 & 0.5 & 0.6 & 0.8 \\
0.2 & m_B([0.0,0.2]) & & & & & & \\
0.3 & m_B([0.0,0.3]) & m_B([0.2,0.3]) & & & & & \\
0.4 & m_B([0.0,0.4]) & m_B([0.2,0.4]) & m_B([0.3,0.4]) & & & & \\
0.5 & m_B([0.0,0.5]) & m_B([0.2,0.5]) & m_B([0.3,0.5]) & m_B([0.4,0.5]) & & & \\
0.6 & m_B([0.0,0.6]) & m_B([0.2,0.6]) & m_B([0.3,0.6]) & m_B([0.4,0.6]) & m_B([0.5,0.6]) & & \\
0.8 & m_B([0.0,0.8]) & m_B([0.2,0.8]) & m_B([0.3,0.8]) & m_B([0.4,0.8]) & m_B([0.5,0.8]) & m_B([0.6,0.8]) & \\
1.0 & m_B([0.0,1.0]) & m_B([0.2,1.0]) & m_B([0.3,1.0]) & m_B([0.4,1.0]) & m_B([0.5,1.0]) & m_B([0.6,1.0]) & m_B([0.8,1.0]),
\end{array}
\tag{10.60}
$$

respectively.

The information for a provided by the two sources (see Equation 10.39 and Equation 10.40) can be summarized by the following matrices $\mathbf{A}_1$ and $\mathbf{A}_2$ of the form shown in Equation 10.59:

$$
\mathbf{A}_1 = \begin{bmatrix} 0 & & & \\ 0 & 0 & & \\ 0 & 0 & 1 & \\ 0 & 0 & 0 & 0 \end{bmatrix} \quad \text{and} \quad \mathbf{A}_2 = \begin{bmatrix} 0.2 & & & \\ 0 & 0 & & \\ 0 & 0 & 0 & \\ 0 & 0.8 & 0 & 0 \end{bmatrix}. \tag{10.61}
$$

Similarly, the information for b provided by the three sources (see Equation 10.42 through Equation 10.44) can be summarized by the following matrices $\mathbf{B}_1$, $\mathbf{B}_2$, and $\mathbf{B}_3$ of the form shown in Equation 10.60:

$$
\mathbf{B}_1 = \begin{bmatrix} 0 & & & & & & \\ 0 & 0 & & & & & \\ 0 & 0 & 0 & & & & \\ 0 & 0 & 0.1 & 0 & & & \\ 0 & 0 & 0 & 0 & 0 & & \\ 0 & 0 & 0 & 0 & 0 & 0.9 & \\ 0 & 0 & 0 & 0 & 0 & 0 & 0 \end{bmatrix}, \quad \mathbf{B}_2 = \begin{bmatrix} 0 & & & & & & \\ 0 & 0 & & & & & \\ 0 & 0.1 & 0 & & & & \\ 0 & 0 & 0 & 0 & & & \\ 0 & 0 & 0 & 0.7 & 0 & & \\ 0 & 0 & 0 & 0 & 0 & 0 & \\ 0 & 0 & 0 & 0 & 0 & 0.2 & 0 \end{bmatrix},
$$

$$
\text{and } \mathbf{B}_3 = \begin{bmatrix} 0.333 & & & & & & \\ 0 & 0 & & & & & \\ 0 & 0.333 & 0 & & & & \\ 0 & 0 & 0.333 & 0 & & & \\ 0 & 0 & 0 & 0 & 0 & & \\ 0 & 0 & 0 & 0 & 0 & 0 & \\ 0 & 0 & 0 & 0 & 0 & 0 & 0 \end{bmatrix}. \tag{10.62}
$$

The BPAs for all unspecified subsets of $\mathcal{A}$ and $\mathcal{B}$ are zero.

10.3.3.2 Combination of Evidence

Combining the BPAs for the $\mathcal{A}_i$'s to obtain a BPA for $\mathcal{A}$ and combining the BPAs for the $\mathcal{B}_i$'s to obtain a BPA for $\mathcal{B}$ is now considered. The issue of combination of evidence, also referred to as *aggregation of evidence* or *data fusion*, is a topic closely related to evidence theory itself. After the introduction of evidence theory by Dempster in 1967 [61], many researchers believed evidence theory and the issue of combination

Copyright 2005 by CRC Press LLC

of evidence were essentially the same topic. This view was reinforced by the close relationship between evidence theory and Dempster's rule of combination of evidence. In fact, much of the criticism of evidence theory has actually been directed at Dempster's rule of combination. It is now recognized that combination of evidence is a separate topic of growing importance in many fields [50, 52, 64, 82–89]. Combination of evidence takes on even more importance in newer theories of uncertainty, such as evidence theory, because many of the newer theories can deal more directly with large epistemic uncertainty than the traditional application of probability theory. The manner in which conflicting evidence is combined can have a large impact on the results of an uncertainty analysis, particularly when evidence theory is used.

In this presentation, the emphasis is on comparing uncertainty estimation results from the traditional application of probability theory and evidence theory. As a result, evidence from the various sources is combined in the same manner as was done for the solution using probability theory. The equivalent formulation to Equation 10.48 and Equation 10.49 for the matrices $\mathbf{A}_i$ and $\mathbf{B}_i$ is

$$\mathbf{A} = \sum_{i=1}^{2} \mathbf{A}_i/2 \quad \text{and} \quad \mathbf{B} = \sum_{i=1}^{3} \mathbf{B}_i/3. \tag{10.63}$$

Applying these equations to Equation 10.61 and Equation 10.62, respectively, we have

$$\mathbf{A} = \begin{bmatrix} 0.1 & & & \\ 0 & 0 & & \\ 0 & 0 & 0.5 & \\ 0 & 0.4 & 0 & 0 \end{bmatrix} \tag{10.64}$$

$$\text{and } \mathbf{B} = \begin{bmatrix} 0.111 & & & & & & \\ 0 & 0 & & & & & \\ 0 & 0.144 & 0 & & & & \\ 0 & 0 & 0.144 & 0 & & & \\ 0 & 0 & 0 & 0.233 & 0 & & \\ 0 & 0 & 0 & 0 & 0 & 0.3 & \\ 0 & 0 & 0 & 0 & 0 & 0.067 & 0 \end{bmatrix}, \tag{10.65}$$

with the additional specification that $m_A(\mathcal{E}) = 0$ if $\mathcal{E}$ is a subset of $\mathcal{A}$ without an assigned BPA in **A** and $m_B(\mathcal{E}) = 0$ if $\mathcal{E}$ is a subset of $\mathcal{B}$ without an assigned BPA in **B**.

10.3.3.3 Construction of Basic Probability Assignments for the Product Space

The variables *a* and *b* are specified as being independent. With the use of Equation 10.21, the BPA $m_C(\mathcal{E})$ defined on $\mathcal{C} = \mathcal{A} \times \mathcal{B}$ is given by

$$m_C(\mathcal{E}) = \begin{cases} m_A(\mathcal{E}_A) m_B(\mathcal{E}_B) & \text{if } \mathcal{E}_A \subset \mathcal{A}, \mathcal{E}_B \subset \mathcal{B} \text{ and } \mathcal{E} = \mathcal{E}_A \times \mathcal{E}_B \\ 0 & \text{otherwise} \end{cases} \tag{10.66}$$

for $\mathcal{E} \subset \mathcal{C}$. The resultant nonzero BPAs and associated subsets of $\mathcal{C}$ are summarized in Table 10.1.

Subset 11 is used to illustrate the entries in Table 10.1. This subset corresponds to the interval [0.5, 1.0] for *a*, and the interval [0.4, 0.6] for *b*. From Equation 10.66,

$$m_C(\mathcal{E}) = m_A([0.5, 1.0]) m_B([0.4, 0.6]), \tag{10.67}$$

Copyright 2005 by CRC Press LLC

TABLE 10.1 Summary of the Nonzero Values of the BPA m_C for $\mathcal{C} = \mathcal{A} \times \mathcal{B}$

	$m_A([0.1, 0.5]) = 0.1$	$m_A([0.5, 1.0]) = 0.4$	$m_A([0.6, 0.9]) = 0.5$
$m_B([0., 0.2]) = 0.111$	0.0111 (subset 1)	0.0444 (subset 2)	0.0555 (subset 3)
$m_B([0.2, 0.4]) = 0.144$	0.0144 (subset 4)	0.0576 (subset 5)	0.0720 (subset 6)
$m_B([0.3, 0.5]) = 0.144$	0.0144 (subset 7)	0.0576 (subset 8)	0.0720 (subset 9)
$m_B([0.4, 0.6]) = 0.233$	0.0233 (subset 10)	0.0932 (subset 11)	0.1165 (subset 12)
$m_B([0.6, 0.8]) = 0.300$	0.0300 (subset 13)	0.1200 (subset 14)	0.1500 (subset 15)
$m_B([0.6, 1.0]) = 0.067$	0.0067 (subset 16)	0.0268 (subset 17)	0.0335 (subset 18)

where the values for $m_A([0.5, 1.0])$ and $m_B([0.4, 0.6])$ appear in the column and row designators associated with subset 11 (i.e., $\mathcal{E} = [0.5, 1.0] \times [0.4, 0.6]$) and are defined by entries in the matrices **A** and **B** in Equation 10.64 and Equation 10.65, respectively. This yields

$$m_C(\mathcal{E}) = (0.4)(0.233) = 0.0932. \tag{10.68}$$

The magnitude of m_C shown for subsets of $\mathcal{C}$ in Table 10.1 indicates the likelihood that can be assigned to a given set, but *not* to any proper subset of that set. As required in the definition of a BPA, the BPAs in Table 10.1 sum to unity.

10.3.3.4 Construction of Belief and Plausibility for the System Response

The belief and plausibility measures for the system outcome y can now be computed. The goal is to obtain an assessment of the likelihood, in the context of evidence theory, that y will be in the failure region. As previously indicated, the threshold of the failure region is $v = 1.7$. Thus, the system failure question is: "How likely is it that y will have a value in the set $\mathcal{Y}_{1.7}$ defined in Equation 10.28?" As indicated in Equation 10.35 and Equation 10.37,

$$Bel_Y(\mathcal{Y}_v) = \sum_{j \in \mathcal{ICCBF}_v} m_C(\mathcal{E}_j) \tag{10.69}$$

and

$$Pl_Y(\mathcal{Y}_v) = \sum_{j \in \mathcal{ICCPF}_v} m_C(\mathcal{E}_j), \tag{10.70}$$

where $\mathcal{E}_j$, $j = 1, 2, \ldots 18$, are the subsets of $\mathcal{C}$ with nonzero BPAs given in Table 10.1. The sets $\mathcal{ICCBF}_v$ and $\mathcal{ICCPF}_v$ are defined in Equation 10.31 and Equation 10.33. In turn, the sets

$$\mathcal{CCBF} = \{[v, Bel_Y(\mathcal{Y}_v)] : v \in \mathcal{Y}\} \tag{10.71}$$

and

$$\mathcal{CCPF} = \{[v, Pl_Y(\mathcal{Y}_v)] : v \in \mathcal{Y}\} \tag{10.72}$$

define the CCBF and the CCPF for y.

The quantities $\mathcal{ICCBF}_v$, $\mathcal{ICCPF}_v$, $Bel_Y(\mathcal{Y}_v)$, and $Pl_Y(\mathcal{Y}_v)$ for the example problem are summarized in Table 10.2. The contour lines of $y = (a+b)^a$ are shown in Figure 10.4a to aid in understanding where the jumps in the CCBF and CCPF occur. Along the edges of Figure 10.4a are the values of y at equal increments

Copyright 2005 by CRC Press LLC

TABLE 10.2 Determination of the CCBF and CCPF for $y = f(a, b)$ with Equation 10.67 and Equation 10.68 and the BPAs in Table 10.1.

v	$\mathcal{ICCBF}_v$	$\mathcal{ICCPF}_v$	$Bel_Y(\mathcal{Y}_v)$	$Pl_Y(\mathcal{Y}_v)$
0.69220	1,2,3,4,5,6,7,8,9,10,11, 12,13,14,15,16,17,18	1,2,3,4,5,6,7,8,9,10,11,12,13,14,15,16,17,18	1.00000	1.00000
[0.69220, 0.70711]	2,3,4,5,6,7,8,9,10,11,12, 13,14,15,16,17,18	1,2,3,4,5,6,7,8,9,10,11,12,13,14,15,16,17,18	0.98889	1.00000
[0.70711, 0.73602]	3,4,5,6,7,8,9,10,11,12, 13,14,15,16,17,18	1,2,3,4,5,6,7,8,9,10,11,12,13,14,15,16,17,18	0.94444	1.00000
[0.73602, 0.81096]	4,5,6,7,8,9,10,11,12,13, 14,15,16,17,18	1,2,3,4,5,6,7,8,9,10,11,12,13,14,15,16,17,18	0.88889	1.00000
[0.81096, 0.83666]	5,6,7,8,9,10,11,12,13, 14,15,16,17,18	1,2,3,4,5,6,7,8,9,10,11,12,13,14,15,16,17,18	0.87444	1.00000
[0.83666, 0.85790]	6,7,8,9,10,11,12,13,14, 15,16,17,18	1,2,3,4,5,6,7,8,9,10,11,12,13,14,15,16,17,18	0.81667	1.00000
[0.85790, 0.87469]	6,8,9,10,11,12,13,14, 15,16,17,18	1,2,3,4,5,6,7,8,9,10,11,12,13,14,15,16,17,18	0.80222	1.00000
[0.87469, 0.88657]	8,9,10,11,12,13,14,15, 16,17,18	1,2,3,4,5,6,7,8,9,10,11,12,13,14,15,16,17,18	0.73000	1.00000
[0.88657, 0.89443]	8,9,10,11,12,13,14,15, 16,17,18	2,3,4,5,6,7,8,9,10,11,12,13,14,15,16,17,18	0.73000	0.98889
[0.89443, 0.89751]	9,10,11,12,13,14,15,16, 17,18	2,3,4,5,6,7,8,9,10,11,12,13,14,15,16,17,18	0.67222	0.98889
[0.89751, 0.93874]	9,11,12,13,14,15,16,17, 18	2,3,4,5,6,7,8,9,10,11,12,13,14,15,16,17,18	0.64889	0.98889
[0.93874, 0.94868]	11,12,13,14,15,16,17,18	2,3,4,5,6,7,8,9,10,11,12,13,14,15,16,17,18	0.57667	0.98889
[0.94868, 0.95620]	12,13,14,15,16,17,18	2,3,5,6,7,8,9,10,11,12,13,14,15,16,17,18	0.48333	0.97444
[0.95620, 1.00000]	12,14,15,17,18	2,3,5,6,7,8,9,10,11,12,13,14,15,16,17,18	0.44667	0.97444
[1.00000, 1.04881]	14,15,17,18	2,3,5,6,8,9,10,11,12,13,14,15,16,17,18	0.33000	0.96000
[1.04881, 1.08957]	15,18	2,3,5,6,8,9,11,12,13,14,15,16,17,18	0.18333	0.93667
[1.08957, 1.11560]	15,18	2,5,6,8,9,11,12,13,14,15,16,17,18	0.18333	0.88111
[1.11560, 1.14018]		2,5,6,8,9,11,12,13,14,15,16,17,18	0.00000	0.88111
[1.14018, 1.20000]		2,5,6,8,9,11,12,14,15,16,17,18	0.00000	0.85111
[1.20000, 1.22474]		5,6,8,9,11,12,14,15,16,17,18	0.00000	0.80667
[1.22474, 1.26634]		5,6,8,9,11,12,14,15,17,18	0.00000	0.80000
[1.26634, 1.35368]		5,8,9,11,12,14,15,17,18	0.00000	0.72778
[1.35368, 1.40000]		5,8,11,12,14,15,17,18	0.00000	0.65556
[1.40000, 1.44040]		8,11,12,14,15,17,18	0.00000	0.59778
[1.44040, 1.50000]		8,11,14,15,17,18	0.00000	0.48111
[1.50000, 1.60000]		11,14,15,17,18	0.00000	0.42333
[1.60000, 1.61214]		14,15,17,18	0.00000	0.33000
[1.61214, 1.78188]		14,17,18	0.00000	0.18000
[1.78188, 1.80000]		14,17	0.00000	0.14667
[1.80000, 2.00000]		17	0.00000	0.02667
2.00000			0.00000	0.00000

of a and b along the boundary of their domain. Also note that these y values are only given to two significant figures. These contour lines approximately define the sets $f^{-1}(\mathcal{Y}_v)$ for selected values of v. For example, $f^{-1}(\mathcal{Y}_{1.04})$ is indicated in Figure 10.4b through Figure 10.4d. The sets $\mathcal{ICCBF}_v$ and $\mathcal{ICCPF}_v$ are obtained by determining the j for which $\mathcal{E}_j \subset f^{-1}(\mathcal{Y}_v)$ and $\mathcal{E}_j \cap f^{-1}(\mathcal{Y}_v) \neq \varnothing$, respectively. Thus, as an examination of Figure 10.4b through Figure 10.4d shows,

$$\mathcal{ICCBF}_{1.04} = \{14, 15, 17, 18\} \tag{10.73}$$

and

$$\mathcal{ICCPF}_{1.04} = \{2, 3, 5, 6, 8, 9, 10, 11, 12, 13, 14, 15, 16, 17, 18\}, \tag{10.74}$$

Copyright 2005 by CRC Press LLC

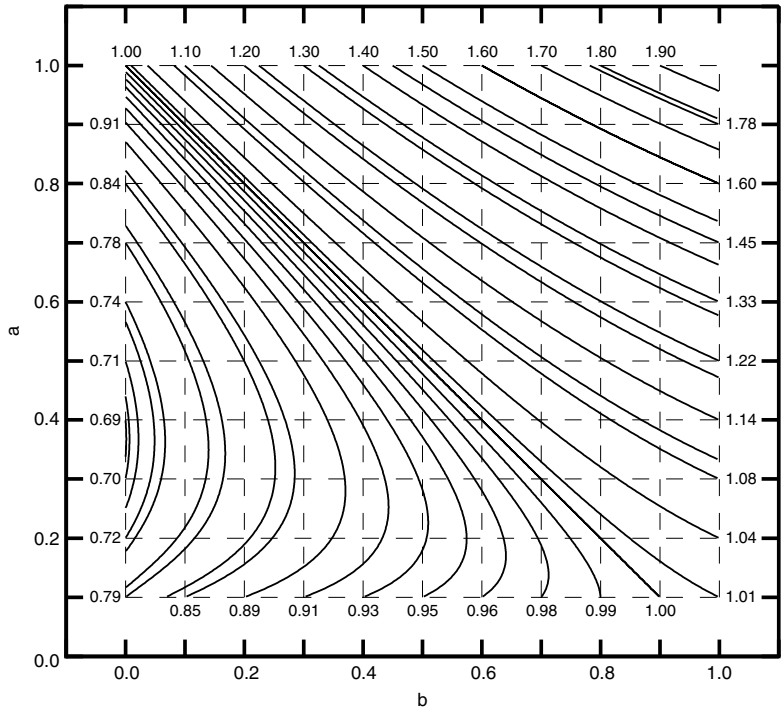

(a) Contour Lines of $y = (a + b)^a$

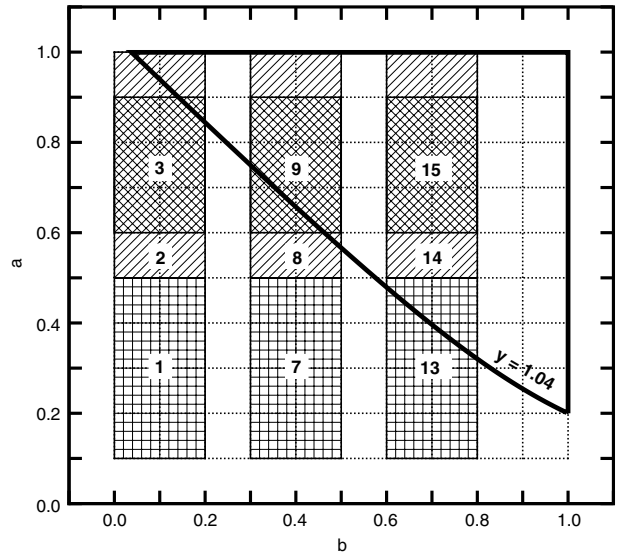

(b) Subsets 1, 2, 3, 7, 8, 9, 13, 14, and 15

FIGURE 10.4 Contour lines of $y = (a + b)^a$ and subsets 1, 2,…, 18 of $\mathcal{C} = \mathcal{A} \times \mathcal{B}$ with nonzero BPAs indicated in Table 10.1: (a) contour lines of $y = (a + b)^a$; (b) subsets 1, 2, 3, 7, 8, 9, 13, 14, and 15; (c) subsets 4, 5, 6, 16, 17, and 18; and (d) subsets 10, 11, and 12. (Originially published in *Investigation of Evidence Theory for Engineering Applications,* Oberkampf, W.L. and Helton, J.C., 4th Nondeterministic Approaches Forum, Denver, AIAA-2002-1569. Copyright © 2002 by the American Institute of Aeronautics and Astronautics, Inc. Reprinted with permission.)

Copyright 2005 by CRC Press LLC

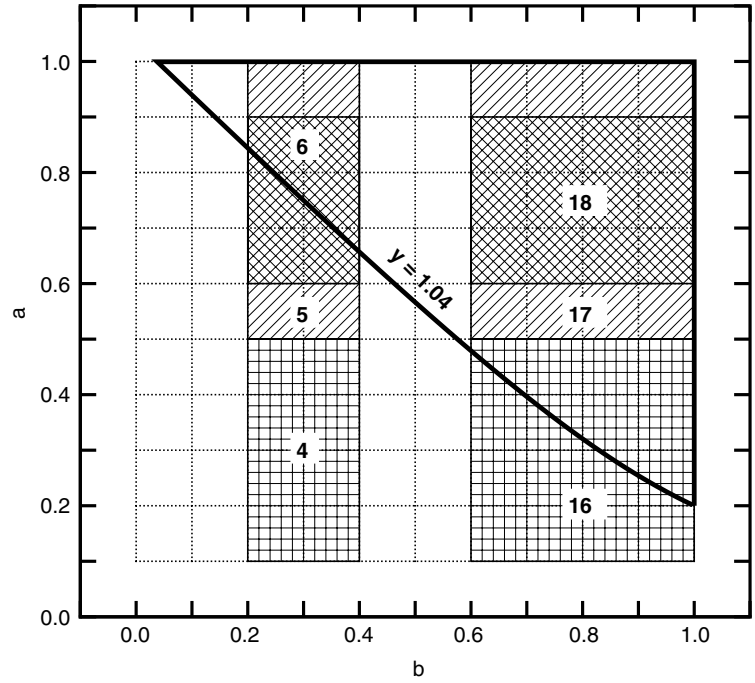

(c) Subsets 4, 5, 6, 16, 17, and 18

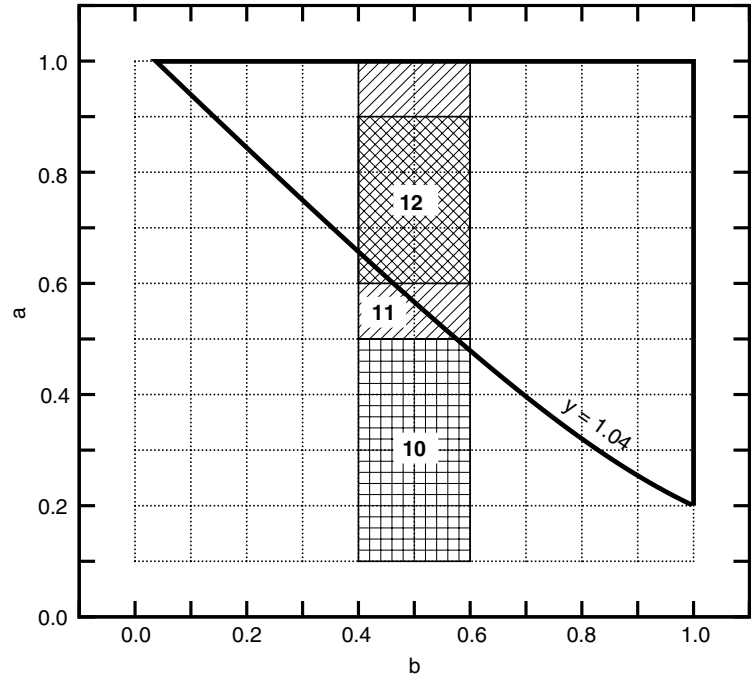

(d) Subsets 10, 11, and 12

FIGURE 10.4 (*Continued*)

Copyright 2005 by CRC Press LLC

which correspond to the values indicated in Table 10.2 for $\mathcal{ICCBF}_{1.04}$ and $\mathcal{ICCPF}_{1.04}$. In turn,

$$\begin{aligned} Bel_{1.04}(\mathcal{Y}_v) &= \sum\nolimits_{j \in \mathcal{ICCBF}_{1.04}} m_C(\mathcal{E}_j) \\ &= m_C(\mathcal{E}_{14}) + m_C(\mathcal{E}_{15}) + m_C(\mathcal{E}_{17}) + m_C(\mathcal{E}_{18}) \\ &= 0.1200 + 0.1500 + 0.0268 + 0.0335 \\ &= 0.3303 \end{aligned} \tag{10.75}$$

and

$$\begin{aligned} Pl_Y(\mathcal{Y}_{1.04}) &= \sum\nolimits_{j \in \mathcal{ICCPF}_{1.04}} m_C(\mathcal{E}_j) \\ &= m_C(\mathcal{E}_2) + m_C(\mathcal{E}_3) + m_C(\mathcal{E}_5) + m_C(\mathcal{E}_6) + m_C(\mathcal{E}_8) + \ldots + m_C(\mathcal{E}_{18}) \\ &= 0.9591. \end{aligned} \tag{10.76}$$

The resultant CCBF and CCPF are provided by plots of the points contained in the sets $\mathcal{CCBF}$ and $\mathcal{CCPF}$ defined in Equation 10.71 and Equation 10.72 and are shown in Figure 10.5. We stress that the jumps, or discontinuities, in the CCBF and CCPF shown in Figure 10.5 are accurate and consistent with evidence theory. Using Monte Carlo sampling for traditional probability theory, one occasionally sees jumps or stair-steps in the CCDF. However, these jumps are typically numerical artifacts, that is, numerical approximations due to use of a finite number of samples to compute the CCDF. In evidence theory, the jumps are *not* numerical artifacts but are due to discontinuous assignments of BPAs across the boundaries of subsets.

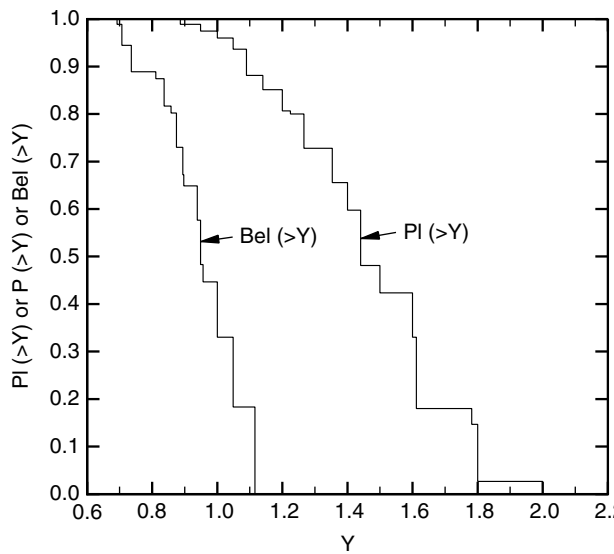

FIGURE 10.5 CCBF and CCPF for example problem $y = (a + b)^a$. (Originially published in *Investigation of Evidence Theory for Engineering Applications,* Oberkampf, W.L. and Helton, J.C., 4th Nondeterministic Approaches Forum, Denver, AIAA-2002-1569. Copyright © 2002 by the American Institute of Aeronautics and Astronautics, Inc. Reprinted with permission.)

Copyright 2005 by CRC Press LLC

10.3.4 Comparison and Interpretation of Results

For the present example, the solution using probability theory is obtained by numerically evaluating Equation 10.55 using Monte Carlo sampling. A random sample of size of one million was used so that an accurate representation of the CCDF could be obtained for probabilities as low as 10^{-4}. The CCDF for y is shown in Figure 10.6. In essence, the CCDF is constructed by plotting the pairs $[v, p_Y(\mathcal{Y}_v)]$ for an increasing sequence of values for v. The resultant CCDF indicates that the probability of the unsafe region, $y > 1.7$, is 0.00646.

Also shown in Figure 10.6 is the CCPF and the CCBF from evidence theory for the example problem. It can be seen in Figure 10.6, and also in Table 10.2, that the highest and lowest probabilities for the unsafe region using evidence theory are 0.18 and 0.0, respectively. That is, the absolutely highest probability that is consistent with the interval data for a and b is 0.18, and the absolutely lowest probability that is consistent with the interval data is 0.0. Stated differently, given the large epistemic uncertainty in the values for a and b, the probability of the unsafe region can *only* be bounded by 0.0 and 0.18. By comparing these interval valued probabilities with the traditional probabilistic result, it is seen that evidence theory states that the likelihood of the unsafe region could be 28 times higher than that indicated by the traditional analysis, or possibly as low as zero.

The key difference between the results obtained with probability theory and evidence theory is that in the probability-based analysis, it was assumed that all values in each specified interval for a and b were equally likely. Stated differently, the probability-based analysis assumed that the probability density function (PDF) was given by a piecewise uniform distribution; whereas in the evidence theory analysis, no additional assumptions were made beyond the uncertainty information supplied by the original sources. In essence, evidence theory permits the specification of partial (i.e., not completely defined)

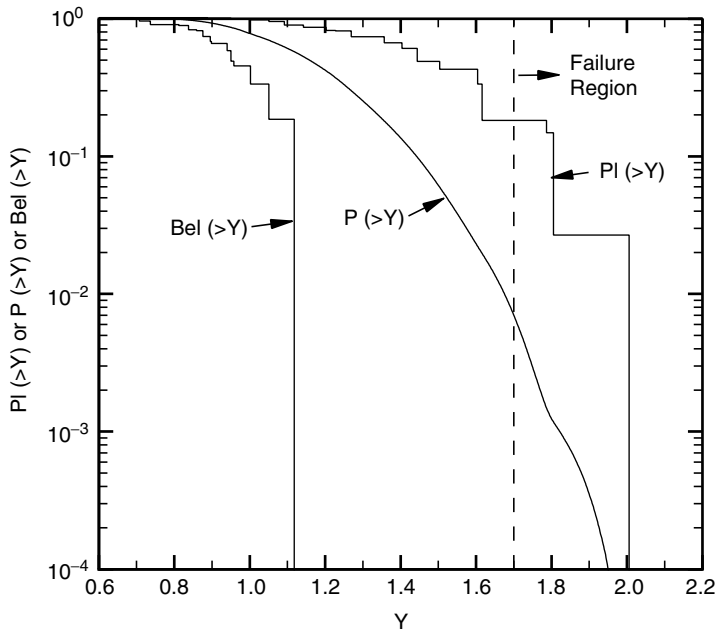

FIGURE 10.6 CCDF, CCPF, and CCBF for example problem $y = (a + b)^a$. (Originially published in *Investigation of Evidence Theory for Engineering Applications,* Oberkampf, W.L. and Helton, J.C., 4th Nondeterministic Approaches Forum, Denver, AIAA-2002-1569. Copyright © 2002 by the American Institute of Aeronautics and Astronautics, Inc. Reprinted with permission.)

Copyright 2005 by CRC Press LLC

probability distributions for a and b. Thus, evidence theory can be viewed as allowing the propagation of partially specified PDFs through the model of the system, in this case $(a + b)^a$, resulting in a range of likelihoods for y. The structure of evidence theory allows the incomplete specification of probability distributions, or more precisely, the complete determination of all possible probability distributions consistent with the input data.

As a final comment, both solution approaches relied on one additional common assumption: namely, that the information from each of the sources of data for a and b could be combined by a simple averaging procedure. As mentioned, a variety of methods have been developed for combining evidence. The results of an uncertainty analysis can strongly depend on which combination method is chosen for use. The selection of an appropriate combination method is an important open issue in uncertainty estimation. Research is needed to provide guidance for the appropriate selection of a combination method given the particular characteristics of a specific analysis and the type of information. Whatever method of combination is chosen in a given situation, the choice should primarily depend on the nature of the information to be combined. For a recent review of methods for combination of evidence, see [89, 90].

10.4 Research Topics in the Application of Evidence Theory

Although evidence theory possesses some advantages compared to the traditional application of probability theory, there are several prominent open issues that must be investigated and resolved before evidence theory can be confidently and productively used in large-scale engineering analyses. First, consider the use sampling techniques to propagate basic probability assignments (BPAs) through "black-box" computational models. An important practical issue arises: what is the convergence rate of approximations to belief and plausibility in the output space as a function of the number of samples? Our preliminary experience using traditional sampling techniques, such as Monte Carlo or Latin Hypercube, indicates that these techniques are reliable for evidence theory, but they are also expensive from the standpoint of function evaluations. Possibly faster convergence techniques could be developed for a wide range of black-box functions. Second, how can sensitivity analyses be conducted in the context of evidence theory? Rarely is a nondeterministic analysis conducted simply for the purpose of estimating the uncertainty in specified system response variables. A more common question is: what are the primary contributors to the uncertainty in the system response? Thus, sensitivity analysis procedures must be available for use in conjunction with uncertainty propagation procedures. Third, for situations of pure epistemic uncertainty (i.e., no aleatory uncertainty) in input parameters, such as the present example problem with interval data, how does one properly interpret belief and plausibility in the output space as minimum and maximum probabilities, respectively? A closely related question is: how does the averaging technique for aggregating conflicting expert opinion, which is the common technique in classical probabilistic thinking, affect the interpretation of interval valued probabilities in the output space?

The issue of combination of evidence from multiple sources is a separate issue from evidence theory itself. Evidence theory has been criticized in the past because there is no unique method for combining multiple sources of evidence. However, combination of evidence in probability theory is also nonunique and open to question. Further research is needed into methods of combining different types of evidence, particularly highly conflicting evidence from different sources. We believe that the method of combination of evidence chosen in a given situation should be context dependent. Stated differently, there is no single method appropriate for combining all types of evidence in all situations dealing with epistemic uncertainty.

Finally, evidence theory may have advantages over the traditional application of probability theory with regard to representing model form uncertainty (i.e., uncertainty due to lack of knowledge of the physical process being mathematically modeled). Because model form uncertainty is just a special case of epistemic uncertainty, any benefits that evidence theory has in the representation of epistemic uncertainty in general should also apply to model form uncertainty. Although this topic was not specifically addressed in this presentation, evidence theory has the capability to leave unspecified the probability assigned to any given mathematical model among alternative candidate models.

Copyright 2005 by CRC Press LLC

Acknowledgments

We thank Jay Johnson of ProStat, Inc., for computation of the results and generation of the figures. This work was performed at Sandia National Laboratories, which is a multiprogram laboratory operated by Sandia Corporation, a Lockheed Martin Company, for the United States Department of Energy's National Nuclear Security Administration under contract DE-AC04-AL85000.

References

1. AIAA, Guide for the verification and validation of computational fluid dynamics simulations, American Institute of Aeronautics and Astronautics, Reston, VA, AIAA-G-077-1998, 1998.
2. Kleijnen, J.P.C., Verification and validation of simulation models, *European Journal of Operational Research*, 82, 145–162, 1995.
3. Oberkampf, W.L. and Trucano, T.G., Verification and validation in computational fluid dynamics, *Progress in Aerospace Sciences*, 38, 209–272, 2002.
4. Oberkampf, W.L. and Trucano, T.G., Verification, validation, and predictive capability in computational engineering and physics, Sandia National Laboratories, Albuquerque, NM, SAND2003-3769, 2003.
5. Knupp, P. and Salari, K., *Verification of Computer Codes in Computational Science and Engineering*, Chapman & Hall/CRC, Boca Raton, FL, 2002.
6. Roache, P.J., *Verification and Validation in Computational Science and Engineering*, Hermosa Publishers, Albuquerque, NM, 1998.
7. Hora, S.C. and Iman, R.L., Expert opinion in risk analysis: the NUREG-1150 methodology, *Nuclear Science and Engineering*, 102, 323–331, 1989.
8. Hauptmanns, U. and Werner, W., *Engineering Risks Evaluation and Valuation*, 1st ed., Springer-Verlag, Berlin, 1991.
9. Beckjord, E.S., Cunningham, M.A., and Murphy, J.A., Probabilistic safety assessment development in the United States 1972–1990, *Reliability Engineering and System Safety*, 39, 159–170, 1993.
10. Modarres, M., *What Every Engineer Should Know about Reliability and Risk Analysis*, Marcel Dekker, New York, 1993.
11. Kafka, P., Important issues using PSA technology for design of new systems and plants, *Reliability Engineering and System Safety*, 45, 205–213, 1994.
12. Breeding, R.J., Helton, J.C., Murfin, W.B., Smith, L.N., Johnson, J.D., Jow, H.-N., and Shiver, A.W., The NUREG-1150 probabilistic risk assessment for the Surry Nuclear Power Station, *Nuclear Engineering and Design,* 135, 29–59, 1992.
13. Kumamoto, H. and Henley, E.J., *Probabilistic Risk Assessment and Management for Engineers and Scientists*, 2nd ed., IEEE Press, New York, 1996.
14. Helton, J.C., Uncertainty and sensitivity analysis in performance assessment for the Waste Isolation Pilot Plant, *Computer Physics Communications*, 117, 156–180, 1999.
15. Paté-Cornell, M.E., Conditional uncertainty analysis and implications for decision making: the case of WIPP, *Risk Analysis*, 19, 1003–1016, 1999.
16. Helton, J.C. and Breeding, R.J., Calculation of reactor accident safety goals, *Reliability Engineering and System Safety*, 39, 129–158, 1993.
17. Ross, T.J., *Fuzzy Logic with Engineering Applications*, McGraw-Hill, New York, 1995.
18. Melchers, R.E., *Structural Reliability Analysis and Prediction*, 2nd ed., John Wiley & Sons, New York, 1999.
19. Hoffman, F.O. and Hammonds, J.S., Propagation of uncertainty in risk assessments: the need to distinguish between uncertainty due to lack of knowledge and uncertainty due to variability, *Risk Analysis*, 14, 707–712, 1994.
20. Rowe, W.D., Understanding uncertainty, *Risk Analysis*, 14, 743–750, 1994.
21. Helton, J.C., Treatment of uncertainty in performance assessments for complex systems, *Risk Analysis*, 14, 483–511, 1994.

Copyright 2005 by CRC Press LLC

22. Ayyub, B.M., The Nature of Uncertainty in Structural Engineering, in *Uncertainty Modelling and Analysis: Theory and Applications*, B. M. Ayyub and M. M. Gupta, Eds., 1st ed., Elsevier, New York, 1994, 195–210.
23. Hora, S.C., Aleatory and epistemic uncertainty in probability elicitation with an example from hazardous waste management, *Reliability Engineering and System Safety*, 54, 217–223, 1996.
24. Frey, H.C. and Rhodes, D.S., Characterizing, simulating, and analyzing variability and uncertainty: an illustration of methods using an air toxics emissions example, *Human and Ecological Risk Assessment,* 2, 762–797, 1996.
25. Ferson, S. and Ginzburg, L.R., Different methods are needed to propagate ignorance and variability, *Reliability Engineering and System Safety*, 54, 133–144, 1996.
26. Ferson, S., What Monte Carlo methods cannot do, *Human and Ecological Risk Assessment*, 2, 990–1007, 1996.
27. Rai, S.N., Krewski, D., and Bartlett, S., A general framework for the analysis of uncertainty and variability in risk assessment, *Human and Ecological Risk Assessment*, 2, 972–989, 1996.
28. Parry, G.W., The characterization of uncertainty in probabilistic risk assessments of complex systems, *Reliability Engineering and System Safety*, 54, 119–126, 1996.
29. Helton, J.C., Uncertainty and sensitivity analysis in the presence of stochastic and subjective uncertainty, *Journal of Statistical Computation and Simulation*, 57, 3–76, 1997.
30. Paté-Cornell, M.E., Uncertainties in risk analysis: six levels of treatment, *Reliability Engineering and System Safety*, 54, 95–111, 1996.
31. Cullen, A.C. and Frey, H.C., *Probabilistic Techniques in Exposure Assessment: A Handbook for Dealing with Variability and Uncertainty in Models and Inputs*, Plenum Press, New York, 1999.
32. Frank, M.V., Treatment of uncertainties in space nuclear risk assessment with examples from Cassini Mission applications, *Reliability Engineering and System Safety*, 66, 203–221, 1999.
33. Haimes, Y.Y., *Risk Modeling, Assessment, and Management*, John Wiley & Sons, New York, 1998.
34. Ang, A.H.S. and Tang, W.H., *Probability Concepts in Engineering Planning and Design: Vol. I Basic Principles*, 1st ed., John Wiley & Sons, New York, 1975.
35. Ditlevsen, O., *Uncertainty Modeling with Applications to Multidimensional Civil Engineering Systems*, 1st ed., McGraw-Hill, New York, 1981.
36. Ang, A.H.S. and Tang, W.H., *Probability Concepts in Engineering Planning and Design: Vol. II Decision, Risk, and Reliability*, John Wiley & Sons, New York, 1984.
37. Neelamkavil, F., *Computer Simulation and Modelling*, 1st ed., John Wiley & Sons, New York, 1987.
38. Haldar, A. and Mahadevan, S., *Probability, Reliability, and Statistical Methods in Engineering Design*, John Wiley & Sons, New York, 2000.
39. Oberkampf, W.L., DeLand, S.M., Rutherford, B.M., Diegert, K.V., and Alvin, K.F., Error and uncertainty in modeling and simulation, *Reliability Engineering and System Safety*, 75, 333–357, 2002.
40. Oberkampf, W.L., DeLand, S.M., Rutherford, B.M., Diegert, K.V., and Alvin, K.F., Estimation of total uncertainty in computational simulation, Sandia National Laboratories, Albuquerque, NM, SAND2000-0824, 2000.
41. Oberkampf, W.L., Helton, J.C., and Sentz, K., Mathematical representation of uncertainty, *3rd Non-deterministic Approaches Forum,* Seattle, WA, AIAA-2001-1645, 2001.
42. Zadeh, L.A., Fuzzy sets as a basis for a theory of possibility, *Fuzzy Sets and Systems*, 1, 3–28, 1978.
43. Manton, K.G., Woodbury, M.A., and Tolley, H.D., *Statistical Applications Using Fuzzy Sets*, John Wiley & Sons, New York, 1994.
44. Onisawa, T. and Kacprzyk, J., Eds., *Reliability and Safety Analyses under Fuzziness*, Physica-Verlag, Heidelberg, 1995.
45. Klir, G.J., St. Clair, U., and Yuan, B., *Fuzzy Set Theory: Foundations and Applications*, Prentice Hall PTR, Upper Saddle River, NJ, 1997.
46. Dubois, D. and Prade, H., *Fundamentals of Fuzzy Sets*, Kluwer Academic, Boston, 2000.
47. Moore, R.E., *Methods and Applications of Interval Analysis*, SIAM, Philadelphia, PA, 1979.

Copyright 2005 by CRC Press LLC

48. Kearfott, R.B. and Kreinovich, V., Eds., *Applications of Interval Computations*, Kluwer Academic, Boston, 1996.
49. Shafer, G., *A Mathematical Theory of Evidence*, Princeton University Press, Princeton, NJ, 1976.
50. Guan, J. and Bell, D.A., *Evidence Theory and Its Applications*, Vol. I., North Holland, Amsterdam, 1991.
51. Krause, P. and Clark, D., *Representing Uncertain Knowledge: An Artificial Intelligence Approach*, Kluwer Academic Publishers, Dordrecht, The Netherlands, 1993.
52. Kohlas, J. and Monney, P.-A., *A Mathematical Theory of Hints — An Approach to the Dempster-Shafer Theory of Evidence*, Springer, Berlin, 1995.
53. Almond, R.G., *Graphical Belief Modeling*, 1st ed., Chapman & Hall, London, 1995.
54. Klir, G.J. and Wierman, M.J., *Uncertainty-Based Information: Elements of Generalized Information Theory*, Physica-Verlag, Heidelberg, 1998.
55. Kramosil, I., *Probabilistic Analysis of Belief Functions*, Kluwer, New York, 2001.
56. Dubois, D. and Prade, H., *Possibility Theory: An Approach to Computerized Processing of Uncertainty*, Plenum Press, New York, 1988.
57. de Cooman, G., Ruan, D., and Kerre, E.E., *Foundations and Applications of Possibility Theory*, World Scientific Publishing Co., Singapore, 1995.
58. Walley, P., *Statistical Reasoning with Imprecise Probabilities*, Chapman & Hall, London, 1991.
59. Klir, G.J. and Yuan, B., *Fuzzy Sets and Fuzzy Logic*, Prentice Hall, Saddle River, NJ, 1995.
60. Klir, G.J. and Smith, R.M., On measuring uncertainty and uncertainty-based information: recent developments, *Annals of Mathematics and Artificial Intelligence*, 32, 5–33, 2001.
61. Dempster, A.P., Upper and lower probabilities induced by a multivalued mapping, *Annals of Mathematical Statistics*, 38, 325–339, 1967.
62. Wasserman, L.A., Belief functions and statistical inference, *The Canadian Journal of Statistics*, 18, 183–196, 1990.
63. Halpern, J.Y. and Fagin, R., Two views of belief: belief as generalized probability and belief as evidence, *Artifical Intelligence*, 54, 275–317, 1992.
64. Yager, R.R., Kacprzyk, J., and Fedrizzi, M., Eds., *Advances in Dempster-Shafer Theory of Evidence*, John Wiley & Sons, New York, 1994.
65. Dong, W.-M. and Wong, F.S., From uncertainty to approximate reasoning. 1. Conceptual models and engineering interpretations, *Civil Engineering Systems*, 3, 143–154, 1986.
66. Dong, W.-M. and Wong, F.S., From uncertainty to approximate reasoning. 3. Reasoning with conditional rules, *Civil Engineering Systems*, 4, 45–53, 1987.
67. Lai, K.-L. and Ayyub, B.M., Generalized uncertainty in structural reliability assessment, *Civil Engineering Systems*, 11, 81–110, 1994.
68. Tonon, F. and Bernardini, A., A random set approach to the optimization of uncertain structures, *Computers & Structures*, 68, 583–600, 1998.
69. Tanaka, K. and Klir, G.J., A design condition for incorporating human judgement into monitoring systems, *Reliability Engineering and System Safety*, 65, 251–258, 1999.
70. Tonon, F., Bernardini, A., and Elishakoff, I., Concept of random sets as applied to the design of structures and analysis of expert opinions for aircraft crash, *Chaos, Solitons, & Fractals*, 10, 1855–1868, 1999.
71. Rakar, A., Juricic, D., and Ball, P., Transferable belief model in fault diagnosis, *Engineering Applications of Artificial Intelligence*, 12, 555–567, 1999.
72. Fetz, T., Oberguggenberger, M., and Pittschmann, S., Applications of possibility and evidence theory in civil engineering, *International Journal of Uncertainty*, 8, 295–309, 2000.
73. Oberkampf, W.L. and Helton, J.C., Investigation of evidence theory for engineering applications, *4th Nondeterministic Approaches Forum,* Denver, CO, AIAA-2002-1569, 2002.
74. Helton, J.C., Oberkampf, W.L., and Johnson, J.D., Competing failure risk analysis using evidence theory, *5th Nondeterministic Approaches Forum,* Norfolk, VA, AIAA-2003-1911, 2003.
75. Feller, W., *An Introduction to Probability Theory and Its Applications*, Vol. 2, John Wiley & Sons, New York, 1971.

Copyright 2005 by CRC Press LLC

76. Ash, R.B. and Doléans-Dade, C.A., *Probability and Measure Theory*, 2nd ed., Harcourt/Academic Press, New York, 2000.
77. Joslyn, C. and Kreinovich, V., Convergence properties of an interval probabilistic approach to system reliability estimation, *International Journal of General Systems*, in press.
78. McKay, M.D., Beckman, R.J., and Conover, W.J., A comparison of three methods for selecting values of input variables in the analysis of output from a computer code, *Technometrics*, 21, 239–245, 1979.
79. Iman, R.L., Uncertainty and sensitivity analysis for computer modeling applications, *Reliability Technology*, 28, 153–168, 1992.
80. Helton, J.C. and Davis, F.J., Latin hypercube sampling and the propagation of uncertainty in analyses of complex systems, *Reliability Engineering and System Safety*, 81, 23–69, 2003.
81. Luo, W.B. and Caselton, W., Using Dempster-Shafer theory to represent climate change uncertainties, *Journal of Environmental Management*, 49, 73–93, 1997.
82. Kacprzyk, J. and Fedrizzi, M., *Multiperson Decision Making Models Using Fuzzy Sets and Possibility Theory*, Kluwer Academic Publishers, Boston, 1990.
83. Abidi, M.A. and Gonzalez, R.C., *Data Fusion in Robotics and Machine Intelligence*, Academic Press, San Diego, 1992.
84. Goodman, I.R., Mahler, R.P.S., and Nguyen, H.T., *Mathematics of Data Fusion,* Kluwer Academic Publishers, Boston, 1997.
85. Goutsias, J., Mahler, R.P.S., and Nguyen, H.T., *Random Sets, Theory and Applications*, Springer, New York, 1997.
86. Slowinski, R., *Fuzzy Sets in Decision Analysis, Operations Research and Statistics*, Kluwer Academic Publishers, Boston, 1998.
87. Bouchon-Meunier, B., Aggregation and fusion of imperfect information, in *Studies in Fuzziness and Soft Computing*, J. Kacprzyk, Ed., Springer-Verlag, New York, 1998.
88. Ferson, S., Kreinovich, V., Ginzburg, L., Myers, D.S., and Sentz, K., Constructing probability boxes and Dempster-Shafer structures, Sandia National Laboratories, Albuquerque, NM, SAND2003-4015, 2003.
89. Sentz, K. and Ferson, S., Combination of evidence in Dempster-Shafer theory, Sandia National Laboratories, Albuquerque, NM, SAND2002-0835, 2002.

Copyright 2005 by CRC Press LLC

11

Info-Gap Decision Theory for Engineering Design: Or Why "Good" Is Preferable to "Best"

Yakov Ben-Haim
Technion–Israel Institute of Technology

11.1 Introduction and Overview

We call ourselves *Homo sapiens*, in part because we value our ability to optimize, but our sapience is not limited to the persistent pursuit of unattainable goals. Rather, what eons have taught the species is the lesson of balancing goals against the constraints of resources, knowledge, and ability. Indeed, the conjunction of reliability analysis and system design is motivated precisely by the need to balance idealized goals and realistic constraints.

The reliability analyst/system designer seeks to optimize the design, so the question is: What constitutes feasible optimization? First we must recognize that even our best models are wrong in ways we perhaps cannot even imagine. In addition, our most extensive data is incomplete and especially lacks evidence about surprises—catastrophes as well as windfalls—that impact the success and survival of the system. These model

Copyright 2005 by CRC Press LLC

and data deficiencies are information gaps (info gaps), or epistemic uncertainties. We will show that optimization of performance is always accompanied by minimization of robustness to epistemic uncertainty. That is, performance and robustness are antagonistic attributes and one must be traded off against the other. A performance-maximizing option will have less robustness against unmodeled information gaps than some suboptimal option, when both are evaluated against the same aspiration for performance. The conclusion is that the performance-suboptimal design is preferable over the performance-optimal design.

The principles just mentioned are explained with four examples in Sections 11.2 through 11.5. These sections can be read independently, although the examples supplement one another by emphasizing different applications, aspects of the problem, and methods of analysis. A theoretical framework is provided in Section 11.6.

Section 11.2 considers the design of the profile of a cantilever that is subjected to uncertain static loads. We first formulate a traditional design analysis, in the absence of uncertainty, which leads to a family of performance-optimal designs. These designs are Pareto-efficient trade-offs between minimizing the stress and minimizing the weight of the beam. We then show that these Pareto-efficient designs in fact have no immunity to info gaps in the load. Robustness to load uncertainty is obtained only by moving off the Pareto-optimal design surface. We also consider the windfall gains that can be garnered from load uncertainty, and examine the relation between robust and opportune designs.

Section 11.3 examines the maneuvering of a vibrating system whose impulse response function is incompletely known. The emphasis is not on control technology, but rather on modeling and managing unstructured info gaps in the design-base model of the system. We formulate a traditional performance optimization of the control input based on the best-available model. We demonstrate that this performance optimization has no immunity to the info gaps that plague the design-base dynamic model. This leads to the analysis of performance-suboptimal designs, which magnify the immunity to uncertainty in the dynamic behavior of the system. A simple numerical example shows that quite large robustness can be achieved with suboptimal designs, while satisficing the performance (making the performance good enough) at levels not too much less than the performance optimum.

Section 11.4 differs from the previous engineering design examples and considers the process of updating the parameters of a system model, based on data, when the basic structure of the model is inaccurate. The case examined is the impact of unmodeled quadratic nonlinearities. We begin by formulating a standard model updating procedure based on maximizing the fidelity between the model and the data. We then show that the result of this procedure has no robustness to the structural deficiencies of the model. We demonstrate, through a simple numerical example, that fidelity-suboptimal models can achieve substantial robustness to model structure errors, while satisficing the fidelity at levels not too far below the fidelity optimum.

Section 11.5 considers hybrid uncertainty: a combination of epistemic info-gaps and explicit (although imprecise) probability densities. A go/no-go decision is to be made based on the evaluation of the probability of failure. This evaluation is based on the best available probability density function. However, this probability density is recognized as imperfect, which constitutes the info-gap that beleaguers the go/no-go decision. An info-gap analysis is used to address the question: How reliable is the probabilistic go/no-go decision, with respect to the unknown error in the probability density? In short, the info-gap robustness analysis supervises the probabilistic decision.

The examples in Sections 11.2 through 11.4 illustrate the assertion that performance optimization will lead inevitably to minimization of immunity to information gaps. This suggests that performance should be satisficed—made adequate but not optimal—and that robustness should be optimized. Section 11.6 provides a rigorous theoretical basis for these conclusions.

11.2 Design of a Cantilever with Uncertain Load

In this section we formulate a simple design problem and solve it by finding the design that optimizes a performance criterion. We then show that this solution has no robustness to uncertainty: infinitesimal deviations (of the load, in this example) can cause violation of the design criterion. This will illustrate the

Copyright 2005 by CRC Press LLC

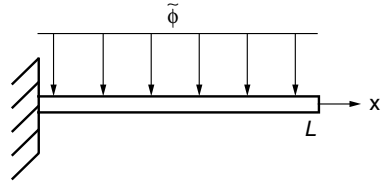

FIGURE 11.1 Cantilever with uniform load.

general conclusion (to be proven later) that optimizing the performance in fact minimizes the robustness to uncertainty. Stated differently, we observe that a designer's aspiration for high performance must be accompanied by the designer's acceptance of low robustness to failure. Conversely, feasible solutions will entail suboptimal performance. Again stated differently, the designer faces an irrevocable trade-off between performance and robustness to failure: demand for high performance is vulnerable to uncertainty; modest performance requirements are more immune to uncertainty.

11.2.1 Performance Optimization

Consider a uniform cantilever of length L [m] subject to a continuous uniform load density $\tilde{\phi}$ [N/m] applied in a single plane perpendicular to the beam axis, as in Figure 11.1. The beam is rectangular in cross section. The beam width, w [m], is uniform along the length and determined by prior constraints, but the thickness in the load plane, $T(x)$ [m], may be chosen by the designer to vary along the beam. The beam is homogeneous and its density is known. The designer wishes to choose the thickness profile to minimize the mass of the beam and also to minimize the maximum absolute bending stress in the beam. These two optimization criteria for selecting the thickness profile $T(x)$ are:

$$\min_{T(x)>0} \int_0^L T(x)dx \tag{11.1}$$

$$\min_{T(x)>0} \max_{0\le x\le L} |\sigma_T(x)| \tag{11.2}$$

where $\sigma_T(x)$ is the maximum bending stress in the beam section at x. The positivity constraint on $T(x)$ arises because the thickness must be positive at every point, otherwise the "beam" is not a beam.

These two design criteria are in conflict, so a trade-off between mass and stress minimization will be needed. To handle this, we will solve the stress minimization with the mass constrained to a fixed value. We then vary the beam mass. Consider the following set of thickness profiles corresponding to fixed mass:

$$\Theta(\theta) = \left\{ T(x): \int_0^L T(x)dx = \theta \right\} \tag{11.3}$$

For any given value of θ, which determines the beam mass, we choose the thickness profile from $\Theta(\theta)$ to minimize the maximum stress. The performance criterion by which a design proposal $T(x)$ is evaluated is:

$$R(T) = \max_{0\le x\le L} |\sigma_T(x)| \tag{11.4}$$

The design that optimizes the performance from among the beams in $\Theta(\theta)$, which we denote $\hat{T}_\theta(x)$, is implicitly defined by:

$$R(\hat{T}_\theta) = \min_{T(x)\in\Theta(\theta)} \max_{0\le x\le L} |\sigma_T(x)| \tag{11.5}$$

Copyright 2005 by CRC Press LLC

From the small-deflection static analysis of a beam with thickness profile $T(x)$, one finds the magnitude of the maximum absolute bending stress at section x to be:

$$|\sigma_T(x)| = \frac{3\tilde{\phi}(L-x)^2}{wT^2(x)}[\text{Pa}] \tag{11.6}$$

where $x = 0$ at the clamped end of the beam.

In light of the integral constraint on the thickness profile, $T(x) \in \Theta(\theta)$ in Equation 11.3, and of the demand for optimal performance, Equation 11.5, we find that the optimal design makes the stress uniform along the beam and as small as possible. The optimal profile is a linear taper:

$$\hat{T}_\theta(x) = \frac{2\theta(L-x)}{L^2}[\text{m}] \tag{11.7}$$

The performance obtained by this design is:

$$R(\hat{T}_\theta) = \frac{3\tilde{\phi}L^4}{4w\theta^2}[\text{Pa}] \tag{11.8}$$

To understand Equation 11.7, we note from Equation 11.6 that the linear taper is the only thickness profile that achieves the same maximum stress at all sections along the beam. From Equation 11.6 we know that we could reduce the stress in some regions of the beam by increasing the thickness profile in those regions. However, the mass-constraint, Equation 11.3, would force a lower thickness elsewhere, and in those other regions the stress would be augmented. Because the performance requirement is to minimize the maximal stress along the beam, the uniform stress profile is the stress-minimizing solution at this beam mass. Equation 11.8, the performance obtained by this optimal design, is the value of the stress in Equation 11.6 with the optimal taper of Equation 11.7.

We can think of Equation 11.8 as a curve, $R(\hat{T}_\theta)$ vs. θ, representing the trade-off between minimal stress and minimal mass, as shown in Figure 11.2. As the beam mass, θ, is reduced, the least possible maximum stress, $R(\hat{T}_\theta)$, increases. Every point along this curve is optimal in the Pareto sense that either of the design criteria—mass or stress minimization—can be improved only by detracting from the other criterion.

Consider a point P on this optimal design curve, corresponding to the min-max stress σ_1 of a beam of mass θ_1. That is, $\sigma_1 = R(\hat{T}_{\theta_1})$. Let Q be a point to the right of P. Q represents beams whose mass is $\theta_2 > \theta_1$ and whose min-max stress is still only σ_1. These beams are suboptimal: at this min-max stress, they have excessive mass. Alternatively, consider the point R lying above P, which represents beams of

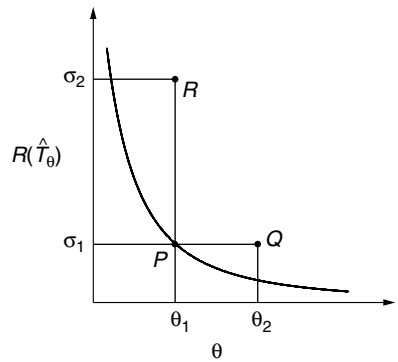

FIGURE 11.2 Optimal (min-max) stress $R(\hat{T}_\theta)$ vs. mass-parameter θ, Equation 11.8.

Copyright 2005 by CRC Press LLC

mass θ_1 whose min-max stress exceeds the optimum for this mass: $\sigma_2 > R(\hat{T}_{\theta_1})$. This again is suboptimal. We can interpret any suboptimal beam as either mass excessive for its min-max stress, or stress excessive for its mass. Finally, because the curve is a Pareto frontier, there are no beams corresponding to points below the curve.

11.2.2 Robustness to Uncertain Load

Now we depart from the performance optimization analysis described above. Any designer wants better performance rather than worse, but aspirations are tempered by the need for feasibility, the need for reliable design. We now consider the very common situation in which the load profile is uncertain and, in response, we will develop a *robust satisficing* design strategy. We are particularly interested in the relation between the optimal design under this strategy, and the performance-maximizing design described in Section 11.2.1.

The designer will choose a thickness profile, $T(x)$, which *satisfices* the aspiration for good performance, that is, which attempts to guarantee that the maximum stress is no greater than a specified level, for a given beam mass. Satisficing is not an optimization, so an element of design freedom still remains. The designer then uses this degree of freedom to maximize the immunity to error in the design-base load. The design specification is *satisficed,* while the robustness to failure is *maximized.*

To implement this we first define an info-gap model of uncertainty and then define the robustness function.

Let $\phi(x)$ [N/m] represent the unknown actual load-density profile, and let $\check{\phi}(x)$ denote the designer's best estimate of $\phi(x)$. For example, the nominal estimate may be the constant load density used in Section 11.2.1. Let $\mathcal{U}(\alpha,\check{\phi})$ be a set of load profiles $\phi(x)$, containing the nominal estimate $\check{\phi}(x)$. An *info-gap model* for the designer's uncertainty about $\phi(x)$ is a *family of nested sets* $\mathcal{U}(\alpha,\check{\phi})$, $\alpha \geq 0$. As α grows, the sets become more inclusive:

$$\alpha \leq \alpha' \quad \text{implies} \quad \mathcal{U}(\alpha,\tilde{\phi}) \subseteq \mathcal{U}(\alpha',\tilde{\phi}) \tag{11.9}$$

Also, the nominal load belongs to all the sets in the family:

$$\check{\phi}(x) \in \mathcal{U}(\alpha,\check{\phi}) \quad \text{for all} \quad \alpha \geq 0 \tag{11.10}$$

The nesting of the uncertainty-sets imbues α with its meaning as a ***horizon of uncertainty.*** A large α entails great variability of the potential load profiles $\phi(x)$ around the nominal estimate $\check{\phi}(x)$. Because α is unbounded ($\alpha \geq 0$), the family of uncertainty sets is likewise unbounded. This means that we cannot identify a worst case, and the subsequent analysis is *not* a worst-case analysis in the ordinary sense, and does *not* entail a min-max as in Equation 11.5. We will see an example of an info-gap model of uncertainty shortly. Info-gap models may obey additional axioms as well [1].

Now we define the *info-gap robustness function.* The designer's aspiration (or requirement) for performance is that the bending stress not exceed the critical value σ_c anywhere along the beam of specified mass. That is, the condition $\sigma(x) \leq \sigma_c$ is needed for "survival"; better performance ($\sigma(x) \ll \sigma_c$) is desirable but is not a design requirement. The designer will choose the critical stress σ_c as small as necessary, but no smaller than needed. The designer attempts to satisfy the design specification with the choice of the thickness profile $T(x)$ from the set $\Theta(\theta)$ in Equation 11.3, but because the actual load profile $\phi(x)$ is unknown when $T(x)$ is chosen, the maximum bending stress is also unknown. The *robustness* of thickness profile $T(x)$ is the greatest horizon of uncertainty, α, at which the maximum stress is guaranteed to be no greater than the design requirement:

$$\hat{\alpha}(T,\sigma_c) = \max\left\{\alpha: \max_{\phi \in \mathcal{U}(\alpha,\check{\phi})} \rho(T,\phi) \leq \sigma_c\right\} \tag{11.11}$$

Copyright 2005 by CRC Press LLC

where:

$$\rho(T, \phi) = \max_{0 \le x \le L} |\sigma_{\phi,T}(x)| \tag{11.12}$$

which is the analog of Equation 11.4 for the current case of unknown load profile. $\sigma_{\phi,T}(x)$ denotes the maximum stress in the beam section at x, given load profile $\phi(x)$ and thickness profile $T(x)$.

We can 'read' Equation 11.11 from left to right: The robustness $\hat{\alpha}(T, \sigma_c)$ of thickness profile $T(x)$, given design specification (or aspiration) σ_c, is the maximum horizon of uncertainty α such that the worst performance $\rho(T(x), \phi(x))$, for any realization $\phi(x)$ of the actual load profile up to α is no greater than σ_c. This is a worst-case-up-to-α analysis, but because α is unknown, what we are doing is determining the greatest α that does not allow failure.

More robustness to failure is better than less, provided the design requirements are satisfied. An info-gap robust-optimal design is an allowed thickness profile, $\hat{T}_\theta(x) \in \Theta(\theta)$, which maximizes the robustness while also satisficing the performance:

$$\hat{\alpha}(\hat{T}_\theta, \sigma_c) = \max_{T \in \Theta(\theta)} \hat{\alpha}(T, \sigma_c) \tag{11.13}$$

This is the info-gap analog of the optimal design criterion in Equation 11.5. Note that, unlike Equation 11.5, we are not minimizing the maximum stress. Rather, we are maximizing the robustness to uncertainty; the stress-requirement is satisficed to σ_c by the robustness function $\hat{\alpha}(T, \sigma_c)$.

Let us consider a concrete example. Suppose that the known nominal load density is the constant non-negative value $\tilde{\phi}$, and that we are also aware that the actual load profile $\phi(x)$ may deviate from $\tilde{\phi}$, but we have no information about this deviation. One representation of this load uncertainty is the envelope-bound info-gap model, which is the following family of nested sets of load profiles:

$$\mathcal{U}(\alpha, \tilde{\phi}) = \{\phi(x): |\phi(x) - \tilde{\phi}| \le \alpha\}, \quad \alpha \ge 0 \tag{11.14}$$

$\mathcal{U}(\alpha, \tilde{\phi})$ is the set of load profiles whose deviation from the nominal profile is bounded by α. Because the horizon of uncertainty, α, is unbounded, we have an unbounded family of nested sets of load profiles. Note that $\mathcal{U}(\alpha, \tilde{\phi})$ satisfies the nesting and inclusion properties of Equation 11.9 and Equation 11.10.

The maximum absolute stress in the beam section at x, $|\sigma_{\phi,T}(x)|$, given load profile $\phi(x)$ and thickness profile $T(x)$, is found to be:

$$|\sigma_{\phi,T}(x)| = \frac{6}{wT^2(x)} \int_x^L (v - x)\phi(v)\, dv \tag{11.15}$$

Employing this relation with Equation 11.12 in Equation 11.11 yields, after some manipulation, the following expression for the robustness of thickness profile $T(x)$ with design specification σ_c:

$$\hat{\alpha}(T, \sigma_c) = \frac{w\sigma_c/3}{\max_{0 \le x \le L} \left(\frac{L - x}{T(x)} \right)^2} - \tilde{\phi} \tag{11.16}$$

provided this expression is positive. A negative value arises if the maximum stress in response to the nominal load exceeds the design requirement, σ_c. A negative value means that, even without uncertainty, the design requirement cannot be achieved. In this case, the robustness to uncertainty vanishes and we define $\hat{\alpha}(T, \sigma_c) = 0$.

Copyright 2005 by CRC Press LLC

11.2.3 Info-Gap Robust-Optimal Design: Clash with Performance-Optimal Design

We now discuss the robustness-maximizing design, $\hat{T}_\theta(x)$ in Equation 11.13. We will find the beam-shape that maximizes the robustness for any choice of the stress-requirement σ_c. Significantly, this beam-shape will be the linear taper that maximizes the performance. However, we will find that when σ_c is chosen on the Pareto-optimal curve, the robustness of this linear taper is precisely zero. That is, performance optimization entails robustness minimization. This motivates the choice of performance suboptimal designs as the only way to obtain positive robustness to uncertainty.

Consider beams of mass θ whose maximum bending stress is no greater than σ_c. We are considering *any* σ_c, so (θ, σ_c) is not necessarily Pareto-optimal and does not necessarily fall on the optimal-design curve of Figure 11.2. From examination of Equation 11.16 we find that the thickness profile in the allowed-mass set $\Theta(\theta)$ that maximizes the robustness and satisfices the stress (at stress requirement σ_c) is precisely the profile which maximizes the performance: the linear taper $\hat{T}_\theta(x)$ in Equation 11.7. With this robustness-maximizing thickness profile, the robustness in Equation 11.16 becomes:

$$\hat{\alpha}(\hat{T}_\theta, \sigma_c) = \frac{4w\theta^2\sigma_c}{3L^4} - \tilde{\phi} \tag{11.17}$$

Figure 11.3 illustrates this optimal robustness vs. the maximum-stress design requirement, σ_c.

Figure 11.3 demonstrates one of the most important universal properties of the robustness function: robustness decreases monotonically as the performance requirement becomes more stringent. A small value of σ_c is a demanding specification, while a large value of σ_c is more lenient. A modest stress requirement will be quite robust, while a demanding design will be prone to failure. The value of σ_c at which the robustness becomes zero is denoted in Figure 11.3 by σ^*. This is such an exacting requirement that even infinitesimal deviations of the actual load profile from the nominal profile may entail violation of the design requirement. Clearly, choosing the requirement $\sigma_c = \sigma^*$ is infeasible and unrealistic because σ_c is defined as a stress level that must not be exceeded.

The value of σ^* is obtained by equating $\hat{\alpha}(\hat{T}_\theta, \sigma_c)$, in Equation 11.17, to zero and solving for σ_c. The result is:

$$\sigma^* = \frac{3\tilde{\phi}L^4}{4w\theta^2}[\text{Pa}] \tag{11.18}$$

which is precisely the minimal stress obtained by the performance-optimizing design, Equation 11.8. We see here an instance of another general phenomenon of great importance: a design that *optimizes the*

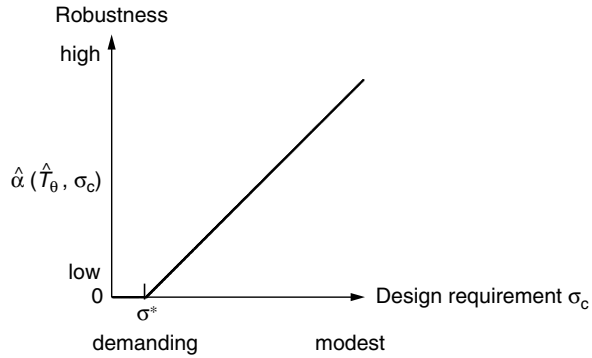

FIGURE 11.3 Optimal robustness curve, $\hat{\alpha}(\hat{T}_\theta, \sigma_c)$, vs. the maximum-stress design requirement σ_c, Equation 11.17.

Copyright 2005 by CRC Press LLC

performance (as in Section 11.2.1) also *minimizes the robustness*. That is, the locus of (θ,σ) values on the optimal-design curve of Figure 11.2 coincides with the zero-robustness points $(\sigma^*,0)$ in Figure 11.3. A point with positive robustness on the curve in Figure 11.3 ($\hat{\alpha}(\hat{T}_\theta,\sigma_2)>0$) corresponds to a point *above* the Pareto-optimal curve like *R* on Figure 11.2 for which $\sigma_2>\sigma(\theta)$. Performance optimization leads to the least feasible of all realizable designs. The designer is therefore strongly motivated to *satisfice the performance and maximize the robustness,* as we have done in this section. We explore this further in the next subsection.

11.2.4 Resolving the Clash

We will seek a thickness profile, $T^*(x)$, that has two properties:

1. The design has positive robustness to load-uncertainty, so that $\hat{\alpha}(T^*,\sigma_c)$ in Equation 11.16 is positive.
2. The design has suboptimal performance, so it is not on the optimal trade-off curve between mass and stress, Equation 11.8. This is necessary in order to enable positive robustness.

If the beam mass is constrained to $\Theta(\theta)$, then the min-max stress is given by Equation 11.8. Let us adopt this value, σ^* in Equation 11.18, as the design requirement. We know from our analysis in Section 11.2.3 that we must accept a beam-mass in excess of θ in order to satisfice this stress requirement with positive robustness. That is, following our discussion of Equation 11.8 and Figure 11.2, we must choose a design point to the right of the optimum-performance design curve, such as point *Q* in Figure 11.2.

From Equation 11.16, the condition for positive robustness is:

$$\frac{w\sigma^*/3}{\max\limits_{0\le x\le L}\left(\dfrac{L-x}{T(x)}\right)^2}>\tilde{\phi} \tag{11.19}$$

When $T(x)$ is the performance-optimal linear taper, $\hat{T}_\theta(x)$ of Equation 11.7, and σ^* is given by Equation 11.18, we obtain equality in Equation 11.19 and hence zero robustness, so we must choose the thickness profile so that:

$$T(x)\ge\frac{2\theta(L-x)}{L^2}=\hat{T}_\theta(x) \tag{11.20}$$

with strict inequality over at least part of the beam. There are many available solutions; we consider one simple class of solutions:

$$T^*(x)=\hat{T}_\theta(x)+\gamma \tag{11.21}$$

where $\gamma\ge 0$. From Equation 11.16, the robustness of this profile is:

$$\hat{\alpha}(T^*,\sigma^*)=\frac{w\sigma^*}{3L^2}\left(\frac{2\theta}{L}+\gamma\right)^2-\tilde{\phi} \tag{11.22}$$

With σ^* from Equation 11.18, this robustness becomes:

$$\hat{\alpha}(T^*,\sigma^*)=\frac{\tilde{\phi}L^2}{4\theta^2}\left(\frac{2\theta}{L}+\gamma\right)^2-\tilde{\phi} \tag{11.23}$$

whose positivity is controlled by γ, which also controls the extent of deviation of T^* from the performance-optimum solution $\hat{T}_\theta$. When γ is zero, the beam shape lies on the performance-optimal curve,

Copyright 2005 by CRC Press LLC

Equation 11.8: it has minimal mass for the stress requirement σ_c. However, at $\gamma = 0$, the robustness to load uncertainty is zero. As γ becomes larger, the robustness increases but the beam also becomes more mass-excessive.

In Equation 11.20 through Equation 11.23 we have derived a performance-suboptimal design that has positive robustness. This design is formulated as a point Q to the right of the performance-optimal curve in Figure 11.2: we have increased the mass while holding the stress requirement fixed. Another approach to defining designs that are performance-suboptimal and yet have positive robustness is to seek points R that are above the curve. Positive robustness is obtained if the inequality in Equation 11.19 is satisfied. This can be obtained with the linear beam shape of Equation 11.7, and with a stress requirement σ_c in excess of the minimal (optimal) stress for this beam mass given by σ^* in Equation 11.18 (or equivalently by $R(\hat{T}_\theta)$ in Equation 11.8). One way to understand this alternative approach is in terms of the relation between points P and R in Figure 11.2. The mass-optimal linear taper is used, Equation 11.7 with θ_1, but the aspiration for stress performance is weakened: rather than adopting the optimal-stress requirement (σ_1 in Figure 11.2), the designer adopts a less demanding stress requirement (σ_2 in Figure 11.2).

The added beam thickness, γ in Equation 11.21, can be thought of as a safety factor.[1] The designer who proceeded according to the performance-optimization procedure of Section 11.2.1 may add the thickness γ as an ad hoc protection. However, Equation 11.23 enables one to evaluate this deviation from the optimum-performance design in terms of the robustness to uncertainty that it entails. The robustness, $\hat{\alpha}(T^*, \sigma^*)$ in Equation 11.23, is the greatest value of the uncertainty parameter, α in the info-gap model of Equation 11.14, which does not allow the maximum bending stress to exceed $\sigma^*(\theta)$ of Equation 11.18. $\hat{\alpha}$ is the interval of load-amplitude within which the actual load profile, $\phi(x)$, may deviate from the design-base nominal load profile, $\tilde{\phi}$, without exceeding the stress requirement. Suppose the designer desires that the robustness, $\hat{\alpha}$, be equal to a fraction f of the nominal load: $\hat{\alpha} = f\tilde{\phi}$. The thickness safety factor that is needed is obtained by inverting Equation 11.23 to obtain:

$$\gamma = \frac{2\theta}{L}(\sqrt{1+f} - 1) \tag{11.24}$$

$f = 0$ means that no robustness is needed, and this causes $\gamma = 0$, meaning that the optimal performance design, $\hat{T}_\theta$, is obtained. f is increased to represent greater demanded robustness to uncertainty, causing the safety factor, γ, to increase from zero.

11.2.5 Opportunity from Uncertain Load

In Section 11.2.2 we defined the robustness function: $\hat{\alpha}(T, \sigma_c)$ is the greatest horizon of uncertainty that design $T(x)$ can tolerate without failure, when σ_c is the maximum allowed stress. The robustness function addresses the adverse aspect of load uncertainty. It evaluates the immunity to failure, which is why a large value of robustness is preferred to a small value, when the stress limit is fixed.

In this section we explore the idea that uncertainty may be propitious: unknown contingencies may be favorable. The "opportunity function" that we will formulate is also an immunity function: it assesses the immunity against highly desirable windfall outcomes. Because the opportunity function is the immunity against sweeping success, a small value is preferred over a large value. Each immunity function — robustness and opportunity — generates its own preference ranking on the set of available designs. We will see that, in general, these rankings may or may not agree.

As before, σ_c is the greatest acceptable bending stress. Let σ_w be a smaller stress that, if not exceeded at any point along the beam, would be a desirable *windfall* outcome. It is not necessary that the stress be as small as σ_w, but this would be viewed very favorably. The nominal load produces a maximum bending stress that is greater than σ_w. However, favorable fluctuations of the load could produce a

[1] The author is indebted to Prof. Eli Altus, of the Technion, for suggesting this interpretation.

Copyright 2005 by CRC Press LLC

maximum bending stress as low as σ_w. The *opportunity function* is the lowest horizon of uncertainty at which the maximum bending stress at any section of the beam can be as low as σ_w:

$$\hat{\beta}(T, \sigma_w) = \min\left\{\alpha: \min_{\phi \in \mathcal{U}(\alpha, \tilde{\phi})} \rho(T, \phi) \le \sigma_w\right\} \tag{11.25}$$

where $\rho(T, \phi)$ is the maximum absolute bending stress occurring in the beam, specified in Equation 11.12. $\hat{\beta}(T, \sigma_w)$ is the lowest horizon of uncertainty that must be accepted in order to enable maximum stress as low as σ_w. $\hat{\beta}(T, \sigma_w)$ is the immunity to windfall: a small value implies that windfall performance is possible (although not guaranteed) even at low levels of uncertainty. The opportunity function is the dual of the robustness function in Equation 11.11.

Employing Equation 11.12 we can write the opportunity function more explicitly as:

$$\hat{\beta}(T, \sigma_w) = \min\left\{\alpha: \min_{\phi \in \mathcal{U}(\alpha, \tilde{\phi})} \max_{0 \le x \le L} |\sigma_{\phi,T}(x)| \le \sigma_w\right\} \tag{11.26}$$

The evaluation of the opportunity function requires a bit of caution because, in general, the order of the inner "min" and "max" operators cannot be reversed. In the current example, however, a simplification occurs.

Let us define a constant load profile, $\phi^* = \tilde{\phi} - \alpha$, that belongs to $\mathcal{U}(\alpha, \tilde{\phi})$ for all $\alpha \ge 0$. One can readily show that this load profile minimizes the maximum stress at all sections, *x*. That is:

$$|\sigma_{\phi^*, T}(x)| = \min_{\phi \in \mathcal{U}(\alpha, \tilde{\phi})} |\sigma_{\phi,T}(x)| \tag{11.27}$$

Because this minimizing load profile, ϕ^*, is the same for all positions *x*, we can reverse the order of the operators in Equation 11.26 as:

$$\min_{\phi \in \mathcal{U}(\alpha, \tilde{\phi})} \max_{0 \le x \le L} |\sigma_{\phi,T}(x)| = \max_{0 \le x \le L} \min_{\phi \in \mathcal{U}(\alpha, \tilde{\phi})} |\sigma_{\phi,T}(x)| \tag{11.28}$$

$$= \max_{0 \le x \le L} |\sigma_{\phi^*, T}(x)| \tag{11.29}$$

$$= \max_{0 \le x \le L} \frac{3(\tilde{\phi} - \alpha)(L - x)^2}{wT^2(x)} \tag{11.30}$$

The opportunity function is the smallest horizon of uncertainty, α, for which the right-hand side of Equation 11.30 is no greater than σ_w. Equating this expression to σ_w and solving for α yields the opportunity for design $T(x)$ with windfall aspiration σ_w:

$$\hat{\beta}(T, \sigma_w) = \tilde{\phi} - \frac{w\sigma_w/3}{\max_{0 \le x \le L}\left(\frac{L - x}{T(x)}\right)^2} \tag{11.31}$$

This expression is nonnegative unless the right-hand side of Equation 11.30 is less than σ_w at $\alpha = 0$, which occurs if and only if the nominal load entails maximal stress less than σ_w; in this case we define $\hat{\beta}(T, \sigma_w) = 0$.

We have already mentioned that each immunity function—robustness and opportunity—generates its own preference ranking of available designs. Because "bigger is better" for the robustness function, we will prefer T over T' if the former design is more robust than the latter. Concisely:

$$T \succ_r T' \quad \text{if} \quad \hat{\alpha}(T, \sigma_c) > \hat{\alpha}(T', \sigma_c) \tag{11.32}$$

Copyright 2005 by CRC Press LLC

The opportunity function is the immunity against windfall performance, so "big is bad." This means that we will prefer T over T' if the former design is more opportune than the latter:

$$T \succ_{\text{o}} T' \quad \text{if} \quad \hat{\beta}(T, \sigma_w) < \hat{\beta}(T', \sigma_w) \tag{11.33}$$

The generic definitions of the immunity functions do not imply that the preference-rankings in Equation 11.32 and Equation 11.33 agree. The immunity functions are said to be *sympathetic* when their preference rankings agree; they are *antagonistic* otherwise. Both situations are possible. In the present example, the immunities are sympathetic, as we see by combining Equation 11.16 and Equation 11.31 as:

$$\hat{\beta}(T, \sigma_w) = \underbrace{-\frac{\sigma_w}{\sigma_c}\hat{\alpha}(T, \sigma_c)}_{A} + \underbrace{\left(1 - \frac{\sigma_w}{\sigma_c}\right)\tilde{\phi}}_{B} \tag{11.34}$$

Expression "B" does not depend upon the design, $T(x)$, and expression "A" is nonnegative. Consequently, any change in the design that causes $\hat{\alpha}$ to increase (that is, robustness improves) causes $\hat{\beta}$ to decrease (which improves opportunity). Likewise, robustness and opportunity deteriorate together. These immunity functions are sympathetic for any possible design change, although they do not necessarily improve at the same rate; marginal changes may be greater for one than for the other.

In general, robustness and opportunity functions are not necessarily sympathetic. Their sympathy in the current example is guaranteed because B in Equation 11.34 is independent of the design. This need not be the case. If B increases due to a design-change which causes $\hat{\alpha}$ to increase, the net effect may be an increase in $\hat{\beta}$, which constitutes a decrease in opportunity. For an example, see [1, p. 52].

11.3 Maneuvering a Vibrating System with Uncertain Dynamics

In Section 11.2 we considered the design and reliability analysis of a static system subject to uncertain loads. We now consider the analysis and control of a simple vibrating system whose dynamic equations are uncertain. That is, the best model is known to be wrong or incomplete in some poorly understood way, and an info-gap model represents the uncertainty in this system model. Despite the uncertainty in the system model, the designer must choose a driving function that efficiently "propels" the system as far as possible.

11.3.1 Model Uncertainty

Consider a one-dimensional linear system whose displacement $x(t)$ resulting from forcing function $q(t)$ is described by Duhamel's relation:

$$x(t; q, h) = \int_0^t q(\tau) h(t - \tau)\, d\tau \tag{11.35}$$

where $h(t)$ is the impulse response function (IRF).

The best available model for the IRF is denoted $\tilde{h}(t)$, which may differ substantially from $h(t)$ due to incomplete or inaccurate representation of pertinent mechanisms. For example, for the undamped linear harmonic oscillator:

$$\tilde{h}(t) = \frac{1}{m\omega} \sin \omega t \tag{11.36}$$

where m is the mass and ω is the natural frequency. This IRF is seriously deficient in the presence of damping, which is a complicated and incompletely understood phenomenon.

Copyright 2005 by CRC Press LLC

Let $\mathcal{U}(\alpha, \tilde{h})$ be an info-gap model for uncertainty in the IRF. That is, $\mathcal{U}(\alpha,\tilde{h})$, $\alpha \geq 0$, is a family of nested sets of IRFs, all containing the nominal best model, $\tilde{h}(t)$. That is:

$$\alpha < \alpha' \quad \text{implies} \quad \mathcal{U}(\alpha, \tilde{h}) \subset \mathcal{U}(\alpha', \tilde{h}) \tag{11.37}$$

and

$$\tilde{h}(t) \in \mathcal{U}(\alpha, \tilde{h}) \quad \text{for all} \quad \alpha \geq 0 \tag{11.38}$$

As an example we now construct a Fourier ellipsoid-bound info-gap model of uncertainty in the system dynamics. Actual IRFs are related to the nominal function by:

$$h(t) = \tilde{h}(t) + \sum_i c_i \sigma_i(t) \tag{11.39}$$

where the $\sigma_i(t)$ are known expansion functions (e.g., cosines, sines, polynomials, etc.) and the c_i are unknown expansion coefficients. Let c and $\sigma(t)$ denote the vectors of expansion coefficients and expansion functions, respectively, so that Equation 11.39 becomes:

$$h(t) = \tilde{h}(t) + c^T \sigma(t) \tag{11.40}$$

A Fourier ellipsoid-bound info-gap model for uncertainty in the IRF is a family of nested ellipsoids of coefficient vectors:

$$\mathcal{U}(\alpha, \tilde{h}) = \{h(t) = \tilde{h}(t) + c^T \sigma(t) : c^T V c \leq \alpha^2\}, \quad \alpha \geq 0 \tag{11.41}$$

where V is a known, real, symmetric, positive definite matrix that determines the shape of the ellipsoids of c-vectors. V is based on fragmentary information about the dispersion of the expansion coefficients. The size of each ellipsoid is determined by the (unknown) horizon-of-uncertainty parameter α.

11.3.2 Performance Optimization with the Best Model

We now consider the performance-optimal design of the driving function $q(t)$ based on the model $\tilde{h}(t)$ of Equation 11.36, which is, for the purpose of this example, the best-known IRF of the system. The goal of the design is to choose the forcing function $q(t)$ to achieve large displacement $x(T; q, \tilde{h})$ at specified time T with low control effort $\int_0^T q^2(t)dt$. Specifically, we would like to select $q(t)$ so as to achieve an optimal balance between the following two conflicting objectives:

$$\max_{q(t)} x(T; q, \tilde{h}) \tag{11.42}$$

$$\min_{q(t)} \int_0^T q^2(t)\, dt \tag{11.43}$$

Let $\mathcal{Q}(E)$ denote the set of all control functions $q(t)$ whose control effort equals E:

$$\mathcal{Q}(E) = \left\{ q(t) : E = \int_0^T q^2(t) dt \right\} \tag{11.44}$$

Using the Schwarz inequality, one can readily show that the q-function in $\mathcal{Q}(E)$ that maximizes the displacement $x(T;q,\tilde{h})$ at time T is:

$$q_E^*(t) = \frac{\sqrt{f_0 E}}{m\omega} \sin \omega(T-t) \tag{11.45}$$

Copyright 2005 by CRC Press LLC

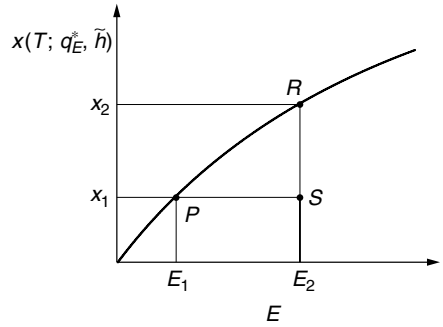

FIGURE 11.4 Maximal displacement $x(T; q_E^*, \tilde{h})$ vs. control effort E, Equation 11.47.

where:

$$f_0 = \frac{4m^2\omega^3}{2\omega T - \sin 2\omega T} \tag{11.46}$$

From this one finds that the greatest displacement at time T, obtainable with any control function in $\mathcal{Q}(E)$, is:

$$x(T; q_E^*, \tilde{h}) = \sqrt{\frac{E}{f_0}} \tag{11.47}$$

Equation 11.47 expresses the trade-off between control effort E and maximal displacement x: large displacement is obtained only at the expense of large effort, as shown in Figure 11.4. Like Figure 11.2, this relationship expresses the Pareto-optimal design options: any improvement in control effort (making E smaller) is obtained only by relinquishing displacement (making x smaller).

Points above the curve in Figure 11.4 are inaccessible: no design can realize those (E, x) combinations. Points on the curve are Pareto-optimal and points below the curve are suboptimal designs. For example, point P on the curve is Pareto-optimal: E_1 is the lowest control effort that can achieve displacement as large as x_1. Point S is suboptimal and represents excessive control effort $(E_2 > E_1)$ to achieve displacement x_1. Likewise, point R is Pareto-optimal: x_2 is the greatest displacement that can be attained with control effort E_2. So again, S is suboptimal: greater displacement $(x_2 > x_1)$ could be achieved with effort E_2.

11.3.3 Robustness Function

We now develop an expression for the robustness, of the displacement $x(T; q, h)$, to uncertainty in the system dynamics $h(t)$.

The first design goal, Equation 11.42, implies that a large value of displacement is needed. The second design goal, Equation 11.43, conflicts with the first and calls for small control effort. In Section 11.3.2 we found that performance optimization leads to a Pareto trade-off between these two criteria, expressed in Equation 11.47 and Figure 11.4. In this section, in light of the uncertainty in the IRF, we take a different approach. For any given control function $q(t)$, we "satisfice" the displacement by requiring that the displacement be at least as large as some specified and satisfactory value x_c. Because $x(T; q, h)$ depends on the unknown IRF, we cannot guarantee that the displacement will be satisfactory. However, we can answer the following question: for given forcing function $q(t)$, by how much can the best model $\tilde{h}(t)$ err without jeopardizing the achievement of adequate displacement? More specifically, given $q(t)$, what is the greatest horizon of uncertainty, α, up to which every model $h(t)$ causes the displacement to be at least as large as x_c? The answer to this question is the robustness function:

$$\hat{\alpha}(q, x_c) = \max\left\{\alpha: \min_{h \in \mathcal{U}(\alpha, \tilde{h})} x(T; q, h) \geq x_c\right\} \tag{11.48}$$

Copyright 2005 by CRC Press LLC

We can "read" this relation from left to right: the robustness $\hat{\alpha}(q, x_c)$ of control function $q(t)$ with displacement-aspiration x_c is the greatest horizon of uncertainty α such that every system-model $h(t)$ in $\mathcal{U}(\alpha, \tilde{h})$ causes the displacement $x(T; q, h)$ to be no less than x_c. If $\hat{\alpha}(q, x_c)$ is large, then the system is robust to model uncertainty and $q(t)$ can be relied upon to bring the system to at least x_c at time T. If $\hat{\alpha}(q, x_c)$ is small, then this driving function cannot be relied upon and the system is vulnerable to uncertainty in the dynamics.

Using Lagrange optimization, one can readily show that the smallest displacement, for any system model $h(t)$ up to uncertainty α, is:

$$\min_{h \in \mathcal{U}(\alpha, \tilde{h})} x(T; q, h) = x(T; q, \tilde{h}) - \alpha \sqrt{b^T V b} \tag{11.49}$$

where we have defined the following vector:

$$b = \int_0^T q(t) \sigma(T - t)\, dt \tag{11.50}$$

Equation 11.49 asserts that the least displacement, up to uncertainty α, is the nominal, best-model displacement $x(T; q, \tilde{h})$, decremented by the uncertainty term $\alpha \sqrt{b^T V b}$. If the nominal displacement falls short of the demanded displacement x_c, then uncertainty only makes things worse and the robustness to uncertainty is zero. If $x(T; q, \tilde{h})$ exceeds x_c, then the robustness is found by equating the right-hand side of Equation 11.49 to x_c and solving for α. That is, the robustness of driving function $q(t)$ is:

$$\hat{\alpha}(q, x_c) = \begin{cases} 0 & \text{if} \quad x(T; q, \tilde{h}) \le x_c \\ \dfrac{x(T; q, \tilde{h}) - x_c}{\sqrt{b^T V b}} & \text{else} \end{cases} \tag{11.51}$$

Equation 11.51 documents the trade-off between robustness, $\hat{\alpha}(q, x_c)$, and aspiration for performance, x_c, as shown in Figure 11.5. A large and demanding value of x_c is accompanied by a low value of immunity to model uncertainty, meaning that aspirations for large displacements are unreliable and infeasible. Modest requirements (small values of x_c) are more feasible because they have greater immunity to uncertainty. The value of x_c at which the robustness vanishes, x^* in the figure, is precisely the displacement predicted by the best model, $x(T; q, \tilde{h})$. That is:

$$\hat{\alpha}\left(q, x(T; q, \tilde{h})\right) = 0 \tag{11.52}$$

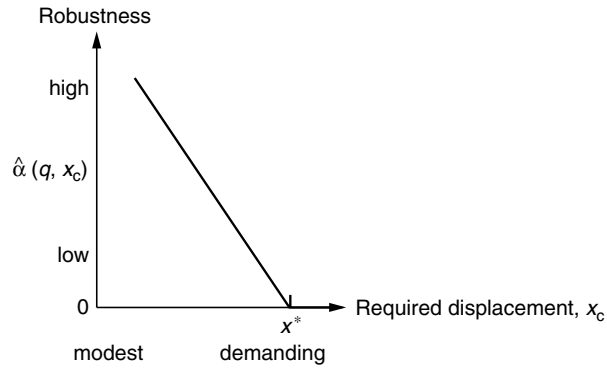

FIGURE 11.5 Robustness $\hat{\alpha}(q, x_c)$ vs. the demanded displacement x_c, Equation 11.51.

Copyright 2005 by CRC Press LLC

This means that, for *any* driving function $q(t)$, the displacement predicted by the best available model $\tilde{h}(t)$ cannot be relied upon to occur. Shortfall of the displacement may occur due to an infinitesimally small error of the model. Because this is true for any $q(t)$, it is also true for the performance-optimum control function $q_E^*(t)$ in Equation 11.45:

$$\hat{\alpha}(q_E^*, x(T; q_E^*, \tilde{h})) = 0 \tag{11.53}$$

While $q_E^*(t)$ is, according to $\tilde{h}(t)$, the most effective driving function of energy E, and while $x(T; q_E^*, \tilde{h})$ is, again according to $\tilde{h}(t)$, the resulting displacement, Equation 11.53 shows that this prediction has no immunity to modeling errors.

It is important to recognize that ordered pairs such as $(E, x(T; q_E^*, \tilde{h}))$ correspond to points such as P and R on the Pareto-optimal design surface in Figure 11.4. That is, E and $x(T; q_E^*, \tilde{h})$ are related by Equation 11.47. Hence, Equation 11.53 shows that all of the performance-optimal designs on the Pareto surface have no immunity to errors in the design-base model of the system. These Pareto-efficient designs are not feasible or reliable predictions of the system performance.

The conclusion from Equations 11.52 and 11.53 is likely to be that, because $x(T; q_E^*, \tilde{h})$ cannot be relied upon to occur, one must moderate one's aspirations and accept a lower value of displacement. The designer might "travel" up and to the left on the robustness curve in Figure 11.5 until finding a value of $x_c < x^*$ at which the robustness is satisfactorily large. But then the question arises: what driving function $q(t)$ *maximizes* the robustness at this selected aspiration for displacement? The optimization studied in Section 11.3.2 was optimization of *performance* (displacement and control effort). We now consider satisficing these quantities and optimizing the *robustness*. Specifically, for any displacement-aspiration x_c, the *robust-optimal* control function $\hat{q}_E(t)$ of energy E maximizes the robustness function:

$$\hat{\alpha}(\hat{q}_E, x_c) = \max_{q(t) \in \mathcal{Q}(E)} \hat{\alpha}(q, x_c) \tag{11.54}$$

This robust optimum may not always exist, or it may be inaccessible for practical reasons. In any case, one will tend to prefer more robust over less robust solutions. More specifically, if $q_1(t)$ is more robust than $q_2(t)$, while satisficing the performance at the same level x_c, then $q_1(t)$ is preferred over $q_2(t)$:

$$q_1(t) \succ q_2(t) \quad \text{if} \quad \hat{\alpha}(q_1, x_c) > \hat{\alpha}(q_2, x_c) \tag{11.55}$$

Relating this to our earlier discussion, suppose that E is an accessible control effort and that x_c is a satisfactory level of performance. For x_c to be feasible, it must be less than the best performance obtainable with effort E, namely, $x_c < x(t; q_E^*, \tilde{h})$. This assures that the robustness of the performance-optimal control function, $q_E^*(t)$, will be positive: $\hat{\alpha}(q_E^*, x_c) > 0$. However, we might well ask if there is some other control function in $\mathcal{Q}(E)$ whose robustness is even greater. This will often be the case, as we illustrate in the next subsection.

11.3.4 Example

To keep things simple, suppose that $\sigma(t)$ in the unknown part of the IRF in Equation 11.40 is a single, linearly decreasing function:

$$\sigma(t) = \eta(T - t) \tag{11.56}$$

where η is a positive constant. Thus, c is a scalar and the shape-matrix in the info-gap model of Equation 11.41 is simply $V = 1$.

The performance-optimal control function of effort E is $q_E^*(t)$ in Equation 11.45, which is a sine function at the natural frequency of the nominal IRF, $\tilde{h}(t)$. From Equation 11.51, the robustness of this

Copyright 2005 by CRC Press LLC

control function is:

$$\hat{\alpha}(q_E^*, x_c) = \frac{\frac{1}{m\omega}\int_0^T q_E^*(t)\sin\omega(T-t)dt - x_c}{\left|\eta\int_0^T q_E^*(t)(T-t)dt\right|} \tag{11.57}$$

Similarly, the robustness of any arbitrary control function $q(t)$ is:

$$\hat{\alpha}(q, x_c) = \frac{\frac{1}{m\omega}\int_0^T q(t)\sin\omega(T-t)dt - x_c}{\left|\eta\int_0^T q(t)(T-t)dt\right|} \tag{11.58}$$

(Presuming the numerator is positive.) In light of our discussion of Equation 11.55 we would like to find a control function $q(t)$ in $\mathcal{Q}(E)$ whose robustness is substantially greater than the robustness of $q_E^*(t)$.

We will illustrate that very substantial robustness benefits can be achieved by abandoning the performance-optimal function $q_E^*(t)$. We will not consider the general maximization of $\hat{\alpha}(q, x_c)$, but only a parametric case. Consider functions of the form:

$$q_\mu(t) = A\sin\mu(T-t) \tag{11.59}$$

where $0 < \mu < \omega$ and A is chosen to guarantee that $q(t)$ belongs to $\mathcal{Q}(E)$ (which was defined in Equation 11.44):

$$A = \sqrt{\frac{4\mu E}{2\mu T - \sin 2\mu T}} \tag{11.60}$$

For the special case that $\omega T = \pi$ the robustness functions of Equations 11.57 and 11.58 become:

$$\hat{\alpha}(q_E^*, x_c) = \frac{\pi\sqrt{\omega E} - \sqrt{2\pi}\, m\omega^2 x_c}{2m\eta\sqrt{\omega E}} \tag{11.61}$$

$$\hat{\alpha}(q_\mu, x_c) = \frac{A\mu^2\left(\frac{\sin[\pi(\mu-\omega)/\omega]}{2(\mu-\omega)} - \frac{\sin[\pi(\mu+\omega)/\omega]}{2(\mu+\omega)}\right) - m\omega\mu^2 x_c}{\eta m A[\omega\sin(\pi\mu/\omega) - \pi\mu\cos(\pi\mu/\omega)]} \tag{11.62}$$

Figure 11.6 shows the ratio of the robustnesses of the suboptimal to the performance-optimal control functions, vs. the frequency of the control function. The robustness at control frequencies μ much less than the nominal natural frequency ω, is substantially greater than the robustness of the performance-maximizing function. For example, at point P, $\mu = 0.2$ and the robustness ratio is $\hat{\alpha}(q_\mu, x_c)/\hat{\alpha}(q_E^*, x_c) = 4.0$, meaning that $q_\mu(t)$ can tolerate a horizon of model-uncertainty four times greater than the uncertainty that is tolerable for $q_E^*(t)$, when satisficing the displacement at x_c. $q_E^*(t)$ maximizes the displacement according to the best IRF, $\tilde{h}(t)$. However, this displacement optimization of the control function leaves little residual immunity to uncertainty in the IRF at this value of x_c. A control function such as $q_\mu(t)$, for $\mu < \omega$, belongs to $\mathcal{Q}(E)$, as does $q_E^*(t)$, but $q_\mu(t)$ is suboptimal with respect to displacement. That is, $x(T; q_\mu, \tilde{h}) < x(T; q_E^*, \tilde{h})$. However, because $q_\mu(t)$ is suboptimal, there are many functions with control effort E that cause displacement as large as $x(T; q_\mu, \tilde{h})$. In other words, there is additional design freedom with which to amplify the immunity to uncertainty. What Figure 11.6 shows is that large robustness-amplification can be achieved. This answers, by way of illustration, the question raised at the end of Section 11.3.3.

Copyright 2005 by CRC Press LLC

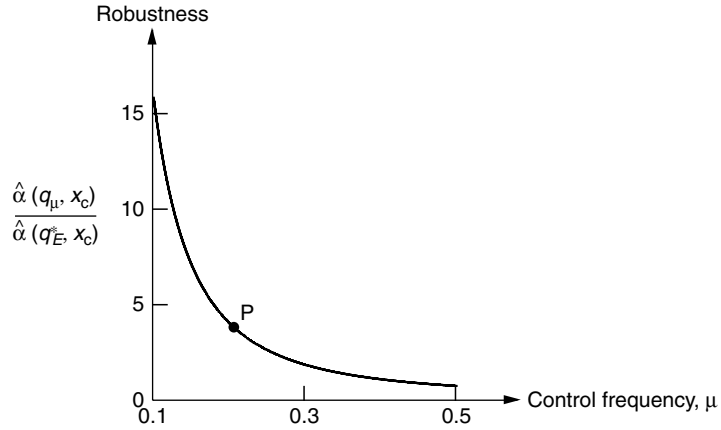

FIGURE 11.6 Ratio of the robustnesses of the suboptimal to performance-optimal control functions, vs. frequency of control function. $x_c = 0.5,\ \omega = E = \eta = m = 1.\ \hat{\alpha}(q_E^*, x_c) = 0.94$.

11.4 System Identification

A common task encountered by engineering analysts is the updating of a system-model, based on measurements. The question we consider in this section is, given that the structure of the model is imperfect, what constitutes optimal estimation of the parameters? More precisely, is it sound procedure to maximize the fidelity between the model and the measurements if the model structure is wrong (in unknown ways, of course)?

11.4.1 Optimal Identification

We begin by formulating a fairly typical framework for optimal identification of a model for predicting the behavior of a system. We then consider an example.

Let y_i be a vector of measurements of the system at time or state i, for $i = 1, \ldots, N$. Let $f_i(q)$ denote the model-prediction of the system in state i, which should match the measurements if the model is good. The vector q, containing real and linguistic variables, denotes the parameters and properties of the model that can be modified to bring the model into agreement with the measurements. We will denote the set of measurements by $Y = \{y_1, \ldots, y_N\}$ and the set of corresponding model-predictions by $F(q) = \{f_1(q), \ldots, f_N(q)\}$.

The overall performance of the predictor is assessed by a function $R[Y, F(q)]$. For example, this might be a mean-squared prediction error:

$$R[Y, F(q)] = \frac{1}{N} \sum_{i=1}^{N} \| f_i(q) - y_i \|^2 \tag{11.63}$$

A performance-optimal model, q^*, minimizes the performance-measure:

$$R[Y, F(q^*)] = \min_q R[Y, F(q)] \tag{11.64}$$

11.4.2 Uncertainty and Robustness

The model $f_i(q)$ is undoubtedly wrong, perhaps fundamentally flawed in its structure. There may be basic mechanisms that act on the system but which are not represented by $f_i(q)$. Let us denote more general

Copyright 2005 by CRC Press LLC

models, some of which may be more correct, by:

$$\phi_i = f_i(q) + u_i \tag{11.65}$$

where u_i represents the unknown corrections to the original model, $f_i(q)$. We have very little knowledge about u_i; if we had knowledge of u_i we would most likely include it in $f_i(q)$. So, let us use an info-gap model of uncertainty to represent the unknown variation of possible models:

$$\phi_i \in \mathcal{U}(\alpha, f_i(q)), \quad \alpha \geq 0 \tag{11.66}$$

The centerpoint of the info-gap model, $f_i(q)$, is the known model, parameterized by q. The horizon of uncertainty, α, is unknown. This info-gap model is a family of nested sets of models. These sets of models become ever more inclusive as the horizon of uncertainty increases. That is:

$$\alpha \leq \alpha' \quad \text{implies} \quad \mathcal{U}(\alpha, f_i(q)) \subset (\alpha', f_i(q)) \tag{11.67}$$

In addition, the update model is included in all of the uncertainty sets:

$$f_i(q) \in \mathcal{U}(\alpha, f_i(q)), \quad \text{for all} \quad \alpha \geq 0 \tag{11.68}$$

As before, the model prediction of the system output in state i is $f_i(q)$, and the set of model predictions is denoted $F(q) = \{f_1(q), \ldots, f_N(q)\}$. More generally, the set of model predictions with unknown terms $u_1, \ldots, u_N$ is denoted $F_u(q) = \{f_1(q) + u_1, \ldots, f_N(q) + u_N\}$.

We wish to choose a model, $f_i(q)$ for which the performance index, $R[Y, F_u(q)]$, is small. Let r_c represent an acceptably small value of this index. We would be willing, even delighted, if the prediction-error is smaller, but an error larger than r_c would be unacceptable.

The *robustness to model uncertainty,* of model q with error-aspiration r_c, is the greatest horizon of uncertainty, α, within which all models provide prediction error no greater than r_c:

$$\hat{\alpha}(q, r_c) = \max\left\{\alpha : \max_{\substack{\phi_i \in \mathcal{U}(\alpha, f_i(q)) \\ i=1,\ldots,N}} R[Y, F_u(q)] \leq r_c\right\} \tag{11.69}$$

When $\hat{\alpha}(q, r_c)$ is large, the model $f_i(q)$ may err fundamentally to a great degree, without jeopardizing the accuracy of its predictions; the model is robust to info gaps in its formulation. When $\hat{\alpha}(q, r_c)$ is small, then even small errors in the model result in unacceptably large prediction errors.

Let q^* be an optimal model, which minimizes the prediction error as defined in Equation 11.64, and let r_c^* be the corresponding optimal prediction error: $r_c^* = R(Y, F(q^*))$. Using model q^*, we can achieve prediction error as small as r_c^*, and no value of q can produce a model $f_i(q)$ that performs better. However, the robustness to model uncertainty, of this optimal model, is zero:

$$\hat{\alpha}(q^*, r_c^*) = 0 \tag{11.70}$$

This is a special case of the theorem to be discussed in Section 11.6 that, by optimizing the performance, one minimizes the robustness to info gaps. By optimizing the performance of the model predictor, $f_i(q)$, we make this predictor maximally sensitive to errors in the basic formulation of the model.

In fact, Equation 11.70 is a special case of the following proposition. For any q, let $r_c = R[Y, F(q)]$ be the prediction-error of model $f_i(q)$. The preliminary lemma in Section 11.6 shows that:

$$\hat{\alpha}(q, r_c) = 0 \tag{11.71}$$

Copyright 2005 by CRC Press LLC

That is, the robustness of *any* model, $f_i(q)$, to uncertainty in the structure of that model, is precisely equal to zero, if the error aspiration r_c equals the value of the performance function of that model. No model can be relied upon to perform at the level indicated by its performance function, if that model is subject to errors in its structure or formulation. $R[Y, F(q)]$ is an unrealistically optimistic assessment of model $f_i(q)$, unless we have reason to believe that no auxiliary uncertainties lurk in the mist of our ignorance.

11.4.3 Example

A simple example will illustrate the previous general discussion.

We begin by formulating a *mean-squared-error estimator* for a one-dimensional linear model. The measurements y_i are scalars, and the model to be estimated is:

$$f_i(q) = iq \tag{11.72}$$

The performance function is the mean-squared error between model and measurements, Equation 11.63, which becomes:

$$R[Y, F(q)] = \frac{1}{N}\sum_{i=1}^{N}(iq - y_i)^2 \tag{11.73}$$

$$= \underbrace{\frac{1}{N}\sum_{i=1}^{N} y_i^2}_{\eta_2} - 2q\underbrace{\frac{1}{N}\sum_{i=1}^{N} iy_i}_{\eta_1} + q^2\underbrace{\frac{1}{N}\sum_{i=1}^{N} i^2}_{\eta_0} \tag{11.74}$$

which defines the quantities η_0, η_1, and η_2. The performance-optimal model defined in Equation 11.64, which minimizes the mean-squared error, is:

$$q^* = \frac{\eta_1}{\eta_0} \tag{11.75}$$

Now we introduce *uncertainty into the model.* The model that is being estimated is linear in the "time" or "sequence" index i: $f_i = iq$. How robust is the performance of our estimator, to modification of the structure of this model? That is, how much can the model err in its basic structure without jeopardizing its predictive power?

Suppose that the linear model of Equation 11.72 errs by lacking a quadratic term:

$$\phi_i = iq + i^2 u \tag{11.76}$$

where the value of u is unknown. The uncertainty in the quadratic model is represented by an interval-bound info-gap model, which is the following unbounded family of nested intervals:

$$\mathcal{U}(\alpha, iq) = \left\{\phi_i = iq + i^2 u\colon\ |u| \le \alpha\right\}, \quad \alpha \ge 0 \tag{11.77}$$

The robustness of nominal model $f_i(q)$, with performance-aspiration r_c, is the greatest value of the horizon of uncertainty α at which the mean-squared error of the prediction is no greater than r_c for any model in $\mathcal{U}(\alpha, iq)$:

$$\hat{\alpha}(q, r_c) = \max\left\{\alpha\colon \quad \max_{|u|\le\alpha} R[Y, F_u(q)] \le r_c\right\} \tag{11.78}$$

Copyright 2005 by CRC Press LLC

The mean-squared error of a model with nonlinear term i^2u is:

$$R[Y, F_u(q)] = \frac{1}{N}\sum_{i=1}^{N}(iq + i^2u - y_i)^2 \tag{11.79}$$

$$= \underbrace{\frac{1}{N}\sum_{i=1}^{N}(iq - y_i)^2}_{\xi_2} + 2u\underbrace{\frac{1}{N}\sum_{i=1}^{N} i^2(iq - y_i)}_{\xi_1} + u^2\underbrace{\sum_{i=1}^{N} i^4}_{\xi_0} \tag{11.80}$$

which defines ξ_0, ξ_1 and ξ_2.

Some manipulations show that the maximum mean-squared error, for all quadratic models ϕ_i up to horizon of uncertainty α, is:

$$\max_{|u|\le\alpha} R[Y, F_u(q)] = \xi_2 + 2\alpha|\xi_1| + \alpha^2\xi_0 \tag{11.81}$$

Referring to Equation 11.78, the robustness to an unknown quadratic nonlinearity i^2u, of the linear model $f_i(q)$, is the greatest value of α at which this maximum error is no greater than r_c.

First we note that the robustness is zero if r_c is small:

$$\hat{\alpha}(q, r_c) = 0, \quad r_c \le \xi_2 \tag{11.82}$$

This is because, if $r_c \le \xi_2$, then max R in Equation 11.81 exceeds r_c for any positive value of α. One implication of Equation 11.82 is that some nonlinear models have prediction errors in excess of ξ_2. If it is required that the fidelity between model and measurement be as good as or better than ξ_2, then no modeling errors of the quadratic type represented by the info-gap model of Equation 11.77 can be tolerated. Recall that ξ_2 is the mean-squared error of the nominal linear predictor, $f_i(q)$. Equation 11.82 means that there is no robustness to model uncertainty if the performance-aspiration r_c is stricter or more exacting than the performance of the nominal, linear model.

For $r_c \ge \xi_2$, the robustness is obtained by equating the right-hand side of Equation 11.81 to r_c and solving for α, resulting in:

$$\hat{\alpha}(q, r_c) = \frac{|\xi_1|}{\xi_0}\left(-1 + \sqrt{1 + \frac{\xi_0(r_c - \xi_2)}{\xi_1^2}}\right), \quad \xi_2 \le r_c \tag{11.83}$$

Relation 11.83 is plotted in Figure 11.7 for synthetic data[2] y_i and for two values of the model parameter q. The figure shows the robustness to model uncertainty, $\hat{\alpha}(q, r_c)$, against the aspiration for prediction error, r_c. The robustness increases as greater error is tolerated. Two curves are shown, one for the optimal linear model, $q^* = 2.50$ in Equation 11.75, whose mean-squared error $r_c^* = R[Y, F(q^*)] = 4.82$ is the lowest obtainable with any linear model. The other model, $q' = 2.60$, has a greater mean-squared error $r_c' = R[Y, F(q')] = 4.94$, so $r_c' > r_c^*$. However, the best performance (the smallest r_c-value) with each of these models, q' and q^*, has no robustness to model uncertainty: $0 = \hat{\alpha}(q^*, r_c^*) = \hat{\alpha}(q', r_c')$.

More importantly, the robustness curves cross at a higher value of r_c (corresponding to lower aspiration for prediction fidelity), as seen in Figure 11.7. If prediction-error $r_c^\circ = 5.14$ is tolerable, then the suboptimal model q' is more robust than, and hence preferable over, the mean-squared optimal model q^*, at the same performance-aspiration. In other words, because $0 = \hat{\alpha}(q^*, r_c^*)$, the analyst recognizes that performance as good as r_c^* is not reliable or feasible with the optimal linear model q^*, and some larger r_c value (representing poorer fidelity between model and measurement) must be accepted; the analyst is motivated

[2] $N = 5$ and $y_1, \ldots, y_5 = 1.4, 2.6, 5.6, 8.6, 15.9$.

Copyright 2005 by CRC Press LLC

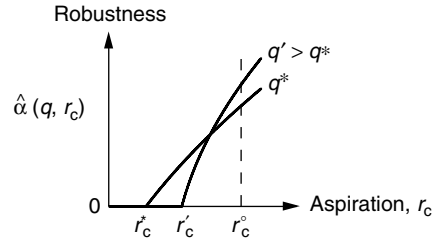

FIGURE 11.7 Robustness vs. prediction-aspiration, Equation 11.83; q fixed.

to "move up" along the q^*-robustness curve. If r_c° is an acceptable level of fidelity, then the suboptimal model q' achieves this performance with greater robustness than the optimal model q^*. In particular, $\hat{\alpha}(q', r_c^\circ) = 0.021$ which is small but still twice as large as $\hat{\alpha}(q^*, r_c^\circ) = 0.011$. In this case, "good" (that is, q') is preferable to "best" (q^*).

We see the robustness preference for a suboptimal model explicitly in Figure 11.8, which shows the robustness vs. the linear model parameter q, for fixed aspiration $r_c = 5.5$ (which is larger than the r_c-values in Figure 11.7, so q^* has positive robustness). The least-squares optimal parameter, $q^* = 2.50$, minimizes the mean-squared error $R[Y, F(q)]$, while the robust-optimal parameter, $\hat{q}_c = 2.65$, maximizes the robustness function $\hat{\alpha}(q, r_c)$. q^* has lower robustness than $\hat{q}_c$, at the same level of model-data fidelity, r_c. Specifically, $\hat{\alpha}(q^*, r_c) = 0.033$ is substantially less than $\hat{\alpha}(\hat{q}_c, r_c) = 0.045$. The mean-squared error of $\hat{q}_c$ is $R[Y, F(\hat{q}_c)] = 5.09$, which is only modestly worse than the least-squares optimum of $R[Y, F(q^*)] = 4.82$. In short, the performance-suboptimal model has only moderately poorer fidelity to the data than the least-squares optimal model $q*$, while the robustness to model uncertainty of $\hat{q}_c$ is appreciably greater than the robustness of q^*.

In summary, we have established the following conclusions from this example.

First, the performance-optimal model, $f_i(q^*)$, has no immunity to error in the basic structure of the model. The model $f_i(q^*)$, which minimizes the mean-squared discrepancy between measurement and prediction, has zero robustness to modeling errors at its nominal prediction fidelity, r_c^*.

Second, this is actually true of *any* model, $f_i(q')$. The value of its mean-squared error is r_c' which, as in Figure 11.7, has zero robustness.

Third, the robustness curves of alternative linear models can cross, as in Figure 11.7. This shows that a suboptimal model such as $f_i(q')$ can be more robust to model uncertainty than the mean-squared optimal model $f_i(q^*)$, when these models are compared at the same aspiration for fidelity between model and measurement, r_c° in the figure.

Fourth, the model that maximizes the robustness can be substantially more robust than the optimal model q^*, which minimizes the least-squared error function, as shown in Figure 11.8. This robustness curve is evaluated at a fixed value of the performance-satisficing parameter r_c.

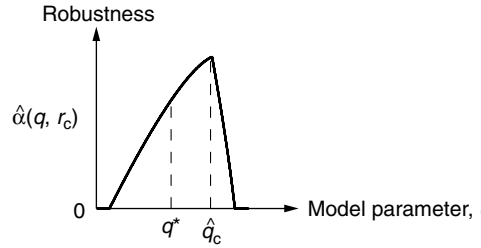

FIGURE 11.8 Robustness vs. model parameter, Equation 11.83; r_c fixed.

Copyright 2005 by CRC Press LLC

11.5 Hybrid Uncertainty: Info-Gap Supervision of a Probabilistic Decision

11.5.1 Info-Gap Robustness as a Decision Monitor

In Sections 11.2 and 11.3 we considered the reliability of technological systems. We now consider the reliability of a decision algorithm itself. Many decisions are based on probabilistic considerations. A foremost class of examples entails acceptance tests based on the evaluation of a probability of failure. Paradigmatically, a go/no-go decision hinges on whether the probability of failure is below or above a critical threshold:

$$P_f(p) \underset{\text{no-go}}{\overset{\text{go}}{\lessgtr}} P_c \tag{11.84}$$

where p is a probability density function (PDF) from which the probability of failure, $P_f(p)$, is evaluated.

This is a valid and meaningful decision procedure when the PDF is well known and when the probability of failure can be assessed with accurate system models. However, a decision algorithm such as Equation 11.84 will be unreliable if the PDF is uncertain (which will often be the case, especially regarding the extreme tails of the distribution) and if the critical probability of failure P_c is small (which is typically the case with critical components). When the PDF is imprecisely known, the reliability of the probabilistic decision can be assessed using the info-gap robustness function.

Let $\tilde{p}$ be the best estimate of the PDF, which is recognized to be wrong to some unknown extent. For the sake of argument, let us suppose that, with $\tilde{p}$, the probability of failure is acceptably small:

$$P_f(\tilde{p}) \le P_c \tag{11.85}$$

That is, the nominal PDF implies "all systems go." However, because $\tilde{p}$ is suspect, we would like to know how immune this decision is to imperfection of the PDF.

Let $\mathcal{U}(\alpha, \tilde{p})$, $\alpha \ge 0$, be an info-gap model for the uncertain variation of the actual PDF with respect to the nominal, best estimate, $\tilde{p}$. (We will encounter an example shortly.) The robustness, to uncertainty in the PDF, of decision algorithm Equation 11.84, is the greatest horizon of uncertainty up to which all PDFs lead to the same decision:

$$\hat{\alpha}(P_c) = \max\left\{\alpha: \max_{p \in \mathcal{U}(\alpha,\tilde{p})} P_f(p) \le P_c\right\} \tag{11.86}$$

$\hat{\alpha}(P_c)$ is the greatest horizon of uncertainty in the PDF, up to which all densities p in $\mathcal{U}(\alpha, \tilde{p})$ yield the same decision as $\tilde{p}$. If $\hat{\alpha}(P_c)$ is large, then the decision based on $\tilde{p}$ is immune to uncertainty in the PDF and hence reliable. Alternatively, if $\hat{\alpha}(P_c)$ is small, then a decision based on $\tilde{p}$ is of questionable validity. We see that the robustness function $\hat{\alpha}(P_c)$ is a decision evaluator: it supports the higher-level judgment (how reliable is the probabilistic algorithm?) that hovers over and supervises the ground-level go/no-go decision.

If the inequality in Equation 11.85 were reversed and $\tilde{p}$ implied "no-go," then we would modify Equation 11.86 to:

$$\hat{\alpha}(P_c) = \max\{\alpha: \min_{p \in \mathcal{U}(\alpha,\tilde{p})} P_f(p) \ge P_c\} \tag{11.87}$$

The meaning of the robustness function as a decision monitor would remain unchanged. $\hat{\alpha}(P_c)$ is still the greatest horizon of uncertainty up to which the decision remains constant.

Copyright 2005 by CRC Press LLC

We can formulate the robustness slightly differently as the greatest horizon of uncertainty at which the probability of failure does not differ more than π_c:

$$\hat{\alpha}(\pi_c) = \max\{\alpha : \max_{p \in \mathcal{U}(\alpha, \tilde{p})} |P_f(p) - P_f(\tilde{p})| \le \pi_c\} \tag{11.88}$$

Other variations are also possible [2], but we now proceed to a simple example of the use of the info-gap robustness function in the supervision of a probabilistic decision with an uncertain PDF.

11.5.2 Nonlinear Spring

Consider a spring with the following nonlinear relationship between displacement x and force f:

$$f = k_1 x + k_2 x^2 \tag{11.89}$$

The spring fails if the magnitude of the displacement exceeds x_c and we require the probability of failure not to exceed P_c.

The loading force f is nonnegative but uncertain, and the best available PDF is a uniform density:

$$\tilde{p}(f) = \begin{cases} 1/F & \text{if} \quad 0 \le f \le F \\ 0 & \text{if} \quad F \le f \end{cases} \tag{11.90}$$

where the value of F is known. However, it is recognized that forces greater than F may occur. The probability of such excursions, although small, is unknown, as is the distribution of this high-tail probability. That is, the true PDF, shown schematically in Figure 11.9, is:

$$p(f) = \begin{cases} \text{constant} & \text{if} \quad 0 \le f \le F \\ \text{variable} & \text{if} \quad F \le f \end{cases} \tag{11.91}$$

The first question we must consider is how to model the uncertainty in the PDF of the force f. What we **do know** is that f is nonnegative, that $p(f)$ is constant for $0 \le f \le F$, and the value of F. What we **do not know** is the actual constant value of $p(f)$ for $0 \le f \le F$ and the behavior of $p(f)$ for $f > F$. We face an info gap.

Let $\mathcal{P}$ denote the set of all nonnegative and normalized PDFs on the interval $[0, \infty)$. Whatever form $p(f)$ takes, it must belong to $\mathcal{P}$. An info-gap uncertainty model that captures the information as well as the info gaps about the PDF is:

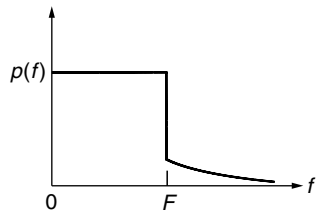

FIGURE 11.9 Uncertain probability density function of the load, Equation 11.91.

$$\mathcal{U}(\alpha, \tilde{p}) = \left\{ p(f) : \quad p(f) \in \mathcal{P}; \quad \int_F^\infty p(f)\,df \le \alpha; \right.$$
$$\left. p(f) = \frac{1}{F}\left(1 - \int_F^\infty p(f)\,df\right), \; 0 \le f \le F \right\}, \quad \alpha \ge 0 \tag{11.92}$$

Copyright 2005 by CRC Press LLC

The first line of Equation 11.92 states that $p(f)$ is a normalized PDF whose tail above F has weight no greater than α. The second line asserts that $p(f)$ is constant over the interval $[0, F]$ and the weight in this interval is the complement of the weight on the tail.

The spring fails if x exceeds the critical displacement x_c. This occurs if the force f exceeds the critical load f_c, which is:

$$f_c = k_1 x_c + k_2 x_c^2 \tag{11.93}$$

With PDF $p(f)$, the probability of failure is:

$$P_f(p) = \text{Prob}(f \geq f_c \mid p) \tag{11.94}$$

We require that the failure probability not exceed the critical probability threshold:

$$P_f(p) \leq P_c \tag{11.95}$$

The robustness of the determination of this threshold exceedence, based on the nominal PDF, is $\hat{\alpha}(P_c)$ given by Equation 11.86. The value of this robustness depends on the values of F and f_c. After some algebra, one finds:

$$\hat{\alpha}(P_c) = \begin{cases} 0 & \text{if } f_c \leq (1-p_c)F \\ 1 - \dfrac{1-P_c}{f_c/F} & \text{if } (1-P_c)F < f_c \leq F \\ P_c & \text{if } F < f_c \end{cases} \tag{11.96}$$

The first line of Equation 11.96 arises when the critical force, f_c, is small enough so that $P_f(p)$ can exceed P_c even when the nominal PDF, $\tilde{p}$, is correct. The third line arises when f_c is so large that only the tail could account for failure. The second line covers the intermediate case. $\hat{\alpha}(P_c)$ is plotted schematically in Figure 11.10.

As we explained in Section 11.5.1, the value of the robustness $\hat{\alpha}(P_c)$ indicates whether the go/no-go threshold decision, based on the best-available PDF, is reliable or not. A large robustness implies that the decision is insensitive to uncertainty in the PDF, while a small value of $\hat{\alpha}(P_c)$ means that the decision can err as a result of small error in $\tilde{p}$. From Equation 11.96 and Figure 11.10 we see that the greatest value that $\hat{\alpha}(P_c)$ can take is P_c itself, the critical threshold value of failure probability. In fact, $\hat{\alpha}(P_c)$ may be much less, depending on the critical force f_c. From Equation 11.86 we learn that $\hat{\alpha}(P_c)$ and α have the

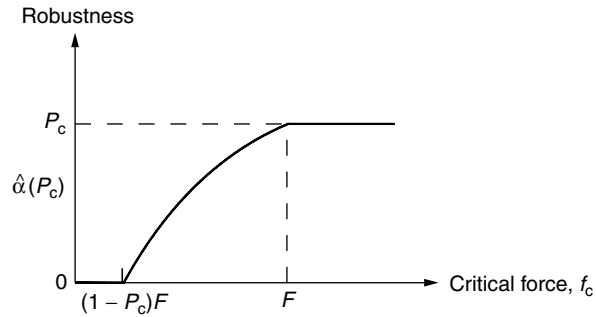

FIGURE 11.10 Robustness vs. critical force, Equation 11.96.

Copyright 2005 by CRC Press LLC

same units. The first line of Equation 11.92 indicates that α is a probability: the statistical weight of the upper tail. Consequently, $\hat{\alpha}(P_c)$ is the greatest tolerable statistical weight of the unmodeled upper tail of $p(f)$. $\hat{\alpha}(P_c)$ must be "large" in order to warrant the go/no-go decision; the judgment whether $\hat{\alpha}(P_c)$ is "small" or "large" depends on a judgment of how wrong $\tilde{p}(f)$ could be. As the tolerable probability of failure, P_c, becomes smaller, the tolerance against probability "leakage" into the upper tail becomes lower as well. $\hat{\alpha}(P_c)$ establishes a quantitative connection between the critical force f_c, the nominally maximum force F, the critical probability P_c, and the reliability of the go/no-go decision.

An additional use of the robustness function is in choosing technical modifications of the system itself that enhance the reliability of the go/no-go decision in the face of load uncertainty. Examination of Equation 11.96 reveals that $\hat{\alpha}(P_c)$ is improved by increasing f_c (if $f_c < F$). Let us consider the choice of the two stiffness coefficients, k_1 and k_2. From Equation 11.93 we note that:

$$\frac{\partial f_c}{\partial k_1} = x_c > 0 \tag{11.97}$$

$$\frac{\partial f_c}{\partial k_2} = x_c^2 > 0 \tag{11.98}$$

Thus, f_c is increased and thereby $\hat{\alpha}(P_c)$ is improved, by increasing either k_1 or k_2 or both. Equation 11.96 quantifies the robustness-enhancement from a design change in k_1 or k_2.

Equation 11.94 implies that increasing f_c causes a reduction in the probability of failure, $P_f(p)$, regardless of how the load is distributed. Thus, a change in the system that reduces the probability of failure also makes the prediction of the failure probability more reliable. There is a sympathy between *system reliability* and *prediction reliability*. This is, in fact, not just a favorable quirk of this particular example. It is evident from the definition of robustness in Equation 11.94 that any system modification which decreases $P_f(p)$ will likewise increase (or at least not decrease) the robustness $\hat{\alpha}(P_c)$.

11.6 Why "Good" Is Preferable to "Best"

The examples in Sections 11.2 through 11.4 illustrated the general proposition that optimization of performance is associated with minimization of immunity to uncertainty. This led to the conclusion that performance should be satisficed—made adequate but not optimal—and that robustness should be optimized. In the present section, we put this conflict between performance and robustness on a rigorous footing.

11.6.1 The Basic Lemma

The designer must choose values for a range of variables. These variables may represent materials, geometrical dimensions, devices or components, design concepts, operational choices such as "go" or "no-go," etc. Some of these variables are expressible numerically, some linguistically. We will represent the collection of the designer's decisions by the decision vector q.

In contrast to q, which is under the designer's control, the designer faces uncontrollable uncertainties of many sorts. These may be uncertain material coefficients, unknown and unmodeled properties such as nonlinearities in the design-base models, unknown external loads or ambient conditions, uncertain tails of a probability distribution, and so on. The uncertainties are all represented as vectors or functions (which may be vector-valued). We represent the uncertain quantities by the uncertain vector u. The uncertainties associated with u are represented by an info-gap model $\mathcal{U}(\alpha, \tilde{u})$, $\alpha \geq 0$. The centerpoint of the info-gap model is the known vector, which is the nominal value of the uncertain quantity u.

Info-gap models are suitable for representing ignorance of u for both practical and fundamental reasons. Practically, probability models defined on multidimensional function spaces tend to be cumbersome and informationally intensive. More fundamentally, info-gap models entail no measure functions, while measure-theoretic representation of ignorance can lead to contradictions [3, Chapter 4].

Copyright 2005 by CRC Press LLC

Many design specifications can be expressed as a collection of inequalities on scalar valued functions. For example, the mechanical deflection must not exceed a given value, while each of the three lowest natural frequencies must be no greater than various thresholds. For a design choice q, and for a specific realization of the uncertainty u, the performance of the system is expressed by the real-valued *performance functions* $R_i(q, u),\ i = 1, \ldots, N$, where the design specification is the following set of inequalities:

$$R_i(q,u) \le r_{c,i} \quad \text{for all} \quad i = 1, \ldots, N \tag{11.99}$$

The $r_{c,i}$ are called *critical thresholds,* which are represented collectively by the vector r_c. These thresholds may be chosen either small or large, to express either demanding or moderate aspirations, respectively.

Definition 11.1 A performance function $R_i(q, u)$ is *upper unsatiated* at design q if its maximum, up to horizon of uncertainty α, increases strictly as α increases:

$$\alpha < \alpha' \Rightarrow \max_{u \in \mathcal{U}(\alpha, \tilde{u})} R_i(q,u) < \max_{u \in \mathcal{U}(\alpha', \tilde{u})} R_i(q,u) \tag{11.100}$$

Upper unsatiation is a type of monotonicity: the maximum of the performance function strictly increases as the horizon of uncertainty increases. This monotonicity in α does not imply monotonicity of $R(q,u)$ in either q or u. Upper unsatiation results from the nesting of the sets in the info-gap model $\mathcal{U}(\alpha, \tilde{u})$.

By definition, the robustness of design q, with performance requirements r_c, is the greatest horizon of uncertainty at which all the performance functions satisfy their critical thresholds:

$$\hat{\alpha}(q, r_c) = \max \{\alpha: \max_{u \in \mathcal{U}(\alpha, \tilde{u})} R_i(q,u) \le r_{c,i}, \quad \text{for all} \quad i = 1, \ldots, N\} \tag{11.101}$$

We now assert the following basic lemma. (Proofs appear in Section 11.6.4.)

Lemma 11.1 Given:

- An info-gap model $\mathcal{U}(\alpha, \tilde{u}),\ \alpha \ge 0$.
- Performance functions $R_i(q, u),\ i = 1, \ldots, N$, which are all upper unsatiated at q.
- Critical thresholds equaling the performance functions evaluated at the centerpoint of the info-gap model:

$$r_{c,i} = R_i(q, \tilde{u}), \quad i = 1, \ldots, N \tag{11.102}$$

Then the robustness-to-uncertainty of design q vanishes:

$$\hat{\alpha}(q, r_c) = 0 \tag{11.103}$$

$\tilde{u}$ is the centerpoint of the info-gap model: the known, nominal, "best estimate" of the uncertainties accompanying the problem. If $\tilde{u}$ precisely represents the values of these auxiliary variables, then the performance aspirations in Equation 11.102 will be achieved by decision q. However, Equation 11.103 asserts that this level of performance has no immunity to unknown variations in the data and models upon which this decision is based. Any unmodeled factors, such as the higher-order terms in Equation 11.76, jeopardize the performance level vouched for in Equation 11.102. Probabilistically, one would say that things could be worse than the expected outcome. However, our assertion is stronger, because we are considering not only random uncertainties, but rather the info gaps in the entire epistemic infrastructure of the decision, which may include info gaps in model structures and probability densities.

This result is particularly significant when we consider performance-optimization, to which we now turn.

Copyright 2005 by CRC Press LLC

11.6.2 Optimal-Performance vs. Optimal Robustness: The Theorem

We are particularly interested in the application of lemma 11.1 to optimal-performance design. The lemma will show that a design that optimizes the performance will have zero robustness to uncertainty. This means that high aspirations for performance are infeasible in the sense that these aspirations can fail to materialize due to infinitesimal deviations of the uncertain vector from its nominal value. It is true that failure to achieve an ultimate aspiration may entail only a slight reduction below optimal performance. Nonetheless, the gist of the theorem is that zenithal performance cannot be relied upon to occur; a design specification corresponding to an extreme level of performance has no robustness to uncertainty. The designer cannot "sign-off" on a performance-optimizing specification; at most, one can hope that the shortfall will not be greatly below the maximum performance.

Let $\mathcal{Q}$ represent the set of available designs from which the designer must choose a design q. Let $\tilde{u}$ denote the nominal, typical, or design-base value of the uncertain vector u. What is an optimal-performance design, from the allowed set $\mathcal{Q}$, and with respect to the design-base value $\tilde{u}$?

If there is only one design specification, so $N = 1$ in Equation 11.99, then an optimal-performance design q^* minimizes the performance function:

$$R(q^*, \tilde{u}) = \min_{q \in \mathcal{Q}} R(q, \tilde{u}) \tag{11.104}$$

If there are multiple design specifications ($N > 1$), then such a minimum may not hold simultaneously for all the performance functions. One natural extension of Equation 11.104 employs the idea of *Pareto efficiency*. Pareto efficiency is a "short blanket" concept: if you pull up your bed covers to warm your nose, then your toes will get cold. A design q^* is Pareto efficient if any other design q' that improves (reduces) one of the performance functions detracts from (increases) another:

$$\text{If:} \quad R_i(q', \tilde{u}) < R_i(q^*, \tilde{u}) \quad \text{for some} \quad i \tag{11.105}$$

$$\text{Then:} \quad R_j(q', \tilde{u}) > R_j(q^*, \tilde{u}) \quad \text{for some} \quad j \neq i \tag{11.106}$$

A Pareto-efficient design does not have to be unique, so let us denote the set of all Pareto efficient designs by Q^*. For the case of a single design specification, let Q^* denote all the designs that minimize the performance function, as in Equation 11.104. The following theorem, which is derived directly from lemma 11.1, asserts that any design that is performance-optimal (Equation 11.104) or Pareto efficient (Equations 11.105 and 11.106) has no robustness to uncertain deviation from the design-base value $\tilde{u}$.

Theorem 11.1 Given:

- A set of Pareto-efficient or performance-optimal designs, with respect to the design-base value $\tilde{u}$.
- An info-gap model $\mathcal{U}(\alpha, \tilde{u})$, $\alpha \geq 0$, whose centerpoint is the nominal or design-base value $\tilde{u}$.
- Performance functions $R_i(q^*, u)$, $i = 1, \ldots, N$, which are all upper unsatiated at some $q^* \in Q^*$.
- Critical thresholds equaling the performance functions evaluated at the centerpoint of the info-gap model and at this q^*:

$$r_{c,i} = R_i(q^*, \tilde{u}), \quad i = 1, \ldots, N \tag{11.107}$$

Then the robustness to uncertainty of this performance-optimal design q^* vanishes:

$$\hat{\alpha}(q^*, r_c) = 0 \tag{11.108}$$

Theorem 11.1 is really just a special case of lemma 11.1. We know from lemma 11.1 that whenever the critical thresholds, $r_{c,i}$, are chosen at the nominal values of the performance-functions, $R_i(q, \tilde{u})$, and

Copyright 2005 by CRC Press LLC

when that nominal value, $\tilde{u}$, is the centerpoint of the info-gap model, $\mathcal{U}(\alpha,\tilde{u})$, then any design has zero robustness. Theorem 11.1 just specializes this to the case where q is Pareto-efficient or performance-optimal.

We can understand the special significance of this result in the following way. The functions $R_i(q^*,\tilde{u})$ represent the designer's best-available representation of how design q^* will perform. $R_i(q^*,\tilde{u})$ is based on the best-available models, and is the best estimate of all residual (and possibly recalcitrant) uncertain factors or terms. We know from lemma 11.1 that any performance-optimal design we choose will have zero robustness to the vagaries of those residual uncertainties. However, the lesson to learn is **not** to choose the design whose performance is optimal; theorem 11.1 makes explicit that this design also cannot be depended upon to fulfill our expectations. To state it harshly, choosing the performance optimum is just wishful thinking, unless we are convinced that no uncertainties lurk behind our models. The lesson to learn, if we seek a design whose performance can be reliably known in advance, is to move off the surface of Pareto-efficient or performance-optimal solutions. For example, referring again to Figure 11.2, we must move off the optimal-performance curve to a point *Q* or *R*. We can evaluate the robustness of these suboptimal designs with the robustness function, and we can choose the design to satisfice the performance and to maximize the robustness.

11.6.3 Information-Gap Models of Uncertainty

We have used info-gap models throughout this chapter. In this section we present a succinct formal definition, in preparation for the proof of lemma 11.1 in Section 11.6.4.

An info-gap model of uncertainty is a family of nested sets; Equations 11.14, 11.41, 11.77, and 11.92 are examples. An info-gap model entails no measure functions (probability densities or membership functions). Instead, the limited knowledge about the uncertain entity is invested in the structure of the nested sets of events.

Mathematically, an info-gap model is a set-valued function. Let *S* be the space whose elements represent uncertain events. *S* may be a vector space or a function space. Let $\Re$ denote the set of nonnegative real numbers. An info-gap model $\mathcal{U}(\alpha,u)$ is a function from $\Re\times S$ into the class of subsets of *S*. That is, each ordered pair (α,u), where $\alpha\geq 0$ and $u\in S$, is mapped to a set $\mathcal{U}(\alpha,u)$, which is a subset of *S*.

Two axioms are central to the definition of info-gap models of uncertainty:

Axiom 11.1 Nesting. An info-gap model is a family of nested sets:

$$\alpha\leq\alpha'\Rightarrow\mathcal{U}(\alpha,u)\subseteq\mathcal{U}(\alpha',u) \tag{11.109}$$

We have already encountered this property of info-gap models in Equations 11.9, 11.37, and 11.67 where we noted that this inclusion means that the uncertainty sets $\mathcal{U}(\alpha,u)$ become more inclusive as the "uncertainty parameter" α becomes larger. Relation 11.109 means that α is a *horizon of uncertainty.* At any particular value of α, the corresponding uncertainty set defines the range of variation at that horizon of uncertainty. The value of α is unknown, so the family of nested sets is typically unbounded, and there is no "worst case."

All info-gap models of uncertainty share an additional fundamental property.

Axiom 11.2 Contraction. The info-gap set, at zero horizon of uncertainty, contains only the centerpoint:

$$\mathcal{U}(0,u)=\{u\} \tag{11.110}$$

For example, the info-gap model in Equation 11.14 is a family of nested intervals, and the centerpoint is the nominal load, $\tilde{\phi}$, which is the only element of $\mathcal{U}(0,\tilde{\phi})$ and which belongs to the intervals at all positive values of α.

Copyright 2005 by CRC Press LLC

Combining axioms 11.1 and 11.2 we see that u belongs to the zero-horizon set, $\mathcal{U}(0,u)$, and to all "larger" sets in the family.

Additional axioms are often used to define more specific structural features of the info-gap model, such as linear [1, 4], or nonlinear [5] expansion of the sets as the horizon of uncertainty grows. We will not need these more specific axioms. Info-gap models of uncertainty are discussed extensively elsewhere [1, 6].

11.6.4 Proofs

Proof of lemma 11.1. By the contraction axiom of info-gap models, Equation 11.110, and from the choice of the value of $r_{c,i}$:

$$\max_{u\in\mathcal{U}(0,\tilde{u})} R_i(q,u) = r_{c,i} \tag{11.111}$$

Hence, 0 belongs to the set of α-values in Equation 11.101 whose least upper bound equals the robustness, so:

$$\hat{\alpha}(q,r_c) \geq 0 \tag{11.112}$$

Now consider a positive horizon of uncertainty: $\alpha > 0$. Because $R_i(q,r_c)$ is upper unsatiated at q:

$$\max_{u\in\mathcal{U}(0,\tilde{u})} R_i(q,u) < \max_{u\in\mathcal{U}(\alpha,\tilde{u})} R_i(q,u) \tag{11.113}$$

Together with Equation 11.111, this implies that this positive value of α does not belong to the set of α-values in Equation 11.101. Hence:

$$\alpha > \hat{\alpha}(q,r_c) \tag{11.114}$$

Combining Equations 11.112 and 11.114 completes the proof.

Proof of theorem 11.1. Special case of lemma 11.1

11.7 Conclusion: A Historical Perspective

We have focused on the epistemic limitations—information gaps—that confront a designer in the search for reliable performance. The central idea has been that the functional performance of a system must be traded off against the immunity of that system to info gaps in the models and data underlying the system's design. A system that is designed for maximal performance will have no immunity to errors in the models and data underlying the design. Robustness can be obtained only by reducing performance aspirations.

Our discussion is motivated by the recognition that the designer's understanding of the relevant processes is deficient, that the models representing those processes lack pertinent components, and that the available data is incomplete and inaccurate. This very broad conception of uncertainty—including model structure as well as more conventional data "noise"—has received extensive attention in some areas of engineering, most notably in robust control [7]. This scope of uncertainty is, however, a substantial deviation from the tradition of probabilistic analysis that dominates much contemporary thinking.

Least-squares estimation is a central paradigm of traditional uncertainty analysis. The least-squares method was developed around 1800, independently by Gauss (1794–1795) and Legendre (1805–1808), for estimation of celestial orbits [8, 9]. Newtonian mechanics, applied to the heavenly bodies, had established irrevocably that celestial orbits are elliptical, as Kepler had concluded experimentally. However, the data was noisy so it was necessary to extract the precise ellipse that was hidden under the noisy measurements. The data was corrupted, while the model—elliptical orbits—was unchallenged.

Copyright 2005 by CRC Press LLC

Least-squares estimation obtained deep theoretical grounding with the proof of the central limit theorem by Laplace (1812), which established the least-squares estimate as the maximum-likelihood estimate of a normal distribution. The least-squares idea continues to play a major role in modern uncertainty analysis in such prevalent and powerful tools as Kalman filtering, Luenberger estimation [10] and the Taguchi method [11].

What is characteristic of the least-squares method is the localization of uncertainty exclusively on data that is exogenous to the model of the underlying process. The model is unblemished (Newtonian truth in the case of celestial orbits); only the measurements are corrupted. But the innovative designer, using new materials and exploiting newly discovered physical phenomena, stretches models and data to the limits of their validity. The designer faces a serious info gap between partial, sometimes tentative, insights that guide much high-paced modern design, and solid complete knowledge. The present work is part of the growing trend to widen the range of uncertainty analysis to include the analyst's imperfect conceptions and representations. For all our sapience, we are after all only human!

Acknowledgments

The author acknowledges with pleasure the support of the Samuel Neaman Institute for Advanced Studies in Science and Technology. The author is indebted to Professor Eli Altus and Mr. Yakov Saraf of the Technion for useful comments.

References

1. Ben-Haim, Y., *Information-Gap Decision Theory: Decisions Under Severe Uncertainty,* Academic Press, London, 2001.
2. Ben-Haim, Y., Cogan, S., and Sanseigne, L., Usability of Mathematical Models in Mechanical Decision Processes, *Mechanical Systems and Signal Processing.* 12, 121–134, 1998.
3. Keynes, J.M., *Treatise on Probability,* Macmillan & Co. Ltd., London, 1921.
4. Ben-Haim, Y., Set-models of information-gap uncertainty: axioms and an inference scheme, *Journal of the Franklin Institute,* 336, 1093–1117, 1999.
5. Ben-Haim, Y., Robustness of model-based fault diagnosis: decisions with information-gap models of uncertainty, *International Journal of Systems Science,* 31, 1511–1518, 2000.
6. Ben-Haim, Y., *Robust Reliability in the Mechanical Sciences,* Springer-Verlag, Berlin, 1996.
7. Qu, Z., *Robust Control of Nonlinear Uncertain Systems,* Wiley, New York, 1998.
8. Hazewinkel, M., Managing Editor, *Encyclopaedia of Mathematics: An Updated and Annotated Translation of The Soviet "Mathematical Encyclopaedia,"* Kluwer Academic Publishers, Dordrecht, Holland, 1988.
9. Stigler, S.M., *The History of Statistics: The Measurement of Uncertainty before 1900.* The Belknap Press of Harvard University Press, Boston, 1986.
10. Luenberger, D.G., *Optimization by Vector Space Methods,* Wiley, New York, 1969.
11. Taguchi, G., *Introduction to Quality Engineering: Designing Quality into Products and Processes,* translated and published by the Asian Productivity Organization, Tokyo, 1986.

Copyright 2005 by CRC Press LLC

12

Interval Methods for Reliable Computing

Rafi L. Muhanna
Georgia Institute of Technology

Robert L. Mullen
Case Western Reserve University

12.1 Introduction

This chapter explores the use of interval numbers to account for uncertainties in engineering models. We concentrate on models based on finite element discretization of partial differential equations. Results of such models are used ubiquitously in engineering design. Uncertainties in the results of finite element models can be attributed to the following sources:

1. The appropriateness of the partial differential equation
2. Errors associated with discretization of the partial differential equation
3. Uncertainties in the parameters of the engineering model
4. Errors associated with floating point operations on a digital computer

While the appropriateness of a partial differential equation to a given physical problem is beyond the scope of this chapter, the remaining three sources of errors and uncertainties can be bounded using the concept of interval representation and interval numbers. Quantifying the uncertainties in the results of an engineering calculation is essential to provide a reliable computing environment.

Section 12.2 provides a review of interval representation and the mathematics of interval numbers. Section 12.3 contains a description of interval finite element methods that account for uncertain model parameters. Section 12.4 describes methods for bounding errors associated with floating point operations, while Section 12.5 contains information on bounding discretization errors.

0-8493-1180-X/04/$0.00+$1.50

© 2004 by CRC Press LLC

Copyright 2005 by CRC Press LLC

12.2 Intervals and Uncertainty Modeling

12.2.1 Definitions, Applications, and Scope

By definition, an interval number is a closed set in R that includes the possible range of an unknown real number, where R denotes the set of real numbers. Therefore, a real interval is a set of the form

$$x \equiv [x^l, x^u] := \{\tilde{x} \in R \mid x^l \leq \tilde{x} \leq x^u\} \tag{12.1}$$

where x^l and x^u are the lower and upper bounds of the interval number x, respectively, and the bounds are elements of R with $x^l \leq x^u$. Degenerated or thin interval numbers are of the form $[x^l, x^l]$ or $[x^u, x^u]$; they are equivalent to the real numbers x^l and x^u respectively.

Based on the above-mentioned definitions, interval arithmetic is defined on sets of intervals, rather than on sets of real numbers, and interval mathematics can be considered as a generalization of real numbers mathematics. The definition of real intervals and operations with intervals can be found in a number of references [1–4]. However, the main interval arithmetic operations are presented in Appendix 12.1 at the end of this chapter.

Early use of interval representation is associated with the treatment of rounding errors in mathematical computations. The idea was to provide upper and lower bounds on rounding errors. For example, in a computational system with three decimal digit accuracy, the number 3.113 would be represented as a member of the interval [3.11, 3.12]. Intervals can also be used to represent rational bounds on irrational numbers. Archimedes used a "two-sided approximation" to calculate the constant π. He considered inscribed and circumscribed polygons of a circle and obtained an increasing sequence of lower bounds and a decreasing sequence of the upper bounds at the same time. Therefore, stopping the process with polygons each of n sides, he obtained an interval containing the desired result, (i.e., the number π.) By choosing n large enough, an interval of arbitrary small width can be found to contain the number π. Inspired by this method, Moore [2], instead of computing a numerical approximation using limited-precision arithmetic, proceeded to construct intervals known in advance to contain the desired exact results. Several authors independently had the idea of bounding rounding errors using intervals [5, 6]; however, Moore extended the use of interval analysis to bound the effect of errors from different sources, including approximation errors and errors in data (see [7]).

In this section, we try to cover the most significant applications of intervals in the two major areas of *mathematics-computations* and *scientific and engineering modeling*. In addition, we introduce a short review of interval definitions and operations.

In the ***mathematics-computations*** field, there has been increasing interest in solving complex mathematical problems with the aid of digital computers. In general, the solution of these problems is too complicated to be represented in finite terms (floating point representation) or even impossible. But frequently, one is only interested in the existence of a solution within a certain domain or error bounds for the solution (intervals). By the nature of the problems, numerical approximations are insufficient. That motivated the development of interval methods capable of handling the finite representation deficiency. These interval methods are known by different names; for example, self-validating (SV) verification methods or automatic result verification [8]. A detailed introduction of these methods can be found in [4, 8–11]. The goal of self-validating methods, as introduced by Rohn, Rump, and Yamamot [12], is to deliver correct results on digital computers — correct in a mathematical sense, covering all errors such as representation, discretization, rounding errors and others, and more precisely are:

1. To deliver rigorous results
2. In a computing time not too far from a pure numerical algorithm
3. Including the proof of existence (and possibly uniqueness) of a solution

Handling rounding and truncation errors in interval arithmetic is discussed in Section 12.3.

Copyright 2005 by CRC Press LLC

In the area of ***scientific and engineering modeling***, intervals represent a simple, elegant, and computationally efficient tool to handle uncertainty. Recently, the scientific and engineering community has begun to recognize the utility of defining multiple types of uncertainty [13]. While the latest computational advances significantly increased the analysis capabilities, researchers started to encounter the limitations of applying only one mathematical framework (traditional probability theory) to present all types of uncertainty. Traditional probability theory cannot handle situations with incomplete or little information on which to evaluate a probability, or when that information is nonspecific, ambiguous, or conflicting. Because of these reasons, many theories of generalized uncertainty-based information have been developed. There are five major frameworks that use interval-based representation of uncertainty: imprecise probabilities, possibility theory, the Dempster-Shafer theory of evidence, fuzzy set theory, and convex set modeling.

For example, "imprecise probability" is a generic term for the many mathematical models that measure chance or uncertainty without sharp numerical probabilities, represented as an interval included in [0, 1]. The Dempster-Shafer theory offers an alternative to traditional probabilistic theory for the mathematical representation of uncertainty. The significant innovation of this framework is that it allows for the allocation of a probability mass to sets or intervals. To illustrate how intervals are used in the case of possibility theory and fuzzy set theory, despite the differences in their interpretation, let us start with the difference between an ordinary subset A and a fuzzy subset $\boldsymbol{A}$ [14]. Let E be a referential set in R. An ordinary subset A of this referential set is defined by its characteristic function.

$$\forall\, x \in E$$

$$\mu_A(x) \in \{0, 1\}, \tag{12.2}$$

which shows that an element of E belongs to or does not belong to A, according to the value of the characteristic function (1 or 0).

For the same referential set E, a fuzzy subset $\boldsymbol{A}$ will be defined by its characteristic function, called the membership function, which takes its values in the interval [0, 1] instead of in the binary set {0, 1}.

$$\forall\, x \in E:$$

$$\mu_A(x) \in [0, 1], \tag{12.3}$$

that is, that the elements of E belong to $\boldsymbol{A}$ with a level of certainty in the closed set [0, 1].

The concept of fuzzy numbers can be presented in many ways. One way is to construct the membership function in terms of an interval of confidence at several levels of presumption or confidence. The maximum level of presumption is considered to be 1 and the minimum of presumption to be at level 0. The level of presumption α, $\alpha \in [0, 1]$ gives an interval of confidence $A_\alpha = [a_1^{(\alpha)}, a_2^{(\alpha)}]$, which is a monotonic decreasing of α; that is,

$$(\alpha_1 < \alpha_2) \Rightarrow \left(A_{\alpha_2} \subset A_{\alpha_1}\right) \tag{12.4a}$$

or

$$(\alpha_1 < \alpha_2) \Rightarrow \left(\left[a_1^{(\alpha_2)}, a_2^{(\alpha_2)}\right] \subset \left[a_1^{(\alpha_1)}, a_2^{(\alpha_1)}\right]\right) \tag{12.4b}$$

for every $\alpha_1, \alpha_2 \in [0,1]$. Such a situation is shown in Figure 12.1. When a fuzzy membership function is expressed in terms of intervals of confidences, the arithmetic of fuzzy numbers can be constructed from interval operations and the fuzzy number can be considered as nested intervals.

Copyright 2005 by CRC Press LLC

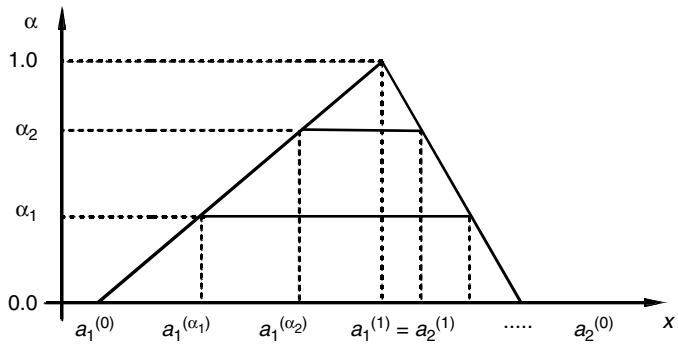

FIGURE 12.1 Definition of fuzzy numbers.

Intervals play a significant role in convex models of uncertainty. To illustrate that, we introduce some basic concepts of the convex sets [15]. A given region is called *convex* if the line segment joining any two points in the region is entirely in the region, and an algebraic formulation of convexity can be presented as follows. Let S be a set of points in n-dimensional Euclidean space, E^n. Then S is convex if all averages of points in S also belong to S. That is, S is convex if, for any points, $p \in S$ and $q \in S$, and any number $0 \le \alpha \le 1$

$$\gamma p + (1 - \gamma)\, q \in S \tag{12.5}$$

The interval models of uncertainty can be seen as an equivalent or a special case of the convex models; for example, within the context of information gap theory [16], the envelope-bound models constrain the uncertain deviations to an expandable envelope. For scalar functions, we can have:

$$\mathcal{U}(\alpha, \tilde{u}) = \{u(t): \quad |u(t) - \tilde{u}(t)| \le \alpha\psi(t)\}, \quad \alpha \ge 0 \tag{12.6}$$

where $\mathcal{U}(\alpha, \tilde{u})$ is the set of all functions whose deviation from the nominal function $\tilde{u}(t)$ is no greater than $\alpha\psi(t)$, $\psi(t)$ is a known function determining the shape of the envelope, and the uncertainty parameter α determines the size. However, envelope-bound models for n-vectors can be formulated by constraining each element of uncertain vector to lie within an expanding envelope:

$$\mathcal{U}(\alpha, \tilde{u}) = \{u_n(t): \quad |u_n(t) - \tilde{u}_n(t)| \le \alpha\psi_n(t), \quad n = 1, \ldots, n\}, \quad \alpha \ge 0 \tag{12.7}$$

in which the interval values of each element of vector u result in a family of n–dimensional expanding boxes.

Interval arithmetic has been developed as an effective tool to obtain bounds on rounding and approximation errors (discussed in the next section). The question now is to what extent interval arithmetic could be useful and effective when the range of a number is due to physical uncertainties (i.e., the range in a material's yield stress or modulus of elasticity), rather than rounding errors. In fact, overestimation is a major drawback in interval computations (overestimation handling discussed in Section 12.3). One reason for such overestimation is that only some of the algebraic laws valid for real numbers remain valid for intervals; other laws only hold in a weaker form [4, pp. 19–21]. There are two general rules for the algebraic properties of interval operations:

1. Two arithmetical expressions that are equivalent in real arithmetic are equivalent in interval arithmetic when a variable occurs only once on each side. In this case, both sides yield the range of the expression. Consequently, the laws of commutativity, associativity, and neutral elements are valid in interval arithmetic.
2. If f and g are two arithmetical expressions that are equivalent in real arithmetic, then the inclusion $f(x) \subseteq g(x)$ holds if every variable occurs only once in f.

Copyright 2005 by CRC Press LLC

In fact, the left-hand side yields the range and the right-hand side encloses the range, thus entailing the invalidity of distributive and cancellation laws in interval arithmetic. However, this property implies a weak form of the corresponding laws from real arithmetic. If a, b, and c are interval numbers, then:

$$a\,(b \pm c) \subseteq ab \pm ac; \quad (a \pm b)\,c \subseteq ac \pm bc, \quad \text{(subdistributivity)}$$

$$a - b \subseteq (a + c) - (b + c); \quad a/b \subseteq (ac)/(bc);$$

$$0 \in a - a; \quad 1 \in a/a \quad \text{(subcancellation)}$$

If we set

$$a = [-2, 2]; \quad b = [1, 2]; \quad c = [-2, 1],$$

we get

$$a\,(b + c) = [-2, 2]([1, 2] + [-2, 1]) = [-2, 2]\,[-1, 3] = [-6, 6]$$

However,

$$ab + ac = [-2, 2][1, 2] + [-2, 2][-2, 1] = [-4, 4] + [-4, 4] = [-8, 8]$$

It can be noticed that the interval number $a(b + c) = [-6, 6]$ is contained in the interval number $ab + ac = [-8, 8]$ but they are not equal. Furthermore, in the case of subcancellation;

$$0 \in b - b = [1, 2] - [1, 2] = [-1, 1]$$

and

$$1 \in b/b = [1, 2]/[1, 2] = [1/2, 2]$$

In the subtraction case, the interval number $[-1, 1]$ is enclosing but not equal to zero; and in the division case, the interval $[1/2, 2]$ is enclosing but not equal to the number 1. The failure of the distributive law is a frequent source of overestimation, and appropriate bracketing is advisable. Clearly, sharp determination for the range of an interval solution requires that extreme care be used to identify interval values that represent a single quantity and prevent the expansion of intervals. Another important source of overestimation in interval computation is dependency.

12.2.2 Dependency

The dependency problem arises when one or several variables occur more than once in an interval expression. Dependency may lead to catastrophic overestimation in interval computations. For example, if we subtract the interval $x = [a, b] = [1, 2]$ from itself, as if we are evaluating the function $f = x - x$, we obtain $[a - b, b - a] = [-1, 1]$ as a result. The result is not the interval $[0, 0]$ as we might expect. Actually, interval arithmetic cannot recognize the multiple occurrence of the same variable x, but it evaluates f as a function of two independent variables: namely, $f(x, y) = \{ f(\tilde{x}, \tilde{y}) = \tilde{x} - \tilde{y} \mid \tilde{x} \in x, \tilde{y} \in y \}$ instead of a function of one variable, that is, $\{ f(\tilde{x}) = \tilde{x} - \tilde{x} \mid x \in \tilde{x} \}$. Thus, interval arithmetic is treating $x - x$ as if evaluating $x - y$ with y equal to but independent of x. Evidently, one should always be aware of this phenomenon and take the necessary precautions to reduce or, if possible, to eliminate its effect. For example, the dependency problem could be avoided in evaluating $x - x$ if it is presented in the form $x\,(1 - 1)$ instead. In addition, overestimation can occur in evaluating a function $f(x, y)$ of the form $(x - y)/(x + y)$, but not if it is rewritten as $1 - 2/(1 + x/y)$. If $f(x, y)$ is evaluated in the latter form, the resulting interval is the exact range of $f(\tilde{x}, \tilde{y})$ for $\tilde{x} \in x$ and $\tilde{y} \in y$ [7, 11]. The reason behind obtaining the exact range is that the multiple occurrences of variables x and y are avoided in the latter form of the function.

Copyright 2005 by CRC Press LLC

12.2.3 Vectors and Matrices

An interval vector is a vector whose components are interval numbers. An interval matrix is a matrix whose elements are interval numbers. The set of $m \times n$ interval matrices is denoted by $IR^{m \times n}$. An interval matrix $A = (A_{ij})$ is interpreted as a set of real $m \times n$ matrices by the convention [4]

$$A = \{\tilde{A} \in R^{m \times n} \mid \tilde{A}_{ij} \in A_{ij} \text{ for } i = 1, ..., m; \ j = 1, ..., n\} \tag{12.8}$$

In other words, an interval matrix contains all real matrices whose elements are obtained from all possible values between the lower and upper bound of its interval elements. One important type of matrix in mechanics is the symmetric matrix. A symmetric interval matrix contains only those real symmetric matrices whose elements are obtained from all possible values between the lower and upper bound of its interval element. This definition can be presented in the following form:

$$A_{sym} = \{\tilde{A} \in R^{n \times n} \mid \tilde{A}_{ij} \in A_{ij} \quad \text{with} \quad \tilde{A}^T = \tilde{A}\} \tag{12.9}$$

An interval vector is an $n \times 1$ interval matrix. The set of real points in an interval vector form an n–dimensional parallelepiped with sides parallel to the coordinate axes. Usually, an interval vector is referred to as a *box* [7]. For more information about algebraic properties of interval matrix operations, the reader may refer to [4, 17, 18].

12.2.4 Linear Interval Equations

Systems of linear interval equations engage considerable attention in engineering applications. It is worthwhile to introduce some main features of their solution. A linear interval equation with coefficient matrix $A \in IR^{n \times n}$ and right-hand side $b \in IR^n$ is defined as the family of linear equations

$$\tilde{A}\tilde{x} = \tilde{b} \quad (\tilde{A} \in A, \tilde{b} \in b) \tag{12.10}$$

Therefore, a linear interval equation represents systems of equations in which the coefficients are unknown numbers ranging in certain intervals. The solution of interest is the enclosure for the solution set of Equation 12.10, given by

$$S(A,b) := \{\tilde{x} \in R^n \mid \tilde{A}\tilde{x} = \tilde{b} \ \text{ for some } \tilde{A} \in A, \ \tilde{b} \in b\}$$

The solution set $S(A, b)$ usually is not an interval vector, and does not need even to be convex; in general, $S(A, b)$ has a very complicated structure. To guarantee that the solution set $S(A, b)$ is bounded, it is required that the matrix A be regular; that is, that every matrix $\tilde{A} \in A$ has rank n. For the solution of a linear interval equation, we usually seek the interval vector x containing the solution set $S(A, b)$ that has the narrowest possible interval components, or what is called the hull of the solution set which can be denoted as

$$A^H b := \Diamond S(A,b) \tag{12.11}$$

where

$$A^H b = \Diamond\{\tilde{A}^{-1} b \mid \tilde{A} \in A, \ \tilde{b} \in b\} \quad \text{for } b \in IR^n \tag{12.12}$$

Copyright 2005 by CRC Press LLC

The expression 12.12 defines a mapping A^H: $IR^n \rightarrow IR^n$ that is called the hull inverse of A. The matrix inverse of a regular interval square matrix $A \in IR^{n\times n}$ is defined by

$$A^{-1} := \Diamond\{\tilde{A}^{-1} \mid \tilde{A} \in A\} \tag{12.13}$$

and it is proven that

$$A^H b \subseteq A^{-1}b, \text{ with equality if } A \text{ is thin} \tag{12.14}$$

Another case of equality in 12.14 occurs when A is a regular diagonal matrix. To illustrate some of the linear interval equation main properties, let us have the following example (adopted from [4, pp. 93]:

Given

$$A := \begin{pmatrix} 2 & [-1, 0] \\ [-1, 0] & 2 \end{pmatrix}, \qquad b := \begin{pmatrix} 1.2 \\ -1.2 \end{pmatrix}$$

Then $\tilde{A} \in A$ iff

$$\tilde{A} := \begin{pmatrix} 2 & -\alpha \\ -\beta & 2 \end{pmatrix} \quad \text{with } \alpha, \beta \in [0, 1]$$

Solving for all possible combinations of α and β, we get the following exact vertices for the solution set:

$$(0.3, -0.6);\ (0.6, -0.6);\ (0.6, -0.3) \quad \text{and} \quad (0.4, -0.4)$$

The solution set is shown in Figure 12.2. Therefore, from Figure 12.2 it can be seen that the hull of the solution set is

$$A^H b = \Diamond S(A, b) = \begin{pmatrix} [0.3,\ 0.6] \\ [-0.6,\ -0.3] \end{pmatrix}$$

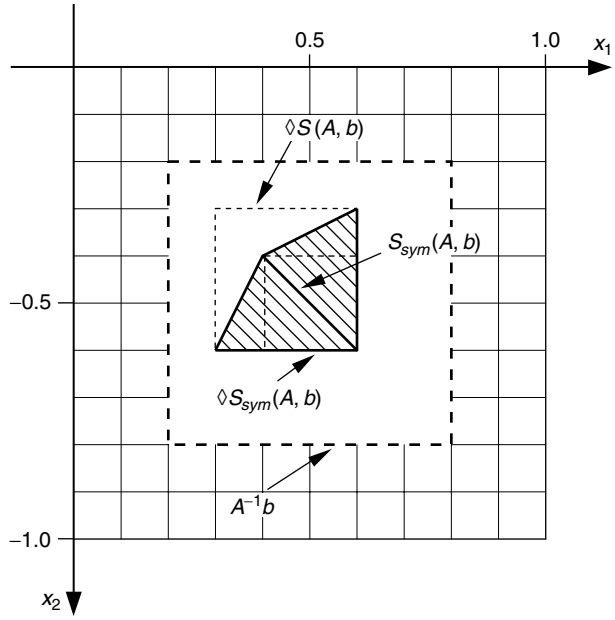

FIGURE 12.2 Solution sets for linear interval equation.

Copyright 2005 by CRC Press LLC

On the other hand,

$$A^{-1} = \begin{pmatrix} [1/2,\ 2/3] & [0,\ 1/3] \\ [0,\ 1/3] & [1/2,\ 2/3] \end{pmatrix}$$

so that

$$A^{-1}b = \begin{pmatrix} [0.2,\ 0.8] \\ [-0.8,\ -0.2] \end{pmatrix} \neq \text{ but } \supset A^H b$$

It is clear that the numerically obtained solution is wider than the actual hull of the solution set $S(A, b)$. In fact, obtaining the exact hull of the solution set for the general case is not known to be achievable. However, obtaining an exact hull of the solution set for the case of interval right-hand side with dependencies is achievable [19].

If the symmetry in A is considered, in that case A stands for the following unknown symmetric matrix:

$$\tilde{A} = \begin{pmatrix} 2 & -\alpha \\ -\alpha & 2 \end{pmatrix}$$

and the solution set will be given by

$$S_{sym}(A,b) = \{\tilde{x} \in R^n \mid \tilde{A}\tilde{x} = \tilde{b} \text{ for some } \tilde{A} \in A, \tilde{b} \in b \text{ with } \tilde{A}^T = \tilde{A}\}$$

The exact solution set is (0.6, –0.6) and (0.4, –0.4), which is smaller than the previous nonsymmetric case, and indicated by a heavy line in Figure 12.2. The hull of the solution set is:

$$\Diamond S_{sym}(A,b) = \begin{pmatrix} [0.4,\ 0.6] \\ [-0.6,\ -0.4] \end{pmatrix} \neq A^H b$$

which is narrower than the hull of the previous general case.

It is clear that care in the application of interval arithmetic to maintain sharp estimate of the interval solution is very important, especially in cases such as bounding the effect of uncertainties on the solution of engineering problems. In general, the sharpest results are obtained when proper bracketing is used, dependency is avoided, and the physical nature of the problem is considered.

12.3 Interval Methods for Predicting System Response Due to Uncertain Parameters

Interval methods are a simple, elegant, and computationally efficient way to include uncertainty when modeling engineering systems with uncertain parameters. As defined earlier, an interval number is the closed set of all real numbers between and including the interval's lower and upper bound [2]. Real-life engineering practice deals with parameters of unknown values: modulus of elasticity, yield stress, geometrical dimensions, density, and gravitational acceleration are some examples. In application to mechanics problems, an interval representation lends itself to the treatment of tolerance specifications on machined parts, components that are inspected, and whose properties will fall within a finite range. For example, the diameter of a rod is given as $D \pm \delta$ or in an interval form as $[D - \delta, D + \delta] = [D^l, D^u]$. In the case of live loads, the value can often be bounded by two extreme values; that is, the live load acting on an office building might be given to be between 1.8 and 2.0 kN/m^2 or in an interval form as [1.8, 2.0] kN/m^2. Experimental data, measurements, statistical analysis, and expert knowledge represent information for

Copyright 2005 by CRC Press LLC

defining bounds on the possible ranges of such quantities. Thus, considering the values of unknown parameters to be defined within intervals that possess known bounds might be a realistic or natural way of representing uncertainty in engineering problems.

Tools that provide sharp predictions of system response including uncertainty in an interval form will provide the infrastructure for wide inclusion of uncertainties in engineering models. However, this will only occur if the sharp results corresponding to the physical problem can be obtained.

12.3.1 Sensitivity Analysis

Sensitivity analysis represents a need when the prediction of system response is required due to variations in the system's parameters. For example [4], if x is a vector of approximate parameters and Δx is a vector containing the bounds for the error in components of x, intervals are a powerful tool to obtain the influence of these parameters' variations on the response function $F(x)$; that is, one is interested in finding a vector ΔF such that, for given Δx,

$$|F(\tilde{x}) - F(x) \leq \Delta F \quad \text{for } |\tilde{x} - x| \leq \Delta x \tag{12.15}$$

Sometimes the dependence of ΔF on Δx is also sought. Stated in the form

$$F(\tilde{x}) \in [F(x) - \Delta F, F(x) + \Delta F] \quad \text{for } \tilde{x} \in [x - \Delta x, x + \Delta x] \tag{12.16}$$

Another interesting example is sensitivity analysis in optimization problems [7]. Consider an unperturbed optimization problem in which the objective function and constraints depend on a vector c of parameters. To emphasize the dependence on c, the problem is introduced as

$$\begin{aligned} &\text{Minimize} \quad f(x,c) \\ &\text{subject to} \quad p_i(x,c) \leq 0 \quad \text{for} \quad i = 1,\ldots,m \\ &\qquad\qquad\quad q_j(x,c) = 0 \quad \text{for} \quad j = 1,\ldots,r \end{aligned}$$

To show the dependence of the solution on c, the solution value is given as $f^*(c)$ and the solution point(s) as $x^*(c)$, where $f(x^*(c), c) = f^*(c)$.

In the perturbed case, c will be allowed to vary over interval vector C. As c varies over the range of C, the obtained set of solution values is

$$f^*(C) = \{f^*(c): \quad c \in C\}$$

and a set of solution points

$$x^*(C) = \{x^*(c): \quad c \in C\}$$

in this case, the width of the interval $f^*(C)$ represents a measure of the sensitivity of the problem to variation of c over the range of C.

12.3.2 Interval Finite Element Methods

Our focus in this section is the introduction of the principal concept for formulation of finite element methods (FEM) using intervals as a way to handle uncertain parameters. Our goal is to capture the behavior of a physical system. Ad-hoc replacement of scalar quantities by intervals will not provide sharp (or correct) measures of the uncertainty in a physical system. We will present various *intervalizations* of finite element methods, and relate these methods to the corresponding implicit assumption about physical parameter uncertainty that each method represents.

Copyright 2005 by CRC Press LLC

Finite element methods have found wide appeal in engineering practice (i.e., [20–22]). They have been used extensively in many engineering applications such as solids, structures, field problems, and fluid flows. Formulation of the Interval Finite Element Method (IFEM) follows the conventional formulation of FEM except that the values of the variables and the parameters of the physical system are assigned interval values. We then proceed with certain assumptions to idealize it into a mathematical model that leads to a set of governing *interval* algebraic equations.

During the past decade, researchers from different engineering disciplines have been contributing significantly to the development of Interval Finite Element Methods. A review of the major IFEM developments can be found in the authors' works [19, 23]. Additional contributions to IFEM include the work of Kupla, Pownuk, and Skalna [24], in which they use intervals to model uncertainty in linear mechanical systems. Also, Pownuk [25] has introduced an interval global optimization method in an attempt to find all stationary global solutions. Akpan et al. [26] developed a fuzzy interval-base finite element formulation and used the response surface method to predict the system response. The system response is calculated for various sets of input values to develop a quadratic functional approximation between the input variables and the response quantities. Combinatorial optimization is performed on the approximate function to determine the binary combinations of the interval variables that result in extreme responses. Such an approximation might give satisfactory results in the case of interval load; however, the general case requires higher-order functions and the work does not provide any evaluation for the possibility of obtaining the right combinations of the input variables. In one of the examples, 13 finite element runs were required compared to 65 runs for all possible combinations. Chen S. et al. [27] introduced an interval formulation for static problems based on a perturbed stiffness neglecting the higher-order parts in the unknown variable approximation. The introduced results are not compared with the exact solutions of the respective problems. A fuzzy structural reliability analysis is introduced in the work of Savoia [28]; this formulation is based on the interval α-cut concept to compute membership functions of the response variables and is not introduced within the context of FEM. The work of Dessombz et al. [29] introduces an interval application, where free vibrations of linear mechanical systems under uncertainty were studied. Special attention has been devoted in this study to the dependency problem. The fixed-point theorem has been used to achieve a conservative enclosure to the system response in the case of narrow intervals. In the case of wide intervals, an interval partition approach is employed that requires costly repetitive runs. A comparison of different methodologies for uncertainty treatment in oil basin modeling has been conducted in the work of Pereira [30], and a successful alternative interval element-by-element finite element formulation for heat conduction problems has been proposed. In addition, as intervals represent a subset of the convex models, Ganzerli and Pantelides [31] developed a load and resistance convex model for optimum design. They [32] also conducted a comparison between convex and interval models within the context of finite elements, restricted to uncertain load. Both works were based on Cartesian product of the convex sets of the uncertain parameters and the load convex model superposition. Although sharp system response can be calculated by a single run of the response convex model, costly computations are required to obtain the response convex model itself. The present review highlights the general effort in the development of interval finite element, and shows that the main application of intervals to mechanical systems using formulations of IFEM has relied on implicit assumptions on the independence of interval quantities and the assumed width of an interval quantity.

However, for IFEM to gain acceptance as an engineering tool, two fundamental questions in the formulation and behavior of interval finite element must be resolved:

1. Does the replacement of the deterministic parameters by corresponding interval parameters lead to a violation of the underlying laws of physics?
2. What physical uncertainty is implied by the introduction of interval parameters?

We will illustrate the finite element *intervalization* using a simple two-element finite element approximation. We will explore the use of interval numbers to represent uncertainties in the values of Young's modulus, E, and the loading function q, (or boundary conditions τ).

Copyright 2005 by CRC Press LLC

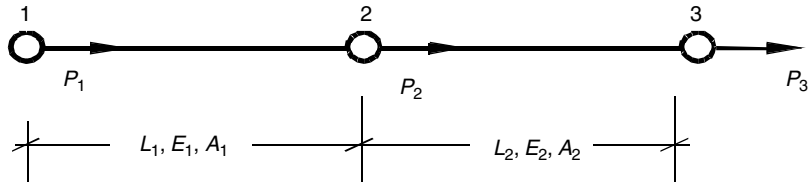

FIGURE 12.3 Two connected linear truss elements.

Figure 12.3 shows the discretization of a bar into two linear truss elements that share node 2. In this example, we assume that the values of E and A are constant over each element. In general, E and A are always positive; thus, as long as the intra-element variation of E is smooth enough and bounded, an interval representation of the integrated element stiffness can be constructed, Dubois, [33].

The resulting noninterval finite element equations are given by

$$\begin{pmatrix} \frac{E_1A_1}{L_1} & -\frac{E_1A_1}{L_1} & 0 \\ -\frac{E_1A_1}{L_1} & \frac{E_1A_1}{L_1}{}_1 + \frac{E_2A_2}{L_2} & -\frac{E_2A_2}{L_2} \\ 0 & -\frac{E_2A_2}{L_2} & \frac{E_2A_2}{L_2} \end{pmatrix} \begin{pmatrix} u_1 \\ u_2 \\ u_3 \end{pmatrix} = \begin{pmatrix} P_1 \\ P_2 \\ P_3 \end{pmatrix} \tag{12.17}$$

Let us consider the case where the values of Young's modulus E and load vector $\boldsymbol{P}$ are uncertain but the bounds of the possible values are known. It is natural to express E and $\boldsymbol{P}$ as an interval quantity and interval vector, respectively. An interval x is a closed set in R defined by:

$$x \equiv [x^l, x^u] := \{\, \tilde{x} \in R \mid x^l \le \tilde{x} \le x^u \} \tag{12.18}$$

where superscripts l and u denote lower and upper bounds, respectively.

Replacement of the scalar E by an interval quantity and vector $\boldsymbol{P}$ by interval vector lead to the following straightforward (**but physically inconsistent**) interval system of equations:

$$\begin{pmatrix} \frac{[E_1^l, E_1^u]A_1}{L_1} & -\frac{[E_1^l, E_1^u]A_1}{L_1} & 0 \\ -\frac{[E_1^l, E_1^u]A_1}{L_1} & \frac{[E_1^l, E_1^u]A_1}{L_1} + \frac{[E_2^l, E_2^u]A_2}{L_2} & -\frac{[E_2^l, E_2^u]A_2}{L_2} \\ 0 & -\frac{[E_2^l, E_2^u]A_2}{L_2} & \frac{[E_2^l, E_2^u]A_2}{L_2} \end{pmatrix} \begin{pmatrix} u_1 \\ u_2 \\ u_3 \end{pmatrix} = \begin{pmatrix} [P_1^l, P_1^u] \\ [P_2^l, P_2^u] \\ [P_3^l, P_3^u] \end{pmatrix} \tag{12.19a}$$

or

$$\boldsymbol{KU} = \boldsymbol{P} \tag{12.19b}$$

with the interval stiffness matrix $K \in IR^{n \times n}$ and the interval load vector $P \in IR^n$. The vector of unknowns $\boldsymbol{U}$ is the interval displacement vector. This linear interval equation is defined as the family of linear equations

$$\tilde{K}\tilde{U} = \tilde{P} \qquad (\tilde{K} \in K, \tilde{P} \in P) \tag{12.20}$$

Copyright 2005 by CRC Press LLC

Thus, in this case we have linear systems of equations in which the coefficients are unknown numbers contained within given intervals. If we do not consider the **underlying physics** of the given system, we will be interested in the enclosure for the solution set of 12.19, given by

$$S(K,P) := \{\tilde{U} \in R^n \mid \tilde{K}\tilde{U} = \tilde{P} \text{ for some } \tilde{K} \in K, \tilde{P} \in P\} \tag{12.21}$$

The exact enclosure for the solution set of 12.19 can be obtained by solving for all possible combinations of the upper and lower bounds of the stiffness matrix coefficients and the right-hand side components.

The stiffness matrix is usually symmetric, and in such a case, the stiffness matrix will be a symmetric *interval* matrix and not an interval matrix in the general sense. The definition of symmetric interval matrix can be found in (Jansson, [34])

$$K_{sym} := \{\tilde{K} \in K, \ \tilde{K}^T = \tilde{K}\} \tag{12.22}$$

and Equation 12.19b takes the form

$$K_{sym}U = P \tag{12.23}$$

We will be interested in the enclosure for the solution set of 12.23, given by

$$S_{sym}(K_{sym}, P) := \{\ \tilde{U} \in R^n \mid \tilde{K}\tilde{U} = \tilde{P} \text{ for some } \tilde{K} \in K, \tilde{P} \in P \text{ with } \ \tilde{K}^T = \tilde{K}\} \tag{12.24}$$

The exact enclosure for the solution set of Equation 12.23 can be obtained by solving for all possible combinations of the upper and lower bounds of the stiffness matrix coefficients with the condition $k_{ij} = k_{ij}$ for $i, j = 1, ..., n, \ i \neq j$ and the right-hand side components.

The solution for both above-mentioned cases (i.e., the *general* and the *symmetric* case) does not represent a correct solution for the given physical problem, even if the solution is based on all possible combinations. Both solutions can overestimate the interval width of the physical problem. This is due to the multiple occurrences of stiffness coefficients in the stiffness matrix. The same physical quantity cannot have two different values (upper and lower bounds) at the same time, and interval arithmetic treats this physical quantity as multiple independent quantities of the same value. In other words, the physical problem has a unique but unknown value of E. Equation 12.19 allows different values of E to exist simultaneously. As will be demonstrated, even exact enclosures of solutions of finite element equations in this form produce physically unacceptable results. Historically, this loss of dependency combined with the well-known computational issues in computing sharp bounds for the solution of interval system of equations encouraged a number of earlier researchers to abandon the application of interval methods to finite element problems.

An alternative method for intervalization of finite element equations is to assume that the same value of Young's modulus E exists in the entire domain. This assumption results in the following interval equation for the two-element problem of Figure 12.2

$$\left([E^l, E^u]\right)\begin{pmatrix} \frac{A_1}{L_1} & -\frac{A_1}{L_1} & 0 \\ -\frac{A_1}{L_1} & \frac{A_1}{L_{1\,1}} + \frac{A_2}{L_2} & -\frac{A_2}{L_2} \\ 0 & -\frac{A_2}{L_2} & \frac{A_2}{L_2} \end{pmatrix}\begin{pmatrix} u_1 \\ u_2 \\ u_3 \end{pmatrix} = \begin{pmatrix} [P_1^l, P_1^u] \\ [P_2^l, P_2^u] \\ [P_3^l, P_3^u] \end{pmatrix} \tag{12.25}$$

Copyright 2005 by CRC Press LLC

Such a formulation leads to an exact solution for the interval system. However, the material property is limited to a constant interval parameter (E) for the entire domain and is not attractive to engineering applications that require solving realistic problems, where the same parameter might vary within the domain itself.

The exact solutions to the interval finite element problems can only be obtained if the *underlying laws of physics are not violated*. Thus, for the considered case, to obtain the exact *physical* enclosure for the solution set of Equation 12.19 we have to trace back the sources of dependency in the formulation of interval finite elements. To illustrate the concept, let us use again, as an example, the two-bar truss of Figure 12.3.

The element interval stiffness matrices can be introduced in the following form:

$$K_1 = \chi_1 \begin{pmatrix} k_1 & -k_1 \\ -k_1 & k_1 \end{pmatrix}, \quad K_2 = \chi_2 \begin{pmatrix} k_2 & -k_2 \\ -k_2 & k_2 \end{pmatrix} \tag{12.26}$$

$$k_i = \frac{E_i A_i}{l_i} \tag{12.27}$$

where $\boldsymbol{K}_i$ = stiffness matrix of i^{th} finite element (for $i = 1, 2$); k_i = stiffness coefficient of the i^{th} element; E_i = modulus of elasticity of the i^{th} element; A_i = cross-sectional area of the i^{th} element; l_i = length of the i^{th} element; and χ_i = the interval multiplier of the i^{th} finite element obtained due to uncertainty in E_i, A_i, and l_i. The presented example represents a simple case of structural problems where the stiffness coefficients are the same for each element and are obtained only from axial stress contribution. However, the general formulation of interval finite element is more involved, where usually the stiffness coefficients are not equal for each element and include contributions from all components of the general stress state. The assemblage of global stiffness matrix can be given by

$$K = \sum_e \left\{ L_e^T \left(\sum_i [\chi_i(\mathrm{k}_i)] \right) L_e \right\} \tag{12.28}$$

where $\boldsymbol{L}_e$ is the element Boolean connectivity matrix with the dimension (number of degrees of freedom per element × total number of degrees of freedom). In this example, the element Boolean connectivity matrix has the following structure

$$L_1 = \begin{pmatrix} 1 & 0 & 0 \\ 0 & 1 & 0 \end{pmatrix}, \quad \text{and} \quad L_2 = \begin{pmatrix} 0 & 1 & 0 \\ 0 & 0 & 1 \end{pmatrix} \tag{12.29}$$

Finally, the global stiffness matrix takes the following form:

$$K_{phys} = \begin{pmatrix} \chi_1 k_1 & -\chi_1 k_1 & 0 \\ -\chi_1 k_1 & \chi_1 k_1 + \chi_2 k_2 & -\chi_2 k_2 \\ 0 & -\chi_2 k_2 & \chi_2 k_2 \end{pmatrix} \tag{12.30}$$

By imposing the boundary conditions, displacement of the first node equals zero in this case, we obtain:

$$K_{phys} = \begin{pmatrix} \chi_1 k_1 + \chi_2 k_2 & -\chi_2 k_2 \\ -\chi_2 k_2 & \chi_2 k_2 \end{pmatrix} \tag{12.31}$$

Copyright 2005 by CRC Press LLC

The interval load vector (right-hand side) can be introduced in the following form:

$$\boldsymbol{P}_{phys} = \begin{pmatrix} \lambda_1 \mathrm{P}_1 \\ \lambda_2 \mathrm{P}_2 \\ \lambda_3 \mathrm{P}_3 \end{pmatrix} \tag{12.32}$$

where

$$\boldsymbol{P}_{phys} = \boldsymbol{P}_c + \boldsymbol{P}_b + \boldsymbol{P}_t \tag{12.33}$$

and $\boldsymbol{P}_c$ = the nodal load vector, $\boldsymbol{P}_b$ = the body force vector, and $\boldsymbol{P}_t$ = traction vector. The body force vector and the traction vector are given by:

$$\boldsymbol{P}_b = \sum_e \left\{ \boldsymbol{L}_e^T \left(\sum_i [\lambda_{ib}(p_{ib})] \right) \boldsymbol{L}_e \right\} \tag{12.34a}$$

$$\boldsymbol{P}_t = \sum_e \left\{ \boldsymbol{L}_e^T \left(\sum_i [\lambda_{it}(\mathrm{p}_{it})] \right) \boldsymbol{L}_e \right\} \tag{12.34b}$$

where p_{ib} is the body force contribution at the i^{th} integration point, and p_{it} is the traction contributions at the i^{th} integration point acting on the surface Γ, and λ is the interval multiplier for each load.

After imposing the boundary conditions, Equation 12.32 takes the following form:

$$\boldsymbol{P}_{phys} = \begin{pmatrix} \lambda_2 P_2 \\ \lambda_3 P_3 \end{pmatrix} \tag{12.35}$$

and the interval form of Equation 12.17 is

$$\boldsymbol{K}_{phys} \boldsymbol{U} = \boldsymbol{P}_{phys} \tag{12.36}$$

The exact enclosure for the solution set of *physical* interval finite Equation 12.36 will be given by

$$\mathrm{S}_{phys}(\boldsymbol{K}_{phys}, \boldsymbol{P}_{phys}) := \{ \tilde{\boldsymbol{U}} \in \boldsymbol{R}^n \mid \tilde{\boldsymbol{K}}_{phys}(\chi)\tilde{\boldsymbol{U}} = \tilde{\boldsymbol{P}}_{phys}(\lambda) \ \text{ for } \ \tilde{\chi}_i \in \chi_i, \ \tilde{\lambda}_i \in \lambda_i \} \tag{12.37}$$

The presented physical solution means that each uncertain parameter throughout the system, regardless of its multiple occurrences, is restricted to take only one unique value within the range of its interval.

The exact enclosure for the solution set of *physical* interval finite equation can be obtained by solving for all possible combinations of lower and upper bounds of uncertain parameters. Such a solution is possible for small size problems (few uncertain parameters); however, engineering applications might require solutions of huge systems where the "all possible combinations" approach is computationally prohibited and such problems are NP-hard problems.

For the solution of interval finite element (IFEM) problems, Muhanna and Mullen [23] introduced an element-by-element interval finite element formulation, in which a guaranteed enclosure for the solution of interval linear system of equations was achieved. A very sharp enclosure for the solution set

Copyright 2005 by CRC Press LLC

due to loading, material and geometric uncertainty in solid mechanics problems was obtained. Element matrices were formulated based on the physics, and the Lagrange multiplier method was applied to impose the necessary constraints for compatibility and equilibrium. Other methods for imposing the constraints (such as the penalty method) might also be used. Most sources of overestimation were eliminated. In this formulation, Equation 12.19b can be introduced in the following form:

$$\begin{pmatrix} K & C^T \\ C & \mathbf{0} \end{pmatrix} \begin{pmatrix} U \\ \lambda \end{pmatrix} = \begin{pmatrix} P \\ \mathbf{0} \end{pmatrix} \tag{12.38}$$

Here, $\boldsymbol{\lambda}$ is the vector of Lagrange multipliers, $C = (0 \quad 1 \quad -1 \quad 0)$, $\boldsymbol{CU} = 0$, and $\boldsymbol{K}$ is introduced as

$$DS = \begin{pmatrix} \chi_1 & 0 & 0 & 0 \\ 0 & \chi_1 & 0 & 0 \\ 0 & 0 & \chi_2 & 0 \\ 0 & 0 & 0 & \chi_2 \end{pmatrix} \begin{pmatrix} \frac{E_1A_1}{L_1} & -\frac{E_1A_1}{L_1} & 0 & 0 \\ -\frac{E_1A_1}{L_1} & \frac{E_1A_1}{L_1} & 0 & 0 \\ 0 & 0 & \frac{E_2A_2}{L_2} & -\frac{E_2A_2}{L_2} \\ 0 & 0 & -\frac{E_2A_2}{L_2} & \frac{E_2A_2}{L_2} \end{pmatrix} \tag{12.39}$$

where χ_i = the interval multiplier of the i^{th} finite element obtained due to uncertainty in E_i, A_i, and l_i. Such a form (i.e., $\boldsymbol{D}\,\tilde{S}$) allows factoring out the interval multiplier resulting with an exact inverse for ($\boldsymbol{D}\,\tilde{S}$).

Equation 12.38 can be introduced in the following equivalent form

$$KU + \tilde{C}^T\lambda = P \tag{12.40a}$$

$$\tilde{C}U = \mathbf{0} \tag{12.40b}$$

If we express K $(n \times n)$ in the form $D\tilde{S}$ and substitute in equation (12.40a)

$$D\tilde{S}U = P - \tilde{C}^T\lambda \tag{12.41}$$

where $D(n \times n)$ is interval diagonal matrix, its diagonal entries are the positive interval multipliers associated with each element, and n = degrees of freedom per element × number of elements in the structure. $\tilde{S}\,(n \times n)$ is a deterministic singular matrix (fixed point matrix). If we multiply Equation 12.40b by $D\tilde{C}^T$ and add the result to Equation 12.41, we get

$$D(\tilde{S}U + \tilde{C}^TCU) = (P - \tilde{C}^T\lambda) \tag{12.42}$$

or

$$\begin{aligned} &D(\tilde{S}U + \tilde{Q}U) = (P - \tilde{C}^T\lambda) \\ &D(\tilde{S} + \tilde{Q})U = (P - \tilde{C}^T\lambda) \\ &D\tilde{R}U = (P - \tilde{C}^T\lambda) \end{aligned} \tag{12.43}$$

where $\tilde{R}$ is a deterministic positive definite matrix, and the displacement vector $\boldsymbol{U}$ can be obtained from Equation 12.43 in the following form

$$U = \tilde{R}^{-1}D^{-1}(P - \tilde{C}^T\lambda) \tag{12.44}$$

Copyright 2005 by CRC Press LLC

where $\tilde{R}^{-1}D^{-1}$ is an exact inverse of the interval matrix $(D\tilde{R})$. Equation 12.44 can be presented in the form

$$U = \tilde{R}^{-1}M\,\delta \tag{12.45}$$

Matrix $\boldsymbol{M}$ has the dimensions ($n \times$ number of elements) and its derivation has been discussed in the previous works of Mullen and Muhanna [19]. The vector δ is an interval vector that has the dimension of (number of elements $\times$ 1): its elements are the diagonal entries of D^{-1} with the difference that every interval value associated with an element is occurring only once. If the interval vector λ can be determined exactly, the solution of Equation 12.45 will represent an exact hull for the solution set of the general interval FE equilibrium equation

$$KU = P \tag{12.46}$$

As a matter of fact, this is the case in statically determinate structures. An exact hull for the solution set can be achieved because vector λ, in the present formulation, represents the vector of internal forces, and in statically determinate structures the internal forces are independent of the structural stiffness. Consequently, using the deterministic value of λ (mid point of λ, the midpoint of an interval a is defined as $a_c = \text{mid}(a) = \frac{a^u + a^l}{2}$) in Equation 12.44 results in an exact hull for the solution set of statically determinate structures with uncertain stiffness. But in the case of statically indeterminate structures, values of λ depend of the structural stiffness and the use of deterministic value of λ results in a very good estimate for the solution, but of course a narrower one. The details for handling the general case is discussed in [23].

This formulation does not allow any violation to the underlying laws of physics, and results in very sharp interval solutions for linear mechanics problems and in exact solutions for one group of these problems (statically determinate problems).

We will illustrate this discussion by numerical results of the following example.

The example is a triangular truss shown in Figure 12.4. The structure is loaded by a deterministic horizontal load 30*KN* and an interval vertical load [50, 100] *KN*, at the top node. The truss has the following data: cross-sectional area $A = 0.001\ m^2$, Young's modulus $E = 200\ GPa$, and 10% uncertainty in E; that is, $E = [190, 200]\ GPa$ was assumed for each element. The results for displacement of selected nodes are given in Table 12.1.

The results show that the general interval solution is wider than the symmetric interval solution. The symmetric interval solution overestimates the physical diameter by 127.2 to 182.5%, while the general interval solution overestimates the exact diameter by 130 to 186.6%.

The above-mentioned discussion illustrates how interval methods can be used for predicting system response due to uncertain parameters. However, different intervalizations of finite element imply different physical uncertainty: the *general interval approach*, which is a naïve replacement of the deterministic

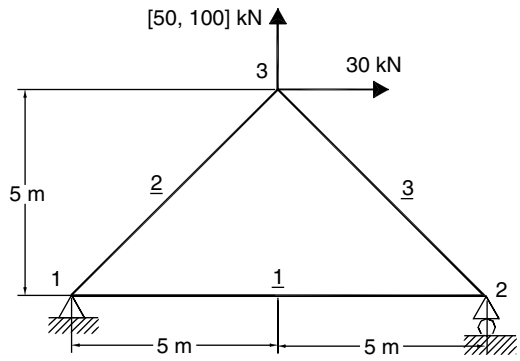

FIGURE 12.4 Triangular truss.

Copyright 2005 by CRC Press LLC

TABLE 12.1 Nodal Displacements of Triangular Truss

	node 2	node 3	
	U	U	V
Node displacements	$U \times 10^{-3}\, m$	$U \times 10^{-3}\, m$	$V \times 10^{-3}$ m
Comb. (physical)	[-1.8421053, -0.4761905]	[-0.0349539, 0.9138331]	[1.9216828, 4.6426673]
Symmetric interval	[-2.7022107, -0.2451745]	[-0.6531157, 1.0781411]	[1.7879859, 5.24493035]
General interval	[-2.7022107, -0.1784592]	[-0.6531157, 1.1173116]	[1.7111129, 5.24493035]
D_{ph}[a]	1.36591	0.94879	2.72098
D_s	2.445704	1.73126	3.46132
D_i	2.52375	1.77043	3.53819
Ds/D_{ph}	1.799	1.825	1.272
Di/De	1.848	1.866	1.300

[a] D_{ph}, D_s and D_i are the diameter of the exact solution, symmetric interval and general interval solution, respectively.

parameters with interval ones, leads to a violation of the physics and even the exact solutions lead to a catastrophic overestimation that does not reflect any realistic evaluation of the system response to the introduced uncertainty. The *symmetric interval approach*, which accounts for symmetry in the system matrix, treats the diagonal interval coefficients as independent ones and, consequently, leads to results of the same nature of the general interval approach. Within the category of what we call physical formulation, two approaches were discussed; the *first* assumes the same interval value of a given parameter exists in the entire domain. Such an assumption limits the variability of parameters within the considered domain to a constant value, and consequently it might not be considered attractive to engineering applications that require solutions that are more realistic. The *second* introduced approach is the element-by-element formulation, where the interval parameters are allowed to vary within the considered domain including different level of variability between elements. This formulation leads to very sharp results and to a realistic propagation of uncertainty in the system with no violation of the physics.

12.4 Interval Methods for Bounding Approximation and Rounding Errors

12.4.1 Approximation Errors

Intervals and ranges of functions over intervals arise naturally in large number of situations [4, 7, 11]. Frequently, approximate mathematical procedures are used in place of the exact ones, using the mean value theorem, an approximate value for the derivative of a real continuously differentiable function $f(x)$ for $x_1 \neq x_2$, is

$$f'(\xi) = \frac{f(x_2) - f(x_1)}{x_2 - x_1} \tag{12.47}$$

for some ξ between x_1 and x_2. To make more than a theoretical or qualitative use of this formula, interval arithmetic can compute or at least bound the range of f'. Another example for interval methods in bounding approximation errors is the use of Taylor's series. It is well known that Taylor's series provides a means to predict a function value at one point in terms of the function value and its derivatives at another point. In particular, the theorem states that any smooth function can be approximated as a polynomial in the following form

$$f(x_{i+1}) = f(x_i) + f'(x_i)h + \frac{f''(x_i)}{2!}h^2 + \cdots + \frac{f^{(n)}(x_i)}{n!}h^n + \frac{f^{(n+1)}(\xi)}{(n+1)!}h^{n+1} \tag{12.48}$$

Copyright 2005 by CRC Press LLC

where $h = (x_{i+1} - x_i)$ and ξ is a value of x between x_i and x_{i+1}. Once again, interval arithmetic can determine the approximation error by computing an enclosure of $f^{(n+1)}(\xi)$, where ξ ranges over the interval $[x_i, x_{i+1}]$.

12.4.2 Rounding-off Errors

Interval arithmetic is a powerful tool to handle rounding-off errors resulting from the finite floating-point representation of numbers on computers. Using floating-point representation, a fractional number is expressed as

$$m \cdot b^e \tag{12.49}$$

where m is the mantissa, b is the base of the number system used, and e is the exponent. For example, the number 254.67 could be represented as 0.25467×10^3 in a floating-point base-10 system. This results in the fact that there is only a finite set $\mathbb{M} \subseteq \mathbb{R}$ of machine-representable numbers. Given any real number x lying between two consecutive machine numbers $x_1, x_2 \in \mathbb{M}$, the interval between these exactly represented numbers Δx will be proportional to the magnitude of the number x being represented. For normalized floating-point numbers (the mantissa has no leading zero digit), this proportionality can be expressed, for cases where chopping is employed, as

$$\frac{|\Delta x|}{|x|} \leq \varepsilon \tag{12.50}$$

and, for cases where rounding is employed, as

$$\frac{|\Delta x|}{|x|} \leq \frac{\varepsilon}{2} \tag{12.51}$$

where ε is referred to as the machine epsilon, which can be computed as

$$\varepsilon = b^{1-L} \tag{12.52}$$

where b is the number base and L is the number of significant digits in the mantissa (mantissa length in bits). The inequalities in Equations 12.50 and 12.51 signify that these are error bounds. For example, computers that use the IEEE format allow 24 bits to be used for the mantissa, which translates into about seven significant base-10 digits of precision; that is

$$\varepsilon = b^{1-24} \approx 10^{-7} \tag{12.53}$$

with range of about 10^{-38} to 10^{39}. However, if the number of computer words used to store floating-point numbers is doubled, such computers can provide about 15 to 16 decimal digits of precision and a range of approximately 10^{-308} to 10^{-308}. Despite the provided high precision, rounding-off errors still represent a crucial problem for achieving numerical solutions for a series of problems, such as root finding, function evaluation, optimization, and the formulation of self-validating methods. One might argue that if computed results, using single and double precision, agree to some number of digits, then those digits are correct. The following example of Rump [35] shows that such an argument is not valid. The evaluated function is

$$f(x, y) = 333.75y^6 + x^2(11x^2y^2 - y^6 - 121y^4 - 2) + 5.5y^8 + \frac{x}{2y} \tag{12.54}$$

for $x = 77617$ and $y = 33096$. The evaluation was done on an S/370 computer. All input data is exactly representable on the computer, so the only rounding-off error occurs during evaluation.

Copyright 2005 by CRC Press LLC

Single, double, and extended precision were used, which were the equivalent of approximately 6, 17, and 34 decimal digit arithmetic. The following values of f were obtained

Single precision: $f = 1.172603\ldots$
Double precision: $f = 1.1726039400531\ldots$
Extended precision: $f = 1.172603940053178\ldots$

All three results agree in the first seven decimal digits. However, they are all completely incorrect. They do not even have the correct sign. The correct value is

$$f = -0.8273960599468213$$

with an error of at most one unit in the last digit.

Interval arithmetic represents an efficient tool to overcome such a numerical difficulty by using what is referred to as rounding-off error control. For an interval arithmetic with floating point endpoints and floating point operations, we need outward rounding. This can be achieved by multiplying the result by some $1 \pm \varepsilon$, ε denoting the relative rounding error unit. Since the establishment of the IEEE 754 arithmetic standard, optimal floating-point operations in a specifiable rounding mode are available. The important rounding modes are ∇ toward $-\infty$, and Δ towards $+\infty$.

Frequently, a processor may be switched into such a rounding mode. This means that subsequent operations are performed in that mode until the next switch. Interval arithmetic uses the notation that an arithmetic expression in parentheses preceded by a rounding symbol implies that all operations are performed in floating-point in the specified rounding mode. Then for a set $\mathbb{M}$ of floating point numbers (e.g., single or double precision including $\pm\infty$), IEEE 754 defines

$$\begin{aligned} &\forall a, b \in \mathbb{M}, \quad \forall \circ \in \{+, -, \cdot, /\} \\ &\nabla(a \circ b) = \max\{x \in \mathbb{M} : x \le a \circ b\} \\ &\Delta(a \circ b) = \min\{x \in \mathbb{M} : a \circ b \le x\} \end{aligned} \tag{12.55}$$

Thus, rounding is correct and best possible. Note that this is true for all floating-point operands and operations.

12.5 Future Developments of Interval Methods for Reliable Engineering Computations

In the previous sections, interval methods have been demonstrated to be an efficient method for the accounting of uncertainty in parameters in engineering models. Interval methods also account for truncation errors from the computer implementation of engineering models. There is also the possibility that intervals can be used to quantify the impact of other sources of errors in engineering models. One such error is the discretization error associated with the generation of approximations to partial differential equations. Discretization errors have been extensively studied; early work on bounding the discretization error was reported by Aziz and Babuska [36]. Following this work, the convergence behavior of most finite element formulations has been determined. Knowledge of the behavior of discretization errors is key to the development of adaptive solutions strategies [37]. We believe that interval representation can be used to incorporate bounds on the solution associated with discretization of a partial differential equation in combination with the other uncertainties identified above.

We will first illustrate this capability using the one-dimensional truss element as describe above. While the truss element is an exact solution to the PDF when loads are restricted to the endpoints of each element, the element is also appropriate for one-dimensional problems with arbitrary loading along the length of the element. In this case, the finite element solution is not exact and one generates discretization errors. Early work by Babuska and Aziz has shown that the global finite element discretization error is bounded by the interpolation error. Thus, one needs only to examine how close the finite element shape

Copyright 2005 by CRC Press LLC

functions can come in representing an exact solution to develop *a priori* error bounds. For example, one can show from simple Taylor theorem calculations [38], the one-dimensional linear element described in Section 12.3, has a discretization error of

$$\|u^h - u\| \le \frac{h^2}{8} \left\| \frac{\partial^2 u}{\partial x^2} \right\| \tag{12.56}$$

Here, u^h is the finite element solution, u the exact solution to the PDE, and h is the length of the element. From the original differential equation, with uniform values of E and A, the bounds can be written.

$$\|u^h - u\| \le \frac{h^2}{8} \left\| \frac{q}{AE} \right\| \tag{12.57}$$

Consider the problem of a rod hanging under its own weight, (i.e., q is the weight per unit length), the exact displacement is given by

$$u(x) = \frac{q}{AE}\left(lx - \frac{x^2}{2} \right) \tag{12.58}$$

On the other hand, a single element FEA model predicts

$$u(x) = \frac{q}{AE}\left(\frac{lx}{2} \right) \tag{12.59}$$

giving a maximum error of $ql^2/8AE$ located at the center of the element. The maximum error as a function of element size is given in Table 12.2.

As can be seen, the predicted errors and the observed errors in this problem are identical. While this example provides insight into the potential of bounding finite element errors, it has several limitations: the problem is one-dimensional, a uniform mesh was used, and the nature of the problem was self-similar — inducing the same error pattern in each element independent of size. The self-similar nature of the error in this problem avoids an important difficulty in bounding discretization errors. Most error estimates are global. They provide bounds on measures such as the error in energy in the solution. Application of global discretization errors to each point in the solution results in loss of sharpness in the resulting bounds, often leading to useless results. Sharper bounds on discretization error can be obtained from *a posteriori* errors [39]. Sharp bounds for the energy norm of the discretization error have been developed by Babuska, Strouboulis, and Gangaraj [40]. They employ an iterative evaluation of the element–residuals and provide *a posteriori* sharp bounds on the reliability interval in the energy norm.

Local error bounds have been developed in terms of an additive combination of "pollution errors" and local element residual errors. *A posteriori* error bounds are calculated on a small patch of elements using local element residual errors. The pollution errors, which represent sources of error outside the small patch of elements, are added to provide sharp local error bounds [41, 42].

TABLE 12.2 Finite Element Errors for a Bar under Its Own Weight

Number of Elements	Max FEA Error	Location(s)	Predicted Error
1	0.125 *ql/EA*	*l*/2	0.125 *ql/EA*
2	0.03125 *ql/EA*	*l*/4 and 3*l*/4	0.03125 *ql/EA*
3	0.013888 *ql/EA*	*l*/6, *l*/2 and 5*l*/6	0.013888 *ql/EA*

Copyright 2005 by CRC Press LLC

Another method of bounding local errors is a concept of attributing all discretization errors to errors in constitutive models [43]. In this method, the governing PDE are considered in terms of separate equilibrium, constitutive, and continuity equations. The displacement finite element solution exactly satisfies the continuity equation. The finite element stress field is transformed into a field that stratifies the equilibrium equation. The changes in the stress field calculated from the FEM and a field that satisfies equilibrium are accommodated by a perturbed constitutive equation. This results in an exact solution to a perturbed problem. All discretization errors are represented by interval bounds on material parameters. In some respects, this method is the inverse problem of IFEM presented in Section 12.3.2.

12.6 Conclusions

Reliable engineering computing is perhaps the only way to ensure a guaranteed solution for engineering problems. A guaranteed solution can be achieved only if all sources of errors and uncertainty are properly accounted for. Errors and uncertainty can be bounded using the concept of interval representation and interval numbers.

Five major frameworks that use interval-based representation of uncertainty have been discussed in this chapter, namely: imprecise probability, possibility theory, the Dempster-Shafer theory of evidence, fuzzy set theory, and convex set modeling. Interval methods for predicting system response under uncertainty were introduced. Sensitivity analysis using intervals has been illustrated; the formulation of Interval Finite Element Method (IFEM) has been discussed, with a focus on dependency problems using Element-By-Element approach. Interval methods for bounding approximation and rounding errors have been introduced. Despite the availability of high-precision computers, rounding-off errors still represent a crucial problem for achieving numerical solutions for a series of problems, such as root finding, function evaluation, optimization, and the formulation of self-validating methods. Intervals show superiority in handling rounding-off errors. There is also the possibility that intervals can be used to quantify the impact of other sources of errors in engineering models. One such error is the discretization errors associated with the generation of approximations to partial differential equations.

Interval representation allows the characterization of uncertainties in model parameters and errors in floating-point representations in digital computers, as well as the potential for representing errors from the discretization of engineering models. This common representation allows for all sources of errors and uncertainty to be represented in a consistent manner. Reliable engineering computations require all sources of uncertainty to be quantified and incorporated into the calculated solutions. Using interval representation may be the only way to accomplish this goal.

References

1. Hansen, E., Interval arithmetic in matrix computation, *J.S.I.A.M., series B, Numerical Analysis*, Part I, 2, 308–320, 1965.
2. Moore, R.E., *Interval Analysis*, Prentice Hall, Englewood Cliffs, NJ, 1966.
3. Alefeld, G. and Herzberger, J., *Introduction to Interval Computations*, Academic Press, New York, 1983.
4. Neumaier, A., *Interval Methods for Systems of Equations*, Cambridge University Press, 1990.
5. Dwyer, P.S., *Computation with Approximate Numbers*, *Linear Computations,* P.S. Dwyer, Ed., Wiley, New York, 1951, 11–34.
6. Sunaga, T., Theory of interval algebra and its application to numerical analysis, *RAAG Memoirs 3*, 29–46, 1958.
7. Hansen, E., *Global Optimization Using Interval Analysis*, Marcel Dekker, New York, 1992.
8. Rump S.M., Self-validating methods, *Journal of Linear Algebra and Its Application,* 324, 3–13, 2001.

Copyright 2005 by CRC Press LLC

9. Alefeld, G. and Herzberger, J., *Introduction to Interval Computations*, Academic Press, New York, 1983.
10. Hansen, E.R., Global optimization using interval analysis — the one-dimensional case, *J. Optim. Theory*, Appl 29, 331–334, 1979.
11. Moore, R.E., *Methods and Applications of Interval Analysis*, SIAM, Philadelphia, 1979.
12. Rohn, Rump, and Yamamot, Preface, *Linear Algebra and Its Applications*, 324, 1–2, 2001.
13. Ferson and Sentz, Combination of Evidence in Dempster-Shafer Theory, *SAND 2002-0835*, 2002.
14. Kaufman and Gupta, *Introduction to Fuzzy Arithmetic, Theory and Applications*, Van Nostrand Reinhold, 1991.
15. Ben-Haim and Elishakoff, *Convex Models of Uncertainty in Applied Mechanics*, Elsevier Science, New York, 1990.
16. Ben-Haim, Yakov, *Information-Gap Decision Theory*, Academic Press, New York, 2001.
17. Apostolatos, N. and Kulisch, U., Grundzüge einer Intervallrechtung für Matrizen und einige Anwwendungen, *Elektron. Rechenanlagen,* 10, 73–83, 1968.
18. Mayer, O., Algebraische und metrische Strukturen in der Intervallrechung und eingine Anwendungen, *Computing,* 5, 144–162, 1970.
19. Mullen, R.L. and Muhanna, R.L., Bounds of structural response for all possible loadings, *Journal of Structural Engineering, ASCE*, 125(1), 98–106, 1999.
20. Bathe, K., *Finite Element Procedures,* Prentice Hall, Upper Saddle River, NJ, 1996.
21. Hughes, T.J.R., *The Finite Element Method,* Prentice Hall, Englewood Cliffs, NJ, 1987.
22. Zienkiewicz, O.C. and Taylor, R.L., *The Finite Element Method,* fourth edition, McGraw-Hill, New York, 1991.
23. Muhanna, R.L. and Mullen, R.L., Uncertainty in mechanics problems — interval-based approach, *Journal of Engineering Mechanics, ASCE,* 127(6), 557–566, 2001.
24. Kulpa, Z., Pownuk, A., and Skalna, I., Analysis of linear mechanical structures with uncertainties by means of interval methods, *Computer Assisted Mechanics and Engineering Sciences,* Vol. 5, Polska Akademia Nauk., 1998.
25. Pownuk, A., New Inclusion Functions in Interval Global Optimization of Engineering Structures, *ECCM-2001 European Conference on Computational Mechanics,* June 26–29, Cracow, Poland, 2001.
26. Akpan, U.O., Koko, T.S., Orisamolu, I.R., and Gallant, B.K., Practical fuzzy finite element analysis of structures, *Finite Elements in Analysis and Design,* 38(2), 93–111, 2001.
27. Chen, S.H., Lian, H.D., and Yang, X.W., Interval static displacement analysis for structures with interval parameters, *International Journal for Numerical Methods in Engineering,* 53(2), 393–407, 2002.
28. Savoia, M., Structural reliability analysis through fuzzy number approach, with application to stability, *Computers & Structures,* 80(12), 1087–1102, 2002.
29. Dessombz, O., Thouverez, F., Laîné, J.P., and Jézéquel, L., Analysis of mechanical systems using interval computations applied to finite elements methods, *Journal of Sound and Vibration,* 239(5), 949–968, 2001.
30. Pereira, S.C.A., *Dealing with Uncertainty in Basin Modeling,* thesis, Department of Civil Engineering, University of Rio De Janeiro, Brazil, 2002.
31. Ganzerli, S. and Pandelides, C.P., Load and resistance convex models for optimum design, *Structural Optimization,* 17, 259–268, 1999.
32. Pantelides, C.P. and Ganzerli, S., Comparison of fuzzy set and convex model theories in structural design, *Mechanical Systems and Signal Processing,* 15(3), 499–511, 2001.
33. Dubios, D. and Prade, H., Towards Fuzzy Differential Calculus Part 2: Intergration on Fuzzy Intervals, *Fuzzy Sets and Systems,* Vol. 8, 105–116, 1982.
34. Jansson, C., Interval Linear System with Symmetric Matricies, Skew-Symmetric Matricies, and Dependencies in the Right Hand Side, *Computing*, 46, 265–274, 1991.
35. Rump, S. M., *Algorithm for Verified Inclusions — Theory and Practice,* Moore, 1988,109–126.

Copyright 2005 by CRC Press LLC

36. Aziz, A.K. and Babuska, I., Part I, Survey lectures on the mathematical foundations of the finite element method, *The Mathematical Foundations of the Finite Element Methods with Applications to Partial Differential Equations,* Academic Press, New York, 1972, 1–362.
37. Zienkiewicz, O.C., Kelly, D.W., Cago, J.P. de S.R., and Babuska, I., The hierarchical finite element approaches, error estimates and adaptive refinement, J.R. Whiteman, Ed., *The Mathematics of Finite Elements and Applications,* Volume IV, Mafelap, 1982, 313–346.
38. Strang, G. and Fix, G., *An Analysis of the Finite Element Method,* Prentice Hall, Englewood Cliffs, NJ, 1972.
39. Babuska, I. and Rheinboldt, W.C., *A posteriori* error estimate for the finite element method, *International J. for Numerical Methods in Engineering,* 12, 1597–1615, 1978.
40. Babuska, I., Strouboulis, T., and Gangaraj, S.K., Guaranteed computable bounds for the exact error in the finite element solution, *Computer Methods in Applied Mechanics and Engineering,* 176, 51–79, 1999.
41. Oden, J.T. and Feng, Y., Local and pollution error estimates for finite element approximations of elliptical boundary value problems, *Journal of Applied and Computations Mathematics,* 74, 245–293, 1996.
42. Liao, X. and Nochetto, R.H., Local *a posteriori* error estimates and adaptive control of pollution effect, *Numerical Methods Partial Differential Equations,* 19, 421–442, 2003.
43. Ladeveze, P., Rougeot, Ph., Blanchard, P., and Moreau, J.P., Local error estimators for finite element linear analysis, *Computer Methods in Applied Mechanics and Engineering,* 176, 231–246, 1999.

Appendix 12.1 Interval Arithmetic Operations

The main arithmetic operations — addition, subtraction, multiplication, and division — are defined as follows [4]:

Suppose that we have the interval numbers: $x = [a,b]$, $y = [c,d]$.

1. Addition:

$$x + y = [a + c, b + d]$$

2. Subtraction:

$$x - y = [a - d, b - c]$$

3. Multiplication: $(x \times y)$

(1)	if $c \geq 0$ and $d \geq 0$ (2)	if $c < 0 < d$ (3)	if $c \leq 0$ and $d \leq 0$ (4)
if $a \geq 0$ and b ≥ 0	$[ac, bd]$	$[bc, bd]$	$[bc, ad]$
if $a < 0 < b$	$[ad, bd]$	$[\min(ad, bc), \max(ac, bd)]$	$[bc, ac]$
if $a \leq 0$ and $b \leq 0$	$[ad, bc]$	$[ad, ac]$	$[bd, ac]$

4. Division: (x/y)

(1)	if $c > 0$ and $d > 0$ (2)	if $c < 0$ and $d < 0$ (3)
if $a \geq 0$ and $b \geq 0$	$[a/d, b/c]$	$[b/d, a/c]$
if $a < 0 < b$	$[a/c, b/c]$	$[b/d, a/d]$
if $a \leq 0$ and $b \leq 0$	$[a/c, b/d]$	$[b/c, a/d]$

Copyright 2005 by CRC Press LLC

On the other hand, only some of the algebraic laws valid for real numbers remain valid for intervals; other laws only hold in a weaker form. The following laws hold for intervals $x, y,$ and z:

1. Commutativity:

$$x + y = y + x$$

$$x \times y = y \times x$$

2. Associativity:

$$(x + y) \pm z = x + (y \pm z)$$

$$(x \times y) \times z = x + (y \pm z)$$

3. Neutral elements:

$$x + 0 = 0 + x = x, \qquad 1 \times x = x \times 1 = x,$$

$$x - y = x + (-y) = -y + x, \qquad x/y = x \times y^{-1} = y^{-1} \times x,$$

$$-(x - y) = y - x, \qquad x \times (-y) = (-x) \times y = -(x \times y),$$

$$x - (y \pm z) + (x - y) \mp z, \qquad (-x)(-y) = x \times y.$$

and the following laws represent weak forms of several laws from the real arithmetic:

1. Subdistributivity:

$$x \times (y \pm z) \subseteq x \times y \pm x \times z, \qquad (x \pm y) \times z \subseteq x \times z \pm y \times z$$

2. Subcancellation:.

$$x - y \subseteq (x + z) - (y + z), \qquad x / y \subseteq (x \times z) / (y \times z)$$

$$0 \in x - x, \qquad 1 \in x/x$$

Copyright 2005 by CRC Press LLC

13

Expert Knowledge in Reliability Characterization: A Rigorous Approach to Eliciting, Documenting, and Analyzing Expert Knowledge

Jane M. Booker
Los Alamos National Laboratory

Laura A. McNamara
Los Alamos National Laboratory

13.1 Introduction

Expert knowledge is technical information provided by qualified people responding to formal elicitation questions that address complex, often under-characterized technical problems or phenomena [1]. Expressions of expert knowledge are of interest to scholars in a wide range of fields: economics, medicine and epidemiology, computational sciences, risk and reliability assessments, engineering, statistics, and others. In its formal expression, expert knowledge is most frequently associated with *expert judgment,* often a significant data source for mathematical and scientific models that attempt to predict or characterize complex, highly uncertain, and rare phenomena—for example, the probability of a nuclear reactor core melt accident. Informally expressed, however, expert knowledge is always a major factor in scientific

Copyright 2005 by CRC Press LLC

research. This form of expert knowledge, which in this chapter is referred to as *expertise*, is articulated in the decisions that scientists and engineers make in selecting phenomena for study, identifying appropriate data sources, designing experiments, and choosing computational models. In short, expert knowledge is never absent from any research process, regardless of how formally it is elicited or expressed.

As such, expert knowledge — whether in the form of expert judgment or as expertise — is a valuable and often untapped source of information for analysts attempting to model complex phenomena. This is particularly true when the analyst is not a "native" speaker of the scientific or engineering community in which he or she is working, which is often the case for statisticians and other consulting analysts. However, formally eliciting, representing, and documenting the conceptual models and judgments that experts use in solving complex technical problems can benefit most analyses, particularly when the phenomenon under study is complex, poorly characterized, multidisciplinary, and involves multiple researchers and research sites — a description that can be applied to an increasing number of engineering projects.

Reliability is defined as the probability or likelihood that a system or product will perform its intended functions within specifications for a specified time. While traditional reliability is strictly defined as a probability, we will allow a more general definition such that other mathematical theories of uncertainty (e.g., possibility theory) could be implemented. As in past efforts [1], the goal of this chapter is to provide a brief but practical overview for researchers who are considering the use of expert knowledge in their reliability analyses. As we discuss below, we have incorporated expert knowledge in evaluating the reliability and performance of complex physical systems, as well as problems related to product manufacturing. These problems are comprised of both parts and processes: missiles in ballistic missile defense, concept designs for automotive systems, aging processes in nuclear weapons, and high cycle fatigue in turbine jet engines.

This chapter draws from our experience as well as from the enormous body of literature concerning the elicitation, documentation, and use of expert knowledge. We present a philosophy and a set of methods for the elicitation of expert knowledge, emphasizing the importance of understanding the "native" conceptual structures that experts use to solve problems and the merging of these methods with the analysis or use of this knowledge in solving complex problems where test or observational data is sparse. The elicitation techniques described herein are derived from ethnography and knowledge representation. They provide guidance for the elicitation and documentation of expert knowledge, as well as for merging information in analyses that involve uncertainty representation using probabilistic or General Information Theories (GITs). (See also Chapter 9 by Joslyn and Booker.)

Section 13.2 of this chapter describes the main definitions and processes involved in knowledge acquisition: identification of an adviser-expert, problem definition, elicitation techniques, representational forms, and model development. These stages typically do not take place in a sequential fashion. Rather, the knowledge acquisition process is iterative, with the analyst's questions becoming more sophisticated as his or her understanding of the problem and the domain increases, and the model itself emerging and being refined throughout.

Section 13.3 discusses expert judgment elicitation, including identification of experts, the development of tools, issues of biases and heuristics, and the documentation and refining of expert assessment. The reader will find that we treat expert judgment elicitation as an extension of the knowledge acquisition (KA) process. We find that expert assessments are best gathered by analysts who have built a working fluency with both the domain and the specific problem under study. Again, the process of eliciting expert judgment is iterative, often bringing about changes in the model structure well after the KA process appears to be complete. We also present an expert-oriented approach [2–5] for eliciting and refining expert assessments.

Section 13.4 focuses on analysis, primarily based on statistical methods, for handling expert judgment. Of particular importance is the expression of uncertainty associated with expert information. Also important is aggregation of expert judgment, which can be problematic when multiple experts give varying opinions or estimates. Moreover, the analyst must be able to combine expert opinion with other forms of data, such as experimental results, computer model outputs, historical performance and reliability data, and other available information sources.

Copyright 2005 by CRC Press LLC

We remind the reader that the field of expert knowledge elicitation, representation, and use is extensive, multidisciplinary, and constantly developing and changing. Throughout the chapter, we discuss some of the newer work in this area, including techniques for teaching experts to perform self-elicitation, knowledge reuse, conceptualization of knowledge, and knowledge management. Although this chapter attempts to cover many of the critical issues in the elicitation, representation, quantification, and aggregation of expert judgment, the reader is encouraged to treat it as a starting point for developing an expert elicitation approach to reliability problems. Suggestions for further reading are provided throughout.

13.2 Definitions and Processes in Knowledge Acquisition

13.2.1 Expert Knowledge Approach: Philosophy, Definitions, Roles, and Stages

13.2.1.1 Philosophy of Local Knowledge

As humans interact with the world in our daily lives, we must make sense of an unrelenting deluge of sensory input: tastes, smells, feelings, written information, the spoken word, nonverbal cues, events, and experiences. Humans are very adept at acquiring, structuring, and applying very large amounts of heterogeneous information in relation to complex and emerging problem situations [6]. Experts in cognitive psychology and artificial intelligence have posited that the human brain processes and applies this deluge of information using mental models, or representational abstractions, that simplify reality into a set of phenomenological categories. In the context of a design team or a research project, these categories enable people to organize and structure emergent knowledge and shared cognitive activities so that they can make appropriate judgments and decisions when approaching complex problems.

Documenting these conceptual structures, and using them to provide guidance in quantitative model development and in the elicitation of expert judgment, constitute the core activities in an expert knowledge approach. Even when expert judgment elicitation is not an explicit goal in the project, cognitive models can still provide the analyst with a great deal of information about structuring and modeling a complex decision area. However, despite the fact that conceptual models play an important role in enabling the integration of communally held knowledge, most communities do not bother to represent these models explicitly. Instead, they tend to take their problem-solving process for granted, as something that newcomers just "learn" through working with more experienced experts. Moreover, cognitive models are locally contingent; that is, the form they take depends on the social context in which activity takes place and the objects around which the community is focused. Hence, these models are constantly being redefined as the community's problem-solving process evolves.

The core problem of knowledge elicitation, then, is to develop explicit representations that capture the tacit, shared conceptual models that structure a community's approach to a problem at a particular point in time. Because this process involves transforming the tacit into something explicit, these representations can themselves impact the problem-solving process, insofar as they establish a focal point around which individuals can discuss and debate the problem. Moreover, the process of building these representations and eliciting formal expressions of expert judgment is necessarily collaborative. The analyst often becomes a full member of the research team, and when this occurs, the model she or he develops can impact how community members engage with each other, with their data, and with new problems.

13.2.1.2 Knowledge Concepts

In this chapter we refer to the following important knowledge concepts and definitions:

- *Domains* are bounded areas of human cognitive activity that are constituted by a mixture of real-world referents (i.e., an object such as a missile motor or a fuel injection system) and the experts' cognitive structures (i.e., the conceptual models that an expert uses when engaging in the problem of designing a fuel injection system) [7].

Copyright 2005 by CRC Press LLC

- The social locus of the domain is the *community of practice:* a group of people who organize their problem-solving activity in pursuit of a shared goal or interest. Communities of practice can be synonymous with an institution, although they can also be located across one or more institutions—for example, a long-established research team composed of contractors from two or more corporations [8–11].
- *Problems* are epistemic challenges through which communities of practice identify limits to domain knowledge. In the realm of reliability, these problems are technical in nature, relating to the performance of a product or system, or its domain. They are critical for the survival of the community as well as the domain, insofar as they provide points of focus for shared human activity. As communities of practice resolve domain-related problems, they extend the skills, understandings, tools, and products that define the domain—and often identify new problems in the process. That is, domains are living entities whose boundaries and focus areas are constantly redefined as individuals within communities of practice engage in the activity of defining and solving problems [8].
- *Example:* Aeronautical engineering is a large knowledge domain instantiated in multiple communities of practice, including government (e.g., FAA, Navy, Air Force), academic (e.g., aerospace engineering departments), and industrial research and production facilities (e.g., engine companies). Individuals within and across these communities of practice identify problems in aeronautical engineering, such as high-cycle fatigue (HCF) in turbine engines. The epistemic challenge arises from the lack of first principles knowledge about HCF, insofar as HCF is not simply an extrapolation of the better known low-cycle fatigue. The process of studying high-cycle fatigue will generate new tools for handling the epistemic uncertainties, techniques for comparing computational models to experiments, and understandings for the engineers involved, thereby extending the domain of aeronautical engineering into areas such as computation, statistics, information theory, materials science, structural dynamics, and expert elicitation, to name a few.

13.2.1.3 Roles

An expert knowledge problem exists within a community of practice, so it is critical to understand how experts "operationalize" key domain concepts in solving problems. This information is then used to structure the statistical analysis or engineering modeling. Collaborators will take on the following important roles:

- *Analyst*. An individual or a team of individuals working to develop a model to support decision making. For readers of this chapter, this model will most likely estimate system reliability. In our experience, the team of analysts consists of a knowledge modeler and one or more statisticians. The knowledge modeler, usually a social scientist, elicits expert knowledge and expert judgment, creates appropriate representations, and develops a qualitative model framework for the problem. The statisticians perform the bulk of the quantitative work, including quantifying the model framework as well as data aggregation and analysis.
- *Adviser-expert*. The analysis team collaborates closely with one or two members of the community of practice. These "native" collaborators are referred to as *adviser-experts*. Such individuals should be well-established members of the community. They will act as guides and hosts, providing access to experts as well as data and information sources. This role is described in greater detail below [1].
- *Decision maker*. The adviser-expert may also be the *decision maker*: the individual who requires the output from the analysis to support a course of action, for example, allocating test resources, making design decisions, timing release of a product.
- *Experts*. Finally, the adviser-expert and the analyst will work closely with the *experts*: individuals within the community who own pieces or areas of the problem and who have substantial experience working in the domain. Depending on the domain, the analyst may consider requesting assistance from experts who are not directly involved in the problem, and even experts who are not immediate members of the community under study. For example, estimating nuclear reactor reliability is a process that often draws on experts from throughout the nuclear energy community, and not just those at a specific plant.

Copyright 2005 by CRC Press LLC

13.2.1.4 Stages in the Approach: An Overview

The decision to use an expert knowledge approach cannot be made on-the-fly or taken lightly. Because the elicitation process must be developed in conjunction with other elements of the analysis, the decision to elicit and use expert judgment in any analysis must be made early in the project timeline, well before the model structure has been chosen and developed. Experts must be courted and trained; questions developed and refined; representation, documentation, and storage techniques and tools developed; the model structure and the data vetted by the experts; in addition to any sensitivity and "what-if" analyses. If the process seems time consuming and labor intensive, it is—but it also opens the door to complex and exciting problems that might otherwise seem intractable.

Briefly, the stages in an expert knowledge problem approach include the following:

- *Problem identification*. Can this problem benefit from an expert knowledge approach?
- *Problem definition*. What is the community trying to achieve? How will the reliability analysis support those goals? How will the project be executed?
- *Model development*. What are the core concepts that structure this problem? How are they related to each other? What class of quantitative models best fits the problem as currently structured?
- *Expert judgment elicitation*. Is expert judgment a viable data source for this problem? What is the best way to elicit expert judgment in a given community?
- *Analysis of expert judgment*. What are the uncertainties associated with judgments? How can judgments from multiple experts be combined?
- *Information integration and analysis*. What additional data sources can be used to characterize this problem? What can the populated model tell us about the system?

Each stage in the approach calls for a particular set of methods. Generally speaking, problem identification, definition, and model development are exploratory efforts that rely at first on open-ended, relatively unstructured interview questions. As the model coheres, the methods become increasingly more structured and quantitative. We provide examples of questions and tools for each stage below.

13.2.2 Problem Identification: Deciding When to Use an Expert Knowledge Approach

The problem identification stage is typically characterized by survey conversations between the analyst, one or more decision makers who are interested in pursuing a collaboration, and perhaps one or more members of the engineering design team.

Example: The analyst meets with a section leader in a large automotive parts corporation. The section leader is concerned about high warranty costs the company has recently incurred on some of its products and wants to develop a way to reduce those costs.

13.2.2.1 Criteria for an Expert Elicitation Approach

Not all problems call for a full-scale expert knowledge approach, which requires a great deal of time and forethought. Indeed, some reliability problems require minimal elicitation of expert knowledge for defining the problem and corresponding structure. If the product to be analyzed has a straightforward reliability structure for its parts and processes, and there is a great deal of available and easily accessible data, then a formal elicitation for expert judgments may be unnecessary.

Example: The reliability of a well-established product, such as an automobile fuel injector, quite naturally lends itself to standard model and representation techniques. An experienced fuel injector design team may be able to construct a reliability block diagram for their system in a relatively short time. The diagram can then be populated with test data and a classic model for reliability, such as the Weibull [12], can propagate part and process reliabilities in each block to get an estimate for the entire system.

However, neatly defined problems with easily available data are increasingly rare as multidisciplinary project teams become the norm in science and engineering. Moreover, we have seen an increasing demand

Copyright 2005 by CRC Press LLC

for predictive analyses to support decision making in experimental and design engineering projects. Predictive analyses are those that estimate system reliability before designs are finalized and tests are performed. Such analyses are particularly useful in design projects where the data is sparse, difficult to access, only indirectly related to the system being designed, or nonexistent. For problems like these, a standard model such as a reliability block diagram might be an inadequate representation of the problem space. Even trickier are complex technical problems where one subsection of the problem is cleanly defined and well characterized, but the larger problem itself is less neat.

Complex problems tend to have one or more of the following characteristics:

- A poorly defined or understood system or process, such as high cycle fatigue effects on a turbine engine
- A process characterized by multiple exogenous factors whose contributions are not fully understood, such as properties of exotic materials
- Any engineered system in the very early stages of design, such as a new concept design for a fuel cell
- Any system, process, or problem that involves experts from different disciplinary backgrounds, who work in different geographical locations, and whose problem-solving tools vary widely, such as the reliability of a manned mission to Mars
- Any problem that brings together new groups of experts in novel configurations for its solution, such as detection of biological agents in war

Any time that multiple experts are involved, their conceptualizations of the problems can differ widely, depending on the tools they possess, their training, and the community of practice to which they belong. A unified model of an emergent problem, then, can be a difficult thing to develop. Moreover, complex problem domains often have tight timelines—for example, when issues of public or consumer safety are involved.

Even a well-understood fuel injector can carry a high degree of complexity. Although the system's parts may be well defined, its operation relies on a series of less clearly defined processes that impact the injector's functioning and hence its reliability. The assembly process and associated quality control and inspection regimes can impact the system's performance. Moreover, as the system is operating, physical processes such as forces, chemical reactions, thermodynamics, and stresses will affect its reliability.

In the past, processes have often been ignored in estimating reliability because they are difficult to specify and incorporate into the problem structure, much less populate with data. In cases where processes contribute significantly to system reliability, an expert elicitation methodology can specify important processes and provide guidance for locating them in the problem structure. These areas can then be populated with expert judgment and other available data sources. Chapter 30 by Griffiths and Tschopp identifies a likely situation where the methods presented in Chapter 13 for eliciting expert judgment can help engineers construct probability distributions for engine excitation variation.

13.2.3 Problem Definition

Once a problem has been identified as one that might benefit from an expert knowledge approach, the next stage is problem definition. During this stage, the analyst works with the community to identify an analytical approach that will support the community's efforts in a particular problem area.

Example: A group of decision makers in the Department of Defense have identified an experimental missile development program as one that could benefit from a predictive reliability analysis. Before the analysis can proceed, the analyst must make contacts with the design team so that he or she can understand how to align the statistical analysis with the design team's goals.

13.2.3.1 Identifying the Adviser-Expert

Developing an expert knowledge approach requires a productive rapport with one or more subject matter experts who can serve as hosts, advisers, and points of entree into the community for the analyst. Therefore, the first and perhaps most important stage in defining the problem is the identification of an *adviser-expert:* a domain native who can act as a guide to the problem as well as the experts, the sources of information,

Copyright 2005 by CRC Press LLC

and data related to the issues under study. Sometimes, the decision maker also plays the adviser-expert role, particularly in smaller corporate or industrial settings. In larger bureaucracies or corporations, the decision maker advocating the analysis may not be a member of the design team. In such cases, the decision maker must suggest one or more candidates within the design team to act as adviser-experts.

There are qualifications for a good adviser-expert, the most important of which is a strong motivation to support the analyst in the elicitation project. A good adviser-expert understands the relationship between the analysis and the problem-solving goals of the community of practice. She or he values the analyst's contributions and is willing to devote time and effort to answering the analyst's questions, assisting the analyst in tool development, locating data sources, reviewing model structure and question formation, identifying reputable experts, and cultivating the community's support for the project. Low motivation on the part of the adviser-expert can make the elicitation process difficult, even impossible.

Experience is another important qualification for the adviser-expert. Because she or he will serve as the analyst's guide to the domain, the adviser-expert must have broad, but not necessarily deep, familiarity with the problem at hand. It goes without saying that a novice will probably not make a good adviser-expert. Rather, the adviser-expert should have a "journeyman's" level of experience within the domain [13]. Ideally, an adviser-expert has been a member of the community for roughly a decade, has direct experience working with problems of the type under study, is well acquainted with the experts assigned to the problem, understands how tasks are distributed among different experts (the social organization of activity), and is respected by other members of the community.

13.2.3.2 Defining a Collaborative Strategy

The first task for the analyst and the adviser-expert is to define the nature and the boundaries of the problem to be addressed. It is important at this stage to differentiate between the goals of the *community* and the *decision maker*, on one hand, and the goals of the *analysis*. For example, a group of engineers working on a new design for a missile might list goals related to the system's reliability and performance: ease of ignition, accuracy of guidance systems, burn time, fuel efficiency, shelf life. The goal of the analysis might be development of a predictive model that enables the engineers to draw on past design experiences to support decision making and resource allocation during the process of designing the new missile. The analyst's goals should be shaped by the community's objectives, so that the two are closely coupled.

Below we offer some questions that we typically use in the problem definition and success/failure stages of elicitation. In Figure 13.1, note that these questions are open-ended interview questions that

PROBLEM DEFINITION QUESTIONS

- What kind of system/process is being developed? How is this similar to past projects? What is this system/process designed to do?
- Who are the customers for this project?
- Who will judge this project's outcomes? What will they use to judge those outcomes?
- What are the motivations in the community for a successful problem outcome (e.g., cash bonus, patent opportunity)?
- Where is this project being conducted? (Single or multiple locations) How many different groups of experts are involved in this project?
- What is the timeline for completing this problem? (Include all milestones.) What constraints does this group face in working this problem (time, financial, human)?
- What is the complexity of the problem space? What parameters must be directly estimated/assessed by the experts? Do the experts have experience with these parameters?
- Do data sources exist? How accessible are existing data sources?
- How much time will people in the organization be willing to devote to this project?

FIGURE 13.1 Sample problem definition questions.

Copyright 2005 by CRC Press LLC

allow the adviser-expert to direct the conversation. At this stage, it is important for the analyst to learn as much as possible from the adviser-expert without making assumptions that could limit the analyst's problem and domain understanding.

Problem definition is not always a straightforward task. If the problem is newly identified or resists definition (we have found this to be the case for many nuclear weapons problems), it is possible that none of the experts will be able to articulate more than a few high-level goals. In this case, it is also likely that the problem definition will change as the project's outlines become clearer. For this reason, we strongly recommend the analyst and the adviser-expert carefully document their problem definition discussions and revisit the topic frequently to assess how changes in the community's problem might impact the goals of the analysis.

13.2.4 Eliciting Expertise for Model Development

The elicitation of expertise and the development of a knowledge model marks the beginning of intensive problem-focused work on the part of the analyst. During this phase, the analyst will focus on developing a qualitative map of the problem area to guide inquiry in subsequent stages of the analysis.

Example: Two design teams in a large aeronautical engineering company are collaborating with a team consisting of one social scientist and two statisticians to develop an expert knowledge approach for making design modifications in their jet engines. Although the engineers share a great deal of information, neither design team is overly familiar with the others' work processes because one team has a parts-oriented design focus, while the other has a manufacturing-oriented design focus. However, the statisticians require a unified representation of the problem, as well as some understanding of the processes the teams use to generate and interpret data. It is also a beneficial learning experience for the two teams with different orientations to learn how the other team views the problem.

13.2.4.1 What Is a Knowledge Model?

A *knowledge model* is a type of knowledge representation designed to capture the key concepts and relationships that make up the community's conceptualization of the problem. As defined by Davis, Schrobe, and Slzolovits [14], a *knowledge representation* is a formally specified medium of human expression that uses symbols to represent a real-world domain. A knowledge representation captures all the categories within a domain, as well as the relationships that define their behavior and interactions, and expresses these in a computationally efficient format. In other words, a representation is a mediating tool that bridges the gap between the as-experienced, real-world domain and a computed version of that domain. In computer science, formally specified knowledge representations play a critical role in the development of databases, query languages, and other common applications. Knowledge representations can also be very useful in developing and specifying statistical models, particularly when the problem under study is very complicated.

Developing a knowledge model is not the same enterprise as developing a statistical model for quantitative analysis, although it provides a foundation for later statistical work. Instead, the knowledge model provides a way to ensure that the primary concepts that comprise the problem space are mapped and documented in a way that all parties involved in the project can come to agreement on what the primary focus areas are, how best to address them, what analytical techniques will be most appropriate, and where to collect data and information [15]. Indeed, developing the knowledge model can be seen as a further iteration of problem definition, albeit a much more detailed one.

The purpose of developing a knowledge model for problem definition is to find out how the community of practice works for solving a problem such as the design of a system or product. The graphical representation should represent the community's knowledge about areas critical to development of a formal model, including the following:

- What level of granularity (detail, resolution) is appropriate for the model?
- Who is responsible for what areas of work?

Copyright 2005 by CRC Press LLC

- Where do data sources exist?
- How do parts in the system relate to produce functions?
- What is the design process?
- How does information flow through the organization?

Developing a knowledge model requires the elicitation of *expertise*. Expertise consists of the information, practices, and background experience that qualified individuals carry to new problems—the implicit ways experts think, make decisions, and solve problems within their community of practice. Expertise is context dependent. It is the distinctive manner and ways that members of a technical community act, make things, perform tasks, and interpret their experience. In other words, expertise is the form of explicit and implicit knowledge that enables expert communities to combine data and information during their problem-solving process. Properly documented, expertise can provide valuable input into model development.

The elicitation and formal representation of expertise has been a key element of software engineering and development since the 1950s. The field of *knowledge acquisition* (KA) emerged as researchers in artificial intelligence and expert systems attempted to elicit and capture experts' problem-solving processes and model them in software applications, such as expert systems. As researchers in these fields quickly realized, the task of eliciting expert knowledge was far more difficult than originally anticipated: experts have a difficult time consciously articulating skills and thought processes that have become automatic. Moreover, many of the bias issues that plague the elicitation of expert judgment can also affect the elicitation of expertise (see discussion below).

Because of these challenges, experts in the field of knowledge acquisition have developed an extensive portfolio of approaches to the elicitation of expert knowledge. In this chapter we provide a general outline of the process below with an emphasis on open-ended and semistructured interview techniques, since this approach can be used with success in most settings. There is an extensive suite of elicitation tools and representational techniques available for capturing expert knowledge. This suite includes methods from fields as diverse as knowledge acquisition and artificial intelligence, statistics, risk analysis, decision analysis, human communication, cognitive science, anthropology and sociology, and other disciplines that study human learning and knowing. Ultimately, the selection of methods is the decision of the analyst, who can draw on many well-established knowledge elicitation techniques (for comprehensive reviews of elicitation techniques, see especially [1, 13, 16]).

13.2.4.2 Process for Eliciting Expertise

The elicitation and representation of expertise is a qualitative, iterative process involving background research on the part of the analyst, and the development of open-ended and semistructured interview schedules. One outcome of the elicitation process is a set of graphical representations that capture the important elements of the knowledge domain (see below). However, the real benefit of the knowledge elicitation process is the opportunity it provides for the analyst and the consulted experts to arrive at an explicit and common understanding of the problem structure and key elements. Briefly, the stages for eliciting expert knowledge include the following:

- Identify key areas and points of contact within the project.
- Gather background materials for project areas.
- Conduct open-ended interviews with experts.
- Develop graphical representations of experts' domain.

As with all elicitation, the analyst should rely on the adviser-expert's assistance in selecting and arranging interviews with experts on the project. A useful tool is to begin with a simple graphical map, similar to an organization chart, that delineates which engineering teams are responsible for what areas of the project. (Note that organizational charts often do not capture project-specific information.) Within each sub-field, the analyst and the adviser-expert should work together to identify points of contact who will provide information and assist in arranging meetings and interviews with specific engineering

Copyright 2005 by CRC Press LLC

SAMPLE QUESTIONS FOR DEVELOPING A KNOWLEDGE MODEL:

A Missile System Example

- If you had to divide this missile into major subsections or components, what would those be?
- Provide a list of clear, measurable goals for missile performance. What are the relative states of success and failure for this system?
- Who are the major groups working on this missile? Are these groups congruous with the missile subsections? Or are they organized differently?
- What information is required to begin the design process in each group?
- Where does that information come from? To whom does it flow?
- How do individual engineers use background information in the design process?
- How is the system assembled? Where? In what order?
- At what level does testing take place (material, component, subsystem)? What kind of data do different tests generate?
- How do you convince yourselves that a part, subsystem, material will work?
- How do you generate appropriate levels of physical processes (temperature, vibration, shock) for your test process?

FIGURE 13.2 Sample questions for a knowledge model.

experts. Before conducting interviews with the experts, the analyst works with the adviser-expert to learn the basic elements of the problem at hand. Background study is important because, as with all human knowledge, expertise is context dependent and its elicitation requires some familiarity with the community of practice. The adviser-expert can provide the analyst with written material about the project, including statements of work, engineering drawings, project management diagrams, organizational charts, material from presentations, internal reports, journal articles, and other written descriptions of the problem, which would include local jargon and terminology. The analyst should study this material to familiarize herself or himself with the domain before developing questions and interviewing the experts. The adviser-expert's role during this time is to support the analyst's learning process and to assist in the development of appropriately worded questions for the experts. Figure 13.2 provides a set of sample questions used in defining the knowledge domain for a missile system.

Once the analyst and adviser-expert have developed a schedule, identified points of contact, and practiced conducting interviews for eliciting the problem structure from the experts, the elicitation process of problem definition can begin. The expert-advisor's role as a conduit into the experts' community comes into play at this time, providing motivation for the experts to participate in the elicitation.

It is particularly important at this stage to define the appropriate level of detail or *granularity* for the problem, which must be related to the goals that are defined for the analysis. For example, a decision maker may only need a rough comparison of a new design to the old to answer the question, "Is the new one at least as good as the old one?" For a problem like this, it may not be necessary to structure the two systems down to the smallest level of physical quantities to make this determination. Also, the extent of information availability (including data and experts) can dictate how levels of detail are identified and chosen for inclusion in the model. If knowledge is completely lacking at a sub-component level, the problem may be defined and structured at the component level. Different levels of focus are possible within a problem; however, very complex structures pose information integration difficulties when combining all levels for the full system analysis.

During the initial phases of knowledge elicitation, the answers provided by the experts may generate further questions for the analyst. Documentation can be done in the form of simple star-graphs, which can leverage the emergence of more formal knowledge representations (see below).

13.2.4.3 Knowledge Representation Techniques for Modeling Expertise

Although computer scientists use formal logic to develop knowledge representations, simple node-and-arc models provide a tractable way to represent expert knowledge. Because most people find it easy to understand nodes, arcs, and arrows, graphical representations of complex relationships can be used to

Copyright 2005 by CRC Press LLC

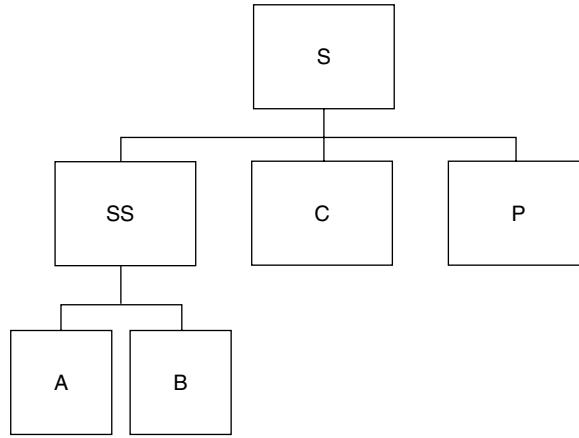

FIGURE 13.3 Reliability block diagram of a simple system.

mediate the negotiation of model structure across communities of experts. Indeed, engineers often communicate with each other using graphical representations and models of their systems, and graphical models are quite common in the field of reliability analysis.

Example: A reliability block diagram uses boxes and connecting lines to represent the intricate relationships in a complex mechanical system. In Figure 13.3, the system, S, is composed of a series of three items: subsystem, SS, component, C, and manufacturing process, P. Subsystem SS is, in turn, a series combination of two other components, A and B.

Some problems can be easily represented in a reliability block diagram. However, others are more complex and require representations that include more information than just parts. The elicitation of knowledge for complex problems should aim at identifying the key concepts and relationships in the knowledge domain and understanding the relationships that tie these concepts together. Even the most complex engineering problems share a core set of concepts and relationships. Some of these concepts will be very easy for the engineers to specify: *component, subsystem, system* may be readily available in design drawings or from tests or vendor documentation. Entities like these, which are explicitly labeled in the community's vocabulary, can be far easier to elicit than entities that are more tacit. For example, *functions* describe what a part or set of parts do as the system is working, but engineering communities rarely specify functions on engineering diagrams and may even lack a formal vocabulary for referring to them. *Processes* are more likely part of the manufacturing community, rather than the design community's everyday language. Processes include the operations required to assemble a system and monitor its quality through inspection or quality control. However, understanding what function a set of parts performs can be critical in developing a system-wide reliability diagram. Similarly, failure modes can be difficult to retrieve from memory.

Simple line graphs are very useful in the initial "brain dump" stages of the elicitation process, as the analyst is working with the adviser-expert to define the problem domain and catalog all the concepts of interest. For example, a *star graph* has a central node to represent the domain and an unlimited number of arcs that radiate outward [17]. Each arc is connected to one of the domain's concepts. Elicitation at this stage is very open-ended: the analyst provides the expert with the concept under study and simply asks the expert to describe it. For example, if the domain under study is high cycle fatigue, a basic star graph that describes the domain might look like Figure 13.4.

Initially, none of the outer nodes are grouped into higher-order categories, nor do additional edges display connections among the outer nodes. Further specifications of the star graph, however, will bring the domain structure into clearer focus. For example, in Figure 13.5, the nodes labeled *blade disk* and *airfoil* might be grouped into a larger category called "parts," while *rotational load, bending, torsion,* and *vibration* can be grouped into a category "stress."

Copyright 2005 by CRC Press LLC

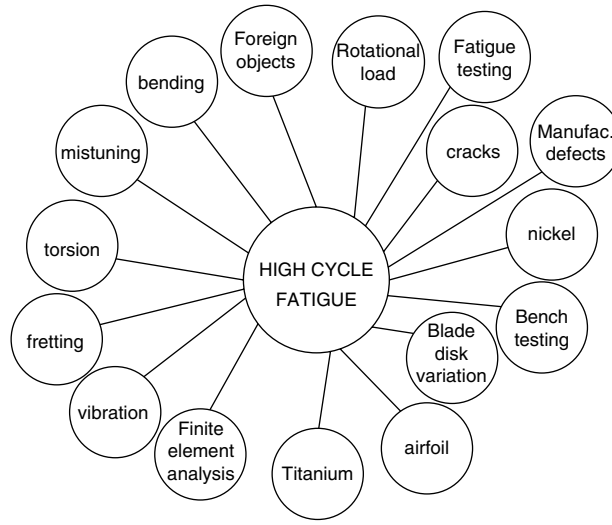

FIGURE 13.4 Star graph for high cycle fatigue.

As the graphical representation is further developed in Figure 13.6, a relationship between the categories "Parts" and "Stress" in the domain "High Cycle Fatigue" can be formed.

A categorical relationship like that specified above can be developed for all areas of the knowledge domain, and will form the structure for the knowledge model. This model, also known as an *ontology* in the field of knowledge representation, displays the basic categories in a domain and the relationships among them. Figure 13.7 is an example of an ontology for a missile system. Note that the lowest level of granularity is "Parts," which are ultimately related to "Events" through "Functions."

As the analyst works through the problem area, the ontology is used to structure later queries that specify instances of each category. For example, the analyst can use the categories to develop a list of all parts, the types of stresses to which they are vulnerable, and potential failure states related to those stresses. Other categories that emerge during the elicitation period, such as "Test" and "Data," can also

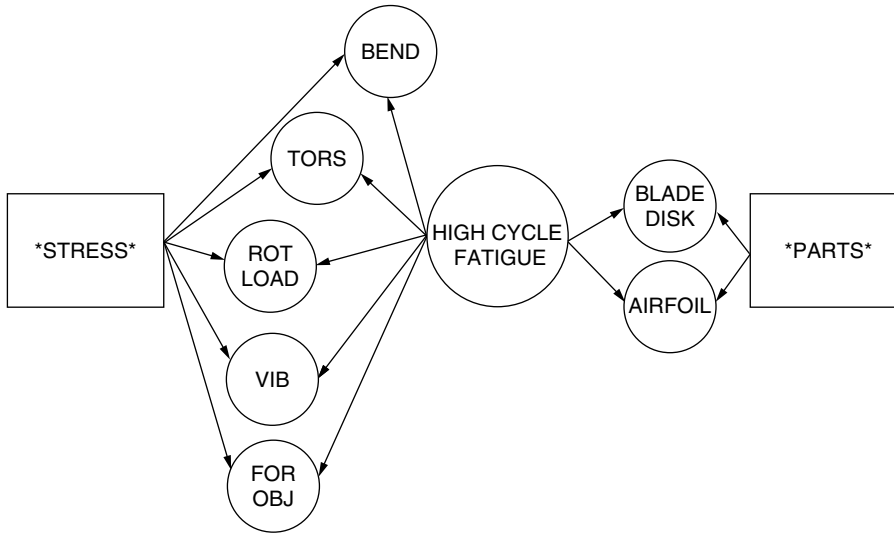

FIGURE 13.5 Grouped representation.

Copyright 2005 by CRC Press LLC

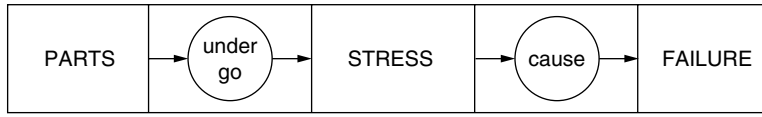

FIGURE 13.6 Fundamental relationship representation.

be represented formally and used to structure further inquiry. The analyst can use these categories to develop a better understanding of how different test processes and data sources are used within the community to generate confidence that parts will not fail under different kinds of stress.

13.2.4.4 Success and Failure for the Problem Area

As part of the knowledge model, it is important to elicit a clear set of definitions for performance—"success" and "failure" of the design team's problem or project, and to have these definitions expressed in terms of clear, discrete, measurable goals. This information, in turn, will guide the analyst in developing an appropriate suite of methods for the consultation and may provide guidance as to what the analysis will be predicting. One tool that we have found very helpful in doing so is a simple *stoplight diagram*: a horizontal chart divided into red, yellow, and green areas that acts as a heuristic for eliciting states of success and failure. The image of a stoplight is commonly used in project management tools and will be familiar to many engineers.

To specify the contents of a stoplight chart, the analyst develops a blank chart and uses it as an elicitation tool with the adviser-expert and the decision maker to identify specific, measurable goals for the project. The event states can be described as catastrophic failure (red), imperfect performance with salvageable outcomes (yellow), or success (green), as in Figure 13.8.

For example, in the missile development ontology, it is possible to identify all the events that the missile designers want their system to perform. The designers can identify red, yellow, and green states elicited for each of these events, which can then be mapped onto the chart. Later, the adviser-expert can

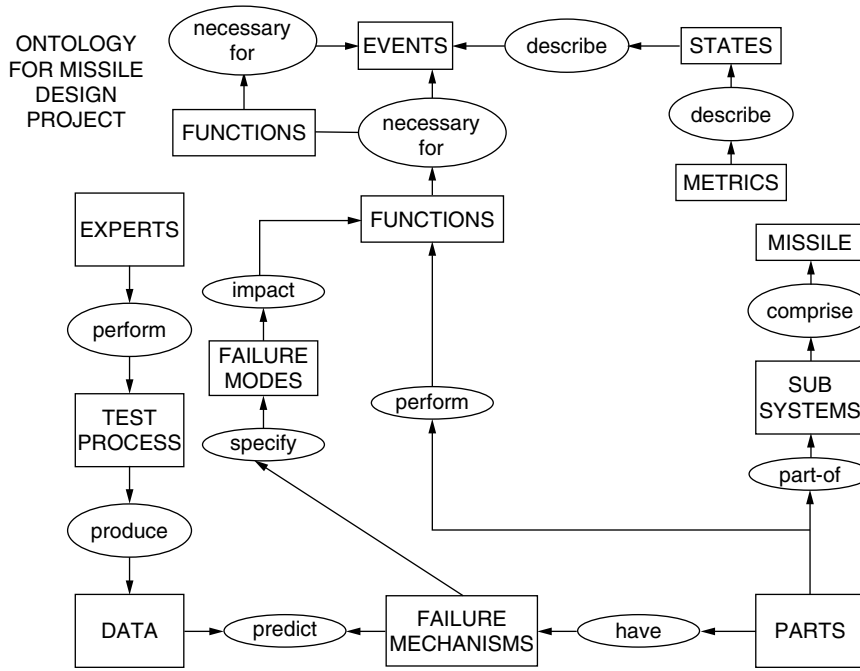

FIGURE 13.7 Ontology for missile design.

Copyright 2005 by CRC Press LLC

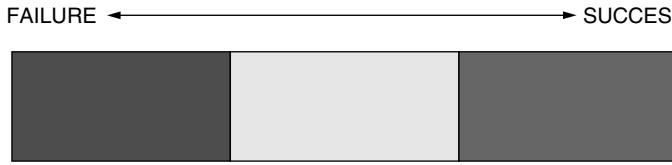

FIGURE 13.8 Stoplight chart.

identify members of the community from whom the analyst can elicit various combinations of failures or functions in the system that would lead to the events and each of the possible states for those events, as described on the stoplight chart.

13.3 Model Population and Expert Judgment

13.3.1 Expert Judgment Elicitation

Eliciting problem structure from experts is usually only the first part of the elicitation process. Extracting the specific knowledge that experts have about the various aspects of the structured problem involves elicitation of expert judgment. We refer to knowledge gathered for this type of elicitation as *populating the structured problem* or *model population*. Although formal quantitative expressions are often the goal of expert judgment elicitation, the elicitation process itself is really a *qualitative* and *inductive* one, insofar as elicitation requires the analyst to understand how experts structure the problem, how they weigh and combine different sources of information (for example, computer models vs. experimental data) in making decisions, and how they conceptualize uncertainty. Ideally, a great deal of this knowledge emerges from the KA process described above, so that the analyst can develop questions and instruments that maximize the experts problem-solving abilities.

For studies that use expert judgment to be accepted as valid, they must be conducted in a formal and rigorous manner, with clear documentation throughout the project. In the remainder of this chapter, we describe the methods we have used for designing, performing, and documenting expert elicitation.

13.3.1.1 What Is Expert Judgment?

In this chapter, we treat expert judgment (also referred to as *expert opinion*) as a very specific form of expert knowledge. It is qualitative or quantitative information that reflects an individual's experience, understanding, and assessment of particular technical issues. It is perhaps best thought of as a snapshot of the expert's knowledge about a particular problem at a particular time [18, 19]. And as the term implies, expert judgment refers to the subjective assessments of individuals who are recognized by their peers as having a great deal of experience and fluency with the phenomenon under study.

Expert judgment can be viewed as a subjective probability—a quantitative statement that reflects an individual's degree of belief in the likelihood of a future and uncertain event, based on the knowledge and experience that the individual holds about similar past events. Because this opinion is subjective, and rooted in the individual's experience within the community of practice, it is critical to elicit information in a way that facilitates the experts' reasoning process.

Example: Three experts are selected to provide their opinions about the reliability of a new circuit design. The adviser-expert and the analyst work together to develop a question format that makes sense to the individuals being consulted. The analyst has developed a set of questions that asks about failures over the course of a year. The adviser-expert explains that engineers in this company commonly think of failures per million hours of operation, information that the analyst uses to revise his or her questions.

We recognize the utility and advocate the use of expert judgment in research problems where data sources are scarce or difficult to access. It can provide a valuable source of information for the analyst. For some classes of events—never observed, one time, or very rare events, and phenomena that do not lend themselves to convenient study—expert predictions may be the only source of data available.

Copyright 2005 by CRC Press LLC

Indeed, expert opinion shares many characteristics with data: it can be quantified, its quality is affected by the process used to gather it, and it has uncertainty that can be characterized and subsequently analyzed. Moreover, expert opinion is always part of any analysis, whether in the form of judgments made about appropriate data sources, model structure, or analytical techniques. Rarely are these tacit choices fully documented (or even acknowledged); instead, they are treated as a "natural" part of the research process. For example, model choice is a realization or form of expert judgment, as is the process of populating the model with quantified expressions of expert estimates from judgments.

It is perhaps ironic, then, that studies that make explicit use of expert opinion as a data source are often criticized for being too "soft." Specifically, expert elicitation projects have lacked formality, rigor, and documentation [19], while analysts have failed to carefully consider and document their choice of "experts" for elicitation on a particular subject area [20]. The strongest critique, however, comes from "human fallacy" research that details the heuristics that humans use in making judgment. *Heuristics* are informal mental rules for assessing information and making predictions. These heuristics give rise to predictable biases, which in turn lead to poor coherency and calibration of expert opinion [21].

Such difficulties are not insurmountable. In the following section, we present our philosophy of expert judgment, as well as a set of general principles and tenets for eliciting, documenting, and refining expert opinion. The basic principles of our approach to elicitation can be summarized with the following key words, each described in this section:

- Bias minimization
- Reliance on advisor-expert
- Pilot test
- Verbal protocol
- Verbal probe
- Decomposition
- Conditional information
- Feedback
- Document

These principles are compared to the Delphi technique for eliciting knowledge from experts in Section 13.3.2.

13.3.1.2 What to Elicit?

One of the most significant questions to consider in designing the elicitation instrument is the design of the model. As a general rule of thumb, expert judgment must be elicited so that the expert assessments fit with the model structure.

Example: Consider a model structure in which a Bayesian hierarchical structure of conditional probabilities is used to assess the performance of a simple mechanical system. When populating such a model with expert judgment, the analyst is interested in knowing the probability that any *child* variable (A) will be in a given range of states ($a_1, a_2, \ldots, a_n$), given the possible range of states for each and all of its *parent* variables (B and C). It makes little sense to elicit probabilities for the states of variable A without taking into consideration the entire range of states for variables B and C, because the model structure specified that the state of A is *conditioned upon* the states of B and C.

As noted in the example above, dependencies among aspects of the model or the structure must be anticipated and included as part of the elicitation process. Dependencies expressed by conditional probabilities can be elicited using a *causal structure:* If event B occurs, then event A will occur with probability p (expressed as $P(a|b) = p$, where a and b are the specific values of A and B, respectively). Conditional probabilities can also be elicited using a *diagnostic structure:* Given that event A has occurred, then event B has occurred with probability p (expressed as $P(b|a) = p$). Bayesian networks [22] are complex structures of such *parent/child* hierarchies that are connected through Bayes theorem.

Copyright 2005 by CRC Press LLC

13.3.1.3 Identifying the Experts

An *expert* can be defined as someone recognized by his peers as having training and experience in his technical field. In our experience, the selection of experts depends on the type of problem facing the analyst, the novelty of the project, and the social organization of tasks in the research setting. The pool of experts may be limited to members of the immediate research or engineering team; for example, in projects that involve a great deal of industrial proprietary or classified information. In cases like these, the analyst works exclusively with all the team members to elicit their expert knowledge.

However, it is often possible to work within a corporation, laboratory, or other research organization to gain information about a system under development from individuals who are not themselves members of the research team, but who may be familiar with one or more of its goals. For example, some corporations have engineers whose job it is to assess the reliability of all electronic parts across programs, and who may be able to provide some prior estimates of the reliability of prototype components being developed within their organization. In some cases, it may even be possible to draw on experts from outside the organization to provide an opinion that can serve as a prior for the model, although again this is not advisable in situations where proprietary information is involved.

All this, however, begs the question of expertise: who is an expert, and what is the best way to assess expertise? Unfortunately, there is no formal test to determine expertise, which, in any case, is problem specific — and therefore not amenable to general assessment tools. One simple way of defining expertise is to assess educational and professional experience: the greater the educational attainment and level of training, the higher the level of expertise. However, some individuals may work for years in a particular field and never be considered true experts within their peer group.

More useful are the definitions given in Hoffman et al. [13]. They draw on the terminology of medieval European guilds to develop a typology of expertise, ranging from *naivette* — one who is totally ignorant of a domain's existence — to master, which they define as an expert whose judgments "set regulations, standards or ideals" for the rest of the community. Between these two extremes lie several intermediate stages where most individuals will reside: initiate, apprentice, journeyman, and expert. The last two — journeyman and expert — are excellent candidates for elicitation because they are members of the community who have achieved an acceptable level of competence so that their peers are comfortable allowing them to work without supervision. More specifically, an expert is one who is called upon to address "tough" cases [13].

Ayyub [23] offers another useful way to think about expertise; an expert, he argues, is an individual who is conscious of ignorance, one who realizes areas of deficiency in her or his own knowledge or that of the community, and strives to amend those gaps. On the other hand, naivettes, initiates, and apprentices tend to be unfamiliar with the knowledge domain and cannot therefore recognize areas of epistemological deficiency. They often solve problems from first principles rather than draw creatively on experience, simply because they lack the domain familiarity of a journeyman, expert, or master.

It is also acceptable to rely on the peer group's opinion. One excellent method is to interview project participants to discover which members of the organization are most frequently tapped for assistance in solving difficult technical problems. Oftentimes, novice or journeyman individuals are excellent sources of information about expertise within an organization because they are often paired with more senior people in mentoring relationships and can identify which individuals are most helpful with difficult problems.

It is also possible to use the ontology to break the problem itself down into a set of subject areas. For example, a missile system might be broken into power subsystems, pneumatic subsystems, software, and other areas. After identifying subject matter experts, the analyst and the adviser-expert can use Hoffman et al.'s typology or a similar tool to identify journeyman-, expert-, and master-level individuals within each topical area. Another alternative is to work with the adviser-expert to determine which individuals are known for making progress on particularly challenging or novel problems — this being a marker of "conscious ignorance" and hence expertise. We have found that it is less helpful to ask individuals to rate their *own* level of expertise, as they frequently tend to downplay or underrate themselves. However, this is another option for the analyst.

Copyright 2005 by CRC Press LLC

No matter what method the analyst chooses in selecting experts for expertise and judgment elicitation, we emphasize again the importance of documenting the rationale and method for doing so. Because expert knowledge projects are often loosely documented, informal, and implicit, they are often criticized for being "soft" or "biased." Careful choice and documentation of the project's methods, rationale, and progress is important throughout, but may become extremely so once the analysis is complete.

13.3.1.4 Single or Multiple Experts?

One of the first considerations in any project is whether to elicit information from single or multiple experts. Statistical sampling theory implies that a greater amount of information can lead to a better understanding of the problem, with corresponding reductions in uncertainty. We are not suggesting that a certain number of experts can represent a statistically valid sample for making inferences about the unknown underlying population. However, logic says that consulting more experts will provide a more diverse perspective on the current state of knowledge.

There are other good reasons to consult multiple experts. While this approach can pose problems of *motivational* bias, it does seem to have some advantage in minimizing *cognitive* bias (see discussion in next section). O'Leary [24] found evidence that judgments acquired from groups of experts are more likely to result in expressions that are consistent with Bayes' theorem [12], and with the axioms of probability, than are judgments elicited from single individuals. One explanation for this phenomenon is that groups of individuals have a wider range of cognitive tools and representations for structuring the problem, enabling individuals in the group to reason more consistently and coherently.

Of course, the answer to the single-vs.-multiple experts may be context dependent. In projects where one or two engineers are the only individuals familiar with the problem or system under discussion, the decision is already made. In others, there may be a great many experts who could proffer opinions, but the project itself may limit participation. For example, in projects that involve classified or proprietary data, there may be little possibility of eliciting information from more than a few experts. Other times, the research setting may offer the chance to gather formal opinions from several experts. In this case, one must decide whether to conduct the elicitation as a focus group, or to interview the experts individually.

Once the decision has been made to conduct elicitation with multiple experts, the next step is to decide if goal of the problem is to seek a *consensus* or a *diversity* of views. Group elicitations can be designed for either situation. However, the analyst must consider the possibility that the experts will have incommensurable views, as is often the case in newly emergent fields. In this case, the challenge of aggregating varying estimates from multiple experts then falls to the analyst. Other issues to consider in expert judgment elicitation are the levels of expertise that individuals bring to the problem. In addition, there may be some sources of inter-expert correlation, so that one must treat them as dependent rather than independent sources of knowledge. These and other issues involved with aggregation are discussed below.

13.3.1.5 Expert Cognition and the Problem of Bias

Perhaps the greatest issue with using expert judgment for predictive modeling is the question of *bias*. Simply put, bias can degrade the quality of elicited data and call into question the validity of using expert judgment as a source of data.

What is bias? Bias in scientific instrumentation means a deviation or drift from the normal or nominal operating conditions. In statistics, bias is understood as a parameter estimation that is off target from its expected value. Similarly, in cognitive science, bias refers to skewing from a reference point or standard. This definition implies the existence of "real" knowledge in the expert's brain, from which the expert deviates due to cognitive or ecological factors.

Since the mid-1950s, researchers in a variety of fields — including statistics, business, and cognitive psychology, among others — have studied human judgment in both experimental and naturalistic settings to assess how individuals make assessments of unknown events with minimal information. Almost without exception, this area of study has benchmarked the quality and utility of expert judgment by comparing human cognitive assessments to the quantitative predictions of probabilistic statistical models.

Copyright 2005 by CRC Press LLC

Set against this standard, early research clearly indicated that human cognition is not consistently logical; instead, it is vulnerable to sources of bias and error that can severely compromise its utility in probabilistic statements. Comparing the accuracy of human clinical assessments to statistical models demonstrated the predictive superiority of the latter, as well as the cognitive inconsistencies of the former (for discussion, see [25]).

Human fallacy research (see discussion in [24]) has shown fairly conclusively that human beings do not reason in accordance with the rules that ground statistical models. On one hand, predictive models must follow the rules of probability theory; however, human cognitive processes for making predictions under uncertainty often violate these rules. Individuals tend not to adequately revise their opinions when provided with new information, which constitutes a failure to reason in accordance with Bayes theorem. Nor do individuals rely instinctively on the axioms of probability. More recently, some researchers [25] have suggested that cognitive studies themselves introduce bias into the results of research on human cognition.

Biases can be broken down into two general categories, relating to their sources and origins. *Cognitive biases* relate to biases of thought processes and problem solving. *Motivational biases* relate to human behavior from circumstances and personal agendas. Both are discussed in detail.

13.3.1.5.1 Cognitive Bias

Some deficiencies in human judgment can be attributed to inherent inconsistencies in cognition. Such cognitive biases become particularly salient when human experts are asked to make judgments under conditions of uncertainty or with incomplete knowledge—a situation that is not uncommon in many decision environments.

In attempting to identify and classify sources of bias in human judgment, Tversky and Kahneman conducted a series of experiments in which they compared predictions made using probabilistic constraints to subjective judgments made by individuals about the same phenomena. In doing so, they identified several significant and consistent types of bias that seem to degrade the quality of human predictive reasoning. They concluded that "Whether deliberate or not, individuals [rely] on natural assessments [as opposed to probabilistic rules] to produce an estimation or a prediction" [26]. Human problem solving is intuitive, not logically extensional; hence, errors in judgment, they argued, were an unavoidable characteristic of the cognitive processes that humans use to integrate information and make predictive assessments.

In defining sources for bias, Tversky and Kahneman identified three primary intuitive heuristics, or cognitive rules of thumb: *representative, availability,* and *adjustment* and *anchoring*.

1. *Representativeness.* Representativeness refers to the tendency to ignore statistically defined probabilities in favor of experientially based, often narrow stereotypes to classify individual phenomena into categories. An expert evaluates the probability of an uncertain event using its most salient properties, leading to misclassification of the event.
   - *Example:* NASA engineers assumed that the Hubble satellite was reliable because it was manufactured by Perkins-Elmer, which had an excellent track record with other national security satellites. In reality, the Hubble faced scientific demands that other satellites did not, making it a far more complicated system—and less reliable [27]. Small samples are particularly vulnerable to representativeness-based biases.
2. *Availability.* Tversky and Kahneman used this term to describe the ease with which humans draw upon certain types of information—recent events, or strikingly memorable examples of some class of events—and over-incorporate them into cognitive assessments without taking into account the relative value of this information. Humans tend to overestimate the likelihood of rare events, particularly when instances of the class of event in the class are catastrophic, traumatic, and recent.
   - *Example:* An individual who has recently been in an automobile accident may overestimate the probability of being in another. Similarly, experts may assign higher likelihoods to the probability of catastrophic events, such as reactor failure, than actual rates of occurrence warrant.

Copyright 2005 by CRC Press LLC

3. *Anchoring.* Anchoring and its counterpart, adjustment, describe the tendency for individuals to undervalue new information when combining it with existing data to make judgments about the likelihood of a particular event. This occurs when experts have a difficult time moving their thinking from preconceptions or baseline experience. For example, an engineer who has never observed aerodynamic stress beyond a particular value may find it difficult to imagine a situation in which higher load levels might occur. Anchoring also appears as an artifact of the elicitation situation, when an expert draws automatically on assumptions or data used in a previous question to answer a new one, regardless of whether or not that data is truly applicable to the new question.
   - *Example:* When asking experts to estimate failure rates for different classes of high explosives, an expert may unconsciously anchor his or her estimate of failure rates for explosive B to the assumptions or data she or he used for explosive A.

In expert judgment situations, these additional heuristics can generate the following forms of bias:

1. *Conjunction fallacy.* Tversky and Kahneman are also credited with pointing out the existence of the *conjunction fallacy*. This term is used to describe situations in which individuals predicted that the co-occurrence of two unrelated phenomena (A and B) was more likely than the occurrence of either one alone — a prediction that directly contradicts a basic axiom of probability, which states the $P(A \text{ and } B) \leq P(A)$.
   - *Example:* A component fails if it is under high pressure and under the stress from an external load. An expert estimates the probability of a component being under pressure and being under loading as 0.25, but estimated the probability of it being under pressure as 0.20.
2. *Conservativism/base rate neglect.* The discovery of the conjunction fallacy led to the identification of another heuristic, *conservativism.* This heuristic emerges when individuals are asked to use limited information to place a sample in the appropriate population. When provided with new information that should lead to the updating of one's beliefs (for example, statistical base rates), individuals tend to undervalue the new information in relation to the old, and therefore fail to revise their estimates appropriately. *Conservativism* is also referred to as *base-rate neglect,* and it directly affects the expert's ability to properly apply Bayes theorem — a probability theorem for updating new data in light of prior information.
   - *Example:* An expert would not alter his or her reliability estimate of new component, A, when given additional information, B, directly affecting A's performance. That is, $P(A) = P(A|B)$, which implies the reliability of A (i.e., $P(A)$) is independent of B.
3. *Inconsistency.* This very common source of bias is both ecological and cognitive in nature. Confusion, fatigue, or memory problems usually lead to inconsistency. As we discuss below, there are some simple steps that the elicitor can take to minimize inconsistency.
   - *Example:* As an interview begins, the expert may make an assumption about initial conditions. However, after an hour of intensive questioning, the expert may forget or change this assumption, resulting in a different value for a temperature than the original assumption would warrant.
4. *Underestimation of uncertainty.* Humans typically believe we know more than we really do and know it with more precision and accuracy.
   - *Example:* A classic and deadly example of overconfidence was that the Titanic could not sink.

13.3.1.5.2 Motivational Bias

Some deficiencies in human judgment can be attributed to environmental factors. Examples of such *motivational* biases might include fatigue or a desire to appear confident in front of a senior expert. Briefly, some common motivational biases include:

1. *Groupthink.* Group or peer social pressure can slant responses or cause silent acquiescence to what is acceptable to that group.
   - *Example:* The classic and deadly example is President Kennedy's decision on the Bay of Pigs. All his advisors told him what they believed he wanted to hear, rather than providing him with their best judgments and estimates.

Copyright 2005 by CRC Press LLC

2. *Misinterpretation.* Misinterpretation is the inadequate translation of elicited knowledge into a response.
   - *Example:* An interviewer records the pressure for vessel burst as 2000 psi when the expert answered the question as an interval from 1500 to 2500 psi.
3. *Wishful thinking.* Experts' hopes influence their judgments and responses. The old adage, *wishing makes it so*, applies here.
   - *Example:* If an expert is defending his or her system design against competitors, she or he may hope and hence state that it will perform beyond requirements.
4. *Impression management.* Experts are motivated to respond according to politically correct interpretations, convincing themselves that this response is correct.
   - *Example:* A manager may verbally choose one design because it is perceived as more environmentally friendly, when she or he knows that this design has a larger cost-to-benefit ratio.

13.3.1.6 Bias Minimization

Like all data sources, the quality of expert judgment is affected by the process used to gather it. Analysts are trained to understand that measurement data must be calibrated to certain standards in order to eliminate instrumentation biases. Similarly, analysts can and should be meticulous in adopting bias minimization techniques to improve the quality of expert judgment. The quality of expert expressions is conditioned on various factors such as question phrasing, information considered by experts, and experts' methods of problem solving. In short, just as experimental design must be considered when attempting to record data, so too does the elicitation process require deliberate planning.

The cognitive and motivational biases affecting how expert knowledge is gathered are addressed by different bias minimization techniques other than physical *calibration*. Studies have shown [21] that for an expert to be calibrated like an instrument, feedback must be frequent, immediate, and relevant to the technical topic. Very few situations, such as in weather prediction, permit calibration. If sufficient data and information exist to calibrate experts, then their expertise is no longer necessary [1].

In minimizing the effects of cognitive bias, awareness is the first step. Anticipating which biases are likely to occur is the next step. Minimizing bias can also be accomplished by informing the experts of what biases are likely to be exhibited in the elicitation. The advisor-expert can help determine which these are and also help in making the other experts aware.

- *Example:* To mitigate impression management:
  - Assess how likely this bias is given the situation (e.g., will experts benefit or suffer respectively from giving an estimate that sounds good/bad).
  - As a general rule, do not allow experts' bosses during the interview because bosses might pressure the expert to adhere to the party line.
  - Consider making judgments nonattributable to a person, maintaining anonymity.
  - Require substantial explanation of reasoning behind the expert's answer, making it more difficult for them to give the party line.

The analyst should constantly monitor for the occurrence of bias. Adjustments can be made during the elicitation if a particular bias is encountered.

Example: If inconsistencies are beginning to appear in a long interview, then fatigue may be the cause. A break can be taken or another session scheduled to mitigate this bias. If a bias is encountered but cannot be mitigated, it should at least be documented.

The use of the formal elicitation principles in this chapter is an important step in bias minimization. It may also be possible to analyze the elicited judgments to determine if a bias is present; however, this usually requires a very controlled elicitation and multiple expert judgments [1].

13.3.1.7 Question Phrasing

The analyst should *pilot test* the interview using the advisor-expert as practice. This exercise helps ensure that the issues are properly specified, background information is sufficient, and definitions are properly

Copyright 2005 by CRC Press LLC

phrased. It also provides an estimate of the length of the interview, which should be kept to a reasonable time (such as an hour) to prevent fatigue and to minimize the impact on the experts' schedules.

Care in question phrasing and asking is an obvious, but important, aspect of implementation. Questions must be nonleading and formulated using the terms and jargon of the expert's field. Likewise, responses must be understood and recorded in as original form as possible.

While the advisor-expert can help formulate the appropriate topics and specific questions, the entire elicitation session should be *pilot tested* — practiced prior to scheduling the first expert. The advisor-expert and representatives from the design team can be used as the subject for this pilot test. It is during this pilot testing that question wording, order, *response mode* (see below), and interview flow can be examined and revised if necessary. Not infrequently, the analyst will have to refine terminology, question structure, and even locate additional background information. The pilot test should also be timed, so that the experts can be told how much time to set aside for completing the elicitation.

Common difficulties in formulating questions include the following: program structure is too vague or goals are too general to permit concise questions; subject areas covered are too broad; too many questions covering too many areas for the amount of time available; and a cumbersome or inappropriate response mode is asked.

The *response mode* refers to the form used to ask experts to provide judgments. Some numeric mechanisms include asking experts to specify probabilities, likelihoods, odds, odds ratios, intervals, ratings, rankings or pairwise comparisons. Qualitative responses include verbal or written descriptions, rules, classifications, categorizations, and preferences. It is important to make sure that the information extracted from experts is not distorted. Asking an expert to express a judgment in unfamiliar terms (e.g., probability) or forcing a response beyond the current state of knowledge can open any number of pitfalls that lead to bias in his or her expressions.

Example: An analyst would ask the advisor-expert if experts were comfortable providing ranges of values to represent uncertainty in the reliability of a new component. The expert-advisor may advise that numerical answers might not be possible given the new design. Then descriptors such as *poor, moderate, good,* or *excellent* could be used as the response mode.

One method to minimize potential distortion is to provide feed back to the experts, demonstrating what was done with their supplied judgments and how these were used.

Example: If the analyst has gathered ranges of values to construct a probability density function (PDF) representing the uncertainty of a particular parameter for a stress mechanics finite element model, the analyst shows the expert the final form of this PDF and explains its interpretation. Explanation may be involved if the expert is unfamiliar with PDFs.

It is possible to train experts to provide responses in a given manner, although this can be a time-consuming undertaking. *Training* in probabilistic reasoning can offset some of the mismatch between human cognition and probability theory. Training experts in probability provides them with a new set of perceptual models for structuring their judgments. Also, groups of individuals can make use of a wider universe of perceptual models in making judgments.

Conducting the elicitation using bias minimization techniques is best done employing *verbal probe* and *verbal protocol*. Verbal protocol analysis or verbal report is a technique from educational psychology requiring the expert to think aloud. It is best used in face-to-face interview situations because the elicitor may have to continually remind the experts to verbalize their thoughts. Some experts are more able to accommodate this request. Verbal probe refers to repeated questioning, utilizing the words spoken by an expert, drilling down into details of a subject. Verbal probe is another educational psychology technique for understanding the expert's problem-solving processes. These two methods help minimize biases by avoiding leading questions, by checking for consistency through detailed questioning, and by understanding the expert's problem solving. An example would be using additional questions to expand the expert's thinking in avoiding anchoring or under-estimation of uncertainty.

Drilling for details on a given topic serves another principle of elicitation: *decomposition*. Studies have shown [28] that experts can better tackle difficult technical issues if that issue is broken down into more manageable pieces.

Copyright 2005 by CRC Press LLC

Regardless of what level of detail or complexity of the technical problem, all information is conditional. Probing for and documenting these conditions is an important task for the elicitor and provides a traceable record for the experts. Said another way, the universe is a complex tapestry of multiple variables, relationships among those variables, and dependent information. While it may not be possible to unravel all the complex issues and their relationships, uncovering their existence should be the goal of every question/answer session. Expert knowledge is often conditioned upon the assumptions used, the information seen, the way problems are solved, and experience [29]. Understanding basic conditional and dependent relationships is often the key to resolving differences in experts' knowledge and for combining expert knowledge with other sources of information (see Section 13.4.2).

In our experience it is best to allow the experts time to reflect, research, model, calculate, or just think about the problem and the questions asked. Situations where real-time answers are required do exist, but hastened or pressured responses are subject to bias.

13.3.1.7 Documentation

The old adage that the three secrets to a good business are location, location, location applies to the three secrets for successful elicitation: document, document, document. Information and knowledge are constantly changing. Documentation provides the means for understanding and updating these changes. Documentation not only includes recording everything during the elicitation, but also recording the preparations and pilot study experiences. It includes the way the analysis was done and feedback to the experts. The primary goal of eliciting and utilizing expert knowledge is to capture the current state of knowledge — accomplished by formal elicitation and thorough documentation.

13.3.2 A Modified Delphi for Reliability Analysis

In this section, we describe the Delphi approach for eliciting expert reliability assessments in complex technical problems.

Example: As part of a larger reliability study, an analyst is working with a group of aerospace engineers to determine the reliability of a new control system for a communication satellite. The design team is working to identify a test series that will provide high-quality reliability data at minimal cost to the project. The company has a number of senior engineers who are not working on this particular project but who are willing to assist in the reliability characterization. Two of these engineers are considered senior experts and are known for having very strong opinions about design issues. The analyst and the adviser-experts are concerned that their opinions may unduly sway those of the design team members.

The Delphi technique is often associated with the elicitation of knowledge from experts who are asked to characterize uncertain trends, events or patterns. It is perhaps most accurately characterized as a technique for "structuring a group communication process so that the process is effective in allowing a group of individuals, as a whole, to deal with a complex problem" [5]. The method was developed at the RAND Corporation after World War II to elicit expert forecasts of technology trends for the United States military. In the past 50 years, researchers in a wide range of fields have adopted and modified the technique as a way of eliciting judgments in situations where experts are geographically dispersed, do not typically communicate with each other, and face-to-face meetings are difficult to arrange. The response mode is usually qualitative.

The Delphi procedure begins by identifying experts and assessing their willingness to work on the project. The analyst then provides the participating experts with a series of questions, usually focused on one or two issues (e.g., physical variables). This can be accomplished in several ways:

- Through a website where the experts can access the questionnaire and record responses
- By providing the experts with electronic copies of a questionnaire to be filled out and returned electronically to the analyst
- With a standard paper questionnaire that the experts will complete and return through the post

Copyright 2005 by CRC Press LLC

Once the expert responses are received, the analyst removes identifying information and compiles the expert opinion into a single document. The analyst then sends this revised document to the experts, who are asked to take their peers' answers into account when considering and revising their initial judgments. This procedure can be repeated until an acceptable level of consensus is reached among the experts.

While Delphi has many advantages — including potential cost savings, its ability to minimize groupthink, and its applicability to emergent, poorly-defined problems — there are many potential pitfalls associated with pursuing a Delphi approach. The method has been criticized not so much for its philosophical basis, but for the ways in which it has been applied [5]. As the attached bibliography indicates, analysts interested in learning more about the history and applications of Delphi elicitation will find a great deal of literature and guidance in journals, on the Internet, and in the library. In this discussion, however, we are interested in exploring the application of a Delphi-style approach for eliciting expressions of expert judgment. This includes the following issues:

- Using an expert-oriented elicitation to estimate reliability for parts and processes
- Designing a pilot-tested questionnaire
- Training experts to respond so that the occurrence of bias is minimized

Delphi can be modified to address the criticisms leveled at it, and the approach can provide the analyst with a valuable tool for eliciting expert assessments. As with all expert opinion, our approach, like Delphi is grounded in a fundamental philosophy that formal methods for eliciting and documenting expert knowledge add rigor and provide defensibility. Moreover, formal elicitation augments the analyst's ability to update information as the state of knowledge within the community changes.

This is particularly true in situations when busy schedules make it impossible to gather a group of experts for a group elicitation, or when complicated social dynamics among experts have the potential to limit the quality and quantity of data collected. Examples of the latter include situations when a single expert tends to dominate other members of the organization, influencing the group's consensus. In other organizations, experts simply may not get along with one another. When grouped around a single table, argumentative experts can easily get "stuck" on a fine point of disagreement while failing to address other aspects of the elicitation. Because of this, Delphi requires that experts *not* be in contact during the elicitation. Hence, it can be quite effective in eliciting opinions from individual experts under conditions of anonymity.

13.4 Analyzing Expert Judgment

13.4.1 Characterizing Uncertainties

The main purpose of eliciting expertise and expert judgments is to establish and gather all that is currently known about a problem. However, this knowledge can be in different forms (qualitative or quantitative), dependent upon the current state of what is known. Where knowledge is vague or weak, expert judgments may only be in the form of natural language statements or rules regarding the performance of a product. For example, an expert may say "*if the temperature is too hot, this component will not work very well*." While this statement is nonnumeric, it contains valuable information, and epistemic uncertainties are inherent in the use of linguistic terms such as *too hot* and *not very well*. Membership functions from Zadeh's fuzzy set theory [30] can be used to characterize the uncertainty associated with these language terms. For example, input membership functions (Figure 13.9) can be constructed to represent the uncertainty in classifying temperatures as *too hot* and output membership functions (Figure 13.10) constructed to classify performance as *not work very well*. *If-then* rules are used to map the input temperatures into the performance descriptions.

Where knowledge is stronger, experts may be able to provide quantitative answers for the physical quantities of interest or for reliability directly. In such cases, quantitative answers for the corresponding uncertainties associated with these quantities may also be elicited. These include *probability, ratings*,

Copyright 2005 by CRC Press LLC

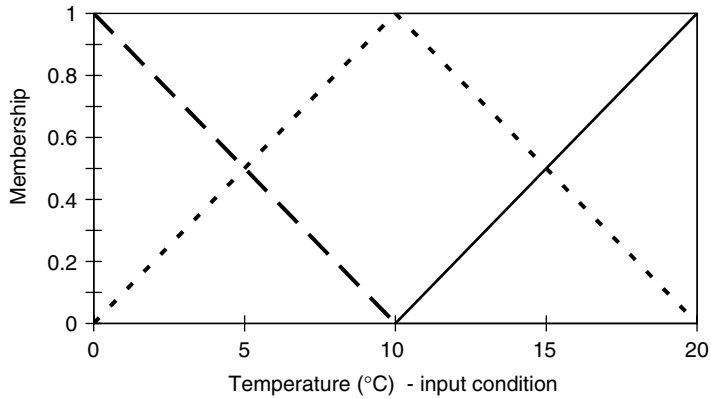

FIGURE 13.9 Input membership functions (— — warm, - - - hot, — too hot).

rankings, *odds ratios*, *log odds*, *weighting factors*, *ranges*, and *intervals*. A convenient, useful, and bias-minimizing tool for guiding experts to provide any of the above quantitative estimates is to have them mark their estimates on a drawn real number line. While humans tend to think in linear terms, directing the use of a simple linear *number line*, some physical phenomena may be on a logarithmic scale, directing a log line use (such as for eliciting *log odds*).

The *number line* elicitation begins with experts providing the scale for the line by specifying its endpoints. Then the expert is asked to mark his best estimate on the line with an *x*. To capture uncertainties, he is then asked to provide the extreme high and low values on the line. It is necessary to carefully guide the expert in specifying extreme values to overcome anchoring and under-estimation of uncertainty biases, without leading him. If the expert wants to shade in regions on the number line (rather than marking specific points) for the best and extreme estimates, permit this because he is expressing uncertainties about the values. At this point the analyst has intervals that could be analyzed using *interval* analysis or *random intervals*. (See Chapter 9 on by Joslyn and Booker on General Information Theories.)

If the expert has sufficient knowledge to specify relative frequencies of occurrence for various values on the number line, an entire uncertainty distribution (such as a probability density function) could be elicited [1, 20]. These distributions could also be formulated indirectly by eliciting information from experts about parameters and uncertainties on those parameters for a chosen model. Such an exercise is described by Booker et al. [31], where the parameters of a Weibull reliability model were elicited, because

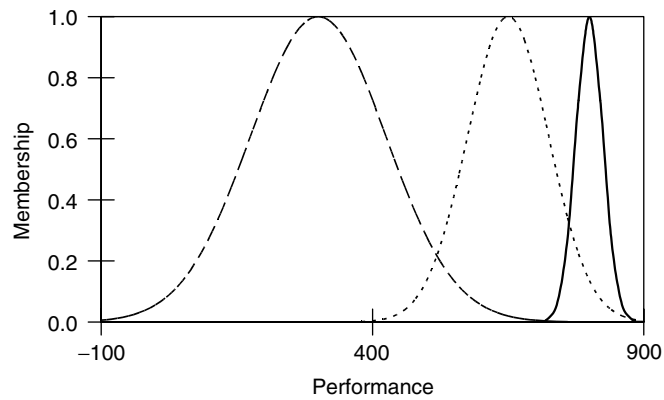

FIGURE 13.10 Output membership functions (— — bad, - - - not well, —— not very well).

Copyright 2005 by CRC Press LLC

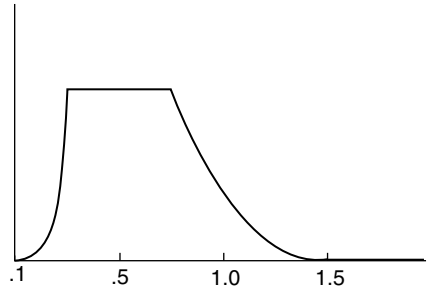

FIGURE 13.11 PDF drawn by hand, expressing an expert's uncertainty about a variable.

the experts customarily thought in terms of failure mechanisms and rates that defined those parameters. It should be noted that elicited PDFs do not necessarily have to follow a particular family or distribution type (e.g., a normal). Empirically based or expert supplied distributions reflect the way experts interpret the likelihood of values associated with the quantity of interest — the variable. Figure 13.11 demonstrates a probability distribution function drawn free-hand by an expert.

Rankings refer to specifying preferences x out of a finite list of n options, alternatives, or similar items. An implicit assumption in using ranks is that the numeric answers are equidistant (i.e., a rank of 4 is twice the rank of 2). If properly directed, experts can use a nonlinear scale (e.g., this rank is "5" out of "50" but "4" through "7" are closer ranked than "1" through "3" or above "8"). Such specifications aid in determining uncertainty.

Rating scales can be used to map words into numbers, percentages, ranks, or ratings. Examples include *Saaty's pairwise comparisons,* which utilize a specified scale description for comparing the degree of comparison between items, two at a time [32]. A scale from Sherman and Kent establishes equivalency between verbal descriptions of likelihood, chances, and percentages. For example, *8 out of 10, 8/10,* or *80%* falls between *probable* and *nearly certain* or between *likely* and *highly likely.* Here again, the vagueness of the verbal description imposes a source of epistemic uncertainty.

Odds ratio takes advantage of the concept of betting and chance. Our experience confirms the results of others, indicating that humans are naturally comfortable thinking in these terms.

Uncertainties can be estimated with rankings, ratings, and odds by eliciting ranges rather than single-valued results. Again, GITs can be used to mathematically represent the uncertainties from these ranges. Possibility distributions, random intervals, upper and lower probabilities, and membership functions are among the alternative forms for PDFs. These theories also offer axioms of how to combine their respective distributions of uncertainty within the operations of each theory. However, only one linkage has been formalized between two of the theories: probability and fuzzy membership functions [33].

Twice now the subject of turning linguistic terms into numbers has emerged in the characterization of uncertainties. As demonstrated in Figure 13.4 and Figure 13.5, membership functions from fuzzy sets can be useful in eliciting natural language information and then quantifying the uncertainty associated with those linguistic terms. Fuzzy sets and their corresponding measure of uncertainty, membership, are designed to best capture uncertainties due to ambiguity of classification. For example, what does it mean to be *too hot*? (See Chapter 9 by Joslyn and Booker on General Information Theories, section on fuzzy sets and membership functions.) In contrast to this type of uncertainty, probability is best designed to capture the uncertainty associated with the outcome of an event or experiment.

As a quantification tool for reliability, membership functions map the condition of a component or system into its performance through the use of knowledge contained in *if-then* rules. The previous example holds: *if the temperature is too hot* (input fuzzy membership function), *then this component will not work very well* (output fuzzy membership function). Membership functions can be used to characterize the conditions (x) and *if-then* rules map those conditions into performance (y) membership functions. A reliability example of how to combine linguistic information from a component supplier with probability expert judgments from designers can be found in Kerscher et al. [34].

Copyright 2005 by CRC Press LLC

13.4.1.1 Probability Theory: The Good and the Bad

Probability theory has become a fundamental theory for characterizing *aleatoric uncertainty* — uncertainty associated with phenomena such as random noise, measurement error, and uncontrollable variation. With aleatoric uncertainty, the common conception is that uncertainty cannot be further reduced or eliminated by additional information (data or knowledge). In communities involved in KA and computational sciences, *epistemic uncertainty* refers to an absence of complete knowledge — uncertainty that can be reduced or eliminated by increasing knowledge or sample size. In following the formal elicitation principles, such as preserving the original form of elicited information, uncertainty characterization should be consistent with the way experts think and hence verbalize. Because experts (even those in science and engineering fields) may not readily think in terms of probability and may not be able to characterize their uncertainties with PDFs, probability may not be adequate for handling either form of uncertainty. Studies [35, 36] have also shown that many humans who are comfortable with probabilistic thinking are not able to think consistently within its axioms. Other GITs are examined below in their applicability for elicited judgments.

Yet probability theory has a rich and long legacy of use in science and engineering and in uncertainty analysis and quantification. To those involved with complex decision problems like Probabilistic Risk Assessment (PRA), the uncertainty embodies both: *aleatoric* (random, irreducible uncertainty) and *epistemic* (lack of knowledge, reducible with more information) uncertainties. This interpretation also encompasses uncertainty caused by errors, mistakes, and miscalculations. The absence of a distinction between aleatoric and epistemic uncertainty is also subscribed to by modern subjective probabilists, or Bayesians, and applies to modern, complex reliability analysis. Probability theory (see Chapter 9 by Joslyn and Booker on GITs) provides a calculus for the uncertainty associated with the outcome of an event or experiment (E), designated as P(E). The theory and its basic axioms do not specify how to determine the value of probability nor how to interpret it. Therefore, numerous historical interpretations are of equal value, including the subjective, personalistic or Bayesian interpretation, which says there is no such thing as a correct probability, or an objective probability. This interpretation is best suited for the way expert probabilities are elicited and used. Data is typically sparse for rare or one-of-a-kind events — the perfect use of subjective probability.

13.4.1.2 General Information Theories: The Good and the Bad

While the mathematical theory of many GITs is well developed, the practical implementation of these to real problems, such as reliability and expert elicitation, is lacking. As has already been noted, these theories can offer alternatives for characterizing uncertainties consistent with information elicited from experts. For example, if the extent of knowledge only permits intervals as answers, and those intervals have imprecise limits, then random intervals could provide a consistent analysis tool. Another example is linguistic information and classification uncertainty that can be best represented by fuzzy membership functions.

However, in any complex reliability problem, available information can be in diverse forms, data, models, expert judgment, historical information, practices, and experience. Accompanying uncertainties may also be best formulated using a variety of GITs, including probability. All this information must be combined to assess the reliability of the entire system, so the uncertainty theories must be linked for combination. Unfortunately, the theory and application of the GITs are insufficient to handle cross linkages. This failing is so severe that analysts are often forced to specify a particular GIT for the entire system and work only within that theory.

13.4.1.3 Aggregation of Expert Judgments

A large body of literature specifies various methods for combining expert judgments from multiple experts. These methods range from the use of elicitation to reach consensus or resolve differences to exact analytical methods [37]. Booker and McNamara [38] detail such a scenario, utilizing the tenets of elicitation. To summarize these, differences between experts can often be resolved by thorough examination of their

Copyright 2005 by CRC Press LLC

assumptions, sources of information used, heuristics, and problem-solving processes. For example, experts with different assumption sets may be solving slightly different problems. Once common assumptions and problem definition are established, differences can be mitigated. Remaining differences among experts after resolution attempts may be representative of the existing (and perhaps large) state of uncertainty.

Aggregation can be achieved by analytical methods, with combination techniques implemented by an analyst, a decision maker, or by the experts themselves. The maximum entropy solution (when no other information is available to determine weighting factors) is to equally weight the experts. The aggregation (like many others) assumes that all experts are independent, in much the same way as a statistician would consider repeated runs of an experiment as independent draws from a probability distribution representing the population of all possible outcomes. However, this classical inference argument has been disputed when applied to experts who have dependencies due to common experience, access to the same data, and similar education and training. The elicitor, advisor expert, decision maker, or analyst may be able to quantify dependence among experts [1]. From this book, studies have shown that experts are quite capable of determining weights for each other and also that expert judgments are well correlated to how experts solve problems, making precise extraction and documentation of problem solving important.

The many analytical expressions for combining expert judgments can be summarized into three basic formulas for aggregating uncertainty distribution functions, f. Each expert contributes to the construction of these functions by either providing information relating to the uncertainty of the random variable, x, or the parameters, θ, of the functions. Common practice in probability theory is to specify these f's as probability density functions; however, f could also refer to any uncertainty function such as a possibility distribution. Rules for combining these f's within their respective theories will alter the basic combination schemes below (which refer to probability theory):

$$f_c(x, \theta) = w_1 \cdot f_1(x, \theta) + w_2 \cdot f_2(x, \theta) + \ldots \tag{13.1}$$

$$f_c(x, \theta) = f([w_1 \cdot x_1 + w_2 \cdot x_2 + \ldots], \theta) \tag{13.2}$$

$$f_c(x, \theta) = f([x_1, x_2, \ldots], \theta) \tag{13.3}$$

Equation 13.1 illustrates a scheme that weights each expert's function for x and θ in a linear combination. Equation 13.2 weights the random variables from each expert, and that weighted combination is mapped through an overall function. That is, in Equation 13.2, the function on the left hand side is the probability density function of the weighted sum of random variables. Equation 13.3 combines the random variables for a given θ using the concept of a joint distribution function.

Example: Two experts each supply PDF's, f_1 and f_2 as uncertainty distributions on the number of failure incidences per 1000 vehicles (IPTV) manufactured for a new electronic circuit, shown in Figure 13.12. Using Equation 13.1 with equal weights, the combined result is shown in Figure 13.13. Combining expert uncertainty functions is an analytical exercise not unlike combining the diverse sources of information using information integration tools.

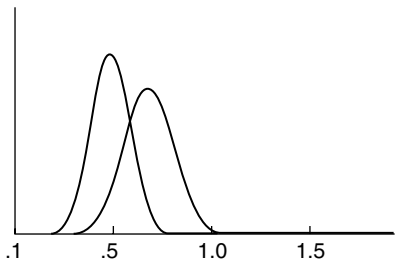

FIGURE 13.12 Two experts' IPTV PDFs.

Copyright 2005 by CRC Press LLC

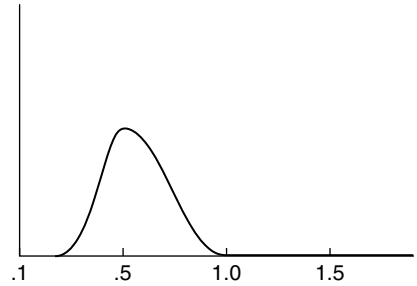

FIGURE 13.13 Equal combination.

13.4.2 Information Integration for Reliability

13.4.2.1 How Expert Knowledge Combines with Other Information

Reliability is typically defined as a probability; specifically, it is the probability that the system will function up to a specified time, t, for given conditions or specifications. This reliability can be denoted as $R(t|\theta)$, where the parameters θ could denote mean time to failure or could refer to two parameters in a Weibull model. In classical (frequentist interpretation of probability) estimation of θ, data is considered as random and θ parameters are considered fixed. In Bayesian (subjective interpretation of probability) estimation, the data is fixed, and θ are random. Either interpretation is valid under the axioms of probability, and in both cases, the process of estimation relies on having *data*. In cases where data are sparse or nonexistent, the estimation process relies on whatever forms of information are available, including expert judgment.

Example: A team of design engineers wants to evaluate the performance of three design ideas for a new actuator on a valve. Design 1 uses a new explosive; design 2 uses a new firing set; and design 3 uses both. Large amounts of data exist on the old explosive and firing sets, making a statistical estimate of reliability possible by calculating successes/tests. No data is available for the new components, but the team estimates a subjective reliability for the new explosive and new firing set. Both the calculated reliability and the experts' subjective reliability values are valid interpretations of probabilities. Both can be used to estimate the performances of the three designs.

Additional information sources could also include historical information about the system, data from similar components, and computer model outputs of physical processes. Systems are composed of more than components and subsystems. Processes are equally important representations of system performance and functioning. If parts are considered the *nouns* of the system, then processes are its *verbs*. Processes include the actions involved in assembly, testing, quality control, inspections, and physical dynamics, to name a few.

Complex or newly designed systems may have one or more parts or processes that have no test or experimental data. Preprototype, preproduction concept design systems may have no relevant test data, resulting in reliance on other information sources to estimate reliability. Information integration techniques have been developed [39] to take advantage of all available information to assess the performance of new, complex, or aging systems for decisions regarding their production, continued use, and maintenance, respectively. Expertise and expert judgment play important roles in these decisions, and expert judgment may be the sole source of information in some cases. A reliability example using this technology can be found in [31].

Information integration techniques are also useful for updating reliability assessments. The state of knowledge is constantly changing, and mathematical updating mechanisms such as Bayes theorem are useful for updating the existing information (under uncertainty) with the new information. Documentation is therefore necessary for all information sources, not just expert judgments, to ensure proper updating with these or any other techniques.

Example: In designing a new fuel pump, the design team of experts used their experience with other fuel pumps to estimate the reliability of one of its new components. They supplied a range of values for the failure

Copyright 2005 by CRC Press LLC

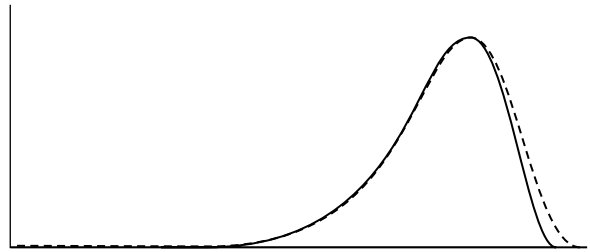

FIGURE 13.14 Experts' prior reliability estimate (solid) and combined estimate with 40 *what-if* test results (dashed) [31].

rate of that component, λ, to be used in a Weibull model for estimating the reliability, R, at time $t = 1$ year:

$$R(t|\lambda) = exp(-\lambda t^{0.8}) \tag{13.4}$$

where the failure rate parameter, λ, decays according to the second parameter in the time exponent with a value of 0.8. To improve reliability, the experts asked *what if* we built 40 prototypes that all passed the testing program; how much would reliability improve? Using Bayes theorem, their initial (prior) reliability distribution (Figure 13.14, solid curve) was combined with a binomial distribution for 40 tests, 0 failures. The resulting posterior for the new combined reliability is the dashed curve (Figure 13.14). Based on the minimal improvement gained from the costly prototype and test program, the decision maker decided not to pursue this program.

13.5 Conclusion

Today's complex reliability problems demand more predictability with less expensive test programs. Awareness of uncertainties and the simple fact that the state of knowledge is constantly changing add to the complexity of these problems. Why not take advantage of an organization's most valuable source of information — the knowledge and expertise of its technical staff. Use of the formal elicitation methods in this chapter provides a traceable, updateable, defensible way to capture this knowledge.

Elicitation methods are used for gathering knowledge and understanding about the structure of a complex problem and for populating that structure with the qualitative and quantitative judgments of the experts. Information integration methods exist to provide a formalism for combining expert knowledge, and its associated uncertainties, with other data or information.

The keys to successful elicitation include the following: Construct an expert-oriented elicitation and analysis that captures the current state of knowledge and permits combination of this knowledge with other data/information. The formal methods outlined in this chapter emphasize bias minimization, capturing knowledge consistent with the way experts think and problem solve, utilizing feedback, and documentation. Finally, the analyst should never compromise the experts' trust.

References

1. Meyer, M.A. and Booker, J.M., *Eliciting and Analyzing Expert Judgment: A Practical Guide*. Philadelphia, PA: Society for Industrial and Applied Mathematics/American Statistical Association, 2001.
2. Helmer, O. and Rescher, N., "On the Epistemology of the Inexact Sciences," *Management Science*, 5 (June), 25–52, 1959.
3. Dalkey, N.C., "An Experimental Study of Group Opinion: The Delphi Method," *Science*, 243, 1668–1673, 1969.
4. Dalkey, N.C. and Helmer, O., "An Experimental Application of the Delphi Method to the User of Experts," *Management Science*, 9(3), 458–67, 1963.

Copyright 2005 by CRC Press LLC

5. Linstone, H.A. and Turoff, M., Eds., *The Delphi Method. Techniques and Applications.* Reading, MA, 1975.
6. Paton, R.C., Nwana, H.S., Shave, M.J.R., and Bench-Capon, T.J.M., "From Real World Problems to Domain Characterisations", *Proceedings of 5th European Knowledge Acquisition Workshop*, Crieff, May, 1991. Reprinted in Linster, M., Ed., *Proceedings of 5th European Knowledge Acquisition Workshop*, GMD-Studien Nr. 211, GMD, Sankt-Augustin, Germany, 1992, 235–256.
7. Paton, R.C., Lynch, S., Jones, D., Nwana, H.S., Bench-Capon, T.J.M., and Shave, M.J.R., "Domain Characterisation for Knowledge Based Systems," *Proceedings of A.I. 94 — Fourteenth International Avignon Conference*, Volume 1, 41–54, 1994.
8. Wenger, E., *Communities of Practice: Learning, Meaning and Identity*. Cambridge, UK: Cambridge University Press, 1998.
9. Chaiklin, S. and Lave, J., Eds., *Understanding Practice: Perspectives on Activity and Context*. Cambridge, UK and New York: Cambridge University Press, 1996.
10. Lave, J. and Wenger, E., *Situated Learning: Legitimate Peripheral Participation.* Cambridge, UK: Cambridge University Press, 1991.
11. Lave, J., *Cognition in Practice*. Cambridge, UK: Cambridge University Press, 1988.
12. Martz, H.F. and Waller, R.A., *Bayesian Reliability Analysis*, New York: John Wiley & Sons, 1982.
13. Hoffman, R.R., Shadbolt, N.R., Burton, A.M., and Klein, G., "Eliciting Knowledge from Experts: A Methodological Analysis," *Organizational Behavior and Decision Management,* 62(2), 129–158, 1995.
14. Davis, R., Shrobe, H., and Szolovits, P., "What Is a Knowledge Representation?" *AI Magazine,* 14(1), 17–33, 1993.
15. Leishman, D. and McNamara, L., "Interlopers, Translators, Scribes and Seers: Anthropology, Knowledge Representation and Bayesian Statistics for Predictive Modeling in Multidisciplinary Science and Engineering Projects," to appear in *Multidisciplinary Studies of Visual Representations and Interpretations.* Malcolm, G. and Paton, R., Eds., Amsterdam: Elsevier Science, 2004.
16. Cooke, N.J., "Varieties of Knowledge Elicitation Techniques," *International Journal of Human-Computer Studies,* 41, 801–849, 1994.
17. Paton, R.C., "Process, Structure and Context in Relation to Integrative Biology," *BioSystems*, 64, 63–72, 2002.
18. Keeney, R.L. and von Winterfeldt, D., "On the Uses of Expert Judgment on Complex Technical Problems," *IEEE Transactions on Engineering Management,* 36, 83–86, 1989.
19. Keeney, R.L. and von Winterfeldt, D., "Eliciting Probabilities from Experts in Complex Technical Problems," *IEEE Transactions on Engineering Management,* 38(3), 191–201, 1991.
20. Kadane, J.B. and Wolfson, L.J., "Experiences in Elicitation," *The Statistician,* 47, 1–20, 1998.
21. Lichtenstein, S., Fischhoff, B., and Phillips, L.D., "Calibration of Probabilities: The State of the Art to 1980," in D. Kahneman, P. Slovic, and A. Tversky, Eds., *Judgment under Uncertainty: Heuristics and Biases,* Cambridge, MA: Cambridge University Press, 1982, 306–334.
22. Jensen, F.V., *An Introduction to Bayesian Networks.* New York: Springer, 1996.
23. Ayyub, B., *Elicitation of Expert Opinions for Uncertainty and Risk*s. Boca Raton, FL: CRC Press, 2001.
24. O'Leary, D., "Knowledge Acquisition from Multiple Experts: An Empirical Study," *Management Science,* 44(8), 1049–1058, 1998.
25. Ayton, P. and Pascoe. E., "Bias in Human Judgment under Uncertainty?" *The Knowledge Engineering Review,* 10(1), 21–41, 1995.
26. Tversky, A. and Kahneman, D., "Extensional versus Intuitive Reasoning: The Conjunction Fallacy in Probability Judgment." *Psychological Review*, 90(4), 293–315, 1983.
27. Nelson, M., "The Hubble Space Telescope Program: Decision-Making Gone Awry," Unpublished Report, Nelson Associates, Del Mar, CA., Available at URL http://home.att.net/~maxoccupancy/, 1992.
28. Armstrong, J.S., *Long-Range Forecasting: From Crystal Ball to Computer*. New York: Wiley-Interscience, 1981.
29. Booker, J.M. and Meyer, M.A., "Sources and Effects of Interexpert Correlation: An Empirical Study," *IEEE Transactions on Systems, Man, and Cybernetics,* 18, 135–142, 1988.

Copyright 2005 by CRC Press LLC

30. Zadeh, L., "Fuzzy Sets," *Information and Control*, 8, 338–353, 1965.
31. Booker, J.M., Bement, T.R., Meyer, M.A., and Kerscher, W.J., "PREDICT: A New Approach to Product Development and Lifetime Assessment Using Information Integration Technology," *Handbook of Statistics: Statistics in Industry*, Volume 22 (Rao and Khattree, Editors), Amsterdam, The Netherlands: Elsevier Science, 2003, Chap. 11.
32. Saaty, T.L., *The Analytic Hierarchy Process: Planning, Priority Setting, and Resource Allocation,* New York: McGraw-Hill, 1980.
33. Singpurwalla, N.D. and Booker, J.M., "Membership Functions and Probability Measures of Fuzzy Sets," *Journal of the American Statistical Association*, September 2004 Volume 99 No. 467, 867–877.
34. Kerscher, W.J., Booker, J.M., Meyer, M.A., and Smith, R.E., "PREDICT: A Case Study Using Fuzzy Logic," *Proceedings of International Symposium on Product Quality & Integrity*, Tampa, FL, January 27–30, 2003, and Los Alamos National Laboratory report, LA-UR-02-0732, 2003.
35. Kahneman, D. and Tversky, A., "Subjective Probability: A Judgment of Representativeness," In Kahneman, D., Slovic, P., and Tversky, A., Eds., *Judgment under Uncertainty: Heuristics and Biases,* 32–47. Cambridge, MA: Cambridge University Press, 1982.
36. Hogarth, R., Cognitive processes and the assessment of subjective probability distributions. *Journal of the American Statistical Association,* 70, 271–291, 1975.
37. Lindley, D.V. and Singpurwalla, N.D., "Reliability and Fault Tree Analysis Using Expert Opinions," George Washington University Report GWU/IRRA/TR-84/10, Washington, D.C., 1984.
38. Booker, J.M. and McNamara, L.A., "Solving the Challenge Problems Using Expert Knowledge Theory & Methods," submitted to *Reliability Engineering and System Safety*, Special Issue: Epistemic Uncertainty Workshop and Los Alamos National Laboratory Report, LA-UR-02-6299 (2002).
39. Meyer, M.A., Booker, J.M., and Bement, T.R., "PREDICT-A New Approach to Product Development," *R&D Magazine*, 41, 161, and Los Alamos National Laboratory document, LALP-99-184, 1999.

Copyright 2005 by CRC Press LLC

14

First- and Second-Order Reliability Methods

Armen Der Kiureghian
University of California, Berkeley

14.1 Introduction

Within the broader field of reliability theory, the class of time-invariant structural reliability problems is characterized by an n-vector of basic (directly observable) random variables $\mathbf{x} = \{x_1, \ldots, x_n\}^{\mathrm{T}}$ and a subset Ω of their outcome space, which defines the "failure" event. The probability of failure, $p_f = P(\mathbf{x} \in \Omega)$, is given by an n-fold integral

$$p_f = \int_{\Omega} f(\mathbf{x}) d\mathbf{x} \tag{14.1}$$

where $f(\mathbf{x})$ is the joint probability density function (PDF) of $\mathbf{x}$. This problem is challenging because for most nontrivial selections of $f(\mathbf{x})$ and Ω, no closed form solution of the integral exists. Furthermore, straightforward numerical integration is impractical when the number of random variables, n, is greater than 2 or 3. Over the past two decades, a number of methods have been developed to compute this probability integral. This chapter introduces two of the most widely used methods: the first-order reliability method, FORM, and the second-order reliability method, SORM. Extensions of the above formulation to time- or space-variant problems and to applications involving finite element analysis are also described in this chapter.

In general, the failure domain Ω is described in terms of continuous and differentiable *limit-state* functions that define its boundary within the outcome space of $\mathbf{x}$. Depending on the nature of the problem, the following definitions apply:

Copyright 2005 by CRC Press LLC

Component problem:

$$\Omega \equiv \{g(\mathbf{x}) \leq 0\} \tag{14.2a}$$

Series system problem:

$$\Omega \equiv \bigcup_k \{g_k(\mathbf{x}) \leq 0\} \tag{14.2b}$$

Parallel system problem:

$$\Omega \equiv \bigcap_k \{g_k(\mathbf{x}) \leq 0\} \tag{14.2c}$$

General system problem:

$$\Omega \equiv \bigcup_k \bigcap_{j \in c_k} \{g_j(\mathbf{x}) \leq 0\} \tag{14.2d}$$

The formulation in 14.2a applies to component reliability problems, which are defined in terms of a single limit-state function, $g(\mathbf{x})$. Any outcome $\mathbf{x}$ of the random variables, for which the limit-state function is nonpositive, constitutes the failure of the component. The simplest example for this class of problems is the limit-state function $g(x_1, x_2) = x_1 - x_2$, where x_1 denotes a capacity quantity and x_2 denotes the corresponding demand. More generally, the limit-state function is defined by considering the mechanical conditions under which the failure may occur. For example, the failure due to yielding of a two-dimensional continuum according to the von Mises yield criterion is defined by the limit-state function $g(\mathbf{x}) = \sigma_{\text{yld}}^2 - (\sigma_x^2 + \sigma_y^2 - \sigma_x\sigma_y + 3\tau_{xy}^2)$, where σ_x, σ_y and τ_{xy} are the components of stress and σ_{yld} is the yield stress, all being functions of some basic random variables $\mathbf{x}$ describing observable quantities, such as material property constants, structural dimensions and loads. The relationship between the stress components and the basic variables, of course, can be complicated and computable only through an algorithmic procedure, such as a finite element code. This aspect of reliability analysis is briefly described in Section 14.6.

The series system problem in 14.2b applies when the failure domain is the union of componential failure events. A structure having multiple failure modes, each defined in terms of a continuous and differentiable limit-state function $g_k(\mathbf{x})$, belongs to this category of problems. Note that the random variables $\mathbf{x}$ are shared by all the components. As a result, the componential failure events in general are statistically dependent. A good example for a series system is a ductile structural framework having multiple failure mechanisms. Such an example is described later in this chapter.

The parallel system problem in 14.2c applies when the failure domain is the intersection of componential failure events. A redundant structure requiring failure of several components, each defined in terms of a continuous and differentiable limit-state function $g_k(\mathbf{x})$, belongs to this category of problems. A good example is a bundle of brittle wires with random strengths and subjected to a random tension load.

Most structural systems are neither series nor parallel. Rather, the system fails when certain combinations of components fail. We define a cut set as any set of components whose joint failure constitutes failure of the system. Let c_k denote the index set of components in the k-th cut set. The intersection event in 14.2d then defines the failure of all components in that cut set. The union operation is over all the cut sets of the system. For an accurate estimation of the failure probability, one must identify all the minimal cut sets. These are cut sets that contain minimum numbers of component indices; that is, if any component index is removed, what remains is not a cut set. Exclusion of any minimum cut set from consideration will result in underestimation of the failure probability. Thus, the cut-set formulation provides an estimate of the failure probability from below. It is noted that this formulation essentially represents the system as a series of parallel subsystems, each subsystem representing a cut set.

Copyright 2005 by CRC Press LLC

An alternate formulation for a general system defines the complement of Ω in terms of link sets. A link set is a set of components whose joint survival constitutes the survival of the system. Letting l_k define the set of indices in the k-th link set, the complement of the failure event, the survival event, is defined as

$$\overline{\Omega} \equiv \bigcup_k \bigcap_{j \in l_k} \{g_j(\mathbf{x}) > 0\} \tag{14.2e}$$

In this formulation, one only needs to include minimal link sets, that is, link sets that do not include superfluous components. The advantage of this formulation is that exclusion of any link set produces a conservative estimate of the failure probability. However, working with the intersection of survival events as in 14.2e is computationally more difficult. For this reason, the formulation in 14.2d is more commonly used.

FORM, SORM, and several other computational reliability methods take advantage of the special properties of the standard normal space. For this reason, these methods involve a transformation of the random variables $\mathbf{x}$ into standard normal variables $\mathbf{u}$ having the joint PDF $\varphi_n(\mathbf{u}) = (2\pi)^{-n/2} \exp(-\|\mathbf{u}\|^2/2)$, where $\|\cdot\|$ denotes the Euclidean norm, as a first step of the reliability analysis. Useful properties of the standard normal space include rotational symmetry, exponentially decaying probability density in the radial and tangential directions, and the availability of formulas for the probability contents of specific sets, including the half space, parabolic sets, and polyhedral sets. The applicable forms of this transformation are described in the following section.

14.2 Transformation to Standard Normal Space

Let $\mathbf{x}$ denote an n-vector of random variables with a prescribed joint PDF $f(\mathbf{x})$ and the corresponding joint cumulative distribution function (CDF) $F(\mathbf{x}) = \int_{-\infty}^{x_n} \cdots \int_{-\infty}^{x_1} f(\mathbf{x}) d\mathbf{x}$. We wish to construct a one-to-one transformation $\mathbf{u} = \mathbf{T}(\mathbf{x})$, such that $\mathbf{u}$ is an n-vector of standard normal variables. As described below, such a transformation exists, although it may not be unique, as long as the joint CDF of $\mathbf{x}$ is continuous and strictly increasing in each argument. For computational purposes in FORM and SORM, we also need the inverse transform $\mathbf{x} = \mathbf{T}^{-1}(\mathbf{u})$ and the Jacobian of the $\mathbf{x} \to \mathbf{u}$ transformation, $\mathbf{J}_{\mathbf{u},\mathbf{x}}$. These are defined in the following subsections for four distinct cases that occur in practice. For this analysis, let $\mathbf{M} = \{\mu_1 \cdots \mu_n\}^{\mathrm{T}}$ denote the mean vector of $\mathbf{x}$ and $\Sigma = \mathbf{DRD}$ denote its covariance matrix, where $\mathbf{D} = \mathrm{diag}[\sigma_i]$ is the $n \times n$ diagonal matrix of standard deviations and $\mathbf{R} = [\rho_{ij}]$ is the correlation matrix having the elements $\rho_{ij}, i, j = 1, \ldots, n$.

14.2.1 Statistically Independent Random Variables

Suppose the random variables $\mathbf{x}$ are statistically independent such that $f(\mathbf{x}) = f_1(x_1) f_2(x_2) \cdots f_n(x_n)$, where $f_i(x_i)$ denotes the marginal PDF of x_i. Let $F_i(x_i) = \int_{-\infty}^{x_i} f_i(x_i) dx_i$ denote the CDF of x_i. The needed transformation in this case is diagonal (each variable is transformed independently of other variables) and has the form

$$u_i = \Phi^{-1}[F_i(x_i)] \qquad i = 1, 2, \ldots, n \tag{14.3}$$

where $\Phi[\cdot]$ denotes the standard normal CDF and the superposed -1 indicates its inverse. Figure 14.1 shows a graphical representation of this transformation. Each point (x_i, u_i) on the curve is obtained by equating the cumulative probabilities $F_i(x_i)$ and $\Phi(u_i)$. Note that this solution of the needed transformation is not unique. For example, an alternative solution is obtained if $F_i(x_i)$ in Equation 14.3 is replaced by $1 - F_i(x_i)$.

The inverse of the transformation in 14.3 is

$$x_i = F_i^{-1}[\Phi(u_i)] \quad i = 1, 2, \ldots, n \tag{14.4}$$

Copyright 2005 by CRC Press LLC

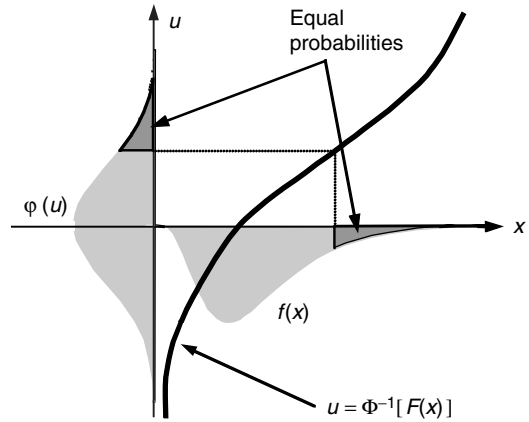

FIGURE 14.1 Transformation to the standard normal space for a single random variable.

If x_i is nonnormal, both transformations 14.3 and 14.4 are nonlinear and may require a numerical root finding algorithm to solve. The Jacobian of the transformation is a diagonal matrix $\mathbf{J}_{\mathbf{u},\mathbf{x}} = \text{diag}[J_{ii}]$ having the elements

$$J_{ii} = \frac{f_i(x_i)}{\varphi(u_i)} \qquad i = 1, 2, \ldots, n \tag{14.5}$$

where $\varphi(u) = (2\pi)^{-1/2} \exp(-u^2/2)$ is the univariate standard normal PDF.

14.2.2 Dependent Normal Random Variables

Suppose random variables **x** are normally distributed with mean vector **M** and covariance matrix **Σ**. In this case, a convenient form of the transformation to the standard normal space is

$$\mathbf{u} = \mathbf{L}^{-1}\mathbf{D}^{-1}(\mathbf{x} - \mathbf{M}) \tag{14.6}$$

where **D** is the diagonal matrix of standard deviations defined earlier and **L** is a lower-triangular matrix obtained by Choleski decomposition of the correlation matrix such that $\mathbf{R} = \mathbf{L}\mathbf{L}^{\mathrm{T}}$. This decomposition is possible provided the covariance matrix is positive definite, which is the case as long as the random variables **x** are not linearly dependent. (If a linear dependence exists, one can eliminate it by reducing the number of random variables.) As can be seen, the transformation in this case is linear. The inverse transform is

$$\mathbf{x} = \mathbf{M} + \mathbf{D}\mathbf{L}\mathbf{u} \tag{14.7}$$

and the Jacobian is

$$\mathbf{J}_{\mathbf{u},\mathbf{x}} = \mathbf{L}^{-1}\mathbf{D}^{-1} \tag{14.8}$$

It is noted that **L** being triangular, its inverse is easy to compute.

14.2.3 Random Variables with Nataf Distribution

A set of statistically dependent random variables x_i, $i = 1, \ldots, n$, with prescribed marginal CDFs $F_i(x_i)$ and correlation coefficients ρ_{ij}, $i, j = 1, \ldots, n$, are said to be Nataf-distributed if the marginally transformed random variables

$$z_i = \Phi^{-1}[F_i(x_i)] \qquad i = 1, 2, \ldots, n \tag{14.9}$$

Copyright 2005 by CRC Press LLC

are jointly normal. Liu and Der Kiureghian [1] have shown that the correlation coefficients of the two sets of random variables are related through the identity

$$\rho_{ij} = \int_{-\infty}^{\infty}\int_{-\infty}^{\infty}\left(\frac{x_i-\mu_i}{\sigma_i}\right)\left(\frac{x_j-\mu_j}{\sigma_j}\right)\varphi_2(z_i,z_j,\rho_{0,ij})\,dz_i dz_j \tag{14.10}$$

where $\rho_{0,ij}$ is the correlation coefficient between z_i and z_j and $\varphi_2(z_i,z_j,\rho_{0,ij})$ is their bivariate normal PDF. For given continuous and strictly increasing marginal CDFs $F_i(x_i)$ and a positive-definite correlation matrix $\mathbf{R}=[\rho_{ij}]$, the Nataf distribution is valid as long as $\mathbf{R}_0=[\rho_{0,ij}]$ is a valid correlation matrix.

Among joint distribution models that are consistent with a set of prescribed marginal distributions and correlation matrix, the Nataf distribution is particularly convenient for reliability applications for two reasons: (1) it can accommodate a wide range of correlations between the random variables $\mathbf{x}$ (see [1] for analysis of the limits on ρ_{ij} for which the Nataf distribution is valid), and (2) the transformation to the standard normal space is simple and independent of the ordering of the random variables. The required transformation is given by

$$\mathbf{u} = \mathbf{L}_0^{-1}\begin{Bmatrix}\Phi^{-1}[F_1(x_1)]\\ \vdots \\ \Phi^{-1}[F_n(x_n)]\end{Bmatrix} \tag{14.11}$$

where $\mathbf{L}_0$ is the Choleski decomposition of the correlation matrix $\mathbf{R}_0$, i.e., $\mathbf{R}_0=\mathbf{L}_0\mathbf{L}_0^{\mathrm{T}}$. It can be seen that the above transformation is a synthesis of transformation 14.3 for independent nonnormal random variables and transformation 14.6 for correlated normal random variables. The inverse transform consists in first finding the intermediate variables $\mathbf{z}=\mathbf{L}\mathbf{u}$ and then using $x_i=F_i^{-1}[\Phi(z_i)]$, $i=1,\ldots,n$. Furthermore, the Jacobian of the transformation is given by

$$\mathbf{J}_{\mathbf{u},\mathbf{x}} = \mathbf{L}_0^{-1}\mathrm{diag}[J_{ii}] \tag{14.12}$$

where J_{ii} is as in Equation 14.5.

14.2.4 Dependent Nonnormal Random Variables

For dependent nonnormal random variables other than those with the Nataf distribution, a different transformation must be used. By sequentially conditioning, the joint PDF of the set of random variables x_i, $i=1,\ldots,n$, can be written in the form

$$f(\mathbf{x}) = f_n(x_n\,|\,x_1,\ldots,x_{n-1})\cdots f_2(x_2\,|\,x_1)f_1(x_1) \tag{14.13}$$

where $f_i(x_i\,|\,x_1,\ldots,x_{i-1})$ denotes the conditional PDF of x_i for given values of $x_1,\ldots,x_{i-1}$. Let

$$F_i(x_i\,|\,x_1,\ldots,x_{i-1}) = \int_{-\infty}^{x_i} f_i(x_i\,|\,x_1,\ldots,x_{i-1})\,dx_i \tag{14.14}$$

denote the conditional CDF of x_i for the given values of $x_1,\ldots,x_{i-1}$. The so-called Rosenblatt transformation [2] is defined by

$$\begin{aligned} u_1 &= \Phi^{-1}[F_1(x_1)]\\ u_2 &= \Phi^{-1}[F_2(x_2\,|\,x_1)]\\ &\cdots\\ u_n &= \Phi^{-1}[F_n(x_n\,|\,x_1,\ldots,x_{n-1})]\end{aligned} \tag{14.15}$$

Copyright 2005 by CRC Press LLC

Note that this is a triangular transformation; that is, u_i is dependent only on x_1 to x_i. Because of this property, the inverse of this transform is easily obtained by working from top to bottom. Specifically, for a given $\mathbf{u} = \{u_1 \cdots u_n\}^{\mathrm{T}}$, the first equation is solved for x_1 in terms of u_1, the second equation is solved for x_2 in terms of u_2 and x_1, etc. Because of the nonlinearity of the transformation, an iterative root-finding scheme must be used to solve each of these equations. The Jacobian of the transformation, $\mathbf{J}_{\mathbf{u},\mathbf{x}}$, is a lower-triangular matrix having the elements

$$\begin{aligned} J_{11} &= \frac{f_1(x_1)}{\varphi(u_1)} \\ J_{ij} &= 0 \qquad \text{for } i < j \\ &= \frac{f_i(x_i \mid x_1, \ldots, x_{i-1})}{\varphi(u_i)} \qquad \text{for } i = j > 1 \\ &= \frac{1}{\varphi(u_i)} \frac{\partial F_i(x_i \mid x_1, \ldots, x_{i-1})}{\partial x_j} \qquad \text{for } i > j \end{aligned} \tag{14.16}$$

It is noted that the above transformation is not unique. For example, any reordering of the random variables will produce an alternative transformation to the standard normal space.

In the reliability community, Equation 14.16 is known as the Rosenblatt transformation. This is due to an early work by Rosenblatt [3], which was used by Hohenbichler and Rackwitz in their pioneering use of this transformation in reliability analysis. It must be noted, however, that the above transformation was used much earlier by Segal [4], among others.

14.3 The First-Order Reliability Method

In the first-order reliability method (FORM), an approximation to the probability integral in Equation 14.1 is obtained by linearizing each limit-state function in the standard normal space at an optimal point. The fundamental assumption is that the limit-state functions are continuous and differentiable, at least in the neighborhood of the optimal point. The following subsections describe this method for component and system reliability problems. Simple examples demonstrate the methodology.

14.3.1 Component Reliability by FORM

Consider the component reliability problem defined by Equations 14.1 and 14.2a, which is characterized by the limit-state function $g(\mathbf{x})$ and the joint PDF $f(\mathbf{x})$. Transforming the variables into the standard normal space, the failure probability integral is written as

$$p_f = \int_{g(\mathbf{x}) \le 0} f(\mathbf{x}) d\mathbf{x} = \int_{G(\mathbf{u}) \le 0} \varphi_n(\mathbf{u}) d\mathbf{u} \tag{14.17}$$

where $G(\mathbf{u}) \equiv g(\mathbf{T}^{-1}(\mathbf{u}))$ is the limit-state function in the standard normal space. The FORM approximation is obtained by linearizing the function $G(\mathbf{u})$ at a point $\mathbf{u}^*$ defined by the constrained optimization problem

$$\mathbf{u}^* = \arg\min\{\|\mathbf{u}\| \mid G(\mathbf{u}) = 0\} \tag{14.18}$$

where "arg min" denotes the argument of the minimum of a function. It is seen that $\mathbf{u}^*$ is located on the limit-state surface, $G(\mathbf{u}) = 0$, and has minimum distance from the origin in the standard normal space. Because equal probability density contours in the standard normal space are concentric circles centered at the origin, $\mathbf{u}^*$ has the highest probability density among all realizations in the failure domain $G(\mathbf{u}) \le 0$.

Copyright 2005 by CRC Press LLC

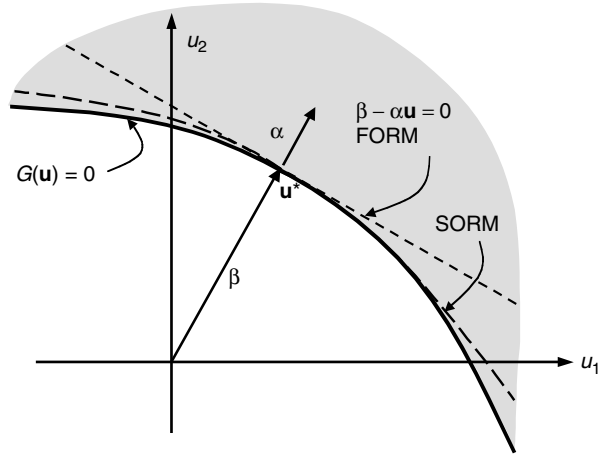

FIGURE 14.2 FORM and SORM approximations for a component problem.

It follows that the neighborhood of this point makes a dominant contribution to the last integral in Equation 14.17. In this sense, $\mathbf{u}^*$ is an optimal point for the linearization of the limit-state function. Another important advantage of this point is that it is invariant of the formulation of the limit-state function, although it may be dependent on the selected form of the transformation from **x** to **u** space. In the reliability community, this point is commonly known as the *design point*, but other names such as *most probable point* (MPP) and *beta point* are also used.

Noting that $G(\mathbf{u}^*) = 0$, the linearized limit-state function is written as

$$G(\mathbf{u}) \cong G_1(\mathbf{u}) = \nabla G(\mathbf{u}^*)(\mathbf{u} - \mathbf{u}^*) = \| \nabla G(\mathbf{u}^*) \| (\beta - \alpha\mathbf{u}) \tag{14.19}$$

where $\nabla G(\mathbf{u}) = [\partial G/\partial u_1, \ldots, \partial G/\partial u_n]$ denotes the gradient row vector[1], $\alpha = -\nabla G(\mathbf{u}^*)/\| \nabla G(\mathbf{u}^*) \|$ is the normalized negative gradient row vector at the design point (a unit vector normal to the limit-state surface at the design point and pointing toward the failure domain), and $\beta = \alpha\mathbf{u}^*$ is the *reliability index*. In essence, the linearization replaces the failure domain $G(\mathbf{u}) \le 0$ by the half space $\beta - \alpha\mathbf{u} \le 0$; see Figure 14.2. The first-order approximation of the failure probability is given by the probability content of the half space in the standard normal space, which is completely defined by the distance β; that is,

$$p_f \cong p_{f1} = \Phi(-\beta) \tag{14.20}$$

where the subscript 1 is used to indicate a first-order approximation. This approximation normally works well because, as mentioned earlier, the neighborhood of the design point makes the dominant contribution to the probability integral 14.17. There are two conditions under which this approximation may not work well: (1) the surface $G(\mathbf{u}) = 0$ is strongly nonflat, and (2) the optimization problem in Equation 14.18 has multiple local or global solutions. A recourse for the first condition is to use a higher-order approximation, such as SORM (see Section 14.4), or a corrective sampling method, such as importance sampling or sampling on the orthogonal plane [5]. All these methods make use of the design point, so they need the FORM solution as a first step. The second condition is quite rare, but it does occur, particularly when dealing with dynamic problems. If the local solutions of Equation 14.18 are

[1] To be consistent with the definition of a Jacobian matrix, the gradient of a function is defined as a row vector. Note that for a set of functions $f_i(x_1, \ldots, x_n)$, $i = 1, \ldots, m$, the Jacobian matrix has the elements $J_{ij} = \partial f_i/\partial x_j$, $i = 1, \ldots, m$, $j = 1, \ldots, n$. The gradient ∇f_i is the i-th row of this matrix. The normalized gradient α is taken as a row vector for the same reason.

Copyright 2005 by CRC Press LLC

significant, i.e., the corresponding distances from the origin are not much greater than β, then one recourse is to use multiple linearizations and a series system formulation to obtain an improved FORM approximation (see, e.g., [6]).

It should be clear by now that solving Equation 14.18 is the main computational effort in FORM. Several well-established iterative algorithms are available for this purpose [7]. Starting from an initial point $\mathbf{u}_1 = \mathbf{T}(\mathbf{x}_1)$, one typically computes a sequence of points using the recursive formula

$$\mathbf{u}_{i+1} = \mathbf{u}_i + \lambda_i \mathbf{d}_i \qquad i = 1, 2, \ldots \tag{14.21}$$

where $\mathbf{d}_i$ is a search direction vector and λ_i is a step size. Algorithms differ in their selections of $\mathbf{d}_i$ and λ_i. One simple algorithm that is especially designed for the objective function in Equation 14.18 uses the search direction

$$\mathbf{d}_i = \left[\frac{G(\mathbf{u}_i)}{||\nabla G(\mathbf{u}_i)||} + \alpha_i \mathbf{u}_i \right] \alpha_i^{\mathrm{T}} - \mathbf{u}_i \tag{14.22}$$

where $\alpha_i = -\nabla G(\mathbf{u}_i)/||\nabla G(\mathbf{u}_i)||$ is the normalized negative gradient row vector. For $\lambda_i = 1$, this algorithm is identical to one originally suggested by Hasofer and Lind [8] and later generalized for nonnormal variables by Rackwitz and Fissler [9]. However, with a unit step size this algorithm does not converge when $1 \le |\beta\kappa_i|$, where κ_i is a principal curvature of the limit-state surface at the design point. The appropriate step size can be selected by monitoring a merit function, $m(\mathbf{u})$. This is any continuous and differentiable function of $\mathbf{u}$, whose minimum occurs at the solution of Equation 14.18 and for which $\mathbf{d}_i$ is a descent direction at $\mathbf{u}_i$ (i.e., the value of the function $m(\mathbf{u})$ decreases as we move a small distance in the direction $\mathbf{d}_i$ starting from $\mathbf{u}_i$). Zhang and Der Kiureghian [10] have shown that a merit function that satisfies these conditions is

$$m(\mathbf{u}) = \frac{1}{2}\|\mathbf{u}\|^2 + c\,|G(\mathbf{u})| \tag{14.23}$$

where the penalty parameter c should be selected at each step to satisfy the condition $c_i > ||\mathbf{u}_i||/||\nabla G(\mathbf{u}_i)||$. Using the merit function, the best step size is obtained as

$$\lambda_i = \arg\min\{m(\mathbf{u}_i + \lambda \mathbf{d}_i)\} \tag{14.24}$$

However, strict solution of the above minimization is costly. In practice, it is sufficient to select $\lambda_i \in (0,1]$ such that $m(\mathbf{u}_i + \lambda \mathbf{d}_i) < m(\mathbf{u}_i)$. A popular rule for this purpose is the Armijo rule [11].

The algorithm described by Equation 14.21 through Equation 14.24 is known as the Improved HL-RF algorithm [10]. For most problems, this algorithm converges in just a few steps. To assure that convergence to the global solution is obtained, it is a good practice to repeat the solution starting from a different initial point $\mathbf{x}_1$. In practice, it is very rare that convergence to a local solution occurs, and when this does occur, usually one can detect it from the context of the problem. Nevertheless, one should keep in mind that optimization algorithms do not guarantee convergence to the global solution and caution should be exercised in interpreting their results.

As we have seen, the FORM solution essentially requires repeated evaluation of the limit-state function $G(\mathbf{u})$ and its gradient $\nabla G(\mathbf{u})$ at selected points $\mathbf{u}_i$, $i = 1, 2, \ldots$. Because the limit-state function is defined in terms of the original random variables $\mathbf{x}$, it is necessary to carry out these calculations in that space. For this purpose, for any point $\mathbf{u}_i$ selected in accordance with the optimization algorithm, the inverse transform $\mathbf{x}_i = \mathbf{T}^{-1}(\mathbf{u}_i)$ is used to compute the corresponding point in the original space. Then, $G(\mathbf{u}_i) = g(\mathbf{x}_i)$ and $\nabla G(\mathbf{u}_i) = \nabla g(\mathbf{x}_i)\mathbf{J}_{\mathbf{u},\mathbf{x}}^{-1}(\mathbf{x}_i)$, where $\mathbf{J}_{\mathbf{u},\mathbf{x}}$ is the Jacobian of the transformation, as described in Section 14.2. Note that $\mathbf{J}_{\mathbf{u},\mathbf{x}}$ being a triangular matrix, its inverse is easy to compute.

Copyright 2005 by CRC Press LLC

TABLE 14.1 Description of Random Variables for Example in Section 14.3.1.1

Variable	Marginal Distribution	Mean	c.o.v.	Correlation Coefficient			
				m_1	m_2	p	y
m_1, kNm	Normal	250	0.3	1.0			
m_2, kNm	Normal	125	0.3	0.5	1.0		
p, kN	Gumbel	2,500	0.2	0.3	0.3	1.0	
y, MPa	Weibull	40	0.1	0.0	0.0	0.0	1.0

14.3.1.1 Example: Reliability Analysis of a Column by FORM

Consider a short column subjected to biaxial bending moments m_1 and m_2 and axial force p. Assuming an elastic perfectly plastic material with yield stress y, the failure of the column is defined by the limit-state function

$$g(\mathbf{x}) = 1 - \frac{m_1}{S_1 y} - \frac{m_2}{S_2 y} - \left(\frac{p}{Ay}\right)^{\theta} \tag{14.25}$$

where $\mathbf{x} = \{m_1, m_2, p, y\}^{\mathrm{T}}$ denotes the vector of random variables, $\theta = 2$ is a limit-state function parameter, $A = 0.190$ m^2 is the cross-sectional area, and $S_1 = 0.030$ m^3 and $S_2 = 0.015$ m^3 are the flexural moduli of the fully plastic column section. Assume m_1, m_2, p, and y have the Nataf distribution with the second moments and marginal distributions listed in Table 14.1. Starting from the mean point, the Improved HL-RF algorithm converges in nine steps with the results $\mathbf{u}^* = \{1.21, 0.699, 0.941, -1.80\}^{\mathrm{T}}$, $\mathbf{x}^* = \{341, 170, 3223, 31.8\}^{\mathrm{T}}$, $\alpha = [0.491, 0.283, 0.381, -0.731]$, $\beta = 2.47$, and $p_{f1} = 0.00682$. The "exact" estimate of the failure probability, obtained with 120,000 Monte Carlo simulations and a coefficient of variation of 3%, is $p_f \cong 0.00931$.

14.3.2 System Reliability by FORM

Consider a series or parallel system reliability problem defined by a set of limit-state functions $g_k(\mathbf{x})$, $k = 1, 2, \ldots, m$, and the failure domain as in Equation 14.2b or 14.2c. Let $G_k(\mathbf{u})$, $k = 1, 2, \ldots, m$, denote the corresponding limit-state functions in the standard normal space. A first-order approximation to the system failure probability is obtained by linearizing each limit-state function $G_k(\mathbf{u})$ at a point $\mathbf{u}_k^*$, $k = 1, 2, \ldots, m$, such that the surface is approximated by the tangent hyperplane

$$\beta_k - \alpha_k \mathbf{u} = 0 \tag{14.26}$$

where $\alpha_k = -\nabla G_k(\mathbf{u}_k^*)/\|\nabla G_k(\mathbf{u}_k^*)\|$ is the unit normal to the hyperplane and $\beta_k = \alpha_k \mathbf{u}_k^*$ is the distance from the origin to the hyperplane. An easy choice for the linearization points $\mathbf{u}_k^*$ is the minimum-distance points from the origin, as defined in Equation 14.18. While this is a good choice for series systems, for parallel systems a better choice is the so-called *joint design point*

$$\mathbf{u}^* = \arg\min\{\|\mathbf{u}\| \,|\, G_k(\mathbf{u}) \le 0, k = 1, \ldots, m\} \tag{14.27}$$

The above is an optimization problem with multiple inequality constraints, for which standard algorithms are available. Figure 14.3 illustrates the above choices for linearization. It is clear that the linearization according to Equation 14.27 will provide a better approximation of the failure domain for parallel systems. Nevertheless, the linearization point according to Equation 14.18 is often used for all system problems because it is much easier to obtain.

Copyright 2005 by CRC Press LLC

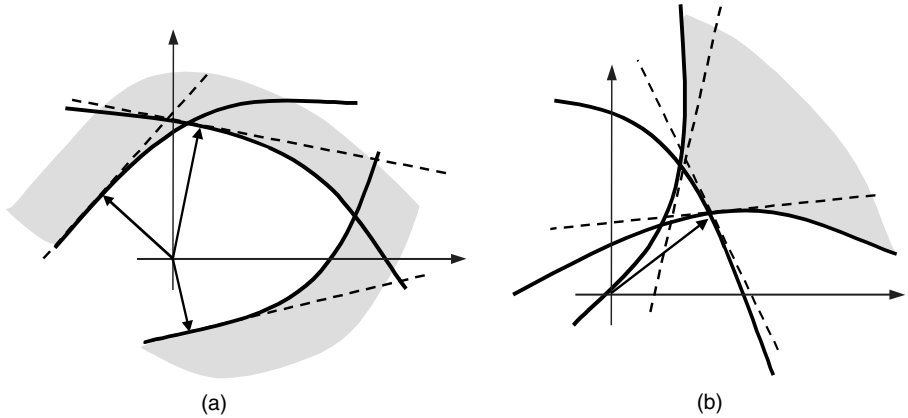

FIGURE 14.3 Linearization points for series and parallel systems: (a) linearization according to Equation 14.18; (b) linearization according to Equation 14.27.

With the limit-state surfaces linearized, the system failure domain is approximated by a hyper-polygon. The corresponding approximations of the failure probability are derived as follows: Let $v_k = \alpha_k \mathbf{u}$, $k = 1, 2, \ldots, m$. It is easy to see that $\mathbf{v} = \{v_1, \ldots, v_m\}^{\mathrm{T}}$ are normal random variables with zero means, unit variances, and correlation coefficients $\rho_{kl} = \alpha_k \alpha_l^{\mathrm{T}}$, $k, l = 1, 2, \ldots, m$. For a series system, one can write [12]:

$$\begin{aligned} p_{f1,\text{series}} &= P\left[\bigcup_{k=1}^{m} (\beta_k \le v_k)\right] \\ &= 1 - P\left[\bigcap_{k=1}^{m} (v_k < \beta_k)\right] \\ &= 1 - \Phi_m(\mathbf{B}, \mathbf{R}) \end{aligned} \tag{14.28}$$

where $\Phi_m(\mathbf{B}, \mathbf{R})$ is the m-variate standard normal CDF with correlation matrix $\mathbf{R} = [\rho_{kl}]$ and evaluated at the thresholds $\mathbf{B} = (\beta_1, \ldots, \beta_m)$. For a parallel system, one can write [12]:

$$\begin{aligned} p_{f1,\text{parallel}} &= P\left[\bigcap_{k=1}^{m} (\beta_k \le v_k)\right] \\ &= P\left[\bigcap_{k=1}^{m} (v_k < -\beta_k)\right] \\ &= \Phi_m(-\mathbf{B}, \mathbf{R}) \end{aligned} \tag{14.29}$$

where use has been made of the symmetry of the standard normal space. Note that for a single component ($m = 1$), the above relations 14.28 and 14.29 both reduce to 14.20.

It is clear from the above analysis that computing the multi-normal probability function is essential for FORM solution of series and parallel systems. For $m = 2$, the bivariate normal CDF can be computed using the single-fold integral

$$\Phi_2(\beta_1, \beta_2, \rho) = \Phi(\beta_1)\Phi(\beta_2) + \int_0^{\rho} \varphi_2(\beta_1, \beta_2, r)\, dr \tag{14.30}$$

Copyright 2005 by CRC Press LLC

where $\varphi_2(\ldots r)$ denotes the bivariate standard normal PDF with correlation coefficient r. For higher dimensions, numerical techniques for computing the multi-normal probability have been developed (see, e.g., [13–15]).

As described in the introduction, a general system can be represented as a series system of parallel subsystems, with each parallel subsystem representing a cut set. Let

$$C_k = \left\{ \bigcap_{j \in c_k} G_j(\mathbf{u}) \le 0 \right\} \tag{14.31}$$

denote the k-th cut-set event, that is, the event that all components within the k-th cut set have failed. The probability of failure of a system with m cut sets can be written as

$$p_{f,\text{general system}} = P\left(\bigcup_{k=1}^{m} C_k \right) \tag{14.32}$$

Several options are available for computing the above probability. If the cut sets are disjoint (i.e., no two cut sets can simultaneously occur), we can write

$$p_{f,\ \text{general system}} = \sum_{k=1}^{m} P(C_k) \tag{14.33}$$

where each term $P(C_k)$ is a parallel system problem and can be solved as described above. The difficulty in this approach is that the disjoint cut sets can be numerous and may contain large numbers of components. A more compact system formulation is obtained in terms of the minimum cut sets, that is, cut sets that do not contain superfluous components. However, such cut sets usually are neither mutually exclusive nor statistically independent. If the number of minimum cut sets is not too large, the inclusion-exclusion rule of probability can be used to write Equation 14.32 as

$$p_{f,\,\text{general system}} = \sum_{k=1}^{m} P(C_k) - \sum_{k=1}^{m-1} \sum_{l=k+1}^{m} P(C_k C_l) + \cdots + (-1)^{m-1} P(C_1 C_2 \cdots C_m) \tag{14.34}$$

Each term in the above expression represents a parallel system reliability problem and can be solved as described earlier. Note, however, that the number of parallel system problems to be solved and the number of components in them will rapidly increase with the number of cut sets, m.

To avoid solving parallel systems with large number of components, bounding formulas for system failure probability have been developed that rely on low-order probabilities. For example, the Kounias-Hunter-Ditlevsen bounds, progressively developed in [16–18], are

$$p_{f,\,\text{general system}} \ge P(C_1) + \sum_{k=2}^{m} \max\left[0,\, P\left(C_k\right) - \sum_{l=1}^{k-1} P(C_k C_l) \right] \tag{14.35a}$$

$$p_{f,\,\text{general system}} \le P(C_1) + \sum_{k=2}^{m} \left[P(C_k) - \max_{l<k} P(C_k C_l) \right] \tag{14.35b}$$

where only joint probabilities of pairs of cut sets are required. Similar formulas involving joint probabilities of three or more cut sets have been developed by Zhang [19]. Recently, Song and Der Kiureghian [20]

Copyright 2005 by CRC Press LLC

developed a linear programming algorithm for computing bounds on general system probability for any given information on the marginal and joint component probabilities. Their approach is guaranteed to produce the narrowest possible bounds for any given information.

In the structural reliability literature, the bounds in Equation 14.35 are often considered in connection with series systems, where each component represents a cut set. The above formulation shows that these bounds are equally applicable to general systems represented in terms of multi-component cut sets.

14.3.2.1 Example: Series System Reliability Analysis of a Frame by FORM

Consider the one-bay frame in Figure 14.4a, which has ductile members and is subjected to random horizontal and vertical loads h and v. The frame has random plastic moment capacities m_i, $i = 1, \ldots, 5$, at the joints shown in the figure. Under the applied loads, this frame may fail in any of the three mechanisms shown in Figure 14.4b. Using the principle of virtual work, these mechanisms are described by the limit-state functions

$$g_1(\mathbf{x}) = m_1 + m_2 + m_4 + m_5 - 5h \tag{14.36a}$$

$$g_2(\mathbf{x}) = m_2 + 2m_3 + m_4 - 5v \tag{14.36b}$$

$$g_3(\mathbf{x}) = m_1 + 2m_3 + 2m_4 + m_5 - 5h - 5v \tag{14.36c}$$

where $\mathbf{x} = \{m_1, \ldots, m_5, h, v\}^{\mathrm{T}}$ is the vector of random variables. Table 14.2 shows the assumed distributions and second moments of the random variables.

The reliability of the frame against the formation of a mechanism represents a series system reliability problem with the limit-state functions shown in 14.36. Using the FORM approximation, we obtain the following $\beta_k \alpha_k$ values for the three components:

$$\beta_1 \alpha_1 = 2.29[-0.238 - 0.174 - 0.044 - 0.131 - 0.112\ 0.939\ 0.000] \tag{14.37a}$$

$$\beta_2 \alpha_2 = 2.87[-0.263 - 0.356 - 0.425 - 0.204\ 0.000\ 0.000\ 0.763] \tag{14.37b}$$

$$\beta_3 \alpha_3 = 2.00[-0.313 - 0.137 - 0.291 - 0.240 - 0.113\ 0.792\ 0.317] \tag{14.37c}$$

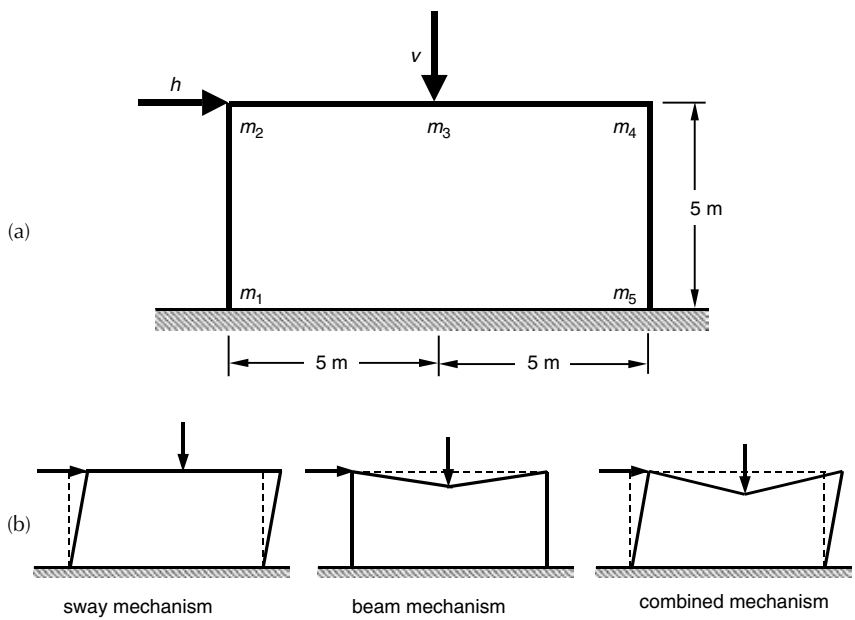

FIGURE 14.4 Ductile frame and its failure mechanisms.

Copyright 2005 by CRC Press LLC

TABLE 14.2 Description of Random Variables for Example in Section 14.3.2.1

Variable	Distribution	Mean	c.o.v.	Correlation
m_i, i=1, …,5, kNm	Joint lognormal	150	0.2	$\rho_{m_i m_j} = 0.3$, $i \neq j$
h, kN	Gumbel	50	0.4	Independent
v, kN	Gamma	60	0.2	Independent

These values are used in Equation 14.28 to obtain the FORM approximation of the failure probability, $p_{f1} = 0.02644$. If the bounds in Equation 14.35 are used, the result is $0.02639 \leq p_{f1} \leq 0.02647$.

14.3.2.2 Example: Reliability Updating of a Frame after Proof Test

Suppose the frame in the example in Section 14.3.2.1 has been proof-tested under a horizontal load of $h_0 = 70$ kN and a vertical load of $v_0 = 72$ kN. Because the frame has survived under these loads, we have observed

$$g_4(\mathbf{x}) = -(m_1 + m_2 + m_4 + m_5 - 5h_0) \leq 0 \tag{14.38a}$$

$$g_5(\mathbf{x}) = -(m_2 + 2m_3 + m_4 - 5v_0) \leq 0 \tag{14.38b}$$

$$g_6(\mathbf{x}) = -(m_1 + 2m_3 + 2m_4 + m_5 - 5h_0 - 5v_0) \leq 0 \tag{14.38c}$$

where h_0 and v_0 are deterministic values, as given above. The updated probability of failure of the frame in light of the proof-test result is the conditional probability

$$p_{f|\text{proof test}} = \frac{P(C_1 \bigcup C_2 \bigcup C_3)}{P(C_4)} \tag{14.39}$$

where the index sets for the cut sets C_k, $k = 1, \ldots, 4$, are $c_1 = (1,4,5,6)$, $c_2 = (2,4,5,6)$, $c_3 = (3,4,5,6)$, and $c_4 = (4,5,6)$, respectively. It is seen that the numerator represents a general system problem, whereas the denominator is a parallel system problem. First-order approximation of the probabilities in Equation 14.39 yields the updated probability $p_{f1|\text{proof test}} = 0.0189$. In light of the positive proof-test observation, this result is smaller than the unconditional failure probability estimated earlier. This example demonstrates the use of general system reliability analysis. It also shows how reliability can be updated in light of real-world observations.

14.3.3 FORM Importance and Sensitivity Measures

An important by-product of FORM is a set of importance and sensitivity measures that provide information as to the order of importance of the random variables and the sensitivities of the reliability index or the first-order approximation of the failure probability with respect to parameters in the probability distribution or limit-state models. This section briefly introduces these measures.

Let $G_1(\mathbf{u}) = \|\nabla G\|(\beta - \alpha\mathbf{u})$ denote the linearized limit-state function as in Equation 14.19. Noting that the mean of $\mathbf{u}$ is zero and its covariance is the identity matrix, we obtain the mean and variance of $G_1(\mathbf{u})$ as

$$\mu_{G_1} = \| \nabla G \| \beta \tag{14.40}$$

$$\sigma_{G_1}^2 = \| \nabla G \|^2 \left(\alpha_1^2 + \alpha_2^2 + \cdots + \alpha_n^2\right) = \|\nabla G\|^2 \tag{14.41}$$

where use has been made of the fact that α is a unit vector. The result verifies that $\beta = \mu_{G_1}/\sigma_{G_1}$ is indeed the reliability index for the linearized problem. More importantly, Equation 14.41 shows that α_i^2 is proportional to the contribution of random variable u_i to the total variance of the linearized limit-state function. Clearly, the larger this contribution, the more important random variable u_i is. Hence, the elements of α provide relative measures of importance of the standard normal variables u_i, $i = 1, \ldots, n$.

Copyright 2005 by CRC Press LLC

Furthermore, considering the expanded expression $G_1(\mathbf{u}) = \|\nabla G\|(\beta - \alpha_1 u_1 - \cdots - \alpha_n u_n)$, it is clear that a positive (negative) value of α_i is an indication that random variable u_i is of load (capacity) type.

When the basic random variables of a reliability problem are statistically independent, there is a one-to-one correspondence between the original random variables x_i and the standard normal random variables u_i. The order of importance and nature (load or capacity) of random variables x_i then are similar to the corresponding u_i and can be determined in terms of the α vector. However, when the random variables $\mathbf{x}$ are statistically dependent, there is no such one-to-one correspondence. In that case, α does not provide information about the relative importance of the random variables $\mathbf{x}$ in the original space. To derive measures of importance for the basic random variables, consider linearizing the transformation $\mathbf{u} = \mathbf{T}(\mathbf{x})$ at the design point $\mathbf{u}^*$:

$$\mathbf{u} \cong \mathbf{u}^* + \mathbf{J}_{\mathbf{u},\mathbf{x}}(\mathbf{x} - \mathbf{x}^*) \tag{14.42}$$

Replacing the approximation by an equality, we can write

$$\mathbf{u} = \mathbf{u}^* + \mathbf{J}_{\mathbf{u},\mathbf{x}}(\hat{\mathbf{x}} - \mathbf{x}^*) \tag{14.43}$$

where $\hat{\mathbf{x}}$ is slightly different from $\mathbf{x}$. Because $\hat{\mathbf{x}}$ is a linear function of $\mathbf{u}$, it must have the joint normal distribution. Its covariance matrix is

$$\hat{\boldsymbol{\Sigma}} = \mathbf{J}_{\mathbf{u},\mathbf{x}}^{-1}\left(\mathbf{J}_{\mathbf{u},\mathbf{x}}^{-1}\right)^{\mathrm{T}} \tag{14.44}$$

The random variables $\hat{\mathbf{x}}$ are considered as "equivalent normals" of $\mathbf{x}$ at the design point. The covariance matrix $\hat{\boldsymbol{\Sigma}}$ in general depends on the design point and is slightly different from the actual covariance matrix $\boldsymbol{\Sigma}$ of $\mathbf{x}$. The magnitude of the difference depends on the degree of nonnormality of $\mathbf{x}$. Now using Equation 14.43 in the expression for $G_1(\mathbf{u})$ and noting that $\beta = \alpha \mathbf{u}^*$, we obtain $G_1(\mathbf{u}) = -\|\nabla G\| \alpha \mathbf{J}_{\mathbf{u},\mathbf{x}}(\hat{\mathbf{x}} - \mathbf{x}^*)$. The variance of $G_1(\mathbf{u})$ can now be written as

$$\sigma_{G_1}^2 = \|\nabla G\|^2 \left(\alpha \mathbf{J}_{\mathbf{u},\mathbf{x}} \hat{\boldsymbol{\Sigma}} \mathbf{J}_{\mathbf{u},\mathbf{x}}^{\mathrm{T}} \alpha^{\mathrm{T}}\right) = \|\nabla G\|^2 \left(\|\alpha \mathbf{J}_{\mathbf{u},\mathbf{x}} \hat{\mathbf{D}}\|^2 + \alpha \mathbf{J}_{\mathbf{u},\mathbf{x}}(\hat{\boldsymbol{\Sigma}} - \hat{\mathbf{D}}\hat{\mathbf{D}}) \mathbf{J}_{\mathbf{u},\mathbf{x}}^{\mathrm{T}} \alpha^{\mathrm{T}}\right) \tag{14.45}$$

where $\hat{\mathbf{D}} = \mathrm{diag}[\hat{\sigma}_{\mathrm{i}}$ is the diagonal matrix of standard deviations of $\hat{\mathbf{x}}$. The first term in the above expression contains the contributions to the variance of $G_1(\mathbf{u})$ arising from the individual variances of the elements of $\hat{\mathbf{x}}$, whereas the second term represents the contributions arising from the covariances of pairs of the random variables. Hence, the elements of the vector $\alpha \mathbf{J}_{\mathbf{u},\mathbf{x}} \hat{\mathbf{D}}$ can be considered to provide relative measures of importance of the elements of $\hat{\mathbf{x}}$, or approximately of $\mathbf{x}$. Normalizing this vector, we define

$$\gamma = \frac{\alpha \mathbf{J}_{\mathbf{u},\mathbf{x}} \hat{\mathbf{D}}}{\left\|\alpha \mathbf{J}_{\mathbf{u},\mathbf{x}} \hat{\mathbf{D}}\right\|} \tag{14.46}$$

as the unit row vector defining the relative importance of the original random variables $\mathbf{x}$. A positive (negative) value for the element γ_i of this vector indicates that x_i is of load (capacity) type. It is easy to show that when the random variables are statistically independent, γ reverts back to α.

We now turn our attention to reliability sensitivity measures. Let $f(\mathbf{x}, \theta_f)$ denote the joint PDF of $\mathbf{x}$, where θ_f is a set of distribution parameters, and $g(\mathbf{x}, \theta_g)$ denote the limit-state function, where θ_g is a set of limit-state parameters. It can be shown (see [21] and [22]) that the gradients of β with respect to these parameters are

$$\nabla_{\theta_f} \beta = \alpha \mathbf{J}_{\mathbf{u},\theta_f}(\mathbf{x}^*, \theta_f) \tag{14.47}$$

$$\nabla_{\theta_g} \beta = \frac{1}{\|\nabla G\|} \nabla_{\theta_g} g(\mathbf{x}^*, \theta_g) \tag{14.48}$$

Copyright 2005 by CRC Press LLC

parameters θ_f, evaluated at the design point. Using Equation 14.20, the corresponding gradients of the first-order probability approximation are obtained from

$$\nabla_\theta p_{f1} = -\varphi(\beta)\nabla_\theta \beta \tag{14.49}$$

where $\theta = \theta_f$ or θ_g.

14.3.3.1 Example: Importance and Sensitivity Measures for a Column

Reconsider the example in Section 14.3.1.1. Using Equation 14.46, the importance vector for the basic random variables $\mathbf{x} = \{m_1, m_2, p, y\}^{\mathrm{T}}$ is $\gamma = [0.269, 0.269, 0.451, -0.808]$. From the signs of the elements of the importance vector, it is seen that the first three random variables are load types, whereas the fourth variable, y, is a capacity variable. This finding is intuitively obvious for this problem. However, in a more complex problem, the nature of the random variables may not be obvious and the information provided by the importance vector can be valuable. Of the four basic random variables, y is the most important variable, followed by p, m_1, and m_2. This is in spite of the fact that y has the smallest coefficient of variation among the four.

Using Equation 14.47, the gradient vector of β with respect to the mean values of the random variables (with the standard deviations fixed) is obtained as $\nabla_{\text{mean}}\beta = 10^{-3}[-3.24, -6.48, -0.546, 0.124]$ and the gradient with respect to the standard deviations (with the means fixed) is obtained as $\nabla_{\text{stdev}}\beta = 10^{-3}$ $[-3.92, -7.84, -0.790, -0.245]$. Furthermore, using Equation 14.48, the sensitivity of the reliability index with respect to the limit-state function parameter θ is obtained as $\partial\beta/\partial\theta = 0.552$. The corresponding sensitivities of the first-order failure probability are obtained from Equation 14.49 by scaling the above sensitivity values by $-\varphi(2.47) = -0.0190$.

14.4 The Second-Order Reliability Method

As its name implies, the second-order reliability method, SORM, involves a second-order approximation of the limit-state function. Consider a Taylor series expansion of the component limit-state function $G(\mathbf{u})$ at the design point $\mathbf{u}^*$,

$$\begin{aligned} G(\mathbf{u}) &\cong \nabla G(\mathbf{u}^*)(\mathbf{u}-\mathbf{u}^*) + \frac{1}{2}(\mathbf{u}-\mathbf{u}^*)^{\mathrm{T}}\mathbf{H}(\mathbf{u}-\mathbf{u}^*) \\ &= ||\nabla G(\mathbf{u}^*)||\left[(\beta-\alpha\mathbf{u}) + \frac{1}{2||\nabla G(\mathbf{u}^*)||}(\mathbf{u}-\mathbf{u}^*)^{\mathrm{T}}\mathbf{H}(\mathbf{u}-\mathbf{u}^*)\right] \end{aligned} \tag{14.50}$$

where α and β are as defined earlier and $\mathbf{H}$ is the second-derivative matrix at the design point having the elements $H_{ij} = \partial^2 G(\mathbf{u}^*)/(\partial u_i \partial u_j)$, $i, j = 1, \ldots, n$. Now consider a rotation of the axes $\mathbf{u}' = \mathbf{P}\mathbf{u}$, where $\mathbf{P}$ is an orthonormal matrix with α as its last row. Such a matrix can be constructed by, for example, the well-known Gram-Schmidt algorithm. This rotation positions the design point on the u_n' axis, such that $\mathbf{u}'^* = [0 \cdots 0\ \beta]^{\mathrm{T}}$. Because $\mathbf{u} = \mathbf{P}^{\mathrm{T}}\mathbf{u}'$, defining $G'(\mathbf{u}') = G(\mathbf{P}^{\mathrm{T}}\mathbf{u}')/||\nabla G(\mathbf{u}^*)||$, we have

$$G'(\mathbf{u}') \cong \beta - \alpha\mathbf{P}^{\mathrm{T}}\mathbf{u}' + \frac{1}{2||\nabla G(\mathbf{u}^*)||}(\mathbf{u}'-\mathbf{u}'^*)^{\mathrm{T}}\mathbf{P}\mathbf{H}\mathbf{P}^{\mathrm{T}}(\mathbf{u}'-\mathbf{u}'^*) \tag{14.51}$$

Noting that $\alpha\mathbf{P}^{\mathrm{T}}\mathbf{u}' = u_n'$ and letting $\mathbf{A} = \mathbf{P}\mathbf{H}\mathbf{P}^{\mathrm{T}}/||\nabla G(\mathbf{u}^*)||$, we have

$$G'(\mathbf{u}') \cong \beta - u_n' + \frac{1}{2}(\mathbf{u}'-\mathbf{u}'^*)^{\mathrm{T}}\mathbf{A}(\mathbf{u}'-\mathbf{u}'^*) \tag{14.52}$$

Copyright 2005 by CRC Press LLC

and the corresponding partition of $\mathbf{A}$, $\mathbf{A} = \begin{bmatrix} \mathbf{A}_{11} & \mathbf{A}_{12} \\ \mathbf{A}_{12}^{\mathrm{T}} & a_{nn} \end{bmatrix}$, where $\mathbf{A}_{11}$ is the $(n-1)\times(n-1)$ matrix formed by the first $n-1$ rows and columns of $\mathbf{A}$. Expanding the matrix product in Equation 14.52 yields

$$G'(\mathbf{u}') \cong \beta - u_n' + \frac{1}{2}\left[\mathbf{u}_1'^{\mathrm{T}}\mathbf{A}_{11}\mathbf{u}_1' + 2(u_n' - \beta)\mathbf{A}_{12}^{\mathrm{T}}\mathbf{u}_1' + a_{nn}(u_n' - \beta)^2\right] \tag{14.53}$$

Because $u_n' - \beta = 0$ is the tangent plane at the design point, for points on the limit-state surface in the neighborhood of the design point, the last two terms inside the square brackets in Equation 14.53 are of smaller order than the first term. Neglecting these terms, we arrive at

$$G'(\mathbf{u}') \cong \beta - u_n' + \frac{1}{2}\mathbf{u}_1'^{\mathrm{T}}\mathbf{A}_{11}\mathbf{u}_1' \tag{14.54}$$

This is the equation of a paraboloid with its apex at the design point. Now consider a rotation of the axes around u_n' defined by the transformation $\mathbf{u}_1'' = \mathbf{Q}\mathbf{u}_1'$, where $\mathbf{Q}$ is an $(n-1)\times(n-1)$ orthonormal matrix. Since $\mathbf{u}_1' = \mathbf{Q}^{\mathrm{T}}\mathbf{u}_1''$, we can write $\mathbf{u}_1'^{\mathrm{T}}\mathbf{A}_{11}\mathbf{u}_1' = \mathbf{u}_1''^{\mathrm{T}}\mathbf{Q}\mathbf{A}_{11}\mathbf{Q}^{\mathrm{T}}\mathbf{u}_1''$. It follows that by selecting $\mathbf{Q}^{\mathrm{T}}$ as the eigenmatrix of $\mathbf{A}_{11}$, the product $\mathbf{Q}\mathbf{A}_{11}\mathbf{Q}^{\mathrm{T}}$ diagonalizes and Equation 14.54 reduces to

$$G'(\mathbf{u}') = G'(\mathbf{Q}^{\mathrm{T}}\mathbf{u}_1'', u_n') \cong \beta - u_n' + \frac{1}{2}\sum_{i=1}^{n-1}\kappa_i u_i''^2 \tag{14.55}$$

where κ_i are the eigenvalues of $\mathbf{A}_{11}$. The preceding expression defines a paraboloid through its principal axes with $\kappa_i, i = 1, \ldots, n-1$, denoting its principal curvatures. This paraboloid is tangent to the limit-state surface at the design point and its principal curvatures match those of the limit-state surface at the design point. Note that, for $\beta > 0$, a positive curvature denotes a surface that curves away from the origin. Because the apex is at the design point, which is the point nearest to the origin, it follows that the inequality $-1 < \beta\kappa_i$ must hold for each principal curvature.

In SORM, the probability of failure is approximated by the probability content of the above-defined paraboloid. Because the standard normal space is rotationally symmetric, this probability, which we denote as p_{f2}, is completely defined by β and the set of curvatures $\kappa_i, i = 1, \ldots, n-1$. Hence, we can write the SORM approximation as

$$p_f \cong p_{f2}(\beta, \kappa_1, \ldots, \kappa_{n-1}) \tag{14.56}$$

Tvedt [23] has derived an exact expression for p_{f2} under the condition $-1 < \beta\kappa_i$. Expressed in the form of a single-fold integral in the complex plane, Tvedt's formula is

$$p_{f2} = \varphi(\beta)\mathrm{Re}\left\{\mathrm{i}\sqrt{\frac{2}{\pi}}\int_0^{\mathrm{i}\infty}\frac{1}{s}\exp\left[\frac{(s+\beta)^2}{2}\right]\prod_{i=1}^{n-1}\frac{1}{\sqrt{1+\kappa_i s}}\,ds\right\} \tag{14.57}$$

where $\mathrm{i} = \sqrt{-1}$. A simpler formula based on asymptotic approximations derived earlier by Breitung [24] is

$$p_{f2} \cong \Phi(-\beta)\prod_{i=1}^{n-1}\frac{1}{\sqrt{1+\psi(\beta)\kappa_i}} \tag{14.58}$$

Copyright 2005 by CRC Press LLC

shown that improved results are obtained by using $\psi(\beta) = \varphi(\beta)/\Phi(\beta)$. Note that in the above formula, each term $1/\sqrt{1+\psi(\beta)\kappa_i}$ acts as a correction factor on the FORM approximation to account for the curvature of the limit-state surface in the principal direction u_i''.

To summarize, the SORM approximation according to the above formulation involves the following steps after the design point has been found: (1) Construct the orthonormal matrix $\mathbf{P}$ with α as its last row. (2) Compute the second-derivative matrix $\mathbf{H} = [\partial^2 G/(\partial u_i \partial u_j)]$ at the design point. Usually, a finite-difference scheme in the $\mathbf{u}$ space is used, with the individual function values computed at the corresponding points in the $\mathbf{x}$ space. (3) Compute the matrix $\mathbf{A} = \mathbf{PHP}^{\mathrm{T}}/||\nabla G(\mathbf{u}^*)||$ and form $\mathbf{A}_{11}$ by deleting the last row and column of $\mathbf{A}$. (4) Compute the eigenvalues of $\mathbf{A}_{11}, \kappa_i, i = 1, \ldots, n-1$. (5) Use either of the formulas in Equation 14.57 or Equation 14.58 to obtain the SORM approximation. The most difficult part of this calculation is the evaluation of the second-derivative matrix. This is particularly the case if the limit-state function involves numerical algorithms, such as finite element calculations. Two issues arise in such applications. One is the cost of computing the full second-derivative matrix by finite differences when the number of random variables is large. The second is calculation noise in the limit-state function due to truncation errors, which could produce erroneous estimates of the curvatures. Two alternative SORM methods that attempt to circumvent these problems are described below.

Der Kiureghian and De Stefano [26] have shown that certain algorithms for finding the design point, including the Improved HL-RF algorithm described earlier, have the property that the trajectory of trial points $\mathbf{u}_i, i = 1, 2, \ldots$, asymptotically converges on the major principal axis of the limit-state surface, that is, the axis u_i'' having the maximum $|\kappa_i|$ value. Using this property, the major principal curvature can be approximately computed in terms of the quantities that are available in the last two iterations while finding the design point. Suppose convergence to the design point is achieved after r iterations with $\mathbf{u}_{r-1}$ and $\mathbf{u}_r$ denoting the last two trial points and α_{r-1} and α_r denoting the corresponding unit normal vectors. Using the geometry in Figure 14.5, the major principal curvature is approximately computed as

$$\kappa_i \cong \frac{\mathrm{sgn}[\alpha_r(\mathbf{u}_r - \mathbf{u}_{r-1})]\cos^{-1}\left(\alpha_r \alpha_{r-1}^{\mathrm{T}}\right)}{\sqrt{||\mathbf{u}_r - \mathbf{u}_{r-1}||^2 - ||\alpha_r(\mathbf{u}_r - \mathbf{u}_{r-1})||^2}} \tag{14.59}$$

To obtain the second major principal curvature, one repeats the search process (from a randomly selected initial point) in a subspace orthogonal to the major principal axis. The result, using Equation 14.59, is an approximation of the principal curvature having the second-largest absolute value. Next, the search is repeated in a subspace orthogonal to the first two principal axes. The result is the third major principal curvature. This process is continued until all principal curvatures of significant magnitude have been

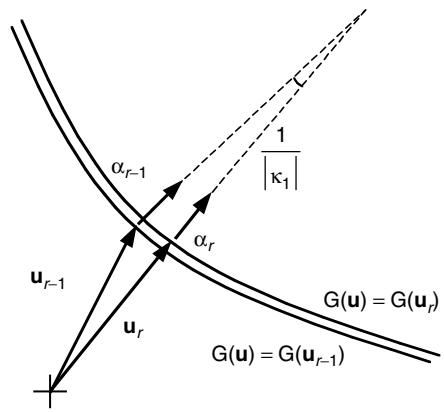

FIGURE 14.5 Geometry for computing the principal curvature.

Copyright 2005 by CRC Press LLC

obtained. The advantages of this approach are twofold: (1) one does not need to compute second derivatives, and (2) one computes the principal curvatures in the order of their importance and can stop the process when the curvature magnitudes are sufficiently small. The latter property is particularly important in problems with large n, where often only a few principal curvatures are significant; that is, the limit-state surface is significantly curved in only a few directions. The reader should consult Der Kiureghian and De Stefano [26] for further details on the implementation of this method.

The SORM method described above constructs the approximating paraboloid by fitting to the principal curvatures at the design point. For this reason, this method is known as the *curvature-fitting* SORM method. As mentioned, there are situations where the computation of the limit-state function involves noise due to truncation errors and computing high-order derivatives is problematic. To circumvent this problem, Der Kiureghian et al. [27] developed a *point-fitting* SORM method, where a piecewise paraboloid surface is defined by fitting to points selected on the limit-state surface on either side of the design point along each axis u'_i, $i = 1, \ldots, n-1$. As shown in Figure 14.6 for a slightly modified version of the method, the points for axis u'_i are selected by searching along a path consisting of lines $u'_i = \pm b$ and a semicircle of radius b centered at the design point. The parameter b is selected according to the rule $b = 1$ if $|\beta| < 1$, $b = |\beta|$ if $1 \le |\beta| \le 3$ and $b = 3$ if $3 < |\beta|$. This rule assures that the fitting points are neither too close nor too far from the design point. Let $(u_i'^-, u_n'^-)$ and $(u_i'^+, u_n'^+)$ denote the coordinates of the fitting points along axis u'_i, where the superscript signs indicate the negative and positive sides of the u'_i axis. Through each fitting point, a semiparabola is defined that is tangent at the design point (see Figure 14.6). The curvature of the semiparabola at the design point is given by

$$a_i^{\mathrm{sgn}(u'_i)} = \frac{2\left(u_n'^{\mathrm{sgn}(u'_i)} - \beta\right)}{\left(u_i'^{\mathrm{sgn}(u'_i)}\right)^2} \tag{14.60}$$

where $\mathrm{sgn}(u'_i)$ denotes the sign of the coordinate on the u'_i axis. The approximating limit-state function is now defined as

$$G'(\mathbf{u}') \cong \beta - u'_n + \frac{1}{2}\sum_{i=1}^{n-1} a_i^{\mathrm{sgn}(u'_i)} u_i'^2 \tag{14.61}$$

When set equal to zero, the above expression defines a piecewise paraboloid surface that is tangent to the limit-state surface at the design point and is coincident with each of the fitting points. Interestingly, this function is continuous and twice differentiable despite the fact that the coefficients $a_i^{\mathrm{sgn}(u'_i)}$ are

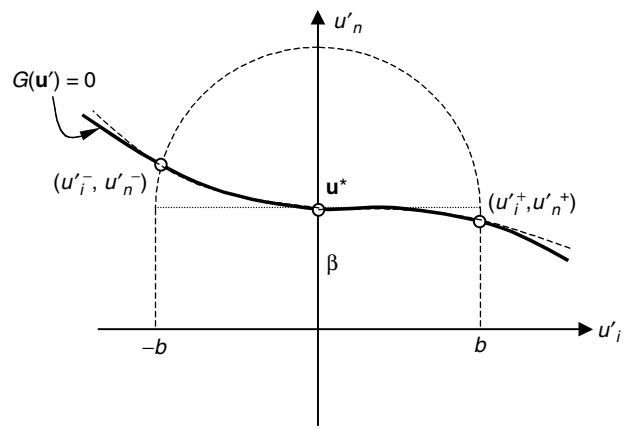

FIGURE 14.6 Definition of fitting points in point-fitting SORM method.

Copyright 2005 by CRC Press LLC

discontinuous. This is because this discontinuity occurs at points where u_i' takes on the zero value. The advantages of this approach are that it is insensitive to noise in the calculation of the limit-state function and it does not require derivative calculations. On the other hand, it requires finding $2(n-1)$ fitting points on the surface. Furthermore, because the fitting points are obtained in the $\mathbf{u}'$ space, the solution may depend on the selected transformation matrix $\mathbf{P}$, which of course is not unique. Der Kiureghian et al. [27] have shown that the maximum error resulting from the worst choice of $\mathbf{P}$ is much smaller than the error in the FORM approximation. That is, even in the worst case, this method improves the FORM approximation.

The above SORM methods are applicable to component reliability problems. For series system reliability problems, a SORM approximation may be obtained by replacing each component reliability index β_k by $\beta_k' = \Phi^{-1}(1-p_{f2})$, while keeping the unit vector α_k unchanged. The formula in Equation 14.28 is then used to obtain the series system probability. This procedure essentially adjusts the distances to the componential hyper-planes such that the half-space probability for each component is equal to the SORM approximation for the component. Unfortunately, a similar approach may not provide an improved result for nonseries systems.

14.4.1 Example: Reliability Analysis of a Column by SORM

For the example in Section 14.3.1.1, a SORM analysis reveals the principal curvatures $\kappa_1 = -0.155$ and $\kappa_2 = -0.0399$, with κ_3 being practically zero. The curvature-fitting SORM estimate of the failure probability according to Tvetd's formula (Equation 14.57) is $p_{f2} = 0.00936$, whereas the result based on Breitung's formula (Equation 14.58) is $p_{f2} \cong 0.00960$. The result based on the point-fitting SORM method is $p_{f2} \cong 0.00913$. All these results closely match the "exact" result given in the example in Section 14.3.1.1.

14.5 Time-Variant Reliability Analysis

Many problems in engineering involve random quantities that vary in time or space. Such quantities are properly modeled as stochastic processes or random fields. If the failure event of interest is defined over a temporal or spatial domain, then the reliability problem is said to be time- or space-variant, respectively. In this section, we only discuss time-variant problems. One-dimensional space-variant reliability problems have similar features. However, multidimensional space-variant problems require more advanced tools (see, e.g., [28]). Our discussion in this section addresses time-variant problems only in the context of FORM analysis. The more general topic of time-variant reliability analysis is, of course, much broader and involves such topics as stochastic differential equations and random vibrations.

Consider a component reliability problem defined by the limit-state function $g[\mathbf{x}, \mathbf{y}(t)]$, where $\mathbf{x}$ is a vector of random variables and $\mathbf{y}(t)$ is a vector of random processes. According to our definition, $\{g[\mathbf{x}, \mathbf{y}(t)] \le 0\}$ describes the failure event at time t. Because, for a given t, $\mathbf{y}(t)$ is a vector of random variables, the *instantaneous* failure probability $p_f(t) = P\{g[\mathbf{x}, \mathbf{y}(t)] \le 0\}$ can be computed by the methods described in this chapter, provided the joint distribution of $\mathbf{x}$ and $\mathbf{y}(t)$ is available.

A more challenging problem results when the failure domain is defined as

$$\Omega = \left\{ \min_{t \in T} g[\mathbf{x}, \mathbf{y}(t)] \le 0 \right\} \tag{14.62}$$

where T denotes an interval of time, say $T = \{t \mid t_1 < t \le t_m\}$. This is the well-known first-passage problem: the failure event occurs when the process $g[\mathbf{x}, \mathbf{y}(t)]$ first down-crosses the zero level. One can easily verify that

$$\max_{t \in T} p_f(t) \le P\left\{ \min_{t \in T} g[\mathbf{x}, \mathbf{y}(t)] \le 0 \right\} \tag{14.63}$$

Copyright 2005 by CRC Press LLC

That is, the maximum of the instantaneous failure probability over an interval only provides a lower bound to the probability of failure over the interval. This is because the failure event can occur at times other than the time at which $p_f(t)$ assumes its maximum. In the following, we present two approaches for approximately solving the above time-variant reliability problem.

A simple way to solve the problem is to "discretize" the time interval and use a series system approximation. Let $t_k, k = 1, \ldots, m$, be a set of time points selected within the interval T. Then,

$$P\left\{\bigcup_{k=1}^{m} g[\mathbf{x}, \mathbf{y}(t_k)] \le 0\right\} \le P\left\{\min_{t \in T} g[\mathbf{x}, \mathbf{y}(t)] \le 0\right\} \tag{14.64}$$

The problem on the left is a series-system reliability problem with m "time-point" components. It can be solved by the FORM methods described in Section 14.3. This involves transforming the entire vector of random variables, $[\mathbf{x}, \mathbf{y}(t_1), \ldots, \mathbf{y}(t_m)]$, to the standard normal space $\mathbf{u}$, finding the design point for each time-point component, and linearizing the corresponding limit-state surfaces such that $g[\mathbf{x}, \mathbf{y}(t_k)] \propto \beta_k - \alpha_k \mathbf{u}, \ k = 1, \ldots, m$, where β_k and α_k are the distance and the unit normal vector defining the plane tangent to the k-th limit-state surface. The quantities β_k and α_k are used in Equation 14.28 to compute the FORM approximation to the probability on the left side of Equation 14.64. The result is an approximate lower bound on the time-variant failure probability. This lower bound can be improved by increasing the number of discrete time points. When $\mathbf{y}(t)$ and, therefore, $g[\mathbf{x}, \mathbf{y}(t)]$ are nonstationary, advantage can be gained by selecting time points at which the instantaneous failure probability, $p_f(t)$, is high. However, selecting time points that are too closely spaced is not necessary because the failure events associated with such points are strongly correlated (the α_k vectors are nearly coincident) and, therefore, they would not significantly add to the series-system probability. One can increase the number of time points gradually until no appreciable increase in the system probability is observed. The result, then, provides a narrow lower bound approximation to the time-variant failure probability. Obviously, this method can become cumbersome when the process $g[\mathbf{x}, \mathbf{y}(t)]$ has a short correlation length relative to the interval T, because in that case a large number of points are necessary to obtain a good approximation. The main computational effort is in finding the design points associated with the discrete time steps $t_k, \ k = 1, \ldots, m$, by use of an iterative algorithm, such as the one described in Section 14.3. In this analysis, significant saving is achieved by finding the design points in sequence and using each preceding solution as the initial trial point in the search for the next design point.

An entirely different approach for computing the time-variant failure probability uses the mean rate of down-crossings of the process $g[\mathbf{x}, \mathbf{y}(t)]$ below the zero level. Consider a small time interval $[t, t + \delta t)$ and let $\nu(t)\delta t$ denote the mean number of times that the process $g[\mathbf{x}, \mathbf{y}(t)]$ down-crosses the level zero during this interval. Let $p(k)$ denote the probability that k down-crossings occur during the interval. We can write

$$\nu(t)\delta t = 0 \times p(0) + 1 \times p(1) + 2 \times p(2) + \cdots \tag{14.65}$$

For a sufficiently small δt, assuming the process $g[\mathbf{x}, \mathbf{y}(t)]$ has a smoothly varying correlation structure, the probability of more than one down-crossing can be considered negligible in relation to the probability of a single down-crossing. Thus, the second- and higher-order terms in the above expression can be dropped. The probability of a single down-crossing is computed by noting that this event will occur if $0 < g[\mathbf{x}, \mathbf{y}(t)]$ and $g[\mathbf{x}, \mathbf{y}(t + \delta t)] \le 0$. Hence [29],

$$\nu(t) = \lim_{\delta t \to 0} \frac{P\left\{-g[\mathbf{x}, \mathbf{y}(t)] < 0 \bigcap g[\mathbf{x}, \mathbf{y}(t + \delta t)] \le 0\right\}}{\delta t} \tag{14.66}$$

Copyright 2005 by CRC Press LLC

The probability in the numerator represents a parallel-system reliability problem with two components. This problem can be solved by FORM. The solution essentially requires finding the design points for the instantaneous limit-state functions $-g[\mathbf{x}, \mathbf{y}(t)]$ and $g[\mathbf{x}, \mathbf{y}(t+\delta t)]$ and the associated reliability indices $\beta(t)$ and $\beta(t+\delta t)$ and unit normals $\alpha(t)$ and $\alpha(t+\delta t)$, respectively. To avoid dealing with the highly correlated random vectors $\mathbf{y}(t)$ and $\mathbf{y}(t+\delta t)$, one can use the approximation $\mathbf{y}(t+\delta t) \cong \mathbf{y}(t) + \delta t\, \dot{\mathbf{y}}(t)$, where $\dot{\mathbf{y}}(t)$ denotes the derivative vector process. Furthermore, for small δt, we have $\beta(t+\delta t) \cong -\beta(t) = b$ and the inner product of $\alpha(t)$ and $\alpha(t+\delta t)$, which defines the correlation coefficient between the two component events, is nearly −1. For this limiting case, one can show (see [30]) that Equation 14.30 reduces to

$$\Phi_2(-b, b, \rho) \cong \frac{1}{4}\exp\left(-\frac{b^2}{2}\right)\left(1 + \frac{\sin^{-1}\rho}{\pi/2}\right) \tag{14.67}$$

This procedure is repeated for a grid of time points to compute $\nu(t)$ as a function of time. Normally, $\nu(t)$ is a smooth function and a coarse grid of time points is sufficient.

With the mean down-crossing rate computed, two options are available for estimating the time-variant failure probability. One is the well known upper bound defined by

$$P\left\{\min_{t\in T}[\mathbf{x}, \mathbf{y}(t)] \le 0\right\} \le P\left\{g[\mathbf{x}, \mathbf{y}(t_0)] \le 0\right\} + \int_{t\in T} \nu(t)dt \tag{14.68}$$

where $P\{g[\mathbf{x}, \mathbf{y}(t_0)] \le 0\}$ is the instantaneous probability of failure at the start of the interval, a time-invariant problem. This expression usually provides a good approximation of the time-variant failure probability when the process $g[\mathbf{x}, \mathbf{y}(t)]$ is not narrow band and the mean rate $\nu(t)$ is small. The second approach is based on the assumption that the down-crossing events are Poisson, which implies statistical independence between these events. This approximation works only if the limit-state process is ergodic.[2] Thus, for this approximation to work, the random variables $\mathbf{x}$ should not be present and $\mathbf{y}(t)$ must be ergodic. The Poisson-based approximation then is

$$P\left\{\min_{t\in T} g[\mathbf{y}(t)] \le 0\right\} \cong \exp\left[-\int_{t\in T} \nu(t)dt\right] \tag{14.69}$$

Provided ergodicity holds, this approximation normally works well when the mean down-crossing rate is small and the limit-state process is not narrow band.

14.5.1 Example: Mean Out-Crossing Rate of a Column under Stochastic Loads

Reconsider the example in Section 14.3.1.1. Assume the applied loads $\mathbf{y}(t) = \{m_1(t), m_2(t), p(t)\}^{\mathrm{T}}$ represent a vector of stationary Gaussian processes with the second moments described in Table 14.1. Also assume the zero-mean stationary Gaussian vector process $\dot{\mathbf{y}}(t)$ has the root-mean square values $300\,\pi$ kNm/s, $150\,\pi$ kNm/s and $2{,}500\,\pi$ kN/s, and the correlation coefficients $\rho_{1,2} = 0.4$, $\rho_{1,3} = \rho_{2,3} = 0.2$. Assuming the yield stress is a deterministic value $y = 40$ MPa, using Equation 14.66, the mean out-crossing rate is obtained as $\nu = 0.00476$ s^{-1}, which is of course independent of time due to the stationarity of the process. If y is considered to be random as in Table 14.1, the estimate of the mean out-crossing rate is $\nu = 0.00592$ s^{-1}. This value is slightly greater due to the added uncertainty of the yield stress.

[2] A random process is ergodic if its ensemble averages equal its corresponding temporal averages.

Copyright 2005 by CRC Press LLC

14.6 Finite Element Reliability Analysis

The finite element (FE) method is widely used in engineering practice to solve boundary-value problems governed by partial differential equations. Essentially, the method provides an algorithmic relation between a set of input variables $\mathbf{x}$ and processes $\mathbf{y}(t)$ and a set of output responses $\mathbf{s}$, that is, an implicit relation of the form $\mathbf{s} = \mathbf{s}(\mathbf{x}, \mathbf{y}(t))$. When $\mathbf{x}$ and $\mathbf{y}(t)$ are uncertain, $\mathbf{s}$ is also uncertain. Reliability methods can then be used to compute the probability associated with any failure event defined in terms of the response vector $\mathbf{s}$. This may include time- or space-variant problems, in which the failure event is defined over a temporal or spatial domain.

In using FORM or SORM to solve FE reliability problems, one essentially needs to repeatedly solve for the response and the response gradients for a sequence of selected realizations of the basic random variables. In FORM, the realizations of the random variables are selected in accordance to the algorithm for finding the design point (see Section 14.3). The number of such repeated FE solutions usually is not large (e.g., of the order of several tens); furthermore, this number is independent of the magnitude of the failure probability and the number of random variables. In SORM, the number of repeated FE solutions is directly governed by the number of random variables. In either case, if the failure probability is small, the amount of needed computations is usually much smaller than that needed in a straightforward Monte Carlo simulation approach.

An important issue in FORM solution of FE reliability problems is the computation of the response gradients, $\nabla_{\mathbf{x}}\mathbf{s}$ and $\nabla_{\mathbf{y}}\mathbf{s}$, which are needed in computing the gradient of the limit-state function. A finite difference approach for computing these gradients is often costly and unreliable due to the presence of computational noise arising from truncation errors. For this reason, direct differentiation methods (DDM) have been developed [31, 32]. These methods compute the response gradients directly, using the derivatives of the governing equations. Of course, this implies coding all the derivative equations in the FE code, for example, the derivatives of the constitutive laws, of the element stiffness and mass matrices, etc. A few modern finite element codes possess this capability. In particular, the OpenSees code developed by the Pacific Earthquake Engineering Research (PEER) Center is so enabled. Furthermore, it embodies the necessary routines for defining probability distributions for input variables or processes and for reliability analysis by FORM and two sampling methods [33]. This code is freely downloadable at http://opensees.berkeley.edu/.

FE reliability analysis by FORM and SORM entails a number of challenging problems, including convergence issues having to do with the discontinuity of gradients for certain nonlinear problems, computational efficiency, processing of large amounts of data, definition of failure events, and solution of time- and space-variant problems. A fuller description of these issues is beyond the scope of this chapter. The reader is referred to [28, 33, 34, 35].

References

1. Liu, P.-L. and Der Kiureghian, A. (1986). Multivariate distribution models with prescribed marginals and covariances. *Probabilistic Engineering Mechanics*, 1(2),105–112.
2. Hohenbichler, M. and Rackwitz, R. (1981). Nonnormal dependent vectors in structural safety. *J. Engineering Mechanics*, ASCE, 107(6), 1227–1238.
3. Rosenblatt, M. (1952). Remarks on a multivariate transformation. *Annals Math. Stat.*, 23, 470–472.
4. Segal, I.E. (1938). Fiducial distribution of several parameters with applications to a normal system. *Proceedings of Cambridge Philosophical Society*, 34, 41–47.
5. Engelund, S. and Rackwitz, R. (1993). A benchmark study on importance sampling techniques in structural reliability. *Structural Safety*, 12(4), 255–276.
6. Der Kiureghian, A. and Dakessian, T. (1998). Multiple design points in first- and second-order reliability. *Structural Safety*, 20(1), 37–49.
7. Liu, P.-L. and Der Kiureghian, A. (1990). Optimization algorithms for structural reliability. *Structural Safety*, 9(3), 161–177.

Copyright 2005 by CRC Press LLC

8. Hasofer, A.M. and Lind, N.C. (1974). Exact and invariant second-moment code format. *J. Engineering Mechanics Division*, ASCE, 100(1), 111–121.
9. Rackwitz, R. and Fiessler, B. (1978). Structural reliability under combined load sequences. *Computers & Structures*, 9, 489–494.
10. Zhang, Y. and Der Kiureghian, A. (1995). Two improved algorithms for reliability analysis. In *Reliability and Optimization of Structural Systems*, Proceedings of the 6th IFIP WG 7.5 Working Conference on Reliability and Optimization of Structural Systems, 1994, (R. Rackwitz, G. Augusti, and A. Borri, Eds.), 297–304.
11. Luenberger, D.G. (1986). *Introduction to Linear and Nonlinear Programming*, Addison-Wesley, Reading, MA.
12. Hohenbichler, M. and Rackwitz, R. (1983). First-order concepts in system reliability. *Structural Safety*, 1(3), 177–188.
13. Gollwitzer, S. and Rackwitz, R. (1988). An efficient numerical solution to the multinormal integral. *Probabilistic Engineering Mechanics*, 3(2), 98–101.
14. Ambartzumian, R.V., Der Kiureghian, A., Oganian, V.K., and Sukiasian, H.S. (1998). Multinormal probability by sequential conditioned importance sampling: theory and application. *Probab. Engrg. Mech.*, 13(4), 299–308.
15. Pandey, M.D. (1998). An effective approximation to evaluate multinormal integrals. *Structural Safety*, 20, 51–67.
16. Kounias, E.G. (1968). Bounds for the probability of a union, with applications. *Am. Math. Stat.*, 39(6), 2154–2158.
17. Hunter, D. (1976). An upper bound for the probability of a union. *J. Applied Probability*, 13, 597–603.
18. Ditlevsen, O. (1979). Narrow reliability bounds for structural systems. *J. Structural Mechanics*, 7(4), 453–472.
19. Zhang, Y.C. (1993). High-order reliability bounds for series systems and application to structural systems. *Computers & Structures*, 46(2), 381–386.
20. Song, J. and Der Kiureghian, A. (2003). Bounds on system reliability by linear programming. *Engineering Mechanics*, ASCE, 129(6), 627–636.
21. Hohenbichler, M. and Rackwitz, R. (1986). Sensitivity and importance measures in structural reliability. *Civil Engineering Systems*, 3, 203–210.
22. Bjerager, P. and Krenk, S. (1989). Parametric sensitivity in first-order reliability theory. *J. Engineering Mechanics*, ASCE, 115(7), 1577–1582.
23. Tvedt, L. (1990). Distribution of quadratic forms in normal space, application to structural reliability. *J. Engineering Mechanics*, ASCE, 116(6), 1183–1197.
24. Breitung, K. (1984). Asymptotic approximations for multinormal integrals. *J. Engineering Mechanics*, ASCE, 110(3), 357–366.
25. Hohenbichler, M. and Rackwitz, R. (1988). Improvement of second-order reliability estimates by importance sampling. *J. Engineering Mechanics*, ASCE, 114(12), 2195–2199.
26. Der Kiureghian, A. and DeStefano, M. (1991). Efficient algorithm for second-order reliability analysis. *J. Engineering Mechanics*, ASCE, 117(12), 2904–2923.
27. Der Kiureghian, A., Lin, H.S., and Hwang, S.-J. (1987). Second-order reliability approximations. *J. Engineering Mechanics*, ASCE, 113(8), 1208–1225.
28. Der Kiureghian, A. and Zhang, Y. (1999). Space-variant finite element reliability analysis. *Comp. Methods Appl. Mech. Engrg.*, 168(1–4), 173–183.
29. Hagen, O. and Tvedt, L. (1991). Vector process out-crossing as parallel system sensitivity measure. *J. Engineering Mechanics*, ASCE, 117(10), 2201–2220.
30. Koo, H. and Der Kiureghian, A. (2003). FORM, SORM and Simulation Techniques for Nonlinear Random Vibrations. *Report No. UCB/SEMM-2003/01*, Department of Civil & Environmental Engineering, University of California, Berkeley, CA, February.
31. Zhang, Y. and Der Kiureghian, A. (1993). Dynamic response sensitivity of inelastic structures. *Computer Methods in Applied Mechanics and Engineering*, 108(1), 23–36.

Copyright 2005 by CRC Press LLC

32. Kleiber, M., Antunez, H., Hien, T.D., and Kowalczyk, P. (1997). *Parameter Sensitivity in Nonlinear Mechanics*. John Wiley & Sons, West Sussex, U.K.
33. Haukaas, T. and Der Kiureghian A. (2004). Finite element reliability and sensitivity methods for performance-based earthquake engineering. PEER Report 2003/4, Pacific Earthquake Engineering Research Center, University of California, Berkeley, CA, April.
34. Liu, P.L. and Der Kiureghian, A. (1991). Finite-element reliability of geometrically nonlinear uncertain structures. *J. Engineering Mechanics*, ASCE, 117(8), 1806–1825.
35. Sudret, B. and Der Kiureghian, A. (2002). Comparison of finite element reliability methods. *Probabilistic Engineering Mechanics*, 17(4), 337–348.

Copyright 2005 by CRC Press LLC

15

System Reliability

Palle Thoft-Christensen
Aalborg University, Aalborg, Denmark

15.1 Introduction

A fully satisfactory estimate of the reliability of a structure is based on a system approach. In some situations, it may be sufficient to estimate the reliability of the individual structural members of a structural system. This is the case for statically determinate structures where failure in any member will result in failure of the total system. However, failure of a single element in a structural system will generally not result in failure of the total system, because the remaining elements may be able to sustain the external load by redistribution of the internal load effects. This is typically the case of statically indeterminate (redundant) structures, where failure of the structural system always requires that more than one element fail. A structural system will usually have a large number of failure modes, and the most significant failure modes must be taken into account in an estimate of the reliability of the structure.

From an application point of view, the reliability of structural systems is a relatively new area. However, extensive research has been conducted in the past few decades and a number of effective methods have been developed. Some of these methods have a limited scope and some are more general. One might

Copyright 2005 by CRC Press LLC

argue that this area is still in a phase of development and therefore not yet sufficiently clarified for practical application. However, a number of real practical applications have achieved success. This chapter does not try to cover all aspects of structural system reliability. No attempt is made to include all methods that can be used in estimating the reliability of structural systems. Only the β-unzipping method is described in detail here, because the author has extensive experience from using that method.

This section is to some degree based on the books by Thoft-Christensen and Baker [1] and Thoft-Christensen and Murotsu [2].

15.2 Modeling of Structural Systems

15.2.1 Introduction

A real structural system is so complex that direct exact calculation of the probability of failure is completely impossible. The number of possible different failure modes is so large that they cannot all be taken into account; and even if they could all be included in the analysis, exact probabilities of failure cannot be calculated. It is therefore necessary to idealize the structure so that the estimate of the reliability becomes manageable. Not only the structure itself, but also the loading must be idealized. Because of these idealizations it is important to bear in mind that the estimates of, for example, probabilities of failure are related to the idealized system (the model) and not directly to the structural system. The main objective of a structural reliability design is to be able to design a structure so that the probability of failure is minimized in some sense. Therefore, the model must be chosen carefully so that the most important failure modes for the real structures are reflected in the model.

It is assumed that the total reliability of the structural system can be estimated by considering a finite number of failure modes and combining them in complex reliability systems. The majority of structural failures are caused by human errors. Human errors are usually defined as serious mistakes in design, analysis, construction, maintenance, or use of the structure, and they cannot be included in the reliability modeling presented in this chapter. However, it should be stated that the probabilities of failure calculated by the methods presented in this book are much smaller than those observed in practice due to gross errors. The failures included in structural reliability theory are caused by random fluctuations in the basic variables, such as extremely low strength capacities or extremely high loads.

Only truss and frame structures are considered, although the methods used can be extended to a broader class of structures. Two-dimensional (plane) as well as three-dimensional (spatial) structures are treated. It is assumed that the structures consist of a finite number of bars and beams, and that these structural elements are connected by a finite number of joints. In the model of the structural system, the failure elements are connected to the structural elements (bars, beams, and joints); see Section 15.2.3. For each of the structural elements, a number of different failure modes exist. Each failure mode results in element failure, but systems failure will, in general, only occur when a number of simultaneous element failures occur. A more precise definition of system failure is one of the main objects of this chapter. It is assumed that the reliability of a structural system can be estimated on the basis of a series system modeling, where the elements are failure modes. The failure modes are modeled by parallel systems.

15.2.2 Fundamental Systems

Consider a statically determinate (nonredundant) structure with n structural elements and assume that each structural element has only one failure element; see Figure 15.1. The total number of failure elements is therefore also n. For such a structure, the total structural system fails as soon as any structural element fails. This is symbolized by a series system.

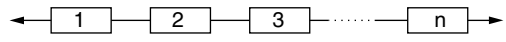

FIGURE 15.1 Series system with n elements.

Copyright 2005 by CRC Press LLC

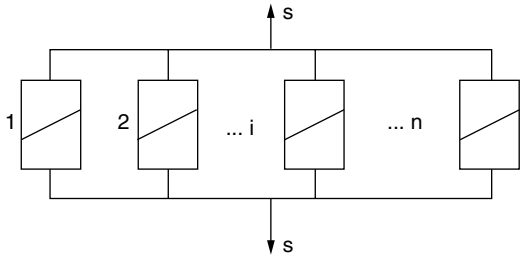

FIGURE 15.2 Parallel system with n elements.

For a statically indeterminate (redundant) structure, failure in a single structural element will not always result in failure of the total system. The reason for this is that the remaining structural elements will be able to sustain the external loading by redistribution of the load effects. For statically indeterminate structures, total failure will usually require that failure takes place in more than one structural element. It is necessary to define what is understood by total failure of a structural system. This problem will be addressed in more detail, but formation of a mechanism is the most frequently used definition. If this definition is used here, failure in a set of failure elements forming a mechanism is called a failure mode. Formation of a failure mode will therefore require simultaneous failure in a number of failure elements. This is symbolized by a parallel system, see Figure 15.2.

In this section it is assumed that all basic variables (load variables and strength variables) are normally distributed. All geometrical quantities and elasticity coefficients are assumed deterministic. This assumption significantly facilitates the estimation of the failure probability, but, in general, basic variables cannot be modeled by normally distributed variables at a satisfactory degree of accuracy. To overcome this problem, a number of different transformation methods have been suggested. The most well-known method was suggested by Rackwitz and Fiessler [3]. One drawback to these methods is that they increase the computational work considerably due to the fact that they are iterative methods. A simpler (but also less accurate) method, called the multiplication factor method, has been proposed by Thoft-Christensen [4]. The multiplication factor method does not increase the computational work. Without loss of generality, it is assumed that all basic variables are standardized; that is, the mean value is 0 and the variance 1.

The β-unzipping method is only used for trussed and framed structures but it can easily be modified to other classes of structures. The structure is considered at a fixed point in time, so that only static behavior has been addressed. It is assumed that failure in a structural element (section) is either pure tension/compression or failure in bending. Combined failure criteria have also been used in connection with the β-unzipping method, but only little experience has been obtained until now.

Let the vector $\overline{X} = (X_1, \ldots, X_n)$ be the vector of the standardized normally distributed basic variables with the joint probability density function φ_n and let failure of a failure element be determined by a failure function $f: \omega \to R$, where ω is the n-dimensional basic variable space. Let f be defined in such a way that the space ω is divided into a failure region $\omega_f = \{\overline{x} : f(\overline{x}) \le 0\}$ and a safe region $\omega_s = \{\overline{x} : f(\overline{x}) > 0\}$ by the failure surface (limit state) $\partial\omega = \{\overline{x} : f(\overline{x}) > 0\}$, where the vector $\overline{x}$ is a realization of the random vector $\overline{X}$. Then the probability of failure P_f for the failure element in question is given by

$$P_f = P(f(\overline{X}) \le 0) = \int_{\omega_f} \varphi_n(\overline{x}) d\overline{x}. \tag{15.1}$$

If the function f is linearized at the so-called design point at the distance β to the origin of the coordinate system, then an approximate value for P_f is given by

$$P_f \approx P(\alpha_1 X_1 + \ldots + \alpha_n X_n + \beta \le 0) = P(\alpha_1 X_1 + \ldots + \alpha_n X_n \le -\beta) = \Phi(-\beta) \tag{15.2}$$

Copyright 2005 by CRC Press LLC

where $\overline{\alpha} = (\alpha_1, \ldots, \alpha_n)$ is the vector of directional cosines of the linearized failure surface. β is the Hasofer-Lind reliability index, and Φ is the standardized normal distribution function. The random variable

$$M = \alpha_1 X_1 + \ldots + \alpha_n X_n + \beta \tag{15.3}$$

is the *linearized safety margin* for the failure element.

Next consider a *series system* with k elements. An estimate of the failure probability P_f^s of this series system can be obtained on the basis of the linearized safety margin of the form in Equation 15.3 for the k elements

$$\begin{aligned} P_f^s &= P\left(\bigcup_{i=1}^{k}(\overline{\alpha}_i\overline{X} + \beta_i \le 0)\right) = P\left(\bigcup_{i=1}^{k}(\overline{\alpha}_i\overline{X} \le -\beta_i)\right) = 1 - P\left(\bigcap_{i=1}^{k}(\overline{\alpha}_i\overline{X} > -\beta_i)\right) \\ &= 1 - P\left(\bigcap_{i=1}^{k}(-\overline{\alpha}_i\overline{X} < \beta_i)\right) = 1 - \Phi_k(\overline{\beta}; \overline{\overline{\rho}}) \end{aligned} \tag{15.4}$$

where $\overline{\alpha}_i$ and β_i are the directional cosines and the reliability index for failure element i, $i = 1,...,k$, respectively, and where $\overline{\beta} = (\beta_1, \ldots, \beta_k)$. $\overline{\overline{\rho}} = \{\rho_{ij}\}$ is the correlation coefficient matrix given by $\rho_{ij} = \overline{\alpha}_i^T \overline{\alpha}_j$ for all $i \neq j$. Φ_k is the standardized k-dimensional normal distribution function. Series systems will be treated in more detail in Section 15.3.

For a *parallel system* with k elements, an estimate of the failure probability P_f^p can be obtained in the following way

$$P_f^p = P\left(\bigcap_{i=1}^{k}(\overline{\alpha}_i\overline{X} + \beta_i \le 0)\right) = P\left(\bigcap_{i=1}^{k}(-\overline{\alpha}_i\overline{X} < -\beta_i)\right) = \Phi_k(\overline{\beta}; \overline{\overline{\rho}}) \tag{15.5}$$

where the same notations as above are used. Parallel systems will be treated in more detail in Section 15.4.

It is important to note the approximation behind Equation 15.4 and Equation 15.5; namely, the linearization of the general nonlinear failure surfaces at the distinct design points for the failure elements. The main problem in connection with application of Equation 15.4 and Equation 15.5 is numerical calculation of the n-dimensional normal distribution function Φ_n for $n \ge 3$. This problem is addressed later in this chapter where a number of methods to get approximate values for Φ_n are mentioned.

15.2.3 Modeling of Systems at Level N

Clearly, the definition of failure modes for a structural system is of great importance in estimating the reliability of the structural system. In this section, failure modes are classified in a systematic way convenient for the subsequent reliability estimate. A very simple estimate of the reliability of a structural system is based on failure of a single failure element, namely the failure element with the lowest reliability index (highest failure probability) of all failure elements. Failure elements are structural elements or cross-sections where failure can take place. The number of failure elements will usually be considerably higher than the number of structural elements. Such a reliability analysis is, in fact, not a system reliability analysis, but from a classification point of view it is convenient to call it *system reliability analysis at level* 0. Let a structure consist of n failure elements and let the reliability index (see, e.g., Thoft-Christensen and Baker [1]) for failure element i be β_i then the system reliability index β_S^0 at level 0 is

$$\beta_S^0 = \min_{i=1,\ldots,n} \beta_i. \tag{15.6}$$

Clearly, such an estimate of the system reliability is too optimistic. A more satisfactory estimate is obtained by taking into account the possibility of failure of any failure element by modeling the structural

Copyright 2005 by CRC Press LLC

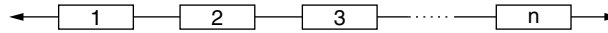

FIGURE 15.3 System modeling at level 1.

system as a series system with the failure elements as elements of the system (see Figure 15.3). The probability of failure for this series system is then estimated on the basis of the reliability indices β_i, $i = 1, 2, \ldots, n$, and the correlation between the safety margins for the failure elements. This reliability analysis is called *system reliability analysis at level* 1. In general, it is only necessary to include some of the failure elements in the series system (namely, those with the smallest β-indices) to get a good estimate of the system failure probability P_f^1 and the corresponding generalized reliability index β_S^1, where

$$\beta_S^1 = -\Phi^{-1}\left(P_f^1\right) \tag{15.7}$$

and where Φ is the standardized normal distribution function. The failure elements included in the reliability analysis are called *critical failure elements.*

The modeling of the system at level 1 is natural for a statically determinate structure, but failure in a single failure element in a structural system will not always result in failure of the total system, because the remaining elements may be able to sustain the external loads due to redistribution of the load effects. This situation is characteristic of statically indeterminate structures.

For such structures, *system reliability analysis at level* 2 or higher levels may be reasonable. At level 2, the system reliability is estimated on the basis of a series system where the elements are parallel systems each with two failure elements — so-called *critical pairs of failure elements* (see Figure 15.4). These critical pairs of failure elements are obtained by modifying the structure by assuming, in turn, failure in the critical failure elements and adding fictitious loads corresponding to the load-carrying capacity of the elements in failure. If, for example, element i is a critical failure element, then the structure is modified by assuming failure in element i and the load-carrying capacity of the failure element is added as fictitious loads if the element is ductile. If the failure element is brittle, no fictitious loads are added. The modified structure is then analyzed elastically and new β-values are calculated for all the remaining failure elements. Failure elements with low β-values are then combined with failure element i so that a number of critical pairs of failure elements are defined.

Analyzing modified structures where failure is assumed in critical pairs of failure elements now continues the procedure sketched above. In this way, *critical triples of failure elements* are identified and a *reliability analysis at level* 3 can be made on the basis of a series system, where the elements are parallel systems each with three failure elements (see Figure 15.5). By continuing in the same way, reliability estimates at levels 4, 5, etc. can be performed, but, in general, analysis beyond level 3 is of minor interest.

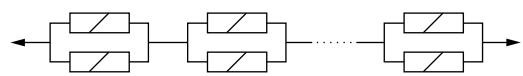

FIGURE 15.4 System modeling at level 2.

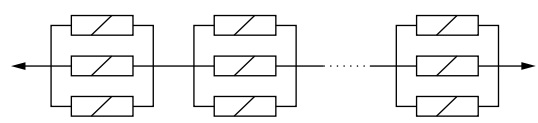

FIGURE 15.5 System modeling at level 3.

Copyright 2005 by CRC Press LLC

15.2.4 Modeling of Systems at Mechanism Level

Many recent investigations in structural system theory concern structures that can be modeled as elastic-plastic structures. In such cases, failure of the structure is usually defined as formation of a mechanism. When this failure definition is used, it is of great importance to be able to identify the most significant failure modes because the total number of mechanisms is usually much too high to be included in the reliability analysis. The β-unzipping method can be used for this purpose, simply by continuing the procedure described above until a mechanism has been found. However, this will be very expensive due to the great number of reanalyzes needed. It turns out to be much better to base the unzipping on reliability indices for fundamental mechanisms and linear combination of fundamental mechanisms.

When system failure is defined as formation of a mechanism, the probability of failure of the structural system is estimated by modeling the structural system as a series system with the significant mechanisms as elements (see Figure 15.6). Reliability analysis based on the mechanism failure definition is called *system reliability analysis at mechanism level.*

For real structures, a mechanism will often involve a relatively large number of yield hinges and the deflections at the moment of formation of a mechanism can usually not be neglected. Therefore, the failure definition must be combined with some kind of deflection failure definition.

15.2.5 Formal Representation of Systems

This section gives a brief introduction to a new promising area within the reliability theory of structural systems called *mathematical theory of system reliability.* Only in the past decade has this method been applied to structural systems, but it has been applied successfully within other reliability areas. However, a lot of research in this area is being conducted and it can be expected that this mathematical theory will also be useful also for structural systems in the future. The presentation here corresponds, to some extent, to the presentation given by Kaufmann, Grouchko, and Cruon [5].

Consider a structural system S with n failure elements $E_1, \ldots, E_n$. Each failure element E_i, $i = 1, \ldots, n$, is assumed to be either in a "state of failure" or in a "state of nonfailure". Therefore, a so-called Boolean variable (indicator function) e_i defined by

$$e_i = \begin{cases} 1 & \text{if the failure element is in a nonfailure state} \\ 0 & \text{if the failure element is in a failure state} \end{cases} \tag{15.8}$$

is associated with each failure element E_i, $i = 1, \ldots, n$.

The state of the system S is therefore determined by the *element state vector*

$$\bar{e} = (e_1, \ldots, e_n). \tag{15.9}$$

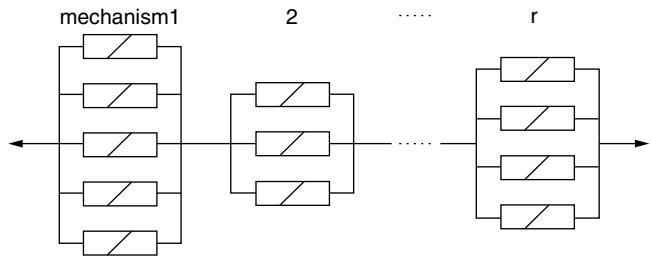

FIGURE 15.6 System modeling at mechanism level.

Copyright 2005 by CRC Press LLC

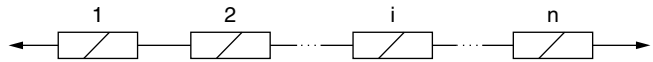

FIGURE 15.7 Series system with n elements.

The system S is also assumed to be either in a "state of failure" or in a "state of nonfailure". Therefore, a Boolean variable s, defined by

$$s = \begin{cases} 1 & \text{if the system is in a nonfailure state} \\ 0 & \text{if the system is in a failure state} \end{cases} \tag{15.10}$$

is associated with the system S. Because the state of the system S is determined solely by the vector $\bar{e}$, there is a function called the *systems structure function*, $\varphi: \bar{e} \rightarrow s$; that is,

$$s = \varphi(\bar{e}). \tag{15.11}$$

$-\sqcup-$

Example 15.1

Consider a series system with n elements as shown in Figure 15.7. This series system is in a safe (nonfailure) state if and only if all elements are in a nonfailure state. Therefore, the structural function s_S for a series system is given by

$$s_S = \varphi_S(\bar{e}) = \prod_{i=1}^{n} e_i \tag{15.12}$$

where $\bar{e}$ is given by Equation 15.9. Note that s_S can also be written

$$s_S = \min(e_1, e_2, \ldots, e_n). \tag{15.13}$$

Example 15.2

Consider a *parallel system* with n elements, as shown in Figure 15.8. This parallel system is in a safe state (nonfailure state) only if at least one of its elements is in a nonfailure state. Therefore, the structural function s_p for a parallel system is given by

$$s_P = \varphi_P(\bar{e}) = 1 - \prod_{i=1}^{n} (1 - e_i) \tag{15.14}$$

where $\bar{e}$ is given by Equation 15.9. Note that s_P can also be written

$$s_P = \max(e_1, e_2, \ldots, e_n). \tag{15.15}$$

$-\sqcup-$

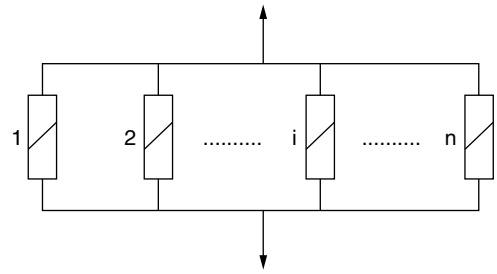

FIGURE 15.8 Parallel system with n elements.

Copyright 2005 by CRC Press LLC

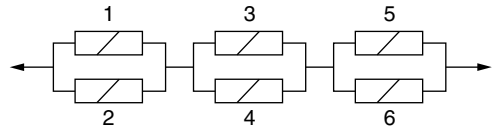

FIGURE 15.9 A level 2 system modeling.

It is easy to combine the structural functions of the system s_S and s_P shown in Equation 15.12 and Equation 15.14 so that the structural function for a more complicated system can be obtained. As an example, consider the system used in system modeling at *level* 2 and shown in Figure 15.9. It is a series system with three elements and each of these elements is a parallel system with two failure elements. With the numbering shown in Figure 15.9, the structural function becomes

$$s_S = s_{P_1} s_{P_2} s_{P_3} = [1-(1-e_1)(1-e_2)][1-(1-e_3)(1-e_4)][1-(1-e_5)(1-e_6)] \tag{15.16}$$

where s_{p_i}, $i = 1, 2, 3$, is the structural function for the parallel system i and where e_i, $i = 1, \ldots, 6$, is the Boolean variable for element i.

Consider a structure S with a set of n failure elements $E = \{E_1, \ldots, E_n\}$ and let the structural function of the system s be given by

$$s = \varphi(\bar{e}) = \varphi(e_1, \ldots, e_n) \tag{15.17}$$

where $\bar{e} = (e_1, \ldots, e_n)$ is the element state vector. A subset, $A = \{E_i \,|\, i \in I\,|\}$, I $\subset$ {l, 2, … , n}, of E is called a *path set* (or a *link set*) if

$$\left.\begin{aligned} e_i &= 1, i \in I \\ e_i &= 0, i \notin I \end{aligned}\right\} \Rightarrow s = 1. \tag{15.18}$$

According to the definition, a subset $A \subset E$ is a path set if the structure is in a nonfailure state and all elements in $E \backslash A$ are in a failure state.

–⊔–

Example 15.3

Consider the system shown in Figure 15.10. Clearly, the following subsets of $E = \{E_1, \ldots, E_6\}$ are all path sets: $A_1 = \{E_1, E_2, E_4\}$, $A_2 = \{E_1, E_2, E_5\}$, $A_3 = \{E_1, E_2, E_6\}$, $A_4 = \{E_1, E_3, E_4\}$, $A_5 = \{E_1, E_3, E_5\}$, and $A_6 = \{E_1, E_3, E_6\}$. The path set A_1 is illustrated in Figure 15.11.

–⊔–

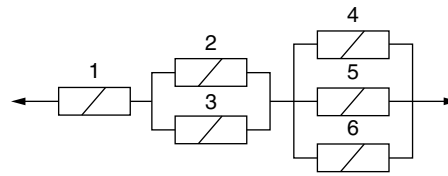

FIGURE 15.10 Example 15.3 system.

Copyright 2005 by CRC Press LLC

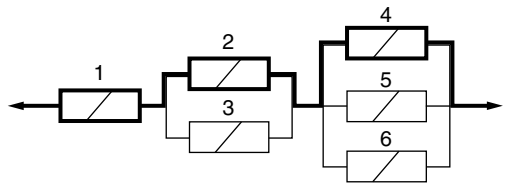

FIGURE 15.11 Path set A_1.

If a path set $A \subset E$ has the property that a subset of A, which is also a path set, does not exist then A is called a *minimal path set.* In other words, a path set is a minimal path set if failure of any failure element in A results in system failure.

Another useful concept is the *cut set* concept. Consider again a structure S defined by Equation 15.17 and let $A \subset E$ be defined by

$$A = \{E_i \,|\, i \in I\}, \quad I \subset \{1, 2, \ldots, n\}. \tag{15.19}$$

A is then called a cut set, if

$$\left.\begin{aligned} e_i &= 0, i \in I \\ e_i &= 1, i \notin I \end{aligned}\right\} \Rightarrow s = 0. \tag{15.20}$$

According to the definition (Equation 15.20) a subset $A \subset E$ is a cut set if the structure is in a failure state when all failure elements in A are in a failure state and all elements in $E \backslash A$ are in a nonfailure state.

–⊔–

Example 15.4

Consider again the structure shown in Figure 15.10. Clearly, the following subsets of $E = \{E_1, \ldots, E_6\}$ are all cut sets: $A_1 = \{E_1\}$, $A_2 = \{E_2, E_3\}$, and $A_3 = \{E_4, E_5, E_6\}$. The cut set A_2 is illustrated in Figure 15.12.

–⊔–

A cut set $A \subset E$ is called a *minimal cut set*, if it has the property that a subset of A is also a cut set. That is a cut set A is a minimal cut set if nonfailure of any failure element in A results in system nonfailure.

It is interesting to note that one can easily prove that any n-tuple $(e_1, \ldots, e_n)$ with $e_i = 0$ or 1, $i = 1, \ldots, n$, corresponds to either a path set or a cut set.

For many structural systems, it is convenient to describe the state of the system by the state of the failure elements on the basis of the system function as described in this section. The next step is then to

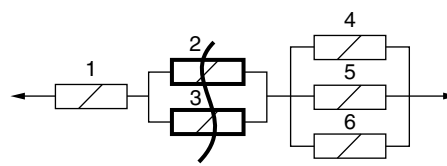

FIGURE 15.12 Cut set A_2.

Copyright 2005 by CRC Press LLC

estimate the reliability of the system when the reliabilities of the failure elements are known. The reliability R_i of failure element E_i is given by

$$R_i = P(e_i = 1) = 1 \times P(e_i = 1) + 0 \times P(e_i = 0) = E[e_i] \tag{15.21}$$

where e_i, the Boolean variable for failure element E_i, is considered a random variable and where $E[e_i]$ is the expected value of e_i.

Similarly, the reliability R_S of the system S is

$$R_S = P(s = 1) = 1 \times P(s = 1) + 0 \times P(s = 0) = E[s] = E[\varphi(\bar{e})] \tag{15.22}$$

where the element state vector $\bar{e}$ is considered a random vector and where φ is the structural function of the system.

Unfortunately, an estimate of $E[\varphi(\bar{e})]$ is only simple when the failure elements are uncorrelated and when the system is simple, for example, a series system. In civil engineering, failure elements will often be correlated. Therefore, the presentation above is only useful for very simple structures.

15.3 Reliability Assessment of Series Systems

15.3.1 Introduction

To illustrate the problems involved in estimating the reliability of systems, consider a structural element or structural system with two potential failure modes defined by safety margins $M_1 = f_1(X_1, X_2)$ and $M_2 = f_2(X_1, X_2)$, where X_1 and X_2 are standardized normally distributed basic variables. The corresponding failure surface and reliability indices β_1 and β_2 are shown in Figure 15.13.

Realizations (x_1, x_2) in the dotted area ω_f will result in failure, and the probability of failure P_f is equal to

$$P_f = \int_{\omega_f} \varphi_{X_1, X_2}(x_1, x_2; 0)\, d\bar{x} \tag{15.23}$$

where φ_{X_1, X_2} is the bivariate normal density function for the random vector $\bar{X} = (X_1, X_2)$. Let $\beta_2 < \beta_1$ as shown in Figure 15.13, and assume that the reliability index β for the considered structural element or

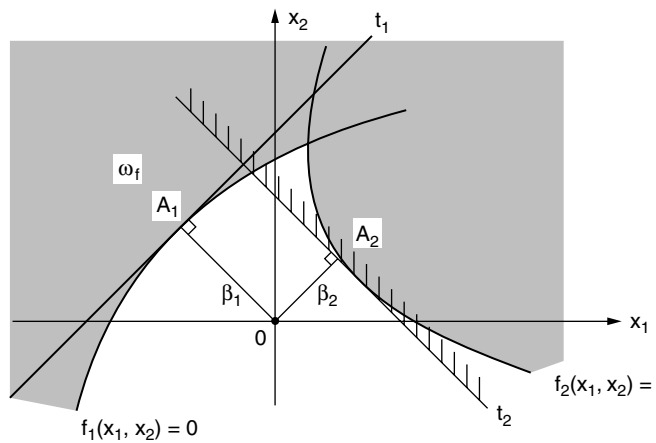

FIGURE 15.13 Illustration of series system with two failure elements.

Copyright 2005 by CRC Press LLC

structural system is equal to the shortest distance from the origin 0 to the failure surface. That is, $\beta = \beta_2$. Estimating the probability of failure by the formula

$$P_f \approx \Phi(-\beta) = \Phi(-\beta_2) \tag{15.24}$$

will then correspond to integrating over the hatched area (to the right of the tangent t_2). Clearly, the approximation (15.2) will in many cases be very different from the exact P_f calculated by (15.1). It is therefore of great interest to find a better approximation of P_f and then define a reliability index β by

$$\beta = -\Phi^{-1}(P_f). \tag{15.25}$$

Let the two failure modes be defined by the safety margins $M_1 = f_1 (X_1, X_2)$ and $M_1 = f_2 (X_1, X_2)$ and let $F_i = \{M_i \le 0\}$, $i = 1, 2$. Then, the probability of failure P_f of the structural system is

$$P_f = P(F_1 \cup F_2) \tag{15.26}$$

corresponding to evaluating the probability of failure of a series system with two elements. An approximation of P_f can be obtained by assuming that the safety margins M_1 and M_2 are linearized at their respective design points A_1 and A_2

$$M_1 = a_1 X_1 + a_2 X_2 + \beta_1 \tag{15.27}$$

$$M_2 = b_1 X_1 + b_2 X_2 + \beta_2 \tag{15.28}$$

where β_1 and β_2 are the corresponding reliability indices when $\overline{a} = (a_1, a_2)$ and $\overline{b} = (b_1, b_2)$ are chosen as unit vectors. Then, an approximation of P_f is

$$\begin{aligned} P_f &\approx P\left(\left\{\overline{a}^T \overline{X} + \beta_1 \le 0\right\} \cup \left\{\overline{b}^T \overline{X} + \beta_2 \le 0\right\}\right) = P\left(\left\{\overline{a}^T \overline{X} \le -\beta_1\right\} \cup \left\{\overline{b}^T \overline{X} \le -\beta_2\right\}\right) \\ &= 1 - P\left(\left\{\overline{a}^T \overline{X} > -\beta_1\right\} \cap \left\{\overline{b}^T \overline{X} > -\beta_2\right\}\right) = 1 - P\left(\left\{-\overline{a}^T \overline{X} < \beta_1\right\} \cap \left\{\overline{b}^T \overline{X} < \beta_2\right\}\right) \\ &= 1 - \Phi_2(\beta_1, \beta_2; \rho) \end{aligned} \tag{15.29}$$

where $\overline{X} = (X_1, X_2)$ is an independent standard normal vector, and ρ is the correlation coefficient given by

$$\rho = \overline{a}^T \overline{b} = a_1 b_1 + a_2 b_2. \tag{15.30}$$

Φ_2 is the bivariate normal distribution function defined by

$$\Phi_2(x_1, x_2; \rho) = \int_{-\infty}^{x_1} \int_{-\infty}^{x_2} \varphi_2(t_1, t_2; \rho) dt_1 dt_2 \tag{15.31}$$

where the bivariate normal density function with zero mean φ_2 is given by

$$\varphi_2(t_1, t_2; \rho) = \frac{1}{2\pi\sqrt{1-\rho^2}} \exp\left(-\frac{1}{2(1-\rho^2)}(t_1^2 + t_2^2 - 2\rho t_1 t_2)\right). \tag{15.32}$$

A formal reliability index β for the system can then be defined by

$$\beta = -\Phi^{-1}(P_f) \approx -\Phi^{-1}\left(1 - \Phi_2(\beta_1, \beta_2; \rho)\right). \tag{15.33}$$

Copyright 2005 by CRC Press LLC

The reliability of a structural system can be estimated based on modeling by a series system where the elements are parallel systems. It is therefore of great importance to have accurate methods by which the reliability of series systems can be evaluated. In this section it will be shown how the approximation of P_f by Equation 15.29 can easily be extended to a series system with n elements. Further, some bounding and approximate methods are presented.

15.3.2 Assessment of the Probability of Failure of Series Systems

Consider a series system with n elements as shown in Figure 15.3 and let the safety margin for element i be given by

$$M_i = g_i(\overline{X}), \quad i = 1, 2, \ldots, n \tag{15.34}$$

where $\overline{X} = (X_1, \ldots, X_k)$ are the basic variables and where g_i, $i = 1, 2, \ldots, n$ are nonlinear functions.

The probability of failure P_f of *element i* can then be estimated in the following way. Assume that there is a transformation $\overline{Z} = \overline{T}(\overline{X})$ by which the basic variables $\overline{X} = (\overline{X}_1, \ldots, \overline{X}_k)$ are transformed into independent standard normal variables $\overline{Z} = (Z_1, \ldots, Z_k)$ so that

$$P_{f,i} = P(M_i \le 0) = P(f_i(\overline{X}) \le 0) = P(f_i(\overline{T}^{-1}(\overline{Z})) \le 0) = P(h_i(\overline{Z}) \le 0) \tag{15.35}$$

where h_i is defined by Equation 15.35. An approximation of $P_{f,i}$ can then be obtained by linearization of h_i at the design point

$$P_{f,i} = P(h_i(\overline{Z}) \le 0) \approx P(\overline{\alpha}_i^T \overline{Z} + \beta_i \le 0) \tag{15.36}$$

where $\overline{\alpha}_i$ is the unit normal vector at the design point and β_i the Hasofer-Lind reliability index.

The approximation in Equation 15.36 can be written

$$P_{f,i} \approx P\left(\overline{\alpha}_i^T \overline{Z} + \beta_i \le 0\right) = P\left(\alpha_i^{-T} \overline{Z} \le -\beta_i\right) = \Phi(-\beta_i) \tag{15.37}$$

where Φ is the standard normal distribution function.

Return to the *series system* shown in Figure 15.3. An approximation of the probability of failure P_{fs} of this system can then be obtained using the same transformation $\overline{T}$ as for the single elements and by linearization of

$$h_i(\overline{Z}) = g_i(\overline{T}^{-1}\overline{Z})), \quad i = 1, 2, \ldots, n \tag{15.38}$$

at the design points for each element. Then (see, e.g., Hohenbichler and Rackwitz [6])

$$\begin{aligned} P_{fs} &= P\left(\bigcup_{i=1}^{n}\{M_i \le 0\}\right) = P\left(\bigcup_{i=1}^{n}\{f_i(\overline{X}) \le 0\}\right) = P\left(\bigcup_{i=1}^{n}\{f_i(\overline{T}^{-1}(\overline{Z})) \le 0\}\right) \\ &= P\left(\bigcup_{i=1}^{n}\{h_i(\overline{Z}) \le 0\}\right) \approx P\left(\bigcup_{i=1}^{n}\left\{\overline{\alpha}_i^T \overline{Z} + \beta_i \le 0\right\}\right) = P\left(\bigcup_{i=1}^{n}\left\{\overline{\alpha}_i^T \overline{Z} \le -\beta_i\right\}\right) \\ &= 1 - P\left(\bigcap_{i=1}^{n}\left\{\overline{\alpha}_i^T \overline{Z} \le -\beta_i\right\}\right) = 1 - P\left(\bigcap_{i=1}^{n}\left\{\overline{\alpha}_i^T \overline{Z} < \beta_i\right\}\right) = 1 - \Phi_n(\overline{\beta}; \overline{\overline{\rho}}) \end{aligned} \tag{15.39}$$

Copyright 2005 by CRC Press LLC

where $\overline{\beta} = (\beta_1, \ldots, \beta_n)$ and where $\overline{\overline{\rho}} = [\rho_{ij}]$ is the correlation matrix for the linearized safety margins; that is, $\rho_{ij} = \overline{\alpha}_i^T \overline{\alpha}_j$. Φ_n is the n-dimensional standardized normal distribution function.

Using Equation 15.39, the calculation of the probability of failure of a series system with linear and normally distributed safety margins is reduced to calculation of a value of Φ_n.

15.3.3 Reliability Bounds for Series Systems

It has been emphasized several times in this chapter that numerical calculation of the multi-normal distribution function Φ_n is extremely time consuming or perhaps even impossible for values of n greater than, say, four. Therefore, approximate techniques or bounding techniques must be used. In this section, the so-called *simple bounds* and *Ditlevsen bounds* are derived.

15.3.3.1 Simple Bounds

First, the simple bounds are derived. For this purpose, it is convenient to use the Boolean variables introduced in Section 15.2.5. Consider a series system S with n failure elements $E_1, \ldots, E_i, E_{i+1}, E_n$. For each failure element E_i, $i = 1, \ldots, n$, a Boolean variable e_i is defined by (see Equation 15.8)

$$e_i = \begin{cases} 1 & \text{if the failure element is in a nonfailure state} \\ 0 & \text{if the failure element is in a failure state.} \end{cases} \tag{15.40}$$

Then the probability of failure P_{fs} of the series system is

$$\begin{aligned} P_{fs} &= 1 - P\left(\bigcap_{i=1}^{n} e_i = 1\right) = 1 - P(e_1 = 1)\frac{P(e_1 = 1 \cap e_2 = 1)}{P(e_1 = 1)} \cdots \frac{P(e_1 = 1 \cap \ldots \cap e_n = 1)}{P(e_1 = 1 \cap \ldots \cap e_{n-1} = 1)} \\ &\le 1 - \prod_{i=1}^{n} P(e_i = 1) = 1 - \prod_{i=1}^{n} (1 - P(e_i = 0)). \end{aligned} \tag{15.41}$$

If

$$P(e_i = 1 \cap e_2 = 1) \ge P(e_1 = 1)P(e_2 = 1) \tag{15.42}$$

etc., or in general,

$$P\left(\bigcap_{j=1}^{i+1} e_j = 1\right) \ge P\left(\bigcap_{j=1}^{i} e_j = 1\right) P(e_{i+1} = 1) \tag{15.43}$$

for all $1 \le i \le n-1$. It can be shown that Equation 15.43 is satisfied when the safety margins for E_i, $i = 1, \ldots, n$, are normally distributed and positively correlated. When Equation 15.43 is satisfied, an upper bound of P_{fs} is given by Equation 15.41. A simple lower bound is clearly the maximum probability of failure of any failure element E_i, $i = 1, \ldots, n$. Therefore, the following simple bounds exist when Equation 15.43 is satisfied

$$\max_{i=1}^{n} P(e_i = 0) \le P_{fs} \le 1 - \prod_{i=1}^{n} (1 - P(e_i = 0)). \tag{15.44}$$

Copyright 2005 by CRC Press LLC

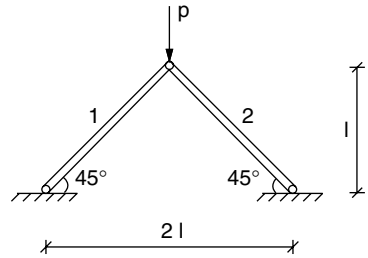

FIGURE 15.14 Structural system for Example 15.5.

The lower bound in Equation 15.44 is equal to the exact value of P_{fs} if there is full dependence between all elements ($\rho_{ij} = 1$ for all i and j) and the upper bound in Equation 15.44 corresponds to no dependence between any pair of elements ($\rho_{ij} = 0$, $i \neq j$).

Example 15.5

Consider the structural system shown in Figure 15.14 loaded by a single concentrated load p. Assume that system failure is failure in compression in element 1 or in element 2. Let the load-carrying capacity in the elements 1 and 2 be $1.5 \times n_F$ and n_F, respectively, and assume that p and n_F are realizations of independent normally distributed random variables P and N_F with

$$\mu_P = 4kN \quad \sigma_P = 0.8kN$$

$$\mu_{N_F} = 4kN \quad \sigma_{N_F} = 0.8kN.$$

Safety margins for elements 1 and 2 are

$$M_1 = \frac{3}{2}N_F - \frac{\sqrt{2}}{2}P, \quad M_2 = N_F - \frac{\sqrt{2}}{2}P$$

or expressed by standardized random variables $X_1 = (N_F - 4)/0.4$ and $X_2 = (P - 4)/0.8$, where the coefficients of X_1 and X_2 are chosen so that they are components of unit vectors. The reliability indices are $\beta_1 = 3.85$ and $\beta_2 = 1.69$ and the correlation coefficient between the safety margins is $\rho = 0.728 \times 0.577 + 0.686 \times 0.816 = 0.98$.

Therefore, the probability of failure of the system is

$$P_{fs} = 1 - \Phi_2(3.85, 1.69; 0.98).$$

The probabilities of failure of the failure elements E_i, $i = 1, 2$, are

$$P_{f1} = P(e_1 = 0) = \Phi(-3.85) = 0.00006, \quad P_{f2} = P(e_2 = 0) = \Phi(-1.65) = 0.04947.$$

Bounds for the probability of failure P_{fs} are then according to Equation 15.44

$$0.04947 \leq P_{fs} \leq 1 - (1 - 0.00006)(1 - 0.04947) = 0.04953.$$

For this series system, $\rho = 0.98$. Therefore, the lower bound can be expected to be close to P_{fs}.

15.3.3.2 Ditlevsen Bounds

For small probabilities of element failure, the upper bound in Equation 15.44 is very close to the sum of the probabilities of failure of the single elements. Therefore, when the probability of failure of one

Copyright 2005 by CRC Press LLC

failure element is predominant in relation to the other failure element, then the probability of failure of series systems is approximately equal to the predominant probability of failure, and the gap between the upper and lower bounds in Equation 15.44 is narrow. However, when the probabilities of failure of the failure elements are of the same order, then the simple bounds in Equation 15.44 are of very little use and there is a need for narrower bounds.

Consider again the above-mentioned series system S shown in Figure 15.7 and define the Boolean variable s by Equation 15.37. Then it follows from Equation 15.12 that

$$\begin{aligned} s &= e_1 \times e_2 \times \ldots \times e_n = e_1 \times e_2 \times \ldots \times e_{n-1} - e_1 \times e_2 \times \ldots \times e_{n-1}(1-e_n) \\ &= e_1 - e_1(1-e_2) - e_1 \times e_2(1-e_3) - \ldots - e_1 \times e_2 \times \ldots \times e_{n-1}(1-e_n). \end{aligned} \tag{15.45}$$

Hence, in accordance with Equation 15.22,

$$\begin{aligned} P_{fs} &= 1 - R_S = 1 - E[s] \\ &= E[1-e_1] + E[e_1(1-e_2)] + E[e_1e_2(1-e_3)] + \ldots + E[e_1e_2 \ldots e_{n-1}(1-e_n)]. \end{aligned} \tag{15.46}$$

It is easy to see that

$$1 - ((1-e_1)(1-e_2) + \ldots + (1-e_n)) \le e_1e_2 \ldots e_n \le e_i \quad \text{for} \quad i = 1, 2, \ldots, n. \tag{15.47}$$

It is then seen from Equation 15.46

$$P_{fs} \le \sum_{i=1}^{n} P(e_i = 0) - \sum_{i=2}^{n} \max_{j<i} P(e_i = 0 \bigcap e_j = 0) \tag{15.48}$$

and

$$P_{fs} \ge P(e_1 = 0) + \sum_{i=2}^{n} \max P(e_i = 0) - \sum_{j=1}^{i-1} P(e_i = 0 \bigcap e_j = 0, 0). \tag{15.49}$$

These bounds have been suggested in a slightly different form by Kounias [7]. In structural reliability, they are called *Ditlevsen bounds* [8]. The numbering of the failure elements may influence the bounds in Equation 15.48 and Equation 15.49. However, experience suggests that it is a good choice to arrange the failure elements so that $P(e_1 = 0) \ge P(e_2 = 0) \ge \ldots \ge P(e_n = 0)$, that is, according to decreasing probability of element failure.

The gap between the Ditlevsen bounds of Equation 15.48 and Equation 15.49 is usually much smaller than the gap between the simple bounds in Equation 15.44. However, the bounds of Equation 15.48 and Equation 15.49 require calculation of the joint probabilities $P(e_i = 0 \bigcap e_j = 0)$ and these calculations are not trivial. Usually, a numerical technique must be used.

15.3.4 Series Systems with Equally Correlated Elements

The n-dimensional standardized normal distribution function $\Phi_n(\bar{x}; \bar{\bar{\rho}})$ can be easily evaluated when $\rho_{ij} = \rho > 0$, $i = 1, \ldots, n$, $j = 1, \ldots, n$, $i \ne j$, that is, when

$$\bar{\bar{\rho}} = \begin{bmatrix} 1 & \rho & \cdots & \rho \\ \rho & 1 & \cdots & \rho \\ \vdots & \vdots & \ddots & \vdots \\ \rho & \rho & \cdots & 1 \end{bmatrix}. \tag{15.50}$$

Copyright 2005 by CRC Press LLC

By the correlation matrix in Equation 15.50, it has been shown by Dunnett and Sobel [9] that

$$\Phi_n(\bar{x}:\bar{\bar{\rho}}) = \int_{-\infty}^{\infty} \varphi(t) \prod_{i=1}^{n} \Phi\left(\frac{x_i - \sqrt{\rho t}}{\sqrt{1-\rho}} \right) dt. \tag{15.51}$$

Equation 15.50 can be generalized to the case where $\rho_{ij} = \lambda_i \lambda_j$, $i \neq j$, $|\lambda_i| \leq 1$, $|\lambda_j| \leq 1$, that is,

$$\bar{\bar{\rho}} = \begin{bmatrix} 1 & \lambda_1\lambda_2 & \cdots & \lambda_1\lambda_n \\ \lambda_2\lambda_1 & 1 & \cdots & \lambda_2\lambda_n \\ \vdots & \vdots & \ddots & \vdots \\ \lambda_n\lambda_1 & \lambda_n\lambda_2 & \cdots & 1 \end{bmatrix}. \tag{15.52}$$

For such correlation matrices, Dunnett and Sobel [9] have shown that

$$\Phi_n(\bar{x}:\bar{\bar{\rho}}) = \int_{-\infty}^{\infty} \varphi(t) \prod_{i=1}^{n} \Phi\left(\frac{x_i - \lambda_i t}{\sqrt{1-\lambda_i^2}} \right) dt. \tag{15.53}$$

For series systems with equally correlated failure elements, the probability of failure P_{fs} can then be written (see Equation 15.39)

$$P_{fs} = 1 - \Phi_n(\bar{\beta};\bar{\bar{\rho}}) = 1 - \int_{-\infty}^{\infty} \varphi(t) \prod_{i=1}^{n} \Phi\left(\frac{x_i - \sqrt{\rho t}}{\sqrt{1-\rho}} \right) dt \tag{15.54}$$

where $\bar{\beta} = (\beta_1, \ldots, \beta_n)$ are the reliability indices for the single failure elements and ρ is the common correlation coefficient between any pair of safety margins M_i and M_j, $i \neq j$.

A further specialization is the case where all failure elements have the same reliability index β_e, that is, $\beta_i = \beta_e$ for $i = 1, \ldots, n$. Then

$$P_{fs} = 1 - \int_{-\infty}^{\infty} \varphi(t) \left[\Phi\left(\frac{\beta_e - \sqrt{\rho t}}{\sqrt{1-\rho}} \right) \right]^n dt. \tag{15.55}$$

–⊔–

Example 15.6

Consider a series system with $n = 10$ failure elements, common element reliability index β_e and common correlation coefficient ρ. The probability of failure P_{fs} of this series system as a function of ρ is illustrated in Figure 15.15 for $\rho = 2.50$ and 3.00. Note that, as expected, the probability of failure P_{fs} decreases with ρ.

–⊔–

To summarize for a series system with equally correlated failure elements where the safety margins are linear and normally distributed, the probability of failure P_{fs} can be calculated by Equation 15.54. A formal reliability index β_S for the series system can then be calculated by

$$P_{fs} = \Phi(-\beta_S) \Leftrightarrow \beta_S = -\Phi^{-1}(P_{fs}). \tag{15.56}$$

Copyright 2005 by CRC Press LLC

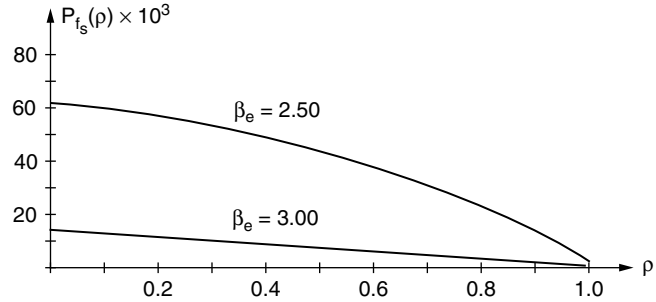

FIGURE 15.15 Probability of failure of series system with ten elements as a function of the correlation coefficient.

15.3.5 Series Systems with Unequally Correlated Elements

It has been investigated by Thoft-Christensen and Sørensen [10] whether an equivalent correlation coefficient can be used in Equation 15.55 with satisfactory accuracy when the failure elements are unequally correlated (or Equation 15.54 if the reliability indices are not equal).

Define the *average correlation coefficient P* by

$$\bar{\rho} = \frac{1}{n(n-1)} \sum_{\substack{i,j=1 \\ i \neq j}}^{n} \rho_{ij} \tag{15.57}$$

$\bar{\rho}$ is the average of all ρ_{ij}, $i \neq j$. Using $\bar{\rho}$ corresponds to the approximation

$$\Phi_n(\bar{\beta}; \bar{\bar{\rho}}) \approx \Phi_n(\bar{\beta}; [\bar{\rho}]) \tag{15.58}$$

where the correlation matrix $[\bar{\rho}]$ is given by

$$[\bar{\rho}] = \begin{bmatrix} 1 & \bar{\rho} & \cdots & \bar{\rho} \\ \bar{\rho} & 1 & \cdots & \bar{\rho} \\ \vdots & \vdots & \ddots & \vdots \\ \bar{\rho} & \bar{\rho} & \cdots & 1 \end{bmatrix}. \tag{15.59}$$

Thoft-Christensen and Sørensen [10] have shown by extensive simulation that in many situations,

$$\Phi_n(\bar{\beta}; [\bar{\rho}]) \leq \Phi_n(\bar{\beta}; [\bar{\bar{\rho}}]) \tag{15.60}$$

so that an estimate of the probability of failure P_{fs} using the average correlation coefficient will in such cases be conservative. Ditlevsen [11] has investigated this more closely by a Taylor expansion for the special case $\beta_i = \beta_e$, $i = 1, \ldots, n$ with the conclusion that Equation 15.60 holds for most cases, when $\beta_e > 3$, $n < 100$, $\bar{\rho} < 0.4$.

Thoft-Christensen and Sørensen [10] have shown that a better approximation can be obtained by

$$\Phi_n(\bar{\beta}; \bar{\bar{\rho}}) \approx \Phi_n(\bar{\beta}; [\bar{\rho}]) + \Phi_2(\beta_e, \beta_e; \rho_{\max}) - \Phi_2(\beta_e, \beta_e; \bar{\rho}) \tag{15.61}$$

where $\bar{\beta} = (\beta_e, \ldots, \beta_e)$ and where

$$\rho_{\max} = \max_{\substack{i,j=1 \\ i \neq j}}^{n} \rho_{ij}. \tag{15.62}$$

Copyright 2005 by CRC Press LLC

By this equation, the probability of failure P_{fs} is approximated by

$$P_{fs} \approx P_{fs}([\rho_{i,j}]) = P_{fs}([\bar{\rho}]) + P_{fs}(n=2, \rho=\rho_{\max}) - P_{fs}(n=2, \rho=\bar{\rho}) \tag{15.63}$$

–⌴–

Example 15.7

Consider a series system with five failure elements and common reliability index β_e = 3.50 and the correlation matrix

$$\bar{\bar{\rho}} = \begin{bmatrix} 1 & 0.8 & 0.6 & 0 & 0 \\ 0.8 & 1 & 0.4 & 0 & 0 \\ 0.6 & 0.4 & 1 & 0.1 & 0.2 \\ 0 & 0 & 0.1 & 1 & 0.7 \\ 0 & 0 & 0.2 & 0.7 & 1 \end{bmatrix}.$$

Using Equation 15.58 with $\bar{\rho} = 0.28$ then gives $P_{fs} \approx 0.00115$. It can be shown that the Ditlevsen bounds are $0.00107 \le P_{fs} \le 0.00107$. The approximation in Equation 15.63 gives $P_{fs} \approx 0.00111$.

–⌴–

15.4 Reliability Assessment of Parallel Systems

15.4.1 Introduction

As mentioned earlier, the reliability of a structural system may be modeled by a series system of parallel systems. Each parallel system corresponds to a failure mode, and this modeling is called system modeling at level N, $N = 1, 2, \ldots$ if all parallel systems have the same number N of failure elements. In Section 15.5 it is shown how the most significant failure modes (parallel systems) can be identified by the β-unzipping method. After identification of significant (critical) failure modes (parallel systems), the next step is an estimate of the probability of failure P_{fp} for each parallel system and the correlation between the parallel systems. The final step is the estimate of the probability of failure P_f of the series system of parallel systems by the methods discussed in Section 15.3.

Consider a parallel system with only two failure elements and let the safety margins be $M_1 = f_1(X_1, X_2)$ and $M_2 = f_2(X_1, X_2)$, where X_1 and X_2 are independent standard normally distributed random variables. If $F_i = \{M_i \le 0\}$, $i = 1, 2$, then the probability of failure P_{fp} of the parallel system is

$$P_{fp} = P(F_1 \cap F_2). \tag{15.64}$$

An approximation of P_{fp} is obtained by assuming that the safety margins M_1 and M_2 are linearized at their respective design points A_1 and A_2 (see Figure 15.16)

$$M_1 = a_1 X_1 + a_2 X_2 + \beta_1 \tag{15.65}$$

$$M_2 = b_1 X_1 + b_2 X_2 + \beta_2 \tag{15.66}$$

where β_1 and β_2 are the corresponding reliability indices when $\bar{a} = (a_1, a_2)$ and $\bar{b} = (b_1, b_2)$ are chosen as unit vectors. Then an approximation of P_{fp} is

$$\begin{aligned} P_{fp} &\approx P\left(\left\{\bar{a}^T \bar{X} + \beta_1 \le 0\right\} \cap \left\{\bar{b}^T \bar{X} + \beta_2 \le 0\right\}\right) \\ &= P\left(\left\{\bar{a}^T \bar{X} \le -\beta_1\right\} \cap \left\{\bar{b}^T \bar{X} \le -\beta_2\right\}\right) = \Phi_2(-\beta_1, -\beta_2; \rho) \end{aligned} \tag{15.67}$$

Copyright 2005 by CRC Press LLC

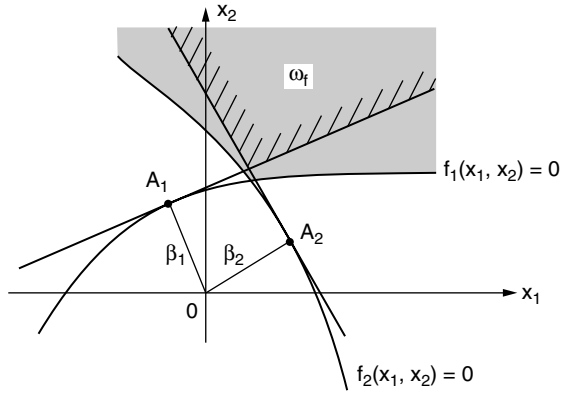

FIGURE 15.16 Illustration of parallel system with two failure elements.

where $\overline{X} = (X_1, X_2)$ and where ρ is the correlation coefficient given by $\rho = \overline{a}^T \overline{b} = a_1 b_1 + a_2 b_2$. Φ_2 is the bivariate normal distribution function defined by Equation 15.32. A formal reliability index β_p for the parallel system can then be defined by

$$\beta_p = -\Phi^{-1}(P_{fp}) \approx -\Phi^{-1}(\Phi_2(-\beta_1, -\beta_2; \rho)). \tag{15.68}$$

Equation 15.67, which gives an approximate value for the probability of failure of a parallel system with two failure elements, will be generalized in Section 15.4.2 to the general case where the parallel system has n failure elements and where the number of basic variables is k.

15.4.2 Assessment of the Probability of Failure of Parallel Systems

Consider a parallel system with n elements as shown in Figure 15.17 and let the safety margin for element i be given by

$$M_i = g_i(\overline{X}), \quad i = 1, \ldots, n \tag{15.69}$$

where $X = (X_1, \ldots, X_k)$ are basic variables and where g_i, $i = 1, 2, \ldots, n$ are nonlinear functions.

The probability of failure P_{fi} of *element i* can then be estimated in the similar way as shown on page 15-12. An approximation of the probability of failure P_{fp} of the parallel system in Figure 15.17 can then be obtained by using the same transformation as for the single elements and by linearization of

$$h_i(\overline{Z}) = g_i(\overline{T}^{-1}(\overline{Z})), \quad i = 1, \ldots, n \tag{15.70}$$

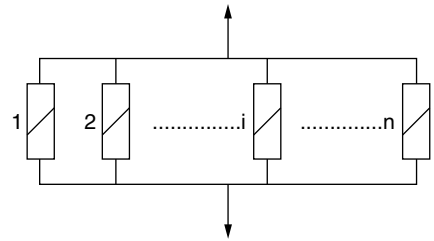

FIGURE 15.17 Parallel system with n elements.

Copyright 2005 by CRC Press LLC

at the design points for each element. Then (see, e.g., Hohenbichler and Rackwitz [6])

$$\begin{aligned} P_{fp} &= P\left(\bigcap_{i=1}^{n}\{M_i \le 0\}\right) = P\left(\bigcap_{i=1}^{n}\{g_i(\overline{X}) \le 0\}\right) = P\left(\bigcap_{i=1}^{n}\{g_i(\overline{T}^{-1}(\overline{Z})) \le 0\}\right) \\ &= P\left(\bigcap_{i=1}^{n}\{h_i(\overline{Z}) \le 0\}\right) \approx P\left(\bigcap_{i=1}^{n}\left\{\overline{\alpha}_i^T \overline{Z} + \beta_i \le 0\right\}\right) = P\left(\bigcap_{i=1}^{n}\left\{\overline{\alpha}_i^T \overline{Z} \le -\beta_i\right\}\right) \\ &= \Phi_n(-\overline{\beta}; \overline{\overline{\rho}}) \end{aligned} \tag{15.71}$$

where $\overline{\beta} = (\beta_1, \ldots, \beta_n)$, and where $\overline{\overline{\rho}} = [\rho_{if}]$ is the correlation matrix for the linearized safety margins; that is, $\rho_{ij} = \overline{\alpha}_i^T \overline{\alpha}_j$. Φ_n is the n-dimensional standardized normal distribution function.

From Equation 15.71, the calculation of the probability of failure of a parallel system with linear and normally distributed safety margins is reduced to calculation of a value of Φ_n.

15.4.3 Reliability Bounds for Parallel Systems

In general, numerical calculation of the multi-normal distribution function Φ_n is very time consuming. Therefore, approximate techniques or bounding techniques must be used.

Simple bounds for the probability of failure P_{fp} analogous to the simple bounds for series systems Equation 15.44 can easily be derived for parallel systems. Consider a parallel system P with n failure elements $E_1, \ldots, E_n$. For each failure element E_i, $i = 1, \ldots, n$, a Boolean variable e_i is defined by (see Equation 15.8)

$$e_i = \begin{cases} 1 & \text{if the failure element is in a nonfailure state} \\ 0 & \text{if the failure element is in a failure state.} \end{cases} \tag{15.72}$$

Then the probability of failure P_{fp} of the parallel system is

$$\begin{aligned} P_{fp} &= P\left(\bigcap_{i=1}^{n} e_i = 0\right) = P(e_i = 0)\frac{P(e_1 = 0 \cap e_2 = 0)}{P(e_1 = 0)} \cdots \frac{P(e_1 = 0 \cap \ldots \cap e_n = 0)}{P(e_1 = 0 \cap \ldots \cap e_{n-1} = 0)} \\ &\ge \prod_{i=1}^{n} P(e_i = 0) \end{aligned} \tag{15.73}$$

if

$$P(e_1 = 0 \cap e_2 = 0) \ge P(e_1 = 0)P(e_2 = 0) \tag{15.74}$$

etc., or in general,

$$P\left(\bigcap_{j=1}^{i+1} e_j = 1\right) \ge P\left(\bigcap_{j=1}^{i} e_j = 1\right)P(e_{i+1} = 1) \tag{15.75}$$

for all $1 \le i \le n-1$. A simple upper bound is clearly the maximum probability of failure of the minimum probability of failure of any failure element E_i, $i = 1, \ldots, n$. Therefore, the following simple bounds exist when Equation 15.75 is satisfied:

$$\prod_{i=1}^{n} P(e_i = 0) \le P_{fp} \le \min_{i=1}^{n} P(e_i = 0). \tag{15.76}$$

Copyright 2005 by CRC Press LLC

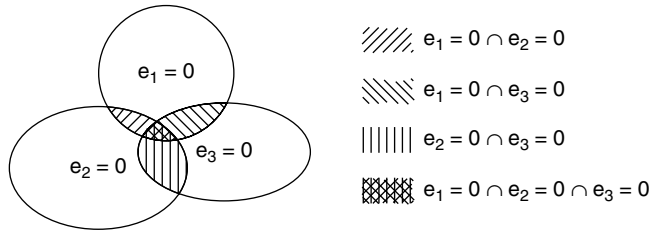

FIGURE 15.18 Derivation of Murotsu's upper bound.

The lower bound in Equation 15.76 is equal to the exact value of P_{fp} if there is no dependence between any pair of elements ($\rho_{ij} = 0, i \neq j$), and the upper bound in Equation 15.76 corresponds to full dependence between all elements ($\rho_{ij} = 1$ for all i and j).

The simple bounds in Equation 15.76 will in most cases be so wide that they are of very little use. A better upper bound of P_{fp} has been suggested by Murotsu et al. [12].

$$P_{fp} \leq \min_{i.j=1}^{n} [P(e_i = 0) \bigcap P(e_j = 0)]. \tag{15.77}$$

The derivation of Equation 15.77 is very simple. For the case $n = 3$, Equation 15.77 is illustrated in Figure 15.18.

–⌴–

Example 15.8

Consider a parallel system with the reliability indices $\overline{\beta} = (3.57, 3.41, 4.24, 5.48)$ and the correlation matrix:

$$\overline{\overline{\rho}} = \begin{bmatrix} 1.00 & 0.62 & 0.91 & 0.62 \\ 0.62 & 1.00 & 0.58 & 0.58 \\ 0.91 & 0.58 & 1.00 & 0.55 \\ 0.62 & 0.58 & 0.55 & 1.00 \end{bmatrix}.$$

Further, assume that the safety margins for the four elements are linear and normally distributed. The probability of failure of the parallel system then is $P_{fp} = \Phi_4(-3.57, -3.41, -4.24, -5,48; \overline{\overline{\rho}})$.

The simple bounds in Equation 15.76 are

$$(1.79 \times 10^{-4}) \times (3.24 \times 10^{-4}) \times (0.11 \times 10^{-4}) \times (0.21 \times 10^{-7}) \leq P_{fp} \leq 0.21 \times 10^{-7}$$

or $0 \leq P_{fp} \leq 0.21 \times 10^{-7}$. The corresponding bounds of the formal reliability index β_p are $5.48 \leq \beta_p \leq \infty$. With the ordering of the four elements shown above, the probabilities of the intersections of e_1 and e_2 can be shown as

$$[P(e_i = 0 \bigcap e_j = 0)] = \begin{bmatrix} - & 1.71 \times 10^{-5} & 9.60 \times 10^{-6} & 9.93 \times 10^{-9} \\ 1.71 \times 10^{-5} & - & 1.76 \times 10^{-6} & 9.27 \times 10^{-9} \\ 9.60 \times 10^{-6} & 1.76 \times 10^{-6} & - & 1.90 \times 10^{-9} \\ 9.93 \times 10^{-9} & 9.27 \times 10^{-9} & 1.90 \times 10^{-9} & - \end{bmatrix}.$$

Copyright 2005 by CRC Press LLC

Therefore, from Equation 15.77: $\beta_P \geq -\Phi^{-1}(1.90 \times 10^{-9}) = 5.89$.

–␣–

15.4.4 Equivalent Linear Safety Margins for Parallel Systems

In Section 15.4.2 it was shown how the probability of failure of a parallel system can be evaluated in a simple way when the safety margin for each failure element is *linear* and normally distributed. Consider a parallel system with n such failure elements. Then, the probability of failure P_{fp} of the parallel system is (see Equation 15.71):

$$P_{fp} = \Phi_n(-\overline{\beta}; \overline{\overline{\rho}}) \tag{15.78}$$

where $\overline{\beta} = (\beta_1, \ldots, \beta_n)$ is a vector whose components are the reliability indices of the failure elements, and where $\overline{\overline{\rho}}$ is the correlation matrix for the *linear* and normally distributed safety margins of the failure elements.

When the reliability of a structural system is modeled by a series system of parallel systems (failure modes), the reliability is evaluated by the following steps:

- Evaluate the probability of failure of each parallel system by Equation 15.78.
- Evaluate the correlation between the parallel systems.
- Evaluate the probability of failure of the series system by Equation 15.39.

Evaluation of the correlation between a pair of parallel systems can easily be performed if the safety margins for the parallel systems are linear. However, in general, this will clearly not be the case. It is therefore natural to investigate the possibility of introducing an *equivalent linear safety margin* for each parallel system. In this section, an equivalent linear safety margin suggested by Gollwitzer and Rackwitz [13] is described.

Consider a parallel system with n elements as shown in Figure 15.17 and let the safety margin for element i, $i = 1, 2, \ldots, n$ be linear

$$M_i = \alpha_i Z_1 + \ldots + \alpha_{ik} Z_k + \beta_i = \sum_{j=1}^{k} \alpha_{ij} Z_j + \beta_i \tag{15.79}$$

where the basic variables Z_i, $i = 1, \ldots, k$ are independent standard normally distributed variables where $\overline{\alpha}_i = (\alpha_{i1}, \ldots, \alpha_{ik})$ is a unit vector, and where β_i is the Hasofer-Lind reliability index. A formal (generalized) reliability index β_P for the parallel system is then given by

$$\beta_P = -\Phi^{-1}(\Phi_n(-\overline{\beta}; \overline{\overline{\rho}})) \tag{15.80}$$

where $\overline{\beta} = (\beta_1, \ldots, \beta_n)$ and $\overline{\overline{\rho}} = [\rho_{ij}] = \left[\overline{\alpha}_i^T \overline{\alpha}_j\right]$.

The equivalent linear safety margin M^e is then defined in such a way that the corresponding reliability index β^e is equal to β_P and so that it has the same sensitivity as the parallel system against changes in the basic variables Z_i, $i = 1, 2, \ldots, k$.

Let the vector $\overline{Z}$ of basic variables be increased by a (small) vector $\overline{\varepsilon} = (\varepsilon_1, \ldots, \varepsilon_k)$. Then the corresponding reliability index $\beta_P(\overline{\varepsilon})$ for the parallel system is

$$\begin{aligned} \beta_P(\overline{\varepsilon}) &= -\Phi^{-1}\left(P\left(\bigcap_{i=1}^{n} \left\{ \sum_{j=1}^{k} \alpha_{ij}(Z_j + \varepsilon_j) + \beta_i \leq 0 \right\} \right) \right) \\ &= -\Phi^{-1}(\Phi_n(-\overline{\beta} - \overline{\overline{\alpha}}\,\overline{\varepsilon}; \overline{\overline{\rho}})) \end{aligned} \tag{15.81}$$

where $\overline{\overline{\alpha}} = [\alpha_{ij}]$.

Copyright 2005 by CRC Press LLC

Let the equivalent linear safety margin M^e be given by

$$M^e = \alpha_1^e Z_1 + \ldots + \alpha_k^e Z_k + \beta^e = \sum_{j=1}^{k} \alpha_j^e Z_j + \beta^e \tag{15.82}$$

where $\bar{\alpha}^e = (\alpha_1^e, \ldots, \alpha_k^e)$ is a unit vector and where $\beta^e = \beta_P$. With the same increase $\bar{\varepsilon}$ of the basic variables, the reliability index $\beta^e(\bar{\varepsilon})$ is

$$\beta_P(\bar{\varepsilon}) = -\Phi^{-1}(\Phi(-\beta^e - \bar{\alpha}^{eT}\bar{\varepsilon})) = \beta^e + \alpha_1^e \varepsilon_1 + \ldots + \alpha_k^e \varepsilon_k. \tag{15.83}$$

It is seen from Equation 15.83 and by putting $\beta_P(\bar{0}) = \beta^e(\bar{0})$ that

$$\alpha_i^e = \frac{\left.\dfrac{\partial \beta_P}{\partial \varepsilon_i}\right|_{\bar{\varepsilon}=\bar{0}}}{\sqrt{\displaystyle\sum_{j=1}^{n} \left(\left.\dfrac{\partial \beta_P}{\partial \varepsilon_i}\right|_{\bar{\varepsilon}=\bar{0}} \right)^2}}, \quad i = 1, \ldots, k. \tag{15.84}$$

An approximate value of α_i^e, $i = 1, \ldots, k$ can easily be obtained by numerical differentiation as shown in Example 15.9.

–⌴–

Example 15.9

Consider a parallel system with two failure elements and let the safety margin for the failure elements be

$$M_1 = 0.8\,Z_1 - 0.6\,Z_2 + 3.0 \quad \text{and} \quad M_2 = 0.1\,Z_1 - 0.995\,Z_2 + 3.5$$

where Z_1 and Z_2 are independent standard normally distributed variables. The correlation ρ between the safety margins is

$$\rho = 0.8 \times 0.1 + 0.6 \times 0.9950 = 0.68.$$

Then, the reliability index β_P of the parallel system is

$$\beta_P = -\Phi^{-1}(\Phi_2(-3.0, -3.5; 0.68)) = 3.83.$$

To obtain the equivalent linear safety margin, Z_1 and Z_2 are in turn given an increment $\varepsilon_i = 0.1$, $i = 1, 2$. With $\bar{\varepsilon} = (0.1, 0)$, one gets

$$-\bar{\beta} - \bar{\bar{\alpha}}\bar{\varepsilon} = \begin{bmatrix} -3.0 \\ -3.5 \end{bmatrix} - \begin{bmatrix} 0.8 & -0.6 \\ 0.1 & -0.995 \end{bmatrix} \begin{bmatrix} 0.1 \\ 0 \end{bmatrix} = \begin{bmatrix} -3.08 \\ -3.51 \end{bmatrix}$$

and by Equation 15.81 $\beta_P = -\Phi^{-1}(\Phi_2(-3.08, -3.51; 0.68)) = 3.87$.

Therefore,

$$\left.\frac{\partial \beta_P}{\partial \varepsilon_1}\right|_{\bar{\varepsilon}=\bar{0}} \approx \frac{3.87 - 3.83}{0.1} = 0.40.$$

Copyright 2005 by CRC Press LLC

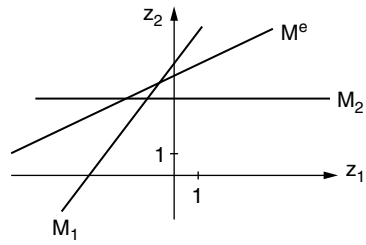

FIGURE 15.19 Safety margins.

Likewise with $\bar{\varepsilon} = (0, 0.1)$,

$$P_{fp} = \int_{-\infty}^{\infty} \varphi(t) \left[\Phi\left(\frac{-\beta_e - \sqrt{\rho t}}{\sqrt{1-\rho}} \right) \right]^n dt$$

and $\beta_P(\bar{\varepsilon}) = -\Phi^{-1}(\Phi_2(-2.94, -3.40; 0.68)) = 3.74$.

Therefore,

$$\left. \frac{\partial \beta_P}{\partial \varepsilon_2} \right|_{\bar{\varepsilon}=\bar{0}} \approx \frac{3.74 - 3.83}{0.1} = -0.90.$$

By normalizing $\bar{\alpha}^e = (\alpha_1^e, \alpha_2^e) = (0.4061, -0.9138)$ and the equivalent safety margin is

$$M^e = 0.4061\, Z_1 - 0.9138\, Z_2 + 3.83.$$

The safety margins M_1, M_2, and M^e are shown in Figure 15.19.

–⌴–

15.4.5 Parallel Systems with Equally Correlated Elements

It was shown in Section 15.4.2 that the probability of failure P_{fp} of a parallel system with n failure elements is equal to $P_{fp} \approx \Phi_n(-\bar{\beta}; \bar{\bar{\rho}})$ when the safety margins are linear and normally distributed.

Dunnett and Sobel [9] have shown for the special case where the failure elements are equally correlated with the correlation coefficient ρ; that is,

$$\bar{\bar{\rho}} = \begin{bmatrix} 1 & \rho & \cdots & \rho \\ \rho & 1 & \cdots & \rho \\ \vdots & \vdots & \ddots & \vdots \\ \rho & \rho & \cdots & 1 \end{bmatrix} \tag{15.85}$$

that (see Equation 15.51)

$$\Phi_n(\bar{x}: \bar{\bar{\rho}}) = \int_{-\infty}^{\infty} \varphi(t) \prod_{i=1}^{n} \Phi\left(\frac{x_i - \sqrt{\rho t}}{\sqrt{1-\rho}} \right) dt. \tag{15.86}$$

If all failure elements have the same reliability index β_e, then

$$P_{fp} = \int_{-\infty}^{\infty} \varphi(t) \left[\Phi\left(\frac{-\beta_e - \sqrt{\rho t}}{\sqrt{1-\rho}} \right) \right]^n dt. \tag{15.87}$$

Copyright 2005 by CRC Press LLC

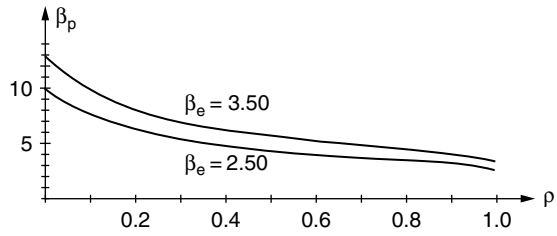

FIGURE 15.20 Safety index of parallel system as a function of correlation coefficient.

A formal reliability index β_P for the parallel system can then be calculated by $\beta_P = -\Phi^{-1}(P_{fp})$.

–⌴–

Example 15.10

Consider a parallel system with $n = 10$ failure elements, and common element reliability index β_e, and common correlation coefficient ρ. The formal reliability index β_P for this parallel system as a function of ρ is illustrated in Figure 15.20 for $\beta_e = 2.50$ and 3.50. Note that, as expected, the reliability index β_P decreases with ρ.

–⌴–

The strength of a *fiber bundle* with n ductile fibers can be modeled by a parallel system as shown in Figure 15.21. The strength R of the fiber bundle is

$$R = \sum_{i=1}^{n} R_i \tag{15.88}$$

where the random variable R_i is the strength of fiber i, $i = 1, 2, \ldots, n$. Let R_i be identically and normally distributed $N(\mu, \sigma)$ with common correlation coefficient ρ. The strength R is then normally distributed $N(\mu_R, \sigma_R)$ where $\mu_R = n\mu$ and $\sigma_R^2 = n\sigma^2 + n(n-1)\rho\sigma^2$.

Assume that the fiber bundle is loaded by a deterministic and time-independent load $S = nS_e$, where S = constant is the load of fiber i, $i = 1, 2, \ldots, n$. The reliability indices of the fibers are the same for all fibers and equal to

$$\beta_e = \frac{\mu - S_e}{\sigma}. \tag{15.89}$$

Therefore, $S = nS_e = n(\mu - \beta_e\sigma)$ and the reliability index β_F for the fiber bundle (the parallel system) is

$$\beta_F = \frac{\mu_R - S}{\sigma_R} = \frac{n\mu - n(\mu - \beta_e\sigma)}{(n\sigma^2 + n(n-1)\sigma^2\rho)^{1/2}} = \beta_e\sqrt{\frac{n}{1+\rho(n-1)}}. \tag{15.90}$$

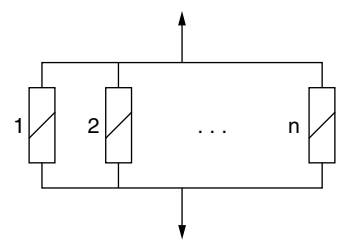

FIGURE 15.21 Modeling of a fiber bundle.

Copyright 2005 by CRC Press LLC

Equation 15.90 has been derived by Grigoriu and Turkstra [14]. In Section 15.4.6 it is shown that Equation 15.90 can easily be modified so that the assumption of the common correlation coefficient ρ can be removed.

15.4.6 Parallel Systems with Unequally Correlated Elements

It was shown earlier that an approximation of the probability of failure of a parallel system with n failure elements with normally distributed safety margins is $P_{fp} \approx \Phi_n(-\overline{\beta}; \overline{\overline{\rho}})$ where $\overline{\beta} = (\beta_1, \ldots, \beta_n)$ is the reliability indices of the failure elements and $\overline{\overline{\rho}} = [\rho_{ij}]$ is the correlation matrix. In Section 15.4.5 it is shown that the reliability index β_F for a *fiber bundle* with n ductile fibers can easily be calculated if the following assumptions are fulfilled:

1. The load S of the fiber bundle is deterministic and constant with time,
2. The strength of the fibers is identically normally distributed $N(\mu, \sigma)$,
3. The fibers have a common reliability index β_e,
4. Common correlation coefficient ρ between the strengths of any pair of fibers. Under these assumptions it was shown that (see Equation 15.90)

$$\beta_F = \beta_e \sqrt{\frac{n}{1+\rho(n-1)}}. \tag{15.91}$$

Now the assumption 4 above will be relaxed. Let the correlation coefficient between fiber i and fiber j be denoted ρ_{ij}. The reliability index β_F for such a fiber bundle with unequally correlated fibers can then be calculated similarly as used in deriving Equation 15.91 in Section 15.4.5 (see Thoft-Christensen and Sørensen [15])

$$\beta_F = \frac{\mu_R - S}{\sigma_R} = \left(n\mu - (n\mu - n\beta_e\sigma)\right)\left(n\sigma^2 + \sigma^2 \sum_{i,j=1,i\neq j}^{n} \rho_{ij}\right)^{-\frac{1}{2}} = \beta_e \sqrt{\frac{n}{1+\overline{\rho}(n-1)}} \tag{15.92}$$

where

$$\overline{\rho} = \frac{1}{n(n-1)} \sum_{i,j=1,i\neq j}^{n} \rho_{ij}. \tag{15.93}$$

By comparing Equation 15.91 and Equation 15.92, it is seen that for systems with unequal correlation coefficients, the reliability index β_{F_p} can be calculated by the simple expression in Equation 15.91 by inserting for ρ the average correlation coefficient $\overline{\rho}$ defined by Equation 15.93. $\overline{\rho}$ is the average of all $\rho_{ij}, i \neq j$.

15.5 Identification of Critical Failure Mechanisms

15.5.1 Introduction

A number of different methods to identify critical failure modes have been suggested (see, e.g., Ferregut-Avila [16], Moses [17], Gorman [18], Ma and Ang [19], Klingmüller [20], Murotsu et al. [21], and Kappler [22]). In this section the β-unzipping method [4], [23]–[25] is used.

The β-unzipping method is a method by which the reliability of structures can be estimated at a number of different levels. The aim has been to develop a method that is at the same time simple to use and reasonably accurate. The β-unzipping method is quite general in the sense that it can be used for

Copyright 2005 by CRC Press LLC

two-dimensional and three-dimensional framed and trussed structures, for structures with ductile or brittle elements, and also in relation to a number of different failure mode definitions.

An estimate of the reliability of a structural system on the basis of failure of a single structural element (namely, the element with the lowest reliability index of all elements) is called system reliability at *level* 0. At level 0, the reliability of a structural system is equal to the reliability of this single element. Therefore, such a reliability analysis is, in fact, not a system reliability analysis, but rather an element reliability analysis. At level 0, each element is considered isolated from the other elements, and the interaction between the elements is not taken into account in estimating the reliability. Let a structure consist of n failure elements (i.e., elements or points where failure can take place) and let the reliability index for failure element i be denoted β_i. Then, at level 0, the system reliability index β_0 is simply given as $\beta_s = \min \beta_i$.

15.5.2 Assessment of System Reliability at Level 1

At *level* 1, the system reliability is defined as the reliability of a series system with n elements — the n failure elements, see Figure 15.1. Therefore, the first step is to calculate β-values for all failure elements and then use Equation 15.39. As mentioned earlier, Equation 15.39 can in general not be used directly. However, upper and lower bounds exist for series systems as shown in Section 15.3.3.

Usually for a structure with n failure elements, the estimate of the probability of failure of the series system with n elements can be calculated with sufficient accuracy by only including some of the failure elements, namely those with the smallest reliability indices. One way of selecting is to include only failure elements with β-values in an interval $[\beta_{\min}, \beta_{\min} + \Delta\beta_1]$, where $\beta_{\min}$ is the smallest reliability index of all failure element indices and where $\Delta\beta_1$ is a prescribed positive number. The failure elements chosen to be included in the system reliability analysis at level 1 are called *critical failure elements.* If two or more critical failure elements are perfectly correlated, then only one of them is included in the series system of critical failure elements.

15.5.3 Assessment of System Reliability at Level 2

At *level* 2, the system reliability is estimated as the reliability of a series system where the elements are parallel systems each with two failure elements (see Figure 15.4) — so-called *critical pairs of failure elements.* Let the structure be modeled by n failure elements and let the number of critical failure elements at level 1 be n_1. Let the critical failure element l have the lowest reliability index β of all critical failure elements. Failure is then assumed in failure element l and the structure is modified by removing the corresponding failure element and adding a pair of so-called fictitious loads F_l (axial forces or moments). If the removed failure element is brittle, no fictitious loads are added. However, if the removed failure element l is ductile, the fictitious load F_l is a stochastic load given by $F_l = \gamma_l R_l$, where R_l is the load-carrying capacity of failure element l and where $0 < \gamma_l \leq 1$.

The modified structure with the loads $P_1, \ldots, P_k$ and the fictitious load F_l (axial force or moment) is then reanalyzed and influence coefficients a_{ij} with respect to $P_1, \ldots, P_k$ and a'_{il} with respect to F_l are calculated. The load effect (force or moment) in the remaining failure elements is then described by a stochastic variable. The load effect in failure element i is called $S_{i|l}$ (load effect in failure element i given failure in failure element l) and

$$S_{i|l} = \sum_{j=1}^{k} a_{ij} P_j + a'_{il} F_l. \tag{15.94}$$

The corresponding safety margin $M_{i|l}$ then is

$$M_{i|l} = \min(R_l^+ - S_{i|l}, R_i^- + S_{i|l}) \tag{15.95}$$

Copyright 2005 by CRC Press LLC

where R_i^+ and R_i^- are the stochastic variables describing the (yield) strength capacity in "tension" and "compression" for failure element *i*. In the following, $M_{i|l}$ will be approximated by either $R_i^+ - S_{i|l}$ or $R_i^+ + S_{i|l}$ depending on the corresponding reliability indices. The reliability index for failure element *i*, given failure in failure element *l*, is

$$\beta_{i/l} = \mu_{M_{i|l}} / \sigma_{M_{i|l}}. \tag{15.96}$$

In this way, new reliability indices are calculated for all failure elements (except the one where failure is assumed) and the smallest β-value is called $\beta_{\min}$. The failure elements with β-values in the interval $[\beta_{\min}, \beta_{\min} + \Delta\beta_2]$, where $\Delta\beta_2$ is a prescribed positive number, are then in turn combined with failure element *l* to form a number of parallel systems.

The next step is then to evaluate the probability of failure for each critical pair of failure elements. Consider a parallel system with failure elements *l* and *r*. During the reliability analysis at level 1, the safety margin M_l for failure element *l* is determined and the safety margin $M_{r|l}$ for failure element *r* has the form in Equation 15.11. From these safety margins, the reliability indices $\beta_1 = \beta_l$ and $\beta_2 = \beta_{r|l}$ and the correlation coefficient $\rho = \rho_{l,r|l}$ can easily be calculated. The probability of failure for the parallel system then is

$$P_f = \Phi_2(-\beta_1, -\beta_2; \rho). \tag{15.97}$$

The same procedure is then, in turn, used for all critical failure elements and further critical pairs of failure elements are identified. In this way, the total series system used in the reliability analysis at level 2 is determined (see Figure 15.4). The next step is then to estimate the probability of failure for each critical pair of failure elements (see Equation 15.97) and also to determine a safety margin for each critical pair of failure elements. When this is done, generalized reliability indices for all parallel systems in Figure 15.4 and correlation coefficients between any pair of parallel systems are calculated. Finally, the probability of failure P_f for the series system (Figure 15.2) is estimated. The so-called equivalent linear safety margin introduced in Section 15.4.4 is used as an approximation for safety margins for the parallel systems.

An important property by the β-unzipping method is the possibility of using the method when brittle failure elements occur in the structure. When failure occurs in a brittle failure element, then the β-unzipping method is used in exactly the same way as presented above, the only difference being that no fictitious loads are introduced. If, for example, brittle failure occurs in a tensile bar in a trussed structure, then the bar is simply removed without adding fictitious tensile loads. Likewise, if brittle failure occurs in bending, then a yield hinge is introduced, but no (yielding) fictitious bending moments are added.

15.5.4 Assessment of System Reliability at Level N > 2

The method presented above can easily be generalized to higher levels $N > 2$. *At level* 3, the estimate of the system reliability is based on so-called *critical triples of failure elements,* that is, a set of three failure elements. The critical triples of failure elements are identified by the β-unzipping method and each triple forms a parallel system with three failure elements. These parallel systems are then elements in a series system (see Figure 15.5). Finally, the estimate of the reliability of the structural system at level 3 is defined as the reliability of this series system.

Assume that the critical pair of failure elements *(l, m)* has the lowest reliability index $\beta_{l,m}$ of all critical pairs of failure elements. Failure is then assumed in the failure elements *l* and *m* adding for each of them a pair of fictitious loads F_l and F_m (axial forces or moments).

The modified structure with the loads $P_1, \ldots, P_k$ and the fictitious loads F_l and F_m are then reanalyzed and influence coefficients with respect to $P_1, \ldots, P_k$ and F_l and F_m are calculated. The load effect in each

Copyright 2005 by CRC Press LLC

of the remaining failure elements is then described by a stochastic variable $S_{i|l,m}$ (load effect in failure element i given failure in failure elements l and m) and

$$S_{i|l,m} = \sum_{j=1}^{k} a_{ij} P_j + a'_{il} F_l + a'_{im} F_m. \tag{15.98}$$

The corresponding safety margin $M_{i|l,m}$ then is

$$M_{i|l,m} = \min(R_i^+ - S_{i|l,m}, R_i^- + S_{i|l,m}) \tag{15.99}$$

where R_i^+ and R_i^- are the stochastic variables describing the load-carrying capacity in "tension" and "compression" for failure element i. In the following, $M_{i|l,m}$ will be approximated by either $R_i^- + S_{i|l,m}$ or $R_i^+ - S_{i|l,m}$ depending on the corresponding reliability indices. The reliability index for failure element i, given failure in failure elements l and m, is then given by

$$\beta_{i|l,m} = \mu_{M_{i|l,m}} / \sigma_{M_{i|l,m}}. \tag{15.100}$$

In this way, new reliability indices are calculated for all failure elements (except l and m) and the smallest β-value is called $\beta_{\min}$. These failure elements with β-values in the interval $[\beta_{\min}\ \beta_{\min} + \Delta\beta_3]$, where $\Delta\beta_3$ is a prescribed positive number, are then in turn combined with failure elements l and m to form a number of parallel systems.

The next step is then to evaluate the probability of failure for each of the critical triples of failure elements. Consider the parallel system with failure elements l, m, and r. During the reliability analysis at level 1, the safety margin M_l for failure element l is determined; and during the reliability analysis at level 2, the safety margin $M_{m|l}$ for the failure element m is determined. The safety margin $M_{r|l,m}$ for safety element r has the form of Equation 15.15. From these safety margins the reliability indices $\beta_1 = \beta_l$, $\beta_2 = \beta_{m|l}$, and $\beta_3 = \beta_{r|l,m}$ and the correlation matrix $\overline{\overline{\rho}}$ can easily be calculated. The probability of failure for the parallel system then is

$$P_f = \Phi_3(-\beta_1, -\beta_2, -\beta_3; \overline{\overline{\rho}}). \tag{15.101}$$

An equivalent safety margin $M_{i,j,k}$ can be determined by the procedure mentioned above. When the equivalent safety margins are determined for all critical triples of failure elements, the correlation between all pairs of safety margins can easily be calculated. The final step is then to arrange all the critical triples as elements in a series system (see Figure 15.5) and estimate the probability of failure P_f and the generalized reliability index β_S for the series system.

The β-unzipping method can be used in exactly the same way as described in the preceding text to estimate the system reliability at levels $N > 3$. However, a definition of failure modes based on a fixed number of failure elements greater than 3 will hardly be of practical interest.

15.5.5 Assessment of System Reliability at Mechanism Level

The application of the β-unzipping method presented above can also be used when failure is defined as formation of a mechanism. However, it is much more efficient to use the β-unzipping method in connection with *fundamental mechanisms*. Experience has shown that such a procedure is less computer time consuming than unzipping based on failure elements.

If unzipping is based on failure elements, then formation of a mechanism can be unveiled by the fact that the corresponding stiffness matrix is singular. Therefore, the unzipping is simply continued until

Copyright 2005 by CRC Press LLC

the determinant of the stiffness matrix is zero. By this procedure, a number of mechanisms with different numbers of failure elements will be identified. The number of failure elements in a mechanism will often be quite high so that several reanalyses of the structure are necessary.

As emphasized above, it is more efficient to use the β-unzipping method in connection with fundamental mechanisms. Consider an elasto-plastic structure and let the number of potential failure elements (e.g., yield hinges) be n. It is then known from the theory of plasticity that the number of fundamental mechanisms is $m = n - r$, where r is the degree of redundancy. All other mechanisms can then be formed by linear combinations of the fundamental mechanisms. Some of the fundamental mechanisms are so-called joint mechanisms. They are important in the formation of new mechanisms by linear combinations of fundamental mechanisms, but they are not real failure mechanisms. Real failure mechanisms are, by definition, mechanisms that are not joint mechanisms.

Let the number of loads be k. The safety margin for fundamental mechanism i can then be written

$$M_i = \sum_{j=1}^{n} |a_{ij}| R_j - \sum_{j=1}^{k} b_{ij} P_j \tag{15.102}$$

where a_{ij} and b_{ij} are the influence coefficients. R_j is the yield strength of failure element j and P_j is load number j. a_{ij} is the rotation of yield hinge j corresponding to the yield mechanism i, and b_{ij} is the corresponding displacement of load j. The numerical value of a_{ij} is used in the first summation at the right-hand side of Equation 15.102 to make sure that all terms in this summation are nonnegative.

The total number of mechanisms for a structure is usually too high to include all possible mechanisms in the estimate of the system reliability. It is also unnecessary to include all mechanisms because the majority of them will in general have a relatively small probability of occurrence. Only the most critical or most significant failure modes should be included. The problem is then how the most significant mechanisms (failure modes) can be identified. In this section, it is shown how the β-unzipping method can be used for this purpose. It is not possible to prove that the β-unzipping method identifies all significant mechanisms, but experience with structures where all mechanisms can be taken into account seems to confirm that the β-unzipping method gives reasonably good results. Note that because some mechanisms are excluded, the estimate of the probability of failure by the β-unzipping method is a lower bound for the correct probability of failure. The corresponding generalized reliability index determined by the β-unzipping method is therefore an upper bound of the correct generalized reliability index. However, the difference between these two indices is usually negligible.

The first step is to identify all fundamental mechanisms and calculate the corresponding reliability indices. Fundamental mechanisms can be automatically generated by a method suggested by Watwood [26]; but when the structure is not too complicated, the fundamental mechanisms can be identified manually.

The next step is then to select a number of fundamental mechanisms as starting points for the unzipping. By the β-unzipping method this is done on the basis of the reliability index $\beta_{\min}$ for the real fundamental mechanism that has the smallest reliability index and on the basis of a preselected constant ε_1 (e.g., $\varepsilon_1 = 0.50$). Only real fundamental mechanisms with β-indices in the interval $[\beta_{\min}; \beta_{\min} + \varepsilon_1]$ are used as starting mechanisms in the β-unzipping method. Let $\beta_1 \le \beta_2 \le \ldots \beta_f$ be an ordered set of reliability indices for f real fundamental mechanisms 1, 2, … , f, selected by this simple procedure. The f fundamental mechanisms selected as described above are now in turn combined linearly with all m (real and joint) mechanisms to form new mechanisms. First, the fundamental mechanism l is combined with the fundamental mechanisms 2, 3, … , m and reliability indices ($\beta_{1,2}, \ldots, \beta_{1,m}$) for the new mechanisms are calculated. The smallest reliability index is determined, and the new mechanisms with reliability indices within a distance ε_2 from the smallest reliability index are selected for further investigation. The same procedure is then used on the basis of the fundamental mechanisms 2, ... , f and a failure tree like the one shown in Figure 15.22 is constructed. Let the safety

Copyright 2005 by CRC Press LLC

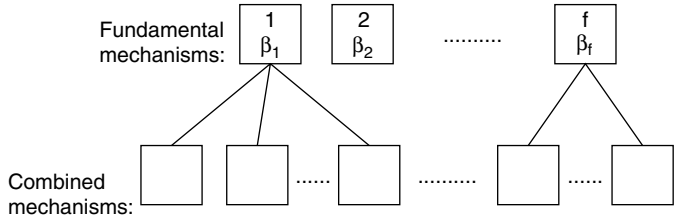

FIGURE 15.22 Construction of new mechanisms.

margins M_i and M_j of two fundamental mechanisms i and j combined as described above (see Equation 15.102) be

$$M_i = \sum_{r=1}^{n} |a_{ir}| R_r - \sum_{s=1}^{k} b_{is} P_s \tag{15.103}$$

$$M_j = \sum_{r=1}^{n} |a_{jr}| R_r - \sum_{s=1}^{k} b_{js} P_s. \tag{15.104}$$

The combined mechanism $i \pm j$ then has the safety margin

$$M_{i\pm j} = \sum_{r=1}^{n} |a_{ir} \pm a_{jr}| R_r - \sum_{s=1}^{k} (b_{is} \pm b_{js}) P_s \tag{15.105}$$

where + or − is chosen dependent on which sign will result in the smallest reliability index. From the linear safety margin Equation 15.105, the reliability index $\beta_{i\pm j}$ for the combined mechanism can easily be calculated.

More mechanisms can be identified on the basis of the combined mechanisms in the second row of the failure tree in Figure 15.22 by adding or subtracting fundamental mechanisms. Note that in some cases it is necessary to improve the technique by modifying Equation 15.105, namely when a new mechanism requires not only a combination with $1 \times$ but a combination with $k \times$ a new fundamental mechanism. The modified version is

$$M_{i\pm+k} = \sum_{r=1}^{n} |a_{ir} \pm k a_{jr}| R_r - \sum_{s=1}^{k} (b_{is} \pm k b_{js}) P_s \tag{15.106}$$

where k is chosen equal to, for example, −1, +1, −2, +2, −3 or +3, depending on which value of k will result in the smallest reliability index. From Equation 15.106 it is easy to calculate the reliability index $\beta_{i\pm+k}$ for the combined mechanism $i + kj$.

By repeating this simple procedure, the failure tree for the structure in question can be constructed. The maximum number of rows in the failure tree must be chosen and can typically be $m + 2$, where m is the number of fundamental mechanisms. A satisfactory estimate of the system reliability index can usually be obtained by using the same ε_2-value for all rows in the failure tree.

During the identification of new mechanisms, it will often occur that a mechanism already identified will turn up again. If this is the case, then the corresponding branch of the failure tree is terminated just one step earlier, so that the same mechanism does not occur more than once in the failure tree.

Copyright 2005 by CRC Press LLC

The final step in the application of the β-unzipping method in evaluating the reliability of an elasto-plastic structure at mechanism level is to select the significant mechanisms from the mechanisms identified in the failure tree. This selection can, in accordance with the selection criteria used in making the failure tree, for example, be made by first identifying the smallest β-value $\beta_{\min}$ of all mechanisms in the failure tree and then selecting a constant ε_3. The significant mechanisms are then, by definition, those with β-values in the interval $[\beta_{\min}; \beta_{\min} + \varepsilon_3]$. The probability of failure of the structure is then estimated by modeling the structural system as a series system with the significant mechanisms as elements (see Figure 15.6).

15.5.6 Examples

15.5.6.1 Two-Story Braced Frame with Ductile Elements

Consider the two-story braced frame in Figure 15.23. The geometry and the loading are shown in the figure. This example is taken from [27] where all detailed calculations are shown. The area A and the moment of inertia I for each structural member are shown in the figure. In the same figure, the expected values of the yield moment M and the tensile strength capacity R for all structural members are also stated. The compression strength capacity of one structural member is assumed to be one half of the tensile strength capacity. The expected values of the loading are $E[P_1] = 100$ kN and $E[P_2] = 350$ kN. For the sake of simplicity, the coefficient of variation for any load or strength is assumed to be $V[\cdot] = 0.1$. All elements are assumed to be perfectly ductile and made of a material having the same modulus of elasticity $E = 0.21 \times 10^9$ kN/m^2.

The failure elements are shown in Figure 15.23. $\times$ indicates a potential yield hinge and | indicates failure in tension/compression. The total number of failure elements is 22, namely $2 \times 6 = 12$ yield hinges in six beams and ten tension/compression possibilities of failure in the ten structural elements. The following pairs of failure elements — (1, 3), (4, 6), (7, 9), (10, 12), (13, 15), and (18, 20) — are assumed fully correlated. All other pairs of failure elements are uncorrelated. Further, the loads P_1 and P_2 are uncorrelated.

The β-values for all failure elements are shown in Table 15.1. Failure element 14 has the lowest reliability index $\beta_{14} = 1.80$ of all failure elements. Therefore, at level 0, the system reliability index is $\beta_S^0 = 1.80$.

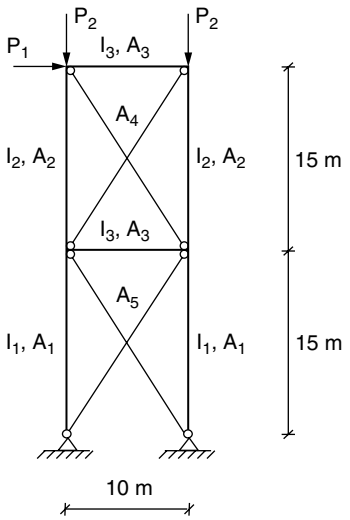

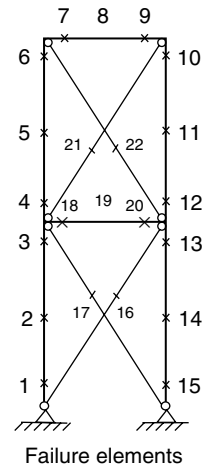

	$A \times 10^3$ m^2	$I \times 10^6$ m^4	$E(M) \times$ kNm	$E(R) \times$ kN
1	4.59	57.9	135	1239
2	2.97	29.4	76	802
3	4.59	4.25	9.8	1239
4	2.6	0	0	702
5	2.8	0	9	756

FIGURE 15.23 Two-story braced frame.

Copyright 2005 by CRC Press LLC

TABLE 15.1 Reliability Indices at Level 0 (and Level 1)

Failure element	2	3	4	5	6	7	8	9	10	11
β-value	8.13	9.96	9.92	4.97	9.98	9.84	9.79	9.86	9.89	1.81
Failure element	12	13	14	16	17	18	19	20	21	22
β-value	9.94	9.97	1.80	9.16	4.67	9.91	8.91	9.91	8.04	3.34

Let $\Delta\beta_1 = 0$. It then follows from Table 15.1 that the critical failure elements are 14, 11, 22, and 17. The corresponding correlation matrix (between the safety margins in the same order) is

$$\bar{\bar{\rho}} = \begin{bmatrix} 1.00 & 0.24 & 0.20 & 0.17 \\ 0.24 & 1.00 & 0.21 & 0.16 \\ 0.20 & 0.21 & 1.00 & 0.14 \\ 0.17 & 0.16 & 0.14 & 1.00 \end{bmatrix}. \tag{15.107}$$

The Ditlevsen bounds for the system probability of failure P_f^1 (see Figure 15.24) are

$$0.06843 \le P_f^1 \le 0.06849.$$

Therefore, a (good) estimate for the system reliability index at level 1 is $\beta_S^1 = 1.49$. It follows from Equation 15.107 that the coefficients of correlation are rather small. Therefore, the simple upper bound in Equation 15.44 can be expected to give a good approximation. One gets $\beta_S^1 = 1.48$. A third estimate can be obtained by Equation 15.54 and Equation 15.57. The result is $\beta_S^1 = 1.49$.

At level 2, it is initially assumed that the ductile failure element 14 fails (in compression) and a fictitious load equal to $0.5 \times R_{14}$ is added (see Figure 15.25). This modified structure is then analyzed elastically

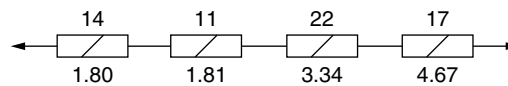

FIGURE 15.24 Series system used in estimating the system reliability at level 1.

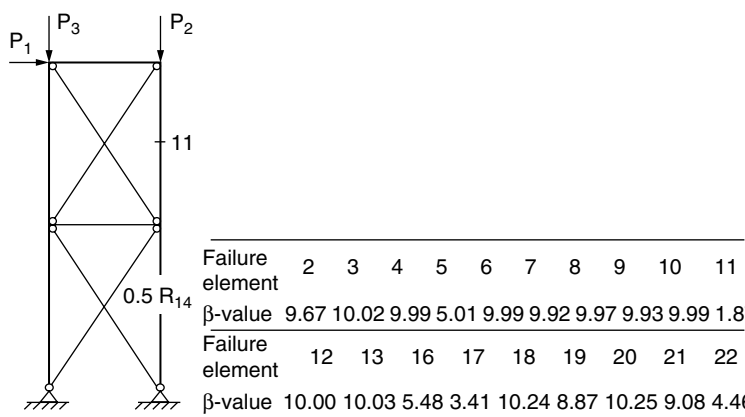

FIGURE 15.25 Modified structure when failure takes place in failure element 14.

Copyright 2005 by CRC Press LLC

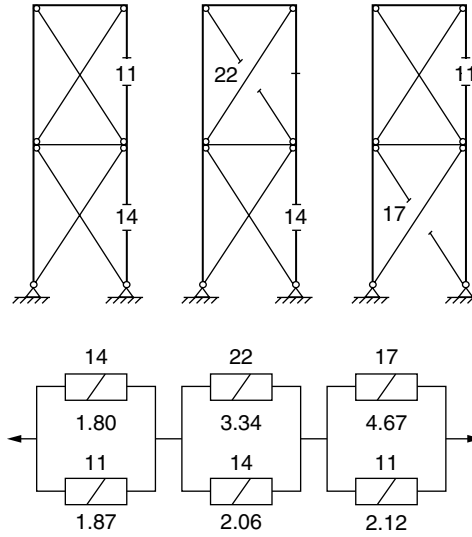

FIGURE 15.26 Failure modes used to estimate the reliability at level 2.

and new reliability indices are calculated for all the remaining failure elements (see Figure 15.25). Failure element 11 has the lowest β-value, 1.87. With $\Delta\beta_2 = 1.00$, failure element 11 is the only failure element with a β-value in the interval $[1.87, 1.87 + \Delta\beta_2]$. Therefore, in this case only one critical pair of failure elements is obtained by initiating the unzipping with failure element 14.

Based on the safety margin M_{14} for failure element 14 and the safety margin $M_{11,14}$ for failure element 11, given failure in failure element 14, the correlation coefficient can be calculated as $\rho = 0.28$. Therefore, the probability of failure for this parallel system is $P_f = \Phi_2(-1.80, -1.87; 0.28) = 0.00347$, and the corresponding generalized index $\beta_{14,11} = 2.70$. The same procedure can be performed with the three other critical failure elements 11, 22, and 17. The corresponding failure modes are shown in Figure 15.26.

Generalized reliability indices and approximate equivalent safety margins for each parallel system in Figure 15.26 are calculated. Then the correlation matrix $\overline{\overline{\rho}}$ can be calculated

$$\overline{\overline{\rho}} = \begin{bmatrix} 1.00 & 0.56 & 0.45 \\ 0.56 & 1.00 & 0.26 \\ 0.45 & 0.26 & 1.00 \end{bmatrix}.$$

The Ditlevsen bounds for the probability of failure of the series system in Figure 15.26 are $0.3488\times10^{-2} \le P_f^2 \le 0.3488\times10^{-2}$. Therefore, an estimate of the system reliability at level 2 is $\beta_S^2 = 2.70$. At level 3 (with $\Delta\beta_3 = 1.00$), four critical triples of failure elements are identified (see Figure 15.27) and an estimate of the system reliability at level 3 is $\beta_S^3 = 3.30$. It is of interest to note that the estimates of the system reliability index at levels 1, 2, and 3 are very different: $\beta_S^1 = 1.49$, $\beta_S^2 = 2.70$, and $\beta_S^3 = 3.30$.

15.5.6.2 Two-Story Braced Frame with Ductile and Brittle Elements

Consider the same structure as in Section 15.5.5.1, but now the failure elements 2, 5, 11, and 14 are assumed brittle. All other data remains unchanged. By a linear elastic analysis, the same reliability indices for all (brittle and ductile) failure elements as in Table 15.1 are calculated. Therefore, the critical failure elements are 14 and 11, and the estimate of the system reliability at level 1 is unchanged, (i.e., $\beta_S^1 = 1.49$).

The next step is to assume brittle failure in failure element 14 and remove the corresponding part of the structure without adding fictitious loads (see Figure 15.28, left). The modified structure is then linear

Copyright 2005 by CRC Press LLC

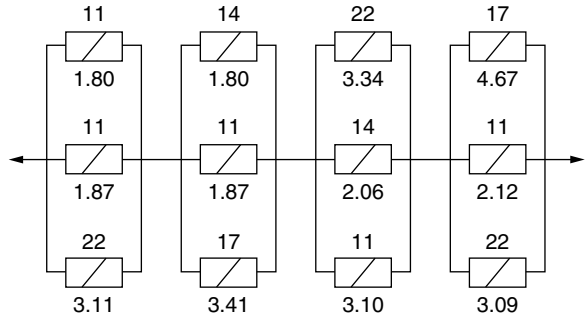

FIGURE 15.27 Reliability modeling at level 3 of the two-story braced frame.

elastically analyzed and reliability indices are calculated for all remaining failure elements. Failure element 17 now has the lowest reliability index, namely the negative value $\beta_{17|14} = -6.01$. This very low negative value indicates that failure takes place in failure element 17 instantly after failure in failure element 14. The failure mode identified in this way is a mechanism and it is the only one when $\Delta\beta_2 = 1.00$. It can be mentioned that $\beta_{16|14} = -3.74$ so that failure element 16 also fails instantly after failure element 14.

Again, by assuming brittle failure in failure element 11 (see Figure 15.28, right), only one critical pair of failure elements is identified, namely the pair of failure elements 11 and 22, where $\beta_{22|11} = -4.33$. This failure mode is not a mechanism. The series system used in calculating an estimate of the system reliability at level 2 is shown in Figure 15.29. Due to the small reliability indices, the strength variables 17 and 22 do not significantly affect the safety margins for the two parallel systems in Figure 15.29 significantly. Therefore, the reliability index at level 2 is unchanged from level 1, namely $\beta_S^2 = 1.49$.

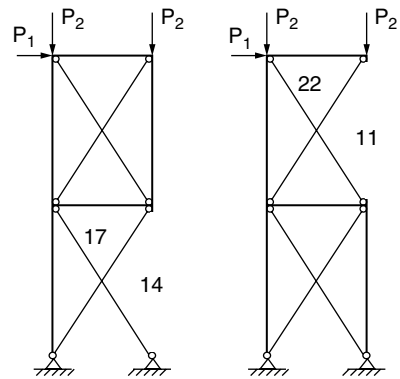

FIGURE 15.28 Modified structures.

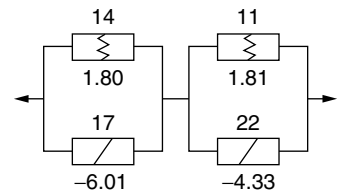

FIGURE 15.29 Modeling at level 2.

Copyright 2005 by CRC Press LLC

As expected, this value is much lower than the value 2.70 (see Section 15.5.5.1) calculated for the structure with only ductile failure elements. This fact stresses the importance of the reliability modeling of the structure.

It is of interest to note that the β-unzipping method was capable of disclosing that the structure cannot survive failure in failure element 14. Therefore, when brittle failure occurs, it is often reasonable to define failure of the structure as failure of just one failure element. This is equivalent to estimating the reliability of the structure at level 1.

15.5.6.3 Elastic-Plastic Framed Structure

In this example, it is shown how the system reliability at mechanism level can be estimated in an efficient way. Consider the simple framed structure in Figure 15.30 with corresponding expected values and coefficients of variation for the basic variables.

The load variables are P_i, $i = 1, \ldots, 4$ and the yield moments are R, $i = 1, \ldots, 19$. Yield moments in the same line are considered fully correlated and the yield moments in different lines are mutually independent. The number of potential yield hinges is $n = 19$ and the degree of redundancy is $r = 9$. Therefore, the number of fundamental mechanisms is $n - r = 10$.

One possible set of fundamental mechanisms is shown in Figure 15.31. The safety margins M_i for the fundamental mechanisms can be written

$$M_i = \sum_{j=1}^{19} |a_{ij}| R_j - \sum_{i=1}^{4} b_{ij} P_j, \qquad i = 1, \ldots, 10 \tag{15.108}$$

where the influence coefficients a_{ij} and b_{ij} are determined by considering the mechanisms in the deformed state.

The reliability indices β_i, $i = 1, \ldots, 10$ for the ten fundamental mechanisms can be calculated from the safety margins, taking into account the correlation between the yield moments. The result is shown in Table 15.2.

With $\varepsilon_1 = 0.50$, the fundamental mechanisms 1, 2, 3, and 4 are selected as starting mechanisms in the β-unzipping and combined, in turn, with the remaining fundamental mechanisms. As an example, consider the combination 1 + 6 of mechanisms 1 and 6. The linear safety margin M_{1+6} is obtained from the linear safety margins M_1 and M_6 by addition, taking into account the signs of the coefficients. The corresponding reliability index is $\beta_{1+6} = 3.74$.

With $\varepsilon_2 = 1.20$, the following new mechanisms 1 + 6, 1 + 10, 2 + 6, 3 + 7, and 4 − 10 are identified by this procedure. The failure tree at this stage is shown in Figure 15.16. It contains 4 + 5 = 9 mechanisms. The reliability indices and the fundamental mechanisms involved are shown in the same figure.

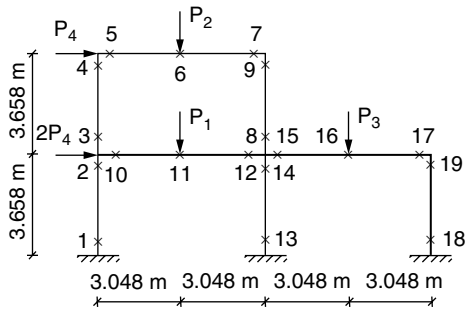

Variables	Expected values	Coefficients of variation
P_1	169 kN	0.15
P_2	89 kN	0.25
P_3	116 kN	0.25
P_4	31 kN	0.25
R_1, R_2, R_{13}, R_{14}, R_{18}, R_{19}	95 kNm	0.15
R_3, R_4, R_8, R_9	95 kNm	0.15
R_5, R_6, R_7	122 kNm	0.15
R_{10}, R_{11}, R_{12}	204 kNm	0.15
R_{15}, R_{16}, R_{17}	163 kNm	0.15

FIGURE 15.30 Geometry, loading, and potential yield hinges (×).

Copyright 2005 by CRC Press LLC

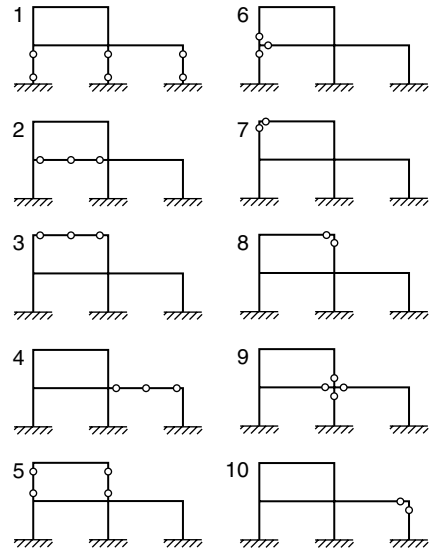

FIGURE 15.31 Set of fundamental mechanisms.

This procedure is now continued as explained earlier by adding or subtracting fundamental mechanisms. If the procedure is continued eight times (up to ten fundamental mechanisms in one mechanism) and if the significant mechanisms are selected by $\varepsilon_3 = 0.31$, then the system modeling at mechanism level will be a series system where the elements are 12 parallel systems. These 12 parallel systems (significant mechanisms) and corresponding reliability indices are shown in Table 15.3. The correlation matrix is

$$\bar{\bar{\rho}} = \begin{bmatrix}
1.00 & 0.65 & 0.89 & 0.44 & 0.04 & 0.91 & 0.59 & 0.97 & 0.87 & 0.81 & 0.86 & 0.92 \\
0.65 & 1.00 & 0.55 & 0.00 & 0.09 & 0.67 & 0.00 & 0.63 & 0.54 & 0.58 & 0.00 & 0.71 \\
0.89 & 0.55 & 1.00 & 0.35 & 0.45 & 0.83 & 0.61 & 0.88 & 0.98 & 0.95 & 0.31 & 0.83 \\
0.44 & 0.00 & 0.35 & 1.00 & 0.00 & 0.03 & 0.00 & 0.45 & 0.37 & 0.04 & 0.89 & 0.08 \\
0.04 & 0.09 & 0.45 & 0.00 & 1.00 & 0.05 & 0.00 & 0.04 & 0.44 & 0.48 & 0.00 & 0.05 \\
0.91 & 0.67 & 0.83 & 0.03 & 0.05 & 1.00 & 0.73 & 0.87 & 0.80 & 0.88 & 0.00 & 0.98 \\
0.59 & 0.00 & 0.61 & 0.00 & 0.00 & 0.73 & 1.00 & 0.58 & 0.60 & 0.65 & 0.00 & 0.64 \\
0.97 & 0.63 & 0.88 & 0.45 & 0.04 & 0.87 & 0.58 & 1.00 & 0.90 & 0.77 & 0.48 & 0.87 \\
0.87 & 0.54 & 0.98 & 0.37 & 0.44 & 0.80 & 0.60 & 0.90 & 1.00 & 0.90 & 0.41 & 0.78 \\
0.81 & 0.58 & 0.95 & 0.04 & 0.48 & 0.88 & 0.65 & 0.77 & 0.90 & 1.00 & 0.00 & 0.88 \\
0.36 & 0.00 & 0.31 & 0.89 & 0.00 & 0.00 & 0.00 & 0.48 & 0.41 & 0.00 & 1.00 & 0.00 \\
0.92 & 0.71 & 0.83 & 0.08 & 0.05 & 0.98 & 0.64 & 0.87 & 0.78 & 0.88 & 0.00 & 1.00
\end{bmatrix}.$$

TABLE 15.2 Reliability Indices for the Fundamental Mechanisms

i	1	2	3	4	5	6	7	8	9	10
β_i	1.91	2.08	2.17	2.26	4.19	10.75	9.36	9.36	12.65	9.12

Copyright 2005 by CRC Press LLC

TABLE 15.3 Correlation Coefficients and Safety Indices of 12 Systems at Mechanism Level

No.	Significant mechanisms	β
1	1 + 6 + 2 + 5 + 7 + 3 − 8	1.88
2	1	1.91
3	1 + 6 + 2 + 5 + 7 + 3 + 4 − 8 − 10	1.94
4	3 + 7 − 8	1.98
5	4 − 10	1.99
6	1 + 6 + 2	1.99
7	2	2.08
8	1 + 6 + 2 + 5 + 7 + 3 + 8	2.09
9	1 + 6 + 2 + 5 + 7 + 3 + 8 + 9 + 4 − 10	2.11
10	1 + 6 + 2 + 5 + 9 + 4 − 10	2.17
11	3	2.17
12	1 + 6 + 2 + 5	2.18

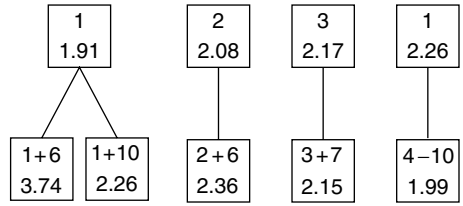

FIGURE 15.32 The first two rows in the failure tree.

The probability of failure P_f for the series system with the 12 significant mechanisms as elements can then be estimated by the usual techniques. The Ditlevsen bounds are $0.08646 \leq P_f \leq 0.1277$. If the average value of the lower and upper bounds is used, the estimate of the reliability index β_s at mechanism level is $\beta_s = 1.25$. Hohenbichler [28] has derived an approximate method to calculate estimates for the system probability of failure P_f (and the corresponding reliability index β_s). The estimate of β_s is $\beta_s = 1.21$. It can finally be noted that Monte Carlo simulation gives $\beta_s = 1.20$.

15.6 Illustrative Examples

15.6.1 Reliability of a Tubular Joint

The single tubular beams in a steel jacket structure will in general at least have three important failure elements; namely, failure in yielding under combined bending moments and axial tension/compression at points close to the ends of the beam and failure in buckling (instability). A tubular joint will likewise have a number of potential failure elements. Consider the tubular K-joint shown in Figure 15.33.

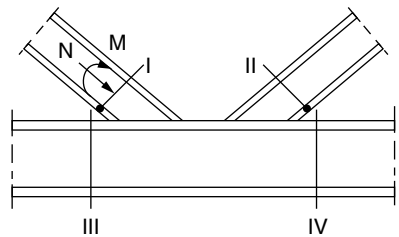

FIGURE 15.33 Tubular K-joint: I through IV are the critical sections and • indicates the hot spots.

Copyright 2005 by CRC Press LLC

This tubular joint is analyzed in more detail in a paper by Thoft-Christensen and Sørensen [29]. It is assumed that the joint has four critical sections as indicated in Figure 15.33 by I, II, III, and IV. The load effects in each critical section are an axial force N and a bending moment M. The structure is assumed to be linear elastic. For this K-joint, 12 failure elements are considered, namely:

- Failure in yielding in the four critical sections I, II, III, and IV
- Punching failure in the braces (cross-sections I and II)
- Buckling failure of the four tubular members (cross-sections I, II, III, and IV)
- Fatigue failure in the critical sections I and II (hot spots are indicated in Figure 15.33)

For these failure elements, safety margins have been formulated by Thoft-Christensen and Sørensen [29]. For failure in yielding the safety margins are of the form

$$M^Y = Z^Y - \left(\left| \frac{M}{M_F} \right| - \cos\left(\frac{\pi}{2} \frac{N}{N_F} \right) \right) \tag{15.109}$$

where M_F and N_F are the yield capacities in pure bending and pure axial loading, and where Z^Y is a model uncertainty variable. For punching failure, the following safety margin is used

$$M^P = Z^P - \left(\left| \frac{N}{Z^N N_U} \right| + \left(\frac{|M|}{Z^M M_U} \right)^{1.2} \right). \tag{15.110}$$

N_U and M_U are ultimate punching capacities in pure axial loading and pure bending, respectively. In this case, three model uncertainty variables Z^P, Z^N, and Z^M are included. The following safety margin is used for buckling failure

$$M^B = Z^B - \left(\frac{N}{N_B} + \frac{M}{M_B} \right) \tag{15.111}$$

where N_B and M_B are functions of the geometry and the yield stress and where Z^B is a model uncertainty variable. Finally, with regard to fatigue failure, the safety margin for each of the two hot points, shown in Figure 15.33, has the form

$$M^F = Z^F - (Z^L)^m K^{-1} (\max(t/32, 1)^{M_1}) g \tag{15.112}$$

where m (= 3) and K are constants in the S-N relation used in Miner's rule. K is modeled as a random variable, t is the wall thickness, M_1 is a random variable, and g is a constant. Z^F and Z^L are model uncertainty variables.

For this particular K-joint in a plane model of a tubular steel jacket structure analyzed by Thoft-Christensen and Sørensen [29], only four failure elements are significant:, namely (referring to Figure 15.33) fatigue in cross-section II ($\beta = 3.62$), punching in the same cross-section II ($\beta = 4.10$), buckling in cross-section II ($\beta = 4.58$), and fatigue in cross-section I ($\beta = 4.69$).

The correlation coefficient matrix of the linearized safety margins of the four significant failure elements is

$$\bar{\bar{\rho}} = \begin{bmatrix} 1 & 0 & 0 & 0.86 \\ 0 & 1 & 0.82 & 0 \\ 0 & 0.82 & 1 & 0 \\ 0.86 & 0 & 0 & 1 \end{bmatrix}$$

Copyright 2005 by CRC Press LLC

and the probability of failure of the joint

$$P_f \approx 1 - \Phi_4(\overline{\beta}, \overline{\overline{\rho}}) = 1.718 \times 10^{-4}$$

The corresponding reliability index for the joint is

$$\beta = -\Phi^{-1}(P_f) = 3.58.$$

It is important to note that in this estimate of the reliability of the *K*-joint, the interaction between the different significant failure elements in, for example, cross-section II is not taken into account. Each failure element (failure mode) is considered independent of the other, although such interaction will influence the reliability of the joint.

15.6.2 Reliability-Based Optimal Design of a Steel-Jacket Offshore Structure

In Thoft-Christensen and Murotsu [2], an extensive number of references to reliability-based optimal design can be found. In this section the optimal design problem is briefly stated and illustrated with an example taken from Thoft-Christensen and Sørensen [30]. In reliability-based optimization, the objective function is often chosen as the weight F of the structure. The constraints can either be related to the reliability of the single elements or to the reliability of the structural system. In the last-mentioned case, the optimization problem for a structure with h elements may be written as

$$\begin{aligned} &\min \quad F(\bar{y}) = \sum_{i=1}^{h} \varphi_i l_i A_i(\bar{y}) \\ &s.t. \quad \beta^s(\bar{y}) \geq \beta_0^s \\ &\qquad y_i^l \leq y_i \leq y_1^u, \quad i = 1, \ldots, n \end{aligned} \tag{15.113}$$

where A_i, l_i and φ_i are the cross-sectional area, the length, and the density of element no. i; $\bar{y} = (y_1, \ldots, y_n)$ are the design variables; β_0^s is the target system reliability index; and y_i^l and y_i^u are lower and upper bounds, respectively, for the design variable y_i, $i = 1, \ldots, n$.

Consider the three-dimensional truss model of the steel-jacket offshore structure shown in Figure 15.34. The load and the geometry are described in detail by Thoft-Christensen and Sørensen [30] and by Sørensen, Thoft-Christensen, and Sigurdsson [31]. The load is modeled by two random variables, and the yield capacities of the 48 truss elements are modeled as random variables with expected values 270×10^6 Nm^{-2} and coefficients of variation equal to 0.15. The correlation structure of the normally distributed variables is described in [31]. The design variables y_i, $i = 1, \ldots, 7$ are the cross-sectional areas (m^2) of the seven groups of structural elements (see Figure 15.34). The optimization problem is

$$\begin{aligned} &\min \quad F(\bar{y}) = 125y_1 + 100y_2 + 80y_3 + 384y_4 + 399y_6 + 255y_7 (m^3) \\ &s.t. \quad \beta^s(\bar{y}) \geq \beta_0^s = 3.00 \\ &\qquad 0 = y_i^l \leq y_i \leq y_1^u = 1, \quad i = 1, \ldots, 7. \end{aligned} \tag{15.114}$$

β^s is the system reliability index at level 1. The solution is $\bar{y}$ = (0.01, 0.001, 0.073, 0.575, 0.010, 0.009, 0.011) m^2 and $F(\bar{y}) = 215$ m^3. The iteration history for the weight function $F(\bar{y})$ and the system reliability index β^s is shown in Figure 15.35.

Copyright 2005 by CRC Press LLC

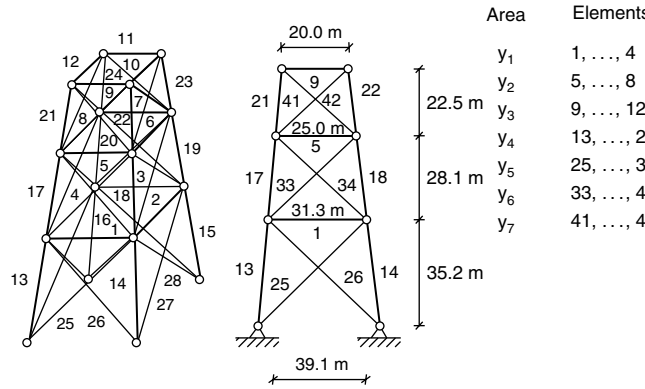

FIGURE 15.34 Space truss tower with design variables.

15.6.3 Reliability-Based Optimal Maintenance Strategies

An interesting application of optimization methods is related to deriving optimal strategies for inspection and repair of structural systems. In a paper by Thoft-Christensen and Sørensen [32], such a strategy was presented with the intention of minimizing the cost of inspection and repair of a structure in its lifetime T under the constraint that the structure has an acceptable reliability. In another paper by Sørensen and Thoft-Christensen [33], this work was extended by including not only inspection costs and repair costs, but also the production (initial) cost of the structure in the objective function.

The purpose of a simple optimal strategy for inspection and repair of civil engineering structures is to minimize the expenses of inspection and repair of a given structure so that the structure in its expected service life has an acceptable reliability. The strategy is illustrated in Figure 15.36, where T is the lifetime of the structure and β is a measure of the reliability of the structure. The reliability β is assumed to be a nonincreasing function with time t. T_i, $i = 1, 2, \ldots, n$ are the inspection times, and $\beta^{\min}$ is the minimum acceptable reliability of the structure in its lifetime.

Let $t_i = T_i - T_{i-1}$, $i = 1, \ldots, n$ and let the quality of inspection at time T_i be q_i, $i = 1, \ldots, n$. Then, with a given number of inspection times n, the design variables are t_i, $i = 1, \ldots, n$ and q_i, $i = 1, \ldots, n$. As an illustration, consider the maintenance strategy shown in Figure 15.36. At time T_1, the solution of the optimization problem is $q_i = 0$; that is, no inspection takes place at that time. Inspection takes place at time T_2; and according to the result of the inspection, it is decided whether or not repair should be performed. If repair is performed, the reliability is improved. If no repair is performed, the reliability is

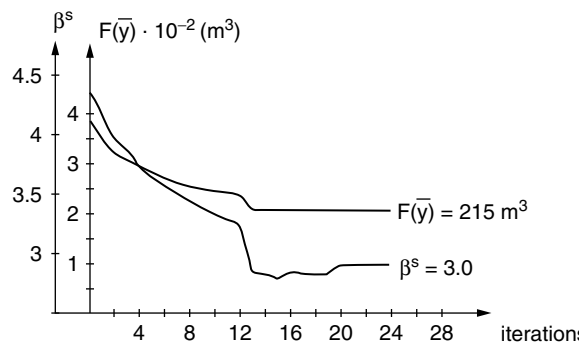

FIGURE 15.35 Iteration history.

Copyright 2005 by CRC Press LLC

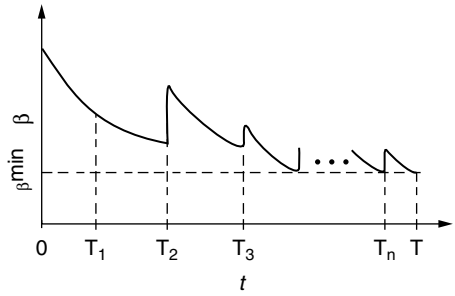

FIGURE 15.36 Maintenance strategy.

also improved because then updating of the strengths of the structural elements takes place. Therefore, the variation of the reliability of the structure with time will be as shown in Figure 15.36. The shape of the curves between inspection times will depend on the relevant types of deterioration, for example, whether corrosion or fatigue is considered.

A very brief description of the application of this strategy is given here, based on [33]. The design variables are cross-sectional parameters $z_1, \ldots, z_m$, inspection qualities $q_1, \ldots, q_N$, and time between inspections $t_1, \ldots, t_{N,}$ where m is the number of cross-sections to be designed and N is the number of inspections (and repairs). The optimization for a structural system modeled by s failure elements can then be formulated in the following way:

$$\min_{\bar{q}=(q_1,\ldots,q_N),\,\bar{t}=(t_1,\ldots,t_N)} C(\bar{z},\bar{q},\bar{t}) = C_I(\bar{z}) + \sum_{i=1}^{N}\sum_{j=1}^{s} C_{IN,j}(q_i)e^{-rT_i} + \sum_{i=1}^{N}\sum_{j=1}^{s} C_{R,j}(\bar{z})E[R_{ij}(\bar{z},\bar{q},\bar{t})]e^{-rT_i} \tag{15.115}$$

$$s.t. \quad \beta^s(T_i) \geq \beta^{\min}, \quad i = 1,\ldots,N,N+1$$

where the trivial bounds on the design variables are omitted; C_I is the initial cost of the structure; $C_{\mathrm{IN},j}(q_i)$ is the cost of an inspection of element j with the inspection quality q_i; $C_{R,j}$ is the cost of a repair of element j; r is the discount rate; and $E[R_{ij}(\bar{z},\bar{q},\bar{t})]$ is the expected number of repairs at the time T_i in element j. $\beta^s(T_i)$ is the system reliability index at level 1 at the inspection time T_i and $\beta^{\min}$ is the lowest acceptable system reliability index.

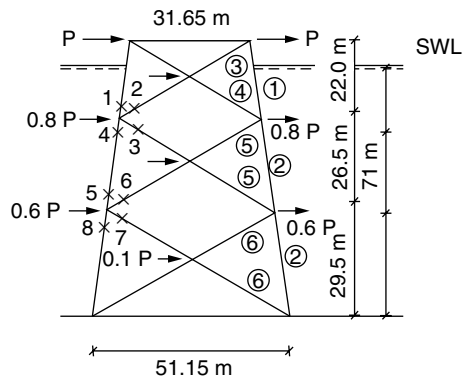

FIGURE 15.37 Plan model of a steel jacket platform.

Copyright 2005 by CRC Press LLC

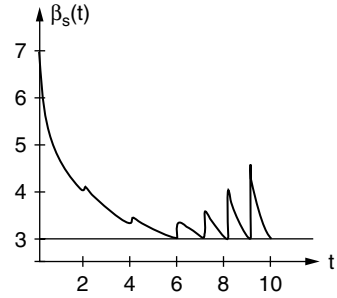

FIGURE 15.38 β^s as a function of the time t for optimal design and inspection variables and for $N = 6$.

Consider the plane model of a steel jacket platform shown in Figure 15.37 (see [33], where all details are described). Due to symmetry, only the eight fatigue failure elements indicated by × in Figure 15.37 are considered. Design variables are the tubular thicknesses of the six groups of elements indicated by ○ in Figure 15.37. Using $\beta^{\min} = 3.00$, $T = 10$ years, $r = 0$, and $N = 6$, the following optimal solution is determined:

$$\bar{t} = (2, 2, 2, 1.19, 0.994, 0.925) \text{ years}$$

$$\bar{q} = (0.1, 0.133, 0.261, 0.332, 0.385, 0.423)$$

$$\bar{z} = (68.9, 62.7, 30.0, 30.0, 50.4, 32.0) \text{ mm}$$

as shown in Figure 15.38.

References

1. Thoft-Christensen, P. and Baker, M. J., *Structural Reliability and Its Applications.* Springer-Verlag, Berlin-Heidelberg-New York, 1982.
2. Thoft-Christensen, P. and Murotsu, Y., *Application of Structural Systems Reliability Theory.* Springer-Verlag, Berlin-Heidelberg-New York, 1986.
3. Rackwitz, R. and Fiessler, B., *An Algorithm for Calculation of Structural Reliability under Combined Loading.* Berichte zur Sicherheitstheorie der Bauwerke, Lab. f. Konstr. Ingb., Tech. Univ. München, München, 1977.
4. Thoft-Christensen, P., *Reliability Analysis of Structural Systems by the β-Unzipping Method.* Institute of Building Technology and Structural Engineering, Aalborg University Centre, Aalborg, Report 8401, March 1984.
5. Kaufmann, A., Grouchko, D., and Cruon R., *Mathematical Models for the Study of the Reliability of Systems.* Academic Press, New York, San Francisco, London, 1977.
6. Hohenbichler, M. and Rackwitz, R., First-Order Concepts in System Reliability. *Structural Safety,* Vol. 1, 1983, pp. 1, 177–188.
7. Kounias, E., Bounds for the Probability of a Union, with Applications. *Annals of Mathematical Statistics,* Vol. 39, 1968, pp. 2154–2158.
8. Ditlevsen, O., Narrow Reliability Bounds for Structural Systems. *J. Struct. Mech.,* Vol. 7(No. 4), 1979, pp. 453–472.
9. Dunnett, C.W. and Sobel, M., Approximations to the Probability Integral and Certain Percentage Points of Multivariate Analogue of Students' t-Distribution. *Biometrika,* Vol. 42, 1955, pp. 258–260.

Copyright 2005 by CRC Press LLC

10. Thoft-Christensen, P. and Sørensen, J. D., Reliability of Structural Systems with Correlated Elements. *Applied Mathematical Modelling,* Vol. 6, 1982, pp. 171–178.
11. Ditlevsen, O., Taylor Expansion of Series System Reliability. *Journal of the Engineering Mechanics,* ASCE, Vol. 110(No. 2), 1984, pp. 293–307.
12. Murotsu, Y., Okada, M., Yonezawa, M., and Taguchi, K., Reliability Assessment of Redundant Structures. *Structural Safety and Reliability, ICOSSAR 81,* Elsevier Scientific, Publishing Company, Amsterdam, 1981, pp. 315–329.
13. Gollwitzer, S. and Rackwitz, R., Equivalent Components in First-Order System Reliability. *Reliability Engineering,* Vol. 5, 1983, pp. 99–115.
14. Grigoriu, M. and Turkstra, C., Safety of Structural Systems with Correlated Resistances. *Applied Mathematical Modelling,* Vol. 3, 1979, pp. 130–136.
15. Thoft-Christensen, P. and Sørensen, J. D., Reliability of Structural Systems with Correlated Elements. *Applied Mathematical Modelling,* Vol. 6, 1982, pp. 171–178.
16. Ferregut-Avila, C. M., *Reliability Analysis of Elasto-Plastic Structures.* NATO Advanced Study Institute, P. Thoft-Christensen, Ed. (ed.), Martinus Nijhoff, The Netherlands, 1983, pp. 445–451.
17. Moses, F., Structural System Reliability and Optimization. *Computers & Structures,* Vol. 7, 1977, pp. 283–290.
18. Gorman, M. R., Reliability of Structural Systems. Report No. 79-2, Case Western Reserve University, Ohio, Ph.D. Report, 1979.
19. Ma, H.-F. and Ang, A. H.-S., Reliability Analysis of Ductile Structural Systems. Civil Eng. Studies, Structural Research Series No. 494, University of Illinois, Urbana, August 1981.
20. Klingmüller, O., Anwendung der Traglastberechnung für die Beurteilung der Sicherheit von Konstruktionen. *Forschungsberichte aus dem Fachbereich Bauwesen.* Gesamthochschule Essen, Heft 9, Sept. 1979.
21. Murotsu, Y., Okada, H., Yonezawa, M., and Kishi, M., Identification of Stochastically Dominant Failure Modes in Frame Structures. *Proc. Int. Conf. on Appl. Stat. and Prob. in Soil and Struct. Eng.,* Universita di Firenze, Italia. Pitagora Editrice 1983, pp. 1325–1338.
22. Kappler, H., Beitrag zur Zuverlässigkeitstheorie von Tragwerken unter Berücksichtigung nichtlinearen Verhaltens. Dissertation, Technische Universität München, 1980.
23. Thoft-Christensen, P., The β-Unzipping Method. Institute of Building Technology and Structural Engineering, Aalborg University Centre, Aalborg, Report 8207, 1982 (not published).
24. Thoft-Christensen, P. and Sørensen, J.D., Calculation of Failure Probabilities of Ductile Structures by the β-Unzipping Method. Institute of Building Technology and Structural Engineering, Aalborg University Centre, Aalborg, Report 8208, 1982.
25. Thoft-Christensen, P. and Sørensen, J.D., Reliability Analysis of Elasto-Plastic Structures. *Proc. 11. IFIP Conf. "System Modelling and Optimization,"* Copenhagen, July 1983. Springer-Verlag, 1984, pp. 556–566.
26. Watwood, V. B., Mechanism Generation for Limit Analysis of Frames. ASCE, *Journal of the Structural Division,* Vol. 105(No. STl), Jan. 1979, pp. 1–15.
27. Thoft-Christensen, P., Reliability of Structural Systems. *Advanced Seminar on Structural Reliability,* Ispra, Italy, 1984. University of Aalborg, Denmark, Report R8401, March 1984.
28. Hohenbichler, M., An Approximation to the Multivariate Normal Distribution Function. *Proc. 155th Euromech on Reliability of Structural Eng. Systems,* Lyngby, Denmark, June 1982, pp. 79–110.
29. Thoft-Christensen, P. and Sørensen, J.D., Reliability Analysis of Tubular Joints in Offshore Structures. *Reliability Engineering,* Vol. 19, 1987, pp. 171–184.
30. Thoft-Christensen, P. and Sørensen, J.D., Recent Advances in Optimal Design of Structures from a Reliability Point of View. *Quality and Reliability Management,* 4, Vol. 4 1987, pp. 19–31.
31. Sørensen, J.D., Thoft-Christensen, P., and Sigurdsson, G., Development of Applicable Methods for Evaluating the Safety of Offshore Structures, Part 2. Institute of Building Technology and Structural Engineering. The University of Aalborg, Paper No. 11, 1985.

Copyright 2005 by CRC Press LLC

32. Thoft-Christensen, P. and Sørensen, J.D., Optimal Strategy for Inspection and Repair of Structural Systems. Civil Engineeringng Systems., Vol. 4, 1987, pp. 94–100.
33. Thoft-Christensen, P., Application of Optimization Methods in Structural Systems Reliability Theory. *Proc. IFIP Conference on "System Modelling and Optimization,"* Tokyo, August/September 1987. Springer-Verlag, 1988, pp. 484–497.

Copyright 2005 by CRC Press LLC

16

Quantum Physics-Based Probability Models with Applications to Reliability Analysis

Erik Vanmarcke
Princeton University

16.1 Introduction

We present herein a class of probability models with considerable potential for useful applications to reliability analysis. The new families of probability density functions (PDFs) have a fundamental basis in quantum physics; they describe the inherent uncertainty of properties of single energy quanta emitted by a "perfect radiator" or "blackbody" with known temperature. The starting point for the derivation of the various PDFs is Planck's blackbody radiation spectrum [1], which expresses how the energy absorbed or emitted in blackbody radiation is distributed among quanta of radiation (photons) with different energies (or frequencies or wavelengths), characterizing the aggregate behavior of very many energy quanta in local thermal equilibrium (LTE).

Section 16.2, providing background, reviews the relationship between the geometric and arithmetic means of any nonnegative random variable. Section 16.3, derives the PDFs of various functionally related random properties of single energy quanta when the local-thermal-equilibrium (LTE) temperature T is known or prescribed. The results apply for any LTE temperature between absolute zero ($T = 0$) and the upper limit on the validity of quantum mechanics and general relativity theory, namely the "Planck temperature" ($T_{Pl} \sim 10^{32} K$). Section 16.4 deals with how to express the intrinsic uncertainty of the "quantum mass ratio," defined as the quotient of the mass (energy/c^2) of a random quantum of energy

Copyright 2005 by CRC Press LLC

and the geometric-mean mass of quanta *given* the LTE-temperature *T*. In Section 16.5, we obtain the probability distribution of the "quantum size ratio," defined as the reciprocal of the quantum mass ratio, representing the relative "sizes" (wavelengths) of single energy quanta sampled from a collection of quanta in (local) thermal equilibrium. Section 16.6 looks into various applications of the probability models to single-mode and system reliability analysis.

16.2 Background: Geometric Mean and Related Statistics

Various random quantities expressed as *products* of random variables can be described efficiently in terms of *geometric* means and related statistics. By definition, the geometric mean $\overline{Y}$ of a nonnegative random variable Y is

$$\overline{Y} \equiv \exp\langle \log Y \rangle = \exp\left\{ \int_0^\infty \log y \, dF_Y(y) \right\}, \tag{16.1}$$

where $\langle \cdot \rangle$ refers to a random quantity's *arithmetic* mean; "log" denotes the natural logarithm; "exp" is the exponential function; and $F_Y(y)$ is the cumulative distribution function (CDF) of Y. The definition in Equation 16.1 implies that the geometric mean of a product of random variables, $Y = Y_1 \ldots Y_n$, equals the product of their geometric means, $\overline{Y} = \overline{Y}_1 \ldots \overline{Y}_n$, and hence that the geometric mean of a power of Y equals $\overline{Y}$ raised to that power. The variability of Y can be quantified in term of its "characteristic value," defined as

$$\widetilde{Y} \equiv \overline{Y} \exp\left\{ \frac{1}{2} Var[\log Y] \right\}, \tag{16.2}$$

which depends on the "logarithmic variance," or the variance of the logarithm, of Y:

$$Var[\log Y] \equiv \langle (\log Y - \langle \log Y \rangle)^2 \rangle = \langle (\log Y)^2 \rangle - \langle \log Y \rangle^2 = 2 \log(\widetilde{Y}/\overline{Y}), \tag{16.3}$$

where the term on the right-hand side is just the inverse of Equation 16.2. Both the logarithmic variance and the "stochasticity factor" $(\widetilde{Y}/\overline{Y})$, the quotient of the characteristic value $\widetilde{Y}$ and the geometric mean $\overline{Y}$, measure the spread of the PDF $f_Y(y)$ of any nonnegative random variable Y; and in case Y is deterministic, $Var[\log Y] = 0$ and $\widetilde{Y}/\overline{Y} = 1$. Common measures of uncertainty based on arithmetic means are the variance $Var[Y] \equiv \langle \{Y - \langle Y \rangle\}^2 \rangle = \langle Y^2 \rangle - \langle Y \rangle^2$, its square root, the standard deviation $\sigma_Y \equiv (Var[Y])^{1/2}$, and the ratio of standard deviation to mean, or the "coefficient of variation," $V_Y \equiv \sigma_Y / \langle Y \rangle$. Note that in case Y is *lognormally* distributed, so the logarithm of Y is normal or Gaussian, the following relations hold: the geometric mean $\overline{Y}$ equals the median (or the fiftieth percentile) of Y, the characteristic value $\widetilde{Y}$ equals the arithmetic mean $\langle Y \rangle$, the stochasticity factor $\widetilde{Y}/\overline{Y}$ is given by $1 + V_Y^2$, and the coefficient of skewness of Y, defined by $\chi_Y \equiv \langle (Y - \langle Y \rangle)^3 \rangle / \sigma_Y^3$, satisfies the relation: $\chi_Y = 3V_Y + V_Y^3$.

16.3 Probability Distributions of the "Quantum Mass Ratio" and Its Logarithm

One of the standard ways of expressing the Planck radiation function [1, 2], characterizing a large number of quanta of radiation (photons) in thermal equilibrium, is in terms of the mean number of quanta per unit volume, dN_λ, having wavelengths within the infinitesimal range between λ and $\lambda + d\lambda$,

$$dN_\lambda = \frac{8\pi}{\lambda^4} d\lambda \Big/ \left[\exp\left\{ \frac{h_P c}{k_B T \lambda} \right\} - 1 \right], \tag{16.4}$$

Copyright 2005 by CRC Press LLC

in which T is the radiation temperature in degrees Kelvin, $c \approx 2.998 \times 10^{10} cm/sec$ is the speed of light, $k_B \approx 8.617 \times 10^{-5} eV$ (electron-volt) per degree Kelvin is Boltzmann's constant, and $h_p \approx 4.14 \times 10^{-15} eV\,sec$ is Planck's constant, the "quantum of action." Integrating over the wavelength intervals $d\lambda$ for values of λ ranging from zero to infinity yields

$$N_{Total} = \int_0^\infty dN_\lambda = 16\pi\zeta(3)\left(\frac{k_B T}{h_p c}\right)^3 \approx 20.288\, T^3\ cm^{-3} \tag{16.5}$$

for the mean total number of energy quanta per unit volume as a function of temperature, in which $\zeta(u) = 1 + 2^{-u} + 3^{-u} + \ldots$ is Riemann's Zeta function [2].

Our interest henceforth focuses on interpreting the Planck radiation spectrum as a description of the random properties of single energy quanta or particles "sampled" from a collection of quanta or particles in local thermal equilibrium with temperature T. Each quantum possesses a set of functionally related random properties: its energy E or mass $m = E/c^2$ (Einstein's famous equation), wavelength $\lambda = h_p c/E = h_p/(mc)$, frequency $\nu = E/h_p = c/\lambda$, and momentum $p = mc = E/c$. Any of these attributes can be expressed, free of units, in terms of the random "quantum mass ratio"

$$W \equiv \frac{E}{\overline{E}} = \frac{m}{\overline{m}} = \frac{\overline{\lambda}}{\lambda}, \tag{16.6}$$

where $\overline{E} \equiv \exp\{\langle \log E \rangle\} = \overline{m}c^2 = h_p c/\overline{\lambda}$, the geometric mean (see Equation 16.1) of the quantum energy, equals the product of $k_B T$ and the constant

$$c_0 \equiv \frac{\overline{E}}{k_B T} = \left(\frac{h_p c}{k_B T}\right)\frac{1}{\overline{\lambda}} \approx 2.134. \tag{16.7}$$

The natural logarithm of W, or the "quantum-mass-ratio logarithm," is

$$L \equiv \log W = \log E - \log \overline{E} = \log\{E/(k_B T)\} - \ell_0, \tag{16.8}$$

where $\ell_0 \equiv \langle \log\{\overline{E}/(k_B T)\} \rangle = \log c_0 \approx 0.758$. (In general, we denote random variables herein by capital letters and their realizations by the lower case; but the rule is broken when symbols have established definitions or serve overriding demands for clarity of presentation, as is the case for the "random wavelength" λ and the "random mass" m in Equations 16.6 and 16.7.)

Combining Equation 16.4 and Equation 16.6 to Equation 16.8 yields the probability density functions of the quantum mass ratio W and its natural logarithm, $L \equiv \log W$, respectively [3],

$$f_W(w) = \frac{c_0}{2\zeta(3)}\frac{(c_0 w)^2}{e^{c_0 w} - 1}, \quad w \geq 0, \tag{16.9}$$

and

$$f_L(\ell) = \frac{1}{2\zeta(3)}\frac{e^{3(\ell_0 + \ell)}}{e^{e^{(\ell_0 + \ell)}} - 1}, \quad -\infty \leq \ell \leq \infty, \tag{16.10}$$

Copyright 2005 by CRC Press LLC

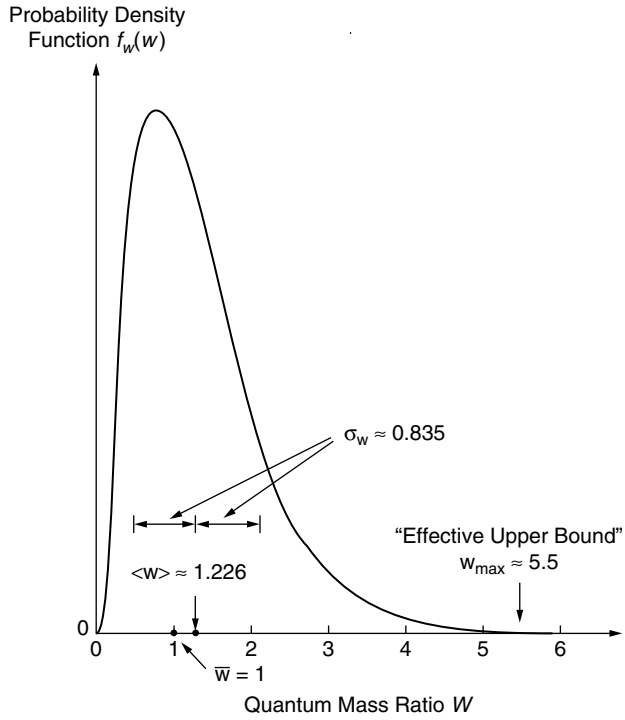

FIGURE 16.1 Probability density function of the "quantum mass ratio" W.

where $c_0[2\zeta(3)]^{-1} \approx 0.8877$ and $[2\zeta(3)]^{-1} \approx 0.416$. The PDFs of W and L are plotted in Figure 16.1 and Figure 16.2, respectively. The expectation of $e^{\imath u L}$, where $\imath = \sqrt{-1}$, defines the "characteristic function" of L; its logarithm $K_L(u) \equiv \log\langle e^{\imath u L}\rangle$ is known as the cumulant function [2], the cumulants of L being the coefficients ($K_{1,L}$, $K_{2,L}$, etc.) in the series expansion of $K_L(u)$:

$$K_L(u) \equiv \log\langle e^{\imath u L}\rangle = (\imath u)K_{1,L} + \frac{(\imath u)^2}{2!}K_{2,L} + \frac{(\imath u)^3}{3!}K_{3,L} + \ldots \tag{16.11}$$

The first three cumulants are the mean, the variance, and the third central moment of L, respectively. The principal property of cumulants is that each cumulant of a sum of independent random variables is itself a sum of component cumulants, so that a sum's cumulant function is also the sum of the component cumulant functions.

16.4 Logarithmic Variance and Other Statistics of the "Quantum Mass Ratio"

In problems involving *products* of (i.i.d.) random variables W, a useful and attractive attribute of the random mass ratio W is that its geometric mean equals one,

$$\overline{W} \equiv \exp\langle \log W\rangle = 1, \tag{16.12}$$

implying $\langle \log W\rangle = \langle L\rangle = 0$. A key measure of uncertainty of the properties of single energy quanta in thermal equilibrium is the logarithmic variance of the quantum mass ratio, or the variance of the

Copyright 2005 by CRC Press LLC

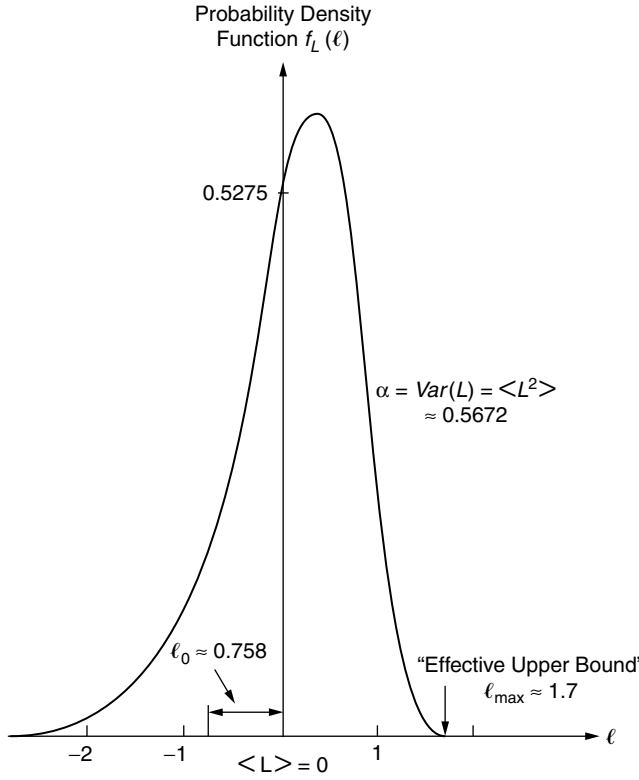

FIGURE 16.2 Probability density function of L, the quantum-mass-ratio logarithm.

mass-ratio logarithm, which we denote by α. We can write:

$$\alpha \equiv Var[\log W] = Var[L] = \sigma_L^2 = \langle L^2 \rangle = \int_0^\infty \ell^2 f_L(\ell) d\ell \approx 0.5672. \tag{16.13}$$

Measuring the variability of the energy (or wavelength or momentum) of single quanta "sampled" from a population of quanta in thermal equilibrium, for any temperature $T \le T_{Planck} \approx 10^{32} K$, the quantity $\alpha \equiv Var[L] \approx 0.5672$ is a basic constant, expressing the Uncertainty Principle in a way that complements, yet differs from, Heisenberg's (1926) formulation; the latter, proposed in the context of atomic physics, is an *inequality* that limits the precision of joint measurements of *two* attributes of a particle, such as position and momentum, and involves Planck's constant, a tiny number. The functions $\ell f_L(\ell)$ and $\ell^2 f_L(\ell)$ are plotted in Figure 16.3 and Figure 16.4, respectively; their complete integrals, from $-\infty$ to $+\infty$, are, respectively, the mean $\langle L \rangle = 0$ and the variance $\alpha \equiv \langle L^2 \rangle \approx 0.5672$ of the quantum-mass-ratio logarithm.

The statistical moments of the quantum mass ratio W, for any real value $s > -2$, not necessarily integers, are given by

$$\langle W^s \rangle = \int_0^\infty w^s f_W(w) dw = \frac{\Gamma(3+s)\zeta(3+s)}{2(c_0)^s \zeta(3)}, \quad s > -2, \tag{16.14}$$

Copyright 2005 by CRC Press LLC

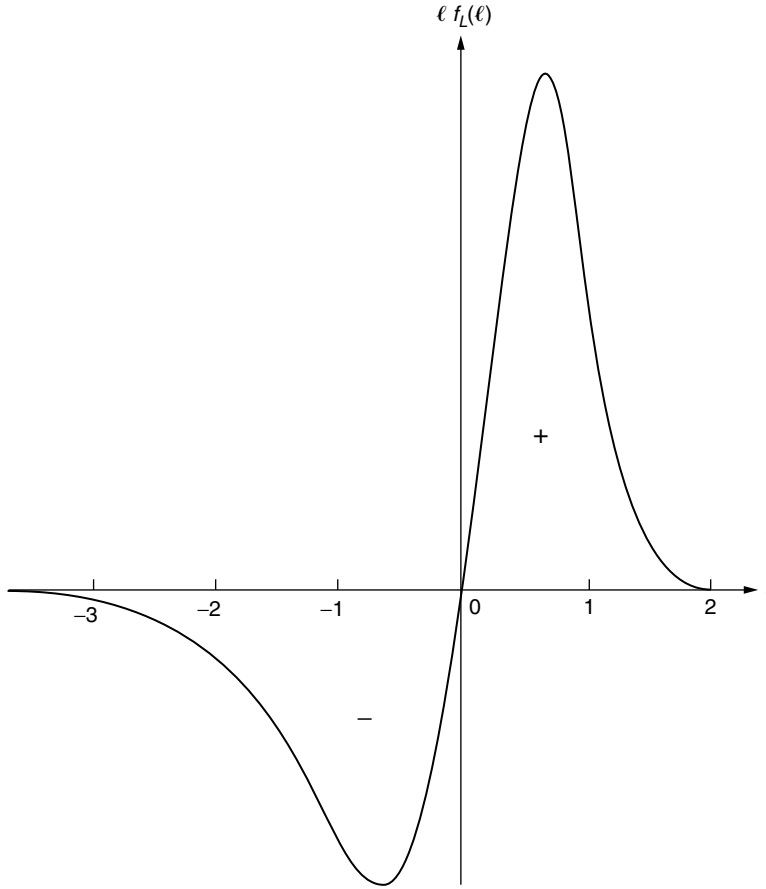

FIGURE 16.3 The function $\ell f_L(\ell)$, whose integral is the (zero) mean of L.

where $\Gamma(\cdot)$ denotes the Gamma function (which for positive integers obeys $\Gamma(m+1)=m!$). The quantities $\langle W^s \rangle$ and its logarithm are plotted in Figure 16.5. The case $s=1$ yields the arithmetic mean $\langle W \rangle \approx 1.226$, while the moment of order $s=-2$ is infinite because $\zeta(1)=\infty$. Other statistics of the mass ratio are its mean square $\langle W^2 \rangle \approx 2.31$, its variance $Var[W]=\langle W^2 \rangle - \langle W \rangle^2 \approx 0.697$, its standard deviation $\sigma_W \equiv (Var[W])^{1/2} \approx 0.835$, and its coefficient of variation $V_W \equiv \sigma_W / \langle W \rangle \approx 0.66$. Also, the quantum-mass-ratio PDF $f_W(w)$ is positively skewed, with coefficient of skewness $\chi_W \approx 1.18$.

The mean energy per particle — in electron-volts (eV) — can be expressed as $\langle E \rangle = c_0 k_B \langle W \rangle T \approx 2.33 \times 10^{-4} T$, where T is the temperature in degrees Kelvin. The mean radiation density per unit volume (in eV/cm^3) is the product of $\langle E \rangle$ and the mean number of quanta per unit volume (given by Equation 16.5), yielding the Stefan-Boltzmann law (expressing mean energy density vs. temperature), namely:

$$u = N_{Total} k_B T c_0 \langle W \rangle = 16\pi\zeta(3) c_0 \langle W \rangle \frac{(k_B T)^4}{(h_P c)^3} \approx 4.723 \times 10^{-3} T^4. \tag{16.15}$$

The function $wf_W(w)$, plotted in Figure 16.6, indicating how energy tends to be distributed among quanta with different w values, is proportional to Planck's energy distribution. (The partial moments of W, such as the partial integral of $wf_W(w)$, are proportional to the Debye functions arising in heat analysis [2].)

Copyright 2005 by CRC Press LLC

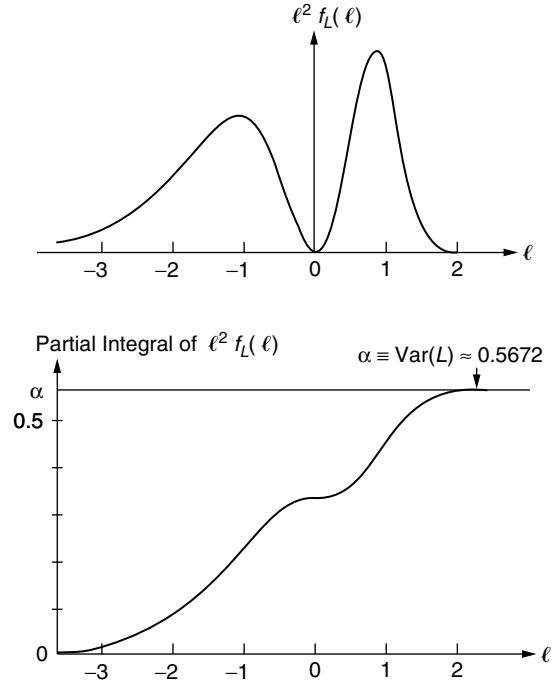

FIGURE 16.4 The function $\ell^2 f_L(\ell)$, whose integral is $\alpha \approx 0.5672$, the variance of L.

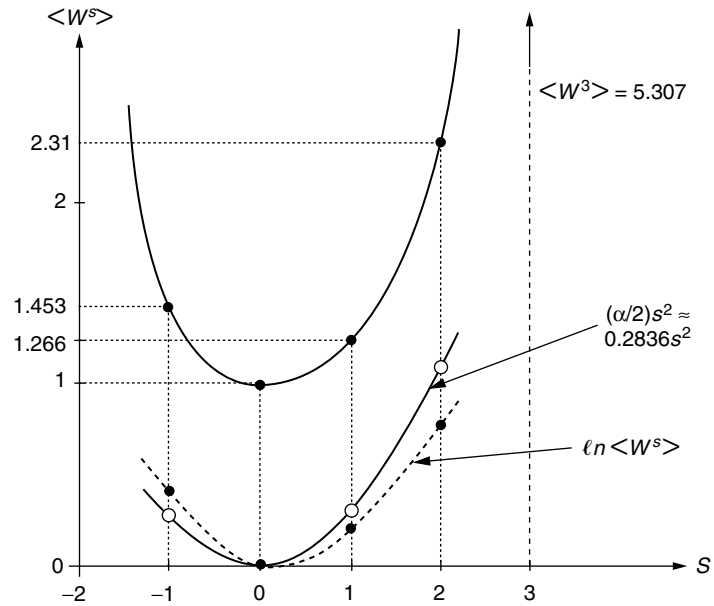

FIGURE 16.5 The moment function of W and its logarithm.

Copyright 2005 by CRC Press LLC

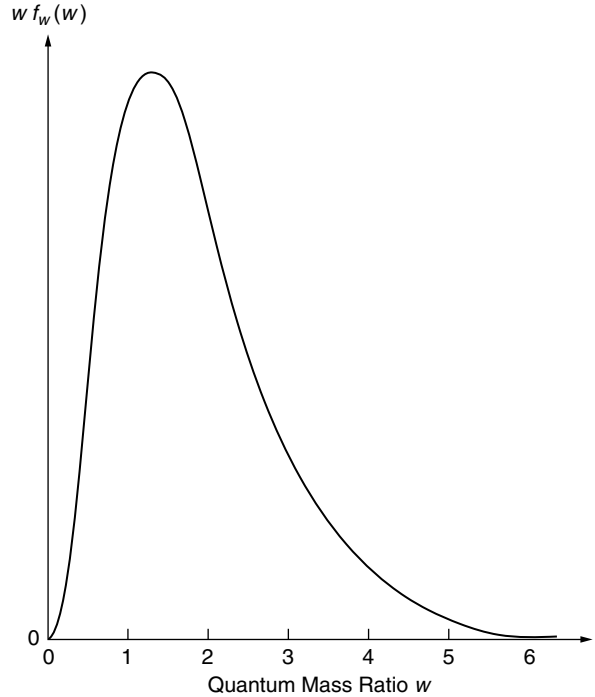

FIGURE 16.6 The function $wf_W(w)$, which indicates how energy tends to be distributed among quanta with different w-values, is proportional to Planck's energy distribution.

The quantum mass ratio W possesses the following geometric statistics: geometric-mean mass ratio $\overline{W} = 1$, logarithmic variance $Var[\log W] \equiv \alpha \approx 0.5672$, and characteristic value (equal to the stochasticity factor) $\tilde{W} = e^{\alpha/2} \approx 1.328$. The *lognormal* formula for the skewness coefficient, $3V_W + V_W^3 \approx 2.27$, is almost twice the true value, $\chi_W \approx 1.18$, the difference reflecting the fast decay of the PDF of W (or the Planck radiation function) in the high-energy range compared to a lognormal PDF with the same geometric mean ($\overline{W} = 1$) and logarithmic variance ($\alpha \approx 0.5672$). The PDF of W is positively skewed ($\chi_W \approx 1.18$) and that of $L = \log W$ negatively, with skewness coefficient $\chi_L \approx -0.879$. Note in Figure 16.1 and Figure 16.2 the lack of symmetry in the tails of either distribution. The fast decay in the high-energy ("Wien") range of the Planck spectrum means that very-high-energy quanta tend to occur much less frequently than very-low-energy ("Jeans-Rayleigh") quanta. The probability that the mass ratio W (of a randomly chosen quantum of energy, *given* the LTE temperature T) exceeds the value w drops very rapidly for w-values exceeding $w \approx 5.5$, corresponding to $\ell = \log 5.5 \approx 1.70$ (see Figure 16.1 and Figure 16.2); these values may be thought of as crude "apparent upper bounds" on the mass ratio W and its logarithm L, respectively. For similar reasons, the Gaussian approximation for $f_L(\ell)$, with mean $\langle L \rangle = 0$ and variance $\langle L^2 \rangle = \alpha$, significantly overestimates the probability that L is larger than ℓ when the latter exceeds its "apparent upper bound" $\ell_{\max} \equiv \log(w_{\max}) = \log(5.5) \approx 1.7 \approx 2.26\sigma_L$.

From the definition of the (quantum-mass-ratio-logarithm) cumulant function $K_L(u) = \log\langle e^{\iota u L} \rangle$, where $\iota = \sqrt{-1}$, taking into account $W = e^L$, we can infer that Equation 16.14 in effect expresses $\langle W^{iu} \rangle = \exp\{K_L(u)\}$, with ιu now substituting for the exponent s. The cumulant function of L is therefore given by

$$K_L(u) = \log\langle W^{\iota u} \rangle = \log\{\Gamma(3 + \iota u)\} + \log\{\zeta(3 + \iota u)\} - \ell_0 \iota u - \log[2\zeta(3)], \tag{16.16}$$

where $\ell_0 \equiv \log c_0 \approx 0.758$ and $\log[2\zeta(3)] \approx 0.877$; also, $K_L(0) = \log\langle W^0 \rangle = 0$. Because the first three cumulants of L are known, $K_{1,L} = \langle L \rangle = 0$, $K_{2,L} = Var[L] = \alpha \approx 0.5672$ and $K_{3,L} = \chi_L \alpha^{3/2} \approx -0.3755$ (where

Copyright 2005 by CRC Press LLC

$\chi_L \approx -0.879$ is the skewness coefficient), the series expansion (Equation 16.11) for the cumulant function starts off as follows:

$$K_L(u) = -\alpha\frac{u^2}{2} + \chi_L\alpha^{3/2}\frac{(\imath u)^3}{3!} + \ldots \approx -0.5672\frac{u^2}{2} - 0.3755\frac{(\imath u)^3}{3!} + \ldots, \tag{16.17}$$

If L actually had a normal (Gaussian) distribution with mean zero and variance α, its cumulant function would obey $K_L(u) = -\alpha u^2/2$, so the higher-order terms in Equation 16.17 represent physically significant deviations from symmetry and normality. The first-term approximation, $\log\langle W^s\rangle = K_L(s/\imath) \approx \alpha s^2/2 \approx 0.2836 s^2/2$, is shown, along with exact values, in Figure 16.5.

16.5 Probability Distribution of the "Quantum Size Ratio"

The wavelengths of individual energy quanta can be thought of as representing the sizes (radii) of elementary "cells." Energetic quanta have relatively small wavelengths or "cell radii" λ and short "lifetimes" $\theta = \lambda/c$. The relative sizes of these energy-quantum-specific cells, *given* the (local-thermal-equilibrium) temperature T, are measured by the "quantum size ratio," defined as the reciprocal of the "quantum mass ratio," $D \equiv \lambda/\bar{\lambda} = 1/W$. The probability density function of the quantum size ratio D is given by $f_D(d) = (1/d^2) f_W(1/d), d \geq 0$, or

$$f_D(d) = \frac{(c_0)^3}{2\zeta(3)}\frac{1}{d^4(e^{c_0/d} - 1)}, \quad d \geq 0, \tag{16.18}$$

matching the *shape* of the Planck spectrum in Equation 16.4. The probability density function of D is plotted in Figure 16.7.

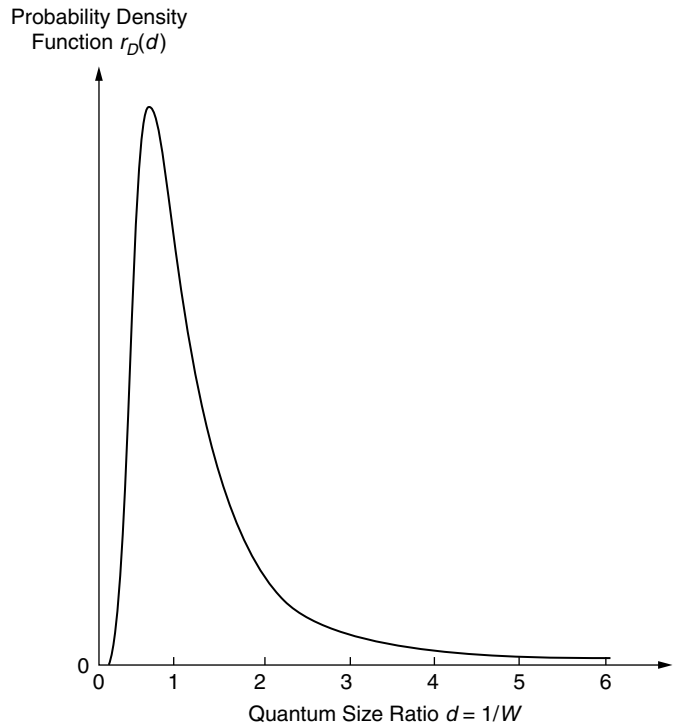

FIGURE 16.7 The probability density function of D, the reciprocal of the quantum mass ration W.

Copyright 2005 by CRC Press LLC

The probability density function $f_{L'}(\ell')$ of the *logarithm* of the quantum size ratio, $L' \equiv \log D = -\log W = -L$, is similar to that of the quantum-mass-ratio logarithm in Equation 16.10. We can write:

$$f_{L'}(\ell') = f_L(-\ell') = \frac{1}{2\zeta(3)} \frac{e^{3(\ell_0 - \ell')}}{e^{e^{(\ell_0 - \ell')}} - 1}, \quad -\infty \le \ell' \le \infty. \tag{16.19}$$

The PDF of L' is as shown in Figure 16.2 *provided* the abscissa's direction is reversed, and the two cumulant functions are similarly related: $K_{L'}(u) = K_L(-u)$. The means of L and L' are both zero, their variances are equal ($\alpha \approx 0.5672$), and their coefficients of skewness have the same absolute value but a different sign: $\chi_{L'} = -\chi_L \approx +0.879$.

The "geometric statistics" of $D = e^{-L}$ are the same as those of the quantum mass ratio ($W = e^L$), namely: geometric mean $\overline{D} = (\overline{W})^{-1} = 1$, characteristic value $\widetilde{D} \approx 1.328$, and logarithmic variance $Var[\log D] \equiv 2\log(\widetilde{D}/\overline{D}) = \alpha \approx 0.5672$. The quantum size ratio's arithmetic mean, $\langle D \rangle = \langle W^{-1} \rangle \approx 1.453$, is the integral of the function $d f_D(d)$. The second moment of the quantum size ratio, $\langle D^2 \rangle = \langle W^{-2} \rangle$, and its variance, $Var[D] = \langle D^2 \rangle - \langle D \rangle^2$, are both *infinite* (corresponding to $s = -2$ in Figure 16.5) due to the slow decay of the upper tail of $f_D(d)$. Closer examination of the asymptotic expression,

$$f_D(d) \to \frac{c_0^2}{2\zeta(3)} \frac{1}{d^3} \approx \frac{1.895}{d^3}, \quad d \gg 1, \tag{16.20}$$

shows that the "truncated" or "conditional" mean square, $\langle D^2 | D < d_0 \rangle$, defined as the integral from 0 to d_0 of the function $d^2 f_D(d)$, shown in Figure 16.8, possesses a term proportional to $\log d_0$, indicating how the "unconditional" mean square $\langle D^2 \rangle$ and variance $Var[D]$ of the quantum size ratio approach infinity. A further consequence is that the conditional or "sample" variance, $Var[D|D < d_0]$, where d_0 represents the size of any actual sampling volume, is predicted to be large but finite. (The predicted sensitivity of size-ratio statistics to the size of sampling regions proves testable in the context of a stochastic model of the so-called inflation phase of the big bang [3]; the model predicts the distribution of radii of "great

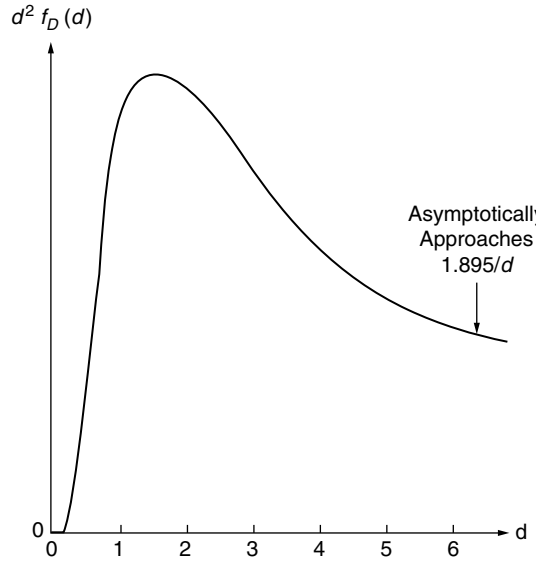

FIGURE 16.8 The function $d^2 f_D(d)$ whose integral, the mean square of D is infinite.

Copyright 2005 by CRC Press LLC

voids" and related geometrical anomalies of the large-scale cosmic structure in terms of basic quantum-size-ratio statistics.)

16.6 Extensions and Applications to Reliability Analysis

Considering a set of quantum-physics-based random variables — a set of W values or L values, for example — that are statistically independent and identically distributed (i.i.d.), one can readily obtain various families of derived probability distributions (and related statistics) for sums or products or extreme values, with the number of i.i.d. random variables (in the sum or product or extremum) serving as a model parameter. Consider, in particular, a set of ν independent and identically distributed (i.i.d.) quantum-mass-ratio logarithms, their common probability density function $f_L(\ell)$ given by Equation 16.10. The probability distribution of the sum, $L_\nu = L_{01} + L_{12} + \ldots + L_{\nu-1,\nu}$, can be obtained by iterative convolution, starting with the PDF of $L_2 = L_{01} + L_{12}$, next that of $L_3 = L_2 + L_{23}$, and so on. The PDF of the corresponding product of i.i.d. quantum mass ratios, $W_\nu \equiv \exp\{L_\nu\} = W_{01} W_{12} \ldots W_{\nu-1,\nu}$, where $W_{i-1,i} = \exp\{L_{i-1,i}\}$ for $i = 1, 2, \ldots, \nu$, can then be found by a single monotonic (one-to-one) transformation. Let us denote $f_{L_\nu}(\ell)$ by $f_{L\nu}(\ell)$ the PDF of the sum of ν independent quantum-mass-ratio logarithms, and by $f_{W\nu}(w)$ the corresponding PDF of the product of ν quantum mass ratios. In the special case $\nu = 1$, we have $f_{L_1}(\ell) \equiv f_L(\ell)$ and $f_{W_1}(w) \equiv f_W(w)$, as given by Equation 16.9 and Equation 16.10, respectively.

An elegant alternative to convolution is to express the cumulant function of L_ν as a sum of cumulant functions, $K_{L_\nu}(u) = \nu K_L(u)$, where $K_L(u)$ denotes the cumulant function of the quantum-mass-ratio logarithm L (given by Equation 16.17), and then compute the inverse-transform of $K_{L_\nu}(u)$ to obtain $f_{L_\nu}(\ell)$. Illustrating a typical set of results, Figure 16.9 shows the PDF of the sum of $\nu = 25$ quantum-mass-ratio logarithms; the dashed line shows the Gaussian probability density function with mean zero and

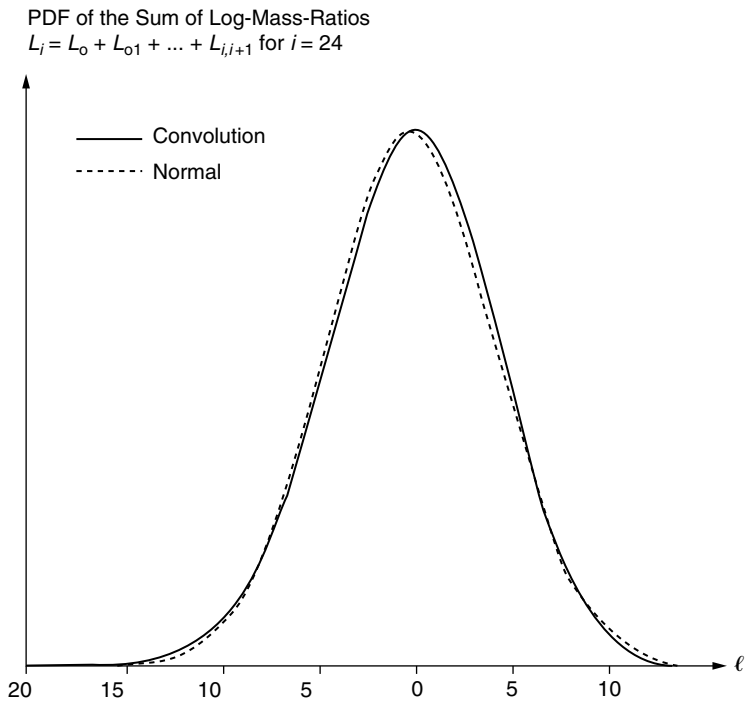

FIGURE 16.9 Probability density function of the sum of $\nu = 25$ quantum-mass-ratio logarithms; the dashed line shows the Gaussian probability density function with matching mean zero and standard deviation $(25\alpha)^{1/2} \approx 3.766$.

Copyright 2005 by CRC Press LLC

standard deviation $(25\alpha)^{1/2} \approx 3.766$. (The subscripts on L are denoted a bit differently in Figure 16.9, without in any way impacting the results.) Note that perceptible differences remain in the tails of the two distributions (displayed in Figure 16.9), which would be highly significant in applications to reliability analysis. Scaling $L_\nu \equiv \log W_\nu$ with respect to its standard deviation, $(\nu\alpha)^{1/2}$, yields a "standardized" random variable, $U^{(\nu)} = L_\nu/(\nu\alpha)^{1/2}$, whose probability distribution, as ν grows, will tend toward the "standard normal" (Gaussian) distribution in its central range. Likewise, the PDF of the derived random variable $V^{(\nu)} \equiv \exp\{U^{(\nu)}\} = \exp\{L_\nu/(\nu\alpha)^{1/2}\}$ should approach the "standard lognormal" PDF in its central range. The coefficient of skewness of L_ν can be expressed in terms of its "cumulants": $\chi_{L_\nu} \equiv \nu K_{3,L}/(\nu K_{2,L})^{3/2} = \chi_L/\sqrt{\nu} \approx -0.879/\sqrt{\nu}$, indicating how the skewness decreases as ν grows (consistent with the Central Limit Theorem), but also the tendency for the negative skewness to persist.

A generalized set of probabilistic models can be obtained by transforming the "standardized" random variable (introduced above), $U^{(\nu)} = L_\nu/(\nu\alpha)^{1/2}$, modifying its zero mean (by adding a constant) and unit variance (by multiplying by another constant); the result is a three-parameter (quantum-physics-based) family of distributions characterized by their mean, variance, and coefficient of skewness, the latter dependent only on ν. A similar transformation of the random variable $V^{(\nu)} \equiv \exp\{U^{(\nu)}\}$ results in a generalized set of PDFs of which $f_{W_\nu}(w)$ are members. These probability models can capture very different types of behavior of random variables (characterized in part by their variability and skewness); the PDFs tend toward the normal (for sums) and lognormal (for products) as the number ν of i.i.d. basic random variables grows. Skewness persists, however, and the tails of the probability distributions, on both the low and high ends, continue to differ greatly from the normal and lognormal distributions, even when ν becomes large. The PDF of the largest (or smallest) value in a group of i.i.d. values of L can also be expressed straightforwardly in terms of the PDF of L and the group size ν.

There appear to be many opportunities for application to system reliability analysis (see, e.g., [4–6]). In single-mode reliability analysis, the focus is often on the *safety margin,* defined as the difference between the random load and the random resistance, or the *safety factor,* defined as the quotient of resistance to load. (A parallel formulation, in economic applications, may be in terms of "supply" and "demand," or "capacity" and "demand".) The two random quantities (i.e., load and resistance) are typically assumed to be statistically independent. The new probability models could be adopted for load and resistance separately, or be applied directly to the safety margin or the safety factor. The safety margin, for example, might be characterized by its mean (above zero) and coefficient of variation; its skewness could also strongly affect the (single-mode) failure probability (i.e., the probability that the actual safety margin is negative). This readily leads to a new set of relationships between, for example, the mean safety margin and the probability of failure (and corresponding reliability indices that depend on the coefficients of variation and skewness).

System reliability concerns the behavior of groups of components or failure modes and the logical relationships between component failures and system failure. In these problem situations as well, the new probabilistic models can be adopted for (or based on data, fitted to) the random "modal" safety margins or safety factors, or the mode-specific loads and resistances, enabling the system reliability to be estimated or bounded (see, e.g., [7]) These bounds are related to the degrees of statistical dependence between the loads and resistances associated with the different failure modes. Here too, the proposed models provide new analytical tools to express statistical dependence. In particular, statistical dependence between, say, component resistances can be realized or simulated by assuming shared (identical) values for some of the basic random variables being summed or multiplied in the process of modeling each failure mode's resistance.

16.7 Conclusion

The probability density functions of a number of functionally related properties of single energy quanta — particles like photons — in thermal equilibrium have been derived from the Planck radiation spectrum. The "quantum mass ratio" W, its reciprocal, the "quantum size ratio" $D = W^{-1}$, and the logarithm $L = \log W = -\log D$ are coupled random properties of individual energy quanta. The ratios W and D have a unit geometric mean, $\overline{W} = \overline{D} = 1$, while the arithmetic mean of their logarithm is

Copyright 2005 by CRC Press LLC

zero, $\langle L \rangle = \langle \log W \rangle = \langle \log D \rangle = 0$. The variance of the mass ratio logarithm, $\alpha \equiv Var[L] \approx 0.5672$, measures the intrinsic uncertainty of properties of single energy quanta in thermal equilibrium, for any LTE temperature in the range $0 < T < T_{Pl} \approx 10^{32} K$.

The idea is that any quantum-producing "engine" simultaneously gives rise to quantum-physical uncertainty. Wherever individual energy quanta are copiously created, the *least* amount of variability realizable is that associated with a single, unique Planck spectrum, with a constant temperature $T = T^*$, characterized by PDFs and variability as measured by $\alpha = Var[L] = Var[\log W] \approx 0.5672$.

Heisenberg's Uncertainty Principle expresses a fundamental constraint on the precision of paired quantum-scale observations: the product of "errors" in joint measurements of, say, a particle's position and momentum must be greater than or equal to the quotient of Planck's constant *hp* and 2π. The measure of inherent uncertainty of the properties of energy quanta in thermal equilibrium, $\alpha = Var[L] = Var[\log W] \approx 0.5672$, differs from Heisenberg's classical formulation in that it (1) expresses an equality instead of an inequality; (2) involves only a single attribute (of a quantum of radiation), or one attribute at a time, instead of two; and (3) does not depend on Planck's constant, a tiny number. A further advantage is that the description of quantum-physical uncertainty in terms of $f_L(\ell)$ or $f_W(w)$ or D extends beyond second-order statistics, thereby enabling one to evaluate the relative likelihood of extreme values, high or low, of quantum properties. We have shown that the new probability models have considerable potential for practical application to single-mode and system reliability analysis.

Acknowledgment

The author is grateful to Ian Buck and Ernesto Heredia-Zavoni for their assistance with the computations needed to generate the figures.

References

1. Planck, M. (1900). *Verh. Deutsche Phys. Ges.,* 2, 237; and in [2] Abramowitz, M. and Stegun, I.A. (1965). *Handbook of Mathematical Functions*, New York: Dover.
2. Abramowitz, M. and Stegun, I.A. (1965). *Handbook of Mathematical Functions*, New York: Dover.
3. Vanmarcke, E.H. (1997), *Quantum Origins of Cosmic Structure*, Rotterdam, Holland and Brookfield, VT: Balkema.
4. Barlow, R.E. and Proschan, F, (1975). *Statistical Theory of Reliability and Life Testing*, New York: Holt, Rinehart and Winston.
5. Freudenthal, A.M. (1947). "The Safety of Structures," *Trans. ASCE*, Vol. 112.
6. Madsen, H.O., Krenk, S., and Lind, N.C. (1986). *Methods of Structural Safety*, Englewood Cliffs, NJ: Prentice Hall.
7. Cornell, C.A. (1967). "Bounds on the Reliability of Structural Systems," *Journal of the Structural Division*, ASCE, 93, 171–200.

Copyright 2005 by CRC Press LLC

17

Probabilistic Analysis of Dynamic Systems

Efstratios Nikolaidis
The University of Toledo

17.1 Introduction and Objectives

Many engineering systems are subjected to loads that are random processes, e.g., random functions. The following are some examples: the wings of an airplane under gust loads, the hull of a ship under wave loads, and an offshore platform under wave loads. Moreover, the properties of many systems, such as their strength (stress at failure) are random and vary in time. The objectives of a random vibration study are to determine the statistics of the response of a system and the probability of failure due to the response. Tools for time invariant reliability problems, such as FORM and SORM, are not directly applicable to random vibration analysis.

Probabilistic analysis of a dynamic system under loads that are random processes involves the following steps:

1. Construct probabilistic models of the excitations. Here we model the excitations using data obtained from measurements and experience. Usually, the excitations are characterized using their means, autocorrelations, and cross-correlations.
2. Calculate the statistics of the response.
3. Calculate of the probability of failure. Failure can occur if the response exceeds a certain level (first excursion failure) or due to accumulation of fatigue damage (fatigue failure). An example of first excursion failure is the collapse of a structure because the stress exceeds a threshold.

This chapter first reviews methods for completing the above three steps, for a general dynamic system with deterministic strength under time varying random excitation. Then the chapter considers special

Copyright 2005 by CRC Press LLC

cases where the system of interest is linear or nonlinear. Finally, this chapter explains how to calculate the reliability of a dynamic system when its strength is uncertain.

This chapter studies methods for analysis of systems in which uncertainties are represented as random processes. Chapter 20, "Stochastic Simulation Methods for Engineering Predictions," and Chapter 21, "Projection Schemes for Stochastic Finite Element Analysis," consider random fields.

17.2 Probabilistic Analysis of a General Dynamic System

This section reviews the theory for representing the excitation of dynamic systems using random processes, finding the response of these systems, and determining their probability of failure.

17.2.1 Modeling Random Processes

17.2.1.1 Random Processes and Random Fields

Random process is a random function, $X(t)$, of one parameter, t. Parameter t is called the *index parameter* of the process and can assume discrete values $\{t_1, \ldots, t_i, \ldots\}$ or continuous values in a range, $t \in [0, \infty]$. In the latter case, the random process is called *continuously parametered* or *continuously indexed*. Parameter t usually represents time, but it can represent some other quantity, such as the distance from a reference point. The value of $X(t)$ at a particular value of parameter $t = t_0$, $X(t_0)$, is a random variable.

We can view a random process as a set of possible *time histories*; each time history (or *sample path*) shows the variation of the process with t for a particular realization of the process.

Example 17.1

Figure 17.1 shows four realizations of the elevation, $X(s)$, of a road covered with concrete slabs as a function of the distance, s, from a reference point. The slabs have fixed length and random height. This set of time histories is called *sample* or *ensemble* of time histories.

The concept of *random fields* is a generalization of the concept of random processes. A random field is a random function of two or more parameters. The modulus of elasticity at a point in a solid, $E(x, y, z)$, varies with the location of the point (x, y, z) and is random. In this case, the modulus of elasticity is a

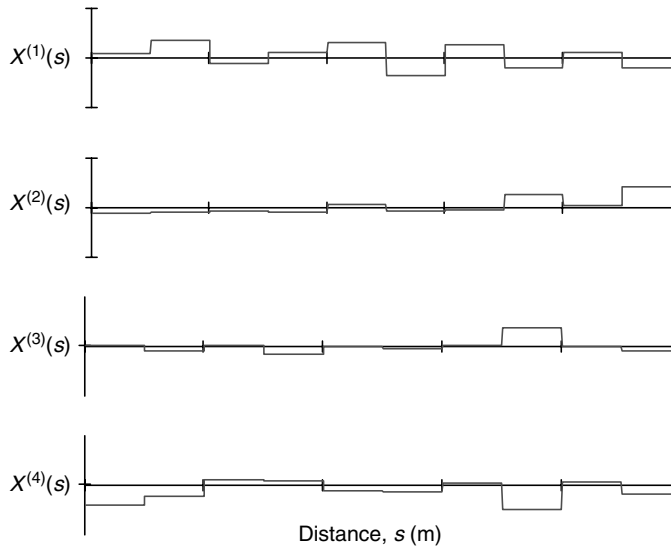

FIGURE 17.1 Four time histories of the elevation of a road covered with concrete labs of fixed length and random height.

Copyright 2005 by CRC Press LLC

random field because it is a random function of the three coordinates of the point of interest. The velocity field in a turbulent flow is also a random field. This is described by the velocity vector $\mathbf{V}(x, y, z, t)$, where (x, y, z) are the coordinates of the point of interest and t is time.

17.2.1.2 Probabilistic Models of Random Processes

A complete probabilistic model of a random process involves the joint probability distribution of the values of the random process for all possible values of the independent parameter. This information is impractical to obtain in most cases. We usually calculate only the first- and second-order statistics of the responses (i.e., their means, autocorrelations, and cross-correlations) because:

- It is impractical to collect sufficient data to determine the higher-order statistics.
- In many problems, we assume that the random processes involved are jointly Gaussian. Then, the first- and second-order statistics define completely the processes.
- Even if the processes involved are not Gaussian, the first two moments contain important information. For example, we can determine an upper bound for the probability that the value of the process at an instant can be outside a given range centered about the mean value using Chebyshev inequality [1, 2].

The first two moments of a single random process include the mean value, $E(X(t))$, and the *autocorrelation* function:

$$R_{XX}(t_1, t_2) = E(X(t_1)X(t_2))$$

where t_1 and t_2 are two time instances at which the value of the process is observed. We can also define the autocorrelation function in terms of parameter $t = t_2$, and the elapsed time between the two observations, $\tau = t_1 - t_2$.

The *autocovariance* of a random process is:

$$C_{XX}(t_1, t_2) = E[(X(t_1) - E(X(t_1)))(X(t_2) - E(X(t_2)))].$$

For two random processes, we also need to define their *cross-correlation*. This function shows the degree to which the two processes tend to move together. The cross-correlation function of two random processes, $X_1(t)$ and $X_2(t)$, is defined as follows:

$$R_{X_1X_2}(t_1, t_2) = E(X_1(t_1)X_2(t_2)).$$

The *cross-covariance* of two random processes is defined as follows:

$$C_{X_1X_2}(t_1, t_2) = E[(X_1(t_1) - E(X_1(t_1)))(X_2(t_2) - E(X_2(t_2)))].$$

In the remainder of this chapter, we will consider only random processes with zero mean values. Therefore, their autocorrelation and cross-correlation are equal to their autocovariance and cross-covariance, respectively. If a random process has nonzero mean, then we transform it into a process with zero mean by subtracting the mean from this process.

Example 17.2

Consider a vehicle traveling with constant speed, $V = 100$ km/hr, on the road made of concrete slabs in Figure 17.1. The length of a slab is 10 m. Assume that the wheels are always in contact with the road. Then, the vertical displacement of a wheel is $X(t)$, where $t = s/V$ and $X(.)$ is the road elevation. Figure 17.2 shows the autocorrelation function of the displacement, $R_{XX}(t + \tau, t)$. The autocorrelation is constant

Copyright 2005 by CRC Press LLC

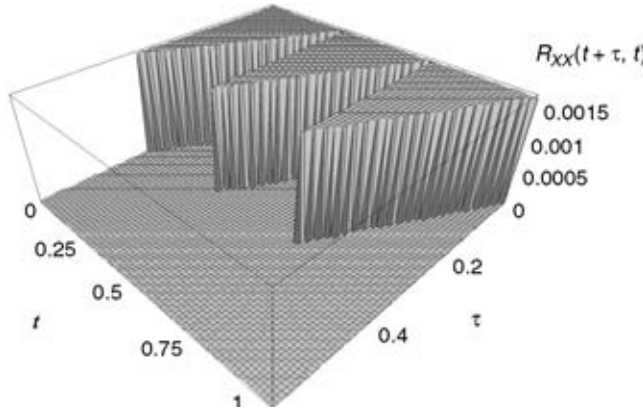

FIGURE 17.2 Autocorrelation of the displacement of the wheel of a car traveling with constant speed on the road made of concrete slabs in Fig. 1.

and equal to the variance of the displacement when the wheel is on the same slab at both instances t and $t + \tau$. Otherwise, it is zero.

A random process can be *stationary* or *nonstationary*. A stationary process is one whose statistics are invariant under time shifts. Otherwise, the process is nonstationary.

The concept of stationarity in random processes corresponds to the concept of steady-state in deterministic functions of time. The wave elevation and the wind speed at a given point in the Atlantic Ocean can be considered stationary during short periods during which weather conditions do not change significantly. The force applied to the landing gear of an airplane during landing is a nonstationary process because this force changes rapidly in time.

A random process, $X(t)$, is called *strictly stationary* if the joint probability density function (pdf) of the process at all possible time instances is invariant under time shifts. Therefore,

$$\begin{aligned} &f_{X(t+\tau)}(x) = f_{X(t)}(x) \\ &f_{X(t_1+\tau),X(t_2+\tau)}(x_1, x_2) = f_{X(t_1),X(t_2)}(x_1, x_2) \\ &\vdots \\ &f_{X(t_1+\tau),X(t_2+\tau),\ldots,X(t_n+\tau)}(x_1, x_2, \ldots, x_n) = f_{X(t_1),X(t_2),\ldots X(t_n)}(x_1, x_2, \ldots, x_n) \end{aligned} \tag{17.1}$$

where $f_{X(t_1),X(t_2),\ldots X(t_n)}(x_1, x_2, \ldots, x_n)$ is the joint PDF of the random process at t_1, t_2, …, and t_n, respectively. In this case, the moments of $X(t)$ are also invariant under time shifts.

Example 17.3

The elevation of the road consisting of concrete slabs in Figure 17.1 is a nonstationary random process. The reason is that the joint pdf of this process at two locations, s_1 and s_2, changes under a distance shift. This is the reason for which the autocorrelation function of the displacement of the wheel in Figure 17.2 varies with t.

Random processes are *jointly stationary* in the strict sense if the joint pdfs of any combinations of values of these processes are invariant under time shifts.

A random process is *stationary in the wide sense* (or *weakly stationary*) if its mean value and autocorrelation function are invariant under shifts of time:

$$E(X(t)) = \text{constant} \tag{17.2}$$

$$R_{XX}(t_1, t_2) = R_{XX}(\tau) \tag{17.3}$$

where $\tau = t_1 - t_2$. Note that the autocorrelation function is an even function of τ.

Copyright 2005 by CRC Press LLC

It is often convenient to work with the *power spectral density* (PSD) function of a weakly stationary process, $X(t)$, instead of the autocorrelation. The reason is that it is easy to find the PSD of the response from that of the input for linear systems. The PSD, $S_{XX}(\omega)$, is the Fourier transform of the autocorrelation:

$$S_{XX}(\omega) = \int_{-\infty}^{+\infty} R_{XX}(\tau) e^{-i\omega\tau} d\tau. \tag{17.4a}$$

The PSD shows the distribution of the energy of a random process over the frequency spectrum. Note that the PSD is a real positive number because it is the Fourier transform of a real, even function. Moreover, the PSD is an even function of the frequency. The autocorrelation function is the inverse Fourier transform of the PSD function:

$$R_{XX}(\tau) = \frac{1}{2\pi} \int_{-\infty}^{+\infty} S_{XX}(\omega) e^{-i\omega\tau} d\omega. \tag{17.4b}$$

Random processes are *jointly stationary in the wide sense* if each of them is stationary and their cross-correlations are functions of τ only. The *cross spectral* density function of two jointly stationary processes is calculated using an equation similar to Equation 17.4b. The *spectral matrix* of a vector of random processes contains the power spectral densities and cross spectral densities of these random processes.

If a random process is stationary in the strict sense, then it is also stationary in the wide sense.

Example 17.4

The elevation of a rough road, X(s), is modeled as a stationary Gaussian random process with autocorelation function $R_{XX}(d) = \sigma^2 \exp(|d|/0.5)$, where d is the distance between two locations, s and $s + d$, in meters (m); and σ is the standard deviation of the road elevation. The standard deviation, σ, is 0.02 m. A car travels on the road with constant speed $V = 16$ m/sec. Find the PSD of the wheel of the car, assuming that it remains always in contact with the ground.

The distance that a wheel travels is $s = V t$. Therefore, the autocorrelation of the elevation of the wheel at two time instances, $t + \tau$ and t, is equal to the autocorrelation function of the road elevation at two locations separated by distance $V\tau$:

$$R_{XX}(\tau) = \sigma^2 e^{-\frac{|V\tau|}{0.5}} = \sigma^2 e^{-32|\tau|}.$$

The units of the autocorrelation are m^2.

The PSD is the Fourier transform of the autocorrelation function. Using Equation 17.4a we find that the PSD is:

$$S_{XX}(\omega) = \sigma^2 \frac{64}{\omega^2 + 32^2}.$$

Figure 17.3 shows the PSD for positive values of frequency.

17.2.2 Calculation of the Response

In the analysis of a dynamic system we construct a mathematical model of the system. For this purpose, we construct a *conceptual model* that simulates the behavior of the actual system. A conceptual model can be an assembly of discrete elements (such as masses, springs, and dampers) or continuous elements (such as beams and plates). By applying the laws of mechanics, we obtain a deterministic mathematical model of the system relating the responses to the excitations. This is usually a set of differential equations relating the response (output) vector, $\mathbf{Y}(t)$, to the excitation (input) vector, $\mathbf{X}(t)$.

Copyright 2005 by CRC Press LLC

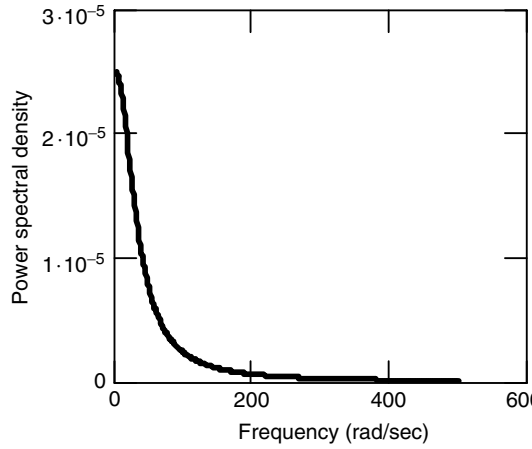

FIGURE 17.3 Power spectral density of road elevation in example 4.

A dynamic system can by thought as a multi-input, multi-output system, such as the one in Figure 17.4. Inputs and outputs are the elements of the excitation vector and response vector, respectively. The following equation relates the response to the excitation:

$$\mathbf{D}(\mathbf{p}, t)[\mathbf{Y}(t)] = \mathbf{X}(t) \tag{17.5}$$

where $\mathbf{D}(\mathbf{p}, t)[.]$ is a matrix of differential operators applied to the elements of the response. The size of $\mathbf{D}(\mathbf{p}, t)[.]$ is $m \times n$, where m is the number of inputs and n is the number of outputs. $\mathbf{p}$ is a set of parameters associated with the system. We can solve Equation 17.5 analytically or numerically to compute the response.

Many single-input, single-output systems can be analyzed using a *Volterra series* expansion:

$$Y(t) = \sum_{i=1}^{\infty} \int_{-\infty}^{t} \cdots \int_{-\infty}^{t} h_i(t, t_1, \ldots, t_i) \prod_{j=1}^{i} X(t_j) dt_j. \tag{17.6}$$

Functions $h_i(t, t_1, \ldots, t_i)$, $i = 1, \ldots, n$ are called *Volterra kernels* of the system.

Systems can be categorized as linear and nonlinear, depending if operator $\mathbf{D}(\mathbf{p}, t)$ is linear or nonlinear. For a linear system, the superposition principle holds and it allows us to simplify greatly the equation

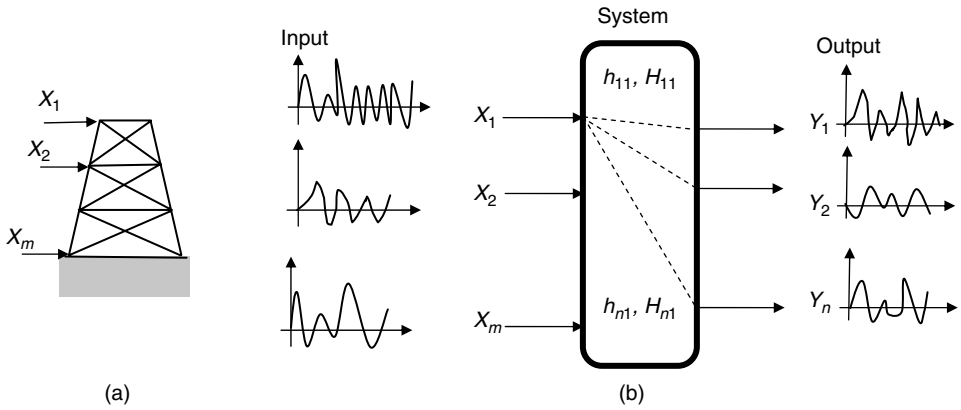

FIGURE 17.4 A structure subjected to excitations $X_1, \ldots, X_m$, and its representation as a multi-input, multi-output system.

Copyright 2005 by CRC Press LLC

for finding the response of the system. Specifically, we can break down the excitation into a series of impulses, find the response to each impulse separately, and then superimpose the responses to find the response of the system. The response can be found as follows:

$$Y(t) = \int_{-\infty}^{t} h(t, t_1) X(t_1) dt_1 \tag{17.7}$$

$h(t, t_1)$ is called *impulse response function*, or *Green's function*. This function represents the response of a system at time t due to a unit impulse that was applied at time t_1. Note that Equation 17.6 reduces to the *convolution integral* in Equation 17.7 if we set $h_i(t, t_1, \ldots, t_i) = 0$ for $i \geq 2$.

Dynamic systems can be also classified under the following categories:

- *Time invariant systems whose parameters are deterministic.* An example is a system that consists of a spring, a mass, and a viscous damper of which the rate of the spring, the mass, and the damping coefficient are deterministic constants. The response of a time invariant system at time t depends only on the elapsed time between the instant at which the excitation occurred and the current time t. Therefore, $h_i(t, t_1, ..., t_i) = h_i(t - t_1, ..., t - t_i)$. If a time invariant system is also linear, the response is:

$$Y(t) = \int_{-\infty}^{t} h(t - t_1) X(t_1) dt_1. \tag{17.8}$$

- *Time invariant systems whose parameters,* **p**, *are random and time invariant.* In this case parameters, **p**, are random variables.
- *Time variant systems whose parameters are deterministic and are functions of time.* An example is a rocket whose mass decreases as fuel is burned.
- *Time variant systems whose parameters are random.* The parameters of these systems can be modeled as random processes.

Clearly, Equation 17.6 through Equation 17.8 cannot be used directly to assess the safety of a dynamic system because the response is random, which means that it is not enough to know the response due to a given output. We need a relation of the statistical properties of the response (such as the mean and autocorrelation function) to the statistical properties of the excitation. We can calculate the statistical properties of the response using Monte Carlo simulation methods or analytical methods. Analytical methods are described in the following two sections for both linear and nonlinear systems.

Example 17.5

Consider a linear single-degree-of-freedom model of the car traveling on the road in Example 17.4. The model consists of a mass, m, representing the sprung mass, a spring, k, and a damper, c, in parallel representing the suspension and tire (Figure, 17.5). Input is the displacement of the wheel, $x(t)$, and output is the displacement, $y(t)$, of mass, m. The system is underdamped; that is $\zeta = c/(2\sqrt{km}) < 1$. Find the impulse response function.

The equation of motion is $m\ddot{y} + c\dot{y} + ky = kx + c\dot{x}$. Therefore, the transfer function is:

$$H(s) = \frac{Y(s)}{X(s)} = \frac{\omega_n^2 + 2\zeta\omega_n s}{s^2 + 2\zeta\omega_n s + \omega_n^2}$$

where $\omega_n = \sqrt{\frac{k}{m}}$ is the natural frequency. $Y(s)$ and $X(s)$ are the Laplace transforms of the displacements of mass m and the wheel, respectively.

Copyright 2005 by CRC Press LLC

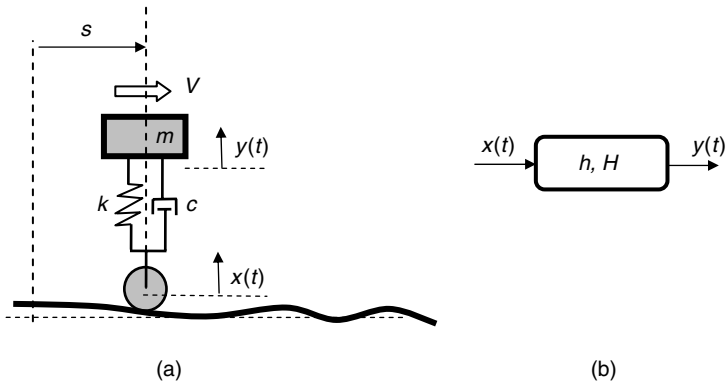

FIGURE 17.5 Model of a vehicle traveling on a rough road and its representation as a single-input, single-output system.

The impulse response function is the inverse Laplace transform of the transfer function:

$$h(\tau) = \frac{\omega_n}{\sqrt{1-\zeta^2}} e^{-\zeta\omega_n\tau} \sin(\omega_d t) - \frac{2\zeta\omega_n}{\sqrt{1-\zeta^2}} e^{-\zeta\omega_n\tau} \sin(\omega_d\, t - \phi)$$

$$\text{where, } \phi = \tan^{-1}\frac{\sqrt{1-\zeta^2}}{\zeta}, \quad \text{and} \quad \omega_d = \omega_n\sqrt{1-\zeta^2}.$$

17.2.3 Failure Analysis

A structure subjected to a random, time-varying excitation can fail in two ways: (1) the response exceeds a certain level (e.g., the wing of an aircraft flying in gusty weather can break if the stress exceeds a maximum allowable value), and (2) the excitation causes fatigue failure. In this section, we only consider failure due to exceedance of a level. This type of failure is called *first excursion failure* (Figure 17.6). The objective of this section is to review methods to calculate the probability of first excursion failure during a given period. Fatigue failure is analyzed in the next section.

In general, the problem of finding the probability of first excursion failure during a period is equivalent to the problem of finding the probability distribution of the maximum of a random vector that contains infinite random variables. These variables are the values of the process at all time instants within the period. No closed form expression exceeds for the first excursion probability for a general random process.

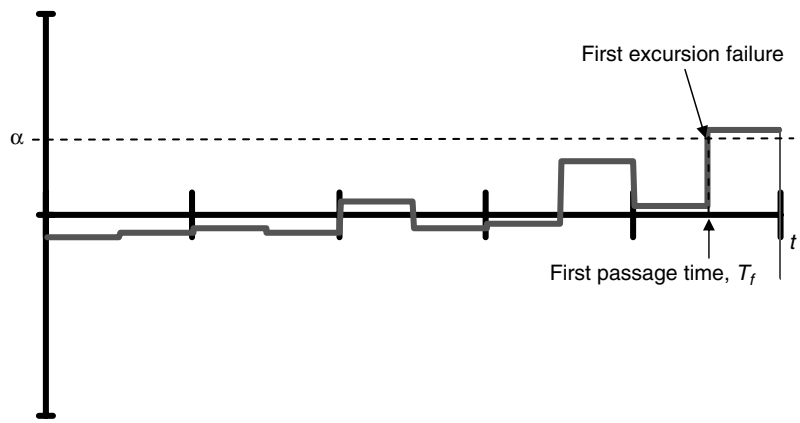

FIGURE 17.6 Illustration of first excursion failure.

Copyright 2005 by CRC Press LLC

Approximate results are available for some special cases. In this section, we review methods to estimate the following quantities for a random process:

- The number of crossings of a level α over a period
- The pdf of the peaks
- The pdf of the first passage time, T_f, which is the time at which the process upcrosses a certain level for the first time (Figure 17.6)

Nigam [1] presents an overview of the methods to estimate the probability of first excursion failure.

17.2.3.1 Number of Crossings of a Level during a Period

Most of the results that we will review have been presented in two seminal papers by Rice [3].

In general, the *average upcrossing rate* (average number of upcrossings of a level α per unit time) at time t is:

$$\nu^+(\alpha, t) = \int_0^\infty \dot{x} f_{X(t),\dot{X}(t)}(\alpha, \dot{x}, t) d\dot{x} \tag{17.9}$$

where $\nu^+(\alpha, t)$ is the average number of upcrossing, and $f_{X(t),\dot{X}(t)}(x, \dot{x}, t)$ is the joint pdf of the process and its velocity.

For a stationary process, this joint density is independent of time: $f_{X(t),\dot{X}(t)}(x, \dot{x}, t) = f_{X(t),\dot{X}(t)}(x, \dot{x})$. Therefore, the average upcrossing rate is also independent of time. The average number of upcrossings over a period T is $\nu^+(\alpha)T$.

17.2.3.2 Probability Density Function of the Peaks

A random process can have several peaks over a time interval T (Figure 17.7). Let $M(\alpha, t)$ be the expected number of peaks above level α per unit time. Then:

$$M(\alpha, t) = \int_\alpha^\infty \int_{-\infty}^0 |\ddot{x}| f_{X(t),\dot{X}(t),\ddot{X}(t)}(\alpha, 0, \ddot{x}) d\ddot{x}\, dx \tag{17.10}$$

where $f_{X(t),\dot{X}(t),\ddot{X}(t)}(x, \dot{x}, \ddot{x})$ is the joint pdf of $X(t)$ and its first two derivatives at t.

The expected number of peaks per unit time regardless of the level, $MT(t)$, is obtained by integrating Equation 17.10 with respect to x from $-\infty$ to $+\infty$:

$$MT(t) = \int_{-\infty}^0 |\ddot{x}| f_{\dot{X}(t),\ddot{X}(t)}(0, \ddot{x}) d\ddot{x}. \tag{17.11}$$

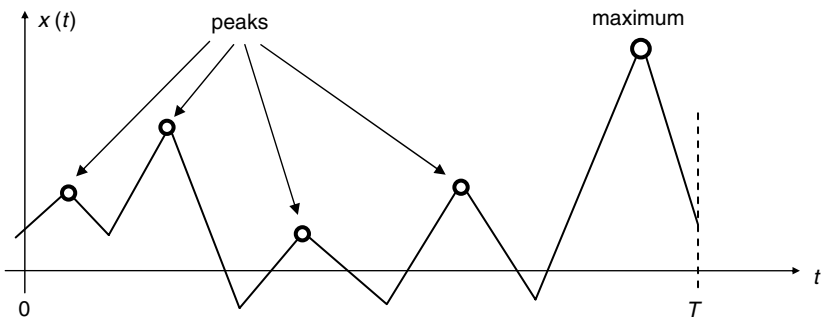

FIGURE 17.7 Local peaks and maximum value of random process, $X(t)$, during period $[0, T]$.

Copyright 2005 by CRC Press LLC

We can find the cumulative probability distribution of a peak at a level by normalizing the expected number of peaks below that level by the expected number of peaks regardless of the level. The pdf of a peak is the derivative of the cumulative distribution of a peak with respect to the level. It can be shown that this pdf of a peak at level α is:

$$f_{peak}(\alpha, t) = \frac{1}{MT(t)} \int_{-\infty}^{0} |\ddot{x}| f_{X(t),\dot{X}(t),\ddot{X}(t)}(\alpha, 0, \ddot{x}) d\ddot{x}. \tag{17.12}$$

17.2.3.3 First Passage Time

Here, the objective is to find the probability distribution of the first passage time, T_f (Figure 17.6). First, we will find the probability distribution of the first passage time for stationary processes and then for nonstationary processes.

Consider a stationary process. If the level is high (e.g., larger than the mean value plus six standard deviations of the process), the upcrossing process can be assumed to be a Poisson process with stationary increments and with interarrival rate $\nu^+(\alpha)$. Then the first passage time, T_f, follows the exponential distribution:

$$F_{T_f}(t) = 1 - e^{-\nu^+(\alpha)t}. \tag{17.13}$$

The average crossing rate can be calculated using Equation 17.9. Both the mean value and standard deviation of the first passage time are equal to the inverse of the average crossing rate.

The probability of first excursion failure, $P(F)$, is the probability that the process will exceed α during the time interval $(0, T)$. This is equal to the probability of the first passage time being less than T:

$$P(F) = 1 - e^{-\nu^+(\alpha)T}. \tag{17.14}$$

The above approach assumes that the peaks of the process are statistically independent. However, subsequent peaks are usually positively correlated, especially if the process is narrowband (e.g., the energy of the process is confined to a narrow frequency range). Yang and Shinozuka [4, 5] proposed a method to account for correlation between subsequent peaks of a process assuming that these peaks are subjected to a Markov chain condition.

If a random process is nonstationary, the average crossing rate is a function of time, $\nu^+(\alpha, t)$. Then the probability of first excursion failure during an interval $[0, T]$ becomes:

$$P(F) = 1 - e^{-\int_0^T \nu^+(\alpha,t)\,dt}. \tag{17.15}$$

The value of the cumulative probability distribution of the first passage time, T_f, is equal to the probability of failure during the period $[0, t]$:

$$F_{T_f}(t) = P(T_f \le t) = P(F) = 1 - e^{-\int_0^t \nu^+(\alpha,\tau)\,d\tau}. \tag{17.16}$$

17.3 Evaluation of Stochastic Response and Failure Analysis: Linear Systems

Closed form, analytical solutions for the response of a linear system to random excitations are available and will be presented here. Results for analysis of failure due to first excursion and fatigue will also be presented.

Copyright 2005 by CRC Press LLC

17.3.1 Evaluation of Stochastic Response

The following two subsections present a method for finding the response of a dynamic system to stationary and nonstationary inputs, respectively.

17.3.1.1 Response to Stationary Inputs

We calculate the autocorrelation and cross-correlations of the responses in three steps:

1. Measure or calculate the PSD of the excitation or the spectral matrix of the excitations. The PSD can be measured directly or it can be derived from the autocorrelation function of the excitation. Similarly, the cross spectral density can be estimated directly or it can be found by calculating the Fourier transform of the cross-correlation.
2. Derive the PSD or the spectral matrix of the response. Consider a linear system with m inputs and n outputs, such as a structure subjected to m loads, for which n stress components are to be calculated. We can consider the structure as a multi-input, multi-output system as shown in Figure 17.4. The second-order statistics of the output are characterized by the spectral matrix of the output, $\mathbf{S_{YY}}(\omega)$, which is calculated as follows:

$$\mathbf{S_{YY}}(\omega) = \mathbf{H}(\omega)\mathbf{S_{XX}}(\omega)\mathbf{H}^{T^*}(\omega). \tag{17.17}$$

   $\mathbf{H}(\omega)$ is an $n \times m$ matrix, whose entry at the i, j position is the sinusoidal transfer function, $H_{ij}(\omega)$, corresponding to the j-th input and i-th output. Sinusoidal transfer function is the Fourier transform of the impulse response function. Superscript T denotes the transpose of a matrix and * complex conjugate. For a single-input, single-output system, the above equation reduces to:

$$S_{YY}(\omega) = |H(\omega)|^2 S_{XX}(\omega) \tag{17.18}$$

   where $S_{XX}(\omega)$ is the PSD of the input, $S_{YY}(\omega)$, is the PSD of the output, and $H(\omega)$ is the sinusoidal transfer function of the system.
2. The autocorrelation and cross-correlation functions of the outputs are the inverse Fourier transforms of the PSDs and cross spectral densities of the corresponding components of the outputs. Using this information we can derive the variances, covariances, and their derivatives with respect to time, which are useful in analysis of failure due to first excursion.

Example 17.6

Find the PSD of the displacement of the vehicle, $Y(t)$, in the Example 17.5. The mass of the vehicle is m = 1,300 kg, the rate of the spring is k = 11,433 m/N, and the viscous damping coefficient is c = 600 N sec/m.

The undamped natural frequency of the system is ω_n = 2.96 rad/sec or 0.472 cycles/sec. The damping ratio is 0.31. The sinusoidal transfer function of this system is:

$$H(\omega) = \frac{k + i\omega c}{-m\omega^2 + k + i\omega c}.$$

Using Equation 17.18 we find the PSD of the displacement $Y(t)$. The PSD is shown in Figure 17.8. Note that the energy of vibration is confined to a narrow range around 3 rad/sec. The reason is that the system acts as a narrowband filter filtering out all frequencies outside a narrow range around 3 rad/sec.

17.3.1.2 Response to Nonstationary Inputs

The inputs are nonstationary in some practical problems. In these problems, the responses are nonstationary.

Copyright 2005 by CRC Press LLC

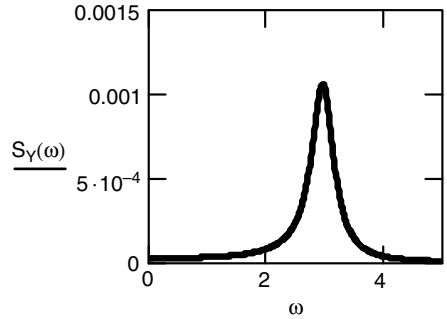

FIGURE 17.8 PSD of the displacement of the mass in Fig. 5.

The *generalized spectral density* of a nonstationary process is defined as the generalized Fourier transform of the covariance, $C_{XX}(t_1, t_2)$, [2]:

$$S_{XX}(\omega_1, \omega_2) = \int_{-\infty}^{+\infty} \int_{-\infty}^{+\infty} C_{XX}(t_1, t_2) e^{-i(\omega_1 t_1 - \omega_2 t_2)} dt_1 dt_2. \tag{17.19}$$

The generalized spectral density of the output of a single-input, single-output linear system can be calculated from the generalized spectral density of the input as follows:

$$S_{YY}(\omega_1, \omega_2) = S_{XX}(\omega_1, \omega_2) H(\omega_1) H^*(\omega_2). \tag{17.20}$$

Note that Equation 17.20 is analogous to Equation 17.17 for the stationary case.

Following are some studies of the response of structures to nonstationary excitation:

- Caughey and Stumpf [6]: study of the transient response of a single-degree-of-freedom system under white noise excitation
- Fung [7]: analysis of stresses in the landing gear of an aircraft
- Amin [8]: analysis of the response of buildings to earthquakes
- Nikolaidis, Perakis, and Parsons [9]: analysis of torsional vibratory stresses in diesel engine shafting systems under a special class of nonstationary processes whose statistics vary periodically with shifts of time

17.3.2 Failure Analysis

17.3.2.1 First Excursion Failure

The average crossing rate for a zero mean, Gaussian, stationary process is:

$$\nu^+(\alpha) = \nu^+(0) e^{-\frac{\eta^2}{2}} \tag{17.21}$$

where $\nu^+(0)$ is the expected rate of zero upcrossings, obtained by the following equation:

$$\nu^+(0) = \frac{1}{2\pi} \cdot \frac{\sigma_{\dot{X}}}{\sigma_X} \tag{17.22}$$

and η = normalized level = $\frac{\alpha}{\sigma_X} \cdot \sigma_X^2$ is the variance of the process and $\sigma_{\dot{X}}^2$ is the variance of the derivative of the process:

$$\sigma_{\dot{X}}^2 = \frac{1}{2\pi} \int_{-\infty}^{+\infty} S_{\dot{X}\dot{X}}(\omega) d\omega = \frac{1}{2\pi} \int_{-\infty}^{+\infty} \omega^2 S_{XX}(\omega) d\omega.$$

Copyright 2005 by CRC Press LLC

Once we have calculated the average upcrossing rate, we can estimate the probability of first excursion failure from Equation 17.14.

The peaks (both positive and negative) of a stationary Gaussian process with zero mean follow the *Rice pdf*. This is a weighted average of a Gaussian pdf and a Rayleigh pdf:

$$f_{peak}(\alpha) = (1-\xi^2)^{1/2} \frac{1}{(2\pi)^{1/2}\sigma_X} e^{-\frac{\alpha^2}{2\sigma_X^2(1-\xi^2)}} + \xi\Phi\left[\frac{\xi\alpha}{\sigma_X(1-\xi^2)^{1/2}}\right]\frac{\alpha}{\sigma_X^2} e^{-\frac{\alpha^2}{2\sigma_X^2}} \tag{17.23a}$$

where $\Phi(.)$ is the cumulative probability distribution function of a standard Gaussian random variable (zero mean, unit standard deviation). Parameter ξ is the ratio of the expected zero upcrossing rate to the expected rate of peaks: $\xi = \nu^+(0)/MT = \sigma_{\dot{X}}^2/(\sigma_X\sigma_{\ddot{X}})$. This parameter is called *bandwidth parameter,* and it expresses the degree to which the energy of the random process is confined to a narrow frequency range. The derivation of the Rice pdf can be found in the book by Lutes and Sarkani [10, pp. 491–492]. $\sigma_{\ddot{X}}^2$ is the variance of the acceleration:

$$\sigma_{\ddot{X}}^2 = \frac{1}{2\pi}\int_{-\infty}^{+\infty} S_{\ddot{X}\ddot{X}}(\omega)d\omega = \frac{1}{2\pi}\int_{-\infty}^{+\infty} \omega^4 S_{XX}(\omega)d\omega.$$

The pdf of the normalized level, $\eta = \alpha/\sigma$, is:

$$f_H(\eta) = f_{peak}(\eta\sigma)\sigma. \tag{17.23b}$$

A narrowband process is a process whose energy is confined to a narrow frequency range. The number of peaks of a narrowband process is almost equal to the number of zero upcrossings. Therefore, the bandwidth parameter is close to one ($\xi \cong 1$). If a stationary Gaussian process is also narrowband, then the peaks follow the Rayleigh pdf:

$$f_{peak}(\alpha) = \frac{\alpha}{\sigma_X^2} e^{-\frac{\alpha^2}{2\sigma_X^2}} \cdot 1(\alpha) \tag{17.24a}$$

where $1(\alpha)$ is a unit step function (e.g., a function that is one for positive values of the independent variable and zero otherwise).

At the other extreme, a broadband process has bandwidth parameter equal to zero ($\xi = 0$). Then the pdf of the peaks reduces to a Gaussian density:

$$f_{peak}(\alpha) = \frac{1}{(2\pi)^{1/2}\sigma_X} e^{-\frac{\alpha^2}{2\sigma_X^2}}. \tag{17.24b}$$

Shinozuka and Yang [11], and Yang and Liu [12] estimated the probability distribution of the peaks of a nonstationary process. If the time period is much longer than the expected period of the process, then the cumulative probability distribution of the peaks at a level α can be approximated using the following equation:

$$F_{peak}(\alpha, t) \cong 1 - \frac{\int_0^t \nu^+(\alpha, \tau)d\tau}{\int_0^t \nu^+(0, \tau)d\tau}. \tag{17.25}$$

Copyright 2005 by CRC Press LLC

The ratio on the right-hand side of Equation 17.25 is the expected number of upcrossings of level α divided by the number of zero upcrossings. Shinozuka and Yang [11] showed that the distribution of the peaks fits very closely the Weibull distribution:

$$F_{peak}(\alpha, T) = 1 - e^{-\left(\frac{\alpha}{\sigma}\right)^{\beta}} \tag{17.26}$$

where parameters β and σ are the shape and scale parameters of the distribution, respectively. These parameters depend on the characteristics of the process and duration *T*.

Example 17.7

Consider the displacement of mass, *m*, of the system in Examples 17.4 through 17.6. Find:

1. The expected rate of zero upcrossings
2. The expected upcrossing rate of a level equal to 5 standard deviations
3. The probability of first excursion failure of the level in question 2 for an exposure period of 50 seconds.

The displacement of the mass is a Gaussian process because the excitation is Gaussian and the system is linear. Therefore, we can use Equations 17.21 and 17.22 to find the expected upcrossing rate. To find the expected number of zero upcrossings, we calculate the standard deviations of the displacement and the derivative of the displacement:

$$\sigma_X = \left(\frac{1}{2\pi} \int_{-\infty}^{+\infty} S_{XX}(\omega) d\omega \right)^{0.5} = 0.016 \text{ m}$$

$$\sigma_{\dot{X}} = \left(\frac{1}{2\pi} \int_{-\infty}^{+\infty} \omega^2 S_{XX}(\omega) d\omega \right)^{0.5} = 0.046 \text{ m}.$$

The zero upcrossing rate is found to be 0.474 upcrossings/sec from Equation 17.22. This is close to the undamped natural frequency of the system, which is 0.472 cycles/sec. The upcrossing rate of the normalized level of five is 1.768×10^{-6} upcrossings/sec.

The probability of first excursion of the level can be found using Equation 17.14:

$$P(F) = 1 - e^{-\nu^{+}(\alpha)T} = 8.84 \times 10^{-5}.$$

Example 17.8

Consider that the PSD of the displacement of mass, *m*, is modified so that it is zero for frequencies greater than 20 rad/sec. This modification helps avoid numerical difficulties in calculating the standard deviation of the acceleration. Find the pdf of the peaks of the displacement and the probability of a peak exceeding a level equal to five standard deviations of the process.

The standard deviations of the displacement and the velocity remain practically the same as those in Example 17.7. The standard deviation of the acceleration is:

$$\sigma_{\ddot{X}} = \left(\frac{1}{2\pi} \int_{-\infty}^{+\infty} \omega^4 S_{XX}(\omega) d\omega \right)^{0.5} = 0.181.$$

The peaks of the displacement follow the Rice pdf in Equations 17.23a and 17.23a. This equation involves the bandwidth parameter of the process, which is found to be 0.751. This indicates that most

Copyright 2005 by CRC Press LLC

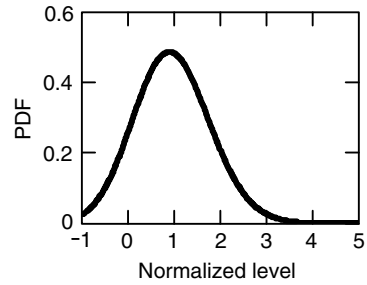

FIGURE 17.9 Probability density function (PDF) of a peak of the displacement normalized by the standard deviation. Since the displacement is a narrowband process, its PDF is close to the Rayleigh PDF.

of the energy of the process is confined to a narrow region (see Figure 17.8). Figure 17.9 shows the pdf of the peaks normalized by the standard deviation of the process. The pdf is a weighted average of the Rayleigh and Gaussian pdfs.

The probability of one peak upcrossing the normalized level, $\eta = 5$, is found to be 2.8×10^{-6} by integrating the pdf of the normalized peaks from 5 to infinity.

17.3.2.2 Fatigue Failure

Fatigue failure is another important failure mode for a vibrating system. This mode is due to accumulation of damage that is inflicted to the system by the oscillating stresses. For example, a spot weld in a car body may fail due to accumulation of damage caused by vibrating stresses. There are two approaches to the problem of fatigue failure: (1) a cumulative damage approach that is usually based on Miner's rule or (2) a fracture mechanics approach. The first approach is popular because it yields reasonably accurate estimates of the lifetime of a component and it is simple. Fracture mechanics-based approaches are more complex. In the following, we use Miner's rule to analyze fatigue failure of a dynamic system under a random, time varying excitation.

Traditionally, the *S-N* curve is used to characterize the behavior of materials in fatigue. This relates the number of stress cycles, which a material can withstand before failing due to fatigue, to the vibration amplitude of these stress cycles:

$$NS^b = c \tag{17.27}$$

where N is the number of stress cycles, S is the amplitude, and b and c are constants that depend on the material type. Exponent b ranges from 3 to 6. Note that the mean stress is assumed zero and the amplitude is assumed constant. Experimental results have shown that the above equation and the values of b and c are independent of the exact shape of the stress time history.

Suppose that a structure is subjected to n cycles of amplitude S, where n is less than N. Then we can define the damage inflicted to the structure as the ratio of n over N:

$$\text{Damage} = D = \frac{n}{N}. \tag{17.28}$$

If the structure is subjected to n_1 cycles of amplitude S_1, n_2 cycles of amplitude $S_2, \ldots,$ n_n, cycles of amplitude S_n, then we can calculate the damage inflicted by each set of stress cycles and then add them to get the total damage using Miner's rule:

$$D = \sum_i \frac{n_i}{N_i} \tag{17.29}$$

where N_i is the number of cycles of amplitude S_i to failure. According to Miner's rule, failure occurs when the damage exceeds 1. According to Miner's rule, D is independent of the order of cycles. Although

Copyright 2005 by CRC Press LLC

experimental evidence has shown that order is important, and several rules that account for the order have been proposed, none of these rules correlates with experimental results better than Miner's rule.

If the stress is a random variable, so is *D*. Then the problem of calculating the probability of fatigue failure is equivalent to that of calculating the probability that *D* exceeds 1. Miles [13] estimated the mean value of the damage for a stationary, narrowband process over a period *T*:

$$E(D(T)) = \nu^{+}(0)T\int_{0}^{\infty}\frac{f_{peak}(\alpha)}{N(\alpha)}\,da \tag{17.30}$$

where $N(\alpha)$ is the number of stress cycles of amplitude α to failure.

If the random process is also Gaussian, then:

$$E(D(T)) = \frac{\nu^{+}(\alpha)T}{c}(\sqrt{2}\sigma_X)^b\Gamma\left(1+\frac{b}{2}\right). \tag{17.31}$$

Mark [14] derived an expression for the variance of the damage in case of a second-order mechanical system subjected to a stationary Gaussian process.

If the applied stress is wideband, we can scale the damage obtained from Equation 17.31 by a correction factor, λ:

$$E(D(t)) = \lambda\frac{\nu^{+}(\alpha)T}{c}(\sqrt{2}\sigma_X)^b\Gamma\left(1+\frac{b}{2}\right). \tag{17.32}$$

Estimates of this factor can be found in Wirsching and Light [15].

17.3.2.3 Practical Estimation of Damage Due to Cyclic Loading and Probability of Fatigue Failure

Most engineering structures, such as airplanes, ships, and offshore platforms, are subjected to nonstationary excitations that are due to changes in weather, loading, and operating conditions. To calculate fatigue damage in these structures, we divide the spectrum of loading and operating conditions into cells. In each cell, these conditions are assumed constant. The time of exposure to the conditions in each cell is estimated using data from previous designs. Then we calculate the fatigue damage corresponding to operation in each cell and add up the damage over all the cells. An alternative approach finds an equivalent stationary load that causes damage equal to the damage due to operations in all the cells and the damage due to the equivalent load. Wirsching and Chen [16] reviewed methods for estimating damage in ocean structures.

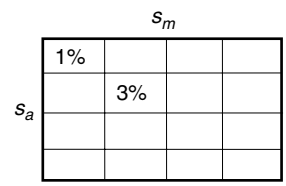

FIGURE 17.10 Load spectrum for alternating and mean stresses.

Consider that the load spectrum (percentage of lifetime during which a structure is subjected to a given mean and alternating load) is given (Figure 17.10). From this spectrum, we can estimate the joint pdf of the mean and alternating stresses, $f_{S_aS_m}(s_a, s_m)$.

For every cell in Figure 17.10, we can find an equivalent alternating stress that causes the same damage as the alternating and mean stresses when they are applied together. This equivalent stress is $(s_{a_i})/[1-(s_{m_j}/S_Y)]$ where s_{a_i} and s_{m_j} are the alternating and mean stresses corresponding to the *i, j* cell, and S_Y is the yield stress. The above expression is obtained using the Goodman diagram. Suppose n_{ij} is the number of cycles corresponding to that cell. Then, the damage due to the portion of the load spectrum

Copyright 2005 by CRC Press LLC

corresponding to the *i, j* cell is $D_{ij} = \frac{n_{ij}}{N_{ij}}$. N_{ij} is the number of cycles at failure when s_{a_i} and s_{m_j} are applied. From the S-N curve we can find the number of cycles:

$$N_{ij}\left[\frac{s_{a_i}}{1-\frac{s_{m_j}}{S_Y}}\right]^b = c \Rightarrow N_{ij} = \frac{c\left(1-\frac{s_{m_j}}{S_Y}\right)^b}{s_{a_i}^b}. \tag{17.33}$$

Therefore, the damage corresponding to the *ij* cell is:

$$D_{ij} = \frac{n_{ij} s_{a_i}^b}{c\left(1-\frac{s_{m_j}}{S_Y}\right)^b}. \tag{17.34}$$

The total damage is:

$$D = \sum_i \sum_j D_{ij} = \sum_i \sum_j \frac{n_{ij} s_{a_i}^b}{c\left(1-\frac{s_{m_j}}{S_Y}\right)^b} = \sum_i \sum_j \frac{p_{ij} s_{a_i}^b}{c\left(1-\frac{s_{m_j}}{S_Y}\right)^b} \tag{17.35}$$

where p_{ij} is the percentage of the number of cycles corresponding to load cell *i, j*. This percentage is obtained from information on the load spectrum (for example, from Figure 17.10).

Sources of uncertainty in the damage include:

- The random nature of the environment and the material properties (e.g., uncertainties in parameters *b* and *c* of the S-N curve)
- Epistemic (modeling) uncertainties, which are due to idealizations in the models of the environment and the structure

Nikolaidis and Kaplan [17] showed that, for ocean structures (ships and offshore platforms), uncertainty in fatigue life is almost entirely due to epistemic (modeling) uncertainties.

17.4 Evaluation of the Stochastic Response of Nonlinear Systems

Analysis of nonlinear systems is considerably more difficult than that of linear systems. A principal reason is that the superposition principle does not hold for nonlinear systems. Closed form solutions have been found for few simple nonlinear systems.

Methods for analysis of nonlinear systems include:

- Methods using the Fokker-Plank equation, which shows how the pdf of the response evolves in time
- Statistical linearization methods [18]
- Methods using state-space and cumulant equations

The above methods are presented in the book by Lutes and Sarkani [10].

Copyright 2005 by CRC Press LLC

17.5 Reliability Assessment of Systems with Uncertain Strength

So far, we have assumed that the strength of a system is deterministic. The probability of failure in this case can be calculated using Equation 17.14 if the random process representing the load is stationary or using Equation 17.15 if the process is nonstationary. Resistance can also be uncertain and in this case the above equations give the conditional probability of failure given that the resistance is $A = \alpha$. Here, an introduction of methods for reliability assessment of systems whose resistance is random is presented. Chapter 18, "Time-Variant Reliability," in this book presents these methods in detail.

Consider the case where the load process is stationary. Using the total probability theorem we find that the probability of failure over a period $[0, T]$ is the average probability of exceedance over the entire range of values of resistance A:

$$P(F) = \int (1 - e^{-\nu^+(\alpha)T}) f_A(\alpha) d\alpha. \tag{17.36}$$

Several random variables can affect the resistance. In such a case, we need to calculate the probability of failure using an equation similar to Equation 17.36 involving nested integrals. This is impractical if there are more than three random variables. Wen [19] recommended two approaches to calculate the probability of failure: (1) the ensemble upcrossing rate method and (2) first- and second-order methods.

In the ensemble method, we calculate an average upcrossing rate considering that α is a random variable and then we use the calculated upcrossing rate in Equation 17.14 to find the probability of failure. This approach tacitly assumes that the crossing events form a Poisson process. This is not true because even if the load process is Poisson, if the resistance is high when a crossing occurs, then it will also be high in the next upcrossing. However, Wen demonstrated using an example that if the crossing rate is low (i.e., the product of the upcrossing rate and the length of the exposure period is considerably less than 1), then this approach can give accurate results.

The second method assumes that we can calculate the probability of failure as a function of the resistance and formulates the problem as a time invariant problem. Specifically, the problem of finding the average probability of failure in Equation 17.36 can be recast into the following problem:

$$P(F) = P(g(\mathbf{A}, U) \le 0)$$

where the performance function g($\mathbf{A}$,U) is:

$$g(\mathbf{A}, U) = U - \Phi^{-1}(P(F/\mathbf{A})). \tag{17.37}$$

$\mathbf{A}$ is the vector of uncertain resistance variables, $P(F/\mathbf{A})$ is the conditional probability of failure given the values of the uncertain resistance variables, and U is a standard Gaussian random variable.

This problem can be solved using a first- or second-order method.

17.6 Conclusion

Many systems are subjected to excitations that should be modeled as random processes (random functions) or random fields.

Probabilistic analysis of dynamic systems involves three main steps: (1) modeling of the excitations, (2) calculation of the statistics of the response, and (3) calculation of the probability of failure. To develop a probabilistic model of a random process, we need to specify the joint probability distribution of the values of a random process for all possible values of the index parameter (e.g., the time). This is often impractical. Therefore, often we determine the second-order statistics of the random process, that is, the mean value, and the autocorrelation function. We have analytical tools, in the form of closed form expressions, for the second-order statistics of linear systems. However, few analytical solutions are available for nonlinear systems.

Copyright 2005 by CRC Press LLC

A system may fail due to first excursion failure, in which the response exceeds a level, and fatigue failure due to damage accumulation. Tools are available for estimating the probability of failure under these two modes. For first excursion failure, we have equations for approximating the average upcrossing rate of a level, the pdf of the local peaks of the response and the pdf of the time to failure. For fatigue failure, we have equations for the cumulative damage.

References

1. Nigam, N.C., 1983, *Introduction to Random Vibrations,* MIT Press, Cambridge, MA.
2. Lin, Y.K., 1967, *Probabilistic Theory of Structural Dynamics,* McGraw-Hill, New York.
3. Rice, S.O., 1944, 1945, "Mathematical Analysis of Random Noise," *Bell Systems Technical Journal,* 23:282–332; 24:46–156. Reprinted in *Selected Papers on Noise and Stochastic Processes,* N. Wax, Ed., 1954. Dover, New York, 133–249.
4. Yang, J.N. and Shinozuka, M., 1971, "On the First Excursion Failure Probability of in Stationary Narrow-Band Random Vibration," *ASME Journal of Applied Mechanics,* 38(4), 1017–1022.
5. Yang, J.N. and Shinozuka, M., 1972, "On the First Excursion Failure Probability in Stationary Narrow-Band Random Vibration — II," *ASME Journal of Applied Mechanics,* 39(4), 733–738.
6. Caughey, T.K. and Stumpf, H.J., 1961, "Transient Response of Dynamic Systems under Random Excitation," *Journal of Applied Mechanics,* 28(4), 563.
7. Fung, Y.C., 1955, "The Analysis of Dynamic Stresses in Aircraft Structures during Landing as Non-stationary Random Processes," *Journal of Applied Mechanics,* 22, 449–457.
8. Amin, M., 1966, "Nonstationary Stochastic Model for Strong Motion Earthquakes," Ph.D. thesis, University of Illinois.
9. Nikolaidis, E., Perakis, A.N., and Parsons, M.G., 1987, "Probabilistic Torsional Vibration Analysis of a Marine Diesel Engine Shafting System: The Input-Output Problem," *Journal of Ship Research,* 31(1), 41–52.
10. Lutes, L.D. and Sarkani, S., 2004, *Random Vibrations,* Elsevier Butterworth-Heinemann, Burlington, MA.
11. Shinozuka, M. and Yang, J.N., 1971, Peak Structural Response to Nonstationary Random Excitations, *Journal of Sound and Vibration,* 14(4), 505–517.
12. Yang, J.N. and Liu, S.C., 1980, "Statistical Interpretation and Application of Response Spectra," *Proceedings 7th WCEE*, 6, 657–664.
13. Miles, J.W., 1954, "On Structural Fatigue under Random Loading," *Journal of Aeronautical Science,* 21, 753–762.
14. Mark, W.D., 1961, "The Inherent Variation in Fatigue Damage Resulting from Random Vibration", Ph.D. thesis, Department of Mechanical Engineering, MIT.
15. Wirsching, P.H. and Light, M.C., 1980, "Fatigue under Wide Band Random Stresses," *Journal of Structural Design,* ASCE, 106(ST7), pp. 1593–1607.
16. Wirsching, P.H. and Chen, Y.-N., 1988, "Considerations of Probability-Based Fatigue Design for Marine Structures," *Marine Structures,* 1, 23–45.
17. Nikolaidis, E. and Kaplan, P., 1992, "Uncertainties in Stress Analyses on Marine Structures, Parts I and II," *International Shipbuilding Progress,* 39(417), 19–53; 39(418), 99–133.
18. Roberts, J.B. and Spanos, P.D., 1990, *Random Vibration and Statistical Linearization,* Wiley, New York.
19. Wen, Y.-K., 1990, *Structural Load Modeling and Combination for Performance and Safety Evaluation,* Elsevier, Amsterdam.

Copyright 2005 by CRC Press LLC

18

Time-Variant Reliability

Robert E. Melchers
The University of Newcastle

Andre T. Beck
Universidade Luterana do Brasil

18.1 Introduction

As discussed already in previous chapters, typically the loads acting on structures vary with time. They may be increasing slowly on average, such as with the gradual increase over many years in vehicular loads on bridges, or more quickly, such as wind loads generating a dynamic structural response. In all cases, the loads are of uncertain magnitude and the actual magnitude at any point in time will be uncertain. Moreover, the structural strength may vary with time — typically, it will decrease as a result of fatigue, corrosion, or similar deterioration mechanism. How to deal with these types of situations for structural reliability estimation is the topic for this chapter.

To be sure, it is not always necessary to use time-variant reliability approaches. For example, if just one load acts on a structure, the load may be represented by its extreme (e.g., its maximum) value and its uncertain nature by the relevant extreme value distribution. It represents the extreme value the load would be expected to occur during a defined time interval (usually the design life of the structure). The probability of failure over a defined lifetime can then be estimated employing the usual *time-invariant* methods such as FOSM, FORM and their developments, as well as in most Monte Carlo work. This has been termed the "time-integrated" approach because it transfers the time dependence effect into the way the load acting on the structure is modeled [1].

A further possibility is to consider not the lifetime of the structure, but some shorter, critical periods, such as the occurrence of a storm event and model the load during that event by an extreme value distribution. By considering the probability of various storm events and using the return period notion or probability bounds similar to those for series systems, the lifetime probability can then be estimated [1].

Copyright 2005 by CRC Press LLC

We will not discuss these simplified methods herein but rather concentrate on introducing concepts from the more general (and rich) stochastic process theory.

The time-integrated simplifications are not valid, in general, when more than one load is applied to a structure. In simple terms, it should be evident that it is very unlikely that the maximum of one load will occur at exactly the same time as the maximum of the second. A proper reliability analysis needs to account for this. One way of doing this is to apply the well-known *load combination rules* found in design codes. However, their usual justification is empirical. As discussed elsewhere, they can be derived, approximately, from time-variant structural reliability theory. A better approach is to use time-variant reliability theory directly.

This chapter provides an overview of time-variant reliability theory. Of necessity, it is brief. Moreover, because of space limitations, we have had to be selective in our selection of material. References must be consulted for more details.

18.2 Loads as Processes: Upcrossings

Examples of loads best modeled as processes include earthquake, wind, snow, temperature, and wave loads. Typically, the process fluctuates about a mean value. For wind or earthquake loading, the mean can be very low and there may be long periods of zero activity. This does not change the essential argument, however. Figure 18.1 shows a typical "realization" (that is, a trace) of a stochastic process.

In probability terms, a process can be described by an *instantaneous* (or average-point-in-time) cumulative probability distribution function $F_X(x,t)$. As usual, it represents the probability that the random process $X(t)$ will take a value lower than (or equal to) x. Evidently, this will depend, in general, on time t. The equivalent probability density function (pdf) is $f_X(x,t)$. Figure 18.1 shows a realization of the random process $X(t)$ and various properties. The instantaneous (average-point-in-time) pdf is shown on the left. Various properties may be derived from $f_X(x,t)$ including the process mean $\mu_X(t) = \int_{-\infty}^{\infty} x f_X(x,t)dx$ and the autocorrelation function $R_{XX}(t_1, t_2) = E[X(t_1)X(t_2)] = \int_{-\infty}^{\infty}\int_{-\infty}^{\infty} x_1 x_2 f_{XX}(x_1, x_2; t_1, t_2)\, dx_1 dx_2$ expressing the correlation relationship between two points in time (t_1, t_2). Here, f_{XX} is the joint probability density function. For (weakly) stationary processes, these two functions are constant in time and R_{XX} becomes dependent on relative time only. In principle, a stationary process cannot start or stop — this aspect usually can be ignored in practical applications provided the times involved are relatively long. Details are available in various texts.

Figure 18.1 also shows a barrier $R = r$. If the process $X(t)$ represents a load process $Q(t)$, say, the barrier can be thought of as the capacity of the structure to resist the load $Q(t)$ at any time t. This is the case for one loading and for a simple time-independent structure. When an event $Q > r$ occurs, the structure "fails."

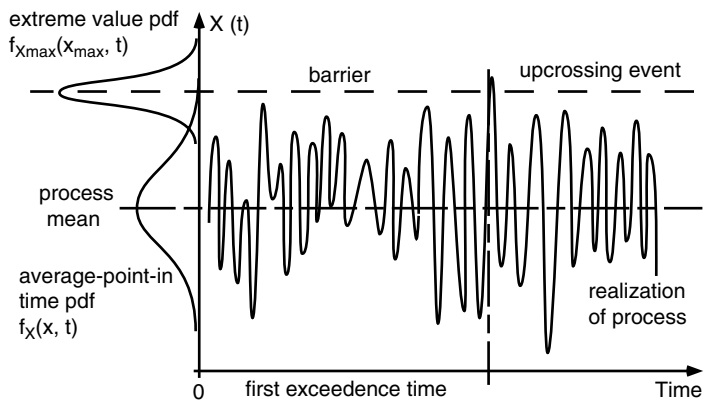

FIGURE 18.1 Realization of a continuous random process (such as windloading) showing an exceedence event and time to first exceedence.

Copyright 2005 by CRC Press LLC

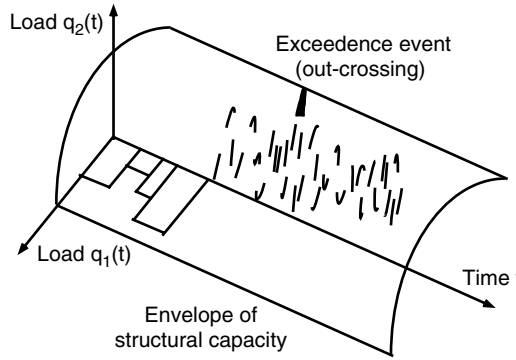

FIGURE 18.2 Envelope of structural strength (resistance) showing a realization of the vector load process and an outcrossing by process $Q_2(t)$.

For a process, this is termed an "upcrossing" or an "exceedence" event. For acceptable structural safety, the time t_1 to the first occurrence of an upcrossing should be sufficiently long. Evidently, t_1 will be a random variable. Estimation of t_1 or its equivalent, the probability of structural failure in a defined time span (the lifetime of the structure), is particularly important for structural reliability estimation, as will be discussed in more detail below. We note that the definition of the failure criterion is a matter for decision by those performing the reliability estimation.

18.3 Multiple Loads: Outcrossings

Most structures are subject to multiple loads, acting individually or in combination, independently or correlated in some way. Moreover, they need not all be modeled as continuous processes such as in Figure 18.1. For example, live loads due to floor loads, car park loads, etc. usually are better modeled as a series of pulses. Each pulse corresponds to a short-term, high-intensity loading event such as an office party or a meeting. Analogous to continuous loading, any one pulse can cause the capacity of the structure to be exceeded.

When several loads act, they can be represented by a vector process $\mathbf{X}(t)$ with corresponding probability density function $f_{\mathbf{X}}(\mathbf{x})$. For Figure 18.2, with loads only as random processes, the corresponding pdf is the vector of load processes $\mathbf{Q}(t)$. Evidently, any one load or any combination of the loads can exceed the structural capacity and produce an exceedence event. This is shown schematically in Figure 18.2 with the outcrossing there being due to the floor load $q_2(t)$. The envelope represents the structural capacity, the region under the envelope is the *safe* domain and the region outside is the *failure* domain. As before, the first exceedence time t_1 is the time until such an exceedence event occurs for the first time, that is, when one of the load processes, or the combined action of the two processes, "outcrosses" the envelope of structural capacity.

18.4 First Passage Probability

The above concepts can be formulated relatively simply using well-established theory of stochastic processes [2, 3]. Let $[0, t_L]$ denote the *design life* for the structure. Then, the probability that the structure will fail during $[0, t_L]$ is the sum of probability that the structure will fail when it is first loaded and the probability that it will fail subsequently, given that it has not failed earlier, or:

$$p_f(t) \le p_f(0, t_L) + [1 - p_f(0, t_L)] \cdot [1 - e^{-\nu t}] \tag{18.1}$$

where ν is the *outcrossing rate*. Already in the expression $[1 - e^{-\nu t}]$ in the second term it has been assumed (not unreasonable) that structural failure events are rare and that such events therefore can be represented

Copyright 2005 by CRC Press LLC

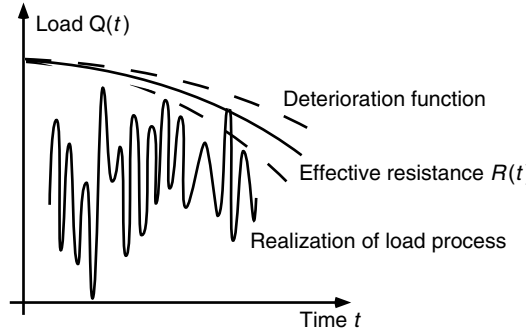

FIGURE 18.3 Exceedence event when there is structural deterioration with time (i.e., when $R = R(t)$).

reasonably closely by a Poisson distribution. Theoretically, this assumption would produce an (asymptotic) upper bound on the actual final term — asymptotic because the bound becomes closer to the true upcrossing probability as the barrier level increases. Despite this, it is has been found that expression 18.1 provides a reasonable estimate for structural failure estimation [4]. However, it would not be appropriate for, say, serviceability failures as these would not, normally, be rare events.

Simulation results tend to confirm that Equation 18.1 is an upper bound. They also show that outcrossings for some types of processes can occur in *clumps.* These are mainly the so-called narrow-band processes because these high values of the peaks of the processes tend to occur together; that is, the high peaks usually are not independent. Various schemes have been proposed for attempting to deal with this problem for different types of process, including being more explicit about individual outcrossings [5].

Equation 18.1 can be applied where the outcrossing rate ν is not constant. This can arise, for example, when there is gradual deterioration (or enhancement) of the structural capacity with time (Figure 18.3). As a result, $p_f(0, t_L)$ and ν become time dependent $\nu = \nu(t)$. Thus, in Equation 18.1, the term νt must be replaced with the time-average upcrossing rate $\int_0^t \nu^+(\tau)d\tau$.

18.5 Estimation of Upcrossing Rates

When the process is a discrete pulse process, such as Borges, Poisson Counting, Filtered Poisson, and Poisson Square Wave and for Renewal processes more generally, it has been possible to directly apply Equation 18.1 to estimate the first passage probability or the level (up)crossing rate for the process acting individually. The results are available in the literature.

For a continuous random process, the outcrossing rate must be estimated using stochastic process theory. The theory is available in standard texts. It is assumed that the process continues indefinitely in time and is stationary. Moreover, it produces an average value of the upcrossing rate over all possible realizations (i.e., the ensemble) of the random process $X(t)$ at any time t. Hence, it is known as the ensemble average value.

Only if the process is ergodic will the estimated upcrossing rate also be the time average frequency of upcrossings. The latter is a useful property because it allows the upcrossing rate to be estimated from a long record of observations of a single process. It is often assumed to hold unless there is evidence to the contrary.

In the special but important case when the random process $X(t)$ is a stationary normal process $N(\mu_X, \sigma_X^2)$, the upcrossing rate for a barrier level a can be

$$\nu_a^+ = \frac{1}{2\pi}\frac{\sigma_{\dot{X}}}{\sigma_X}\left[-\frac{(a-\mu_X)^2}{2\sigma_X^2}\right] = \frac{\sigma_{\dot{X}}}{(2\pi)^{1/2}} f_X\left(\frac{1}{\sigma_X}\phi\left[\frac{(a-\mu_X)}{\sigma_X}\right]\right) \tag{18.2}$$

Copyright 2005 by CRC Press LLC

where $\phi(\,)$ is the standard normal distribution function and $\dot{X}(t)$ is the derivative process distributed as $N(0,\sigma_{\dot{X}}^2)$. Details of the derivation and evaluation of these parameters can be found in standard texts. Suffice to note here simply that

$$\sigma_X^2 = R_{XX}(\tau = 0) - \mu_X^2 \tag{18.3}$$

$$\sigma_{\dot{X}}^2 = -\frac{\partial^2 R_{XX}(0)}{\partial \tau^2} \tag{18.4}$$

where R_{XX} is the autocorrelation function. It can be estimated from observations of the process.

For nonnormal processes there are very few closed solutions. Sometimes, Equation 18.2 is used as an approximation but this can be seriously in error. Numerical solutions often are used.

18.6 Estimation of the Outcrossing Rate

For several discrete pulse processes acting in combination, some results are available. One such application is considered later when dealing with load combinations.

For both discrete and continuous processes, the outcrossing situation is as shown in Figure 18.4, with the outcrossing occurring at point A for a vector of (in this case, two) random processes $\mathbf{X} = \mathbf{X}(t)$ with mean located in the safe domain D_S. The time axis is the third axis in Figure 18.4 and has been compressed onto the page. Closed form solutions are available only for a limited range of cases, dealing mainly with two-dimensional normal processes and open and closed square and circular domains [6]. It has been shown that for an m-dimensional vector process that the outcrossing rate can be estimated from:

$$\nu_D^+ = \int_{D_S} \mathrm{E}(\dot{X}_n \,|\mathbf{X} = \mathbf{x})^+ f_{\mathbf{X}}(\mathbf{x})\, d\mathbf{x} \tag{18.5}$$

In Equation 18.5, the term $()^+$ denotes the (positive) component of $\mathbf{X}$ that crosses out of the safe domain (the other components cross back in and are of no interest). The subscript n denotes the outward normal component of the vector process at the domain boundary and is there for mathematical completeness. Finally, the term $f_{\mathbf{X}}(\mathbf{x})$ represents the probability that the process is actually at the boundary between the safe and unsafe domain (i.e., at the limit state). Evidently, if the process is not at this boundary, it cannot cross out of the safe domain.

There are only a few solutions of Equation 18.5 available for continuous processes, mainly for time-invariant domains; and there is an approximate bounding approach [7, 8]. For n discrete Poisson square

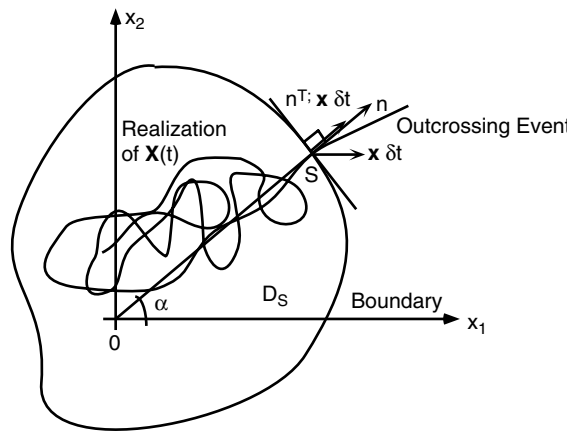

FIGURE 18.4 Vector process realization showing notation for outcrossing and for directional simulation.

Copyright 2005 by CRC Press LLC

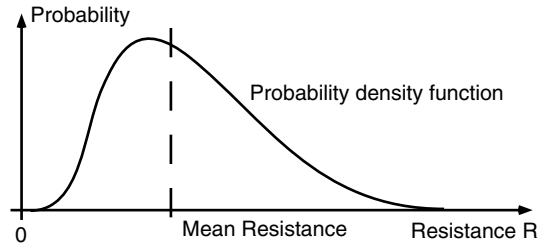

FIGURE 18.5 Schematic probability density function for material strength.

wave processes $\mathbf{X}(t)$ each having pulses of magnitude Y_i normally distributed and having mean arrival rate ν_i the mathematics can be rearranged to [9]:

$$\nu_D^+ = \sum_{i=1}^{n} \nu_i \int_{-\infty}^{\infty} P(\text{outcrossing due to } Y_i) f_{\mathbf{X}^*}(\mathbf{x}) d\mathbf{x} \tag{18.6}$$

where $P(\,) = P[(Y_i, \mathbf{x}^*) \in D_S] \cdot P[(Y_i, \mathbf{x}^*) \notin D_S]$ denotes the probability of a pulse being initially inside the safe domain and then it being outside (i.e., and outcrossing occurs). These are independent events and $\mathbf{X}^*$ denotes the vector without the i-th component that is outcrossing. For various special cases, solutions have been developed for Equation 18.6. These include (1) hyperplanes, (2) hypercubical domains, and (3) linear additions of different processes.

When the safe domain is not convex or cannot be expressed as a linear combination of linear functions, the determination of the outcrossing rate becomes more problematic. Bounding results could be invoked but these tend to be conservative [10]. Nonnormal processes further complicate the problem. Numerical estimation of outcrossing rates must then be used. Figure 18.4 suggests that a procedure using a polar coordinate system is appropriate and indeed this has been developed [11, 12] using simulation (Monte Carlo) methods.

18.7 Strength (or Barrier) Uncertainty

Thus far, attention has focused on estimating the rate at which one or more processes (loads) crosses out of the safe domain — that is, when the loads exceed the capacity of the structure. As previously discussed, actual structures are not of known precise strength or capacity. There are variations in interpretation of design codes, in calculation procedures, and errors of various types can be committed. Moreover, there are variations introduced during construction and materials have variable properties. Hence, when a structure is finally completed, its actual strength R usually is not known precisely.

As a result, the location of the line $R = r$ in Figure 18.1 and Figure 18.3 should be represented as a probabilistic estimate such as shown in Figure 18.5. The line $R = r$ shown in Figure 18.1 and Figure 18.3 is just one "realization" of many possible resistance or strength or capacity outcomes. Because the actual strength outcome is uncertain, all reasonable possibilities must be considered in a time-variant reliability analysis. Moreover, for many realistic situations, the resistance is a function of time $R = R(t)$. This applies, for example, to strength affected by corrosion (of steel, say) or to concrete strength increase with time. Fatigue can be a function of time or, more accurately, of load applications and stress ranges.

18.8 Time-Dependent Structural Reliability

The above concepts can be generalized for random "barriers" and hence applied to estimation of the time dependent reliability of structures. As before, the discussion is limited to relatively high reliability systems such that the outcrossing approach (Equation 18.1) remains valid asymptotically.

The probability of structural failure during a defined structural (nominal) lifetime $[0, t_L]$ can be stated as

$$p_f(t) = P[R(t) \le S(t)] \quad \forall (t \in [0, t_L]) \tag{18.7}$$

Here, $S(t)$ is the load effect (internal action) process derived from the loads. Equation 18.7 can be rewritten by conditioning on the random variable resistance

$$p_f = \int_{\mathbf{r}} p_f(t_L|\,\mathbf{r}) f_{\mathbf{R}}(\mathbf{r}) d\mathbf{r} \tag{18.8}$$

where the conditional failure probability $p_f(t_L|\mathbf{r})$ is a function of the vector of load processes $\mathbf{Q}(t)$ or the vector of load effects $\mathbf{S}(t)$ and $f_{\mathbf{R}}(\mathbf{r})$ is the probability density function for the resistance random vector $\mathbf{R}$. The key requirement then is the evaluation of the conditional failure probability $p_f(t_L|\mathbf{r})$. In general, no simple results exist, although Equation 18.1 can be used to provide an upper bound.

In using Equation 18.1 in Equation 18.8, two matters are of interest for evaluation. The first term in Equation 18.1 is $p_f(0)$, the probability of structural failure on the structure first being loaded. This can be substituted on its own directly into Equation 18.8. The outcome is a standard structural reliability estimation problem that can be solved by any of the time-invariant methods (FOSM, FORM, Monte Carlo, etc.).

The second matter of interest is the evaluation of the outcrossisng rate ν_D^+. This can be obtained, in principle, from Equation 18.5 or Equation 18.6 for a given realization $\mathbf{R} = \mathbf{r}$ of the structural strength. What then remains is the integration as required in Equation 18.8. The techniques available for these two operations are discussed in the section to follow.

18.9 Time-Variant Reliability Estimation Techniques

18.9.1 Fast Probability Integration (FPI)

For a single normal random process in a problem otherwise described only by Gaussian random variables, the upcrossing rate estimation can be obviated by introducing an "auxiliary" random variable, in standard Gaussian (normal) space, defined as $u_{n+1} = \Phi^{-1}[p_f(t|\mathbf{r})]$. The limit state function then is augmented to [13, 14]:

$$g(u_{n+1}, u_n) = u_{n+1} - \Phi^{-1}[p_f(t|\mathrm{T}^{-1}(u_n))] \tag{18.9}$$

where $\mathbf{u} = \mathrm{T}(\mathbf{r})$ is the transformation to the standard normal space of the resistance random variables $\mathbf{R}$.

Equation 18.9 is exact when $p_f(t_L|\mathbf{r})$ and $f_{\mathbf{R}}(\mathbf{r})$ in Equation 18.8 are independent. However, some error is introduced by approximating the (augmented) limit state function by a linear function in FORM (or a quadratic one in SORM). Applications experience shows that when the conditional failure probability is small (as in most structural reliability problems), this technique may present convergence problems [15].

18.9.2 Gaussian Processes and Linear Limit State Functions

For the special case of fixed, known barriers given as linear limit state functions (i.e., hyperplanes in n-dimensional space) and Gaussian continuous random processes and Gaussian random variables, it is possible to use the result of Equation 18.2 to estimate the outcrossing rate for each hyperplane. Allowance must be made for the area each plane contributes and for the requirement that the process must be "at" the limit state for an outcrossing to occur. The latter is represented by the integral over

Copyright 2005 by CRC Press LLC

the hyperplane of $f_X(\boldsymbol{x})$. For k (i.e., multiple) time-invariant hyperplanes each with surface area ΔS_i the result is then [7]

$$\nu_D^+ = \sum_{i=1}^{k} \nu_k^+ = \sum_{i=1}^{k} \left[\frac{\sigma_{\dot{Z}_i} \phi(\beta_i)}{(2\pi)^{1/2} \sigma_{Z_i}} \right] \left[\int_{\Delta S_i} f_{\mathbf{X}}(\mathbf{x}) d\mathbf{x} \right] \tag{18.10}$$

where $\phi(\beta_i)$ represents the usual *safety index* for the i-th hyperplane relative to the origin in standard Gaussian space. The result (Equation 18.10) can be used in Equation 18.1 for fixed (known) barriers. Example calculations are available [17]. The main problem now remaining is the integration over the resistance random variables **R**. The FPI approach could be used, in principle, but for many problems it appears that integration by Monte Carlo simulation is the only practical approach [18]. Of course, $p_f(0, t_L)$ can be estimated directly by the standard FOSM or FORM methods.

18.9.3 Monte Carlo with Conditional Expectation (and Importance Sampling)

The integration in Equation 18.8 can be carried out using Monte Carlo simulation with conditional expectation [19]. The result is obtained by starting with the usual expression for multi-parameter time-invariant failure probability

$$p_f = \int_{D_F} \cdots \int I[G(\mathbf{x}) \le 0] f_{\mathbf{X}}(\mathbf{x}) d\mathbf{x} \tag{18.11}$$

where D_F represents the failure domain. With some manipulation, this can be expressed as

$$p_f = \int \cdots \int_{D_1} p_{f|\mathbf{X}_1=\mathbf{x}_1} f_{\mathbf{X}_1}(\mathbf{x}_1) d\mathbf{x}_1 \tag{18.12}$$

where $\mathbf{X}_1$ is a subset of the random vector $\mathbf{X}$ with corresponding sampling space D_1 and $p_{f|\mathbf{X}_1=\mathbf{x}_1}$ represents a conditional probability of failure for the subset space $D_2 = D - D_1$. If the latter conditional term can be evaluated analytically or numerically for each sampling of vector $\mathbf{x}_1$, variance reduction can be achieved and the Monte Carlo process made more efficient. The integration over D_1 will be performed by Monte Carlo simulation (with importance sampling).

The use of Equation 18.12 lies in recognizing that it has the same form as Equation 18.8, with the components of the random vector **X** in domain D_1 in Equation 18.12 corresponding to the vector of resistance random variables **R** in Equation 18.8. When importance sampling is to be applied, Equation 18.12 is rewritten in the standard form as

$$p_f = \int \cdots \int_{D_1} \frac{p_{f|\mathbf{X}_1=\mathbf{x}_1} f_{\mathbf{X}_1}(\mathbf{x}_1)}{h_{\mathbf{V}}(\mathbf{x}_1)} h_{\mathbf{V}}(\mathbf{x}_1) d\mathbf{x}_1 \tag{18.13}$$

Some simpler applications are available [19].

18.9.4 Directional Simulation

Directional simulation has been shown to be a reasonably efficient approach for Monte Carlo estimation of the time-invariant probabilities of failure, that is, for random variable problems [12, 20]. When stochastic processes are involved, a more intuitive approach is to consider directional simulation applied in the space of the load processes $\mathbf{Q}(t)$ only.

This way of considering the problem follows naturally from Figure 18.4 with the barrier in that figure now interpreted as one realization of the structural strength or capacity **R**. It follows that Equation 18.5 now becomes an estimate conditional on the realization $\mathbf{R} = \mathbf{r}$ of the structural resistance; that is, Equation 18.5 estimates $p_f(t_L|\mathbf{r})$ in Equation 18.8. The structural resistance will

Copyright 2005 by CRC Press LLC

be represented in this formulation in the space of $\mathbf{Q}(t)$ and will be a function of random variables describing individual member capacities, material strength or stiffness values, dimensions, etc. Thus, $\mathbf{R} = \mathbf{R}(\mathbf{X})$. The main challenge is to derive the probabilistic properties $f_{\mathbf{R}}(\mathbf{r})$ for $\mathbf{R}$. In directional simulation terms, this is written, for each direction $\mathbf{A} = \mathbf{a}$ (see Figure 18.4) as $f_{S|A}(s|\mathbf{a})$ where S is the radial (scalar) distance for measuring the structural strength along the corresponding ray. Several approaches have been proposed [21–23].

Once $f_{S|A}(s|\mathbf{a})$ is available, $p_f(t_L|\mathbf{r})$ in Equation 18.8 can be estimated from Equation 18.1, now written in direction simulation terms as

$$p_f(s|a) \le p_f(0, s|a) + \left\{1 - \exp[-\nu_D^+(s|a)t]\right\} \tag{18.14}$$

where, as earlier, $p_f(0,)$ represents the failure probability at time $t = 0$ and ν_D^+ is the outcrossing rate of the vector stochastic process $\mathbf{Q}(t)$ out of the safe domain D. To support directional simulation, Equation 18.8 has been modified to

$$p_f = \int_{\substack{\text{unit} \\ \text{sphere}}} f_{\mathbf{A}}(\mathbf{a}) \left[\int_S p_f(s|a) f_{S|\mathbf{A}}(s|\mathbf{a}) ds \right] d\mathbf{a} \tag{18.15}$$

where $f_{\mathbf{A}}(\mathbf{a})$ is the pdf for the sampling direction $\mathbf{A}$. The limitation to this rewriting of Equation 18.8 is that each directional simulation direction is assumed as an independent one-dimensional probability integration. It is a reasonable approximation for high barrier levels, but generally will overestimate the failure probability. Techniques to deal with the integration directly through Equation 18.8 are under investigation.

In common with most other techniques, it is also implicit in this formulation that the limit state functions are not dependent on the history of the load process realizations; that is, the results are assumed *load-path independent.*

18.9.5 Ensembled Upcrossing Rate (EUR) Approach

In the ensembled upcrossing rate approach, the upcrossing rate of a random process through a resistance barrier is averaged over the probability distribution of the resistance:

$$\nu_{ED}^+(t) = \int_R \nu^+(r, t) f_R(r, t) dr \tag{18.16}$$

which is then substituted into Equation 18.1 to estimate the failure probability. This is not quite the same as the failure probability estimated using Equation 18.8. Taking the mean over the resistance introduces some level of dependency in the upcrossing rate, thus making the Poisson assumption in Equation 18.1 less appropriate. The EUR approximation consists of approximating the arrival rate of upcrossings through a random barrier by the ensemble average of upcrossings [24]. Typically, this leads to an overestimation of the failure probability [25]. In summary, it would be expected that the EUR approximation has the following characteristics:

1. Appropriate for even higher barrier levels and even lower failure probabilities as compared to a deterministic barrier problem
2. More appropriate for situations with time-dependent random variable or random process barriers, as variations in the barrier tend to reduce the dependency error
3. A function of the relative magnitudes of the resistance and the load process variances

Copyright 2005 by CRC Press LLC

The EUR approach is easily generalized to a vector of random variable resistances **R** and multiple processes. In general, an ensemble outcrossing rate is obtained when the integration boundary (limit state) is considered random in the outcrossing rate calculation (e.g., Equation 18.5 and Equation 18.10). This can be done, for example, through directional simulation in the load-space, by writing Equation 18.15 in terms of outcrossing rates rather than failure probabilities. Ensemble outcrossing rates are also obtained when outcrossing rates are computed as a parallel system sensitivity measure [26] with random resistance parameters included in the solution [27].

The EUR approximation significantly simplifies the solution of time-variant reliability problems when resistance degradation is considered because it changes the order of integrations. In the approaches described earlier, the outcrossing rate is integrated over time for the failure probability (Equation 18.1) and then failure probabilities are integrated over random resistance parameters (Equation 18.8). When resistance degradation is considered, or when load processes are nonstationary, the outcrossing rate becomes time dependent. Hence, outcrossing rate evaluation through Equation 18.5, Equation 18.6, and Equation 18.10 must be repeated over time, for each integration point of Equation 18.8. In the EUR solution, the outcrossing rate is first integrated over random resistance parameters (Equation 18.16) and then over time (Equation 18.1). The ensemble outcrossing rate calculation must also be repeated over time, but this calculation generally represents little additional effort to the computation of conditional outcrossing rates (Equation 18.5). The outer integration for resistance parameters is hence avoided. The integration over time is straightforward, as long as ensemble outcrossing rates can be considered independent.

18.9.6 Estimation of the EUR Error

So far, the EUR approximation has received little attention in structural reliability theory. It is important to understand the error involved in this approximation. This problem was considered in [28]. In summary, Monte Carlo simulation was used to estimate the arrival rate of the first crossing over the random barrier. This is assumed to be an "independent" ensemble crossing rate and is termed ν_{EI}^{+} in the sequel. By comparing ν_{ED}^{+} with ν_{EI}^{+}, it was found possible to estimate the error involved using modest numbers of simulations and to extrapolate the results in time.

Figure 18.6 shows a typical comparison of ν_{EI}^{+} and ν_{ED}^{+} for narrowband (NB) and broadband (BB) standard Gaussian load processes with time-invariant Gaussian barriers. It is seen that there is a very rapid reduction in ν_{EI}^{+} with time (cycles), which is nonexistent in ν_{ED}^{+} (because the barrier is time-invariant) and that the reduction is greater for barriers with higher standard deviations. This is evident also in Figure 18.7, which shows the "order of magnitude" error between ν_{EI}^{+} and ν_{ED}^{+}. Similar results were obtained for time variant barriers with deterioration characteristics.

The results show that the error involved in the conventional EUR approach can be significant for both narrow and broad band processes and that it becomes greater as the variance of the barrier increases. The study also shows that the EUR error is governed by the parameter:

$$E_P = \frac{1}{\sigma_S}\sqrt{\frac{\sigma_S\left(\sigma_R^2 + \sigma_S^2\right)}{(\mu_R - \mu_S)}} \tag{18.17}$$

where indexes R and S are used for resistance and load parameters, respectively. This result is strictly valid only for scalar problems involving Gaussian load processes and Gaussian barriers. It allows establishing practical guidelines for the use of the EUR approximation. For example, the EUR error is known to be smaller than one order of magnitude when $E_P \leq 0.65$. The extension of these results to multidimensional problems and to nonGaussian barriers and processes is under investigation.

18.9.7 Summary of Solution Methods

It should be clear that the estimation of the outcrossing rate for general systems with unrestricted probability descriptions of the random variables and of the stochastic processes involved remains a challenging problem. Some solution techniques are available, however, for special cases.

Copyright 2005 by CRC Press LLC

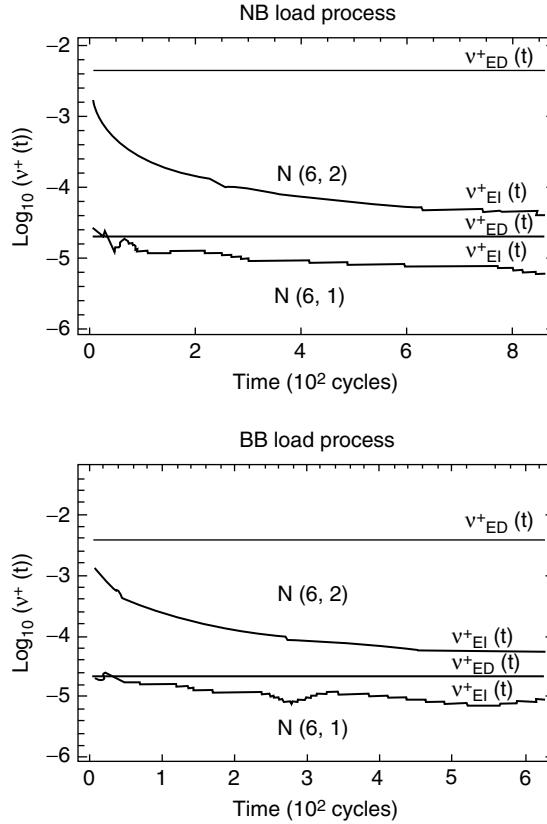

FIGURE 18.6 Ensemble upcrossing rates ν^+_{ED} and ν^+_{EI} for Gaussian random barriers with parameters $N(\mu,\sigma)$ [28].

Only a few analytical solutions exist for estimating the outcrossing rate. The usual approach is through Monte Carlo simulation, including employment of methods of variance reduction [12, 19, 22]. However, it is fair to say that the theoretically accurate results have a high computational demand. Proposals to reduce this all involve various simplifications, often but not always conservative ones.

18.10 Load Combinations

A special but important application of time-variant reliability analysis concerns the possibility of giving the load combination rules used in design codes some degree of theoretical rationality. At the simplest level, the rules provide an equivalent load to represent the combination of two stochastic loads $Q_1(t)$ and $Q_2(t)$, say. As before, these loads are very unlikely to have peak values at the same time.

The stress resultants (internal actions) $S_1(t)$ and $S_2(t)$ from the loads can be taken as additive. Thus, interest lies in the probability that the sum $S_1(t) + S_2(t)$ exceeds some barrier level a. If the two processes each have Gaussian amplitudes and are stationary, the sum will be Gaussian also and Equation 18.10 applies directly.

More generally, Equation 18.5 can be applied for the additive combination of two processes with instantaneous (i.e., arbitrary-point-in-time) pdfs given by $f_{Q_1}(q_1)$ and $f_{Q_2}(q_2)$, respectively. However, this requires joint pdf information that is seldom available. Nevertheless, a reasonably good upper bound is [16]:

$$\nu^+_{\mathbf{Q}}(a) \le \int_{-\infty}^{\infty} \nu_1(u) f_{Q_2}(a-u)\,du + \int_{-\infty}^{\infty} \nu_2(u) f_{Q_1}(a-u)\,du \tag{18.18}$$

Copyright 2005 by CRC Press LLC

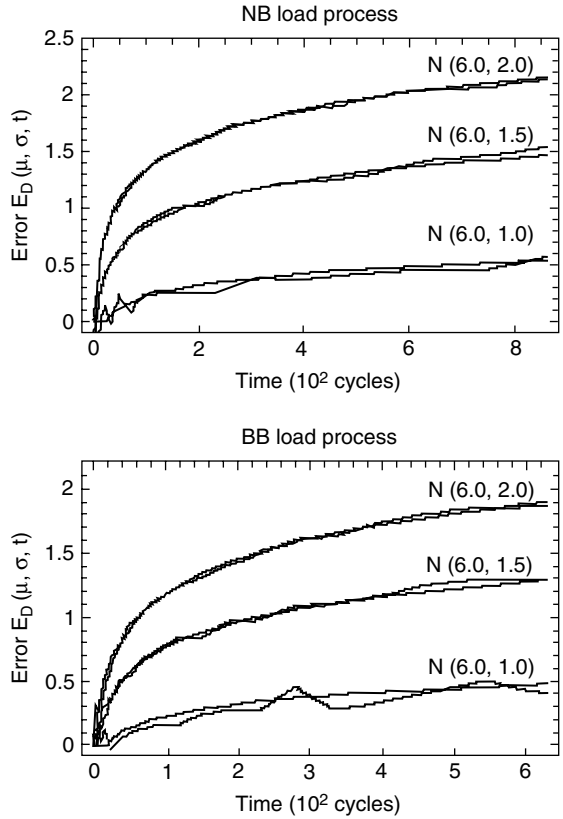

FIGURE 18.7 Ensemble upcrossing rate error as a function of time, numerical result, and analytical approximation.

where $\nu_i(u)$ is the upcrossing rate for the process $Q_i(t)$ $(i = 1, 2)$, evaluated using the theory for single processes. Equation 18.18 is known as a point-crossing formula, and it is exact, mainly for cases where one or both processes has a discrete distribution [29]. For these, the individual process upcrossing rates have a relatively simple form. For example, for the sum of two nonnegative rectangular renewal processes with a probability $p_i(i = 1, 2)$ of zero load value (so-called mixed processes) (see Figure 18.8), the

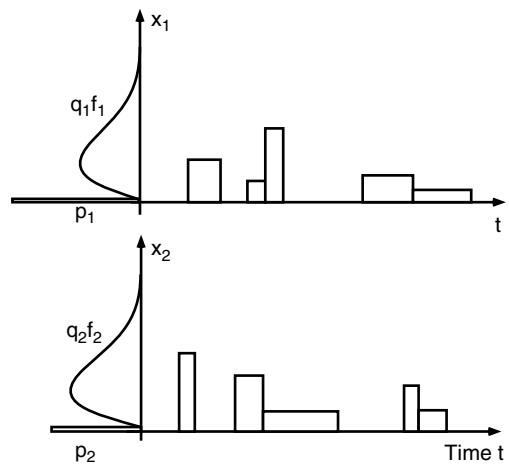

FIGURE 18.8 Realizations of two "mixed" rectangular renewal processes having the shown pdfs.

Copyright 2005 by CRC Press LLC

upcrossing rate is:

$$\nu_{\mathbf{Q}}^{+}(a) = \nu_i[p_i + q_i F_i(a)]\,[q_i(1 - F_1(a)]] \tag{18.19}$$

where $\nu_i q_i$ and $F_i(\,)$ are the mean arrival rate and the cdf of the i-th process, respectively. In this case, the arbitrary-point-in-time probability density function (pdf) for the i-th process is given by $f_{Q_i}(q_i) = p_i\delta(q_i) + q_i f_i(q_i)$, where $\delta(\,)$ is the Dirac-delta function and $q_i = 1 - p_i$ (see Figure 18.8).

Combining Equation 18.18 and Equation 18.19 and making the reasonable assumption that all pulses return to zero after application and that the high pulses are of relatively short duration relative to the life of the structure leads to the approximate result [30]

$$\nu_{\mathbf{Q}}^{+}(a) \approx \nu_1 q_1 G_1(a) + \nu_2 q_2 G_2(a) + (\nu_1 q_1)(\nu_2 q_2) G_{12}(a) \tag{18.20}$$

where $G_i(\,) = 1 - F_i(\,)$ and $\mathrm{F}_{12}(\,)$ is the cdf for the total of the two pulses. In Equation 18.20, the first term represents upcrossings of the first process, the second term those of the second process, and the third term upcrossings involving both processes acting at the same time. Typically, when the pulses are of short duration, the joint mean arrival rate $(\nu_1 q_1)(\nu_2 q_2)$ is very low and the third term can be neglected. Under this assumption, Equation 18.20 can be interpreted as one example of the conventional design code load combination formula although it is phrased in terms of the upcrossing rate.

Noting that the extreme of a process in a time interval $[0, t_L]$ can be represented approximately by $F_{\max}(a) \approx e^{-\nu t_L} \approx 1 - \nu t_L$, where $F_{\max}(\,) = P(X_{\max} < a)$ is the cdf for the maximum of the process in $[0, t_L]$, it follows that

$$G_{\max X}(a) = 1 - F_{\max X}(a) \approx \nu_X^{+}(a) \cdot t_L \tag{18.21}$$

which shows that the upcrossing rate is related directly to the maximum value of a process in a given time interval $[0, t_L]$. Thus, Equation 18.20 can be recast in terms of maximum loads $Q_{i\max}$ (e.g., greater than the barrier level) or their combinations and the average point-in-time values $\overline{Q}_i$

$$Q_{\max} \approx \max[(Q_{1\max} + \overline{Q}_2); (Q_{2\max} + \overline{Q}_1)] \tag{18.22}$$

This is known as Turkstra's rule [31]. Although it is of limited validity for accurate structural reliability estimation, it provides an approximate theoretical justification for the intuitive load combination rules in structural design codes.

18.11 Some Remaining Research Problems

It should be clear from the above that the estimation of time-variant structural reliability is a much more complex matter than for time-invariant problems. Much of the effort has gone into the use of classical stochastic process theory and the asymptotic outcrossing estimates available through it. Monte Carlo solutions have been built on this theory but the computational effort involved is significant. It is possible, of course, just to use brute-force Monte Carlo by simulating very many realizations of the processes in a problem and noting the number of outcrossings obtained for a given time period. This requires very extensive computational power but may be attractive in some applications.

For certain discrete pulse processes, there are exact solutions and reasonably good bounds available but the situation is less satisfactory for continuous processes. For these, upper bound solutions based on the asymptotic approximation are available, for fixed barriers particularly. For normal processes but for random variable barriers, integration over the relevant PDF is still required. This includes efforts to recast the problem to more directly in processes-only spaces.

Copyright 2005 by CRC Press LLC

Progress in this area is considered to require a better understanding of the errors involved in the various methods developed so far, improvements in dealing with integration over the resistance random variables and the possibility of employing response surface methodologies to circumvent the high computational requirements.

For nonstationary processes and deteriorating systems, the form and uncertainty characterization of the time-dependence function has only recently begun to receive serious attention. Almost certainly, the conventional design assumptions about material deterioration and about load (and other) process nonstationarity will not be sufficient for high-quality structural reliability analyses [32]. Much remains to be done in this area also.

References

1. Melchers, R.E. (1999). *Structural Reliability Analysis and Prediction*, second edition, John Wiley & Sons, Chichester (reprinted June 2001).
2. Rice, S.O. (1944). Mathematical analysis of random noise, *Bell System Tech. J.*, **23**, 282–332; (1945), **24**, 46–156. Reprinted in Wax, N. (1954) *Selected Papers on Noise and Stochastic Processes*, Dover Publications.
3. Vanmarcke, E.H. (1975). On the distribution of the first-passage time for normal stationary processes, *J. Applied Mech.*, ASME, **42**, 215–220.
4. Engelund, S., Rackwitz, R., and Lange, C. (1995). Approximations of first-passage times for differentiable processes based on higher-order threshold crossings, *Probabilistic Engineering Mechanics*, **10**, 53–60.
5. Kordzakhia, N., Melchers, R.E., and Novikov, A. (1999). First passage analysis of a 'Square Wave' filtered Poisson process, in *Proc. Int. Conf. Applications of Statistics and Probability,* Melchers, R.E. and Stewart, M.G., Eds., Balkema, Rotterdam, 35–43.
6. Hasofer, A.M. (1974). The upcrossing rate of a class of stochastic processes, *Studies in Probability and Statistics*, Williams, E.J., Ed., North-Holland, Amsterdam, 151–159.
7. Veneziano, D., Grigoriu, M., and Cornell, C.A. (1977), Vector-process models for system reliability, *J. Engineering Mechanics Div.*, ASCE, **103**, (EM3) 441–460.
8. Hohenbichler, M. and Rackwitz, R. (1986). Asymptotic outcrossing rate of Gaussian vector process into intersection of failure domains, *Prob. Engineering Mechanics,* **1**(3), 177–179.
9. Breitung, K. and Rackwitz, R. (1982). Nonlinear combination load processes, *J. Structural Mechanics*, **10**(2), 145–166.
10. Rackwitz, R. (1984). Failure rates for general systems including structural components, *Reliab. Engg.*, **9**, 229–242.
11. Deák, I. (1980). Fast procedures for generating stationary normal vectors, *J. Stat. Comput. Simul.*, **10**, 225–242.
12. Ditlevsen, O., Olesen, R., and Mohr, G. (1987). Solution of a class of load combination problems by directional simulation, *Structural Safety*, **4**, 95–109.
13. Madsen, H.O. and Zadeh, M. (1987). Reliability of plates under combined loading, *Proc. Marine Struct. Rel. Symp., SNAME*, Arlington, VA, 185–191.
14. Wen, Y.-K. and Chen, H.C. (1987). On fast integration for time variant structural reliability, *Prob. Engineering Mechanics,* **2**(3), 156–162.
15. Marley, M.J. and Moan, T. (1994). *Approximate Time Variant Analysis for Fatigue, Structural Safety and Reliability,* Schueller, Shinozuka and Yao, Eds.
16. Ditlevsen, O. and Madsen, H.O. (1983). Transient load modeling: clipped normal processes, *J. Engineering Mechanics Div.*, ASCE, **109**(2), 495–515.
17. Ditlevsen, O. (1983). Gaussian outcrossings from safe convex polyhedrons, *J. Engineering Mechanics Div.*, ASCE, **109**(1), 127–148.
18. Rackwitz, R. (1993). On the combination of nonstationary rectangular wave renewal processes, *Structural Safety*, **13**(1+2) 21–28.

Copyright 2005 by CRC Press LLC

19. Mori, Y. and Ellingwood, B.R. (1993). Time-dependent system reliability analysis by adaptive importance sampling, *Structural Safety*, **12**(1) 59–73.
20. Ditlevsen, O., Melchers, R.E., and Gluver, H. (1990). General multi-dimensional probability integration by directional simulation, *Computers & Structures*, **36**(2), 355–368.
21. Melchers, R.E. (1991). Simulation in time-invariant and time-variant reliability problems, *Proc. 4th IFIP Conference on Reliability and Optimization of Structural Systems*, Rackwitz, R. and Thoft-Christensen P., Eds, Springer, Berlin, 39–82.
22. Melchers, R.E. (1995). Load space reliability formulation for Poisson pulse processes, *J. Engineering Mechanics*, ASCE, **121**(7), 779–784.
23. Guan, X.L. and Melchers, R.E. (1999). A load space formulation for probabilistic finite element analysis of structural reliability, *Prob. Engrg. Mech.,* **14**, 73–81.
24. Pearce, H.T. and Wen, Y.K. (1984). Stochastic combination of load effects, *Journal of Structural Engineering,* ASCE, **110**(7), 1613–1629.
25. Wen, Y.K. and Chen, H.C. (1989). System reliability under time-varying loads: I, *Journal of Engineering Mechanics,* ASCE, **115**(4), 808–823.
26. Hagen, O. and Tvedt, L. (1991). Vector process out-crossing as a parallel system sensitivity measure, *Journal of Engineering Mechanics,* ASCE, **117**(10), 2201–2220.
27. Sudret, B., Defaux, G., Lemaire, M., and Andrieu, C. (2002). Comparison of methods for computing the probability of failure in time-variant reliability using the out-crossing approach, *Fourth International Conference on Computational Stochastic Mechanics,* Kerkyra (Corfu), Greece, June 2002.
28. Beck, A.T. and Melchers, R.E. (2002). On the ensemble up-crossing rate approach to time variant reliability analysis of uncertain structures, *Fourth International Conference on Computational Stochastic Mechanics,* Kerkyra (Corfu), Greece, June.
29. Larrabee, R.D. and Cornell, C.A. (1981). Combination of various load processes, *J. Structural Div.*, ASCE, **107**(ST1). 223–239.
30. Wen, Y.-K. (1977) Probability of extreme load combination, *J. Structural Div.*, ASCE, **104**(ST10) 1675–1676.
31. Turkstra, C.J. (1970). *Theory of Structural Design Decisions Study No. 2*, Solid Mechanics Division, University of Waterloo, Waterloo, Ontario.
32. Melchers, R.E. (2001). Assessment of existing structures — some approaches and research needs, *J. Struct. Engrg.*, ASCE, **127**(4), 406–411.

Copyright 2005 by CRC Press LLC

19

Response Surfaces for Reliability Assessment

Christian Bucher
Bauhaus-University Weimar

Michael Macke
Bauhaus-University Weimar

19.1 Introduction

Structural reliability assessment requires one to estimate probabilities of failure that, in general, are of rather small magnitude. Moreover, structural failure is most typically assessed by means of nonlinear, possibly time-variant analyses of complex structural models. In such cases, the computational cost incurred for one single analysis — to decide whether or not a structure is safe — may become quite demanding. Consequently, the application of direct (or even advanced) Monte Carlo simulation — being the most versatile solution technique available — is quite often not feasible. To reduce computational costs, therefore, it has been suggested to utilize the response surface method for structural reliability assessment [1].

Let us assume that the reliability assessment problem under consideration is governed by a vector $\mathbf{X}$ of n basic random variables X_i ($i = 1, 2, \ldots, n$), that is,

$$\mathbf{X} = (X_1, X_2, \ldots, X_n)' \tag{19.1}$$

where $(\cdot)'$ is transpose. Assuming, furthermore, that the random variables $\mathbf{X}$ have a joint probability density function $f(\mathbf{x})$, then the probability of failure $P(F)$ — that is the probability that a limit state will be reached — is defined by

$$P(F) = \int_{g(\mathbf{x})\le 0} \ldots \int f(\mathbf{x}) d\mathbf{x} \tag{19.2}$$

Copyright 2005 by CRC Press LLC

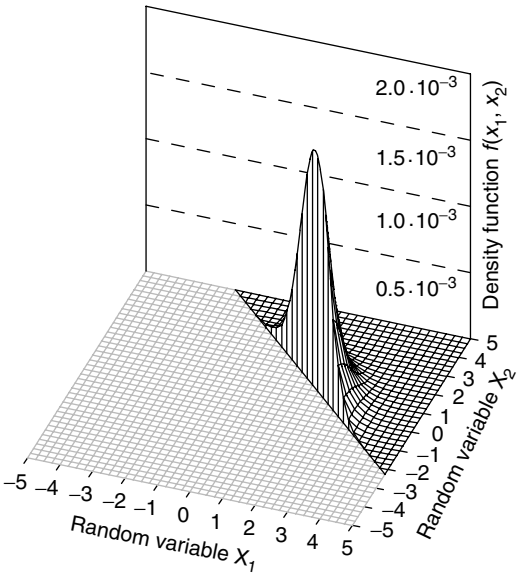

FIGURE 19.1 Integrand for calculating the probability of failure for $g(x_1, x_2) = 3 - x_1 - x_2$.

whereby $g(\mathbf{x})$ is the limit state function that divides the n-dimensional probability space into a failure domain $F = \{\mathbf{x} : g(\mathbf{x}) \leq 0\}$ and a safe domain $S = \{\mathbf{x} : g(\mathbf{x}) > 0\}$. As already mentioned, the computational challenge in determining the integral of Equation 19.2 lies in evaluating the limit state function $g(\mathbf{x})$, which for nonlinear systems usually requires an incremental/iterative numerical approach. The basic idea in utilizing the response surface method is to replace the true limit state function $g(\mathbf{x})$ by an approximation $\eta(\mathbf{x})$, the so-called response surface, whose function values can be computed more easily.

In this context it is important to realize that the limit state function $g(\mathbf{x})$ serves the sole purpose of defining the bounds of integration in Equation 19.2. As such, it is quite important that the function $\eta(\mathbf{x})$ approximates this boundary sufficiently well, in particular in the region that contributes most to the failure probability $P(F)$. As an example, consider a two-dimensional problem with standard normal random variables X_1 and X_2, and a limit state function $g(x_1, x_2) = 3 - x_1 - x_2$. In Figure 19.1, the integrand of Equation 19.2 in the failure domain is displayed. It is clearly visible that only a very narrow region around the so-called design point $\mathbf{x}^*$ really contributes to the value of the integral (i.e., the probability of failure $P(F)$). Even a relatively small deviation of the response surface $\eta(\mathbf{x})$ from the true limit state function $g(\mathbf{x})$ in this region may, therefore, lead to significantly erroneous estimates of the probability of failure. To avoid this type of error, it must be ensured that the important region is sufficiently well covered when designing the response surface.

The response surface method has been a topic of extensive research in many different application areas since the influential paper by Box and Wilson in 1951 [2]. Whereas in the formative years the general interest was on experimental designs for polynomial models (see, e.g., [2, 3]), in the following years nonlinear models, optimal design plans, robust designs, and multi-response experiments — to name just a few — came into focus. A fairly complete review on existing techniques and research directions of the response surface methodology can be found in [4–7]. However, traditionally, the application area of the response surface method is not structural engineering, but, for example, chemical or industrial engineering. Consequently, the above-mentioned special requirement for structural reliability analysis — that is, the high degree of accuracy required in a very narrow region — is usually not reflected upon in the standard literature on the response surface method [8–10].

One of the earliest suggestions to utilize the response surface method for structural reliability assessment was made in [1]. Therein, Lagrangian interpolation surfaces and second-order polynomials are rated as useful response surfaces. Moreover, the importance of reducing the number of basic variables and error

Copyright 2005 by CRC Press LLC

checking is emphasized. Support points for estimating the parameters of the response surface are determined by spherical design. In [11], first-order polynomials with interaction terms are utilized as response surfaces to analyze the reliability of soil slopes. The design plan for the support points is saturated — either by full or by fractional factorial design. Another analysis with a saturated design scheme is given in [12], where quadratic polynomials without interaction terms are utilized to solve problems from structural engineering. Polynomials of different order in combination with regression analysis are proposed in [13], whereby fractional factorial designs are utilized to obtain a sufficient number of support points. The validation of the chosen response surface model is done by means of analysis of variance.

In [14] it has been pointed out that for reliability analysis it is most important to obtain support points for the response surface very close to or exactly at the limit state $g(\mathbf{x}) = 0$. This finding has been further extended in [15, 16]. In [17], the response surface concept has been applied to problems involving random fields and nonlinear structural dynamics. It has been shown that a preliminary sensitivity analysis using simplified structural analysis models may help to significantly reduce the computational effort. Because random field problems are typically characterized by a large number of mutually highly correlated variables, a spectral decomposition of the covariance matrix [18] can also considerably reduce the number of random variables required for an appropriate representation of the uncertainties.

In addition to polynomials of different order, piecewise continuous functions such as hyperplanes or simplices can also be utilized as response surface models. For the class of reliability problems defined by a convex safe domain, secantial hyperplane approximations such as presented in [19, 20] yield conservative estimates for the probability of failure. Several numerical studies indicate, however, that in these cases the interpolation method converges slowly from above to the exact result with increasing number of support points. The effort required for this approach is thereby comparable to Monte Carlo simulation based on directional sampling [21].

19.2 Response Surface Models

19.2.1 Basic Formulation

Response surface models are more or less simple mathematical models designed to describe the possible experimental outcome (e.g., the structural response in terms of displacements, stresses, etc.) of a more or less complex structural system as a function of quantitatively variable factors (e.g., loads or system conditions), which can be controlled by an experimenter. Obviously, the chosen response surface model should give the best possible fit to any collected data. In general, we can distinguish two different types of response surface models: regression models (e.g., polynomials of varying degree or nonlinear functions such as exponentials) and interpolation models (e.g., polyhedra).

Let us denote the response of any structural system to a vector $\mathbf{x}$ of n experimental factors or input variables x_i $(i = 1, 2, \ldots, n)$ (i.e., $\mathbf{x} = (x_1, x_2, \ldots, x_n)'$), by $z(\mathbf{x})$. In most realistic cases, it is quite likely that the *exact* response function will not be known. Therefore, it must be replaced by a flexible function $q(\cdot)$ that will express satisfactorily the relation between the response z and the input variables x. Taking into account a (random) error term ε, the response can be written over the region of experimentation as

$$z = q(\theta_1, \theta_2, \ldots, \theta_p; x_1, x_2, \ldots, x_n) + \varepsilon \tag{19.3}$$

where $\theta_j (j = 1, 2, \ldots, p)$ are the parameters of the approximating function $q(\cdot)$. Taking now expectations, that is,

$$\eta = \mathrm{E}[z] \tag{19.4}$$

then the surface represented by

$$\eta = q(\theta_1, \theta_2, \ldots, \theta_p; x_1, x_2, \ldots, x_n) = q(\boldsymbol{\theta}; \mathbf{x}) \tag{19.5}$$

Copyright 2005 by CRC Press LLC

is called a *response surface*. The vector of parameters $\boldsymbol{\theta} = (\theta_1, \theta_2, \ldots, \theta_p)'$ must be estimated from the experimental data in such a way that Equation 19.4 is fulfilled. In the following we will investigate the most common response surface models, methods to estimate their respective parameters, and, most significant, techniques for determining whether a chosen response surface model is suitable or should be replaced by a more appropriate one.

19.2.2 Linear Models and Regression

Let us assume that an appropriate response surface model $q(\cdot)$ has been chosen to represent the experimental data. Then, for estimating the values of the parameters $\boldsymbol{\theta}$ in the model, the method of maximum likelihood can be utilized. Under the assumptions of a Gaussian distribution of the random error terms ε, the method of maximum likelihood can be replaced by the more common method of least squares [8]. In the latter case, the parameters $\boldsymbol{\theta}$ are determined in such a way that the sum of squares of the differences between the value of the response surface $q(\boldsymbol{\theta}; \mathbf{x}^{(k)})$ and the measured response $z^{(k)}$ at the m points of experiment

$$\mathbf{x}^{(k)} = \left(x_1^{(k)}, \ldots, x_n^{(k)}\right)', \qquad k = 1, 2, \ldots, m \tag{19.6}$$

becomes as small as possible. That is, the sum of squares function

$$s(\boldsymbol{\theta}) = \sum_{k=1}^{m} \left(\mathrm{z}^{(k)} - q(\boldsymbol{\theta}; \mathbf{x}^{(k)})\right)^2 \tag{19.7}$$

must be minimized. This corresponds to a minimization of the variance of the random error terms ε. The minimizing choice of $\boldsymbol{\theta}$ is called a *least-squares estimate* and is denoted by $\hat{\boldsymbol{\theta}}$.

The above regression problem becomes more simple to deal with when the response surface model is linear in its parameters $\boldsymbol{\theta}$. Let us assume that the response surface is given by

$$\eta = \theta_1 q_1(\mathbf{x}) + \theta_2 q_2(\mathbf{x}) + \cdots + \theta_p q_p(\mathbf{x}) \tag{19.8}$$

The observations $z^{(k)}$ made at the points of experiment $\mathbf{x}^{(k)}$ can be represented by this response surface model as

$$\mathbf{z} = \begin{bmatrix} z^{(1)} \\ z^{(2)} \\ \vdots \\ z^{(m)} \end{bmatrix} = \begin{bmatrix} q_1(\mathbf{x}^{(1)}) & q_2(\mathbf{x}^{(1)}) & \cdots & q_p(\mathbf{x}^{(1)}) \\ q_1(\mathbf{x}^{(2)}) & q_2(\mathbf{x}^{(2)}) & \cdots & q_p(\mathbf{x}^{(2)}) \\ \vdots & \vdots & & \vdots \\ q_1(\mathbf{x}^{(m)}) & q_2(\mathbf{x}^{(m)}) & \cdots & q_p(\mathbf{x}^{(m)}) \end{bmatrix} \begin{bmatrix} \theta_1 \\ \theta_2 \\ \vdots \\ \theta_p \end{bmatrix} + \begin{bmatrix} \varepsilon^{(1)} \\ \varepsilon^{(2)} \\ \vdots \\ \varepsilon^{(m)} \end{bmatrix} = \mathbf{Q}\boldsymbol{\theta} + \boldsymbol{\varepsilon} \tag{19.9}$$

with $\boldsymbol{\varepsilon}$ as a vector of random error terms. Assuming that the random error terms are normally distributed and statistically independent with constant variance σ^2, i.e.,

$$\mathrm{E}[\varepsilon^{(k)}] = 0, \quad \mathrm{Var}[\varepsilon^{(k)}] = \sigma^2 \quad \text{and} \quad \mathrm{Cov}[\varepsilon^{(k)}, \varepsilon^{(l)}] = 0 \quad \text{for} \quad k \neq l \tag{19.10}$$

then the covariance matrix of the observations $\mathbf{z}$ is

$$\mathrm{Cov}[\mathbf{z}] = \mathrm{E}[(\mathbf{z} - \mathrm{E}[\mathbf{z}])(\mathbf{z} - \mathrm{E}[\mathbf{z}])'] = \sigma^2 \mathbf{I} \tag{19.11}$$

with $\mathbf{I}$ as an identity matrix.

The least square estimates $\hat{\boldsymbol{\theta}} = (\hat{\theta}_1, \ldots, \hat{\theta}_p)'$ of the parameter vector $\boldsymbol{\theta}$ are determined such that

$$L = (\mathrm{z} - \mathbf{Q}\hat{\boldsymbol{\theta}})'(\mathbf{z} - \mathbf{Q}\hat{\boldsymbol{\theta}}) = \mathbf{z}'\mathbf{z} - 2\mathbf{z}'\mathbf{Q}\hat{\boldsymbol{\theta}} + (\mathbf{Q}\hat{\boldsymbol{\theta}})'\mathbf{Q}\hat{\boldsymbol{\theta}} \tag{19.12}$$

Copyright 2005 by CRC Press LLC

becomes minimal. A necessary condition is that

$$\frac{\partial L}{\partial \hat{\theta}} = -2\mathbf{z}'\mathbf{Q} + 2(\mathbf{Q}\hat{\theta})'\mathbf{Q} = 0 \tag{19.13}$$

From this follows that

$$\mathbf{Q}'\mathbf{Q}\hat{\theta} = \mathbf{Q}'\mathbf{z} \tag{19.14}$$

The fitted regression model is consequently

$$\hat{\mathbf{z}} = \mathbf{Q}\hat{\theta} \tag{19.15}$$

If the matrix $\mathbf{Q}'\mathbf{Q}$ is not rank deficit (i.e., rank $(\mathbf{Q}'\mathbf{Q}) = p \leq m$), then there exists a unique solution to the above system of equations. The estimated parameter vector is given by

$$\hat{\theta} = (\mathbf{Q}'\mathbf{Q})^{-1}\mathbf{Q}'\mathbf{z} \tag{19.16}$$

This estimator is unbiased; that is,

$$\mathrm{E}[\hat{\boldsymbol{\theta}}] = \boldsymbol{\theta} \tag{19.17}$$

with covariance

$$\mathrm{Cov}[\hat{\theta}] = \sigma^2(\mathbf{Q}'\mathbf{Q})^{-1} \tag{19.18}$$

If the above made assumptions with respect to the random error terms ε do not hold—for example, the error terms are correlated or nonnormally distributed—then a different minimizing function L than given in Equation 19.12 has to be utilized. Typical examples thereof are given in [8].

19.2.3 Analysis of Variance

Because a response surface is only an approximation of the functional relationship between the structural response and the basic variables, it should be evident that, in general, there is always some *lack of fit* present. Therefore, a crucial point when utilizing response surfaces for reliability assessment is to check whether the achieved fit of the response surface model to the experimental data suffices or if the response surface model must be replaced by a more appropriate one. Therefore, different measures have been proposed in the past for testing different aspects of response surface models. In the following, a short overview of the most common measures is given. The basic principle of these measures is to analyze the variation of the response data in comparison to the variation that can be reproduced by the chosen response surface model—that is why this kind of response surface testing is also referred to as *analysis of variance*. Further and more advanced measures or checking procedures can be found in[8–10, 22].

Let us start with a measure of overall variability in a set of experimental data, the *total sum of squares* s_t. It is defined as the sum of squared differences $(z^{(k)} - \bar{z})$ between the observed experimental data $z^{(k)}$ $(k = 1, 2, \ldots, m)$ and its average value

$$\bar{z} = \frac{1}{m}\sum_{k=1}^{m} z^{(k)} \tag{19.19}$$

Copyright 2005 by CRC Press LLC

that is,

$$s_t = \mathbf{z}'\mathbf{z} - \frac{1}{m}(\mathbf{1}'\mathbf{z})^2 \tag{19.20}$$

where **1** is a vector of ones. If we divide s_t by the appropriate number of degrees of freedom, that is, $(m-1)$, we obtain the sample variance of the z's, which is a standard measure of variability.

The total sum of squares can be partitioned into two parts, the *regression sum of squares* s_r, which is the sum of squares explained by the utilized response surface model, and the *error sum of squares* s_e, which represents the sum of squares unaccounted for by the fitted model. The regression sum of squares is defined as the sum of squared differences $(\hat{z}^{(k)} - \bar{z})$ between the value $\hat{z}^{(k)}$ predicted by the response surface and the average value $\bar{z}$ of the observed data; that is,

$$s_r = (\mathbf{Q}\hat{\boldsymbol{\theta}})'\boldsymbol{\zeta} - \frac{1}{m}(\mathbf{1}'\boldsymbol{\zeta})^2 \tag{19.21}$$

If the response surface model has p parameters, then the number of degrees of freedom associated with the measure s_r is $(p-1)$.

The sum of squares unaccounted for in the model — called error sum of squares or, sometimes also, residual sum of squares — is defined as the squared difference $(z^{(k)} - \hat{z}^{(k)})$ between the observed experimental data $z^{(k)}$ and the value $\hat{z}^{(k)}$ predicted by the response surface, that is,

$$s_e = \mathbf{z}'\mathbf{z} - (\mathbf{Q}\hat{\boldsymbol{\theta}})'\mathbf{z} \tag{19.22}$$

Obviously, the error sum of square s_e is the difference between the total sum of squares s_t and the regression sum of squares s_r; that is, $s_e = s_t - s_r$. Consequently, the degrees of freedom associated with the measure s_e are $(m-p) = (m-1) - (p-1)$. Moreover, it can be shown that

$$\mathbf{E}[s_e] = \sigma^2(m-p) \tag{19.23}$$

Thus, an unbiased estimator of σ^2 is given by

$$\hat{\sigma}^2 = \frac{s_e}{m-p} \tag{19.24}$$

From the above defined sums of squares, different kinds of statistics can be constructed that measure certain aspects of the utilized response surface. The first of such measures is the *coefficient of (multiple) determination*

$$r^2 = \frac{s_r}{s_t} = 1 - \frac{s_e}{s_t} \tag{19.25}$$

which measures the portion of the total variation of the values $z^{(k)}$ about the mean $\bar{z}$ which can be explained by the fitted response surface model. We can easily see that $0 \le r^2 \le 1$. A large value of r^2 is supposed to indicate that the regression model is a good one. Unfortunately, adding an additional variable to an existing response surface model will always increase r^2 — independent of its relevancy to the model [10]. Therefore, an adjusted r^2-statistic has been proposed, defined as

$$r_A^2 = 1 - \frac{\mathbf{E}[s_e]}{\mathbf{E}[s_t]} = 1 - \frac{s_e}{s_t}\frac{(m-1)}{(m-p)} \tag{19.26}$$

Copyright 2005 by CRC Press LLC

As has been pointed out in [10], in general the measure r_A^2 does not increase when terms are added to the model, but in fact decreases often if these additional terms are unnecessary.

A different measure, which allows one to test the significance of the fitted regression equation, is the ratio of the mean regression sum of squares and the mean error sum of squares; that is,

$$F_0 = \frac{\mathbf{E}[s_r]}{\mathbf{E}[s_e]} = \frac{s_r}{s_e}\,\frac{(m-p)}{(p-1)} \tag{19.27}$$

the so-called *F*-statistic, which follows an *F*-distribution. The *F*-statistic allows to test the null hypothesis

$$H_0: \quad \theta_1 = \theta_2 = \cdots = \theta_p = 0 \tag{19.28}$$

against the alternative hypothesis

$$H_1: \quad \theta_j \neq 0 \text{ for at least one value of } \theta_j \; (j = 1, 2, \ldots, p) \tag{19.29}$$

For a specified level of significance α, the hypothesis H_0 is rejected if

$$F_0 > F_{\alpha, p-1, m-p} \tag{19.30}$$

(here, $p-1$ represents the degrees of freedom numerator and $m-p$ represents the degrees of freedom denominator) and we can conclude that at least one or more of the terms of the response surface model are able to reproduce a large extent of the variation observed in the experimental data. Or, if the hypothesis H_0 is not rejected, a more adequate model has to be selected, because none of the terms in the model seem to be of indispensable nature.

In addition to the test with the above-mentioned *F*-statistic, which tests all parameters at once, we are also often interested in the question if an *individual* parameter θ_j is significant to our model. That is, we would like to test if the model can be improved by adding an additional term, or if we can delete one or more variables to make our model more effective. As has been mentioned already above, when one parameter is added to a response surface model, the error sum of squares always decreases. However, adding an unimportant parameter to the model can increase the mean square error, thereby reducing the usefulness of the response surface model [10]. It is therefore an important task to decide if a certain parameter should be used in a response surface model — or better be rejected.

The hypothesis testing concerning individual parameters is performed by comparing the parameter estimates $\hat{\theta}_j$ in the fitted response surface model to their respective estimated variances $\text{Var}[\hat{\theta}_j]$ — these are the diagonal elements of the covariance matrix $\text{Cov}[\hat{\boldsymbol{\theta}}]$ in Equation 19.18. Testing of the null hypothesis

$$H_0: \quad \theta_j = 0 \tag{19.31}$$

is performed by determining the value of the *t*-statistic

$$t_0 = \frac{\hat{\theta}_j}{(\text{Var}\,[\hat{\theta}_j])^{1/2}} \tag{19.32}$$

and compare it with a percentile value α of the *t*-distribution with $(m-p)$ degrees of freedom, which corresponds to the number of degrees of freedom of the unbiased estimator of $\hat{\sigma}^2$ in Equation 19.24. Depending on the alternative hypothesis H_1, that is, if we utilize a two-sided test with

$$H_1: \quad \theta_j \neq 0 \tag{19.33}$$

Copyright 2005 by CRC Press LLC

or a one-sided-test with either

$$H_1: \quad \theta_j < 0 \quad \text{or} \quad H_1: \quad \theta_j > 0 \tag{19.34}$$

the null hypothesis H_0 is rejected at a confidence level α if, respectively,

$$|t_0| > t_{\alpha/2,m-p} \tag{19.35}$$

or

$$|t_0| > t_{\alpha,m-p} \tag{19.36}$$

If H_0 is rejected, then this indicates that the corresponding term can be dismissed from the model. It should be noted that this is a partial test, because the value of the tested parameter depends on all other parameters in the model. Further tests in a similar vein can be found in [8–10].

We conclude this section with a reminder that the estimated parameters $\hat{\boldsymbol{\theta}}$ are least square estimates; that is, there is a certain likelihood that the true parameter $\boldsymbol{\theta}$ has a different value than the estimated one. Therefore, it is sometimes quite advisable to determine confidence intervals for the parameters. The $(1-\alpha)$ confidence interval for an individual regression coefficient θ_j is given by [10]

$$\hat{\theta}_j - (\mathrm{Var}[\hat{\theta}_j])^{1/2} t_{\alpha/2,m-p} \le \theta_j \le \hat{\theta}_j + (\mathrm{Var}[\hat{\theta}_j])^{1/2} t_{\alpha/2,m-p} \tag{19.37}$$

(Joint confidence regions for several regression coefficients are given, e.g., in [10].) Consequently, when utilizing response surfaces in reliability assessment, we should be aware that all predictions — may it be the structural response for a certain design or a reliability measure — show respective prediction intervals.

19.2.4 First- and Second-Order Polynomials

As already mentioned, response surfaces are designed such that a complex functional relation between the structural response and the basic variables is described by an appropriate, but — preferably — as simple as possible mathematical model. The term "simple" means, in the context of response surfaces, that the model should be continuous in the basic variables and should have a small number of terms, whose coefficients can be easily estimated. Polynomial models of low order fulfill such demands. Therefore, in the area of reliability assessment, the most common response surface models are first- and second-order polynomials (see [1, 12, 15, 16]).

The general form of a first-order model of a response surface η, which is linear in its n basic variables x_i, is

$$\eta = \theta_0 + \sum_{i=1}^{n} \theta_i x_i \tag{19.38}$$

with θ_i ($i = 0, 1, \ldots, n$) as the unknown parameters to be estimated from the experimental data. The parameter θ_0 is the value of the response surface at the origin or the center of the experimental design, whereas the coefficients θ_i represent the gradients of the response surface in the direction of the respective basic variables x_i. As can be seen from Equation 19.38, the first-order model is not able to represent even the simplest interaction between the input variables.

If it becomes evident that the experimental data cannot be represented by a model whose basic variables are mutually independent, then the first-order model can be enriched with (simple) interaction terms, such that

$$\eta = \theta_0 + \sum_{i=1}^{n} \theta_i x_i + \sum_{i=1}^{n-1} \sum_{j=i+1}^{n} \theta_{ij} x_i x_j \tag{19.39}$$

Copyright 2005 by CRC Press LLC

The total number of parameters to be estimated is given by $1 + n(n + 1)/2$. In the response surface model of Equation 19.39, there is some curvature present, but only from the twisting of the planes of the respective input variables. If a substantial curvature is required as well, then the above model can be further enriched by n quadratic terms to a complete second-order model of the form

$$\eta = \theta_0 + \sum_{i=1}^{n} \theta_i x_i + \sum_{i=1}^{n} \sum_{j=i}^{n} \theta_{ij} x_i x_j \tag{19.40}$$

The total number of parameters to be estimated is, therewith, given by $1 + n + n(n + 1)/2$. In most common cases, either the first-order or the complete second-order model is utilized as the response surface function.

19.2.5 Exponential Relationships

Although polynomial approximations of the response are most common in reliability assessment, there is also some interest in other forms of approximating functions—most notable in exponential relationships (see, e.g., [13, 23]). There may exist mechanical or mathematical justifications for utilizing exponential relationships (e.g., when approximating solutions of differential equations or probability functions); nevertheless, in most cases, the choice is clearly dominated by an engineer's habit to take the logarithm of the input variables or the response to achieve a better fit of a linear model when the fit so far has not been satisfactory.

Most exponential relationships have been treated in a completely different way as compared to polynomial relationships; nevertheless, they often can be included in the polynomial family. Take, for example, two of the most popular exponential relationships of the form

$$\eta = \theta_0 + \sum_{i=1}^{n} \theta_i \exp(x_i) \tag{19.41}$$

and

$$\eta = \theta_0 \prod_{i=1}^{n} \exp(\theta_i x_i) + \theta_{n+1} \tag{19.42}$$

The model of Equation 19.41 is linear in its parameters. Moreover, by taking the logarithm of the input variables, that is,

$$\eta = \theta_0 + \sum_{i=1}^{n} \theta_i \exp(\log(\tilde{x}_i)) = \theta_0 + \sum_{i=1}^{n} \theta_i \tilde{x}_i \tag{19.43}$$

where $\tilde{x}_i$ are the transformed input variables, the model can be reduced to the first-order polynomial type. In case of Equation 19.42, the same linear form can be obtained by utilizing a logarithmic transformation for the response surface η, that is,

$$\tilde{\eta} = \log(\eta - \theta_{n+1}) = \log(\theta_0) + \sum_{i=1}^{n} \theta_i x_i = \tilde{\theta}_0 + \sum_{i=1}^{n} \theta_i x_i \tag{19.44}$$

where $\tilde{\eta}$ is the transformed response and $\tilde{\theta}_0$ is the transformed parameter θ_0.

When utilizing transformations for a reparametrization of a chosen response surface model, we should take into account that, in general, also the random error terms ε are affected, (i.e., transformed).

Copyright 2005 by CRC Press LLC

Consequently, the assumptions made for the nontransformed model in the regression analysis or the analysis of variance must be revised for the transformed model. Further examples of exponential relationships or other nonlinear models can be found (e.g., in [5, 9]).

19.2.6 Polyhedral Models

In addition to the above-mentioned regression models, there are also interpolation models available for describing response surfaces. A special type of such models are polyhedra, that is, an assemblage of continuous functions. The given rationale for utilizing such models is that they are more flexible to local approximations and should, therefore, indeed converge in the long run to the exact limit state function [19, 20]. This flexibility is an important feature in reliability assessment, where the estimated reliability measure depends quite considerably on a sufficiently accurate representation of the true limit state function in the vicinity of the design point. Therefore, these models utilize only points on the limit state surface $g(\mathbf{x}) = 0$, which separates the failure domain from the safe domain.

Typical examples of such polyhedral models are: *tangential planes* [19] defined by a point on the limit state surface $g(\mathbf{x}) = 0$ and the gradients with respect to the basic variables at this point; *normal planes* [20] defined by one point on the limit state surface $g(\mathbf{x}) = 0$ and the normal vector whose direction is defined by the point on the limit state surface and the origin in standard normal space; and *simplices* [20] defined in n-dimensional random variable space by n nondegenerated points on the limit state surface $g(\mathbf{x}) = 0$. All these polyhedral models allow, by including additional points on the limit state surface, an adaptive refinement of the approximating response surface and, consequently, an improvement of the estimator of the failure probability. However, this refinement is often marred by an excessive need for additional points on the limit state surface.

19.3 Design of Experiments

19.3.1 Transformations

Having chosen an appropriate response surface model, support points $\mathbf{x}^{(k)}$ $(k = 1, 2, \ldots, m)$ have to be selected to estimate in a sufficient way the unknown parameters of the response surface. Thereto, a set of samples of the basic variables is generated. In general, this is done by applying predefined schemes, so-called *designs of experiments*. The schemes shown in the following are saturated designs for first- and second-order polynomials, as well as full factorial and central composite designs. As is quite well known from experiments regarding physical phenomena, it is most helpful to set up the experimental scheme in a space of dimensionless variables. The schemes as described in the following perform experimental designs in a space of dimension n, where n is equal to the number of relevant basic variables.

The selected design of experiments provides a grid of points defined by the dimensionless vectors $\boldsymbol{\xi}^{(k)} = (\xi_1^{(k)}, \xi_2^{(k)}, \ldots, \xi_n^{(k)})'$. This grid must be centered around a vector $\mathbf{c} = (c_1, c_2, \ldots, c_n)'$. In the absence of further knowledge, this center point can be chosen equal to the vector of mean values $\boldsymbol{\mu} = (\mu_1, \mu_2, \ldots, \mu_n)'$ of the basic random variables X_i $(i = 1, 2, \ldots, n)$. As will be shown below, when further knowledge about the reliability problem becomes available, other choices of the center point are, in general, more appropriate. The distances from the center are controlled by the scaling vector $\mathbf{s} = (s_1, s_2, \ldots, s_n)$. In many cases, it is useful to choose the elements s_i of this scaling vector equal to the standard deviations σ_i of the random variables X_i. So, in general, a support point $\mathbf{x}^{(k)}$ $(k = 1, 2, \ldots, m)$ is defined as

$$\mathbf{x}^{(k)} = \begin{bmatrix} x_1^{(k)} \\ x_2^{(k)} \\ \vdots \\ x_n^{(k)} \end{bmatrix} = \begin{bmatrix} c_1 + \xi_1^{(k)} s_1 \\ c_2 + \xi_2^{(k)} s_2 \\ \vdots \\ c_n + \xi_n^{(k)} s_n \end{bmatrix} \tag{19.45}$$

The number m of generated support points depends on the selected method.

Copyright 2005 by CRC Press LLC

Depending on the type of probability functions $F(x_i)$ associated with the random variables X_i, this scheme may generate support points outside the range for which the random variables are defined (such as, e.g., negative values of coordinates for log-normally distributed random variables). To circumvent this type of problem, it may be helpful to transform first all random variables X_i into standardized normal random variables U_i by means of

$$u_i = \Phi^{-1}[F(x_i)] \tag{19.46}$$

whereby $\Phi^{-1}(\cdot)$ is the inverse of the normal distribution function

$$\Phi(u) = \frac{1}{\sqrt{2\pi}} \int_{-\infty}^{u} \exp\left(-\frac{y^2}{2}\right) dy \tag{19.47}$$

Equation 19.46 assumes that the random variables X_i are mutually independent. In normal random variable space, the design would be carried out using, for example, $u_i^{(k)} = \xi_i^{(k)}$ and the corresponding values of $x_i^{(k)}$ can be computed from the inverse of Equation 19.46; that is,

$$x_i^{(k)} = F^{-1}\left[\Phi\left(u_i^{(k)}\right)\right] \tag{19.48}$$

Note that both approaches yield the same support points if the random variables are independent and normally distributed. Nevertheless, for continuous distribution functions, there always exist suitable transfomations $\mathbf{T}(\cdot)$ that allow one to transform a vector of random variables $\mathbf{X}$ into a vector of mutually independent standard normal variables $\mathbf{U} = \mathbf{T}(\mathbf{X})$ [24].

19.3.2 Saturated Designs

Saturated designs provide a number of support points just sufficient to represent a certain class of response functions exactly. Hence, for a linear saturated design, a linear function will be uniquely defined. Obviously, $m = n + 1$ samples are required for this purpose (see Figure 19.2). The factors $\xi_i^{(k)}$ for $n = 3$ are given by

$$\boldsymbol{\xi} = (\boldsymbol{\xi}^{(1)}, \boldsymbol{\xi}^{(2)}, \boldsymbol{\xi}^{(3)}, \boldsymbol{\xi}^{(4)}) = \begin{bmatrix} 0 & +1 & 0 & 0 \\ 0 & 0 & +1 & 0 \\ 0 & 0 & 0 & +1 \end{bmatrix} \tag{19.49}$$

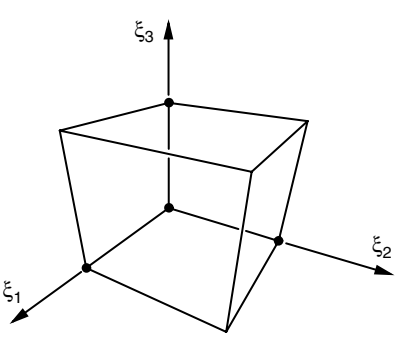

FIGURE 19.2 Saturated linear experimental scheme.

Copyright 2005 by CRC Press LLC

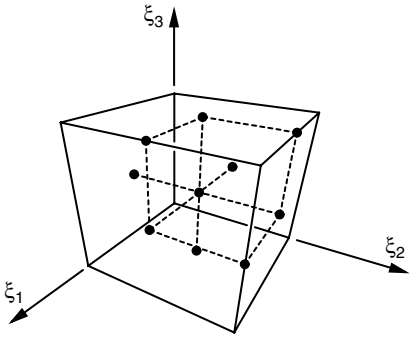

FIGURE 19.3 Saturated quadratic design scheme for $n = 3$.

Here, each column represents one support point. Of course, any variation of the factors above in which some or all values of (+1) were replaced by (−1) would also constitute a valid linear saturated design. Obviously, there is some arbitrariness in the design scheme that can usually be resolved only by introducing additional knowledge about the system behavior.

A saturated quadratic design (Figure 19.3) generates $m = n(n+1)/2 + n + 1$ support points $\mathbf{x}^{(k)}$. The factors $\xi_i^{(k)}$ for $n = 3$ are given by

$$\xi = (\xi^{(1)}, \xi^{(2)}, \ldots, \xi^{(10)}) = \begin{bmatrix} 0 & +1 & 0 & 0 & -1 & 0 & 0 & +1 & +1 & 0 \\ 0 & 0 & +1 & 0 & 0 & -1 & 0 & +1 & 0 & +1 \\ 0 & 0 & 0 & +1 & 0 & 0 & -1 & 0 & +1 & +1 \end{bmatrix} \tag{19.50}$$

Again, each column represents one support point. As mentioned, any change of sign in the pairwise combination would also lead to a saturated design, so that the final choice is somewhat arbitrary and should be based on additional problem-specific information.

19.3.3 Redundant Designs

Redundant experimental design methods provide more support points than required to define the response surface, and thus enable error checking procedures as outlined in the preceding section. Typically, regression is used to determine the coefficients of the basis function. Here also, linear and quadratic functions are being utilized.

The *full factorial* method (Figure 19.4) generates q sample values for each coordinate, thus producing a total of $m = q^n$ support points $\mathbf{x}^{(k)}$ ($k = 1, 2, \ldots, m$). Note that even for moderate values of q and n,

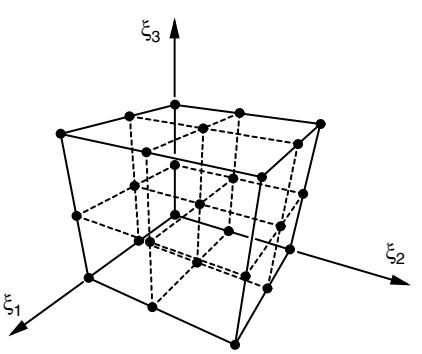

FIGURE 19.4 Full factorial desing scheme for $q = 3$ and $n = 3$.

Copyright 2005 by CRC Press LLC

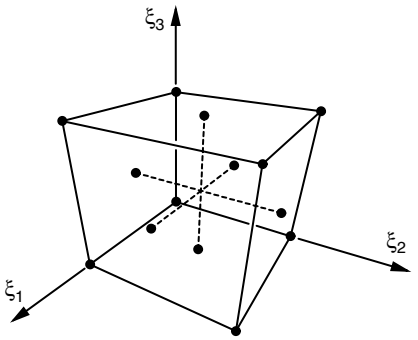

FIGURE 19.5 Central composite design scheme for $n = 3$.

this may become prohibitively expensive. Therefore frequently subsets are chosen that lead to *fractional factorial* designs.

The *central composite* design method (Figure 19.5) superimposes a full factorial design with $q = 2$ and a collection of all center points on the faces of an n-dimensional hypercube. Thus, it generates $m = (2^n + 2n)$ support points $\mathbf{x}^{(k)}$. The factors for $n = 3$ are given by

$$\xi = \begin{bmatrix} +1 & +1 & +1 & +1 & -1 & -1 & -1 & -1 & +1 & 0 & 0 & -1 & 0 & 0 \\ +1 & +1 & -1 & -1 & +1 & +1 & -1 & -1 & 0 & +1 & 0 & 0 & -1 & 0 \\ +1 & -1 & +1 & -1 & +1 & -1 & +1 & -1 & 0 & 0 & +1 & 0 & 0 & -1 \end{bmatrix} \tag{19.51}$$

D-optimal designs attempt to maximize the information content if only a small subset of the otherwise preferable full factorial design can be utilized, for example, due to restrictions on computer capacity. Given a set of candidate factors $\xi^{(k)}$, a subset of size m' is chosen in order to maximize the following function

$$D = \det(\mathbf{Q}'\mathbf{Q}) \tag{19.52}$$

In this equation, $\mathbf{Q}$ denotes a matrix containing values of the basis functions for the response surface evaluated at the selected support points (see Equation 19.9). Typically, the number m' is chosen to be 1.5-times the corresponding number of a saturated design.

19.3.4 Comparison

Table 19.1 shows the number of support points as a function of the number of variables for different experimental schemes. It is quite clear that factorial schemes—especially the full factorial—can become quite unattractive due to the exponential growth of the number of support points with increasing dimension of the problem. On the other hand, the more economical saturated designs do not allow for sufficient redundancy, which is needed to provide error control on the basis of the analysis of variance as outlined in a previous section. Therefore, moderately redundant schemes (such as *D*-optimal design) may provide the most appropriate solution.

TABLE 19.1 Numbers of Support Points for Different Experimental Designs

n	Linear	Quadratic	Full Factorial $q = 2$	Central Composite	Full Factorial $q = 3$
1	2	3	2	4	3
2	3	6	4	8	9
3	4	10	8	14	27
4	5	15	16	24	81
5	6	21	32	42	243

Copyright 2005 by CRC Press LLC

19.4 Reliability Computation

19.4.1 Choice of Method

Based on a chosen type of response surface and an appropriate design of experiments, an approximation for the limit state function is obtained. The subsequent reliability analysis usually can be performed with any available solution technique, such as first- and second-order method or Monte Carlo simulation. Because the cost of computation for one sample is extremely low, no special consideration needs to be given to achieve high efficiency. It should be carefully noted, however, that in the case of quadratic functions, unexpected phenomena might appear. A quadratic response surface $\eta(\mathbf{x})$ can generally be written in the form of

$$\eta(\mathbf{x}) = \boldsymbol{\theta}_0 + \boldsymbol{\theta}'\mathbf{x} + \mathbf{x}'\Theta\mathbf{x} \tag{19.53}$$

Here, the scalar coefficient $\boldsymbol{\theta}_0$, the vector θ, and the matrix $\boldsymbol{\Theta}$ have been obtained as outlined in the preceding sections. Unfortunately, there is no guarantee that the matrix $\boldsymbol{\Theta}$ is positive definite. If it turns out to be indefinite (i.e., it has both positive and negative eigenvalues), then the approximated limit state function is a hyperbolic surface. Hyperbolic surfaces are not simply connected, so they consist of several disjoint parts. Such surfaces may cause severe problems for optimization procedures, which are typically used in conjunction with the first-order reliability method. Generally, Monte Carlo-based methods are rather insensitive to the specific shape of the response surface and can be recommended. Adaptive sampling [25] provides a convenient importance sampling method that does not depend on the success of the first-order reliability method approach.

19.4.2 Error Checking and Adaptation of the Response Surface

In view of the statements made regarding the accuracy of the response surface near the region of the largest contribution to $P(F)$ (see Figure 19.1), it is mandatory to make sure that this region has been covered by the design of experiment scheme. Adaptive sampling utilizes the mean value vector $\boldsymbol{\mu}_F$ of the generated samples conditional on the failure domain F; that is,

$$\boldsymbol{\mu}_F = \mathbf{E}[\mathbf{X}|\mathbf{X} \in F] \tag{19.54}$$

If this vector lies outside the region covered by the experimental design scheme, it is advisable to repeat the experimental design around $\boldsymbol{\mu}_F$. This leads to an adaptive scheme in which the response surfaces are updated based on the results of the reliability analysis. A simple concept in this vein has been suggested in [12]. This is sketched in Figure 19.6. As indicated in Figure 19.6, the experimental design shifts all support points closer to the limit state $g(\mathbf{x}) = 0$. Ideally, some support points should lie on the limit state. A repeated calculation of $\boldsymbol{\mu}_F$ can be utilized as an indicator for convergence of the procedure.

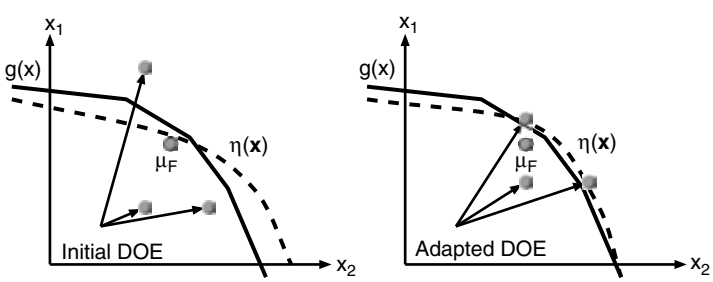

FIGURE 19.6 Simple adaptive response surface scheme.

Copyright 2005 by CRC Press LLC

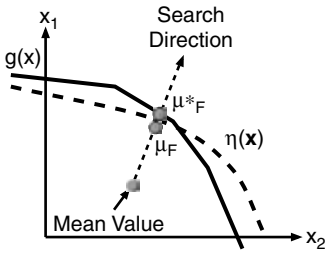

FIGURE 19.7 Simple error check for response surface.

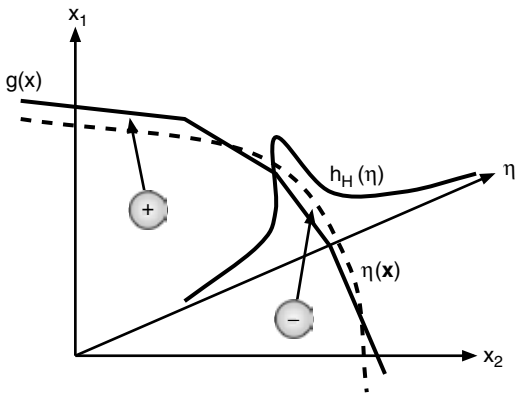

FIGURE 19.8 Correction to response surface using conditional sampling.

If computational resources are extremely limited so that a repetition of the design of experiment scheme is not feasible, it is recommended to at least check that the conditional mean $\boldsymbol{\mu}_F$ (which lies close to $\eta(\mathbf{x}) = 0$) is really close to the exact limit state $g(\mathbf{x}) = 0$. One possibility for that is to perform one single incremental analysis along the direction from the mean values of $\mathbf{X}$ to $\boldsymbol{\mu}_F$ resulting in a point $\boldsymbol{\mu}_F^*$ on the limit state (see Figure 19.7). If the distance between $\boldsymbol{\mu}_F$ and $\boldsymbol{\mu}_F^*$ is small, it may be concluded that the response surface is acceptable.

A somewhat different concept has been presented in [26]. Here, the concept of conditional sampling as introduced by [14] is utilized to generate random samples close to the approximate limit state $\eta(\mathbf{x}) = 0$. For this purpose, an importance sampling function $h(\eta)$ is introduced that allows the generation of suitable samples $\mathbf{x}^{(k)}$. For each of these samples, the exact limit state condition is checked. These samples are utilized to improve the estimate for the failure probability as obtained from the response surface approach. If the sample lies in the failure domain, the estimate for the failure probability is increased, if the sample lies in the safe domain, the estimate is decreased (see the positive and negative symbols in Figure 19.8).

19.5 Application to Reliability Problems

19.5.1 Linear Response Surface

As a first example, a truss-type structure under random static loads $F_1 = X_8$ and $F_2 = X_9$ is investigated (see Figure 19.9) . The loads are assumed to be independent, whereby their distribution function is of the Gumbel type with mean $\mu = 2 \cdot 10^7$ N and standard deviation $\sigma = 2 \cdot 10^6$ N. The characteristic length of the structure is $l = 1$ m. Whereas the elasticity modulus E of each truss is assumed to be a deterministic quantity with $E = 2 \cdot 10^{11}$ N/m^2, the respective areas A_1 to A_7 are mutually independent random quantities that are log-normally distributed with mean $\mu = 0.01$ m^2 and standard deviation $\sigma = 0.001$ m^2 ($A_i = X_i$, $i = 1, 2, \ldots, 7$).

Copyright 2005 by CRC Press LLC

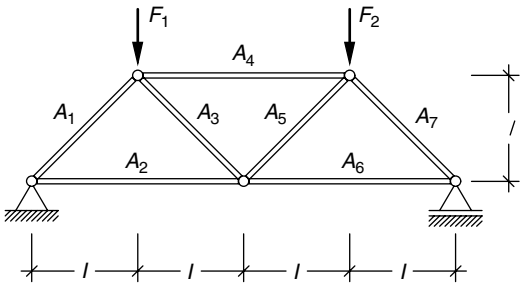

FIGURE 19.9 Truss-type structure.

In the following we are interested in the probability that the midspan deflection exceeds a value of 0.1 m. As the response surface we utilize a first-order polynomial of the form

$$\eta(\mathbf{u}) = \theta_0 + \sum_{i=1}^{9} \theta_i u_i \tag{19.55}$$

whereas u_i are the random variables x_i transformed to standard normal space, that is, $u_i = \mathbf{\Phi}^{-1}[F(x_i)]$. As design of experiments we choose a 2^{9-5}_{III} fractional factorial design [27] in standard normal space, that is,

$$\mathrm{u}' = \begin{bmatrix} -1 & -1 & -1 & -1 & -1 & -1 & +1 & -1 & -1 \\ -1 & -1 & +1 & -1 & +1 & +1 & -1 & +1 & -1 \\ -1 & -1 & +1 & +1 & -1 & +1 & -1 & -1 & +1 \\ -1 & -1 & -1 & +1 & +1 & -1 & +1 & +1 & +1 \\ +1 & -1 & +1 & +1 & +1 & -1 & -1 & -1 & -1 \\ +1 & -1 & -1 & +1 & -1 & +1 & +1 & +1 & -1 \\ +1 & -1 & -1 & -1 & +1 & +1 & +1 & -1 & +1 \\ +1 & -1 & +1 & -1 & -1 & -1 & -1 & +1 & +1 \\ -1 & +1 & -1 & +1 & +1 & +1 & -1 & -1 & -1 \\ -1 & +1 & +1 & +1 & -1 & -1 & +1 & +1 & -1 \\ -1 & +1 & +1 & -1 & +1 & -1 & +1 & -1 & +1 \\ -1 & +1 & -1 & -1 & -1 & +1 & -1 & +1 & +1 \\ +1 & +1 & +1 & -1 & -1 & +1 & +1 & -1 & -1 \\ +1 & +1 & -1 & -1 & +1 & -1 & -1 & +1 & -1 \\ +1 & +1 & -1 & +1 & -1 & -1 & -1 & -1 & +1 \\ +1 & +1 & +1 & +1 & +1 & +1 & +1 & +1 & +1 \end{bmatrix} \tag{19.56}$$

An adaptation of the response surface is performed by determining in each step the design-point $\mathbf{u}^* = (u_1^*, u_2^*, \ldots, u_9^*)'$ for the approximating response surface $\eta(\mathbf{u})$ and repeat the experimental design centered at this design-point. As the start point we utilize the origin in standard normal space.

In Table 19.2 the first two steps of the adaptive response surface method as well as the converged result are displayed and compared with the result from first-order reliability method. As can be seen, the response surface provides a very good approximation of the true limit state function already in the second step (i.e., after the first adaptation). To verify that the chosen response surface model is appropriate, we

Copyright 2005 by CRC Press LLC

TABLE 19.2 Analysis of Variance (Truss-Type Structure)

	First-Order Reliability method	Response Surface		
		1. Step	2. Step	Last Step
s_t	—	$4.91 \cdot 10^{-4}$	$4.43 \cdot 10^{-3}$	$2.34 \cdot 0^{-3}$
s_r	—	$4.90 \cdot 10^{-4}$	$4.42 \cdot 10^{-3}$	$2.34 \cdot 10^{-3}$
s_e	—	$8.69 \cdot 10^{-7}$	$9.70 \cdot 10^{-6}$	$5.16 \cdot 10^{-6}$
r^2	—	0.99	0.99	0.99
r_A^2	—	0.99	0.99	0.99
F_0	—	375.83	304.02	302.23
u_1^*	−0.64	−1.44	−0.60	−0.62
u_2^*	−0.44	−1.02	−0.41	−0.43
u_3^*	0.00	0.00	0.00	0.00
u_4^*	−0.93	−2.07	−0.93	−0.93
u_5^*	0.00	−0.10	−0.08	−0.08
u_6^*	−0.44	−1.02	−0.41	−0.43
u_7^*	−0.64	−1.50	−0.66	−0.67
u_8^*	2.55	3.22	2.56	2.37
u_9^*	2.55	3.22	2.56	2.37
β	3.89	5.61	3.89	3.65

determine in each step the coefficient r^2, its adjusted form r_A^2, and the F-statistic. Both r^2 and r_A^2 show values approaching 1, clearly indicating that the response surface model is capable of reproducing the variation in the experimental data almost to its entirety. This is also supported by the F-statistic, because when choosing a confidence level of $\alpha = 1\%$, we can clearly reject the hypothesis, because always $F_0 > F_{0.01,9,6} = 7.98$.

19.5.2 Nonlinear Response Surface

Given is a tension bar with known load $T = 1$, random diameter X_1 and yield strength X_2. The dimensionless limit state function is given as

$$g(x_1,\ x_2) = \frac{\pi x_1^2}{4} x_2 - T = 0 \tag{19.57}$$

The random variables X_1 and X_2 are independent. X_1 is log-normally distributed with distribution function $F(x) = \Phi[(\ln(x) - 1)/2],\ x > 0$. X_2 obeys the Rayleigh distribution function $F(x) = 1 - \exp[-\pi x^2/(4\mu^2)],\ x \geq 0$, with mean $\mu = 200$. The response surface model we want to use in the following is a first-order polynomial of the form

$$\eta(\mathbf{u}) = \theta_0 + \theta_1 u_1 + \theta_2 u_2 \tag{19.58}$$

whereas u_1 and u_2, respectively, are the random variables x_1 and x_2 transformed to standard normal space (i.e., $u_i = \Phi^{-1}[F(x_i)]$). As design of experiments we utilize a 2^2-factorial design with one center run in standard normal space, that is,

$$\mathbf{u} = \begin{bmatrix} -1 & +1 & -1 & +1 & 0 \\ -1 & -1 & +1 & +1 & 0 \end{bmatrix} \tag{19.59}$$

As the method for adaptation, we again determine in each step the design-point $\mathbf{u}^* = (u_1^*, u_2^*)'$ for the approximating response surface $\eta(\mathbf{u})$ and repeat the experimental design centered at this design-point. As the start point we utilize the origin in standard normal space.

When applying this scheme we perform again an accompanying analysis of variance; that is, we determine in each step the coefficient r^2, its adjusted form r_A^2, and the F-statistic. As can be seen from Table 19.3, the

Copyright 2005 by CRC Press LLC

TABLE 19.3 Analysis of Variance (Tension Bar)

	Original Scale			Transformed Scale		
	1. Step	2. Step	Last Step	1. Step	2. Step	Last Step
s_t	$6.60 \cdot 10^9$	$3.19 \cdot 10^8$	16.95	17.41	19.40	22.90
s_r	$5.04 \cdot 10^9$	$2.38 \cdot 10^8$	10.95	17.40	19.38	22.86
s_e	$1.56 \cdot 10^9$	$0.81 \cdot 10^8$	6.00	0.01	0.02	0.04
r^2	0.76	0.74	0.64	0.99	0.99	0.99
r_A^2	0.53	0.49	0.29	0.99	0.99	0.99
F_0	3.23	2.92	1.82	2044.73	857.02	631.24
u_1^*	–0.68	–1.30	–3.54	–4.10	–3.75	–3.41
u_2^*	–0.37	–0.79	–3.51	–1.21	–1.73	–2.24
β	0.77	1.52	4.98	4.27	4.13	4.08

above-mentioned measures indicate a nonsatisfactory performance of the chosen response surface model. Not only do the values of r^2 and r_A^2 differ considerably from each other, but they are also clearly different from the optimal value of 1. This indicates that the model is not able to reproduce appropriately the variation in the experimental data. Furthermore, when testing the null hypothesis H_0 of Equation 19.28 at a confidence level of $\alpha = 1\%$, we cannot reject the hypothesis, because clearly $F_0 < F_{0.01,2,2} = 99$. In other words, the chosen response surface model is not appropriate for the experimentally gained data. This can also be noticed when investigating Figure 19.10, which displays the limit state function $g(\mathbf{u})$ in standard normal space for different values of T. As can be seen, the limit state function is highly nonlinear.

Nevertheless, when taking the logarithm of the response values, a linear response surface would represent a good approximation of the true limit state function. Therefore, a more adequate response surface model would be of the form

$$\eta(\mathbf{u}) = \theta_0 \exp(\theta_1 u_1 + \theta_2 u_2) - 1 \tag{19.60}$$

which can be transformed to its linear form by

$$\tilde{\eta}(\mathbf{u}) = \ln(\eta + 1) = \ln(\theta_0) + \theta_1 u_1 + \theta_2 u_2 = \hat{\theta}_0 + \theta_1 u_1 + \theta_2 u_2 \tag{19.61}$$

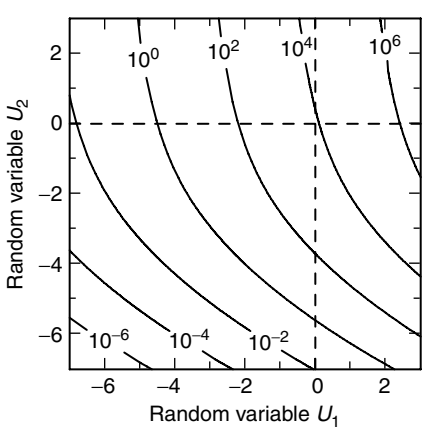

FIGURE 19.10 Limit state function $g(\mathbf{u})$ in standard normal random variable space for different values of T.

Copyright 2005 by CRC Press LLC

When using this response surface model, all measures displayed in Table 19.3 show satisfactory values. Moreover, already in the second step (i.e., after the first adaptation), a reasonable approximation of the exact result can be achieved. The response surface method converges to the point $\mathbf{u}^* = (-3.41, -2.24)'$, which relates to a reliability index $\beta = 4.08$. These results are an excellent approximation of the true design-point $\mathbf{u}^* = (-3.46, -2.29)'$ and the true reliability index $\beta = 4.15$. It should also be noted that if we would have dismissed the indicators in the original scaling as being not relevant, the response surface analysis would not provide a satisfactory result, as can be seen from Table 19.3.

19.5.3 Nonlinear Finite Element Structure

A simple three-dimensional steel frame subjected to three random loadings is considered as shown in Figure 19.11. The three-dimensional frame is modeled by 24 physically nonlinear beam elements (linear elastic-ideally plastic material law, elasticity modulus $E = 2.1 \cdot 10^{11}$ N/m^2, yield stress $\sigma_Y = 2.4 \cdot 10^8$ N/m^2). The cross section for the girder is a box (width 0.2 m, height 0.15 m, wall thickness 0.005 m) and the columns are I-sections (flange width 0.2 m, web height 0.2 m, thickness 0.005 m). The columns are fully clamped at the supports. The static loads acting on the system p_z, F_x, and F_y are assumed to be random variables. Their respective properties are given in Table 19.4. The failure condition is given by total or partial collapse of the structure. Numerically, this is checked either by tracking the smallest eigenvalue of the global tangent stiffness matrix (it becomes 0 at the collapse load) or by failure in the global Newton iteration indicating loss of equilibrium. Because this type of collapse analysis is typically based on a discontinuous function (convergence vs. nonconvergence), it is imperative that the support points for the response surface be located exactly at the limit state. A bisection procedure is utilized to determine collapse loads with high precision (to the accuracy of 1% of the respective standard deviation).

The geometry of the limit state separating the safe from the failure domain is shown in Figure 19.12. The limit points were obtained from directional sampling using 500 samples. The size of the dots indicates the visual distance from the viewer. It can be easily seen that there is considerable interaction between the random variables F_x and F_y at certain levels. The region of most importance for the probability of failure (this is where most of the points from the directional sampling are located) is essentially flat, and mainly governed by the value of F_y. This is clearly seen in Figure 19.13. The box in this figure indicates a space of ± 5 standard deviations around the mean values. The probability of failure obtained from directional sampling is $P(F) = 2.3 \cdot 10^{-4}$, with an estimation error of 20%.

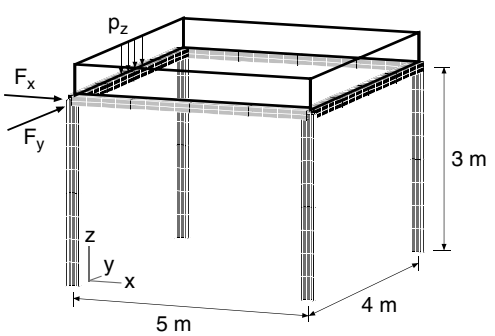

FIGURE 19.11 Three-dimensional steel frame structure.

TABLE 19.4 Random Variables Used in Three-Dimensional Frame Analysis

Random Variable	Mean Value	Standard Deviation	Distribution Type
p_z [kN/m]	12.0	0.8	Gumbel
F_x [kN]	30.0	2.4	Gumbel
F_y [kN]	40.0	3.2	Gumbel

Copyright 2005 by CRC Press LLC

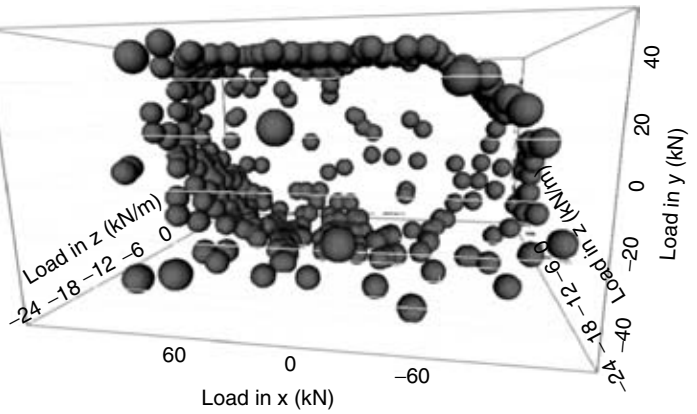

FIGURE 19.12 Visualization of limit state function $g(\mathbf{x})$.

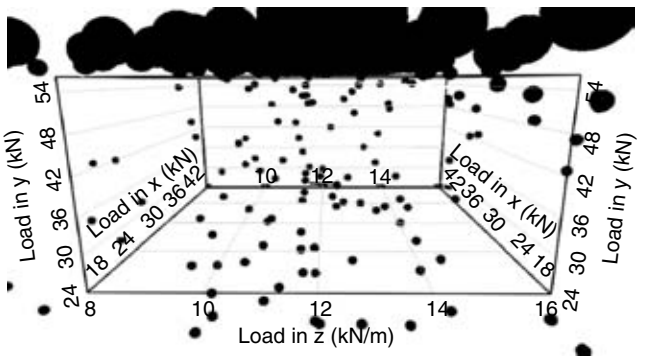

FIGURE 19.13 Visualization of limit state function $g(\mathbf{x})$, details near mean.

A saturated quadratic scheme including pairwise interactions is utilized for the initial layout of the experimental design scheme. The support points thus generated are interpreted as direction vectors along which all loads are incremented. Starting from the mean values, and incrementing along this direction, lead to a set of nine support points on the limit state function. These support points (see Table 19.5) have a function value of $g(\mathbf{x}) = 0$. By adding the mean value as first support point with a function value of $g(\mathbf{x}) = 1$, a quadratic response surface can be defined. Considering lines 2 through 7 in Table 19.5, it was decided to consider combination terms in which all variables are incremented up from the mean. This leads to the final three support points given in lines 7 through 10 of Table 19.5.

TABLE 19.5 Support Points for Response Surface

i-th Support Point $\mathbf{x}^{(i)}$	p_z [kN/m]	F_x [kN]	F_y [kN]	$g(\mathbf{x}^{(i)})$
1	12.000	30.000	40.000	1
2	21.513	30.000	40.000	0
3	−21.516	30.000	40.000	0
4	12.000	113.180	40.000	0
5	12.000	−81.094	40.000	0
6	12.000	30.000	59.082	0
7	12.000	30.000	−59.087	0
8	19.979	109.790	40.000	0
9	13.527	30.000	59.084	0
10	12.000	45.275	59.094	0

Copyright 2005 by CRC Press LLC

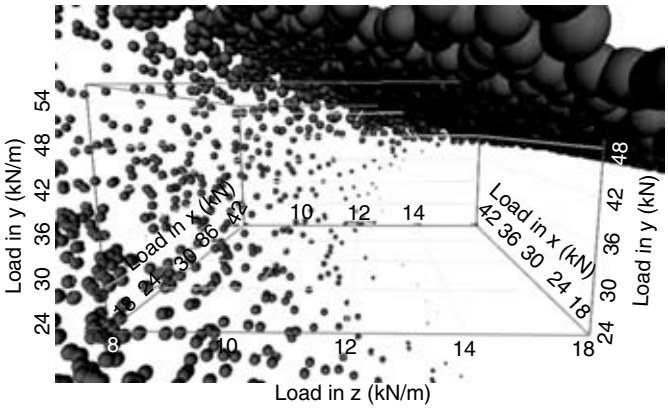

FIGURE 19.14 Visualization of response surface $\eta(\mathbf{x})$, details near mean.

A Monte Carlo simulation based on this quadratic surface is carried out. The sampling scheme utilized is adaptive sampling [25], which iteratively updates the importance sampling density. The resulting probability of failure from three consecutive runs with 3000 samples each was found to be $P(F) = 1.7 \cdot 10^{-4}$, with an estimation error of 2%. Alternatively, directional sampling with 1000 samples was carried out, yielding the same value for $P(F)$. As a by-product, simple visualizations of the response surface can easily be obtained from the directional sampling procedure because this procedure calculates the location of a failure point in a randomly simulated direction. Figure 19.14 shows that the response surface is almost flat in the important region. Consequently, the resulting failure probability matches the exact result very well. The conditional mean vector of the samples in the failure domain is found to be

$$\boldsymbol{\mu}_F = (13.457, 30.160, 59.977)' \tag{19.62}$$

and an incremental search in the direction from the mean values to $\boldsymbol{\mu}_F$ yields a point at the exact limit state

$$\boldsymbol{\mu}_F^* = (13.391, 30.153, 59.080)' \tag{19.63}$$

so that the distance δ between these two points (measured in multiples of the standard deviations) is $\delta = 0.29$. This can be considered reasonably small.

19.6 Recommendations

Based on the examples shown above, the following guidelines and recommendations for the successful application of response surface methods in structural reliability analyses can be given:

- Utilize all available knowledge about the structural behavior, especially sensitivity analysis to eliminate unimportant or unnecessary random variables. In this context, the following hints may be helpful:
  - Use engineering judgment to eliminate random variables whose coefficient of variation is significantly smaller compared to others.
  - Use simple parameter variations, one variable at a time in the magnitude of 1 to 2 standard deviations to assess the sensitivity.
  - Reduce the structural model to include only relevant failure mechanisms.
- Choose an experimental design scheme that is compatible with the type of response surface you wish to utilize.

Copyright 2005 by CRC Press LLC

- Make sure that the experimental design scheme yields support points well within the range of definition of the random variables.
- In general, highly redundant experimental designs do not improve the results significantly over saturated or moderately redundant designs.
- Utilize a simple experimental and a simple response surface with the possibility of adaptation, rather than a complex design of experiments and a complex response surface.
- Make sure that the response surface obtained is "well-behaved" in the sense that its mathematical properties do not interfere with reliability computation. This is of particular importance when using a calculation technique based on the first order reliability method.
- Allow for sufficient computational power to perform some adaptation of the response surface or at least simple error checking.

References

1. Rackwitz, R., *Response Surfaces in Structural Reliability*, Berichte zur Zuverlässigkeitstheorie der Bauwerke, Heft 67, München, 1982.
2. Box, G.E.P. and Wilson, K.B., On the experimental attainment of optimum conditions, *Journal of the Royal Statistical Society, Series B*, 13, 1–45, 1951.
3. Box, G.E.P. and Draper, N.R., A basis for the selection of a response surface design, *Journal of the American Statistical Association*, 54, 622–654, 1959.
4. Hill, W.J. and Hunter, W.G., A review of response surface methodology: a literature survey, *Technometrics*, 8, 571–590, 1966.
5. Mead, R. and Pike, D.J., A review of response surface methodology from a biometric viewpoint, *Biometrics*, 31, 803–851, 1975.
6. Myers, R.H., Khuri, A.I., and Carter, Jr., W.H., Response surface methodology: 1966–1988, *Technometrics*, 31, 137–157, 1989.
7. Myers, R.H., Response surface methodology — Current status and future directions, *Journal of Quality Technology*, 31, 30–44, 1999.
8. Box, G.E.P. and Draper, N.R., *Empirical Model-Building and Response Surfaces*, Wiley, New York, 1987.
9. Khuri, A.I. and. Cornell, J.A., *Response Surfaces: Designs and Analyses*, Dekker, New York, 1996.
10. Myers, R.H. and Montgomery, D.C., *Response Surface Methodology: Process and Product Optimization Using Designed Experiments*, Wiley, New York, 2002.
11. Wong, F.S., Slope reliability and response surface method, *Journal of Geotechnical Engineering*, 111, 32–53, 1985.
12. Bucher, C.G. and Bourgund, U., A fast and efficient response surface approach for structural reliability problems, *Structural Safety*, 7, 57–66, 1990.
13. Faravelli, L., Response-surface approach for reliability analysis, *Journal of Engineering Mechanics, ASCE*, 115, 2763–2781, 1989.
14. Ouypornprasert, W., Bucher, C.G., and Schuëller, G.I., On the application of conditional integration in structural reliability analysis, in *Proc. 5th Int. Conf. on Structural Safety and Reliability*, San Francisco, Ang, A.H.-S., Shinozuka, M., and Schuëller, G.I., Eds., ASCE, New York, 1989, 1683–1689.
15. Kim, S.-H. and. Na, S.-W., Response surface method using vector projected sampling points, *Structural Safety*, 19, 3–19, 1997.
16. Zheng, Y. and Das, P.K., Improved response surface method and its application to stiffened plate reliability analysis, *Engineering Structures*, 22, 544–551, 2000.
17. Brenner C.E. and Bucher, C., A contribution to the SFE-based reliability assessment of nonlinear structures under dynamic loading, *Probabilistic Engineering Mechanics*, 10, 265–273, 1995.
18. Ghanem, R. and Spanos, P.D., *Stochastic Finite Elements — A Spectral Approach*, Springer, New York, 1991.

Copyright 2005 by CRC Press LLC

19. Guan, X.L. and Melchers, R.E., Multitangent-plane surface method for reliability calculation, *Journal of Engineering Mechanics, ASCE*, 123, 996–1002, 1997.
20. Roos, D., Bucher, C., and Bayer, V., Polyhedra response surfaces for structural reliability assessment, in *Proc. 8th Int. Conf. on Applications of Statistics and Probability*, Sydney, Melchers, R.E. and Stewart, M.G., Eds., Balkema, Rotterdam, 2000, 109–115.
21. Bjerager, P., Probability integration by directional simulation, *Journal of Engineering Mechanics, ASCE*, 114, 1285–1302, 1988.
22. Böhm, F. and Brückner-Foit, A., On criteria for accepting a response surface model, *Probabilistic Engineering Mechanics*, 7, 183–190, 1992.
23. Yao, T.H.-J. and Wen, Y.K., Response surface method for time-variant reliability analysis, *Journal of Structural Engineering, ASCE*, 122, 193–201, 1996.
24. Hohenbichler, M. and Rackwitz, R., Nonnormal dependent vectors in structural safety, *Journal of the Engineering Mechanics Division, ASCE*, 107, 1227–1238, 1981.
25. Bucher, C.G., Adaptive sampling — An iterative fast Monte Carlo procedure, *Structural Safety*, 5, 119–126, 1988.
26. Schuëller, G.I. and Bucher, C.G., Computational stochastic structural analysis — A contribution to the software development for the reliability assessment of structures under dynamic loading, *Probabilistic Engineering Mechanics*, 6, 134–138, 1991.
27. Montgomery, D.C., *Design and Analysis of Experiments*, Wiley, New York, 1997.

Copyright 2005 by CRC Press LLC

20

Stochastic Simulation Methods for Engineering Predictions

Dan M. Ghiocel
Ghiocel Predictive Technologies, Inc.

20.1 Introduction

The term "simulation" comes from the Latin word *simulatio*, which means to imitate a phenomenon or a generic process. In the language of mathematics, the term "simulation" was used for the first time during the World War II period at the Los Alamos National Laboratory by the renowned mathematicians Von Neumann, Ulam, Metropolis and physicist Fermi, in the context of their nuclear physics research for the atomic bomb. About the same time they also introduced an exotic term in mathematics, namely "Monte Carlo" methods. These were defined as numerical methods that use artificially generated statistical selections for reproducing complex random phenomena and for solving multidimensional integral problems. The name "Monte Carlo" was inspired by the famous Monte Carlo casino roulette, in France, that was the best available generator of uniform random numbers.

In scientific applications, stochastic simulation methods based on random sampling algorithms, or Monte Carlo methods, are used to solve two types of problems: (1) to generate random samples that belong to a given stochastic model, or (2) to compute expectations (integrals) with respect to a given distribution. The expectations might be probabilities, or discrete vectors or continuous fields of probabilities or in other words, probability distributions. It should be noted that if the problem is solved,

Copyright 2005 by CRC Press LLC

so that random samples are available, then the solution to the problem, to compute expectations, becomes trivial because expectations can be approximated by the statistical averaging of the random samples.

The power of Monte Carlo methods manifests visibly for multidimensional probability integration problems, for which the typical deterministic integration algorithms are extremely inefficient. For very low-dimensional problems, in one dimension or two, Monte Carlo methods are too slowly convergent and therefore there is no practical interest in employing them. For a given number of solution points N, the Monte Carlo estimator converges to the exact solution with rate of the order $O(N^{-1/2})$ in comparison with some deterministic methods that converge much faster with rates up to the order $O(N^{-4})$ or even $O(\exp(-N))$. Unfortunately, for multidimensional problems, the classical deterministic integration schemes based on regular discretization grids fail fatally. The key difference between stochastic and deterministic methods is that the Monte Carlo methods are, by their nature, meshless methods, while the deterministic integration methods are regular grid-based methods. The problem is that the classical grid-based integration methods scale very poorly with the space dimensionality.

The fact that the Monte Carlo estimator convergence rate is independent of the input space dimensionality makes the standard Monte Carlo method very popular for scientific computing applications. Although the statistical convergence rate of the Monte Carlo method is independent of the input space dimensionality, there are still two difficulties to address that are dependent on the input space dimensionality: (1) how to generate uniformly distributed random samples in the prescribed stochastic input domain, and (2) how to control the variance of Monte Carlo estimator for highly "nonuniform" stochastic variations of the integrand in the prescribed input domain. These two difficulties are becoming increasingly important as the input space dimensionality increases. One can imagine a Monte Carlo integration scheme as a sort of a random fractional factorial sampling scheme or random quadrature that uses a refined cartesian grid of the discretized multidimensional input domain with many unfilled nodes with data, vs. the deterministic integration schemes or deterministic quadratures that can be viewed as complete factorial sampling schemes using cartesian grids with fully filled nodes with data. Thus, a very important aspect to get good results while using Monte Carlo is to ensure as much as possible a *uniform filling* of the input space domain grid with statistically independent solution points so that the potential local subspaces that can be important are not missed. The hurting problem of the standard Monte Carlo method is that for high-dimensional spaces, it is difficult to get uniform filling of the input space. The consequence of a nonuniform filling can be a sharp increase in the variance of the Monte Carlo estimator, which severely reduces the attraction for the method.

The classical way to improve the application of Monte Carlo methods to high-dimensional problems is to partition the stochastic input space in subdomains with uniform statistical properties. Instead of dealing with the entire stochastic space, we deal with subdomains. This is like defining a much coarser grid in space to work with. The space decomposition in subdomains may accelerate substantially the statistical convergence for multidimensional problems. Stratified sampling and importance sampling schemes are different sampling weighting schemes based on stochastic space decomposition in partitions. Using space decomposition we are able to control the variation of the estimator variance over the input domain by focusing on the most important stochastic space regions (mostly contributing to the integrand estimate) and adding more random data points in those regions.

Another useful way to deal with the high dimensionality of stochastic space is to simulate correlated random samples, instead of statistically independent samples, that describe a random path or walk in stochastic space. If the random walk has a higher attraction toward the regions with larger probability masses, then the time spent in a region vs. the time (number of steps) spent in another region is proportional to the probability mass distributions in those regions. By withdrawing samples at equal time intervals (number of steps), we can build an approximation of the prescribed joint probability distribution. There are two distinct classes of Monte Carlo methods for simulating random samples from a prescribed multivariate probability distribution: (1) static Monte Carlo (SMC), which is based on the generation of independent samples from univariate marginal densities or conditional densities; and (2) dynamic Monte Carlo (DMC), which is based on spatially correlated samples that describe the random evolutions of a *fictitious* stochastic dynamic system that has a stationary probability distribution identical

Copyright 2005 by CRC Press LLC

with the prescribed joint probability distribution. Both classes of Monte Carlo methods are discussed herein.

This chapter focuses on the application of Monte Carlo methods to simulate random samples of a variety of stochastic models — from the simplest stochastic models described by one-dimensional random variable models, to the most complex stochastic models described by hierarchical stochastic network-like models. The chapter also includes a solid section on high-dimensional simulation problems that touches key numerical issues including sequential sampling, dynamic sampling, computation of expectations and probabilities, modeling uncertainties, and sampling using stochastic partial-differential equation solutions. The goal of this chapter is to provide readers with the conceptual understanding of different simulation methods without trying to overwhelm them with all the implementation details that can be found elsewhere as cited in the text.

20.2 One-Dimensional Random Variables

There are a large number of simulation methods available to generate random variables with various probability distributions. Only the most popular of these methods are reviewed in this chapter: (1) inverse probability transformation, (2) sampling acceptance-rejection, (3) bivariate functional transformation, and (4) density decomposition. The description of these methods can be found in many textbooks on Monte Carlo simulations [1–5]. Herein, the intention is to discuss the basic concepts of these methods and very briefly describe their numerical implementations. In addition to these classical simulation methods, there is a myriad of many other methods, most of them very specific to particular types of problems, that have been developed over the past decades but for obvious reasons are not included.

20.2.1 Uniform Random Numbers

The starting point for any stochastic simulation technique is the construction of a reliable uniform random number generator. Typically, the random generators produce random numbers that are uniformly distributed in the interval [0, 1]. The most common uniform random generators are based on the linear congruential method [1–5].

The quality of the uniform random number generator reflects on the quality of the simulation results. It is one of the key factors that needs special attention. The quality of a random generator is measured by (1) the uniformity in filling with samples the prescribed interval and (2) its period, which is defined by the number of samples after which the random generator restarts the same sequence of independent random numbers all over again. Uniformity is a crucial aspect for producing accurate simulations, while the generator periodicity is important only when a large volume of samples is needed. If the volume of samples exceeds the periodicity of the random number generator, then the sequence of numbers generated after this is perfectly correlated with initial sequence of numbers, instead of being statistically independent. There are also other serial correlation types that can be produced by different number generators [4]. If we need a volume of samples for simulating a rare random event that is several times larger than the generator periodicity, then the expected simulation results will be wrong due to the serial correlation of the generated random numbers.

An efficient way to improve the quality of the generated sequence of uniform numbers and break their serial correlation is to combine the outputs of few generators into a single uniform random number that will have a much larger sequence periodicity and expectedly better space uniformity. As general advice to the reader, it is always a good idea to use statistical testing to check the quality of the random number generator.

20.2.2 Inverse Probability Transformation

Inverse probability transformation (IPT) is based on a lemma that says that for any random variable x with the probability distribution F, if we define a new random variable y with the probability distribution F^{-1} (i.e., the inverse probability transformation of F), then $y = F^{-1}(u)$ has a probability distribution F.

Copyright 2005 by CRC Press LLC

The argument u of the inverse probability transformation stands for a uniformly distributed random variable.

The general algorithm of the IPT method for any type of probability distribution is as follows:

Step 1: Initialize the uniform random number generator.
Step 2: Implement the algorithm for computing F^{-1}.
Step 3: Generate a uniform random number u in the interval [0, 1].
Step 4: Compute the generated deviate x with the distribution F by computing $x = F^{-1}(u)$.

Because the probability or cumulative distribution functions (CDFS) are monotonic increasing functions, the IPT method can be applied to any type of probability distribution, continuous or discrete, analytically or numerically defined, with any probability density function (PDF) shapes, from symmetric to extremely skewed, from bell-shaped to multimodal-shaped.

Very importantly, IPT can be also used to transform a sequence of Gaussian random deviates into a sequence of nonGaussian random deviates for any arbitrarily shaped probability distribution. A generalization of the IPT method, called the transformation method, is provided by Press et al. [4].

20.2.3 Sampling Acceptance-Rejection

Sampling acceptance-rejection (SAR) uses an auxiliary, trial, or proposal density to generate a random variable with a prescribed distribution. SAR is based on the following lemma: If x is a random variable with the PDF $f(x)$ and y is another variable with the PDF $g(y)$ and the probability of $f(y) = 0$, then the variable x can generated by first generating variable y and assuming that there is a positive constant α such as $\alpha \geq f(x)/g(x)$. If u is a uniform random variable defined on [0, 1], then the PDF of y conditioned on relationship $0 \leq u \leq f(y)/\alpha g(y)$ is identical with $f(x)$.

A typical numerical implementation of the SAR method for simulating a variable x with the PDF $f(x)$ is as follows:

Step 1: Initialize the uniform random number generator and select constant α.
Step 2: Generate a uniform number u on [0, 1] and a random sample of y.
Step 3: If $u > f(y)/\alpha g(y)$, then reject the pair (u, y) and go back to the previous step.
Step 4: Otherwise, accept the pair (u, y) and compute $x = y$.

It should be noted that SAR can be easily extended to generate random vectors and matrices with independent components.

The technical literature includes a variety of numerical implementations based on the principle of SAR [6]. Some of the newer implementations are the weighted resampling and sampling importance resampling (SIR) schemes [6, 7] and other adaptive rejection sampling [8].

20.2.4 Bivariate Transformation

Bivariate transformation (BT) can be viewed as a generalization of the IPT method for bivariate probability distributions. A well-known application of BT is the Box-Muller method for simulating standard Gaussian random variables [9]. Details are provided in [4–6].

20.2.5 Density Decomposition

Density decomposition (DD) exploits the fact that an arbitrary PDF, $f(x)$, can be closely approximated in a linear combination elementary density function as follows:

$$f(x) = \sum_{i=1}^{N} p_i g_i(x) \tag{20.1}$$

in which $0 \leq p_i < 1$, $1 \leq i \leq N$, and $\sum_{i=1}^{N} p_i = 1$.

Copyright 2005 by CRC Press LLC

The typical implementation of DD for a discrete variable x is as follows:

Step 1: Initialize for the generation of a uniform random number and a variable z_i with the PDF $g_i(x)$. This implies that $x = z_i$ with the probability p_i.
Step 2: Compute the values $G_i(x) = \sum_{j=1}^{i} p_j$ for all i values, $i = 1, N$.
Step 3: Generate a uniform random variable u on [0, 1].
Step 4: Loop $j = 1, N$ and check if $u < G_i(x)$. If not, go to the next step.
Step 5: Generate z_j and assign $x = z_j$.

It should be noted that the speed of the above algorithm is highest when the p_i values are ordered in descending order. It should be noted that DD can be combined with SAR. An example of such a combination is the Butcher method [10] for simulating normal deviates.

20.3 Stochastic Vectors with Correlated Components

In this section the numerical simulation of stochastic vectors with independent and correlated components is discussed. Both Gaussian and nonGaussian vectors are considered.

20.3.1 Gaussian Vectors

A multivariate Gaussian stochastic vector $\mathbf{x}$ of size m with a mean vector $\boldsymbol{\mu}$ and a covariance matrix $\boldsymbol{\Sigma}$ is completely described by the following multidimensional joint probability density function (JPDF):

$$f_x(\mu, \Sigma) = \frac{1}{(2\pi)^{\frac{m}{2}} (\det \Sigma)^{\frac{1}{2}}} \exp\left[-\frac{1}{2}(\mathbf{x}-\mu)^T \Sigma^{-1}(\mathbf{x}-\mu)\right] \tag{20.2}$$

The probability distribution of vector $\mathbf{x}$ is usually denoted as $N(\boldsymbol{\mu}, \boldsymbol{\Sigma})$. If the Gaussian vector is a standard Gaussian vector, $\mathbf{z}$, with a zero mean, $\mathbf{0}$, and a covariance matrix equal to an identity matrix, $\mathbf{I}$, then its probability distribution is $N(\mathbf{0}, \mathbf{I})$. The JPDF of vector $\mathbf{z}$ is defined by:

$$f_z(\mathbf{0}, \mathbf{I}) = \frac{1}{(2\pi)^{\frac{m}{2}} (\det \Sigma)^{\frac{1}{2}}} \exp\left(-\frac{1}{2}\mathbf{z}^T\mathbf{z}\right) = \prod_{i=1}^{m} \frac{1}{\sqrt{2\pi}} \exp\left(-\frac{1}{2}z_i^2\right) \tag{20.3}$$

To simulate a random sample of a Gaussian stochastic vector $\mathbf{x}$ (with correlated components) that has the probability distribution $N(\boldsymbol{\mu}, \boldsymbol{\Sigma})$, a two computational step procedure is needed:

Step 1: Simulate a standard Gaussian vector $\mathbf{z}$ (with independent random components) having a probability distribution $N(\mathbf{0}, \mathbf{I})$. This step can be achieved using standard routines for simulating independent normal random variables.
Step 2: To compute the vector $\mathbf{x}$ use the linear matrix equation

$$\mathbf{x} = \boldsymbol{\mu} + \mathbf{S}\mathbf{z} \tag{20.4}$$

where matrix $\mathbf{S}$ is called the *square-root matrix* of the positively definite covariance matrix $\boldsymbol{\Sigma}$. The matrix $\mathbf{S}$ is a lower triangular matrix that is computed using the Choleski decomposition that is defined by the equation $\mathbf{S}\mathbf{S}^T = \boldsymbol{\Sigma}$.

Another situation of practical interest is to generate a Gaussian vector $\mathbf{y}$ with a probability distribution $N(\mu_y, \Sigma_{yy})$ that is conditioned on an input Gaussian vector $\mathbf{x}$ with a probability distribution $N(\mu_x, \Sigma_{xx})$. Assuming that the augmented vector $[\mathbf{x}, \mathbf{y}]^T$ has the mean $\boldsymbol{\mu}$ and the covariance matrix $\boldsymbol{\Sigma}$ defined by

$$\mu = \begin{pmatrix} \mu_y \\ \mu_x \end{pmatrix} \qquad \Sigma = \begin{pmatrix} \Sigma_{yy} & \Sigma_{yx} \\ \Sigma_{xy} & \Sigma_{xx} \end{pmatrix} \tag{20.5}$$

Copyright 2005 by CRC Press LLC

then the statistics of the conditional vector **y** are computed by the matrix equations:

$$\begin{aligned} \mu_y &= \mu_y + \Sigma_{yx} \cdot \Sigma_{xx}^{-1}(\mathbf{x} - \mu_x) \\ \Sigma_{yy} &= \Sigma_{yy} - \Sigma_{yx}\Sigma_{xx}^{-1}\Sigma_{xy} \end{aligned} \tag{20.6}$$

It is interesting to note that the above relationships define a stochastic condensation procedure of reducing the size of a stochastic vector from the size of the total vector $[\mathbf{y}, \mathbf{x}]^T$ with probability distribution $N(\boldsymbol{\mu}, \boldsymbol{\Sigma})$ to a size of the reduced vector **y** with a probability distribution $N(\mu_y, \Sigma_{yy})$. The above simulation procedures employed for Gaussian vectors can be extended to nonGaussian vectors, as shown in the next subsection.

An alternate technique to the Choleski decomposition for simulating stochastic vectors with correlated components is the popular principal component analysis. Principal component analysis (PCA) is based on eigen decomposition of the covariance matrix. If PCA is used, then the matrix equation in the Step 2 shown above is replaced by the following matrix equation

$$\mathbf{x} = \mu + \Phi\lambda^{1/2}\mathbf{z} \tag{20.7}$$

where $\boldsymbol{\lambda}$ and Φ are the eigenvalue and eigenvector matrices, respectively, of the covariance matrix.

20.3.2 NonGaussian Vectors

A nonGaussian stochastic vector is completely defined by its JPDF. However, most often in practice, a nonGaussian vector is only partially defined by its second-order moments (i.e., the mean vector and the covariance matrix) and its marginal probability distribution (MCDF) vector. This definition loses information about the high-order statistical moments that are not defined.

These partially defined nonGaussian vectors form a special class of nonGaussian vectors called translation vectors. Thus, the translation vectors are nonGaussian vectors defined by their second-order moments and their marginal distributions. Although the translation vectors are not completely defined stochastic vectors, they are of great practicality. First, because in practice, most often we have statistical information limited to second-order moments and marginal probability distributions. Second, because they capture the most critical nonGaussian aspects that are most significantly reflected in the marginal distributions. Of great practical benefit is that translation vectors can be easily mapped into Gaussian vectors, and therefore can be easily handled and programmed.

To generate a nonGaussian (translation) stochastic vector **y** with a given covariance matrix $\boldsymbol{\Sigma}_{yy}$ and a marginal distribution vector **F**, first a Gaussian image vector **x** with a covariance matrix $\boldsymbol{\Sigma}_{xx}$ and marginal distribution vector $\boldsymbol{\Phi}(\mathbf{x})$ is simulated. Then, the original nonGaussian vector **y** is simulated by applying IPT to the MCDF vector **F** as follows:

$$\mathbf{y} = \mathbf{F}^{-1}\Phi(\mathbf{x}) = \mathbf{g}(\mathbf{x}) \tag{20.8}$$

However, for simulating the Gaussian image vector we need to define its covariance matrix $\boldsymbol{\Sigma}_{xx}$ as a transform of the covariance matrix $\boldsymbol{\Sigma}_{yy}$ of the original nonGaussian vector. Between the elements of the scaled covariance matrix or correlation coefficient matrix of the original nonGaussian vector, $\rho_{yi,yj}$, and the elements of the scaled covariance or correlation coefficient of the Gaussian image vector, $\rho_{xi,xj}$, there is the following relation:

$$\rho_{yi,yj} = \frac{1}{\sigma_{yi}\sigma_{yj}} \int_{-\infty}^{\infty}\int_{-\infty}^{\infty} \left[F_i^{-1}\Phi(x_i) - \mu_{yi}\right]\left[F_i^{-1}\Phi(x_j) - \mu_{yj}\right]\phi(x_i, x_j)\, dx_i dx_j \tag{20.9}$$

Copyright 2005 by CRC Press LLC

where the bivariate Gaussian probability density is defined by:

$$\phi(x_i, x_j) = \frac{1}{2\pi\left(1-\rho_{xi,xj}^2\right)^{0.5}\sigma_{xi}\sigma_{xj}} \exp\left(-\frac{1}{2}\frac{(x_i-\mu_{xi})^2/\sigma_{xi}^2 - 2\rho_{xi,xj}/\sigma_{xi}\sigma_{xj} + (x_j-\mu_{xj})^2/\sigma_{xj}^2}{\left(1-\rho_{xi,xj}^2\right)}\right) \quad (20.10)$$

Two probability transformation options are attractive: (1) the components of the Gaussian image stochastic vector have means and variances equal to those of the original nonGaussian vector (i.e., $\mu_y = \mu_x$ and $\sigma_y = \sigma_x$), or (2) the Gaussian image vector is standard Gaussian vector (i.e., $\mu_x = \mathbf{0}$ and $\boldsymbol{\sigma}_x = \mathbf{1}$). Depending on the selected option, the above equations take a simpler form.

Thus, problem of generating nonGaussian vectors is a four-step procedure for which the two steps are identical with those used for generating a Gaussian vector:

Step 1: Compute the covariance matrix of Gaussian vector **x** using Equation 20.9.
Step 2: Generate a standard Gaussian vector **z.**
Step 3: Generate a Gaussian vector **x** using Equation 20.4 or Equation 20.7.
Step 4: Simulate a nonGaussian vector **y** using the following inverse probability transformation of the MCDF, $\mathbf{y} = \mathbf{F}^{-1}\boldsymbol{\Phi}(\mathbf{x})$.

Sometimes in practice, the covariance matrix transformation is neglected, assuming that the correlation coefficient matrix of the original nonGaussian vector and that of the image Gaussian vector are identical. This assumption is wrong and may produce a violation of the physics of the problem. It should be noted that calculations of correlation coefficients have indicated that if $\rho_{xi,xj}$ is equal to 0 or 1, then $\rho_{yi,yj}$ is also equal to 0 or 1, respectively. However, when $\rho_{xi,xj}$ is −1, then $\rho_{yi,yj}$ is not necessarily equal to −1. For significant negative correlations between vector components, the effects of covariance matrix transformation are becoming significant, especially for nonGaussian vectors that have skewed marginal PDF shapes. Unfortunately, this is not always appreciated in the engineering literature. There are a number of journal articles on probabilistic applications for which the significance of covariance matrix transformation is underestimated; for example, the application of the popular Nataf probability model to nonGaussian vectors with correlated components neglects the covariance matrix transformation. Grigoriu [11] showed a simple example of a bivariate lognormal distribution for which the lowest value of the correlation coefficient is −0.65, and not −1.00, which is the lowest value correlation coefficient for a bivariate Gaussian distribution.

For a particular situation, of a nonGaussian component y_i and a Gaussian component x_j, the correlation coefficient $\rho_{yi,xj}$ can be computed by

$$\rho_{yi,xj} = \frac{1}{\sigma_{yi}\sigma_{xj}} \int_{-\infty}^{\infty}\int_{-\infty}^{\infty} [F^{-1}\Phi(x_i) - \mu_{yi}](x_j - \mu_{xj})\phi(x_i, x_j)dx_i dx_j \quad (20.11)$$

As shown in the next section, the above probability transformation simulation procedure can be extended from nonGaussian vectors to multivariate nonGaussian stochastic fields. The nonGaussian stochastic fields that are partially defined by their mean and covariance functions and marginal distributions are called translation stochastic fields.

Another way to generate nonGaussian stochastic vectors is based on the application of the SAR method described for one-dimensional random variables to random vectors with correlated components. This application of SAR to multivariate cases is the basis of the Metropolis-Hastings algorithm that is extremely popular in the Bayesian statistics community. Importantly, the Metropolis-Hastings algorithm [12] is not limited to translation vectors. The basic idea is to sample directly from the JPDF of the nonGaussian vector using an adaptive and important sampling strategy based on the application of SAR. At each

Copyright 2005 by CRC Press LLC

simulation step, random samples are generated from a simple proposal or trial JPDF that is different than the target JPDF and then weighted in accordance with the important ratio. This produces dependent samples that represent a Markov chain random walk in the input space. The Metropolis-Hastings algorithm is the cornerstone of the Markov chain Monte Carlo (MCMC) simulation discussed in Section 20.5 of this chapter.

To move from vector sample or state $\mathbf{x}^t$ to state $\mathbf{x}^{t+1}$, the following steps are applied:

Step 1: Sample from the trial density, $\mathbf{y} \approx q(\mathbf{x}^t, \mathbf{y})$, that is initially assumed to be identical to the conditional density $q(\mathbf{y}|\mathbf{x}^t)$.

Step 2: Compute acceptance probability

$$\alpha(\mathbf{x}^t, \mathbf{y}) = \min\left(1, \frac{\pi(\mathbf{y})q(\mathbf{y}, \mathbf{x}^t)}{\pi(\mathbf{x}^t)q(\mathbf{x}^t, \mathbf{y})}\right) \tag{20.12}$$

where π is the target JPDF.

Step 3: Compute $\mathbf{x}^{t+1} = \mathbf{y}$ for sampling acceptance, otherwise $\mathbf{x}^{t+1} = \mathbf{x}^t$ for sampling rejection.

Based on the ergodicity of the simulated Markov chain, the random samples of the target JPDF are simulated by executing repeated draws at an equal number of steps from the Markov chain movement in the stochastic space. There is also the possibility to use multiple Markov chains simultaneously.

A competing algorithm with the Metropolis-Hastings algorithm is the so-called Gibbs sampler [13]. The Gibbs sampler assumes that the probability of sampling rejection is zero; that is, all samples are accepted. This makes it simpler but less flexible when compared with the Metropolis-Hastings algorithm. One step of the Gibbs sampler that moves the chain from state $\mathbf{x}^t$ to state $\mathbf{x}^{t+1}$ involves the following simulation steps by breaking the vector $\mathbf{x}$ in its k components:

$$\begin{aligned}
&\text{Step 1: Sample } x_1^{t+1} \approx \pi\left(x_1 | x_2^t, \ldots, x_k^t\right).\\
&\text{Step 2: Sample } x_2^{t+1} \approx \pi\left(x_2 | x_1^{t+1}, x_3^t, \ldots, x_k^t\right).\\
&\quad\vdots\\
&\text{Step j: Sample } x_j^{t+1} \approx \pi\left(x_j | x_1^{t+1}, \ldots, x_{j-1}^{t+1}, x_{j+1}^t, \ldots, x_k^t\right).\\
&\quad\vdots\\
&\text{Step k: Sample } x_k^{t+1} \approx \pi\left(x_k | x_1^{t+1}, \ldots, x_{k-1}^{t+1}\right).
\end{aligned} \tag{20.13}$$

To ensure an accurate vector simulation for both the Metropolis-Hastings and the Gibbs algorithms, it is important to check the ergodicity of the generated chain, especially if they can be stuck in a local energy minimum. Gibbs sampler is the most susceptible to getting stuck in different parameter space regions (metastable states).

Most MCMC researchers are currently using derivative of the Metropolis-Hastings algorithms. When implementing the Gibbs sampler or Metropolis-Hastings algorithms, key questions arise: (1) How do we need to block components to account for the correlation structure and dimensionality of the target distribution? (2) How do we choose the updating scanning strategy: deterministic or random? (3) How do we devise the proposal densities? (4) How do we carry out convergence and its diagnostics on one or more realizations of the Markov chain?

20.4 Stochastic Fields (or Processes)

A stochastic process or field is completely defined by its JPDF. Typically, the term "stochastic process" is used particularly in conjunction with the time evolution of a dynamic random phenomenon, while the term "stochastic field" is used in conjunction with the spatial variation of a stochastic surface. A space-time stochastic process is a stochastic function having time and space as independent arguments. The term "space-time stochastic process" is synonymous with the term "time-varying stochastic field." More generally, a stochastic function is the output of a complex physical stochastic system. Because a stochastic output can be described by a stochastic surface in terms of input parameters (for given

Copyright 2005 by CRC Press LLC

ranges of variability), it appears that the term "stochastic field" is a more appropriate term for stochastic function approximation. Thus, *stochastic field* fits well with stochastic boundary value problems. *Stochastic process* fits well with stochastic dynamic, phenomena, random vibration, especially for stochastic stationary (steady state) problems that assume an infinite time axis. The term "stochastic field" is used hereafter.

Usually, in advanced engineering applications, simplistic stochastic models are used for idealizing component stochastic loading, material properties, manufacturing geometry and assembly deviations. To simplify the stochastic modeling, it is often assumed that the *shape* of spatial random variations is deterministic. Thus, the spatial variability is reduced to a single random variable problem, specifically to a random scale factor applied to a deterministic spatial shape. Another simplified stochastic model that has been extensively used in practice is the traditional response surface method based on quadratic regression and experimental design rules (such as circumscribed central composite design, CCCD, or Box-Benken design, BBD). The response surface method imposes a global quadratic trend surface for approximating stochastic spatial variations that might violate the physics of the problem. However, the traditional response surface method is practical for mildly nonlinear stochastic problems with a reduced number of random parameters.

From the point of view of a design engineer, the simplification of stochastic modeling is highly desired. A design engineer would like to keep his stochastic modeling as simple as possible so he can understand it and simulate it with a good confidence level (obviously, this confidence is subjective and depends on the analyst's background and experience). Therefore, the key question of the design engineer is: Do I need to use stochastic field models for random variations, or can I use simpler models, random variable models? The answer is yes and no on a case-by-case basis. Obviously, if by simplifying the stochastic modeling the design engineer significantly violates the physics behind the stochastic variability, then he has no choice; he has to use refined stochastic field models. For example, stochastic field modeling is important for turbine vibration applications due to the fact that blade mode-localization and flutter phenomena can occur. These blade vibration-related phenomena are extremely sensitive to small spatial variations in blade properties or geometry produced by the manufacturing or assembly process. Another example of the need for using a refined stochastic field modeling is the seismic analysis of large-span bridges. For large-span bridges, the effects of the nonsynchronicity and spatial variation of incident seismic waves on structural stresses can be very significant. To capture these effects, we need to simulate the earthquake ground motion as a dynamic stochastic field or, equivalently, by a space-time stochastic process as described later in this section.

A stochastic field can be homogeneous or nonhomogeneous, isotropic or anisotropic, depending on whether its statistics are invariant or variant to the axis translation and, respectively, invariant or variant to the axis rotation in the physical parameter space. Depending on the complexity of the physics described by the stochastic field, the stochastic modeling assumptions can affect negligibly or severely the simulated solutions. Also, for complex problems, if the entire set of stochastic input and stochastic system parameters is considered, then the dimensionality of the stochastic space spanned by the stochastic field model can be extremely large.

This chapter describes two important classes of stochastic simulation techniques of continuous multivariate stochastic fields (or stochastic functionals) that can be successfully used in advanced engineering applications. Both classes of simulation techniques are based on the decomposition of the stochastic field in a set of elementary uncorrelated stochastic functions or variables. The most desirable situation from an engineering perspective is to be able to simulate the original stochastic field using a reduced number of elementary stochastic functions or variables. The dimensionality reduction of the stochastic input is extremely beneficial because it also reduces the overall dimensionality of the engineering reliability problem.

This chapter focuses on stochastic field simulation models that use a limited number of elementary stochastic functions, also called *stochastic reduced-order models.* Many other popular stochastic simulation techniques, used especially in conjunction with random signal processing — such as discrete autoregressive process models AR, moving-average models MA, or combined ARMA or ARIMA models, Gabor

Copyright 2005 by CRC Press LLC

transform models, wavelet transform models, and many others — are not included due to space limitation. This is not to shadow their merit.

In this chapter two important types of stochastic simulation models are described:

1. *One-level hierarchical stochastic field (or stochastic functional) model.* This simulation model is based on an *explicit* representation of a stochastic field. This representation is based on a statistical function (causal relationship) approximation by nonlinear regression. Thus, the stochastic field is approximated by a stochastic hypersurface **u** that is conditioned on the stochastic input **x**. The typical explicit representation of a stochastic field has the following form:

$$\mathbf{u}|\mathbf{x} = \mathbf{u}(\mathbf{x}) = \boldsymbol{\mu}_{u|x} + [\mathbf{u}(\mathbf{x}) - \boldsymbol{\mu}_{u|x}] \tag{20.14}$$

   In the above equation, first the conditional mean term, $\boldsymbol{\mu}_{u|x}$, is computed by minimizing the global mean-square error over the sample space. Then, the randomly fluctuating term $[\mathbf{u}(\mathbf{x}) - \boldsymbol{\mu}_{u|x}]$ is treated as a zero-mean decomposable stochastic field that can be factorized using a Wiener-Fourier series representation. This type of stochastic approximation, based on regression, is limited to a convergence in mean-square sense.

   In the traditional response surface method, the series expansion term is limited to a single term defined by a stochastic residual vector defined directly in the original stochastic space (the vector components are the differences between exact and mean values determined at selected sampling points via experimental design rules).

2. *Two-level hierarchical stochastic field (or stochastic functional) model.* This simulation model is based on an *implicit* representation of a stochastic field. This representation is based on the Joint Probability Density Function (JPDF) (non-causal relationship) estimation. Thus, the stochastic field **u** is described by the JPDF of an augmented stochastic system $[\mathbf{x}, \mathbf{u}]^T$ that includes both the stochastic input **x** and the stochastic field **u**. The augmented stochastic system is completely defined by its JPDF $f(\mathbf{x}, \mathbf{u})$. This JPDF defines implicitly the stochastic field correlation structure of the field. Then, the conditional PDF of the stochastic field $f(\mathbf{u}|\mathbf{x})$ can be computed using the JPDF of augmented system and the JPDF of the stochastic input $f(\mathbf{x})$ as follows:

$$f(\mathbf{u}|\mathbf{x}) = f(\mathbf{x}, \mathbf{u}) / f(\mathbf{x}) \tag{20.15}$$

The JPDF of the augmented stochastic system can be conveniently computed using its projections onto a stochastic space defined by a set of locally defined, overlapping JPDF models. The set of local or conditional JPDF describe completely the local structure of the stochastic field. This type of stochastic approximation is based on the joint density estimation convergences in probability sense.

There are few key aspects that differentiate the two stochastic field simulation models. The one-level hierarchical model is based on statistical function estimation that is a more restrictive approximation problem than the density estimation employed by the two-level hierarchical model. Statistical function estimation based on regression can fail when the stochastic field projection on the input space is not convex. Density estimation is a much more general estimation problem than a statistical function estimation problem. Density estimation is always well-conditioned because there is no causal relationship implied.

The two-level hierarchical model uses the local density functions to approximate a stochastic field. The optimal solution rests between the use of a large number of small-sized isotropic-structure density functions (with no correlation structure) and a reduced number of large-sized anisotropic-structure density functions (with strong correlation structure). The preference is for a reduced number of local density functions. Cross-validation or Bayesian inference techniques can be used to select the optimal stochastic models based either on error minimization or likelihood maximization.

Copyright 2005 by CRC Press LLC

20.4.1 One-Level Hierarchical Simulation Models

To simulate complex pattern nonGaussian stochastic fields (functionals), it is advantageous to represent them using a Wiener-Fourier type series [14–16]:

$$\mathbf{u}(\mathbf{x},\theta)=\sum_{i=0}^{\infty}\mathbf{u}_i(\mathbf{x})\mathrm{f}_i(\theta)=\sum_{i=0}^{\infty}\mathbf{u}_i(\mathbf{x})\mathbf{f}_i(\mathbf{z}(\theta)) \tag{20.16}$$

where argument **z** is a set of independent standard Gaussian random variables and **f** is a set of orthogonal basis functions (that can be expressed in terms of a random variable set **z**). A simple choice is to take the set of stochastic basis functions **f** equal to the random variables set **z**. There are two main disadvantages when using the Wiener-Fourier series approximations. First, the stochastic orthogonal basis functions f_i are multidimensional functions that require intensive computations, especially for high-dimensional stochastic problems for which a large number of coupling terms need to be included to achieve adequate convergence of the series.

Generally, under certain integrability conditions, a stochastic function can be decomposed in an orthogonal structure in a probability measure space. Assuming that the uncorrelated stochastic variables z_i, $i=1, 2, \ldots, m$ are defined on a probability space and that $u(z_1,\ldots,z_m)$ is a square-integrable function with respect to the probability measure and if $\{p_{i,k}(z_i)\}$, $i = 1, 2, \ldots, m$ are complete sets of square-integrable stochastic functions orthogonal with respect to the probability density $P_i(dz_i)/dz_i = f_z(z_i)$, so that $E[p_k(z_i)p_l(z_i)]=0$ for all $k\neq 1 = 0, 1, \ldots$ and $i = 1, \ldots m$, then, the function $u(z_1,\ldots,z_m)$ can be expanded in a generalized Wiener-Fourier series:

$$u(z_1,\ldots z_m)=\sum_{k_1=0}^{\infty}\cdots\sum_{k_m=0}^{\infty}u_{k_1\ldots k_m}p_{k_1}(z_1)\ldots p_{k_m}(z_m) \tag{20.17}$$

where $\{p_{k_1}(z_1),\ldots, p_{k_m}(z_m)\}, k_1,\ldots,k_m=0,1,\ldots$, are complete sets of stochastic orthogonal (uncorrelated) functions. The generalized Wiener-Fourier series coefficients can be computed by solving the integral

$$u_{k_1\ldots k_m}=\int\ldots\int u(z_1,\ldots,z_m)p_{k_1}(z_1)\ldots p_{k_m}(z_m)\ u_1(z_1)\ldots u_m(z_m)dz_1\ldots dz_m \tag{20.18}$$

The coefficients $u_{k_1\ldots k_m}$ have a key minimizing property, specifically the integral difference

$$D=\int\ldots\int\left[u(z_1,\ldots,z_m)-\sum_{k_1=0}^{M_1}\ldots\sum_{k_m=0}^{M_m}g_{k_1\ldots k_m}p_{k_m}(z_m)\right]^2 f_z(z_1)\ldots f_z(z_m)dz_1\ldots dz_m \tag{20.19}$$

reaches its minimum only for $g_{k_1\ldots k_m}p_{k_m}=u_{k_1\ldots k_m}p_{k_m}$.

Several factorization techniques can be used for simulation of complex pattern stochastic fields. An example is the use of the Pearson differential equation for defining different types of stochastic series representations based on orthogonal Hermite, Legendre, Laguerre, and Cebyshev polynomials. These polynomial expansions are usually called Askey chaos series [16]. A major application of stochastic field decomposition theory is the spectral representation of stochastic fields using covariance kernel factorization. These covariance-based techniques have a large potential for engineering applications because they can be applied to any complex, static, or dynamic nonGaussian stochastic field. Herein, in addition to covariance-based factorization techniques, an Askey polynomial chaos series model based on Wiener-Hermite stochastic polynomials is presented. This polynomial chaos model based on Wiener-Hermite series has been extensively used by many researchers over the past decade [15–17].

Copyright 2005 by CRC Press LLC

20.4.1.1 Covariance-Based Simulation Models

Basically, there are two competing simulation techniques using the covariance kernel factorization: (1) the Choleski decomposition technique (Equation 20.4), and (2) the Karhunen-Loeve (KL) expansion (Equation 20.7). They can be employed to simulate both static and dynamic stochastic fields. A notable property of these two simulation techniques is that they can handle both real-valued and complex-valued covariance kernels. For simulating space-time processes (or dynamic stochastic fields), the two covariance-based techniques can be employed either in the time-space domain by decomposing the cross-covariance kernel or in the complex frequency-wavelength domain by decomposing the complex cross-spectral density kernel. For real-valued covariance kernels, the application of the KL expansion technique is equivalent to the application of the Proper Orthogonal Decomposition (POD expansion) and Principal Component Analysis (PCA expansion) techniques [17, 18].

More generally, the Choleski decomposition and the KL expansion can be applied to any arbitrary square-integrable, complex-valued stochastic field, $u(\mathbf{x}, \theta)$. Because the covariance kernel of the complex-valued stochastic field $\mathrm{Cov}[u(\mathbf{x}, \theta), u(\mathbf{x}', \theta)]$ is a Hermitian kernel, it can be factorized using either Choleski or KL decomposition.

If the KL expansion is used, the covariance function is expanded in the following eigenseries:

$$\mathrm{Cov}[u(\mathbf{x}, \theta), u(\mathbf{x}', \theta)] = \sum_{n=0}^{\infty} \lambda_n \Phi_n(\mathbf{x}) \Phi_n(\mathbf{x}') \tag{20.20}$$

where λ_n and $\Phi_n(\mathbf{x})$ are the eigenvalue and the eigenvector, respectively, of the covariance kernel computed by solving the integral equation (based on Mercer's theorem) [19]:

$$\int \mathrm{Cov}[u(\mathbf{x}, \theta), u(\mathbf{x}', \theta)] \Phi_n(\mathbf{x}) d\mathbf{x} = \Phi_n(\mathbf{x}') \tag{20.21}$$

As a result of covariance function being Hermitian, all its eigenvalues are real and the associated complex eigenfunctions that correspond to distinct eigenvalues are mutually orthogonal. Thus, they form a complete set spanning the stochastic space that contains the field u. It can be shown that if this deterministic function set is used to represent the stochastic field, then the stochastic coefficients used in the expansion are also mutually orthogonal (uncorrelated).

The KL series expansion has the general form

$$u(\mathbf{x}, \theta) = \sum_{i=0}^{n} \sqrt{\lambda_i} \Phi_i(\mathbf{x}) z_i(\theta) \tag{20.22}$$

where set $\{z_i\}$ represents the set of uncorrelated random variables that are computed by solving the stochastic integral:

$$z_i(\theta) = \frac{1}{\sqrt{\lambda_i}} \int_D \Phi_n(\mathbf{x})\, u(\mathbf{x}, \theta)\, d\mathbf{x} \tag{20.23}$$

The KL expansion is an optimal spectral representation with respect to the second-order statistics of the stochastic field. Equation 20.23 indicates that the KL expansion can be applied also to nonGaussian stochastic fields if sample data from it are available. For many engineering applications on continuum mechanics, the KL expansion is fast mean-square convergent; that is, only a few expansion terms need to be included.

An important practicality aspect of the above covariance-based simulation techniques is that they can be easily applied in conjunction with the marginal probability transformation (Equation 20.8 and Equation 20.9)

Copyright 2005 by CRC Press LLC

to simulate nonGaussian (translation) stochastic fields, either static or dynamic. For nonGaussian (translation) stochastic fields, two simulation models can be employed:

1. *Original space expansion*. Perform the simulation in the original nonGaussian space using the covariance-based expansion with a set $\{z_i\}$ of uncorrelated nonGaussian variables that can be computed as generalized Fourier coefficients by the integral

$$z_i(\theta) = \int_D u_i(\mathbf{x}) u(\mathbf{x}, \theta)\, d\mathbf{x} \tag{20.24}$$

   In particular, for the KL expansion, the Equation 20.23 is used.

2. *Transformed space expansion*. Perform the simulation in the transformed Gaussian space using the covariance-based expansion with a set $\{z_i\}$ of standard Gaussian variables and then transform the Gaussian field to nonGaussian using the marginal probability transformation (Equation 20.8 and Equation 20.9).

In the engineering literature there are many examples of the application of covariance-based expansions for simulating either static or dynamic stochastic fields. In the civil engineering field, Choleski decomposition and KL expansion were used by several researchers, including Yamazaki and Shinozuka [20], Deodatis [21], Deodatis and Shinozuka [22], and Ghiocel [23] and Ghiocel and Ghanem [24], to simulate the random spatial variation of soil properties and earthquake ground motions. Shinozuka [25] and Ghiocel and Trandafir [26] used Choleski decomposition to simulate stochastic spatial variation of wind velocity during storms. Ghiocel and Ghiocel [27, 28] employed the KL expansion to simulate the stochastic wind fluctuating pressure field on large-diameter cooling towers using a nonhomogeneous, anisotropic dynamic stochastic field model. In the aerospace engineering field, Romanovski [29], and Thomas, Dowell, and Hall [30] used the KL expansion (or POD) to simulate the unsteady pressure field on aircraft jet engine blades. Ghiocel [31, 32] used the KL expansion as a stochastic classifier for jet engine vibration-based fault diagnostics.

An important aerospace industry application is the stochastic simulation of the engine blade geometry deviations due to manufacturing and assembly processes. These random manufacturing deviations have a complex stochastic variation pattern [33]. The blade thickness can significantly affect the forced response of rotating bladed disks [34–36]. Due to the cyclic symmetry geometry configuration of engine bladed disks, small manufacturing deviations in blade geometries produce a mode-localization phenomenon, specifically called mistuning, that can increase the airfoil vibratory stresses up to a few times. Blair and Annis [37] used the Choleski decomposition to simulate blade thickness variations, assuming that the thickness variation is a homogeneous and isotropic field. Other researchers, including Ghiocel [38, 39], Griffiths and Tschopp [40], Cassenti [41], and Brown and Grandhi [35], have used the KL expansion (or POD, PCA) to simulate more complex stochastic blade thickness variations due to manufacturing. Ghiocel [36] applied the KL expansion, both in the original, nonGaussian stochastic space and transformed Gaussian space. It should be noted that the blade thickness variation fields are highly nonhomogeneous and exhibit multiple, localized anisotropic directions due to the manufacturing process constraints (these stochastic variations are also technology dependent). If different blade manufacturing technology datasets are included in the same in a single database, then the resultant stochastic blade thickness variations could be highly nonGaussian, with multimodal, leptoqurtique, and platiqurtique marginal PDF shapes. More generally, for modeling the blade geometry variations in space, Ghiocel suggested a 3V-3D stochastic field model (three variables Δx, Δy, Δz, in three dimensions x, y, z). For only blade thickness variation, a 1V-2D stochastic field (one variable, thickness, in two dimensions, blade surface grid) is sufficient. It should be noted that for multivariate-multidimensional stochastic fields composed of several elementary one-dimensional component fields, the KL expansion must be applied to the entire covariance matrix of the stochastic field set that includes the coupling of all the component fields.

One key advantage of the KL expansion over the Choleski decomposition, that makes the KL expansion (or POD, PCA) more attractive for practice, is that the transformed stochastic space obtained using the

Copyright 2005 by CRC Press LLC

KL expansion typically has a highly reduced dimensionality when compared with the original stochastic space. In contrast, the Choleski decomposition preserves the original stochastic space dimensionality. For this reason, some researchers [29, 30] consider the KL expansion (or POD, PCA) a *stochastic reduced-order model* for simulating complex stochastic patterns. The KL expansion, in addition to space dimensionality reduction, also provides great insight into the stochastic field structure. The eigenvectors of the covariance matrix play, in stochastic modeling, a role similar to the vibration eigenvectors in structural dynamics; complex spatial variation patterns are decomposed in just a few dominant spatial variation *mode shapes*. For example, blade thickness variation *mode shapes* provide great insight into the effects of technological process variability. These insights are very valuable for improving blade manufacturing technology.

The remaining part of this subsection illustrates the application of covariance-based stochastic simulation techniques to generate dynamic stochastic fields. Specifically, the covariance-based methods are used to simulate the stochastic earthquake ground surface motion at a given site.

To simulate the earthquake ground surface motion at a site, a nonstationary, nonhomogeneous stochastic vector process model is required. For illustrative purposes, it is assumed that the stochastic process is a nonhomogeneous, nonstationary, 1V-2D space-time Gaussian process (one variable, acceleration in an arbitrary horizontal direction, and two dimensions for the horizontal ground surface). The space-time process at any time moment is completely defined by its evolutionary cross-spectral density kernel. For a seismic acceleration field $u(\mathbf{x}, t)$, the cross-spectral density for two motion locations i and k is:

$$\mathbf{S}_{ui,uk}(\omega, t) = [\mathbf{S}_{ui,ui}(\omega, t)\mathbf{S}_{uk,uk}(\omega, t)]^{1/2} Coh_{ui,uk}(\omega, t) \quad \exp[-i\omega(X_{D,i} - X_{D,k})/V_D(t)] \tag{20.25}$$

where $\mathbf{S}_{uj,uk}(\omega)$ is the cross-spectral density function for point motions u_i and u_k, and $\mathbf{S}_{uj,uj}(\omega)$, $j = i$, k is the auto-spectral density for location point j. The function $Coh_{ui,uk}(\omega, t)$ is the stationary or "lagged" coherence function for locations i and k. The "lagged" coherence is a measure of the similarity of the two point motions including only the amplitude spatial variation. Herein, it is assumed that the frequency-dependent spatial correlation structure of the stochastic process is time-invariant. The exponential factor $\exp[i\omega(D_1 - D_2)/V_D(t)]$ represents the wave passage effect in the direction D expressed in the frequency domain by a phase angle due to two motion delays at two locations X_i and X_j. The parameter $V_D(t)$ is the apparent horizontal wave velocity in the D direction. Most often in practice, the nonstationary stochastic models of ground motions are based on the assumption that the "lagged" coherence and the apparent directional velocity are independent of time. However, in real earthquakes, the coherence and directional wave velocity are varying during the earthquake duration, depending on the time arrivals of different seismic wave packages hitting the site from various directions.

Because the cross-spectral density is Hermitian, either the Choleski decomposition or the KL expansion can be applied. If the Choleski decomposition is applied, then

$$\mathbf{S}(\omega, t) = \mathbf{C}(\omega, t)\mathbf{C}^*(\omega, t) \tag{20.26}$$

where the matrix $\mathbf{C}(\omega, t)$ is a complex-valued lower triangular matrix. Then the space-time nonstationary stochastic process can be simulated using the trigonometric series as the number of frequency components $NF \to \infty$ [21,22]:

$$u_i(t) = 2\sum_{k=1}^{NL}\sum_{j=1}^{NF} |C_{i,k}(\omega_j, t)| \sqrt{\Delta\omega} \cos[\omega_j t - \theta_{i,k}(\omega_j, t) + \Phi_{k,j}], \quad \text{for } i = 1, 2, \ldots NL \tag{20.27}$$

In the above equation, NL is the number of space locations describing the spatial variation of the motion. The first phase angle term in Equation 20.27 is computed by

$$\theta_{i,k}(\omega, t) = \tan^{-1}\left\{\frac{\mathrm{Im}\,|C_{i,k}(\omega, t)|}{\mathrm{Re}\,|C_{i,k}(\omega, t)|}\right\} \tag{20.28}$$

Copyright 2005 by CRC Press LLC

and the second phase angle term $\Phi_{k,j}$ is a random phase angle uniformly distributed in [0, 2π] (uniform random distribution is consistent with Gaussian assumption). The above procedure can be used for any space-time stochastic process. For nonGaussian processes, the procedure can be applied in conjunction with the inverse probability equation transformation (Equation 20.8 and Equation 20.9).

If the complex-valued coherence function (including wave passage effects) is used, then its eigenfunctions are complex functions. Calculations have shown that typically one to five coherence function modes are needed to get an accurate simulation of the process [23, 24]. The number of needed coherence function modes depends mainly on the soil layering stiffness and the frequency range of interest; for high-frequency components, a larger number of coherence modes are needed.

20.4.1.2 Polynomial Chaos Series-Based Simulation Models

Ghanem and Spanos [15] discussed theoretical aspects and key details of the application Polynomial Chaos to various problems in their monograph on spectral representation of stochastic functionals.

Polynomial chaos expansion models can be formally expressed as a nonlinear functional of a set of standard Gaussian variables or, in other words, expanded in a set of stochastic orthogonal polynomial functions. The most popular polynomial chaos series model is that proposed by Ghanem and Spanos [15] using a Wiener-Hermite polynomial series:

$$u(\mathbf{x}, t, \theta) = a_0(\mathbf{x}, t)\Gamma_0 + \sum_{i_1=1}^{\infty} a_{i_1}(\mathbf{x}, t)\Gamma_1(z_{i_1}(\theta)) + \sum_{i_1=1}^{\infty}\sum_{i_2=1}^{i_1} a_{i_1 i_2}(\mathbf{x}, t)\Gamma_2(z_{i_1}(\theta), z_{i_2}(\theta)) + \ \ldots \tag{20.29}$$

The symbol $\Gamma_n(z_{i_1}, \ldots, z_{i_n})$ denotes the polynomial chaoses of order n in the variables $(z_{i_1}, \ldots, z_{i_n})$. Introducing a one-to-one mapping to a set with ordered indices denoted by $\{\psi_i(\theta)\}$ and truncating the polynomial chaos expansion after the p^{th} term, Equation 20.29 can be rewritten

$$u(\mathbf{x}, t, \theta) = \sum_{j=0}^{p} u_j(\mathbf{x}, t)\psi_j(\theta) \tag{20.30}$$

The polynomial expansion functions are orthogonal in L_2 sense that is, their inner product with respect to the Gaussian measure that defines their statistical correlation, $E[\psi_j\psi_k]$, is zero. A given truncated series can be refined along the random dimension either by adding more random variables to the set $\{z_i\}$ or by increasing the maximum order of polynomials included in the stochastic expansion. The first refinement takes into account higher frequency random fluctuations of the underlying stochastic process, while the second refinement captures strong nonlinear dependence of the solution process on this underlying process. Using the orthogonality property of polynomial chaoses, the coefficients of the stochastic expansion solution can be computed by

$$u_k = \frac{E[\psi_k u]}{E[\psi_k^2]} \quad \text{for } k = 1, \ldots, K \tag{20.31}$$

A method for constructing polynomial chaoses of order n is by generating the corresponding multidimensional Wiener-Hermite polynomials. These polynomials can be generated using the partial differential recurrence rule defined by

$$\frac{\partial}{\partial z_{ij}}\Gamma_n(z_{i1}(\theta), \ldots, z_{in}(\theta)) = n\Gamma_{n-1}(z_{i1}(\theta), \ldots, z_{in}(\theta)) \tag{20.32}$$

The orthogonality of the polynomial chaoses is expressed by the inner product in L_2 sense with respect to Gaussian measure:

$$\int_{-\infty}^{\infty} \Gamma_n(z_{i1}, \ldots, z_{in})\Gamma_m(z_{i1}, \ldots, z_{in}) \exp\left(-\frac{1}{2}\mathbf{z}^{\mathrm{T}}\mathbf{z}\right) dz = n!\sqrt{2\pi}\,\delta_{mn} \tag{20.33}$$

Copyright 2005 by CRC Press LLC

Although popular in the engineering community, the polynomial chaos series may not necessarily be an efficient computational tool to approximate multivariate nonGaussian stochastic fields. The major problem is the stochastic dimensionality issue. Sometimes, the dimensionality of the stochastic transformed space defined by a polynomial chaos basis can be even larger than the dimensionality of the original stochastic space. Nair [42] discussed this stochastic dimensionality aspect related to polynomial chaos series application. Grigoriu [43] showed that the indiscriminate use of polynomial chaos approximations for stochastic simulation can result in inaccurate reliability estimates. To improve its convergence, the polynomial chaos series can be applied in conjunction with the inverse marginal probability transformation (Equation 20.8 and Equation 20.9) as suggested by Ghiocel and Ghanem [24].

20.4.2 Two-Level Hierarchical Simulation Models

The two-level hierarchical simulation model is based on the decomposition of the JPDF of the implicit input-output stochastic system in local or conditional JPDF models. The resulting stochastic local JPDF expansion can be used to describe, in detail, very complex nonstationary, multivariate-multidimensional nonGaussian stochastic fields. It should be noted that the local JPDF expansion is convergent in a probability sense, in contrast with the Wiener-Fourier expansions, which are convergent only in a mean-square sense.

The stochastic local JPDF basis expansion, or briefly, the local density expansion, can be also viewed as a Wiener-Fourier series of a composite type that provides both a global approximation and a local functional description of the stochastic field. In contrast to the classical Wiener-Fourier series that provides a global representation of a stochastic field by employing global basis functions, as the covariance kernel eigenfunctions in KL expansion or the polynomial chaoses [16], the stochastic local density expansion provides both a global and local representation of a stochastic field.

Stochastic local density expansion can be implemented as a two-layer stochastic neural-network, while Wiener-Fourier series can be implemented as a one-layer stochastic neural-network. It should be noticed that stochastic neural-network models train much faster than the usual multilayer preceptor (MLP) neural-networks. Figure 20.1 describes in pictorial format the analogy between stochastic local JPDF expansion and a two-layer neural-network model.

In the local density expansion, the overall JPDF of the stochastic model is obtained by integration over the local JPDF model space:

$$g(\mathbf{u}) = \int f(\mathbf{u}|\alpha)dp(\alpha) \tag{20.34}$$

where $p(\alpha)$ is a continuous distribution that plays the role of the probability weighting function over the local model space. In a discrete form, the weighting function can be expressed for a number N of local JPDF models by

$$p(\alpha) = \sum_{i=1}^{N} P(\alpha_i)\delta(\alpha - \alpha_i) \tag{20.35}$$

in which $\delta(\alpha - \alpha_i)$ is the Kronecker delta operator. Typically, the parameters α_i are assumed or known, and the discrete weighting parameters $P(\alpha_i)$ are the unknowns. The overall JPDF of the stochastic model can be computed in the discrete form by

$$g(\mathbf{u}) = \sum_{i=1}^{N} g(\mathbf{u}|\alpha_i)P(\alpha_i) \tag{20.36}$$

Copyright 2005 by CRC Press LLC

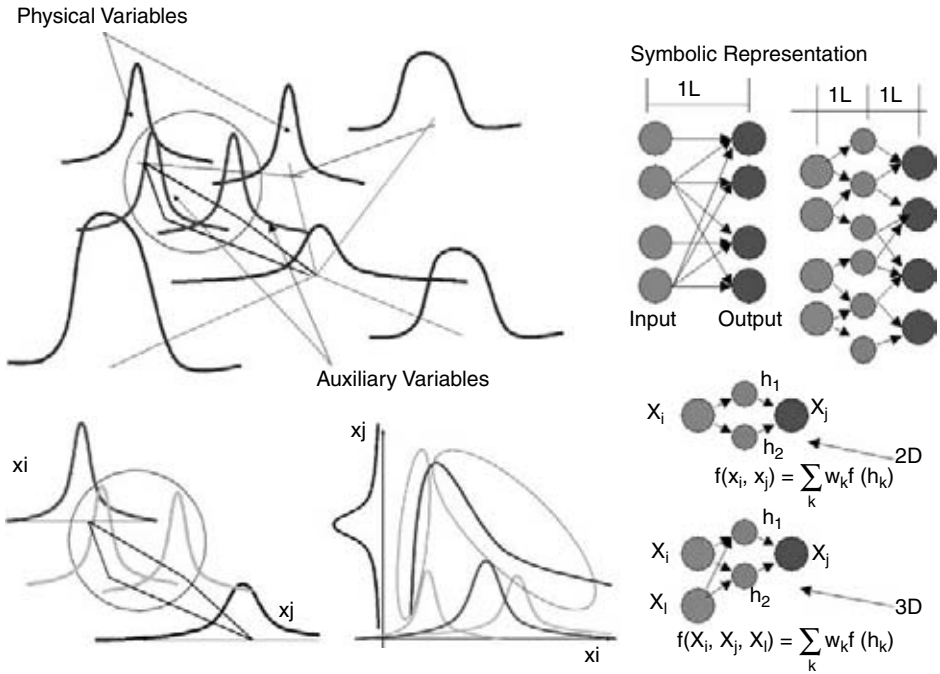

FIGURE 20.1 Analogy betweeen the local JPDF expansion and a two-layer stochastic neural network model.

The parameters α_i can be represented by the second-order statistics (computed by local averaging) of the local JPDF models. Thus, the overall JPDF expression can be rewritten as

$$g(\mathbf{u}) = \sum_{i=1}^{N} f(\mathbf{u} \mid i, \bar{\mathbf{u}}_i, \Sigma_i) P_i \tag{20.37}$$

where $\bar{\mathbf{u}}_i, \Sigma_i$ are the mean vector and covariance matrix, respectively, of the local JPDF model i. Also, $P_i = n_i/N, \sum_{i=1}^{N} P_i = 1$, and $P_i > 0$, for $i = 1, N$. Typically, the types of the local JPDF are assumed and the probability weights are computed from the sample datasets. Often, it is assumed that the local JPDFs are multivariate Gaussian models. This assumption implies that the stochastic field is described locally by a second-order stochastic field model. Thus, nonGaussianity is assumed only globally. It is possible to include nonGaussianity locally using the marginal probability transformation of the local JPDF.

The local JPDF models are typically defined on partially overlapping partitions within stochastic spaces called *soft* partitions. Each local JPDF contributes to the overall JPDF estimate in a localized convex region of the input space. The complexity of the stochastic field model is associated with the number of local JPDF models and the number of stochastic inputs that define the stochastic space dimensionality. Thus, the stochastic model complexity is defined by the number of local JPDFs times the number of input variables. For most applications, the model implementations that are based on a large number of highly localized JPDFs are not good choices because these models have high complexity. For high complexities, we need very informative data to build the locally refined stochastic models. Simpler models with a lesser number of JPDF models have a much faster statistical convergence and are more robust. Thus, the desire is to reduce model complexity at an optimal level.

The complexity reduction of the stochastic field model can be accomplished either by reducing the number of local JPDFs or by reducing their dimensionality. Complexity reduction can be achieved using cross-validation and then removing the local JPDF that produces the minimum variation of the error estimate or the model likelihood estimate. We can also use penalty functions (evidence functions) that

Copyright 2005 by CRC Press LLC

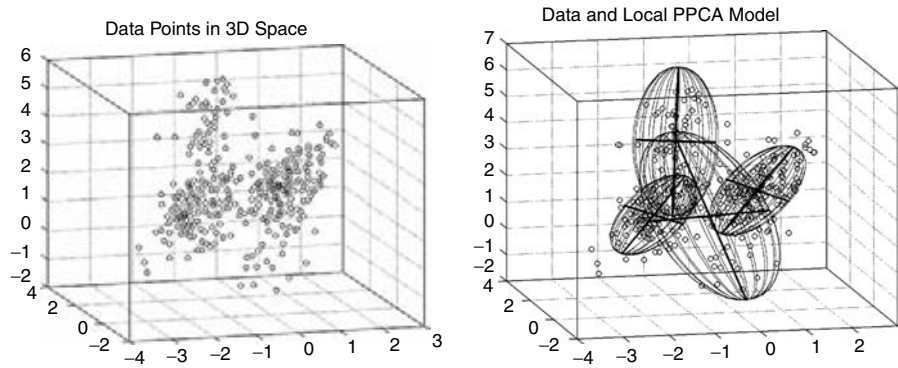

FIGURE 20.2 Sample data and local PPCA models for a trivariate stochastic field.

reduce the model complexity by selecting the most plausible stochastic models based on the evidence coming from sample datasets [44].

Alternatively, we can reduce the model complexity by reducing the dimensionality of local JPDF models using local factor analyzers. Local factor analysis reduces the number of local models by replacing the local variables in the original space by a reduced number of new local variables defined in local transformed spaces using a stochastic linear space projection. If deterministic projection instead of stochastic projection is applied, the factor analysis coincides with PCA. However, in practice, especially for high-dimensional problems, it is useful to consider a stochastic space projection by adding some random noise to the deterministic space projection. Adding noise is beneficial because instead of solving a multidimensional eigen-problem for decomposing the covariance kernel, we can implement an extremely fast convergent iterative algorithm for computing the principal covariance directions. The combination of the local JPDF expansion combined with the local probabilistic PCA decomposition is called herein the local PPCA expansion. Figure 20.2 shows the simulated sample data and the local PPCA models for a complex pattern trivariate stochastic field.

It should be noted that if the correlation structure of local JPDF models is ignored, these local JPDFs lose their functionality to a significant extent. If the correlation is neglected, a loss of information occurs, as shown in Figure 20.3. The radial basis functions, such standard Gaussians, or other kernels ignore the local correlation structure due to their shape constraint. By this they lose accuracy for

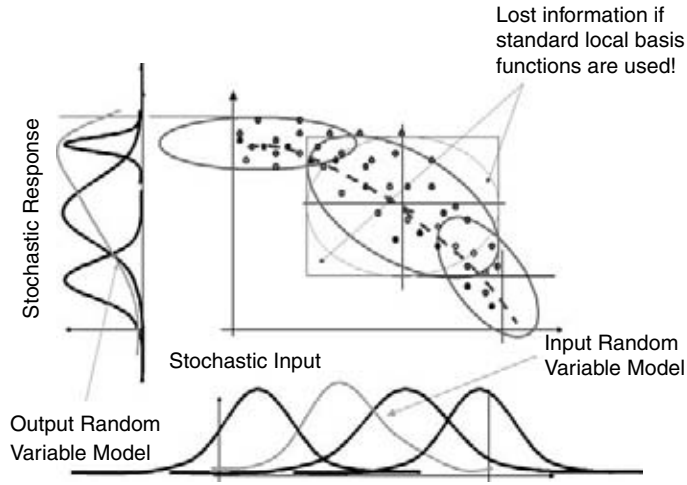

FIGURE 20.3 Loss of information if the local correlation structure is ignored.

Copyright 2005 by CRC Press LLC

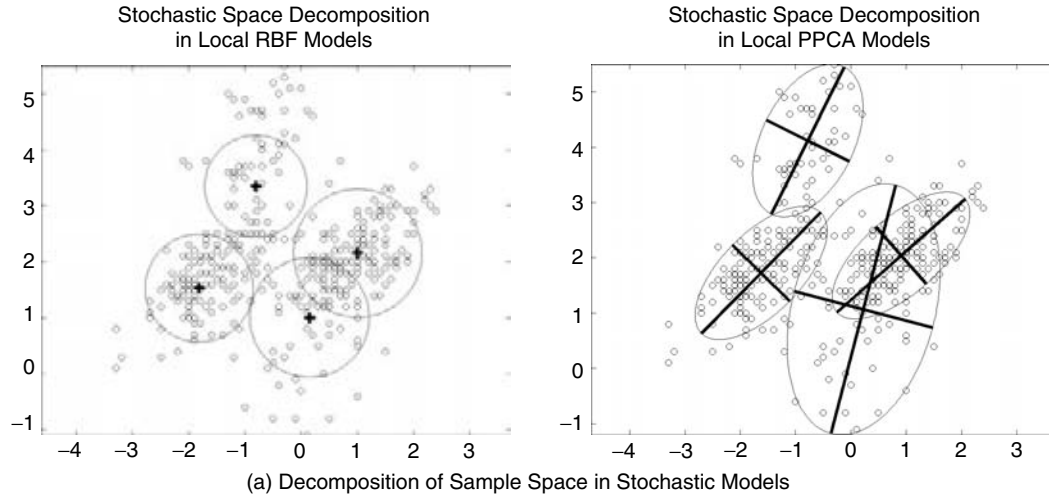

FIGURE 20.4 Local PPCA expansion model versus RBF network model a) decomposition of sample space in local stochastic models b) computed JPDF estimates.

modeling a complex stochastic field. One way to see radial basis function expansions is to look at them as degenerated local JPDF models. These radial functions are commonly used in a variety of practical applications, often in the form of the radial basis function network (RBFN), fuzzy basis function network (FBFN), and adaptive network-based fuzzy inference systems (ANFIS). Figure 20.4 compares the RBFN model with the local PPCA expansion model. The local PPCA expansion model is clearly more accurate and better captures all the data samples, including those that are remote in the tails of the JPDF. For a given accuracy, the local PPCA expansion needs a much smaller number of local models than the radial basis function model. As shown in the figure, the local PPCA models can elongate along long data point clouds in any arbitrary direction. The radial basis functions do not have this flexibility. Thus, to model a long data point cloud, a large number of overlapping radial basis functions are needed. And even so, the numerical accuracy of radial basis function expansions may still not be as good as the accuracy of local PPCA expansions with just few arbitrarily oriented local point cloud models. It should be noted that many other popular statistical approximation models, such as Bayesian Belief Nets (BNN), Specht's Probability Neural Network (PNN), in addition to ANFIS, RBF, and FBF networks, and even the two-layer MLP networks, have some visible conceptual similarities with the more refined local PPCA expansion.

Copyright 2005 by CRC Press LLC

Copyright 2005 by CRC Press LLC

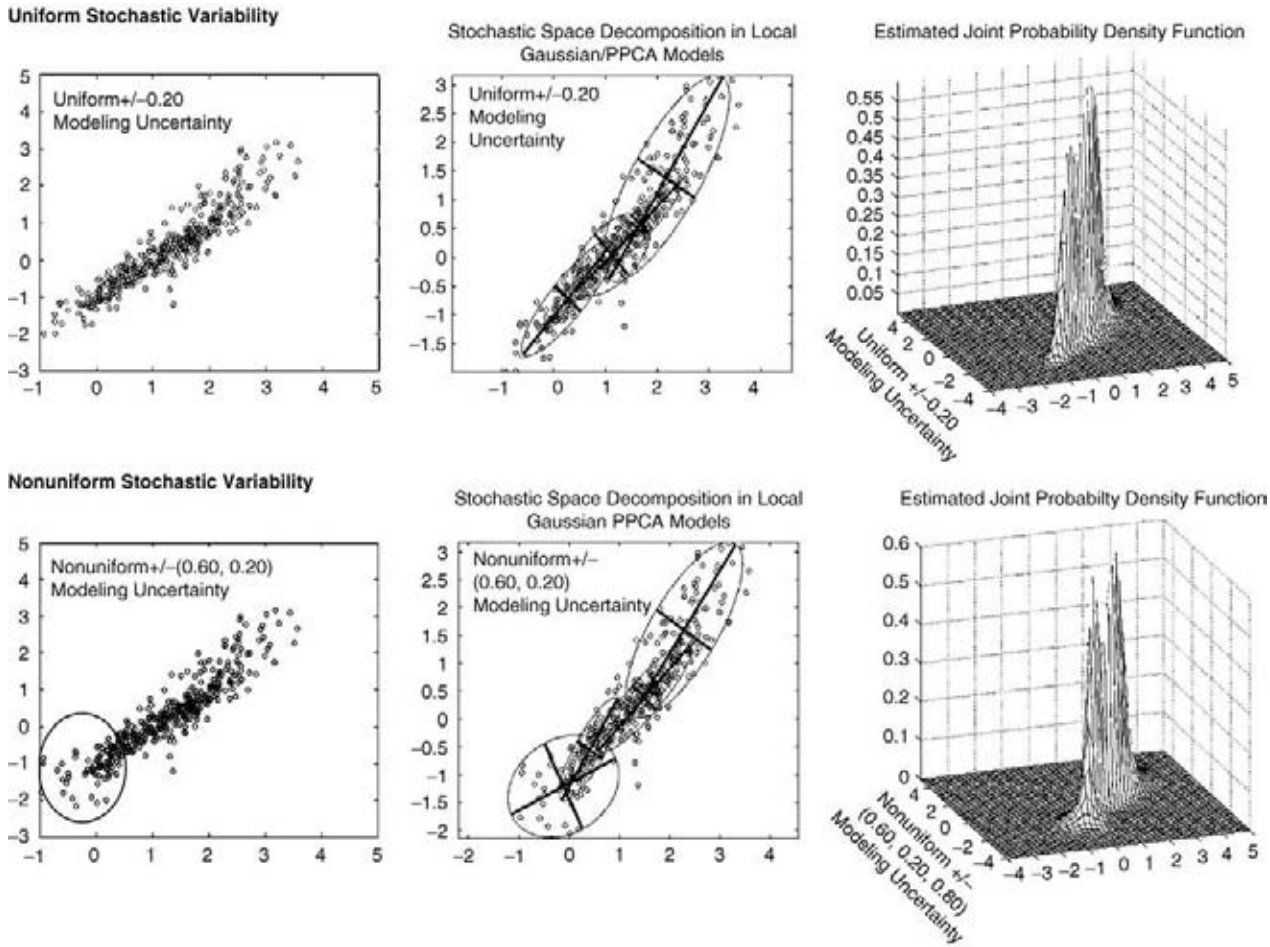

FIGURE 20.5 Local PPCA expansion model captures the nonuniform stochastic variability; a) Initial dataset, uniform data, b) Locally perturbed dataset, nonuniform data.

The stochastic local PPCA expansion is also capable of including accurately local, nonuniform stochastic variations. Figure 20.5 illustrates this fact by comparing the local PPCA expansions for two sample datasets that are identical except for a local domain shown at the bottom left of the plots. For the first dataset (left plots), the local variation was much smaller than for the second dataset (right plots). As seen by comparing the plots, the local PPCA expansion captures well this highly local variability of probabilistic response.

The decomposition of stochastic parameter space in a set of local models defined on soft partitions offers several possibilities for simulating high-dimensional complex stochastic fields. This stochastic sample space decomposition in a reduced number of stochastic local models, also called *states*, opens up a unique avenue for developing powerful stochastic simulation techniques based on stochastic process or field theory, such as dynamic Monte Carlo. Dynamic Monte Carlo techniques are discussed in the next section.

20.5 Simulation in High-Dimensional Stochastic Spaces

In simulating random samples from a joint probability density $g(\mathbf{x})$, in principle there are always ways to do it because we can relate the multidimensional joint density $g(\mathbf{x})$ to univariate probability densities defined by full conditional densities $g(x_j|x_M, \ldots, x_{j+1}, x_{j-1}, \ldots, x_1)$:

$$g(\mathbf{x}) = g(x_1, \ldots, x_K) = \prod_{j=1}^{M} g(x_j|x_{j-1}, \ldots, x_1) \tag{20.38}$$

Unfortunately, in real-life applications, these (univariate) full conditional densities are seldom available in an explicit form that is suitable to direct sampling. Thus, to simulate a random sample from $g(\mathbf{x})$, we have few choices: (1) use independent random samples drawn from univariate marginal densities (static, independent sampling, SMC) to build the full conditionals via some predictive models; or (2) use independent samples from trial univariate marginal and conditional densities (sequential importance sampling, SIS), defined by the probability chain rule decomposition of the joint density, and then adaptively weight them using recursion schemes; or (3) use independent samples drawn from the univariate full conditional densities to produce spatially dependent samples (trajectories) of the joint density using recursion schemes that reflect the stochastic system dynamics (dynamic, correlated sampling, DMC).

For multidimensional stochastic fields, the standard SMC sampling techniques can fail to provide good estimators because their variances can increase sharply with the input space dimensionality. This variance increase depends on stochastic simulation model complexity. For this reason, variation techniques are required. However, classical techniques for variance reductions such as stratified sampling, importance sampling, directional sampling, control variable, antithetic variable, and Rao-Blackwellization methods are difficult to apply in high dimensions.

For simulating complex pattern, high-dimensional stochastic fields, the most adequate techniques are the adaptive importance sampling techniques, such as the sequential importance sampling with independent samples, SIS, or with correlated samples, DMC. Currently, in the technical literature there exists a myriad of recently developed adaptive, sequential, single sample-based or population-based evolutionary algorithms for high-dimensional simulations [6, 45]. Many of these techniques are based on constructing a Markov chain structure of the stochastic field. The fundamental Markov assumption of one-step memory significantly reduces the chain structures of the full or partial conditional densities, thus making the computations affordable. In addition, Markov process theory is well-developed so that reliable convergence criteria can be implemented.

20.5.1 Sequential Importance Sampling (SIS)

SIS is a class of variance reduction techniques based on adaptive important sampling schemes [45, 46]. A useful strategy to simulate a sample of joint distribution is to build up a trial density sequentially until it converges to the target distribution. Assuming a trial density constructed as $g(\mathbf{x}) = g_1(x_1)g_2(x_2|x_1) \ldots g_N(x_N|x_1, \ldots x_{N-1})$

Copyright 2005 by CRC Press LLC

and using the same decomposition for the target density $\pi(\mathbf{x}) = \pi(x_1)\pi(x_2|x_1) \ldots \pi(x_N|x_1, \ldots x_{N-1})$, the importance sampling weight can be computed recursively by

$$w_t(\mathbf{x}_t) = w_{t-1}(\mathbf{x}_{t-1}) \frac{\pi(\mathbf{x}_t|\mathbf{x}_{t-1})}{g_t(\mathbf{x}_t|\mathbf{x}_{t-1})} \tag{20.39}$$

An efficient SIS algorithm is based on the following recursive computation steps, using an improved adaptive sampling weight [6, 46]:

Step 1: Simulate $\mathbf{x}_t$ from $g_t(\mathbf{x}_t|\mathbf{x}_{t-1})$, let $\mathbf{x}_t = (\mathbf{x}_{t-1}, \mathbf{x}_t)$
Step 2: Compute the adaptive sampling weight by

$$w_t = w_{t-1} \frac{\pi_t(\mathbf{x}_t)}{\pi_{t-1}(\mathbf{x}_{t-1}) g_t(\mathbf{x}_t|\mathbf{x}_{t-1})} \tag{20.40}$$

The entire sample of the input $\mathbf{x}$ is adaptively weighted until the convergence of the trial density to the target density is reached.

An important application of the SIS simulation technique is the *nonlinear filtering* algorithm based on the linear state-space model that is very popular in the system dynamics and control engineering community. In this algorithm, the system dynamics consist of two major coupled parts: (1) the state equation, typically represented by a Markov process; and (2) the observation equations, which are usually written as

$$\begin{aligned} x_t &\sim q_t(.|x_{t-1}, \theta) \\ y_t &\sim f_t(.|x_t, \phi) \end{aligned} \tag{20.41}$$

where y_t are observed state variables and x_t are unobserved state variables. The distribution of x_t are computed using the recursion:

$$\pi_t(x_t) = \int q_t(x_t|x_{t-1}) f_t(y_t|x_t) \pi_{t-1}(x_{t-1})\, dx_{t-1} \tag{20.42}$$

In applications, the discrete version of this model is called the Hidden Markov model (HMM). If the conditional distributions q_t and f_t are Gaussian, the resulting model is the called the *linear dynamic model* and the solution can be obtained analytically via recursion and coincides with the popular Kalman filter solution.

To improve the statistical convergence of SIS, we can combine it with resampling techniques, sometimes called SIR, or with rejection control and marginalization techniques.

20.5.2 Dynamic Monte Carlo (DMC)

DMC simulates realizations of a stationary stochastic field (or process) that has a unique stationary probability density identical to the prescribed JPDF. Instead of sampling directly in the original cartesian space from marginal distributions, as SMC does, DMC generates a stochastic trajectory of spatially dependent samples, or a random walk in the state-space (or local model space). Figure 20.6 shows the basic conceptual differences between standard SMC and DMC. The Gibbs sampler and Metropolis-Hastings algorithms presented in Section 20.3.2 are the basic ingredients of dynamic Monte Carlo techniques.

The crucial part of the DMC is how to invent the best ergodic stochastic evolution for the underlying system that converges to the desired probability distribution. In practice, the most used DMC simulation

Copyright 2005 by CRC Press LLC

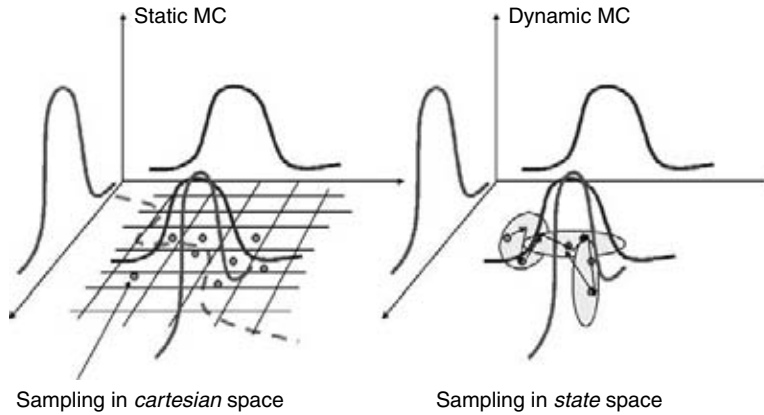

FIGURE 20.6 Conceptual differences between static Monte Carlo and dynamic Monte Carlo.

models are based on irreducible, aperiodic, reversible stationary Markov process models. The DMC simulation based on Markov process models is called Markov Chain Monte Carlo simulation, or briefly MCMC. Higher-order Markov chains or nonMarkovian are more difficult to implement. When using MCMC, a key modeling aspect is how to ensure that the samples of the chain are ergodic, especially when there is a chance that they can be stuck in a local energy minimum. The principal drawback of MCMC is that it has only local moves along its random path. This leads to a very slow convergence to equilibrium or, worse, to a stop in a local state.

A good strategy for improving MCMC movement in space is to combine the local powerful properties of MCMC with the global updating properties of molecular dynamics simulation using a Hamiltonian formulation of system dynamics. This combination is based on the Hamiltonian Markov Chain Monte Carlo (H-MCMC) algorithm [47]. The Hamiltonian MCMC is also called the Hybrid Monte Carlo (HMC). As an alternate to H-MCMC, an MCMC with random jumps has been developed [48].

Herein we describe briefly the H-MCMC algorithm. This algorithm is the preferred MCMC algorithm for high-dimensional stochastic simulation problems. The H-MCMC simulation algorithm can be efficiently implemented in conjunction with conditional PPCA expansion models. Hanson [47] claims in his research paper that "the efficiency of Hamiltonian method does not drop much with increasing dimensionality." Hanson has used H-MCMC for stochastic problems with a parameter space size up to 128 dimensions.

The H-MCMC algorithm is used to simulate a random sample of a canonical (or Gibbs, or Boltzmann) JPDF of the form:

$$\pi(\mathbf{x}) = c \text{ x } \exp(-H(\mathbf{x})) \tag{20.43}$$

This distribution is specific to Gibbs fields or equivalently to Markov fields [49]. In the above equation, $H(\mathbf{x})$ is the Hamiltonian of the dynamic system.

In the Hamiltonian formulation, the evolution of the dynamic system is completely known once the total energy or the Hamiltonian function in generalized coordinates, $H(\mathbf{q}, \mathbf{p})$, is defined:

$$H(\mathbf{q}, \mathbf{p}) = \sum_{i=1}^{n} \frac{p_i^2}{2m_i} + E(\mathbf{q}) \tag{20.44}$$

Copyright 2005 by CRC Press LLC

where **q** and **p** are the vectors of the generalized coordinates and generalized momenta (in the phase space), m_i are the masses associated with the individual particles of the system, and E(**q**) is the potential energy that ensures a coupling between the particles. System dynamics is represented by a trajectory in the phase space. For any arbitrary evolutionary function f(**q**, **p**), its rate of change is expressed by its time derivative:

$$\dot{f}(\mathbf{q},\mathbf{p}) = \sum_{i=1}^{n}\left(\frac{\partial f}{\partial q_i}\dot{q}_i + \frac{\partial f}{\partial p_i}\dot{p}_i\right) = \sum_{i=1}^{n}\left(\frac{\partial f}{\partial q_i}\frac{\partial H}{\partial p_i} - \frac{\partial f}{\partial p_i}\frac{\partial H}{\partial q_i}\right) \tag{20.45}$$

For stationary stochastic dynamics, the Hamiltonian conserves. Now, using the molecular dynamics (MD) approach, we can discretize the Hamiltonian function evolution using finite difference equations over the time chopped in small increments. The most used implementation is the leap-frog scheme [47]:

$$\begin{aligned} p_i\left(t+\frac{1}{2}\Delta t\right) &= p_i(t) - \frac{1}{2}\Delta t\frac{\partial E(q)}{\partial q_i(t)} \quad q_i(t+\Delta t) = q_i(t) + \Delta t p_i\left(t+\frac{1}{2}\Delta t\right) \quad p_i(t+\Delta t) \\ &= p_i\left(t+\frac{1}{2}\Delta t\right) - \frac{1}{2}\Delta t\frac{\partial E(\mathbf{q})}{\partial q_i(t+\Delta t)} \end{aligned} \tag{20.48}$$

The leap-frog scheme is time reversible and preserves the phase space volume. The resulting Hamiltonian-MCMC algorithm is capable of having trajectory jumps between different iso-energy surfaces and converges to a target canonical (or Gibbs, Boltzmann) distribution.

Figure 20.7 and Figure 20.8 show the application of H-MCMC to a simple bivariate stochastic field model composed of three overlapping local Gaussians. Figure 20.7 shows a simulated trajectory using the H-MCMC. The random samples were obtained by drawing sample data at each random walk step. Figure 20.8 compares the target JPDF and the estimated JPDF. The estimated JPDF is computed from the 250 random samples drawn at each step of the Markov chain evolution. It can be observed that there is a visible spatial correlation between the generated random samples. In practice, the random samples should be drawn periodically after a large number of random walk steps, so that the spatial correlation is lost. This improves considerably the convergence in probability of the H-MCMC simulation.

An extremely useful application of the DMC simulation is the stochastic interpolation for stochastic fields with missing data, especially for heavy-tailed nonGaussianity. DMC can be also used to simulate conditional-mean surfaces (response surfaces). Figure 20.9 illustrates the use of H-MCMC in conjunction with the local PPCA expansion for a univariate highly nonGaussian stochastic field with unknown mean. It should be noted that the quality of estimation depends on the data density in the sample space. Figure 20.10 shows another simple example of application of H-MCMC for simulating a univariate stochastic field with known mean using different persistence parameters (that define the magnitude of fictitious generalized momenta). The figure shows the H-MCMC samples and the exact (given) and estimated mean curves. By comparing the two plots in Figure 20.10, it should be noted that larger persistence parameters (larger generalized momenta) improve the simulation results for the mean curve in remote regions where data density is very low. Larger fictitious momenta produce larger system dynamics and, as a result, increase the variance and reduce the bias of the mean estimates. It appears that larger momenta in H-MCMC simulations are appropriate for probability estimations in the distribution tails of the joint distributions. Thus, DMC can be also employed to establish confidence bounds of stochastically interpolated surfaces for different probability levels. From the figure we can note that larger momenta provide less biased confidence interval estimates in the remote area of the distribution tails.

Copyright 2005 by CRC Press LLC

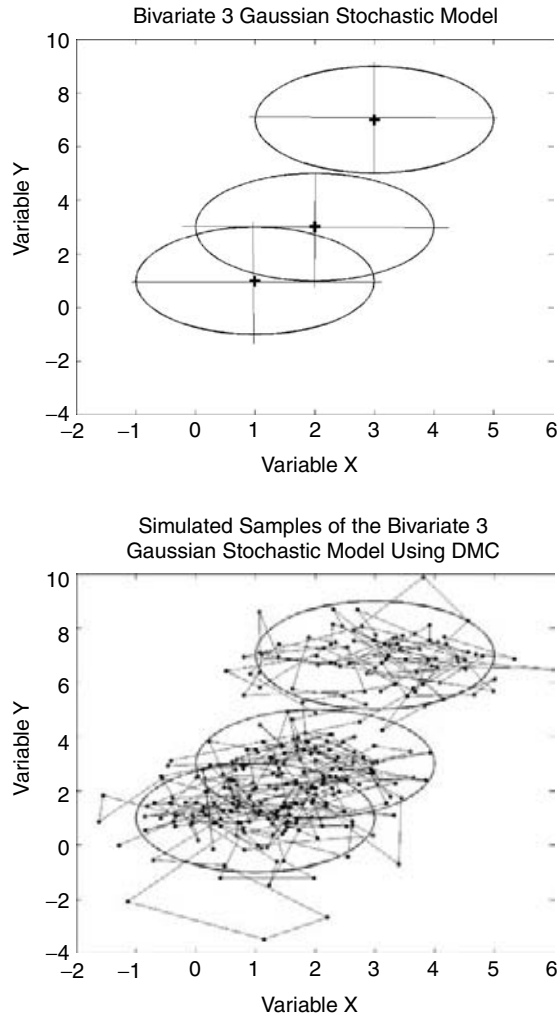

FIGURE 20.7 The prescribed stochastic model and the H-MCMC simulated random samples (drawn point data and random walk).

Other techniques to accelerate the MCMC convergence are simulated tempering and annealing. Simulated tempering and simulated annealing are popular MCMC applications of stochastic simulation to optimization under uncertainty problems. These techniques, which are described in many textbooks, are not discussed herein. This is not to shadow their merit.

20.5.3 Computing Tail Distribution Probabilities

As discussed in the introductory section of this chapter, stochastic simulation can be applied to either (1) simulate random quantities or (2) compute expectations. For probabilistic engineering analyses, both applications of stochastic simulation are of practical interest. For reliability and risk assessment analyses, the second application of simulation is used.

This section addresses the use of stochastic simulation to compute expectations. Only selective aspects are reviewed herein. The focus is on solving high-complexity stochastic problems.

Copyright 2005 by CRC Press LLC

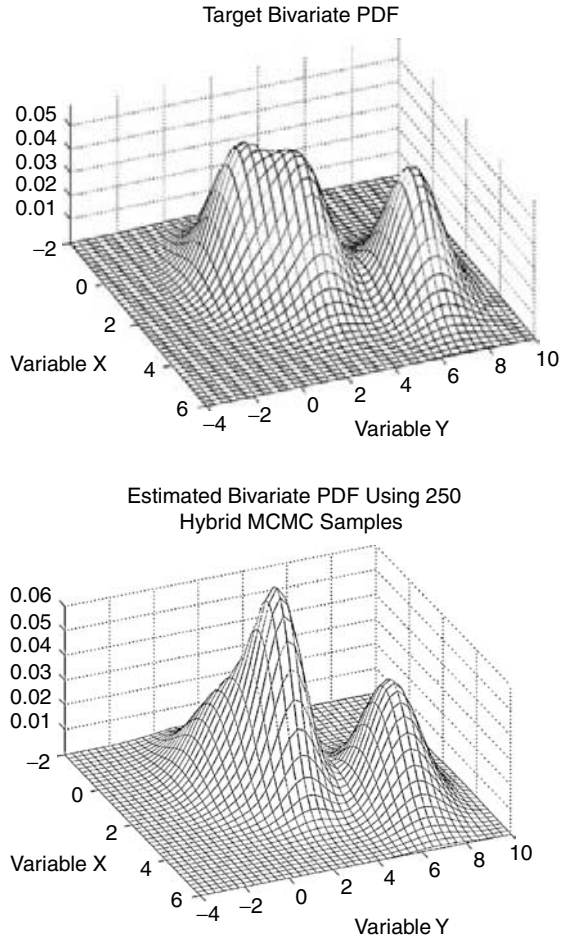

FIGURE 20.8 Target JPDF versus estimated JPDF (using 250 samples drawn at each step).

Expectations can include probability integrals for computing marginal distributions, evidences (normalization constant for the product of likelihood and prior in Bayes theorem), statistical moments, and expectation of functions. Thus, in most stochastic problems, the numerical aspect consists of computing the expected value of a function of interest f(**x**) with respect to a target probability density $g(\mathbf{x})$, where **x** is the stochastic input. Assuming that $x_1, x_2, \ldots, x_N$ are an independent identically distributed sample set from $g(\mathbf{x})$, then the Monte Carlo estimator $\hat{f}$ is computed by simple statistical averaging over the entire sample set:

$$\hat{f} = \frac{1}{N}\sum_{i=1}^{n} f(x_i) \tag{20.49}$$

The estimator $\hat{f}$ is unbiased and has the variance

$$\text{var}(\hat{f}) = \frac{1}{N}\int [f(\mathbf{x}) - E_g(f)]^2 g(\mathbf{x})\, d\mathbf{x} \tag{20.50}$$

Copyright 2005 by CRC Press LLC

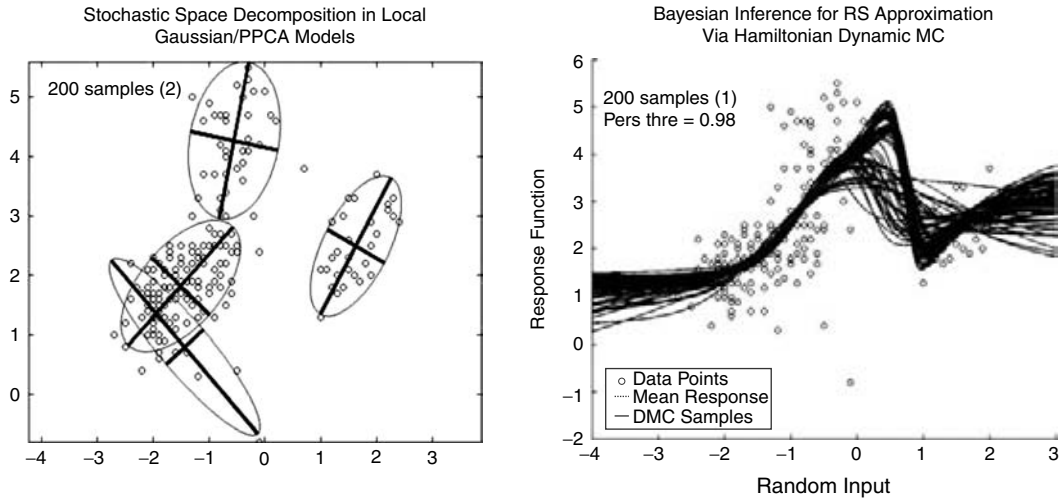

FIGURE 20.9 Stochastic Interpolation Using A Local PPCA Expansion Model via H-MCMC Simulation.

implying that the sampling error, (i.e., standard deviation) of $\hat{f}$ is O($N^{-1/2}$) independent of stochastic space dimensionality. Thus, the MC simulation estimator always converges with a constant rate that is proportional to the square-root of the number of samples. This is a key property of the standard Monte Carlo estimator that makes the SMC simulation method so popular in all engineering fields.

Many textbooks provide suggestions on how to select the required number of samples to estimate the probability of failure for a given percentage error independent of an assumed probability estimate. If the mean probability estimate $\hat{\bar{P}}_f$ has a normal distribution, the number of required samples for the confidence $1 - \alpha/2$ is given by

$$n = t^2_{1-\alpha/2,n-1}\hat{\bar{P}}_f(1-\hat{\bar{P}}_f) \tag{20.51}$$

where t is the T or Student distribution with $n-1$ degrees of freedom.

Thus, it appears that if we respect the above equation and select a small error, then we have nothing to worry about. This is not necessarily true, especially for high-dimensional problems that involve non-Gaussian stochastic fields (or responses). The delicate problem is that for standard stochastic simulation based on SMC, although the convergence rate is independent of space dimensionality, the probability estimate variance is not independent of space dimensionality. In fact, it can increase dramatically with dimensionality increase. The probability estimate variance increase affects most severely the tail probability estimates (low and high fractiles) that typically are dependent on localized probability mass distributions in some remote areas of the high-dimensional space.

Figure 20.11 shows a simple example of the increase of probability estimate variance with space dimensionality. Consider the computation of failure probability integral, I, defined by a volume that is internal to a multivariate standard Gaussian function:

$$I = \int_0^{1/4} \dots \int_0^{1/4} \exp\left(\frac{1}{2}x_1^2 + x_2^2 \dots + x_n^2\right) dx_1 dx_2 \dots dx_n \tag{20.52}$$

Copyright 2005 by CRC Press LLC

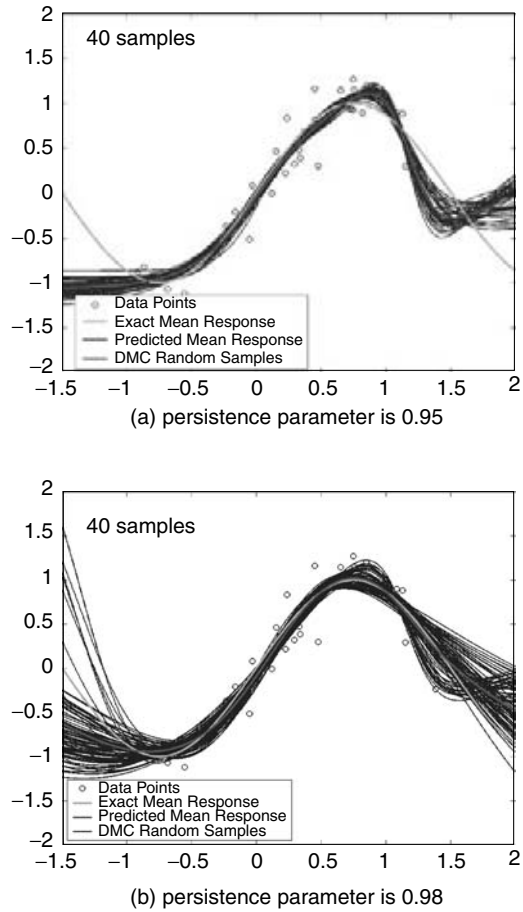

FIGURE 20.10 Effects of persistance (fictitious momenta) on the MCMC stochastic simulations a) persistence parameter is 0.95, b) persistence parameter is 0.98.

Figure 20.11 shows the plot of the coefficient of variation (c.o.v.) and the 90% (normalized) confidence interval (measure of the sampling error) as a function of input space dimension N that varies up to 10. For a number of 10,000 random samples, the c.o.v. of the failure probability estimate increases from about 3% for one dimension to about 87% for ten dimensions.

Thus, for the (random) point estimates of failure probabilities that we are typically getting from our reliability analyses, the use of Equation 20.51 for determining the number of required random samples can be erroneous, and possibly unconservative, as sketched in Figure 20.12. The required number of samples increases with the complexity of the stochastic simulation model, namely with its dimensionality and its nonGaussianity (or nonlinearity of stochastic dependencies).

20.5.4 Employing Stochastic Linear PDE Solutions

A special category of stochastic fields comprises the *physics-based* stochastic fields. These physics-based fields are defined by the output of computational stochastic mechanics analyses. The physics-based stochastic fields, or stochastic functionals, can be efficiently decomposed using *stochastic reduced-order models* (ROM) based on the underlying physics of the problem. This physics is typically described by stochastic partial-differential equations. Stochastic ROMs are computed by projecting

Copyright 2005 by CRC Press LLC

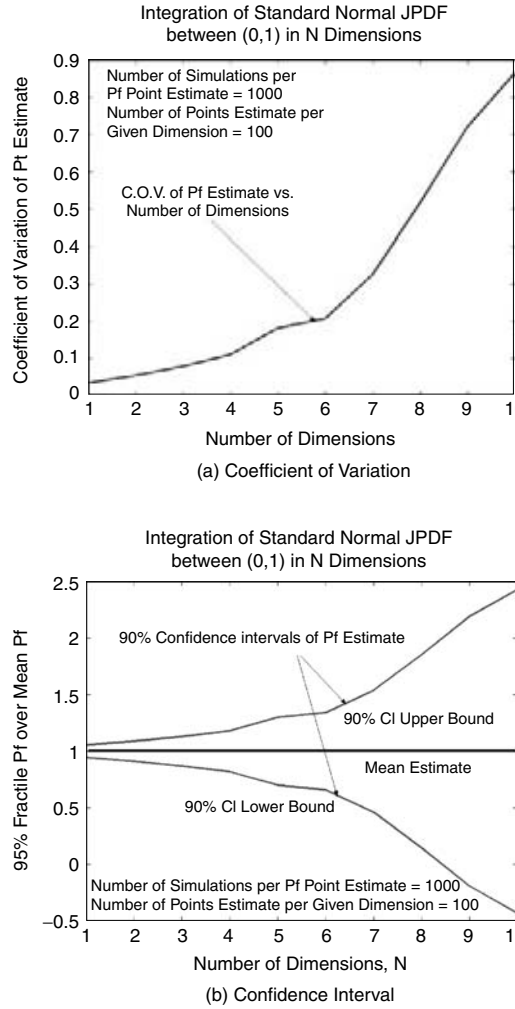

FIGURE 20.11 Effects of stochastic space dimensionality on the computed probability estimates; a) Coefficient of variation, b) Confidence interval.

the original stochastic physical field on reduced-size stochastic subspaces. Iterative algorithms using stochastic preconditioning can be employed in conjunction with physics-based stochastic ROM models.

The most used physics-based stochastic ROM models are those based on stochastic projections in the preconditioned eigen subspace, Taylor subspace, and Krylov subspace. These stochastic subspace projections are accurate for linear stochastic systems (functionals, fields) [42]. Nonlinear variations can be included by stochastically preconditioning Newton-type iterative algorithms. Both approximate and exact solvers can be used as preconditioners in conjunction with either stochastic ROM or full models. The key ingredients of the stochastic ROM implementations are (1) fast-convergent stochastic subspace expansions, (2) stochastic domain decomposition, (3) fast iterative solvers using stochastic preconditioners, and (4) automatic differentiation to compute function derivatives.

A useful industry application example of the stochastic ROM based on a eigen subspace projection is the Subset of Nominal Method (SNM) developed by Griffin and co-workers [50] for computing the mistuned (mode-localization) responses of jet engine bladed-disks due to random manufacturing deviations. The SNM approach is *exact* for proportional small variations of the linear dynamic system mass

Copyright 2005 by CRC Press LLC

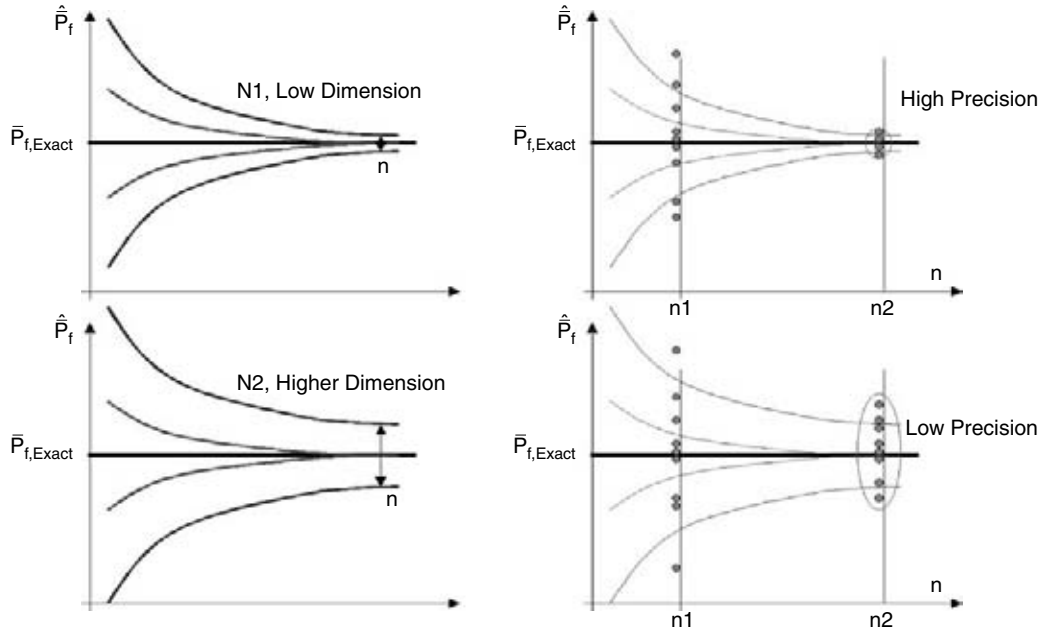

FIGURE 20.12 Space dimensionality effects on the accuracy of the computed probability estimates.

and stiffness matrices. Ghiocel [36] suggested combining the SNM approach with the KL expansion for simulating mistuned responses more realistically by including the effects of nonproportional blade variations due to manufacturing. The main idea is to use the KL expansion to reduce the stochastic input dimensionality and then use SNM iteratively to reduce the stochastic dynamic system dimensionality.

The stochastic field projections in the Taylor and Krylov subspaces can be very efficient for both static and dynamic stochastic applications. Figure 20.13 illustrates the application of the Krylov subspace expansion for computing the vibratory mistuned response of a 72-blade compressor engine blisk system. The system stochasticity is produced by the random variations in airfoil geometry due to manufacturing. Figure 20.13 shows the blade tip stochastic responses in frequency domain (transfer functions) for a given engine order excitation [34, 51]. The stochastic Krylov expansion requires only 14 basis vectors to converge. This means that only a reduced-size system of 14 differential equations must be solved at each stochastic simulation step.

The application of physics-based stochastic ROMs to stochastic simulation is limited to stochastic fields that can be described by *known* linear partial differential equations. It is obvious that the application of these stochastic ROM to computational stochastic mechanics problems is straightforward, as presented by Nair [42]. However, for stochastic fields that have an *unknown* functional structure, the physics-based stochastic ROMs are not directly applicable.

20.5.5 Incorporating Modeling Uncertainties

Engineering stochastic simulation procedures should be capable of computing confidence or variation bounds of probability estimates. The variation of probability estimates is generated by the presence of epistemic or modeling uncertainties due to (1) a lack of sufficient collection of data (small sample size issue); (2) nonrepresentative collection of statistical data with respect to the entire statistical population characteristics or stochastic system physical behavior (nonrepresentative data issue); (3) a lack of fitting the stochastic model with respect to a given statistical dataset, i.e., a bias is typically introduced due to smoothing (model statistical-fitting issue); and (4) a lack of accuracy of the prediction model with respect to real system physical behavior for given input data points, i.e., a bias is introduced at each predicted data point due to prediction inaccuracy (model lack-of-accuracy issue).

Copyright 2005 by CRC Press LLC

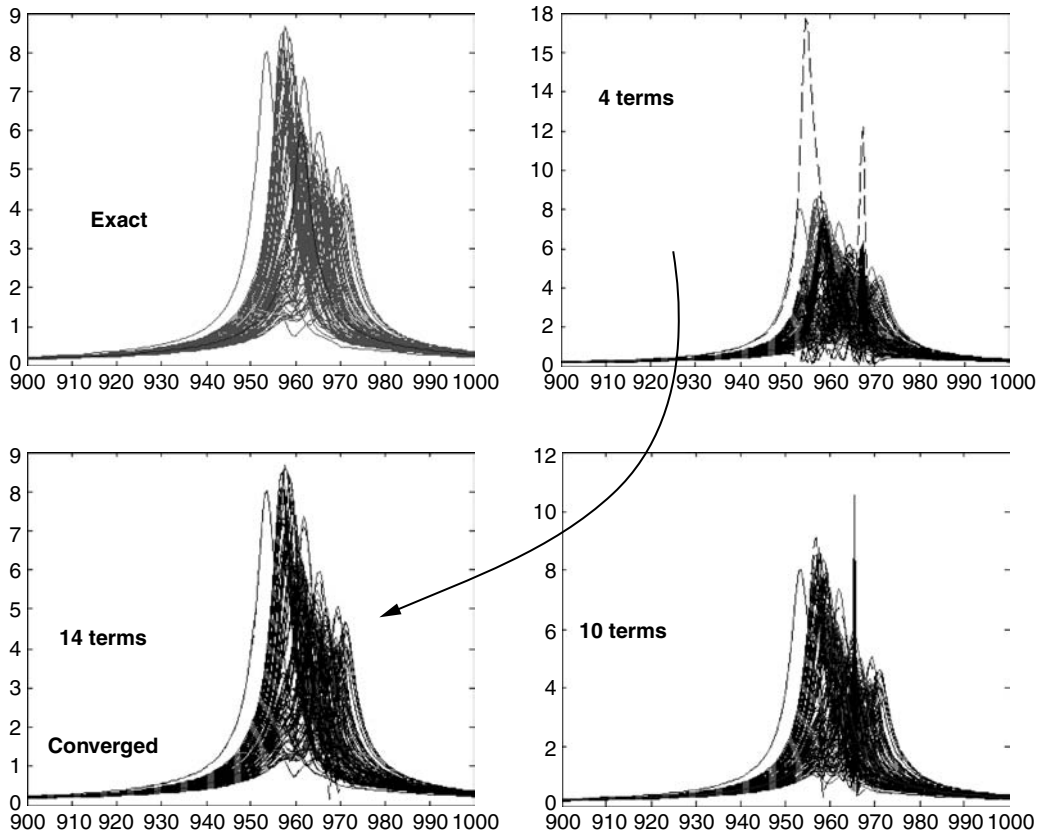

FIGURE 20.13 Convergence of stochastic Krylov subspace expansion for the random mistuned response of the blades compressor engine blisk; solid line is the full-model solution and dashed line is the reduced-model solution.

The first three modeling uncertainty categories are all associated with statistical modeling aspects. The fourth modeling uncertainty category is different. It addresses the prediction uncertainty due to the accuracy limitation of our computational models. In addition to these four uncertainty categories containing information that are objective in nature, there is also an uncertainty category related to the subjective information coming from engineering experience and judgment. Engineering judgment is an extremely useful source of information for situations where only scarce data or no data is available.

The above categories of uncertainties are described in detail in other chapters of the book. The purpose of mentioning these categories is to highlight the necessity of including them in the stochastic simulation algorithms. Unfortunately, this also increases the overall dimensionality of the stochastic simulation problem. Strategies to reduce the overall stochastic space dimensionality are needed [52].

20.6 Summary

Stochastic simulation is a powerful engineering computational tool that allows accurate predictions for complex nondeterministic problems. The most important aspect when employing simulation is to ensure that the underlying stochastic model is compatible with the physics of the problem. By oversimplifying stochastic modeling, one can significantly violate the physics behind stochastic variabilities.

Copyright 2005 by CRC Press LLC

Because the stochastic simulation is an almost endless subject, the focus of this chapter is on the conceptual understanding of these techniques, and not on the implementation details. This chapter reviews only the stochastic simulation techniques that in the author's opinion are the most significant for engineering design applications.

The chapter describes various stochastic simulation models — from simple, one-dimensional random variable models to complex stochastic network-based models. Significant attention is given to the decomposition of stochastic fields (or functionals) in constituent basis functions. Advances of stochastic functional analysis for developing efficient simulation techniques based on stochastic reduced-order models are included.

Another topic of a special attention is the stochastic simulation in high-dimensional spaces. The chapter reviews recent developments in stochastic simulation in high-dimensional spaces based on sequential importance sampling and dynamic simulation via a Hamiltonian formulation. Other key topics that are only briefly discussed include the computation of tail probabilities and the incorporation of epistemic or modeling uncertainties in simulation.

References

1. Hammersley, J.M. and Handscomb, D.C., *Monte Carlo Methods,* Methuen and Co. Ltd., London, 1964.
2. Knuth, D.C., *The Art of Computer Programming*, Addison-Wesley, Reading, MA, 1969.
3. Vaduva, I., *Simulation Models for Computer Applications*, The Series Mathematical Basis of Operational Research, Technical Editure, Bucharest, 1977.
4. Press, W.H., Teukolsky, S.A., Vetterling, W.T., and Flannery, B.P., *Numerical Recipes in FORTRAN: The Art of Scientific Computing,* Cambridge University Press, New York, 1992.
5. Law, A.M. and Kelton, W.D., *Simulation Modeling and Analysis,* McGraw-Hill, New York, 1991.
6. Gamerman, D., "Markov Chain Monte Carlo: Stochastic Simulation for Bayesian Inference," *Text in Statistical Science,* Chapman & Hall, New York, 1997.
7. Rubin, D.B., Using SIR Algorithm to Simulate Posterior Distributions (with discussion), in *Bayesian Statistics, Vol. 3,* Oxford University Press, Oxford, England, 395–402, 1987.
8. Gilks, W.R. and Wild, P., Adaptive Rejection Sampling for Gibbs Sampling, *Applied Statistics,* 41, 337–348, 1992.
9. Box, G.E. and Muller M.E., A Note of the Generation of Random Normal Deviates, *Annals of Mathematical Statistics,* 29, 610–611, 1958.
10. Butcher, J.C., Random Sampling from the Normal Distributions, *Computing Journal*, 3, 1961.
11. Grigoriu M., *Applied Non-Gaussian Processes,* Prentice Hall, Englewood Cliffs, NJ, 1995.
12. Metropolis, N., Rosenbluth, A.W., Rosenbluth, M.N., Teller, A.H., and Teller, E., Equations of State Calculations by Fast Computing Machines, *Journal of Chemical Physics,* 21(6), 1087–1091.
13. Geman, S. and Geman, D., Stochastic Relaxation, Gibbs Distributions and the Bayesian Restoration of Images, *IEEE Transactions on Pattern Analysis and Machine Intelligence,* 6, 721–741, 1984.
14. Ghiocel, D.M., Stochastic Field Models for Advanced Engineering Applications, *42nd AIAA/ASME/ASCE/AHS/ASC Structures, Structural Dynamics, and Materials Conference, AIAA/ASCE/ASME Non-Deterministic Approaches Forum,* Seattle, WA, April 16–19, 2001.
15. Ghanem, R.G. and Spanos, P.D., *Stochastic Finite Elements: A Spectral Approach,* Springer-Verlag, Heidelberg, 1991.
16. Wiener, N., The Homogenous Chaos, *American Journal of Mathematics,* 60, 897–936, 1938.
17. Pearson, K., On Lines and Planes of Closest Fit to Systems of Points in Space, *Philosophical Magazine,* 2, 559–572, 1958.
18. Everitt, B.S. and Dunn, G., *Applied Multivariate Data Analysis,* Arnold, Oxford University Press, London, 2001.
19. Grigoriu, M., *Stochastic Calculus,* Birkhauser, Boston, MA, 2002.

Copyright 2005 by CRC Press LLC

20. Yamazaki, K. and Shinozuka, M., Safety Evaluation of Stochastic Systems by Monte Carlo Simulation *9th SMiRT Conference,* Volume M, Lausanne, August 17–21, 1987.
21. Deodatis, G., Non-Stationary Stochastic Vector Processes: Seismic Ground Motion Applications, *Probabilistic Engineering Mechanics,* 11, 149–168, 1996.
22. Shinozuka, M. and Deodatis, G., Stochastic Process Models for Earthquake Ground Motion, *Journal of Probabilistic Engineering Mechanics,* 3, 191–204, 1988.
23. Ghiocel, D.M., Uncertainties of Seismic Soil-Structure Interaction Analysis: Significance, Modeling and Examples, Invited Paper at the *US–Japan Workshop on Seismic SSI, Organized by the NSF/USGS,* Menlo Park, CA, September 22–24, 1998.
24. Ghiocel, D.M. and Ghanem, R.G., Stochastic Finite Element Analysis for Soil-Structure Interaction, *Journal of Engineering Mechanics,* ASCE, 128(1), January 2002.
25. Shinozuka, M., Stochastic Fields and Their Digital Simulation, in *Stochastic Methods of Structural Dynamics,* Schueller, G.I. and Shinozuka, M., Eds., Martinus Nijhoff, Dordrecht, 1987, 93–133.
26. Ghiocel, D.M. and Trandafir, R., Application of Space-Time Stochastic Processes in Load Modeling for Structural Design of Special Facilities, *6th National Symposium on Informatics in Civil Engineering,* Timisoara, June 1988 (in Romanian).
27. Ghiocel, D.M. and Ghiocel, D., Structural Behavior of Large Cooling Towers on Wind Load, *Scientific Bulletin of Civil Engineering,* Vol. 1, ICB, Bucharest, 1988 (in Romanian).
28. Ghiocel, D.M. and Ghiocel, D., Stochastic Modeling and Simulation of Wind Fluctuating Pressure Field on Large Diameter Cooling Tower Structures, *ASCE Probabilistic Structural Mechanics Conference,* Sandia National Laboratories, Alburquerqe, NM, July 24–26, 2004 (submitted).
29. Romanowski, M., Reduced Order Unsteady Aerodynamic and Aeroelastic Models Using Karhunen-Loeve Eigenmodes, *AIAA Journal,* Paper AIAA 96–3981, 1996.
30. Thomas, J.P., Dowell, E.H., and Hall, K.C., Three Dimensional Transonic Aeroelasticity Using Proper Orthogonal Decomposition-Based Reduced Order Models, *Journal of Aircraft,* 40(3), 544–551, 2003.
31. Ghiocel, D.M., Refined Stochastic Field Models for Jet Engine Vibration and Fault Diagnostics, *Proceedings of International Gas Turbine & Aeroengine Congress,* 2000 TURBO EXPO, Paper 2000-GT-654, Munich, Germany, May 8–11, 2000.
32. Ghiocel, D.M., A New Perspective on Health Management Using Stochastic Fault Diagnostic and Prognostic Models, *International Journal of Advanced Manufacturing Systems, Special Issue on* "*Non-Deterministic Methods for Design and Manufacturing Under Uncertainties,*" Vol. 4, Issue 1, October 2001.
33. Hilbert, G. and Blair, A., Accuracy of Forced Response Prediction of Gas Turbine Rotor Blades, *4th National Turbine Engine HCF Conference,* Monterey, CA, March 6–9, 1999.
34. Ghiocel, D.M., Mistuning Analysis of Bladed-Disks, in *STI BLADE-GT Engineering Research Report for AFRL/PRT at Wright-Patterson Air Force Base,* Proprietary Information, USAF Contract F33615-96-C-2678, Dayton, OH, June 2002.
35. Brown J. and Grandhi, R.V., Probabilistic Analysis of Geometric Uncertainty Effects on Blade-Alone Forced Response, *Proceedings of the 2004 ASME Turbo Expo,* IGTI 2004, Vienna, June 14–17, 2004.
36. Ghiocel, D.M., Critical Probabilistic Modeling and Implementation Issues for Geometry Mistuning in Engine Blisks, presentation at the *6th Annual FAA/AF/NASA/Navy Workshop on the Application of Probabilistic Methods to Gas Turbine Engines,* Solomon Island, MD, March 18–20, 2003.
37. Blair A. and Annis, C., Development of Probabilistic Methods for Campbell Diagram Frequency Placement, presentation at the *7th National Turbine Engine High Cycle Fatigue Conference,* Monterey, CA, April 16–19, 2003.
38. Ghiocel, D.M., Stochastic Modeling of Airfoil Thickness Spatial Variability due to Manufacturing Process, presented at the *6th National Turbine Engine High Cycle Fatigue Conference,* Jacksonville, FL, March, 5–8, 2001.
39. Ghiocel, D.M., Stochastic Field Models for Aircraft Jet Engines, *Journal of Aerospace Engineering,* ASCE, Special Issue on Reliability of Aerospace Structures, Vol. 14, No. 4, October 2001.

Copyright 2005 by CRC Press LLC

40. Griffiths, J.A. and Tschopp, J.A., Selected Topics in Probabilistic Gas Turbine Engine Turbomachinery Design, in *CRC Press Engineering Design Reliability Handbook,* Nikolaidis, E., Ghiocel, D.M., and Singhal, S., Eds., CRC Press, Boca Raton, FL, 2004.
41. Casenti, B., Probabilistic Blade Design, United Technologies — Pratt and Whitney Final Report, USAF Contract F33615-98-C-2928, June 2003.
42. Nair, P.B., Projection Schemes in Stochastic Finite Element Analysis, in *CRC Press Engineering Design Reliability Handbook*, Nikolaidis, E., Ghiocel, D.M., and Singhal, S., Eds., CRC Press, Boca Raton, FL, 2004.
43. Grigoriu, M., Formulation and Solution of Engineering Problems Involving Uncertainty, Invited presentation at the *Biannual SAE Probabilistic Method Committee Meeting*, Detroit, October 7–9, 2003.
44. McKay, D.J.C., *Bayesian Interpolation*, Neural Computation, 1992.
45. Robert, C.P. and Casella, G., *Monte Carlo Statistical Methods*, Springer-Verlag, Heidelberg, 1999.
46. Liu, J., Monte Carlo Strategies in Scientific Computing, *Spring Series in Statistics,* Springer-Verlag, Heidelberg, 2001.
47. Hanson, K.M., Markov Chain Monte Carlo Posterior Sampling with the Hamilton Method, *Proceedings SPIE 4322, Medical Image: Image Processing,* Sonka, M. and Hanson, M.K., Eds., San Diego, CA, 2001, 456–467.
48. Green, P.J., Monte Carlo Methods: An Overview, Invited Paper, *Proceedings of the IMA Conference on Complex Stochastic Systems and Engineering,* Leeds, U.K., September 1993.
49. Fismen, M., Exact Simulation Using Markov Chains, M.Sc. thesis, Norvegian Institute of Technology and Science, Trondheim, December 1997.
50. Yang, M.-T. and Griffin, J.H., A Reduced Order Model of Mistuning Using a Subset of Nominal Modes, *Journal of Engineering for Gas Turbines and Power,* 123(4), 893–900, 2001.
51. Keerti, A., Nikolaidis, E., Ghiocel, D.M., and Kirsch, U., Combined Approximations for Efficient Probabilistic Analysis of Structures, *AIAA Journal,* 2004.
52. Ghiocel, D.M., Combining Stochastic Networks, Bayesian Inference and Dynamic Monte Carlo for Estimating Variation Bounds of HCF Risk Prediction, presentation at the *7th National Turbine Engine High Cycle Fatigue Conference,* Monterey, CA, April 16–19, 2003.

Copyright 2005 by CRC Press LLC